

Regional Geology Reviews



Jacques Varet

Geology of Afar (East Africa)

Regional Geology Reviews

Series editors

Roland Oberhänsli
Maarten J. de Wit
François M. Roure

More information about this series at <http://www.springer.com/series/8643>

Jacques Varet

Geology of Afar (East Africa)

 Springer

Jacques Varet
Géo2d
Orléans
France

ISSN 2364-6438 ISSN 2364-6446 (electronic)
Regional Geology Reviews
ISBN 978-3-319-60863-1 ISBN 978-3-319-60865-5 (eBook)
<https://doi.org/10.1007/978-3-319-60865-5>

Library of Congress Control Number: 2017947821

© Springer International Publishing AG 2018

This work is subject to copyright. All rights are reserved by the Publisher, whether the whole or part of the material is concerned, specifically the rights of translation, reprinting, reuse of illustrations, recitation, broadcasting, reproduction on microfilms or in any other physical way, and transmission or information storage and retrieval, electronic adaptation, computer software, or by similar or dissimilar methodology now known or hereafter developed.

The use of general descriptive names, registered names, trademarks, service marks, etc. in this publication does not imply, even in the absence of a specific statement, that such names are exempt from the relevant protective laws and regulations and therefore free for general use.

The publisher, the authors and the editors are safe to assume that the advice and information in this book are believed to be true and accurate at the date of publication. Neither the publisher nor the authors or the editors give a warranty, express or implied, with respect to the material contained herein or for any errors or omissions that may have been made. The publisher remains neutral with regard to jurisdictional claims in published maps and institutional affiliations.

Printed on acid-free paper

This Springer imprint is published by Springer Nature
The registered company is Springer International Publishing AG
The registered company address is: Gewerbestrasse 11, 6330 Cham, Switzerland

Foreword

The Afar depression in East Africa is one of the most important geological structures on Earth. It is the area of the junction of three major structures of the Earth's crust: the Red Sea, the Gulf of Aden and the East African Rift. Nearly 50 years have passed since January 1968, when a French-Italian team led by Giorgio Marinelli and Haroun Tazieff, of which Jacques Varet and I were young members, initiated the systematic geological exploration of Afar. I am therefore very pleased to write this preface to the book by Jacques on the geology of Afar.

Since our first mission, we have been fascinated by the geology of Afar and by the discovery—along the axis of the depression—of some active volcanic ranges displaying magmatic and tectonic features suggesting that they were oceanic structures, an indication of continental laceration. It was, however, only after some years, when sufficiently wide zones of Afar had been explored, that general structural interpretation could be attempted. Extensive radiometric dating of volcanic rocks, coupled with tectonic, petrological and geochemical studies, enabled us to establish that internal Afar was almost entirely floored by recent volcanic rocks (less than four million years old) and that older formations were outcropping only on the depression margins. We thus proposed a two-stage evolution model: an initial long stage of continental rifting which began in Early Miocene (around 25 million years ago) was followed nearly four million years ago by a stage of continental break-up with the development of oceanic structures.

Detailed investigations on the eastern margin showed that the connection between the Red Sea and the Gulf of Aden spreading axes had to be found within Afar, as a connection through Bab-el-Mandeb strait (as until then believed) was geologically unsustainable. The Southern Red Sea and eastern Afar margin, in fact, have been stable for eight million years and, therefore, had to be considered as an accretion of the Arabian plate.

Volcanic structures, analogous to oceanic ridges and fracture zones, were identified within Afar. Axial ranges—where basalts of a tholeiitic to transitional affinity erupted along open fissures—displayed geochemical, topographical and geophysical similarities to mid-oceanic spreading ridges, therefore marking the zone where new oceanic crust was accreting within Afar. Transverse tectonic lineaments, with subordinate alkali basaltic volcanism, marked along Afar the equivalent of oceanic fracture zones of the same type as those occurring in the equatorial Atlantic Ocean. By analogy with clay experiments, some sets of en échelon faults connecting adjacent axial ranges were interpreted as the surface expression of transform faults. The identification of these structures was the basis for the reconstruction of the present plate boundaries within Afar. A complex picture emerged, with a mosaic of microplates located in the junction zone of the three major Arabian, African and Somalian plates, some of them being deeply affected by deformation even far from the margins.

On the other hand, petrological and geochemical studies revealed a complex variation in the nature of volcanic products from one type of structure to the other, and even within a single structure. These studies showed that axial ranges consisted of basalts and subordinate products of their differentiation, whereas crustal contamination had modified the composition of products erupted in the volcanic complex located near the Afar margins, where attenuated continental crust was present.

The occurrence of complete sequences of rocks from basalts to peralkaline rhyolites enabled the study of the basalt fractionation process. A combined geochemical, petrological and mineralogical approach enabled us to reconstruct the solid–liquid equilibria during the fractionation process and to evaluate the controlling physical-chemical parameters.

These studies also showed that few basalts of the Afar axial ranges (Manda Hararo and Asal) had tholeiitic composition identical to the equivalent rocks of the Red Sea and Gulf of Aden spreading axes. Elsewhere in the Afar axial ranges, basalts tended to be more alkalic, although remaining in the field of transitional basalts; in these ranges, fractionation processes are, in general, more developed. Considering the structural position of the various axial ranges in Afar, we were inclined to relate these differences to variations in the spreading rate. A lower spreading rate would have favoured a lower degree of the mantle partial melting, producing basalts with a more alkalic affinity. In these low-rate spreading segments, shallow magma chambers may have formed where slowly supplied basalts were fractionated, forming various differentiates.

The geological studies carried out in Afar in the last few decades confirmed these basic findings of the French-Italian team, including those on the 2005–2010 tectono-volcanic crisis of Manda Hararo, which represents a typical spreading episode of an oceanic axial range in central Afar.

In 1975 Jacques and I were the first recipients of the Wager Prize, awarded to us by the International Association of Volcanology and Chemistry of the Earth Interior and the Royal Society of London for our “fruitful collaborative study of Afar”. I think that the reason was largely the extraordinary interest of the Afar geology and I am sure that this book will contribute to the diffusion of the knowledge of this beautiful desert.

Franco Barberi
Università degli Studi Roma Tre Rome Italy

Acknowledgements

The author wishes to express his gratitude to all the people who supported him during these years of studies of the Afar region:

- His wife, the late Catherine Sornein, who was always so understanding and supportive during 40 years of life together, with their four children Christohe, Léopold, Sébastien and Caroline. A beautiful volcano in the Erta Ale range (see cover page) was given her name by H. Tazieff and G. Marinelli, and her intelligence and her kindness were equal to her beauty.
- The late Professor Giorgio Marinelli, who not only welcomed the author into his laboratory in Pisa, always providing the most useful advice and research facilities, but also acted as an “adoptive father”, hosting the whole family in his house on the Tyrrhenian Sea every summer to facilitate joint work with the team of the University of Pisa.
- The late Haroun Tazieff, who organised the Afar expeditions with his ability to attract sponsors, thanks to his wide reputation and strong personality, contrasting with the surrounding academic world to which he was contributing.
- Franco Barberi, now emeritus professor at the University of Roma 3, assistant to Giorgio Marinelli at Pisa University at the time the work started in Afar, then Professor at the same university. Later Vice-Minister for natural hazards, he played a major role in the renewal of Earth sciences in Italy. Most of the work presented in this book was developed with him. I also had the honour to share the first Wager prize with him.
- Lul Mengesha Seyoum, “Ras” of Tigré province in Emperor’s Haile Selassie’s time, who identified early on the CNR-CNRS team as a potential contribution to the development of this then unknown region of Afar, and constantly supported our work, not hesitating to come himself driving a bulldozer when the whole team was stuck in thixotropic mud after unforeseen heavy rains! Despite political changes, he kept his interest and convinced the new authorities of Afar and Tigré Regional States to invite Franco and myself again to help to develop geothermal in Afar 30 years after having escaped from the country when the DERG (Coordinating Committee of the Armed Forces, Police and Territorial Army) took power.
- The late Professor Russel Black, who invited me to come for 2 years as Assistant Professor at Addis Ababa University (1970–1972), where I could attract the interest of Ethiopian students for the fantastic Earth sciences opportunities in their country. This brings about special thoughts for our students and colleagues, some of whom survived and succeeded, whereas others were killed by the DERG (such as Johannes and Bill Morton) or while fighting in the bush.
- The late Prof. Robert Brousse who asked me to become his assistant at the age of 22 and allowed me to train on volcanic petrology and mineralogy in the French Massif Central.
- Valuable and so friendly colleagues from Italy such as the late Professor Giorgio Ferrara, Enrico Bonatti and Roberto Santacrose, as well as from France such as the late Françoise Gasse, Michel Treuil (with whom we jointly presented our “State Thesis”), Hélène Bizouard, Jacques Demange and the late Jean-Louis Cheminée—I cannot mention all of them here.

- For the most recent observations in Ethiopian Afar, I benefitted from the support of Ismail Ali Gardo and Colonel Atsede (Anbesit Nebro), co-founders (with Lul Mengesha and myself) of AGAP (the new Afar Geothermal Development Company), from the support of Fouad Aye, Minister of Energy, Water and Natural Resources, and from BGR for renewed works in Djibouti in advising the newly-created ODDEG (Office Djiboutien de Développement de l’Energie Géothermique). I thank his director Dr. Kayad Mousa and his staff as well as my friend Abdourahman Haga.

Contents

Part I Afar: Global Context

1 Global and Regional Geodynamic Context	3
References.	12
2 Relief, Climate, People, Languages, Toponymy and Exploration History	13
2.1 Topography of Surrounding Plateaus	13
2.2 Climate and Ecology	15
2.3 Ethnographic Context	16
2.4 Afar Topographic Maps and Toponymy.	22
2.5 History of Afar Exploration	23
References.	38
3 Geophysical Frame: Mantle Plume(s), Triple Points, Rifting Processes	39
3.1 The Nubian Plateau Uplift and Associated Volcanism	39
3.2 From Continental Doming to Rifting: The Continental Rift Stage	43
3.3 Mantle Plume in Afar and East Africa, Geochemical and Geophysical Approaches	44
3.4 The Afar Triple Junction, a “Textbook Example”?	48
3.5 Geodynamic Relations Between Doming and Rifting Inferred from Petrological Studies	50
References.	53

Part II The Early Afar Geological Formations

4 Pre-Quaternary Geological Frame	57
4.1 The Afro-Arabian Plate Before Doming and Rifting	57
4.2 Geology of the Plateau Margins Surrounding Afar	61
4.2.1 The Nubian Margin	61
4.2.2 The Arabian Margin	65
4.2.3 The Somalian Margin	66
4.2.4 The “Danakil Alps” (or Arrata)	68
4.2.5 The Aisha—Ali-Sabieh Block	71
4.3 The Miocene Peralkaline Granite Intrusions of Afar	74
4.4 The Mio-Pliocene “Polychromatic Formation”	76
4.5 The Adolei Basalts	77
4.6 The Mabla Rhyolites	79
4.7 The Dalha Basalts	82

4.8	The Hadar Formation (Central Western Afar, Awash Basin), a Treasure in Human Palaeontology	89
	References.	90
5	First Stage of Oceanisation of the Afar Floor: The Stratoid Series (4–1 Million Years Ago)	93
5.1	The Basaltic Fissural Piles (Afar Stratoid Series Stricto Sensu)	93
5.2	The Silicic Centres Associated with the Stratoid Series	94
5.3	The Recent Basaltic Flows of the Upper Part of the Stratoid Series.	96
5.4	Spectacular Grabens Delimited by the Faulting Affecting the Stratoid Series in Southern Afar	99
	References.	104
 Part III Afar Quaternary and Presently Active Geological Units		
6	Axial Volcanic Ranges	107
6.1	Afar Axial Ranges (Emerged MOR Analogues)	107
6.2	Erta Ale Axial Range	109
6.2.1	Submarine and Sublacustrine Initial Activity of the Rift Floor	112
6.2.2	Hayli Gub Axial Emitting Fissures and Shield Volcano	117
6.2.3	Erta Ale Shield Volcano.	120
6.2.4	Borale Ale Cumulo-Volcano.	129
6.2.5	Alu and Dala Filla Cumulo-Volcanoes	138
6.2.6	Gada Ale Volcano.	143
6.2.7	Ale Bagu Strato-Volcano	146
6.3	Tat'Ali–Mat'Ala Axial Range.	151
6.4	Alayta Axial Range.	157
6.5	Dabbahu Volcanic Centre	162
6.6	Manda Harraro Axial Range.	167
6.6.1	Geological Description.	167
6.6.2	The 2005 Dabahu–Manda Harraro 2005–2010 Rifting Episode.	175
6.6.3	Manda Harraro in the Context of Afar Volcanic Ranges.	180
6.7	Manda Inakir Axial Range.	181
6.8	Asal Axial Range	187
6.8.1	Geology of the Asal Volcanic Range	187
6.8.2	The Ardoukoba Simo-Volcanic Event, 1978	189
6.8.3	Geothermal Exploration and Undergoing Developments at Asal.	196
6.9	The Gulf of Tadjourah Oceanic Spreading Segments.	197
6.10	Discussion: The Significance of the Axial Ranges.	200
	References.	202
7	Recent and Active Units of the Danakil Sea (Dagad Salt Plain) and Afdera Lake	205
7.1	The Danakil Sea and the Dagad Salt Plain	205
7.1.1	Marine Limestones	205
7.1.2	Gypsum Deposits	208
7.1.3	Salt Deposits	209
7.1.4	Loams and Silts of the Plains	210

7.2	Volcanoes of the Gulf of Zula (Eritrea)	211
7.3	Alid Volcanoes (Eritrea)	211
7.4	Maraho Submarine Volcano in the Dagad Salt Plain	214
7.5	Dallol Hydrothermal Dome in the Dagad Salt Plain.	217
7.6	As Ale Phreatic Explosion Crater in the Dagad Salt Plain	218
7.7	Lake Afdera and Sodonta Plain	218
7.7.1	Lacustrine Limestones and Diatomites	218
7.7.2	Lake Afdera	219
7.8	Comments on the Danakil Sea and Other Sedimentary Areas	221
	References.	225
8	Central Silicic Volcanoes of the Afar Margins	227
8.1	Ma'alalta (Pierre Pruvost)	227
8.2	The Bidu Transverse Alignment	228
8.3	Moussa Ali	235
8.4	Comments About These Volcanic Centres of Afar Margins	236
	References.	239
9	Transverse Volcanic Alignments Along Afar Margins.	241
9.1	Dubbi (Eritrea)	241
9.2	Hanish-Zukur (Red Sea Islands)	241
9.3	Ado Ale (Assab Range, Eritrea)	243
9.4	Gufa (South Eritrea)	244
9.5	Sawābi Islands (Sept Frères, Djibouti)	244
9.6	Dabbayra (Western Afar)	244
9.7	Geodynamic Interpretation of These Transverse Units	245
	References.	251
10	Southern Afar: The Main Ethiopian Rift (MER) Northern Extremity	253
10.1	Sedimentary Plains of Southern Afar.	253
10.1.1	The Yaldi-Hadar Basin	253
10.1.2	The Kalo (Tendaho)-Gobaad Graben	254
10.1.3	The Grabens of Southern Afar	257
10.2	Geodynamics of Tendaho-Gobaad Graben	259
10.2.1	Volcanic Features in the Tendaho-Gobaad Graben.	259
10.2.2	Dama Ale Shield Volcano	260
10.2.3	Discussion of the Geodynamic Significance of the Tendaho-Gobaad Graben.	264
10.3	The MER Volcanic Units of Afar	266
10.3.1	Gabilema.	266
10.3.2	Yangudi.	268
10.3.3	Ayelu-Abida (Called Amoisa in Ahmaric)	269
10.3.4	Angelele-Hertale	272
10.3.5	Dofan	276
10.3.6	Fantale.	279
	References.	281

Part IV Conclusive Remarks

11 Afar, a Hot-Spot for Earth's Geodynamics Studies	285
11.1 The Process of Break-up of a Continent in an Area of Triple Junction	285
11.2 From Continental to Oceanic Rifting	287
11.3 Transform Faults and Fracture Zones.	288
11.4 MOR and Oceanic Island Analogues	289
11.5 Pertinence and Limits of Mantle Plume Models	289
11.6 Proposed Interpretation of the Evolution of Spreading Within Afar	290
References.	293
12 Geological Resources and Socio-Economic Issues	295
12.1 Thermal Manifestations, Geothermal Potential and Development Perspectives	295
12.1.1 Despite Arid Climate, a Gifted Region.	295
12.1.2 Alid (Eritrea)	296
12.1.3 Dallol (North Afar, Ethiopia)	298
12.1.4 Tat'Ali Near Afdera (North Afar, Ethiopia)	299
12.1.5 Dabbahu Near Teru (West Afar, Ethiopia)	299
12.1.6 South Manda Harraro Geothermal Sites (Including Tendaho Graben, Central Afar, Ethiopia).	300
12.1.7 Dama Ale in Ethiopia and Lake Abhe in Djibouti	303
12.1.8 Asal in Djibouti Republic.	303
12.1.9 Other Sites in Djibouti Republic	309
12.1.10 Gawani Area	310
12.1.11 Dofan	311
12.1.12 Fantale.	313
12.1.13 Future Dreams: Drilling Through an Oceanic Ridge from Land	314
12.1.14 General Considerations on Geothermal Development Perspectives in Afar.	316
12.2 Mineral Resources	317
12.2.1 Metallic Resources Associated with the Tectono-Magmatic and Geothermal Context.	317
12.2.2 Mineral Resources Related to Marine or Lacustrine Evaporitic Contexts	317
12.2.3 Metallic Resources Associated with Synsedimentary Hydrothermal Activity	318
References.	321
13 Afar, One Geology, One Culture, Spread in Three Countries, at Present a Melting Pot	323
Conclusion	325
References	327

Introduction

The Afar Triangle is a geological depression that developed in the area of the triple Junction where two oceanic ridges, the Gulf of Aden and the Red Sea, and a continental rift, the East African Rift Valley, meet. It has long been considered to be the northern extremity (“funneling out”, Mohr, 1962, 1967) of the Great Rift Valley. It is also considered to be one of the most important mantle plumes (or “hot spots”) of the Earth system.

For the past 50 years it has attracted the attention of geologists and geophysicists worldwide as all the steps of the formation of an ocean, from the initial up-doming of the continent with associated trap basalts to the initial crustal thinning and continental drifting, and finally development of an oceanic crust through basaltic dike and surface emissions, with identification of well-defined spreading segments, were involved.

It overlaps Eritrea, Djibouti and Ethiopia, and is bordered by the Ethiopian plateau to the west, by the Danakil block that separates the Afar depression from the Red Sea to the north-east, and by the Somalian Plateau, and its northern extension in the Aisha – Ali-Sabieh block to the south (Fig. 1).

It includes the lowest point in Africa, Lake Asal in Djibouti (154 m below sea level). The Awash River is the main water-flow into the area, and ends in Lake Abhe at the Djibouti-Ethiopia boundary. The northern part of the Afar Triangle is also known as the Danakil Depression, with the great salt plain (a former sea) 120 m below sea level. Afar is also known as one of the hottest places on Earth. The climate varies from 30 °C during the rainy season (July–August, when the salt plain is covered with water) to 48 °C during the dry season (most of the year). The best season to visit Afar remains the period from November to January.

Besides its geological particularities described in this book, which make it the only place in the world where an oceanic plate boundary can be observed on land with all its successive steps of development since continental break-up, the Afar Triangle is also known as one of the cradles of the first extinct hominids. The Middle Awash area contains sites of several fossil discoveries, such as the Ardi site of *Ardipithecus ramidus*, Gona, site of the oldest stone tools, and Hadar, site the *Australopithecus afarensis*, better known as *Lucy*.

This book summarises the geological knowledge accumulated on Afar over the last 50 years. The author had the chance to be included, as a young geoscientist, in the “CNR-CNRS Afar team”, a Franco-Italian research group led by Haroun Tazieff (Paris) and Giorgio Marinelli (Pisa). These two strong personalities had different motivations for undertaking these expeditions in this supposedly “hostile” desert part of the planet: the first to discover new active volcanoes, the second to follow his father’s discoveries in eastern Africa. Dainelli and Marinelli (1912) were the first to provide an exhaustive geographical and geological description of the “Geologia dell’ Africa Orientale” (Dainelli 1943). For 10 years the team undertook extensive field works in winter (December–January), when the climate was less torrid, and this was complemented by laboratory work in Orsay and Pisa Universities. This pioneering work benefited from the support of H.H. Ras Mengesha Seyoum, Governor of the Tigré Province which included northern Afar, and of his team including Aberra and Girma who accompanied Franco Barberi and myself in long walks through the rugged lava, as only limited parts of the area was accessible with four-wheel-drive cars.

In December 1967, when the first expedition was organised, little information was available on the geology of the area, and even geographic base maps were lacking. The US 1/250,000



Fig. 1 The Afar depression is a rather striking feature—surrounded by the Ethiopian, Yemen and Somali plateaus, in the area of junction of the Gulf of Aden, the Red Sea and the Ethiopian Rift Valley, as seen on this relief map (extracted from Colorado Geology Photojournal; note the white line drawing the plate boundary is inadequate <http://www.cliffshade.com/colorado/tectonics.htm>)

sheets, the only ones available, did not provide much relevant information in this desert lowland as only rivers and major summits were reported. When the first satellite photographs became available from the Apollo and Gemini space missions, a completely new picture of the Red Sea – Gulf of Aden region was obtainable, providing a new vision of the Afar triangle (Fig. 2). Further missions provided more detailed information, allowing for complementary geological interpretations (Bannert 1972).



Fig. 2 Horn of Africa and Arabia photograph from the Gemini-Titan X1 space mission (1966) showing the first available picture of the Red Sea, Gulf of Aden and Afar area with the Arabian Peninsula (*on left*) and northeast Africa (*on right*) as seen at an altitude of 340 nautical miles, looking southeast. GT-11, Vintage Color—NASA Photo ID: S-66-54536

At the time of the emergence of the plate tectonics theory (Morgan 1968), the symposium organised on March 27–29, 1969 by the Royal Society in London on “The Structure and Evolution of the Red Sea and the Nature of the Red Sea, Gulf of Aden and Ethiopian Rift Junction” (Falcon et al. 1970) showed for the first time that an oceanic floor could be found in Afar. Five years later, the Wager Prize was awarded by the Royal Society and the IAVCEI to Franco Barberi and Jacques Varet for their joint work in Afar. A German team led by A. Pilger and A. Rösler also explored the geology and geophysics of Afar and organised an International Symposium specifically dedicated to “The Afar Region and Related Rift Problems” in Bad Bergzabern, F.R. Germany on April 1–6, 1974. This extensive knowledge was published in 1976 by the Deutsche Forschungs-gemeinschaft (E. Schweizerbart Ed., Stuttgart).

During subsequent years, the political situation in Ethiopia and Eritrea did not allow for new research projects in Afar. However, the new Republic of Djibouti (1977) offered such opportunities, notably after the eruption of Ardoukôba (November 7–14, 1978) and related tectonic events (two metres wide and 20 km long opening) along the axis of the

Asal-Ghoubbet Rift segment. A French research team from IGP developed new tectonic observations and modelling techniques in eastern Afar and Gulf of Tadjourah in the 1990s.

The Manda Harraro event in 2005, when this axial range located in central Afar opened up to 7 m wide over nearly 70 km long, followed by several successive events and eruptions during the next 5 years, attracted renewed scientific opportunities. Following the event, a new team, the “Afar Rift Consortium”, including Ethiopia, US, UK and French researchers, was established and provided a new impetus to geological and geophysical studies, leading to a symposium held in Addis Ababa on January 11–13, 2012 (Fig.3).

Afar is, and remains, a real “hot spot” for geological and geophysical research, providing “open book” access to the Earth’s processes along diverging plate boundaries, study of both continental and oceanic lithosphere and underlying asthenosphere, margins and transitions, including magmatic, volcanic, tectonic, sedimentary and geodynamic processes.

Afar is also an area where important climate changes occurred in the recent Quaternary period, with successions of rather wet periods, characterised by wide lakes extending in the south and western parts of the depression, with arid phases similar to that prevailing at present. This may relate to the fact that it is also one of the major sites of the origin of mankind. As a whole, it is nowadays a place where climate change issues find their most profound illustration.

As well as the study of human pre-history, Afar is also a place where hydrothermal processes display conditions suitable for the study of the most primitive forms of life (archaeobacterial).

It is also one of the spots of the world (together with Iceland) where, thanks to mantle plumes and accreting plate boundaries, the most important quantity of telluric energy is available at the surface for geothermal development.

These processes and others well developed in Afar—such as evaporation—also lead to the development of mineral deposits, eventually of economic interest.

Although not the subject of this book, the fact that Afar is also the area where a singular human population developed, with its own language and culture, adapting to the rugged landscape and extremely dry and hot climate cannot be forgotten. As well as its use for scientists and students the author hopes this book can also serve the needs of the Afar population, presently split into three different countries as a result of recent history, but whose geological resources are of prime interest in the post-fossil era. Geothermal energy can play a major role within renewables, and Afar can become a focus of future world development as, with cheap labour, the places offering the most affordable renewable energy can attract industry and become an industrial centre.

Scientists and engineers from the developed world, while working in the region can help the Afar population, through proper information, education, training and facilities, to develop their skills.

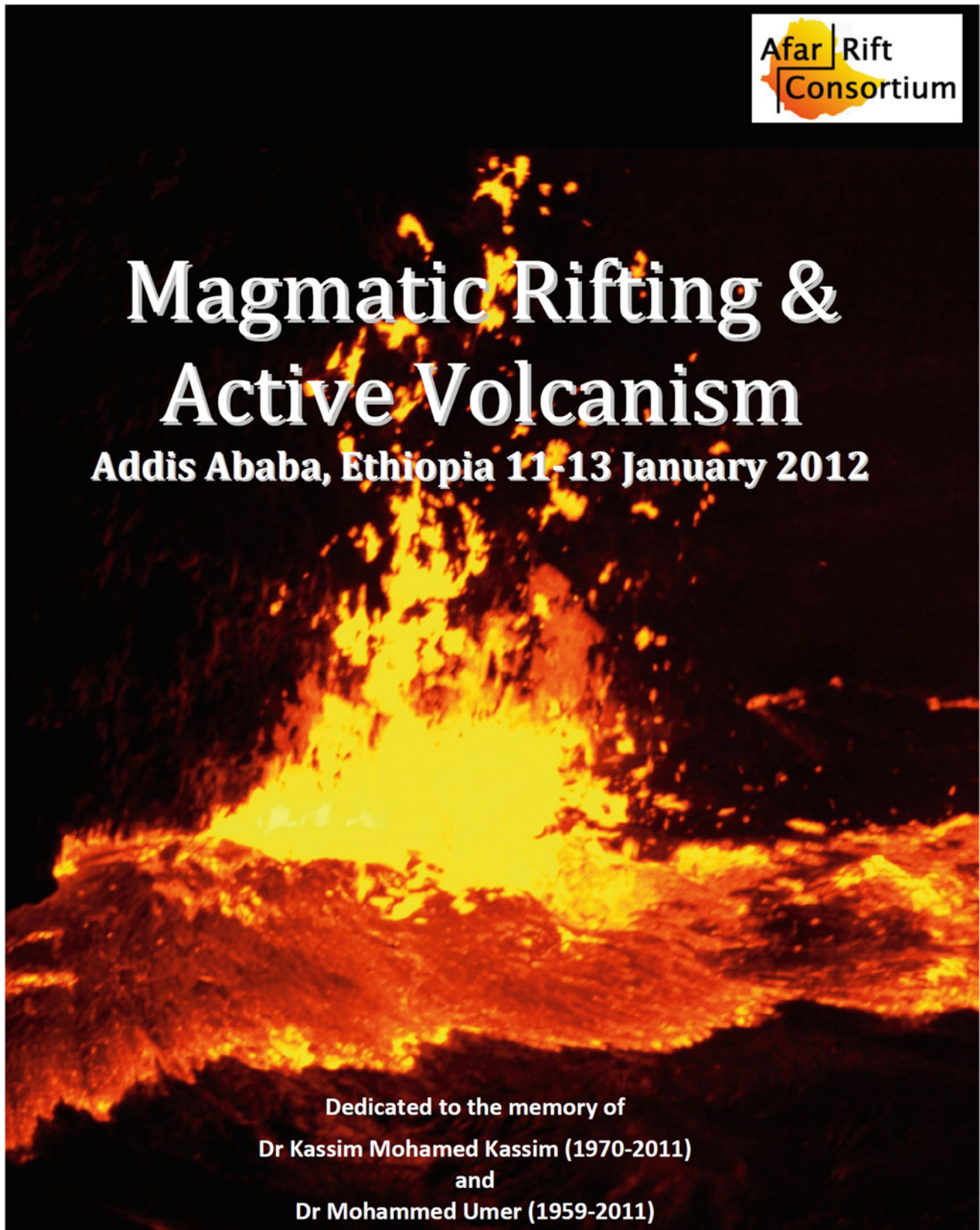


Fig. 3 The Afar Rift Consortium organized the conference entitled “Magmatic Rifting and Active Volcanism in Addis Abeba on January 11–13, 2012, allowing for a new insight on Afar geology and geophysics after the Manda Harraro event. Conference programme and abstract volume available on <http://www.see.leeds.ac.uk/afar/new-afar/conference/conference.html>

References

- Bannert D (1972) Plate drift in the Afar and Issas Territory and Eastern Ethiopia as seen on space photography, NASA, TN. D-6277, 28 p
- Dainelli G (1943) Geologia dell' Africa Orientale, Rend. Acc. It. Roma
- Dainelli G, Marinelli O (1912) Risultati scientifici di un viaggio nella colonia Eritrea. Publ. R. Istit. St. Sup. E ref. di Firenze, 601 p
- Falcon NL, Gass IG, Girdler RW, Laughton AS (1970) A discussion on the structure and evolution of the Red Sea and the Nature of the Red Sea, Gulf of Aden and Ethiopia Rift Junction. Phil. Trans. Royal Soc. London 267(N°1181): 417
- Mohr PA (1962) The Ethiopian rift system. Bull Geophys Observatory Addis Ababa 5:33–62
- Mohr PA (1967) Major volcano-tectonic lineaments in the Ethiopian rift system. Nature 21:664–665
- Morgan WJ (1968) Rises, trenches, great faults and crustal blocks. J Geoph Res 73:1959

Part I

Afar: Global Context

When looking at any picture or map of the area located between Africa and Arabia, the eyes are immediately drawn to a singular place where several peculiarities arise (Figs. 1.1 and 1.2):

1. The sharp change in direction of the Red Sea (trending NNW) with respect to the Gulf of Aden (trending ENE), leaving a sharp “corner” at the level of Yemen.
2. The nearly parallel coast on both sides of the Red Sea and the Gulf of Aden which were interpreted as previously joined by A. Ortelius (Anvers 1596), and identified as resulting from “tensional forces” by the Australian geologist E. Suess in 1891, that is, prior to Wegener’s theory of continental drift (1912).
3. The elevated plateaus surrounding the area on both sides, a striking feature emphasised by Cloos (1913, 1939), a fixist who objected to Wegener’s theory.
4. The presence south of the Red Sea of a depression of broad triangular shape, that is the Afar depression, depicted as early as 2.400 years ago by Heterodotus (Falcon et al. 1970).
5. The East African Rift Valley (EARV), trending NNW, bounded by elevated plateaus on both sides, joining the Red Sea and the Gulf of Aden in Afar, as if “funneling out” (as interpreted by Mohr 1967).

Whereas the Afar area, also called Danakil or even Eritrea, was long, considered by many observers to be a striking earth feature, A. Wegener, basing his work on the observations of his colleague geographer A. Supan, and following several geographers’ and geologists’ observations (including those of A. Ortelius and E. Suess) (Fig. 1.3), was the first to incorporate it in a global Earth model and take it as one of

the most convincing example of continental drift. However, Wegener’s theories did not convince the geological mainstream at that time, and Cloos (1913), more influential in German geological society, was able to show that vertical rather than horizontal movements could explain rift system development. Afar was taken by Cloos as a key example. For him, the “Danakil triangle” jutting out into the Red Sea destroys the congruency with Yemen, making it difficult for Wegener, who objected that the area was mainly basaltic, not granito-gneissic. However, at that time, the idea that ocean floors could be basaltic was not part of theory, and Wegener lost the argument.

The term “rift” was popularised worldwide by the British explorer John Walter Gregory who published the classical book “The Great Rift Valley” in 1896. He also attributed the formation of the rift valley to extensional forces that induced both the continental up-doming and the symmetrical faulting of the rift. As a result, the EARV is also called “the Gregory Rift” by the English speaking community. One should, however, remember that the concept of doming and faulting was proposed a century earlier by Elie de Beaumont (1827) for the Rhine graben, and was further developed by German and Austrian scientists for other parts of the world. However, the term “rift” finally prevailed in the international literature, particularly after plate tectonics selected it for accreting margins, whereas the term “graben” became limited to extensive tectonic faulting.

Carey (1958) was among the few advocate of continental drift and postulated a mechanism for the opening of the Red Sea by tensional forces brought by convection currents in the mantle, and the theory was supported by Swartz and Arden (1960) who proposed a time scale for the rift opening between Africa and Arabia based on geological evidence.

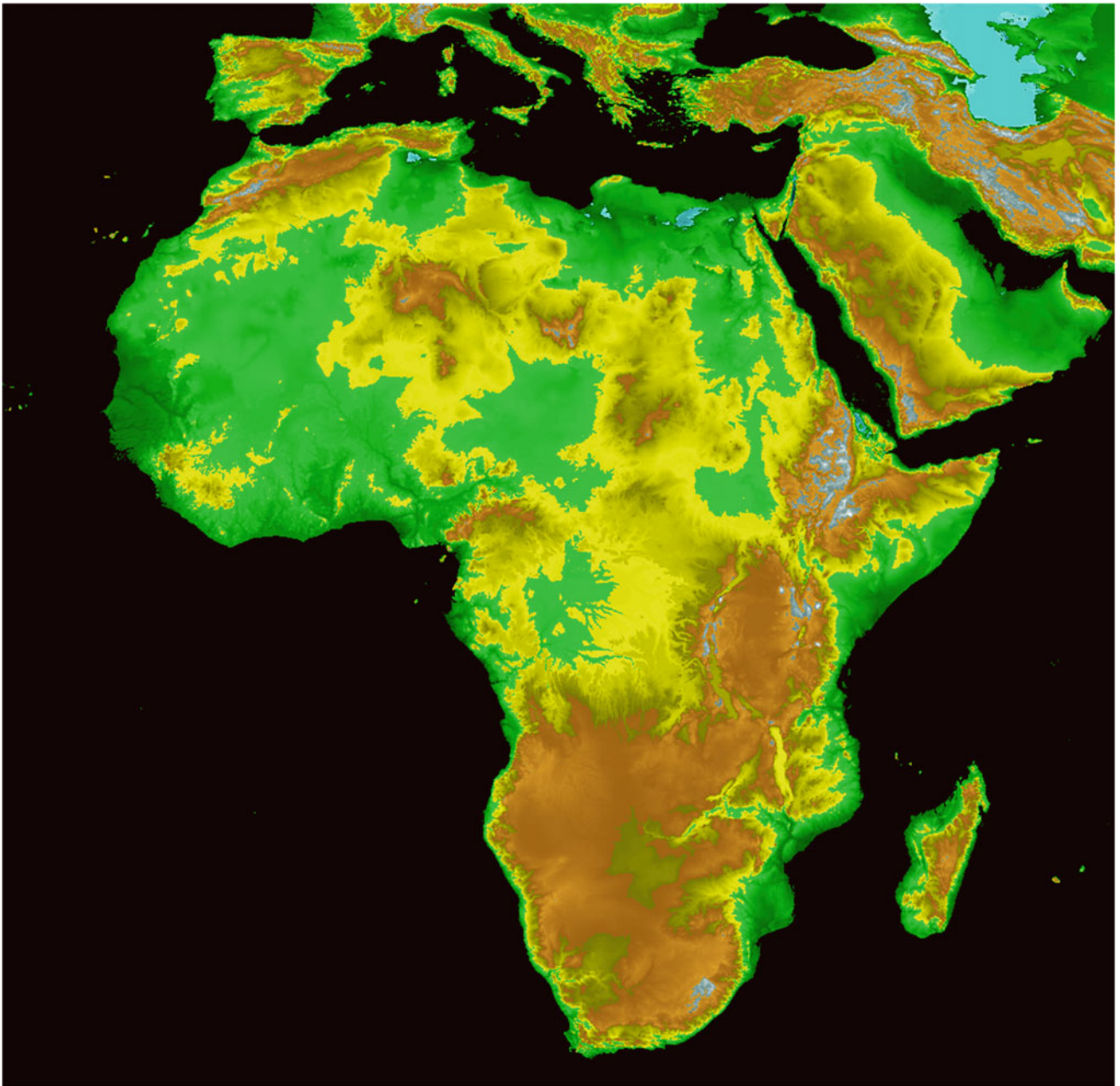


Fig. 1.1 NTM map of the African continent showing the Red Sea, the Gulf of Aden, the East African Rift Valley and the location of the Afar depression, of triangular shape, in the area where these three major geographic and geodynamic features meet. Elevated plateaus of Nubia, Somalia and Yemen surround these three rifts

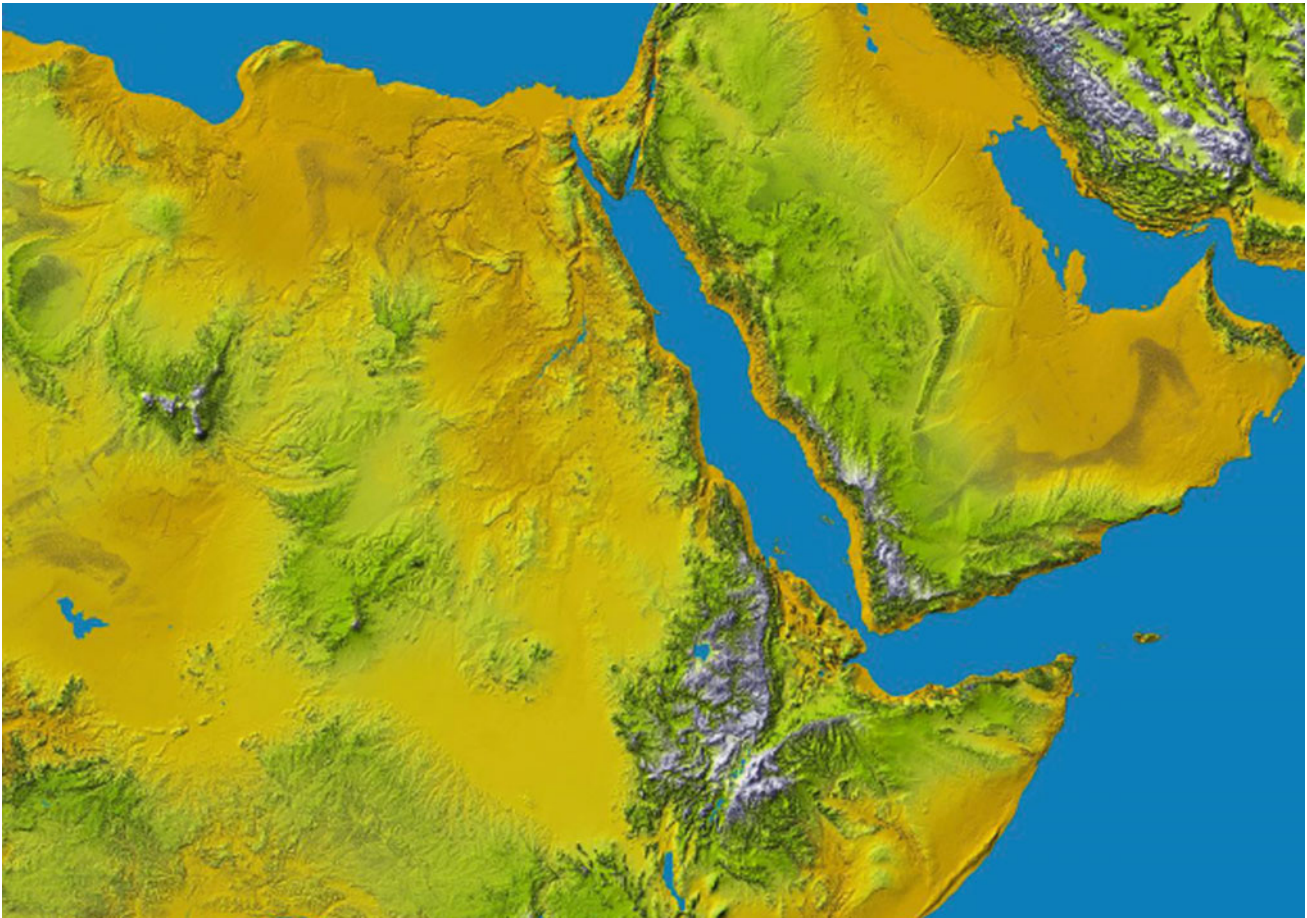


Fig. 1.2 More detailed topographic map of the Red Sea Gulf of Aden showing the connection with the northern termination of the East African Rift Valley in the Afar triangle

They considered that the Arabian continent was subject to compressional forces to the north and tensional stresses developed to the south. They proposed that Arabia moved away from Africa in two steps, the Gulf of Aden starting to open in the Miocene, and the Red Sea and Afar Rift in the Eocene and Oligocene. Their model identified four blocks: Nubia, Somalia, Arabia and Sinai (Fig. 1.4).

Cousteau and co-workers showed the existence of an axial trough as referred to later by Drake and Girdler, with bathymetric profiles across the Red Sea (Tazieff 1952; Cousteau et al. 1953). In 1958 the first magnetic measurements were made in the Red Sea by Drake and Girdler (1964), completed in 1959 and 1961 by Allan et al. (1964). It was shown that the axial trough followed the sinuous coastlines and extended south as far as 15°N, north of Hanish and Zukur Islands, where it disappears where the

coasts start to converge towards the Bab-el-Mandeb strait (Fig. 1.5).

Vine (1966) applied the theory proposed by Vine and Matthews (1963) to the Red Sea data to interpret the magnetic symmetrical lineations about the ridge axis, and found 1 cm/year on each limb (for the axial trough only). Gravity data were also collected and indicated the presence of magnetic dikes forming a veneer between the bottom of the rift and the top (Fig. 1.6).

Even at a broad scale of 1/25,000,000 the geological map of the world issued by the UNESCO/CGMW (second edition, 2000; see Fig. 1.7) clearly makes apparent the geological environment of the Afar triangle. The disappearance of the Red Sea axial trough towards the south is easily visible at the level of Afar to the north as well as the merge of the axis of the Gulf of Aden into Afar to the east (in violet

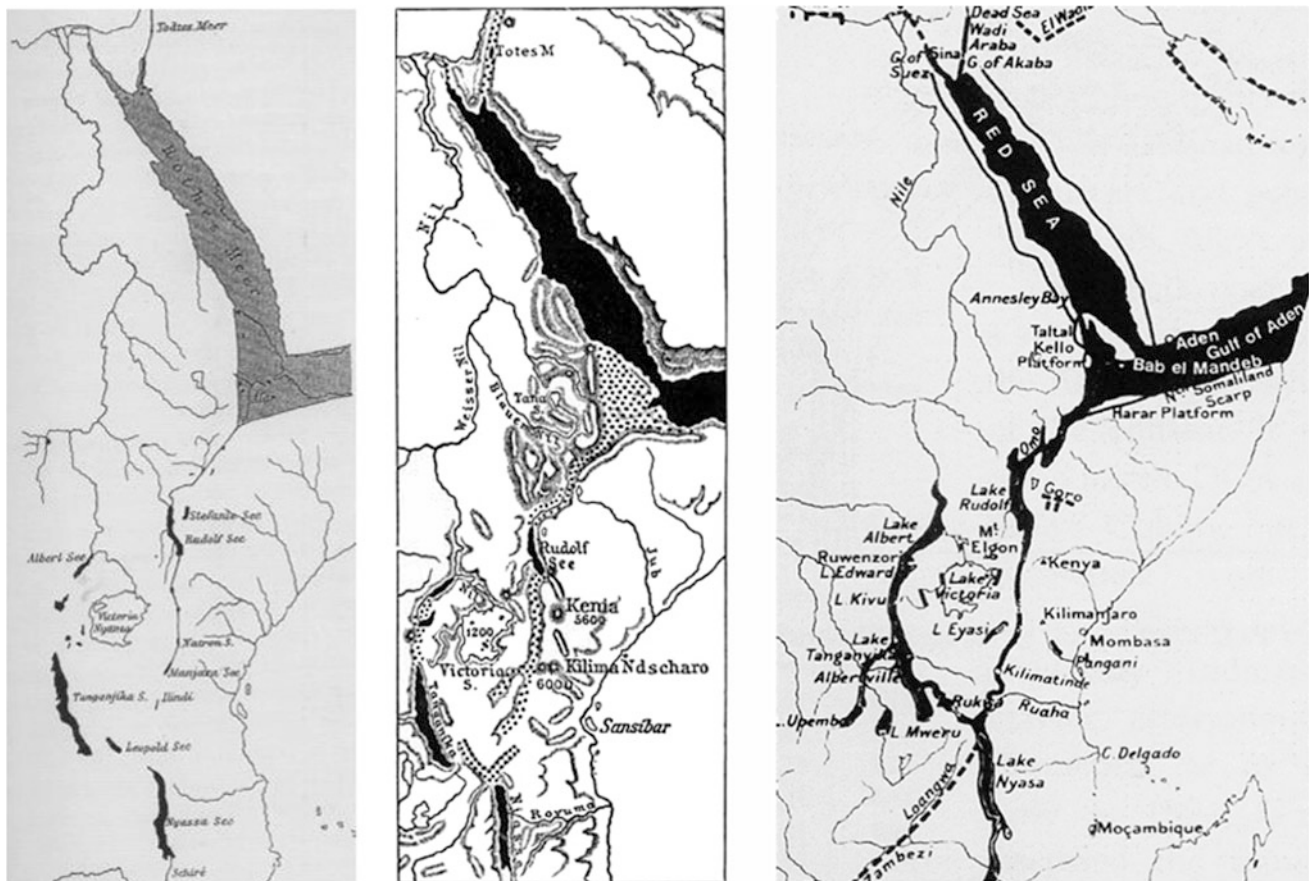


Fig. 1.3 Afar and East African Rift Valley according to Suess (1891), Supan (1899) and Gregory (1920)

and deep blue). Also visible is the East African Rift running through Ethiopia, Kenya and down south to Mozambique (in orange, colour in which Plio-Pleistocene volcanic products from the rift are represented). Some recent basaltic units are also observed in Arabia, both in the Saudis Harrats and in Yemen. Both normal and transverse faultings are shown as red lines on land and offshore and major earthquakes and active volcanic centres are also pictured. The Miocene formations are shown in yellow, including the sediments in the basins and the volcanic traps of the Ethiopian, Somalian and Yemenite plateaus. The Mesozoic sediments are mapped in pale green and the crystalline basement in brown. One can see that the whole pre-Miocene sequence, including the basement and its Mesozoic cover, was lifted up on both sides along the three rift margins, the sedimentary basins generally outcropping away from these structures.

It is apparent, even from this world map, that the active oceanic spreading axis of the Red Sea and the Gulf of Aden do not pass through the Bal-el-Mandeb strait but have to be searched for in Afar, where the map shows faults as well as volcanic and seismic activity but is not detailed enough to show how the three rift systems operate within Afar.

Although at a similarly large scale, the map of the seismicity of the world (only earthquakes with a magnitude above 5 are reported) around the Arabian plate and surrounding regions (Fig. 1.8) clearly shows the earthquakes pattern along the Gulf of Aden and the Red Sea Axis as well as along the EARV. It also quite clearly indicates that the seismicity develops in Afar, entering from the south through the Gulf of Zula and from the east through the Gulf of Tadjourah, whereas the Bab-el-Mandeb strait appears inactive between the Hanish Islands and Obock. The seismic

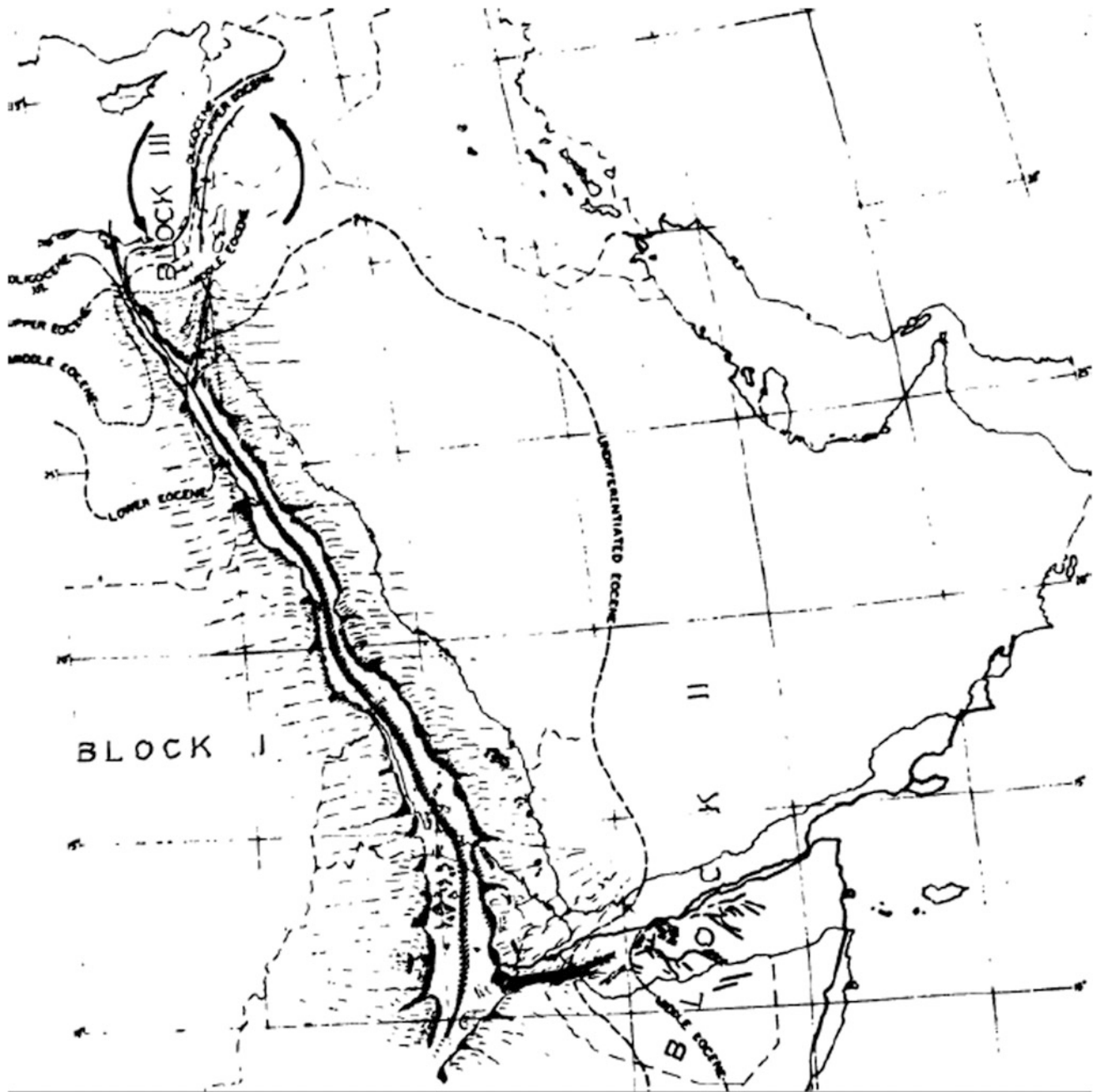


Fig. 1.4 Reconstitution of the Afro-Arabian continent in the pre-Oligocene according to Schwarz and Arden (1960). Although the spreading mechanism is not yet fully explained, Afar is seen as

involved in the same process, and its floor is of similar composition to those of the Red Sea and Gulf of Aden of a rising mantle by Drake and Girdler in 1964 (Fig. 1.6)

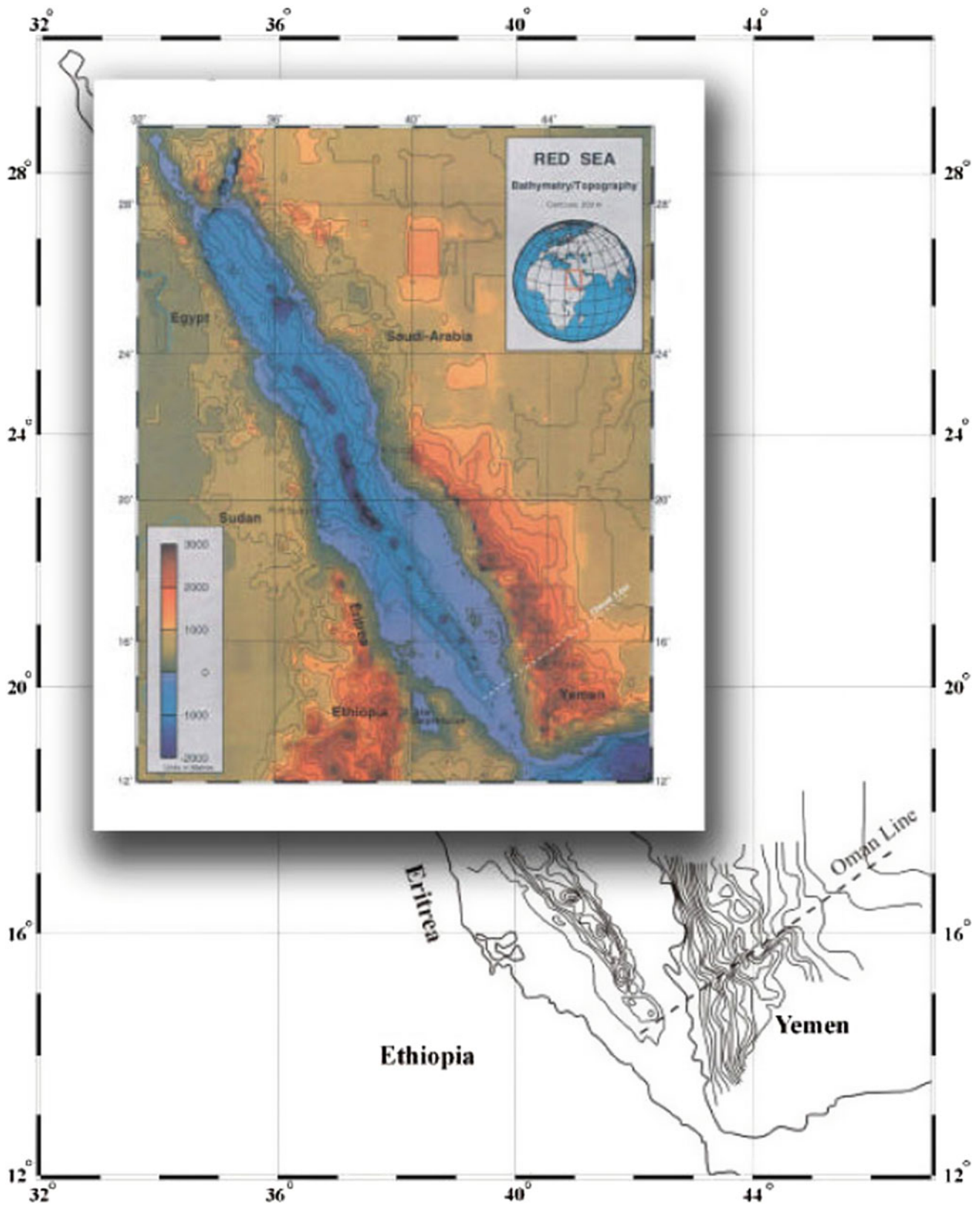


Fig. 1.5 The southern portion of the Red Sea contoured by A.S. Laughton (100 fathom intervals) from data available up to May 1968 from the Hydrographic Ministry of Defence (British Navy). At the level of Afar, the axial valley is less deep when hitting Zebayr Island and disappears at 14°N North of Zukur and Hanish islands. (Reproduced from Derakhshani and Farhoudi 2005)

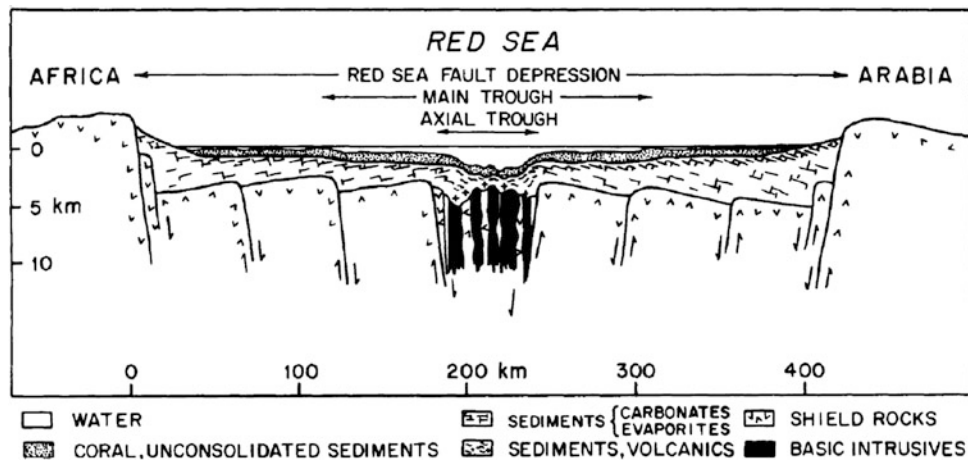


Fig. 1.6 Synthetic interpretation of the Red Sea floor and axial trough by Drake and Girdler (1964)

activity north of the Hanish-Zukur Islands shows that the portion of the southern axis of the Red Sea located between the Zubair and Hanish Islands is still active, in parallel with northern Afar. This delineates a block which corresponds to the “Danakil Alps”, limited to the south by the Dobi-Biddu transverse NE-SW alignment characterised by large calderas (including Nabro) and basaltic fissure fields aligned with the similar volcanic vents forming Hanish Island (as seen on Fig. 1.9, satellite image on the left).

The first charts of the bathymetry and the magnetic anomaly field obtained by Laughton et al. (1970)—together with other data—enabled the evolutionary history of the Gulf of Aden to be determined. These authors have shown that the theory of sea floor spreading satisfactorily accounts for the observed features of the Shaba Ridge over the past 10 million years. Evidence of spreading rates in the direction of the fracture zones were shown to vary from 0.9 to 1.1 cm per year per limb. Between the initial creation of the Gulf and 10 million years ago, the evolution was shown to be less certain, although the geophysical evidence indicated that the crustal structure of the Gulf outside the Sheba Ridge is also oceanic.

Later studies showed that the spreading was not necessarily continuous in the Gulf of Aden, but was rather characterised by stop and go, with the start of oceanic spreading at anomaly 5c (Fig. 1.10), that is, 16 million years ago (Cochran 1981) and a period of transition from rift to drift between 21 and 17 million years ago (Bosworth et al. 2005). It was also made clear after Laughton’s work that the western extremity of the Gulf of Aden (west of 45°) opened later. The Shukra al Sheik Discontinuity was later shown to mark the separation between the early Gulf of Aden (with oceanic floor 16 million years ago) and the western extremity (Tadjourah trench) where the spreading began later, eight million years ago in the Tadjourah trench and 3–1 million years ago in the Gulf of Tadjourah (Richard and Varet 1979).

It appears, as a consequence, that since eight million years ago, oceanic spreading does not occur any more in the southern section of the Red Sea—that is, the Bab-el-Manded strait between the Hanish Islands and the Tadjourah trench—but eventually in Afar itself. This is confirmed by present day seismic activity which concentrates in Afar, the Red Sea and the Gulf of Aden trough, but is nearly absent in this southernmost segment of the Red Sea, as shown in Fig. 1.10.

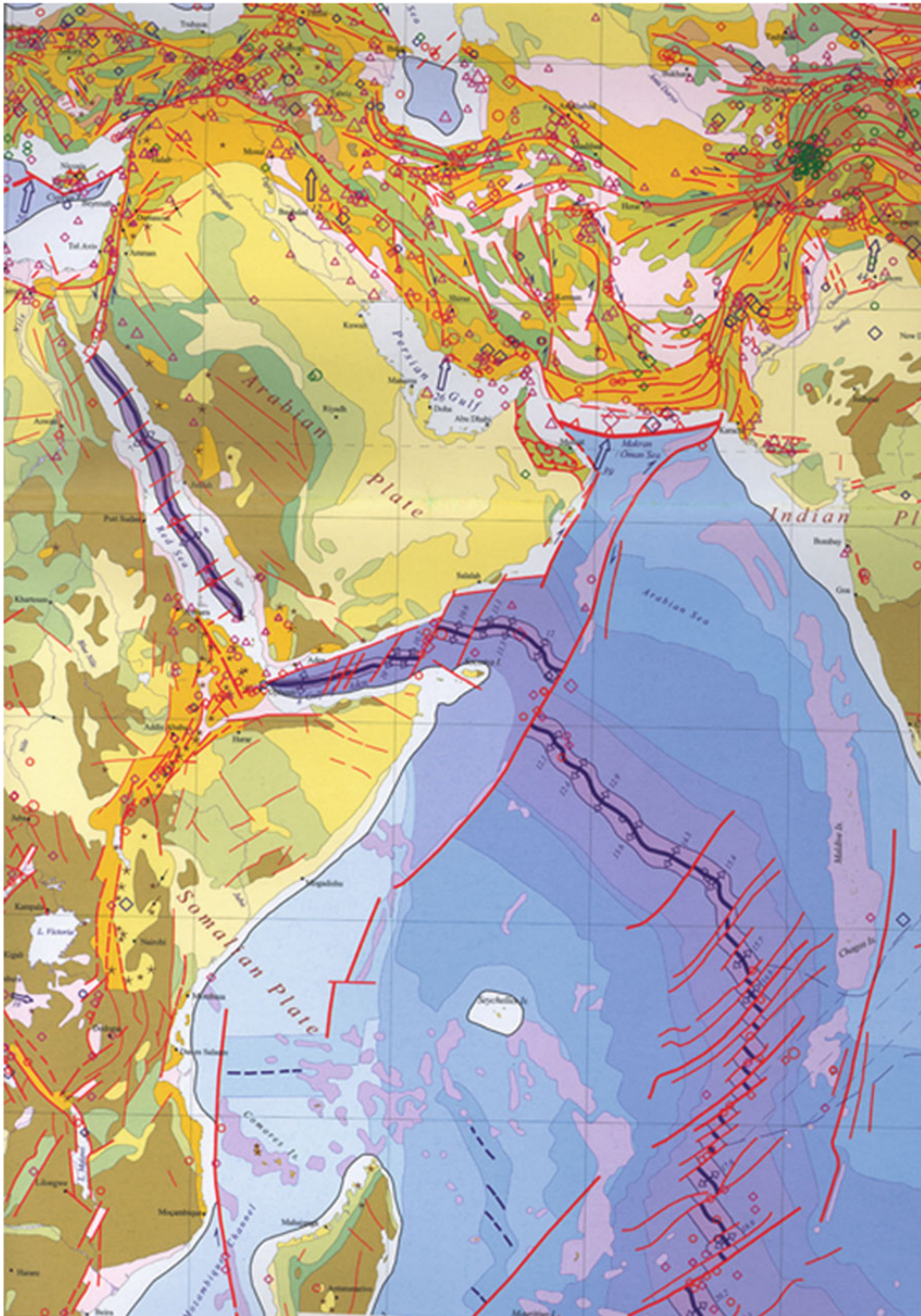


Fig. 1.7 Red Sea, Gulf of Aden and East African rifts surrounding, as seen from the Geological Map of the World (second edition, DGGM/CGMW, Paris, 2000)

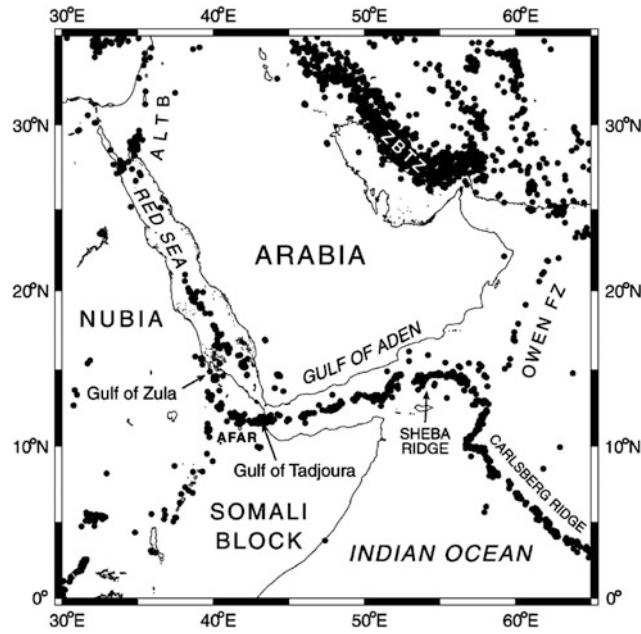


Fig. 1.8 Map of the seismicity (earthquakes over 5 in magnitude) of the Arabian plate and surrounding regions including Owen Fracture Zone and Carlsberg Ridge (after Kanbari 2000)

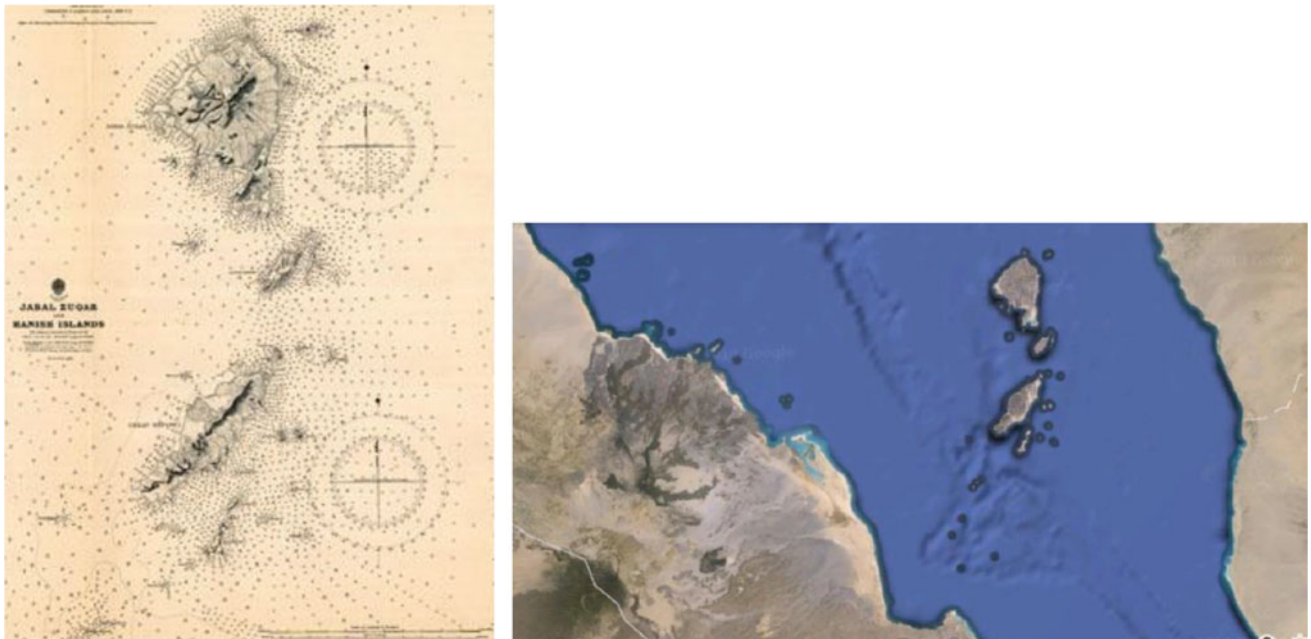


Fig. 1.9 Hanish and Zukur Islands in the Red Sea at 14°N; on the *right*: from Hydrographic Office, U S Navy, 1940; on the *left* Google satellite imagery. All islands clearly show a NW trend corresponding to the direction of the fissures that fed the basaltic hyacloclastite and scoria cones and lava flows, transverse to the Red Sea Rift that does

extend north of the islands but disappears south of them. One also observes on the Erytrean shoreline the basaltic fissural fields of Dubbi that relate to the set of calderas of Bidu and Nabro, also aligned along the same transverse direction

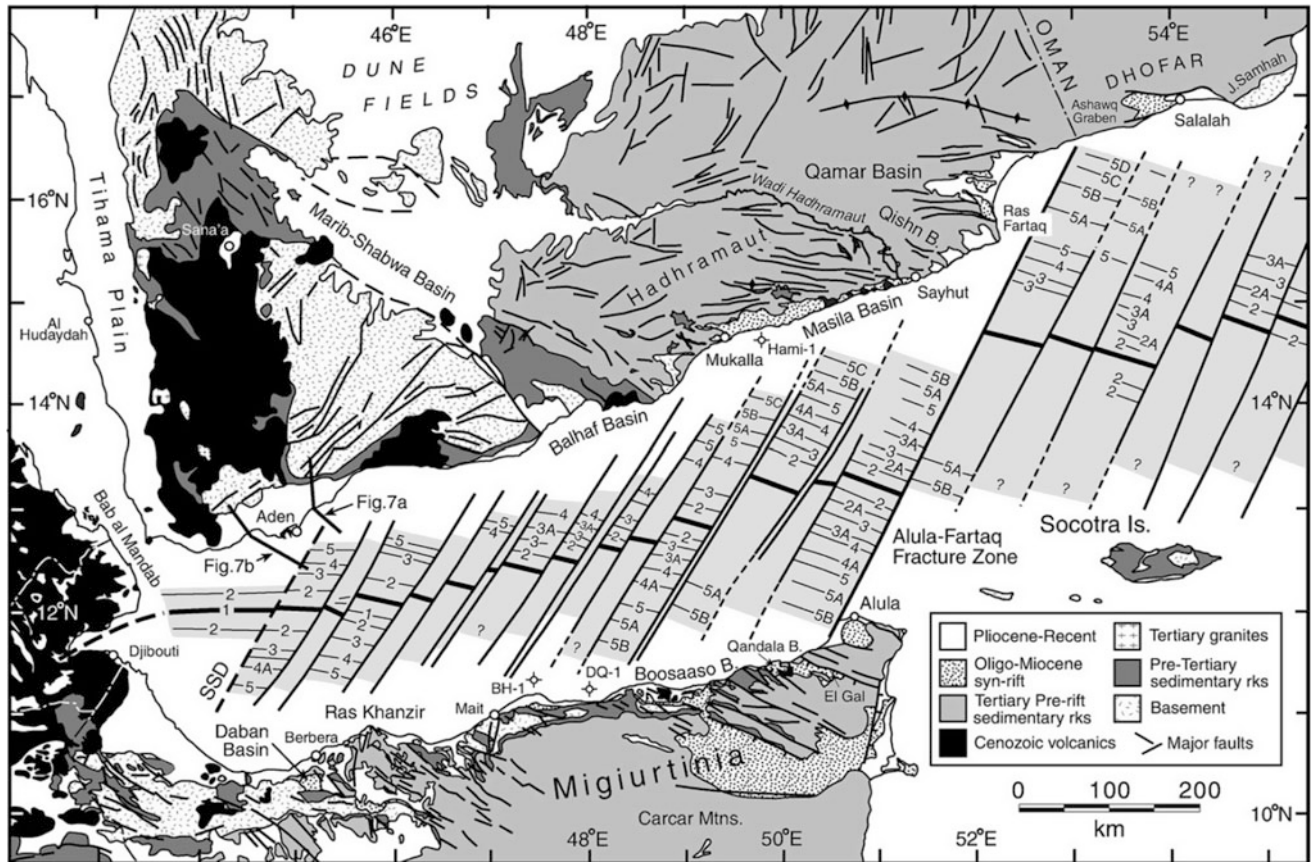


Fig. 1.10 Structural map of the Gulf of Aden (from Bosworth et al. 2005), with simplified geological maps of Yemen and northern Somalia, showing the fractures zones (SSD = Shukra al Sheik Discontinuity) and magnetic anomalies up to 5c (16 million years ago) east from SSD

References

- Allan TD, Charnock H, Morelli C (1964) Magnetic, gravity and depth surveys in the Mediterranean and Red Sea. *Nature* 204:1245–1248
- Bosworth W, Huchon P, McClay K (2005) The Red Sea and Gulf of Aden Basins. *J Afr Earth Sci* 43:334–378
- Carey SW (1958) The tectonic approach to continental drift. In: *Continental Drift: a symposium*. Geology Department, University of Tasmania Publication, pp 177–355
- Cloos H (1913) *Conversation with the Earth*. Translated from German by E.B. Garside. Alfred. A. Knopf, New York, 1953
- Cloos H (1939) Hebung, Spaltung, Vulkanismus. *Geol Rundsch* 30:401–527, 637–640
- Cochran JR (1981) Pre-sea floor spreading development of the Gulf of Aden. *Oceanological Acta Supplement* 4:155–165
- Cousteau JY, Nesteroff W, Tazieff H (1953) Coupes transversales de la mer Rouge. C.G.I. *Comptes Rendus*, 19eme session §IV
- Derakhshani R, Farhoudi G (2005) Existence of the Oman Line in the Empty Quarter of Saudi Arabia and its continuation in the Red Sea. *J Appl Sci* 5:745–752
- Drake CL, Girdler RW (1964) A geophysical study of the Red Sea. *Geophys J* 8:473–495
- Elie de Beaumont L (1827) *Observations géologiques*. *Ann Mines* 2:5–82
- Falcon NL, Gass IG, Girdler RW, Laughton AS (1970) A discussion on the structure and evolution of the Red Sea and the nature of the Red Sea, Gulf of Aden and Ethiopia Rift Junction. *Phil Trans R Soc Lond* 267(1181):417p
- Gregory JW (1920) The African Rift Valleys. *Geogr J Lon* 54:13–47
- Laughton AS, Whitmarsh RB, Jones MT, Habicht JKA (1970) The evolution of the Gulf of Aden (and discussion). *Phil Trans R Soc A* 267:227
- Mohr PA (1967) Major volcano-tectonic lineament in the Ethiopian Rift system. *Nature* 213:664–665
- Ortelius A (1596) *Thesaurus geographicus*, Anvers
- Richard O, Varet J (1979) Study of the transition from deep oceanic to emerged rift zone: gulf of Tadjoura (Republic of Djibouti). *Int Symp Geodyn Evols, Afro-Arabian System*, Roma
- Suess E (1891) Die Brüche des östlichen Africa. In: *Beitrage zur Geologischen Kenntnis des östlichen Africa*, *Denkschriften Kaiserlichen Akademie der Wissenschaftliche Klasse*, Wien, 50:555–556.
- Supan VA (1899) Die Bodenformen des Weltmeeres. *Dr. A. Petermanns Mitteilungen*, 45(8):177–188
- Swartz DH, Arden DD (1960) Geological history of the Red Sea area. *Bull Am Ass Petrol Geol* 44:1621–1637
- Tazieff H (1952) Une récente champagne océanographique dans la Mer rouge. *Bull Soc Belge Geol Pal Hyd* 61:84–90
- Vine FJ (1966) Spreading of the ocean floor: new evidences. *Science*, NY 154:1405–1415
- Vine FJ and Matthews DH (1963) Magnetic anomalies over oceanic ridges. *Nature* 199:947–949
- Wegener A (1912) Die Herausbildung der Grossformen der Erdrinde (Kontinente und Ozeane), auf geophysikalischer Grundlage

2.1 Topography of Surrounding Plateaus

From a geographic point of view, Afar is mostly located in Ethiopia, where it constitutes a Regional State on its own because it is a Federal Republic, but it also occupies the south-eastern part of Eritrea, most of Djibouti and part of Somalia to the east (Fig. 2.1). The Afar depression covers a surface of around 200,000 km² and ranges from 157 m below sea level (Asal salt lake to the east, the lowest point in Africa, in Djibouti Republic) and 120 m below sea level (salt plain to the north, in Ethiopia) up to 800 m above sea level to the south. That is an average elevation of 200 m with the exception of a few mountains, mostly active or recently extinct volcanoes such as Dubi, Nabro (2218 m) and Moussa Ali (2028 m) located along the Eritrean border.

Afar's western margin is characterised by the high Nubian plateau, a fertile highland area where most of the population of Ethiopia (nearly 80 million) live. It varies on average from 1500 to 3000 m above sea level, with several heights above 4000 m, the highest being 4550 m at Ras Dashan, with Tullu Demtu and Mount Batu above 4300 m. Generally, the elevation increases towards Afar and the Rift Valley, so that the drainage system is mostly oriented to the west, feeding the huge Blue Nile basin (and the Mediterranean sea). Lake Tana (2460 m) occupies the centre of the plateau. It was formed from a local Quaternary volcano-tectonic event (emission of alkali basalts closing a basin of the upper Blue Nile to the south of the lake). The Nubian plateau gradually slopes down to the Sudan lowlands to the west, whereas towards Afar the contrast is very sharp, with nearly vertical scarps determined by normal faults that have quickly downthrown the whole pre-rift geological sequence. The division between the Nubian plateau and Afar continues north in Eritrea and marks the limit with the Red Sea. The relief contrast tends to diminish further north. This limit clearly trends NNW, parallel to the Red Sea north of

the Gulf of Zula and Bure peninsula that marks (at 15°N) the northern limit of the Afar depression.

It apparently trends N-S along the Afar margin, following the line of the 40°E meridian for 600 km, but more detailed mapping shows that this results from the succession of en-échelon faults in a NNW direction. At a level of 9°N, the limit of the Nubian plateau changes direction and trends NNE, parallel to the Ethiopian Rift valley that extends south to Kenya through Lake Turkana Rift (surface elevation 360 m, 110 m deep).

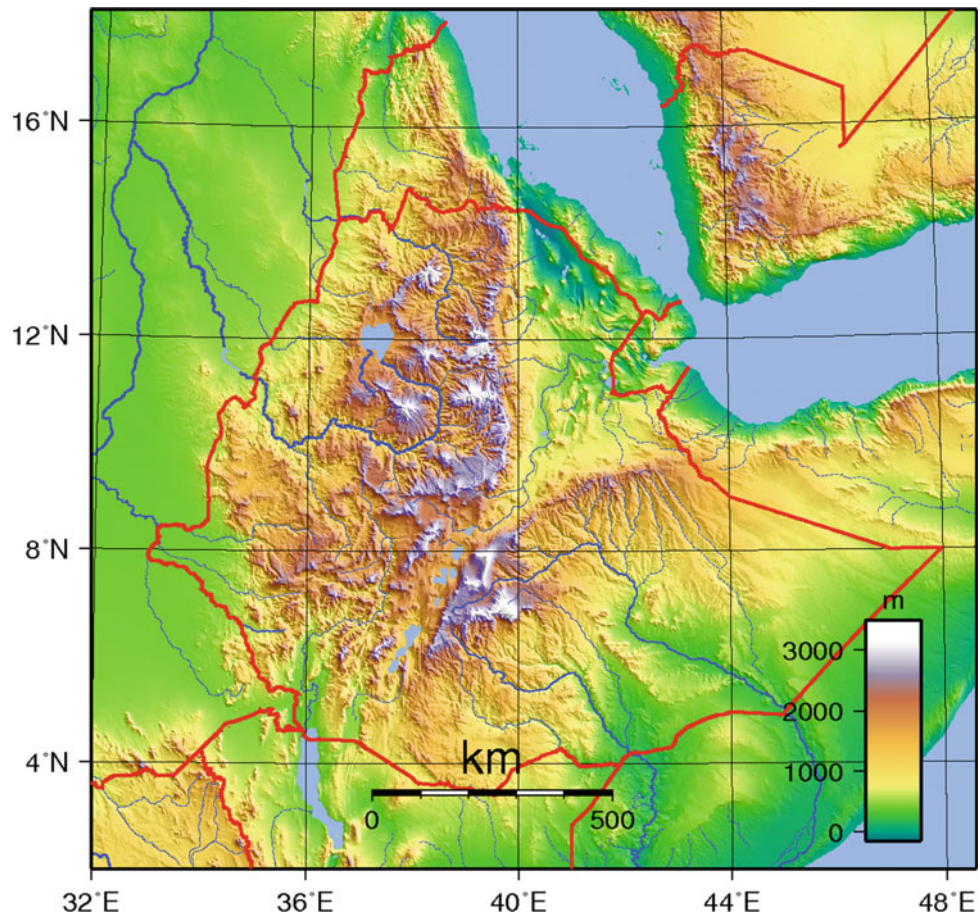
The Nubian plateau is characterised at its northern part by high mountains cut by steep valleys. Parallel with the eastern escarpment are the heights of Mount Biala (3810 m), Abuna Yosef (4190 m) and Kollo (4300 m). West of Lake Tana are Mounts Guna (4210 m), Uara Sahia (3960 m) and Choqa (also called Birhan) (4154 m). South of 10°N, the highlands are more tabular than the northern portion but equally broken.

Despite a few heights between 3000 and 4000 m, the majority do not exceed 2400 m, that is, less than on the eastern side of the rift valley (Somalian plateau border).

The southern margin of Afar is also marked by a sharp escarpment trending nearly 10°N, which corresponds to the NE limit of the Somalian plateau. This plateau, generally less elevated than its Nubian equivalent, is gently inclined towards the SW (down to the Indian Ocean) and is mainly occupied—although with a rather dry climate—by the hydrographic basin of the Wabi Shebele and Jubba rivers. The mountain chain of Ahmar, with an average of 2900 m peaks at 2960 m at Mount Kundudo. The northern limit of the plateau, also marked towards Afar by steep normal faults, trends in a WNW direction and extends west through Somalia, similarly marking the southern limit of the Gulf of Aden.

As observed along the Red Sea western side, the altitude of the plateau gradually decreases away from Afar. Note,

Fig. 2.1 The Afar depression surrounded by the Ethiopian, Yemen and Somalian plateaus, in the area of junction of the Gulf of Aden, the Red Sea and the Main East African Rift Valley, as seen on this relief map, also showing the political boundaries (in red) of concerned countries: Ethiopia, Eritrea, Djibouti Republic, Somalia and Yemen. Observe the mainly diverging flow pattern of the rivers (towards Mediterranean and Indian ocean basins)



however, that a small plateau is observed in the border area of Ethiopia, Somalia and Djibouti (Ali-Sabieh region), known as Aisha Horst.

Towards the west, the border of the Somalian plateau virgates to take a NW direction, parallel to the Ethiopian Rift valley, in symmetry with the Nubian plateau bordering the other side of the valley. That is where the Somalian plateau is the most elevated, forming the Bale Mountains. Tullu Demtu (4377 m) is the second highest mountain in Ethiopia, and this elevated range include Mounts Batu (4307 m), Chilalo (4036 m) and Kaka (3820 m).

The Great Ethiopian Rift Valley runs in a NNE direction from south (Kenya border) to north into Afar. It is a depressed area, on average 1000 m below the borders. The northern half is occupied by the Awash River, which flows northwards into central Afar where it ends in Lake Abhe at the Djibouti border, making a curve in this endoreic basin (Fig. 2.2). The southern part of the valley is occupied by several lakes, a characteristic that is found further south all along the two branches of the East African Rift.

In the southern part of the Ethiopian Rift valley, a parallel rift structure controls the Omo river basin which flows towards south and feeds Lake Turkana, which is larger than all the other Ethiopian Rift valley lakes put together. Omo is a 600 km long perennial river with many affluents and a total fall of about 2000 m, from 2500 m at its source to about 500 m at Lake Turkana level.

Both Awash and Omo river basins developed a strong sedimentation in the Eocene to the present period, with thick detrital sediments which are found intercalated with various lacustrine deposits resulting from the important past climatic variations. This allowed thick sedimentary filling to develop, notably in central Afar, where the floor would otherwise be several hundred metres below sea level.

This situation, together with the normal faulting along the rift margin and successive erosion, allowed for good conditions during Pleistocene both for the first human settlements and for conservation of the resulting fossils. The most ancient fossils of homo species have been extracted from sediments in both Omo and Awash river basins.

Fig. 2.2 The Awash river basin extending over 800 km from Entoto hills near Addis Abeba to Lake Abhe through central Afar. Note that it also receives the tributary of a few smaller rivers including the Mile to the north (Source Wikipedia)



2.2 Climate and Ecology

The Afar triangle is a rather dry region, with desert conditions probably among the hottest and the driest in the world. However, because of the high elevation of the surrounding plateaus in a nearly tropical environment, the upper highlands benefit from a temperate climate. The mountains catch the precipitation of the monsoon winds from the Indian Ocean, producing a rainy season from June to September. Heavy rains cause the Nile and the Awash to flood in the summer, differing from the usual North African conditions.

The Ethiopian Highlands have flora and fauna similar to those of other mountainous regions of Africa but habitats differs on either side of the Great Rift Valley because of the drier climate to the east. The tropical savannas and grasslands in the Rift Valley change to Sahelian Acacia savanna to the northwest.

The Ethiopian plateaus have good fertile soil and are heavily populated, mainly by fixed farming communities that have converted the region to agriculture. In contrast, the

Afar depression is inhabited by scarce nomadic tribes living from cattle, sheep, goat and camel breeding. However, in the last few years, agriculture has tended to develop, albeit with a rather industrial character (sugar and cotton plantations) along the Awash River basin. It is interesting to note that the same ethnic group, speaking the same language, occupies the whole Afar, despite the countries official limits. The total population of Afar can be estimated to be up to two million, as a few areas are more densely populated (Awash valley, flood plains at the bottom of the Ethiopian scarp, and Danakil hills along the Red Sea) than the average desert. However, even in the most remote and desert places, one can find human settlements. As a whole, in the three countries concerned (Ethiopia, Eritrea and Djibouti) this is 1% of the total surrounding communities.

If the Afar depression appears as a simple geographic feature bounded to the west by the edge of the Ethiopian highlands, to the south by the Somali plateau and to the east by the Yemen plateau, its characteristics appear more complex in reality. This striking topography allowed the first

plate tectonics reconstruction to consider the whole Afar triangle as part of the Red Sea—Gulf of Aden oceanic floors (Allan 1970). Two features, however, underline the complexity of this rather simple scheme: the Danakil Alps, which display a clear relief between northern Afar and the Red Sea and the Aisha—Ali-Sabieh horst which separates the southern Afar depression from the Gulf of Aden. These are even more significant when one sees that both consist of pre-Mesozoic formations covering an outcropping Precambrian basement (see Chap. 4). Note, however, that the Danakil Alps are limited to northern Afar. South of the Bidu-Nabro-Dubbi transverse structure, the nature of the area located along the Red Sea appears stable and is made exclusively of volcanic products with no pre-Tertiary formations.

A rather elevated area, peaking at an altitude of 1780 m at Mt Goda, is observed along the northern shoulder of the Ghoubbet Rift which is the last rift segment of the Gulf of Tadjourah, in fact a single rift with the emerged Asal Rift segment (Fig. 2.3). This feature, known for its relict forest (“Forêt du Day”, Fig. 2.4), is frequently interpreted as the southern extremity of the Danakil Alps. It is, however, of quite a different nature and origin. It corresponds in fact to the uplifted shore of this recently formed oceanic rift (less than two million years ago). This Dalha plateau, which extends north and gently downslopes towards NW, is made of basalts, dating from 7 to 4 million years ago, overlying faulted rhyolites (Mabla rhyolites, 12–8 million years ago). However, despite its altitude and level of erosion, no pre-Tertiary formation is observed in the “North Ghoubbet” block.

The Afar depression is otherwise characterised by its rather dry and hot climate. The average waterfall does not exceed 100 mm/year, but rain is generally local, and in some areas there is no rain at all for several years. In this context, in the absence of soil, the geology directly determines the vegetation. The distensive tectonics allows for the development of open fissures and normal faults which may allow for the accumulation of eolian sediments, and eventually some grass and trees (generally acacias). The recent volcanic activity eventually favours spots where vegetation benefits from more favourable environments such as craters or lava channels (Figs. 2.5 and 2.6).

In this generally desert and rugged context, however, we note a few exceptions, found in the Awash River basin, and of a few galleys that descend from the plateaus and allow for flood plains, offering sites where water can be gathered by the nomadic population, allowing for larger settlements and eventually irrigated agricultural developments (Fig. 2.7).

For the local communities in many places in Afar, the only other source of water in the dry climate is the hot springs (and wetlands or irrigated areas around them when not too salty; see Figs. 2.8 and 2.9). The notable exception is the Awash River basin where the availability of water allows

for richer cattle breeding (Fig. 2.10) as well as agro-industrial developments (sugar, cotton etc.). Elsewhere, water can only be obtained by condensation of the steam from fumaroles (sites generally called “Boina”; see Fig. 2.11). The Afar population nearby would dig, build and finally install more or less elaborated systems for water collection from steam (see Figs. 2.12 and 2.13).

In many places in Afar, although groundwater is eventually available, it happens that, because of the active geological context, and in particular the high heat-flow, the groundwater reaches rather high temperatures. At Baloo, Republic of Djibouti near the Ethiopian border, the well drilled near the village produces water at 60°C which requires cooling before it is distributed, and at Karapti San the temperature is so high that the well had to be closed because of the lack of proper high temperature drilling equipment in the Ministry of Agriculture in charge of the drilling (Figs. 2.14 and 2.15).

2.3 Ethnographic Context

From the ethnographic point of view, the region is characterised by its specific nomadic population, which had different names according to the observer. In northern Ethiopia they were long called “Taltal”, a name used by emperor Johannes of the Tigray dynasty who married an Afar girl. In the southern Ethiopian highlands, inhabitants of the depression are still frequently called “Adal”, a word which described the population of southern Afar. The Arabs of the Southern Red Sea called them “Danakils”, a name also used by the Italians during the colonial period and which is still used in northern Afar (see the two-volume book, 1488 pp, by Luca Lupi, IGM, Firenze 2009, entitled “Dancalia¹”) whereas the Somali call them “Oda’Ali”.

As shown by the CNR-CNRS Afar team (1973), the term “Danakil” was first used in the thirteenth century by Ibn Said, the Arab geographer, and this term, currently used by the Arabs, was reported by the first European geographers. The first geographic map printed in Venice in 1541 named the region “Regno de Dangali”, probably from data of Portuguese origin.

However, the people known by outsiders by so many different names call themselves “Afar”. It was therefore reasonable to name this geographic region “Afar”. All Afars, whatever the political boundaries of Ethiopia, Eritrea and Djibouti Republic, belong to the same culture and have the same ethnic roots. Afar is hence a well-defined human and physical geographic entity.

¹Luca Lupi 2009 « Dancalia, l’explorazione dell’Afar, una storia italiana » IGM, Firenze 1488 pp.

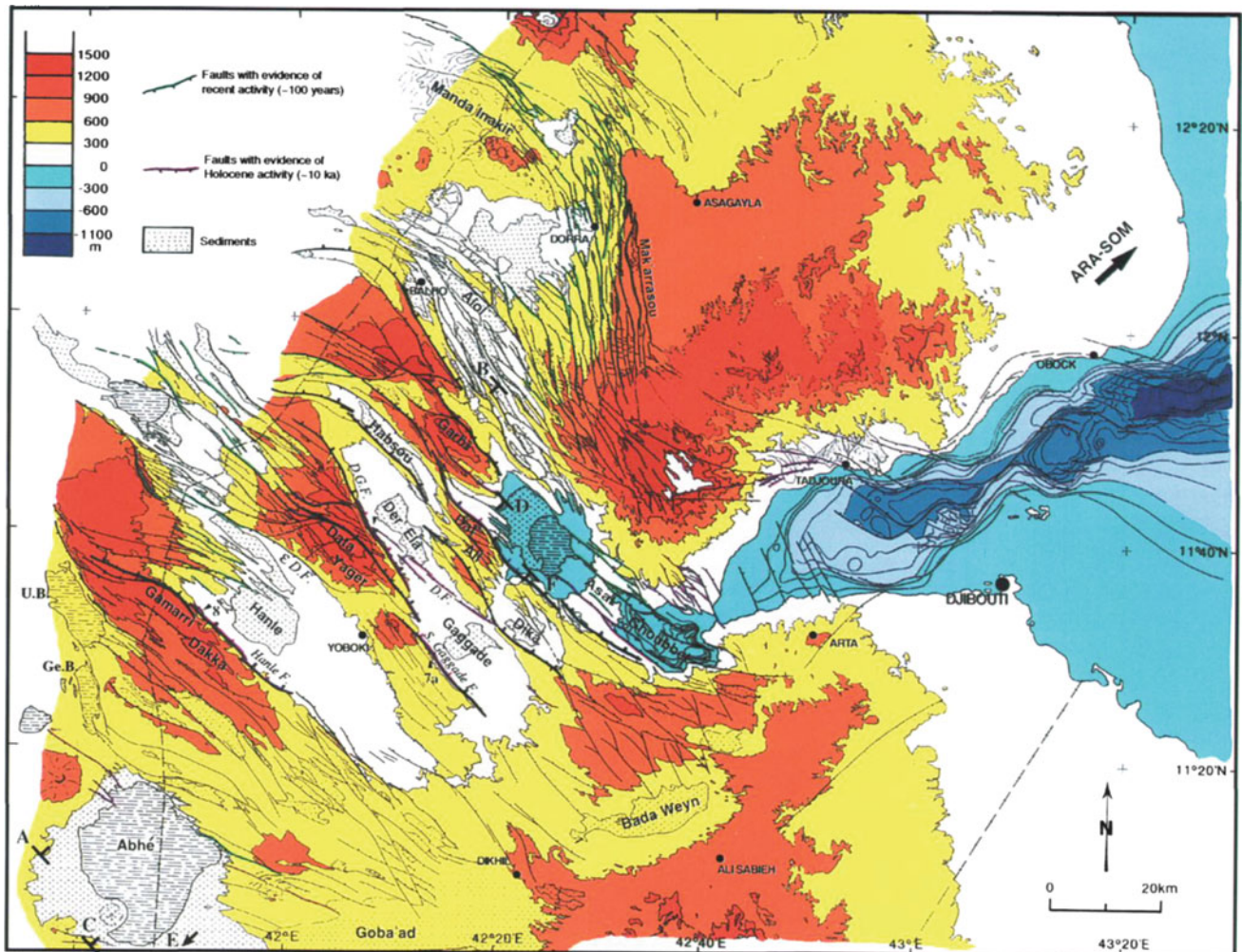


Fig. 2.3 Detailed relief map (redrawn from IGN) of the shoulders of the Ghoubbet-Asal rift and Gulf of Tadjourah (from Manighetti et al. 2001a, b). Observe the high altitude of the Goda massif (Day forest) culminating at 1780 m, and the plateaus gently dipping towards the

NW. Observe also in the bathymetric map of the Gulf of Tadjourah the successive troughs corresponding to the Aden ridge extension towards Afar (with Asal-Ghoubbet as first partly emerged rift segment)

In Ethiopia, the Federal State established after the eviction of the DERG recognised Afar as a “Regional State” (Fig. 2.16), as it was previously divided into several provinces, including the nearby plateaus (Tigré, Wollo, etc.). The Afars number 1,276,867 people (or 1.73% of the total population) in Ethiopia according to the most recent census (2007). The Afars are estimated to make up over one-third of the population of Djibouti Republic, which is approximately 300,000 people, and are considered to be 5% of the population in Eritrea, that is, another 300,000. Therefore, altogether, the Afar population is probably at present (2014) over two million.

Afar people are predominantly Muslim. They have a long history of association with Islam through the various local Muslim politics, and are traditionally pastoralists, raising

goats, sheep, camels and cattle in the desert. Being nomads, they move their houses according to the influence of climate on the pasture land (Fig. 2.17). A few of them practice fishing along the Red Sea coast (Tiho and Edd area, Eritrea). They live in houses made of curved light woods covered with palm fabrics (Figs. 2.18 and 2.19) which can be transported by camels when moving camp. The division of work between men and women is well established, men taking care of looking for pasture lands and protecting the group, women in charge of the households, water and energy supply and food preparation (Figs. 2.20, 2.21, 2.22). Afars are known for their martial prowess. Men traditionally sport the “jile”, their famous curved knife (Fig. 2.23) and are known to have an extensive repertoire of battle songs. All speak the same language that is part of the Cushitic branch

Fig. 2.4 The Day forest, one of the only forested areas in Afar. Observe the deeply eroded trap basalts of the Dalha formation along the Southern slopes of Mt Goda (1780 m)



Fig. 2.5 Typical view of northern Afar. The dry basaltic surfaces do not offer much life support. However, open fissures and normal faults will produce lowlands in which eolian sediments will be fixed, allowing for the presence of some vegetation. Similarly, blocky and Aa flows as well as lava channels may also favour low spots in which some acacia tree may survive (*Photo Marinelli*)





Fig. 2.6 Craters appear as favourable sites for wetlands or even lakes that allow for the development of vegetation of interest for Afar farmers. Three examples from Alayta, Erta Ale (Catherine volcano) and Manda Inakir (*Photos Marinelli*)

Fig. 2.7 The Teru plain, in central western Afar, where the wadies from the Ethiopian plateau hit the axial volcanic range of Alayta, offers a thick green surface where the grass, up to 2 m high, is difficult to penetrate. (F. Barberi and J.Varet, *Photo Marinelli 1969*)



Fig. 2.8 The deeply faulted central Afar is presently affected by a very arid climate. Hot springs offer some of the rare sources of water, which although quite enriched in minerals (which deposit by evaporation, in white), allow for scarce pasture land to be maintained. Alol-Sakalol graben (*Photo Varet 2012*)



Fig. 2.9 Hot-spring irrigated pasture land on the eastern shore of lake Abhe (*Photo Varet 2014*)



Fig. 2.10 The Awash river basin is the exception in Afar economy, with abundant water available for cattle breeding and irrigated agro-industrial developments (Photo credit Imail Ali Gardo)



Fig. 2.11 All over Afar, fumaroles are generally captured by the Afar men with installation of artisanal steam condensation devices allowing the production of the only drinkable water available in this desert environment (Garabayiis, Photo Varet 2012)



of the Afro-Asiatic family of languages. Afar language is hence widely spoken by this population in the whole Afar region of Ethiopia, south-eastern Eritrea and north-western and central Djibouti Republic. They mainly rely upon their cattle for nutrition (mainly milk and also meat from goats, sheep and camels) but may also use some cereals bought in markets from other communities to cook bread in earth-dug and firewood heated ovens.

One should note, however, that in recent years, particularly after the Afar Regional State was established in Ethiopia, the Afar social system underwent important changes, with the development of schools which fixed part of the population in villages and the creation of water points, with cisterns and wells pumping groundwater with solar powered pumps or even extensions of the electric grid. The tendency is therefore for the development of agricultural activities in combination

Fig. 2.12 If the second man is handling the usual gun that Afar men carry on their shoulders, the first is carrying a hoe which is used to dig in the fumarole site to build a water collector condensing steam. The author in 1970. Boina at Ma'alalta. *Photo credit Franco Barberi*



Fig. 2.13 In central Afar, along an open fissure cutting through the Stratoid series, from which the steam surge, producing clay alteration products as well as carbonate and silica deposits, a set of water condensers is being built for drinking water collection and bathing developments (*Photo J. Varet 2015*)



with traditional pastoralism. Artisanal mining also tend to develop, such as salt mining and salt evaporation ponds (e.g. around Lake Afrera). An Afar Geothermal Development Company was even inaugurated in January 2015.

2.4 Afar Topographic Maps and Toponymy

When the geological exploration of Afar started in 1967, no topographic map was accessible, at a proper scale, except for the Djibouti Republic (then still French Territory of Afar

Fig. 2.14 Typical Afar habitat (Photo Varet 2012); observe the rocky and dry surrounding. Near this village called Karapti San, located in the northern extension of the Asal graben, a well drilled by the water department of the ministry of agriculture had to be closed due to its too high temperature (Haga et al. 2012)



and Issas, TFAI) where well-documented 1/100,000 maps were published and sold by IGN. In Ethiopia, one should rely on the 1/1,000,000 scale US aeronautical ONC map as well as the 1/250,000 Joint Operation U.S. Army map. Fortunately, a “topomorphic” map was published in Florence in 1968 from air photographs transcription for Mobil Oil exploration.

Colonel E. Chedeville dedicated his life (1906–1996) to the study of the Afar people and language, which he was teaching at the Paris-Sorbonne Oriental Language Institute (INALCO). Despite the fact that he was forbidden to enter Ethiopia,² he provided the CNR-CNRS Afar team with rather detailed toponymic maps of the whole Afar region, whether in Ethiopia, Eritrea or Djibouti, thanks to his own ability to travel through the country without motor vehicle or escort, benefiting from the Afar people’s hospitality.

In the maps produced with his help, the “restricted” names referring to unusual items such as water point, oued, valley, hill or confluence were printed in small characters whereas “broader” names such as plateaus, grabens and plains were spread over the area to which they refer. The names given to geological entities or formations (volcanic, sedimentary or tectonic units) were from this last category.

²He took a stance against the settlement of the boundary with Ethiopia in 1954 and wrote numerous articles in the period 1948–1954 criticizing the cession of the Afambo area.

A few of the most useful Afar words used in topography are given in Tables 2.1 and 2.2.

2.5 History of Afar Exploration

The history of Afar exploration was recently developed in detail, with numerous illustrations, in a well-documented book edited by the Istituto Geografico Militare (L. Lupi, Firenze 1488p. 2009). Here we recall a few major steps.

The region has long been an area of difficult access for various reasons:

1. The rather hot climate and desert conditions
2. Access for vehicles is rather limited and hazardous
3. The people themselves are hostile towards foreign incursions
4. The political situation and the influence of various outside forces (Italian and French colonisation, Ethiopian imperial influence, Eritrea Liberation Front, etc.)

Even now, parts of Afar are difficult to access, notably around the Eritrean border, whether in Ethiopia or in Djibouti Republic.

For a long time the Afar warriors were considered to be very fierce as several exploring parties were slaughtered by the tribesmen. This was notably the case with the Italian army officer Giulietti who was killed together with all his party of

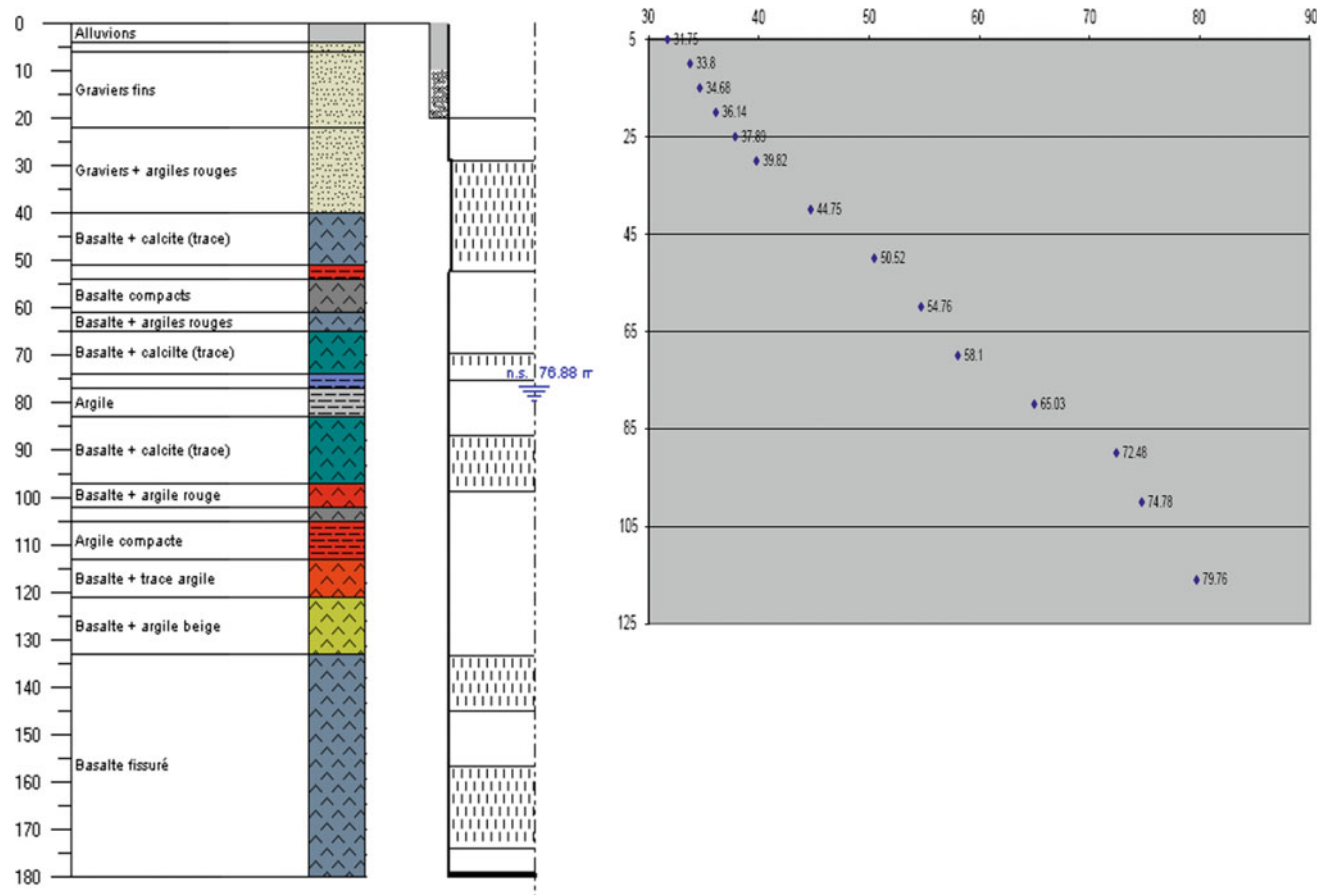


Fig. 2.15 Near the village of Karapti San, located in the northern extension of the Asal graben, a well drilled by the water department of

the ministry of agriculture had to be closed due to its too high temperature (Haga et al. 2012)

14 soldiers at Lake Afrera, therefore called Giulietti in old Italian maps. The access to the Afar depression long being much easier from the coast than from the plateau, geological explorations started from the north (the Gulf of Zula accessible from Massawa) or from the ports located to the south-east (Assab, Tadjourah and Djibouti). The first geological report of the coastal region is that of Salt (1814), followed by Ruppel (1934), Johnston (1884), Issel (1869), Blanford (1870), Zichy (1880) and Aubry (1855) and Justin Visentin and Zanettin (1968). The presence of crystalline basement and Jurassic limestone is known from the Danakil Alps, as well as the recent volcanic rocks and the presence of salt and coralliferous limestone in the depression. This first description of inland Afar was by Munzinger (1869), who gave a detailed description of the salt plain and surrounding area, described as an ancient gulf of the Red Sea, desiccated after obstruction by volcanic events. The basic geological

knowledge of Ethiopia was established by W.T. Blanford, who did not really penetrate Afar. He introduced the term “Aden Series” to describe the volcanic formations located on the Red Sea shore, shown as being distinct from (younger than) the traps of the Yemen and Ethiopian plateaus. The term was later used extensively in the geological literature and maps of Ethiopia for any volcanic rock postdating the trap series of the plateau. It was even used later by Mohr (1967) to describe all volcanoes of the Ethiopian Rift system, whatever their age, petrology or geological position.

Nesbitt (1934) provided the first description of a few recent volcanoes of northern Afar after visits he made to the region with T. Pastori, who provided useful oral information to H. Tazieff and G. Marinelli.

Gortani (1949, 1951) published geological descriptions of the journey he made with Bianchi from Asal to Gawani, and show the presence of heavily faulted trap series



Fig. 2.16 The Afar regional state of Ethiopia



Fig. 2.17 Moving the camp with camel transport of the house spare parts and households (*Photo credit* Ismail Ali Gardo)



Fig. 2.18 Building the wood framework for a house (*Photo credit* Ismail Ali Gardo)

Fig. 2.19 Weaving palm trees fibre for roofing (*Photo credit* Ismail Ali Gardo)





Fig. 2.20 The house seen from outside (Dodom plain, J.Varet 2013) and from inside (Awash basin, *Photo credit* Ismail Ali Gardo)



Fig. 2.21 The house seen from outside (Dodom plain, J.Varet 2013) and from inside (Awash basin, *Photo credit* Ismail Ali Gardo)

covered by recent volcanic action. Basalt samples collected during these expeditions were later studied by Heike Merlin (1950). Desio (1941) also described some volcanoes of central Afar.

Dainelli and Marinelli (1912) were the first to provide a collection of the knowledge of the region and the impressive books published by Dainelli (1943) remain the source of

reference on the information available at the beginning of the twentieth century. Determined to deliver unique information, he concluded his synthesis with these words: “*taking into account the general conditions of the area, it is quite improbable that the geology will ever be systematically studied*”.

Despite this prophetic view, scattered geological information was collected by Gortani (1949, 1951), Justin Visentin and Zanettin (1968), and a gravity traverse was undertaken by Gouin and Mohr (1964). Useful geological descriptions of the sedimentary formations and tectonic environment of the Dallol potash salt mine were published by Holwerda and Hutchinson (1968) and Hutchinson and Engels (1970), and a geological map was published by Bannert et al. (1970) after an important German geological expedition (Brinkmann and Kursten 1969; Bannert and Kedar 1971) (Figs. 2.24, 2.25, 2.26).

It is in this context that a Franco-Italian team was assembled by H. Tazieff and G. Marinelli (Figs. 2.27 and 2.28) with the support of CNR and CRNS to undertake a systematic geological exploration of Afar which started in December 1967 and was continued with yearly winter expeditions (December to January) until 1976. The result of this work was 1/500,000 scale maps of the whole Afar depression (two sheets) and several more detailed maps (1/100,000 scale) of a few relevant units such as the Erta Ale range. As a whole, it was this team that provided the first description and the geological definitions of the major volcanic units of the Afar depression, still of relevance today (Tazieff et al. 1969, 1972; Tazieff and Varet 1969; Barberi and Varet 1970; Barberi et al. 1970, 1972; Marinelli and Varet 1973).

In order to organise the field work, we could benefit from complete air photo coverage of the region both in Ethiopia and Djibouti. Thanks to the desert character of the region, the lack of soil or vegetation, and even frequency of erosion, allow us to differentiate the nature and map the contours of the geological units, notably volcanic units (flows, domes, ignimbrites, tufs, scoria cones, hyaloclastite rings etc.) as well as sedimentary formations (salt, gypsum, diatomite, coral reefs, clay plains or detrital talus etc.), tectonic features (faults, open fissures) or hydrothermal manifestations [hot springs, fumaroles, hot ground showing specific vegetation (“Fialé” herbs)]. The photo-interpretation was carried out in the field using stereoscopes, covering consecutive daily field visits, using four-wheel-drive cars and long marches to reach the targeted sites following itineraries planned the day before. The most inaccessible sites were selected for helicopter visits, frequently organised with two pre-established

Fig. 2.22 Afar family in front of their house, located on a recent basaltic flow (Erta Ale range, Photo Marinelli 1970)



landing sites in the morning and evening after a daily walking itinerary. Mirror signalling to the helicopter was frequently a very useful tool for final positioning.

Fresh rock samples, favouring aphyric lavas—representative of the magmatic liquid evolution—when there was a need for limited loading, were systematically collected and processed and examined as thin sections under a polarizing microscope, using a point counter when necessary for modal analysis. More than 5000 samples were collected over the whole Afar depression and carefully marked on air photographs and field maps, mainly by F. Barberi and J. Varet (Fig. 2.29). The most representative parts of them were crushed and powdered for chemical analysis, age determination, neutronic activation analysis, or selected for microprobe studies. Rocks, powders and thin sections are now stored at the Earth Science Department Afar store of the University of Pisa thanks to the initiative of Roberto Santacroce. Altogether more than 100 scientific papers were

published in various specialised Earth Science Journals in the period 1968–1980).

More recently, renewed interest by Afar studies followed the Asal 1978 tectonic and volcanic event. The seismic crisis, with the earthquake reaching a magnitude of 5.3, and the opening along Asal-Ghoubbet axis reaching 2.4 m wide in the submarine part (Ghoubbet Rift), was well documented because of the seismic and geodetic networks established in 1973 across the rift. The Ardoukoba basaltic eruption (Fig. 2.30) was studied from volcanological, petrological, mineralogical and geochemical standpoints, and placed in the context of the volcano-tectonic and magmatic evolution of the Asal Rift (Demange and Tazieff 1978; Ruegg et al. 1979; Demange et al. 1980).

In February 1980, a scientific colloquium was organised jointly by CNRS (France) and ISERST (Djibouti), attended by 60 geoscientists from Djibouti, France, Italy, Iceland, UK and USA. A volume of the *Bulletin de la Société Géologique*

Fig. 2.23 Young Afar girl carrying water in goat skin water bag (Photo credit Ismail Ali Gardo)



de France was produced including 27 written contributions on all aspects of the event and its geodynamic context (Colloque Rift d'Asal. *Bul. Soc. Geol. Fr.* 1980, (7) XXII, pp. 797–1013).

The 1978 volcano-seismic and tectonic event was followed by a 10-year period of relatively fast opening (6 cm/year) and in 1988 the characteristics changed and the incursion of magma in the Fialé caldera could be documented with several pulses at shallow depth (3.5–2.5 km) which lasted until 2005. The whole event provided further detailed imaging of the magmatic and rifting process (Dobre et al. 2007a, b). Based on satellite imagery processing (including radar interferometry), ground field surveys (GPS, tectonics, palaeomagnetic measurements and age determinations), new bathymetric studies in the Gulf of Tadjourah, detailed seismicity data and seismic profiling, new quantitative models were proposed for the penetration of the Aden oceanic spreading axis within eastern Afar and the deformation of the lithosphere in the south-western part of the Afar floor. Block rotation was shown to occur together with bookshelf faulting affecting the 3.5–1 million years old stratoid series (Manighetti et al. 1997, 1998, 2001a, b),

providing more precise information than the microplate deformation model proposed by Barberi and Varet (1977).

Similarly, the Dabbahu event which affected the northern part of the Manda Harraro range at Da'Ure in September 2005 (Fig. 2.31), followed by successive small basaltic emissions in 2007, 2009 and 2011, allowed for a new geo-scientific investigation into Afar geology and geophysics in the years 2005–2012. This volcanic range, already identified by Varet and Treuil (1973) and Barberi and Varet (1975) as the most active spreading segment in Afar, opened up to 8 m width along a 70-km axis. The event was preceded by an international conference held in Addis Ababa in June 2004 entitled “The East African Rift System: Geodynamics, Resources and Environment”, which was summarised in a special publication (N°259) of the Geological Society of London entitled “The Afar Volcanic Province Within the East African Rift System” edited by Yirgu, Ebinger and Maguire in 2006. This important volume (336 pp) includes 17 articles: Plate kinematic and geodynamic framework of the Afar volcanic province (Part 1), Geochemical constraints on flood basalt and rift processes (Part 2), Rifting in the Afar volcanic province: modelling and kinematics (Part 3) and

Table 2.1 Translation of a few Afar words of use in toponymy

English	Afar
<i>Nouns</i>	
Mountain, massif	‘Ale
Mount, hill	Kôma
Rock, small rocky hill or plateau	Dâ
Large rocks	Deet
Plateau	Râsa
Ridge	Gêra
Summit	San
Cape, point	Damum
Col, pass	Dâba
Hole	Bôdu
Fire	Kira
Plain	Bahari
Powder	Bodo
Valley, oued	Da’ar
Small valley	Dabba
Water, water point	Lê
Well	Ela
Shallow well	Buyyi
Lake, sea	Bad
<i>Adjectives</i>	
Large	Kadda
Small	‘Unda
Black	Data
White	Ado
Red	‘Asa
Yellow	Hurud
Green	Ar’Dar

Rifting in the Afar volcanic province: geophysical studies of crustal structure and processes (Part 4). This initiative helped, following the 2005 event, to establish the “Afar Rift Consortium”, supported by NSF (USA) and NERC (UK). It included American, British, Ethiopian and French geophysical and geological teams who built a research program answering the invitation of the Ethiopian authorities, with heavy involvement of the University of Addis Ababa geology department and geophysical observatory. This allowed the development of a new research approach providing insights on the characteristics and behaviour of the

lithosphere and asthenosphere in the central Afar triple rift junction and mantle plume.

Following the Manda-Hararo sequence of volcano-tectonic events, an international symposium entitled “Magmatic Rifting and Volcanic Activity” was organised in Addis Ababa, Ethiopia on the 11–13 January, 2012, attended by more than 200 geoscientists, including at least 50 Ethiopian research staff and students, and marked the end of the 5-year Afar Rift Consortium project. A total of 67 oral presentations and 66 poster contributions were presented, covering the themes of active magmatic rifting, mid-ocean

Table 2.2 Some useful geological terms

Geological terms	
Earth	Baloo
Basalts (black rocks)	Dâta Deet
Rhyolites (red rocks)	‘Asa Deet
Scoriaceous lava flow (“Aa”)	Manda
Smooth lava flow (Pa Hoe Hoe)	Rasa
Cooked earth	Alayta
Fault	Andidou
Earthquake	Baloo Anguau
Open fissure	Adale Andidou
Necked clay plain	Bôda
Pasture land	Affara Dara
Evaporitic plain	Koubi Adoul
Diatomite (white powder)	Ado Bodo
Travertine	Diikiil
Hot spring	Ni’i Lê
Fumarole	Boïna
Eruption	Badok Tawle
Smoke	‘Irta
Intermittent hot spring (coughing water)	Kahouh Ye
Salty water	Asbo lê
Water spring	Geda Lê
Cold water	Da’Him Lê
Putrefied lake	Abhe Bad
Mer (bad water)	Ad’He bad
Camel hill	Gali Koma
Coloured mountain	Bora’le Ale
Stomach mountain	Ale Bagu
Long mouth	Afdera

ridge processes, rifted continental margins, mantle-lithosphere interactions and the causes of breakup, natural hazards, rifting and climate, and resources from magmatic rifts. The session included: (1) Recent activity in Afar; (2) Structure and origins of Afar, both mainly centred on the Manda Harraro-Dabbahu event; (3) Magmatic rifting in Iceland, allowed for useful comparisons; (4) Resources from magmatic rifts (for which two sessions dealt with geothermal, epithermal gold and oil); (5) Geohazards from volcanic or tectonic origin, including effects on dams in the Awash valley; (6) MOR processes was based on examples from Aden and mid-Atlantic Ridges; (7) Kinematics,

dynamics and structure in Afar and Asal concerned crustal deformation (block rotation) and the active Asal-Goubbet Rift; (8) Mantle-lithosphere interactions was based on seismic imaging, thermal regime and magmatic mantle processes in the East African Rift; (9) Rifting and climate was dedicated to undergoing climate change studies in the East African Rift; (10) Continental rifting and continental margins dealt with Afar margins and comparisons with the Atlantic and the Red Sea; (11) Active magmatic rifting was based on satellite imagery processing, seismic anisotropy, and petrological and geochemical modelling.



Fig. 2.24 Girl carrying the wood (for cooking needs) back home (Photo credit Ismail Ali Gardo)

Several other eruptive events affected the Afar area in recent years, including:

- The Jebel al Tair basaltic eruption in the Southern Red Sea in September 2007.
- The Alu-Dalla Fila eruption in the northern part of the Erta Ale range in November 2008.
- The Dallol phreatic eruption in January 2011 (non-volcanic).
- The major Nabro caldera pyroclastic and lava flow eruption in June 2011.



Fig. 2.25 Young Afar man with the traditional “Jile” (Photo credit Ismail Ali Gardo)

- The submarine hyaloclastite eruption of Zubair giving birth to a new island 180 m high, north of the archipelago in December 2011.
- Not to mention the Erta Ale continuous activity in both lakes, the central one still fluctuating, and the northern one exhibiting a hornito activity (Fig. 2.32). In 2014 an eruptive event occurred with a flow outside the caldera along the northern rim followed by the appearance of a new active pit crater in the northern lava lake (Fig. 2.33). In early 2017, while this book edited, a new fissure appeared along the axis of the wide elliptic caldera collapse located south of Erta Ale caldera followed by an important basaltic eruption, still flowing after 8 month, whereas several new active craters appeared along this NNE-SSW fissure. A new active lava lake appeared in the central part of this wide southern sink.



Fig. 2.26 Afar girls with dough prepared to bake bread in an oven dug in the soil and pre-heated with firewood (*Photo credit* Ismail Ali Gardo)



Fig. 2.27 Haroun Tazieff with H.H. Ras Mengesha Seyoum, Governor of the Tigray province, who supported the CNR-CNRS Afar expeditions (*Photo* Marinelli 1967)



Fig. 2.28 Professor Giorgio Marinelli in the field in Afar (Università di Pisa, Italy; *photo* F. Barberi, 1967)



Fig. 2.29 Franco Barberi and Jacques Varet at Lake Afrera (*Photo Marinelli 1967*). The author had burnt his legs on the fumarolized top of Gada Ale volcano (Erta Ale range)

Fig. 2.30 The eruption of Ardoukoba volcano in the Asal rift axis, November 7–14, 1978 (Demange and Tazieff 1978; Demange et al. 1980); in the background, one of the normal faults bordering the Asal Lake, on the NW side of the rift



Fig. 2.31 Manda Harraro range September 2005 rifting event. View from the north (with people for scale) of the Da'Ure 500 m-long fissure vent formed during Dabbahu's historical eruption. A small pumice dome was formed besides pumice falls. The central part of the Dabbahu volcano is seen on the first horizon line (Vye-Brown et al. 2013)





Fig. 2.32 The Erta Ale volcano, seen from the north, with its two lava lakes, active at least since 1967 when discovered by Tazieff (1968), one located north of and the other to the centre of the elliptic caldera elongated NNW-SSE (Red Sea direction). The southern lava lake is not active. A larger elliptic caldera collapse is observed to the south, where

the Haili Gub rift volcano is also visible, marking the southern extremity of the Erta Ale range (Photo Varet 1972). It is along a fissure affecting the axis of this wide caldera that new basaltic activity is observed and continues for several months



Fig. 2.33 In January 2014, it was observed that the lava lake at the central pit had risen up near to the rim. This was followed by a rise of the lava in the northern crater with basaltic overflow in the northern caldera. This eruption was followed by the appearance of a new pit

crater inside the northern lava lake where the major activity is now located. (Photo from the east, looking SW; Ale Bagu volcano in the back; Geoff Maclay, March 3, 2014)

References

- Allan TD (1970) Magnetic and gravity fields over the Red Sea. *Phil Trans Roy Soc A* 267:153–180
- Aubry A (1855) Observations géologiques sur le pays Danakil, Somalie, le Royaume du Choa et les pays Galla. *Bull. Soc. Geol. Fr.* Vol. XIV.
- Bannert D, Kedar EY (1971) Plate tectonics in the Red Sea region as inferred from space photography. NASA, Washington
- Bannert D, Brinckmann J, Kading K, Ch. et al. (1970) Zur Geologie der danakil-Senke (Nördliches Afar Gebiet, NE-Aethiopen. *Geol Rundsch* 59/2:409–443
- Barberi F, Varet J (1970) The Erta `Ale volcanic range. *Bull Volc* 34:848–917
- Barberi F, Varet J (1975) Volcanological research in Afar (L. R. Wager prize summary lecture). *Bull Volc* 39(2):166–174
- Barberi F, Varet J (1977) Volcanism in Afar: small-scale plate tectonic implications. *Bull Geol Soc Amer* 88:1251–1266
- Barberi F, Borsi S, Ferrara G, Marinelli G, Varet J (1970) Relations between tectonics and magmatology in the northern Danakil Depression (Ethiopia). *Philosophical Trans Royal Soc London* A267:293–311
- Barberi F, Tazieff H, Varet J (1972) Volcanism in the Afar depression: its tectonic and magmatic significance. *Tectonophysics* 15:19–29
- Blanford WT (1870) Observations on the geology and zoology of Abyssinia, made during the progress of the British Expedition to that country in 1867-68. McMillan, London
- Brinckmann J, Kursten M (1969) Geological sketchmap of the Danakil Depression (1:250.000). Budesantalt jur Bodenforschung. Hannover. 4p.
- CNR—CNRS Afar team (1973) Geology of northern Afar (Ethiopia). *Rev Geogr Phys Geol Dyn* 15:443–490
- Dainelli G (1943) Geologia dell' Africa Orientale. *Rend. Acc. It. Roma*
- Dainelli G, Marinelli O (1912) Risultati scientifici di un viaggio nella colonia Eritrea. *Publ. R. Istit. St. Sup. E ref. di Firenze*, p 601
- Demange J, Tazieff H (1978) L'éruption tectonique de l'Ardoukoba (Djibouti). *C.R. Acad Sc Paris* 287:1269–1272
- Demange J, Stieltjes L, Varet J (1980) L'éruption d'Asal de novembre 1978. *Bull Soc Géol France* 12 (6):837–843
- Desio A (1941) Apunti Geomorfologici sulla Dancalia occidentale. *Bol R Soc Geogr Ital* Vol. VI
- Dobre C, Manighetti I, Dorbath C, Dorbath L, Jacques E, Delmond J-C (2007a) Crustal structure and magmato-tectonic processes in an active rift (Asal-Ghoubbet, Afar, East Africa): 1. Insights from a 5-month seismological experiment. *J Geophys Res* 112
- Dobre C, Manighetti I, Dorbath L, Dorbath C, Bertil D, Delmond J-C (2007b) Crustal structure and magmato-tectonic processes in an active rift (Asal-Ghoubbet, Afar, East Africa): 2. Insights from a the 23 year recording of seismicity since the last rifting event. *J Geophys Res* 112
- Gortani M (1949) Il problema delle fosse tettoniche africane e le ricerche italiane in Dancalia. *Ann Hébert et Aug* 7:201–222
- Gortani M (1951) Risultati di una spedizione geologica nella Dancalia meridionale. *Proc XVIIIth sess Intern Geol Congr London, 1948*, XIV:193–198
- Gouin P, Mohr PA (1964) Gravity traverses in Ethiopia. *Bull. Geoph. Obs. Addis Abeba* 3(3):185–240
- Haga AO, Youssouf SK, Varet J (2012) The Manda-Inakir geothermal prospect area, Djibouti Republic. Proceedings of the 4th African Rift Geothermal Conference. Nairobi, Kenya, 21-23 November 2012, 7p
- Heike Merlin O (1950) I basalti dell' Africa Orientale. *Mem Ist Geol Min Univ Padova*, 17
- Holwerda JG, Hutchinson RW (1968) Potash bearing deposits in the Danakil area, Ethiopia. *Econ. Geol.* 63:124–150
- Hutchinson RW, Engels GC (1970) Tectonic significance of regional geology evaporate lithofacies in Northern Ethiopia. *Phil. Trans. Roy. Soc. London A.* 267(1181):313–329
- Issel A (1869) Malacologia del Mar Rosso. Ricerche zoologiche e paleontologiche. Pisa
- Johnston (1884) Travel in southern Ethiopia through the country of Adal and the kingdom of Shoa. London.
- Justin Visentin E, Zanettin B (1968). Prime osservazioni geologico-petrografiche Dancalia interna fra Sardo e Dallol. *St Trent Sc Nat* 45, N°1
- Manighetti I, Tapponnier P, Courtillot V, Gruszow S, Gillot P-Y (1997) Propagation of rifting along the Arabia-Somalia plate boundary: The gulfs of Aden and Tadjourah. *J Geophys Res* 102:2681–2710
- Manighetti I, Tapponnier P, Gillot P-Y, Jacques E, Courtillot V, Armijo R, Ruegg J-C, King G (1998) Propagation of rifting along the Arabia-Somalia plate boundary: Into Afar. *J Geophys Res* 103:4947–4974
- Manighetti I, King GCP, Gaudemer Y, Scholtz CH, Dobre C (2001a) Slip accumulation and lateral propagation of active normal faults in Afar. *J Geophys Res* 106:13,667–13,696
- Manighetti I, Tapponnier P, Courtillot V, Gallet Y, Jacques E, Gillot Y (2001b) Strain transfer between disconnected, propagating rifts in Afar. *J Geophys Res* 106:13,613–13,665
- Marinelli G, Varet J, (1973) Structure et évolution du Sud du "horst Danakil" (TFAI et Ethiopie). *C.R. Acad Sci, (D)* 276:1119–1122
- Mohr PA (1967) Major volcano-tectonic lineament in the Ethiopian Rift system. *Nature* 213:664–665
- Munzinger W (1869) Narrative of a journey through the Afar country. *J Royal Geogr Soc* 39:188–232
- Nesbitt LM (1934) Desert and Forest: the exploration of Abyssinian Danakil (London: Jonathan Cape) pp 450 (Also Published in 1935 by A. A. Knopf, New York, under the title 'Hell-hole of creation: the exploration of the Abyssinian Dankil')
- Ruegg JC, Kasser M, Lépine JC, Tarantola A, (1979). Geodetic measurements of rifting associated with a seismo-volcanic crisis in Afar. *Geophys. Res. Lett.* 6:817–820
- Ruppel E (1934). Skizze der geologischen formationen Abyssiniens. Mus. Senckenberg. 1.
- Salt H (1814) A voyage to Abyssinia and travels into the interior of that country executed under the orders of the British Government in the years 1809 and 1810. Revington, London
- Tazieff H (1968) Relations tectoniques entre l' Afar et al Mer Rouge. *Bull. Soc. Geol. DFr.*, 7 (X):468–477.
- Tazieff, H, Varet, J. (1969) Pétrographie et tectonique de l'Afar septentrional (Ethiopie). Colloque Géol. Africaine Clermont-Ferrand (résumé). *Ann Fac Sc Clermont* (41):54
- Tazieff H, Marinelli G, Barberi F, Varet J (1969) Géologie de l'Afar septentrional Symposium Ass. *Interna. Volcanologie; Canaries. Bull. Volc.*, t. XXXIII-4, pp 1039–1072
- Tazieff H, Barberi F, Giglia G, Varet J (1972) Tectonic significance of the Afar (or Danakil) depression. *Nature* 235:144–147
- Treuil M, Varet J (1973) Critères volcanologiques, pétrologiques et géochimiques de la genèse et de la différenciation des magmas basaltiques exemple de l'Afar. *Bull Soc Géol France* 7(15):506–540
- Varet J (2013) The Afar system and carbonates. Cocard workshop (abstract), Sicily, p 48–49
- Vye-Brown C, Smith K, Wright, T (2013) Active rifting, magmatism and volcanism in the Afar depression, Ethiopia. Large Igneous Province Commission IAVCEI
- Zichy W (1880) Die Danakil Küste. *Petern Mittheil* 26:292

The Arabian plate to the north detached from the Nubian and Somalian plates along the Red Sea and Gulf of Aden oceanic ridges, whereas a continental rift separates the Nubian and Somalian plates. Afar appears to be the place where the oceanic plate boundary linking the Red Sea and the Gulf of Aden emerges and meets the EARS. Therefore Afar, where these three plates meet, is typically considered to be a “triple-junction”, in fact the only one visible on the Earth’s surface.

As a whole, the Afar region and surrounding plateaus allow one to observe all the steps of the development of divergent continental plate boundaries from the stage of the plateau upwarping to the formation of the continental rift valley and the progressive development of an oceanic ridge.

As observed on relief maps of the region (Fig. 1 in ‘Introduction’ and Fig. 1.2), the Afar depression is visible on the Earth’s surface, resulting from the fact that it is surrounded by the three high plateaus of Ethiopia, Yemen and Somalia. This uplift dates back from Miocene, and predates the sinking of Afar. It results from a mantle upwelling, causing the crust to down warp and swell into domes. Mantle upwelling is considered to be produced by the rise of the hotter asthenosphere up into the colder lithosphere.

In the plume theory, this is the cause of continental break-up. However, mantle decompression (and hence uplift) could also result from earlier extension affecting the Afro-Arabian plate, which began in the late Cretaceous and developed in the Palaeogene periods.

The importance of volcanism associated with doming is considered as an argument supporting the plume model.

3.1 The Nubian Plateau Uplift and Associated Volcanism

Detailed geological investigations allowed the correlation of basaltic emissions and dome uplift.

It appears that the first volcanic activity started in southern Ethiopia—away from the uplifted area—with

basaltic emissions dating from the Eocene (45–35 million years ago) (George et al. 1998; George and Rogers 2002).

Until late Cretaceous, the uplift did not exceed 400 m. An early Miocene event produced an uplift estimated to be at least 500 m. However, the main component, a staggering 1500 m in magnitude, dates from late Neogene (Baker et al. 1972) (Fig. 3.1).

The uplift caused by the Ethiopian dome was accompanied by the emission of Palaeogene flood basalts, the erosion features of which characterise the morphology and land use of the Ethiopian plateau (Fig. 3.2). The main pile accumulated 31–30 million years ago in a very short time span, that is, less than one million years (Hoffman et al. 1997). All these basalts are of tholeiitic composition and the associated sub-alkalic rhyolites appear to be genetically linked. At the end of this event, rhyolite ignimbrites were emitted, well known in the landscape as many historical Coptic churches include this material (Fig. 3.3). These ignimbrites correlate with the Yemen thicker silicic piles, were dated from 30–29 million years ago and represent one of the major silicic eruptive events on Earth (Utskins et al. 2002). They were shown to be derived by low pressure crystal fractionation from the same magma source as the associated basalts, combined with minor assimilation from continental crust (Ayalew and Yirgu 2003). In the north-east of the plateau, where it was faulted and tilted, magnesian and alkali basalts, enriched in hygromagmatophile elements, are also found, dating from 30 million years ago.

Uplift totalised 2.2 km, having occurred in the last 30 million years. It was shown that the stratigraphic contact between Jurassic and Cretaceous layers was at around 1 km elevation by the early Oligocene when a 1 km thick sequence of trap basalts was emitted 31 million years ago. This overload may have resulted in a subsidence of 0.15 km. Hence the net rock uplift of the Ethiopian plateau has been 2.05 km (2.2–0.15 km).

This eruptive phase continued with the building of the Simien shield volcanoes (Fig. 3.4). Later volcanic phases (22 million years ago) produced the Choke and Gugufu shield volcanoes made of alkali basalts as their underlying trap units. More recent

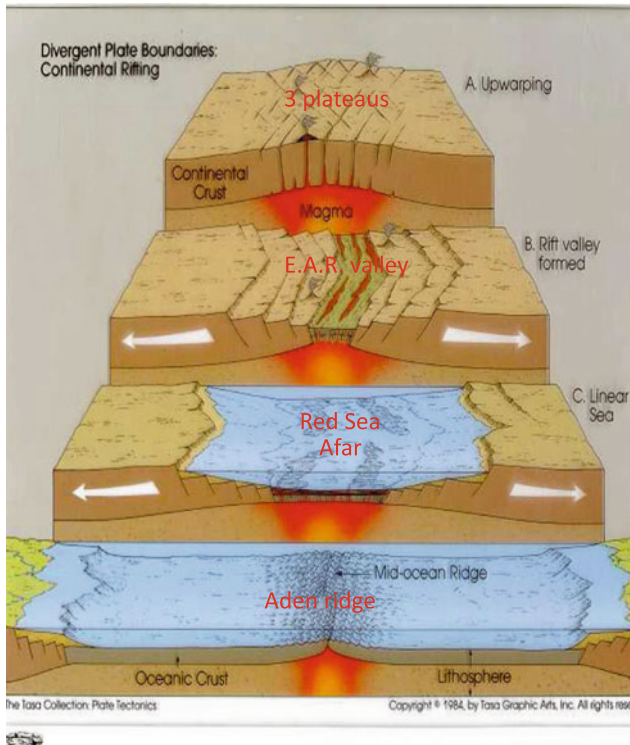


Fig. 3.1 Steps of the development of an oceanic crust after continental crust upwarping, continental rift initiation and oceanic floor development under continuous rifting (modified from Tasa Graphic Art Inc.)

shield volcanoes (such as Mt Guna, 11 million years ago) display even more undersaturated compositions. Younger shield

volcanoes to the south have been dated as young as three million years old (Utskins et al. 2002). They display a variety of rock compositions from alkali basalts to trachytes and phonolites, with abundant porphyritic rock varieties (olivine, plagioclase, pyroxene). South of Lake Tana, highly alkaline lava erupted from a number of Quaternary volcanic centres. The main unit blocked the Blue Nile and was the cause of the curvilinear shape of the upper basin. These lava are olivine-rich basanites. In the Injibara area and west of Nekemte (Dedessa River) they carry abundant mantle xenoliths.

The uplift of the Nubian plateau, combined with the rifting occurring in Afar, resulted in a massive faulting area of more than 2500 m vertical displacement along the Afar margin. The plateau culminates at 2000–3000 m altitude along the upper faulted margin, which also corresponds to the divide between the Mediterranean (Blue Nile) and Afar depression. The Nubian scarp represents the abrupt eastern slope of the generally westwardly tilted plateau and trends N-S between meridians $39^{\circ}45'$ and $40^{\circ}15'$ (Fig. 3.5).

About 40–50 km wide in the northern part of the Afar triangle—where the basement and its Mesozoic cover outcrops (Fig. 3.6)—it becomes slightly larger in the south. This also corresponds to the area where the pre-Mesozoic basement is covered by the trap basalts of the Ethiopian plateau.

Since 29 million years ago, $93,000 \text{ km}^3$ of rocks were removed from the plateau by erosion, in three phases (29–10 million years ago slow uplift, 10–6 million years ago increased uplift and 6 million years ago to the present dramatic plateau rise), that is with an acceleration with time, which

Fig. 3.2 Eroded trap basalts in the Simien mountains (from: www.trekkinginethiopia.com)





Fig. 3.3 Lalibella Coptic church dug in the ignimbrite of the Ethiopian plateau covering the trap basalts as observed in the plans behind (Source www.boundless.com)

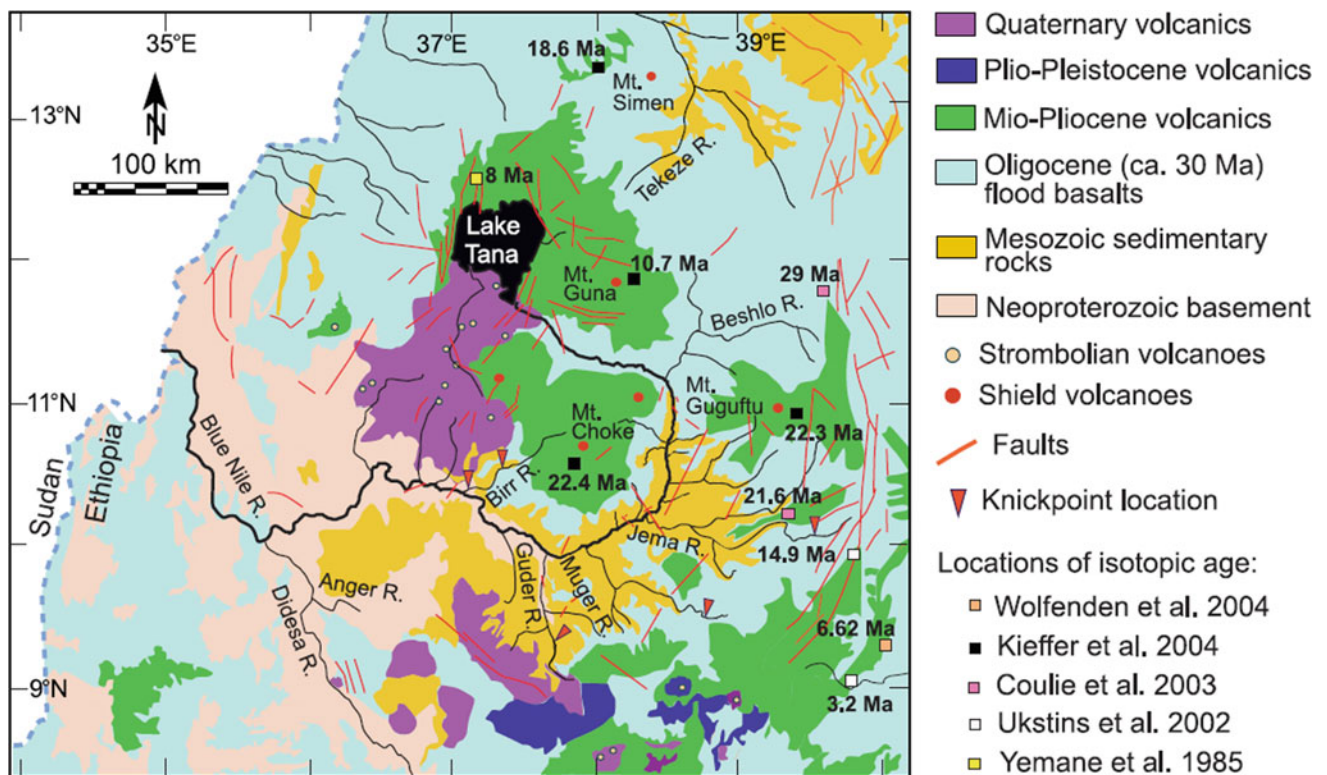


Fig. 3.4 Geologic map of the north-western Ethiopian plateau showing the main volcanic units overlying the Neoproterozoic basement and its Mesozoic sedimentary cover, with indication of radiometric age determinations (from Gani et al. 2007)

Fig. 3.5 Relief map of Afar and neighbouring Ethiopian plateaus. The water divides are indicated in *red*, whereas the political boundaries are drawn in *black*. The whole hydro network of the plateau departs from the rift margin along the Nubian margin, whereas the watershed is very short or absent on the Afar side, with the exception of the Awash river which originates south-west in the Nubian plateau. Observe, the width of the foothill and the presence of marginal depressions where Tertiary and Quaternary sedimentary basins developed as a result of block-faulting and tilting



Fig. 3.6 The Ethiopian plateau as observed along the track from Makale to Dallol, across the 2000 m scarp, showing the faulted Jurassic limestone overlying the Triassic sandstones and the Precambrian basement. (Photo J. Varet 2013)



correlates with the uplift and rifting episodes rather than with climate variations. That is over an area of 250,000 km² with a mean thickness of 0.37 km. This huge amount of sediment removed along the Nile largely fed the delta, eventually influencing the Messinian crisis in the Mediterranean (Gani et al. 2007). The present-day seismic activity (see Fig. 3.9) indicates that the movement of normal faulting (with uplift of the plateau and sinking of the depression) still continues.

3.2 From Continental Doming to Rifting: The Continental Rift Stage

If the first step of continental doming and associated mantle uplift is well expressed by the Nubian plateau, the process of crustal extension results in the formation of a continental rift. This stage is observed at present, south of Afar, in the EARV (from Ethiopia down to Kenya, Uganda and Tanzania) which it is considered to be a plate boundary. The Nubian Plate was identified and makes up most of Africa, and the smaller plate that is pulling away was named the Somalian Plate (Fig. 3.7). Plate analysis suggests that the EARV marks a zone of very slow crustal spreading (1–6 mm/year, increasing from south to north), against nearly 2 cm for the Red Sea and Gulf of Aden and varying from 19 to 7 mm from south-east to north in the Afar link. This model helps to account for many of the peculiar or unique features of this complex continental rift. Slowly moving away from each other, these two continental plates have not yet really separated, as no oceanic floor has been created by basaltic diking in identified segments. In the southern extremity, the mere distinction of two plates is questionable (less than a 1 mm/year in the southern Malawi Rift).

At the level of Lake Turkana, in the area located aside the Ethiopia Kenya border, the rift structural feature attenuates to form a 200 km “basin and range” province (Moore and Davidson 1978) separating the Ethiopian and Kenyan Rifts. This was shown to be an area of crustal thinning with an anomalous low velocity upper mantle, a thermal anomaly related to asthenospheric upwelling during passive extension. The reason for this area not to be affected by doming remains unexplained. Could it relate to the extensive fracture zones present in this area and described below?

South of this, the rift splits into the eastern Gregory Rift and the western Albertine Rift, which are separated by the 1300 km-wide East African Plateau, centred on Lake Victoria, where the small “Victoria Plate” can be identified (Fig. 3.7). This particular behaviour appears to be linked to two major pre-existing geological features (Fig. 3.8):

- One is the change in nature of the geological substratum. Whereas the Afar, Red-Sea and Gulf of Aden and Ethiopian Rift system developed in the Arabian-Nubian

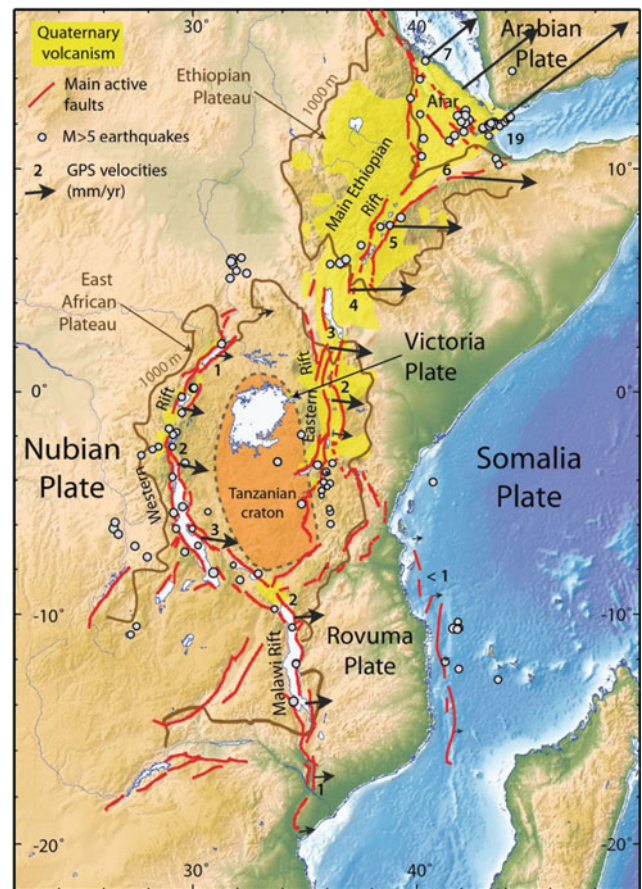
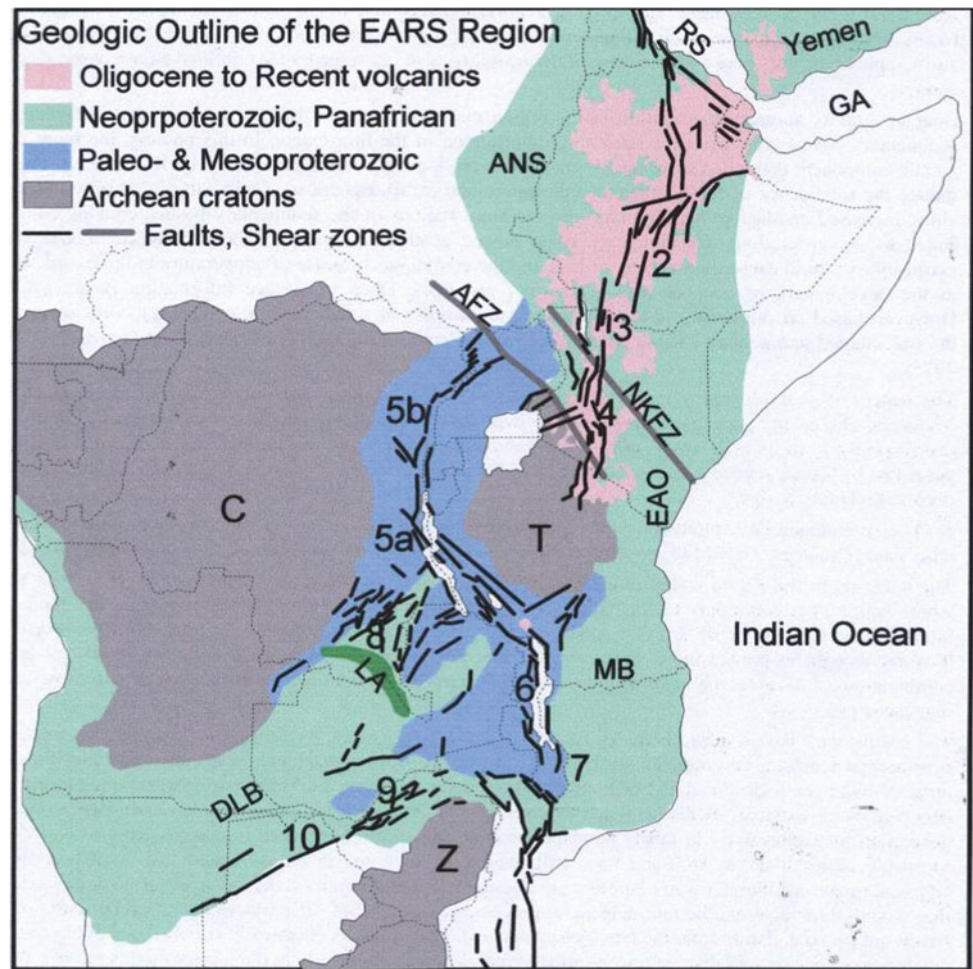


Fig. 3.7 The East African Rift System, with major faults (in red), seismicity (M over 5, as white circles), quaternary volcanism (in yellow) and plate motion vectors with GPS velocities in mm/year (black arrows). From Calais (2016)

shield, in a relatively recent lithosphere of pan-African age, eroded and thinned (650–500 million years ago; Avigad and Gvirtzman 2009), it is when reaching the old, thick and cold Tanzanian Craton of Archean age (3.15–2.75 billion years; Dirks et al. 2003) that it splits. It is as if it was too strong and isotropic to be substantially faulted and rifted to allow upwards heat and mass transfer from the mantle (Demissie 2010). Therefore, when underlain by tumescent mantle, it refracts heat and mass transfer paths into the more mobile peri-cratonic orogenic belts (the Mesoproterozoic belt where the western rift developed).

- The other is the influence of the pre-existing transverse fracture N’Doto-Kaziza-Fault Zone. The N’Doto-Kaziza-Fault Zone, running in a NW–SE direction, apparently corresponds to a line of weakness along which an earlier Cretaceous rift developed (see Fig. 3.8). Despite its apparent aseismic character; this transverse structure appears to have played an important role in the later development of the East African doming and rift system (Fig. 3.9).

Fig. 3.8 The Proterozoic orogenic belts. Cratons: Congo (C), Tanzania (T) and Zimbabwe (Z). Orogenic belts: Paleo- and Mesoproterozoic (blue), Panafrican (green): Damara-Lufilian (DLB), Lufilian Arc (LA), East African (EAO) comprising the Mozambique Belt (MB) and the Arabian-Nubian Shield (ANS). EARS sectors: Afar (1), Main Ethiopian (2), Turkana (3), Main Kenyan (4), Western (5) Malawi (6), Urema (7), SW branches (8) and Zambezi (9); (10) is the Ganzi-Chobe fault (Botswana). RS: Red Sea, GA: Gulf of Aden, ASZ: Aswa Shear Zone, NKFZ: N'Doto-Karisa Fault Zone, TRFZ: Tanganyika Rukwa-Malawi fault zone. Based on the Geological Map of Africa, (UNESCO-CGMW, 1985–1990)



3.3 Mantle Plume in Afar and East Africa, Geochemical and Geophysical Approaches

The two regions of topographic uplift observed (the Ethiopian and Kenyan domes) along the East African Rift System (EARS) section of the African continent are both commonly regarded as the surface expression of one or two mantle plumes.

However, there are still debates among geophysicists and geochemists concerning the characteristics of these mantle plumes. Ritsema et al. (1998) showed the presence in the mantle of a broad low velocity shear anomaly underlying the EARS, which initiates deep in the core mantle boundary beneath South Africa and merges towards the surface beneath Afar (Fig. 3.10). This was interpreted as a “superplume” quite different from the traditional narrow plumes observed elsewhere (Bastow et al. 2008), with mantle wave speeds among the slowest on earth (−4% as shown by Bastow and Keir 2011; Bastow 2012).

Interpretations differ concerning the origin of these seismic wave-speed anomalies, as they appear to be only partly

caused by elevated temperatures. Roomey et al. (2007) show that the anomaly peaked at +170 °C during the first major flood basalt event 30 million years ago, and have slightly fallen since to +140 °C, which is the lowest amongst large igneous provinces. These authors interpreted this as a result of the relatively high production of CO₂ by the superplume in the asthenosphere, which assisted melt production and contributed to the low seismic wave-speeds of the region at depth.

The undersaturated alkali basaltic products associated with phonolites found in the Turkana Rift segment suggest a decompression melting of ascending asthenospheric material which Furman et al. (2006) infer from geochemical analysis to be a mantle plume. The Sr, Nd and Pb isotope ratios of the Mg-rich lava differ from EARS basalts despite a melting at shallower depth, and suggest an initiation in a plume arising from the core-mantle boundary. A superplume of deep origin is not expressed in the topography (Fig. 3.10).

The origin and mode of development of the Ethiopian and Kenyan domes and of related mantle plume(s) are still questioned. According to geochronological data, volcanism

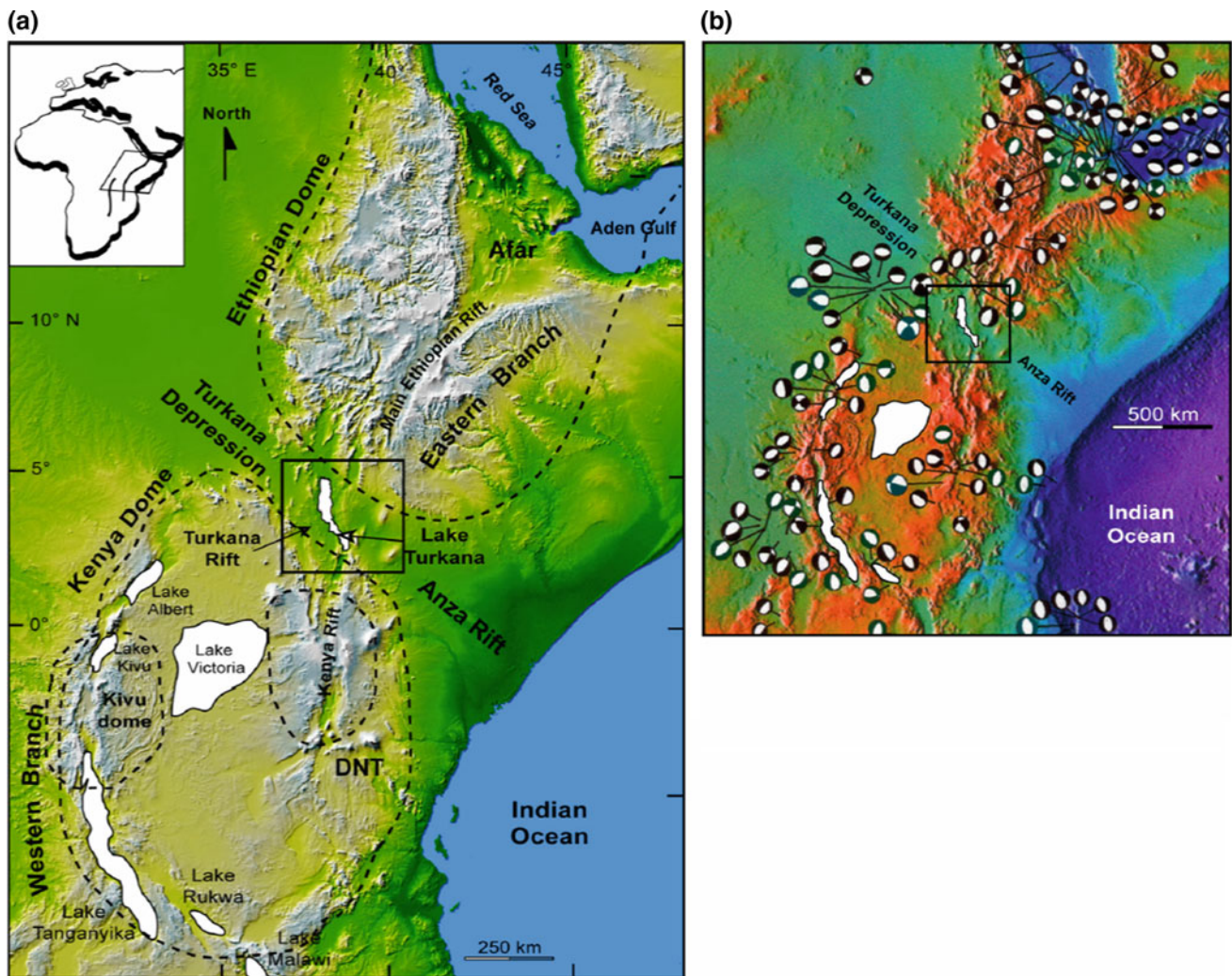


Fig. 3.9 Topographic map of the East African Rift System obtained from SRTM data showing the transverse Turkana depression between the two Ethiopian and Kenyan domes (*black dotted*). The *square* shows the area where the late cretaceous and tertiary Turkana rift of N E

direction developed. Note on the inserted seismic map showing focal mechanisms the relatively aseismic nature of Turkana and Western Kenya rift compared with the western branch and the Afar–Red Sea–Aden area (after Vetel 2005)

and rifting started near the Kenya-Ethiopia border in the surroundings of Lake Turkana 50 million years ago with further spreading towards north and south. It was shown to have migrated south within Kenya around 30 million years ago, reaching the central part of the Kenyan Rift around 15 million years later. Volcanism initiated in southern Kenya 12 million years ago and 8 million years ago in northern Tanzania.

This sequence in space and time was interpreted as resulting from the African plate motion over the megaplume northwards (Vetel 2005). In this model, the development of the two Afar and Kenyan domes are interpreted as resulting from the split of the upper part of the megaplume, which first developed north 35 million years ago, and then also south from 10 million years ago to the present day. The result of

the process is the presently depressed Turkana area despite its role in twin-plume generation (Fig. 3.11).

To account for the relationship between topographic elevation, seismic velocity anomalies and volcanism, a variety of models have been proposed, implying the presence of one or several plumes (Ebinger and Sleep 1998; George et al. 1998; Ritsema et al. 1998; Davis and Slack 2002).

The voluminous flood basalts in Ethiopia, both on the plateau and in Afar, have long been taken as evidence for the activity of a mantle plume (Schilling 1973; Marty et al. 1993; Courtillot et al. 1999).

Rogers et al. (2000) proposed a two distinct plumes model for the Kenyan and Ethiopian domes and rifts, whereas Furman et al. (2004) and Ebinger and Sleep (1998)

Fig. 3.10 Seismic tomography carried along the East African rift allowed a section deep in the mantle to be obtained depicting the African superplume, with shear velocity perturbations between -1.5 and $+1.5\%$ (after Ritsema et al. 1998). It initiates beneath South Africa at the core-mantle boundary and merges in Afar, passing along the East African Rift Valley

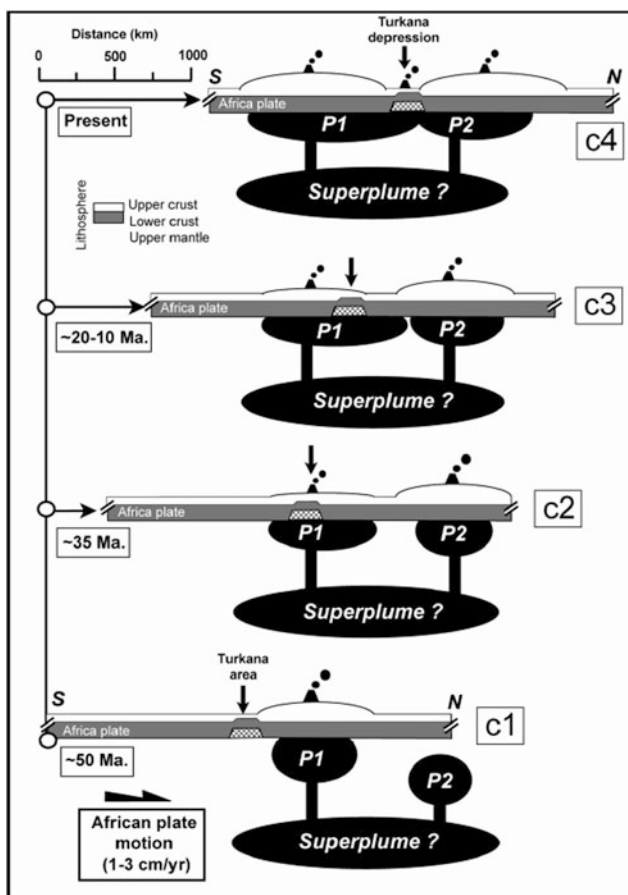
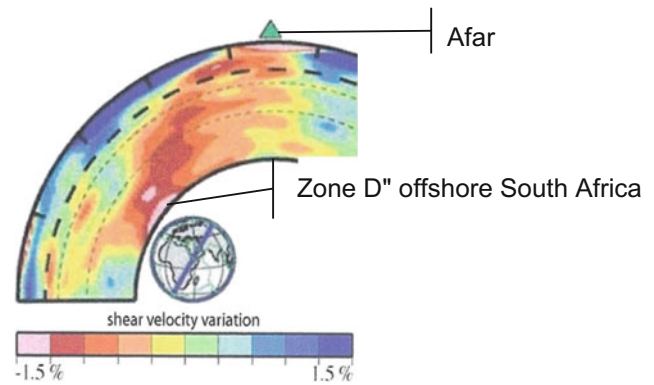


Fig. 3.11 Evolution of the East African megaplume moving northward with time, according to Vetel (2005), showing the first impact in the Lake Turkana area 50 million years ago, followed by the development of the Afar plume (P2, 35 million years ago), with later development of the Kenyan plume (10 million years ago to present)

advocate the presence of a unique long-lived plume under the whole EARV and Afar.

Considerable attention was paid to the important early Oligocene magmas emplaced during an event 31–31 million years ago. A total of $250,000 \text{ km}^3$ of flood basalt was produced in a short time interval, implying an eruption rate of the order of $0.2\text{--}0.3 \text{ km}^3/\text{year}$. Major and trace element analyses of the basalts from the Nubian plateau show the existence of three main magma types spatially zoned according to their TiO_2 content (Pik et al. 1998) and allowed for a more precise definition of their zonal arrangement. Low-Ti basalts with tholeiitic affinity are predominant ($150,000 \text{ km}^3$) in the NW whereas high-Ti transitional basalts predominate to the SW, and ultra-titaniferous transitional basalts and picrites are found in the central Lalibela area. These were shown by Beccaluva et al. (2009) to differ from the magmas issued from the Kenyan plume, supporting a distinct plume origin.

According to the isotopic results obtained by Pik and Marty (1999), two distinct components are involved in the genesis of the two extreme (low-Ti vs high-Ti) magmas: the latter are similar to oceanic island mantle sources, as well as some Afar basalts, whereas the former show a depleted mantle component associated with crustal contamination, but no simple plume model emerges.

Widening the study to include the later magmatic events of more alkalic composition, Kieffer et al. (2004) showed that, despite this larger range of compositional variation, these lava display similar Nd and Sr isotope compositions, whereas Pb varies considerably. They deduced that a conventional model of melting in a mantle plume, or two or more plumes, cannot explain the synchronous emission of the various magmas encountered.

In later studies, Pik et al. (2006) using also He isotopes showed the need to consider the presence of two mantle plumes: a large deep-seated mantle plume originating from the core-mantle boundary, which subsequently interacted with shallower mantle sources to produce the syn-rift volcanism of the Ethiopia-Afar province, and a second-order shallow mantle upwelling effective all over Africa in the various volcanic swells. Relying upon a deep mantle origin of the tritium signal, it contradicts the hypothesis of a shallow origin of this signal and does not support the model of a unique large mantle plume feeding the whole East Africa and Afar volcanic province.

Originally discussed by Treuil and Varet (1973), the Afar geochemical plume model proposed by Schilling, if enriched by isotopic data, became so complex that the plume model itself is questioned.

Rychert et al. (2012) used seismic S-to-P receiver functions to image the mantle structure beneath Afar. Whereas a transition between the lithosphere and the underlying asthenosphere is observed 75 km beneath the flanks of the continental rift, this boundary is absent in the rift itself (Fig. 3.12). Instead, a strong increase of velocities with depth is observed at about 75 km, which is best explained by decompression melting of the mantle in the absence of a strong mantle plume. These authors conclude that if a plume may have once been active, the influence of a thermal plume in Afar today is minimal. This conclusion is in conformity with the earlier geochemical observations by Treuil and

Varet (1973) and Barberi et al. (1975), who explained the variations observed in the basaltic magmas in Afar and surroundings with a decompression model involving melting from a successively more depleted mantle (Fig. 3.13).

Bastow et al. (2008) studied the Main Ethiopian Rift (MER) segment of the EARV, showing a low velocity zone in the asthenosphere which is well expressed at depths of 75–200 km. At greater depths (down to 350 km), tomographic images reveal an enlargement of a low velocity zone (although less anomalous than under the rift at shallower depth) over a 500 km-wide area, which extends beneath the Nubian plateau (Fig. 3.14). In contrast to Rychert et al. (2012), they interpret these low velocities as the expression of the upper mantle continuation of the African superplume, noting that the mantle beneath the region is amongst the slowest worldwide. The MER is, however, located towards the eastern edge of this broad deep low velocity structure and not above its centre. It is even more distant from Afar. This conclusion is in agreement with Chorowicz (2005), who concluded from a morphotectonic approach that the plume is centred under Lake Tana and not Afar.

As a whole, a possible interpretation is that if a mantle plume from deep in the mantle at the core-mantle boundary may account for the whole East Africa volcanic province, and is required in order to explain the initial trap series of the plateau, and eventually initial lithospheric weakening and breaking of the Afar triple junction, it is no more the

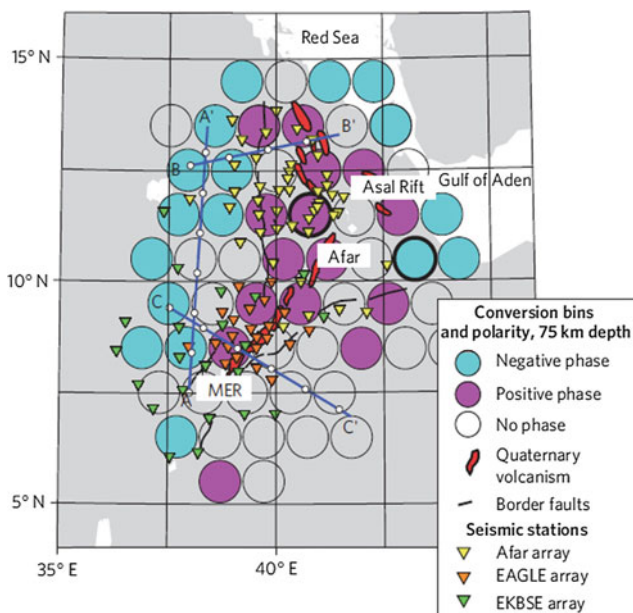


Fig. 3.12 Map of Afar indicating the location of stations with a discontinuity at 75 km depth (blue) and with a continuous low velocity zone showing onset of melting (violet). Seismic stations locations from the three networks (Afar, EAGLE and KBSE) are also indicated (coloured triangles). (Rychert et al. 2012)

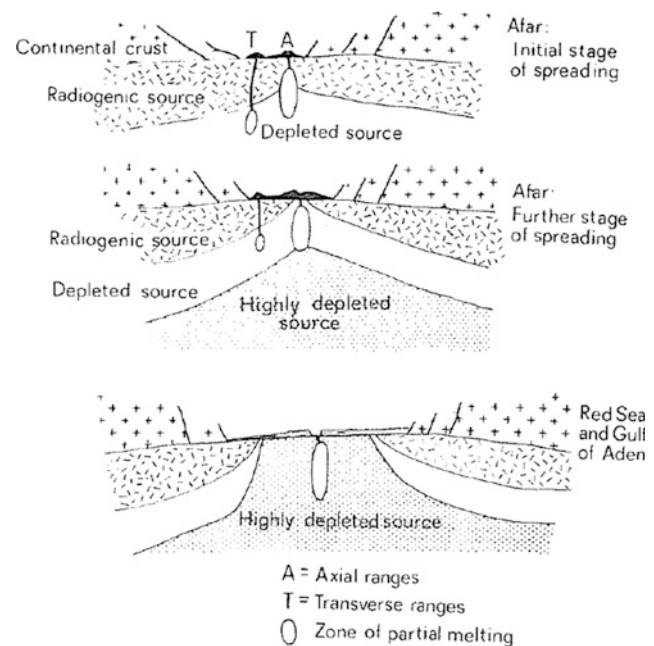


Fig. 3.13 Mantle evolution model from initial (Afar) to advanced stages of spreading (Red Sea trough, Aden ridge) showing the up-rise of highly depleted mantle replacing the radiogenic source that characterised the initial stage of continental crustal spreading (Barberi et al. 1975)

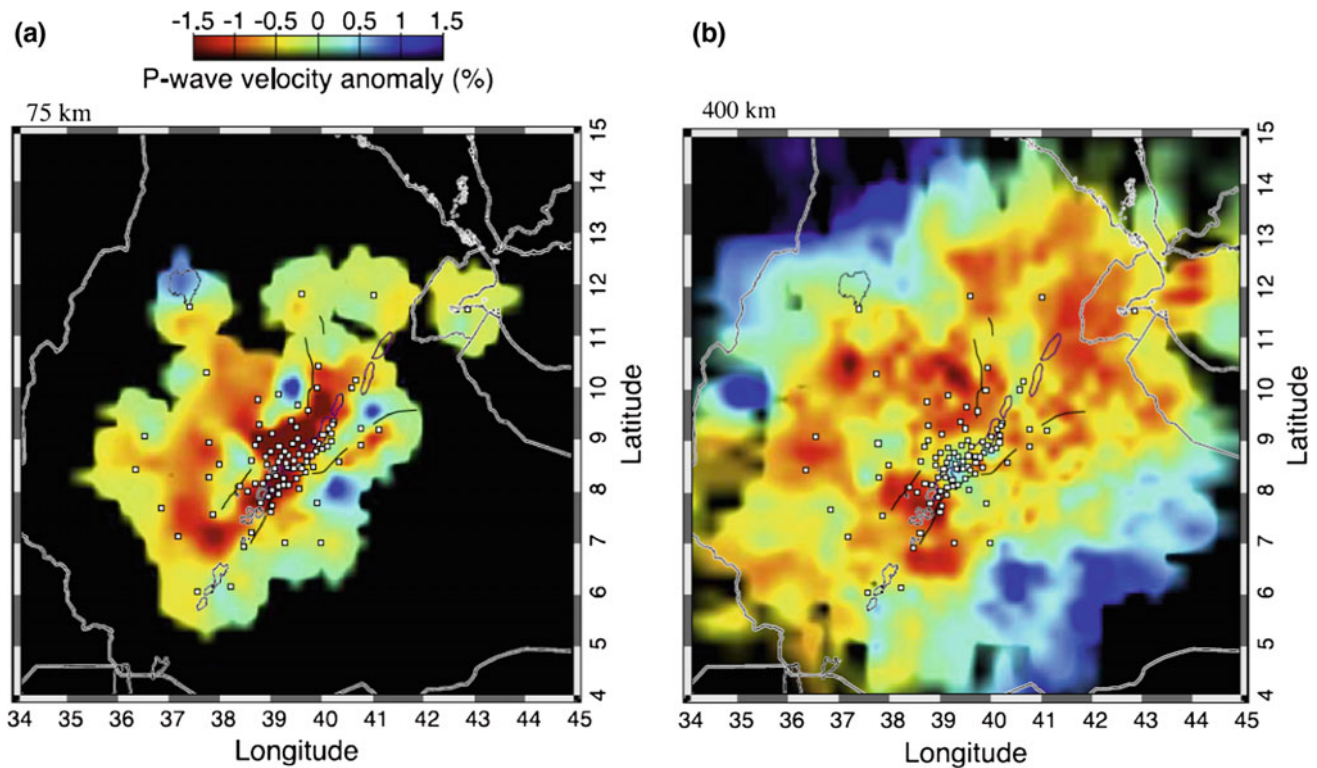


Fig. 3.14 P wave velocity model at 75 and 400 km depth with the location of the stations contributing to the tomographic inversion shown in white squares (from Bastow et al. 2008)

determinant feature of the Afar Rift that better accounts for a simple asthenosphere upwelling and partial melting, similar to what occur elsewhere in the oceanic floor (Fig. 3.15).

3.4 The Afar Triple Junction, a “Textbook Example”?

Afar, where two branches are occupied by the oceanic rifts of the Red Sea and Gulf of Aden, with the East African as a third continental rift branch, is currently taken as a “textbook example” (McKenzie and Morgan 1969; McKenzie et al. 1972) of such a “triple junction”. More precisely, among the numerous theoretical possibilities discussed by these authors, the triple rift “RRR” junctions are common, as rifting along three fractures at 120° is the best way to relieve stresses from uplift at the surface of a sphere (Fig. 3.16). On Earth, stresses similar to these are believed to be caused by the mantle hotspots (or plumes) thought to initiate rifting in continents. The stability of RRR junctions is determined by the fact that the perpendicular bisectors of the sides of a triangle always meet at a single point; the lines ab, bc and ca of a triangle can always be made to meet regardless of relative velocities.

In the case of Afar, which is always taken as an example of RRR triple junctions (and is in fact the only emerged

one), this pattern should result from the impact of a deep mantle plume, hitting the lithosphere and weakening it, allowing for the rifts and plate boundaries to develop.

Hence, several points can be discussed.

1. *The question of the relation of the plume with the triple junction.* Evident at a first sight, it appears less simple when looking at detailed geological data. If global geological thinking holds that bulges are initiated by mantle plumes heating the overlying crust and causing it to expand with fractures created in a pattern of three fracture zones radiating from a point with an angular separation of 120° , the geophysical characteristics of the plume, its location away from central Afar (at the level of lake Tana) and the chronology of the events do not fit at all with this simple model.

Moreover, in itself, the complexity of the plume, the possible existence of two of them and their mere existence do not facilitate the elaboration of a plume-related triple junction.

2. *The question of the relation of the triple junction with the rifts.* In the ideal model, the rifts should initiate at the triple junction centre and progressively propagate along

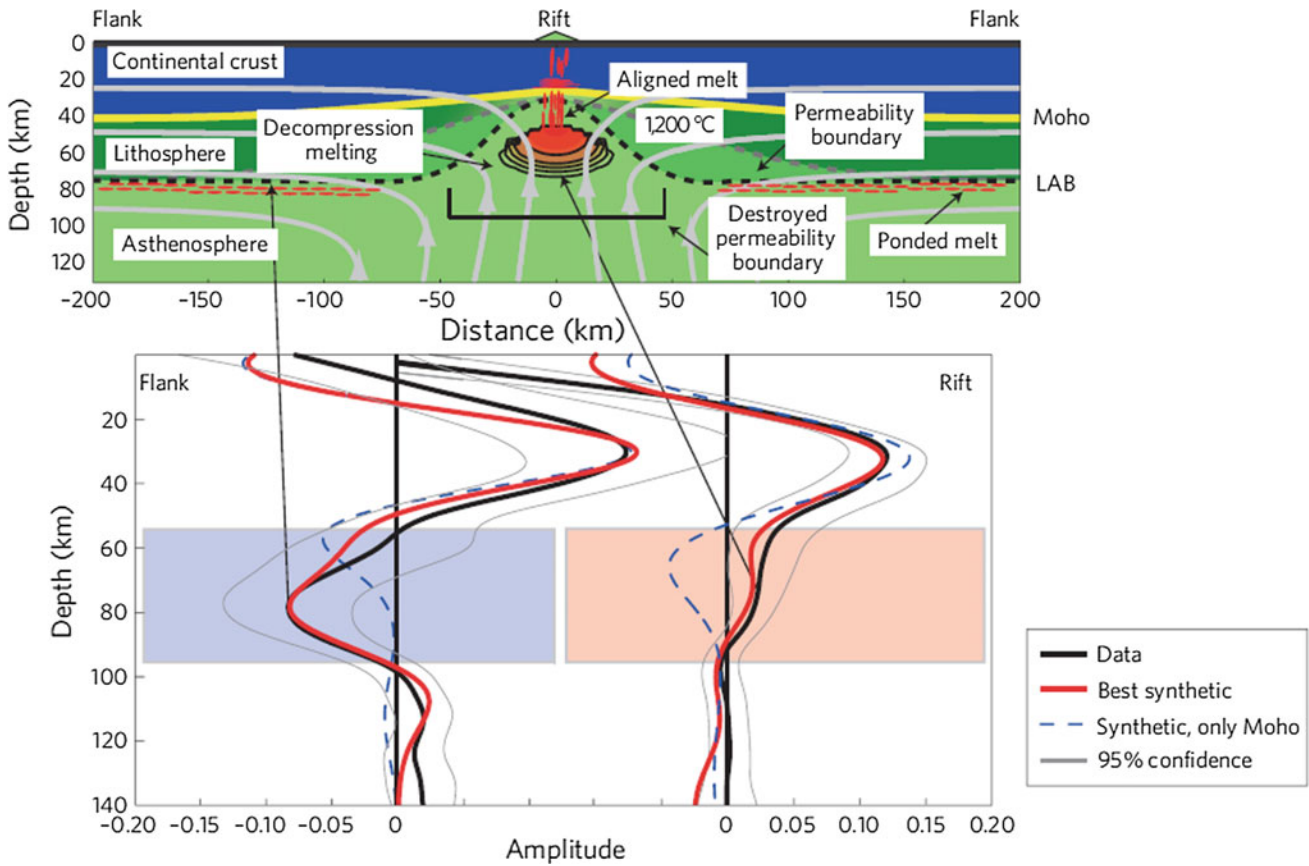


Fig. 3.15 Geodynamic modelling and interpretation of the S to P receiver function data of Afar: Moho (yellow line), flow lines (grey), 1200 °C isotherm (dashed grey line) and interpreted permeability barrier (dashed black line) with underlying melt (red). Melt percentage at 0.2% intervals in the region of decompression melting beneath the

rift is shown for melt volumes 0% (green) to 1% (red). The bottom panel shows the corresponding waveform modelling, with blue dashed line for only Moho discontinuity. Blue and red shaded regions highlight the depth range of interest (Bastow et al. 2008)

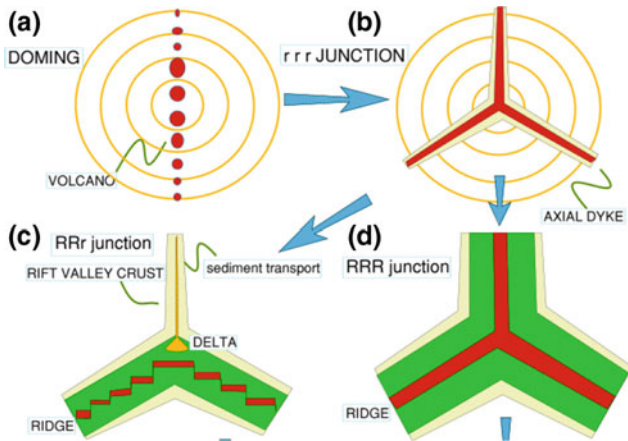


Fig. 3.16 Theoretical schemes of RRR triple junctions and their evolution: A doming, B RRR junction, C oceanic ridges and continental rift valley junction (case of Afar), D triple oceanic ridge junction. (Source <http://www.le.ac.uk/>)

the induced rifts. In fact, the data available from Afar do not fit that well with the model.

We have seen that the East African Rift initiated away from Afar, in the Turkana area, and that the Ethiopian Rift Valley appeared later, after an initial phase of crustal stretching and volcanic activity as early as 45 million years ago (Davidson and Rex 1980, Ebinger et al. 1993), which is even largely before the plume generating the Nubian flood basalts 31 million years ago. Even if real rifting in this area located between the two Ethiopian and Kenyan domes initiated later (20 million years ago according to Pik et al. 2008), it appears that the southern extremity of the MER initiated earlier than its Afar northern extremity. Wolfenden et al. (2004) showed that the northern extremity of the MER initiated 11 million years ago, and deduced that the EARV has propagated northwards over time.

Similarly, the Aden Rift—certainly the oldest of the three as the first discontinuities there appeared since Mesozoic and the rifting was already well developed since early Miocene (i.e. around 45 million years ago) to the east—was shown to have penetrated towards Afar through the Gulf of Tadjourah only in the last 4 million years (Richard and Varet 1979), again the reverse of what would be expected from a diverging triple junction induced by a plume at a triple junction.

As far as the Red Sea is concerned, the situation is rather more complex, as a long phase of crustal stretching and continental rifting preceded the development of the oceanic median trough. It appears that Afar underwent the same evolution, but nothing indicates that the rifting along the Red Sea arm was initiated in Afar and propagated northwards. On the contrary, following Manighetti et al. (2001), several authors reproduced the “Red Sea Propagator” model, implying a north to south penetration of the oceanic spreading in Afar (which does not necessarily fit with the geological data presented in the next chapter).

3. *A non-driving triple junction.* As a whole, the Afar triple junction appear to be the geometric place where these three rifts, with their predetermined geometry, happen to cross rather than the point that initiated the rifting along a 120° angle ideal theoretical pattern.

In the details we see that there have been complex interferences of the three rift systems in the Afar region, with successive phases in which different patterns and relations between the three rift structures prevailed, with no possible identification of a well-defined triple point.

However, despite this complex geological history, it remains that Afar is at present the place where three rifts actually meet, with well-defined boundaries for the three plates: Nubia, Somalia and Arabia. Even the spreading rates of the three plates is now well documented, based not only on models derived from the geometry of the plate margins, geodetic arrays or active axis seismic events (Calais et al. 2006) but also on direct measurements using satellites. Combining GPS with DORIS data, it was possible for Nocquet et al. (2006) to obtain measured values of rifting over a period of 12 years along the East African Rift as well as for the Gulf of Aden and the Red Sea (Fig. 3.17).

Plate tectonic reconstructions show an opening of 250 km along the Sheba Ridge (2.5 cm/year), of 170 km across the central Red Sea (1.7 cm/year) and a strike-slip sinistral motion of 90 km (0.9 cm/year) along the Aquaba-Levant (Bosworth et al. 2005). Using magnetic anomalies from the sea floor, Lemaux et al. (2002) deduced a 23-km opening along the Nubian and Somalia plate over the past 11 million years with a change from NW-SE to E-W

around 3.2 million years ago. This change in extensional stress is consistent with the observed en echelon magmatic axis along the northern MER.

3.5 Geodynamic Relations Between Doming and Rifting Inferred from Petrological Studies

The precise relation between doming, volcanic activity and rifting still needs to be understood fully, and the sequence may differ within the whole rift system. We have seen that early tectonic rifting pre-existed the doming. Volcanic activity started in the central Ethiopian plateau 35 million years ago, long before the Afar and Ethiopian rifting began. This first period of magmatic activity deposited important volumes of flood basalts and rhyolites (500–2000 m thick over very wide surfaces). This trap basalt event was apparently contemporaneous with the uplift of the Ethiopian plateau. Shield volcanoes developed 30–10 million years ago on the Ethiopian plateaus on the top of the trap series with piling of 1000–2000 m of additional material (basalts and differentiated products).

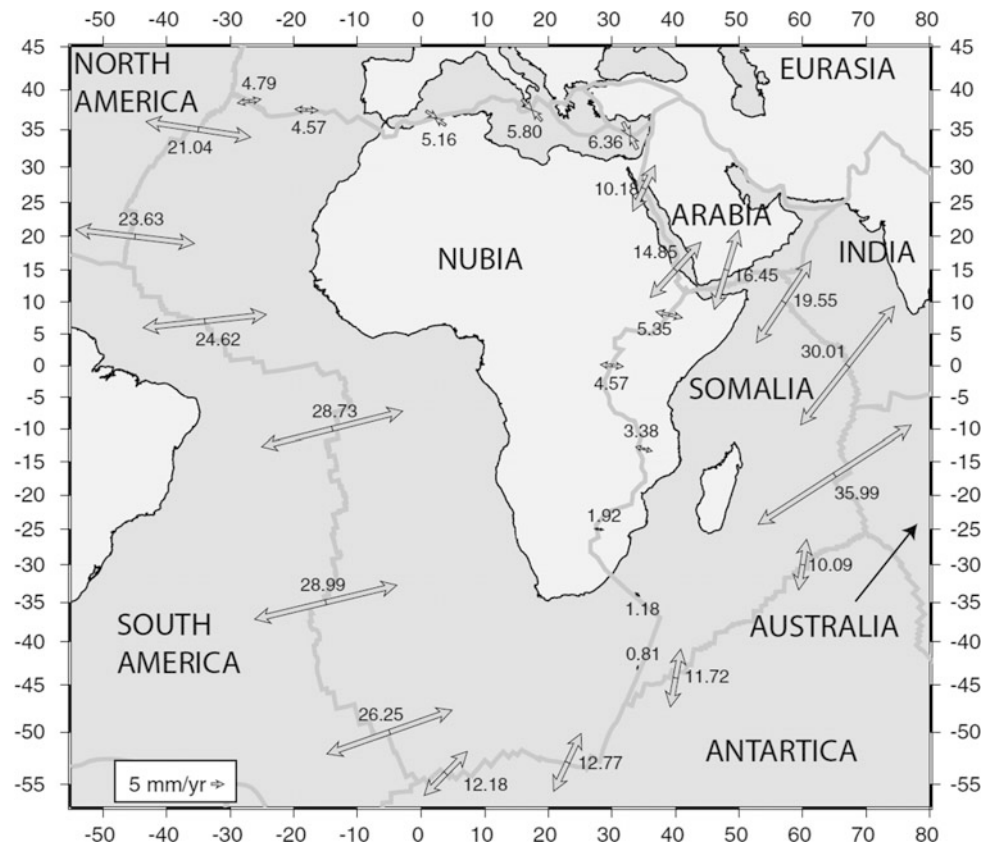
Continental rifting began about 24 million years ago in Afar, 18 million years ago in the south and 11 million years ago in northern parts of the MER, where, from mid-Pleistocene onwards, volcanic activity produced fissure flood basalts associated with a chain of central volcanoes. They now constitute the floor of the Ethiopian Rift throughout its length, dividing it into separate valleys segments.

Several authors tried to use the magmatic characteristics (petrology, geochemistry) of the volcanism to determine the geodynamic relations between doming and rifting initiation and development. Barberi et al. (1979) showed that the nature of the magmas in the whole African rift system, including Afar, appears to be related to both the chronology of the rift development and the geodynamic characteristics of the rifting, in particular the rate of spreading.

On the one hand, with the development of the doming and consequent rifting process, whether in the Kenya or Ethio-Afar region, one can observe that the tendency is for a change from more alkaline lavas (alkali basalts and associated with trachytes and phonolites) at the plateau stage to transitional basalts associated with peralkaline rhyolites (pantellerites) at the continental rift stage, nearly up to tholeiite with associated sub-alkaline rhyolites at the stage of the oceanic floor spreading reached in the axial ranges in Afar.

On the other hand, variation is observed along the whole EARS branch from south to north. Alkali-rich magmas—including carbonatites in Tanzania—associated with abundant

Fig. 3.17 Plate motions obtained from combined GPS and DORIS satellite data over a period of 12 years showing the variation of the plate motions (in mm/year) along the East African Rift Valley, the Red Sea Rift and the Aden ridge (Nocquet et al. 2006)



tephrites and phonolites dominate in the southern part of the EARS, whereas transitional basalts are associated with pantellerites in the Ethiopian Rift, and finally tholeiite-like basalts appear the northern end of the EARS in central Afar.

Of course, this general picture is rather more complex when examining the various portions of the rift and Afar floor in detail:

1. *In Kenya*, the first volcanic events in early Miocene, located along the Kenya–Uganda border, produced nephelinitic central volcanoes, whereas in late Miocene the central rift area was the site of phonolite flood eruptions prior to main doming. The first extensive rifting episodes developed in early to mid-Pliocene produced flood alkali basalts with minor phonolites and trachytes, whereas in late Pliocene, massive eruptions of trachytic ignimbrites occurred in the Naivasha sector. The Gregory Rift developed in mid-Pleistocene accompanied by flood trachytes, followed by the building of central calderas, volcanoes of trachyte, phonolite and sometime rhyolite composition, whereas mildly-alkali basalt fissure eruptions filled part of the rift floor (Williams 1978).

As a whole, the general tendency is for:

- Increasing undersaturation at any time away from the rift axis.
 - Decreasing undersaturation with time with transitional basalts following alkali basalts in the Quaternary along the rift axis (Lippard and Truckle 1978).
 - These evolutions being reflected in both the basalts and associated salic end-products.
2. *In the MER*, fissural mildly-alkali to transitional basalts emitted from an echelon fissures are associated with intermediate products and oversaturated trachytes and peralkali-rhyolites found in central volcanoes. These volcanoes are regularly spaced (55 km) and their position is controlled by transverse tectonics. Volcanism initiated in the early Miocene (30–25 million years ago) and evidence was provided by Barberi et al. (1975) for an initiation of the rifting process around 25 million years ago when peralkaline granites intruded the initial basalts, as observed in Afar. The oldest dates reported in the rift itself from rhyolites outcropping on the inner margins

refer to mid-Miocene (13–10 million years ago), dates which correspond to a first peak of activity. A second peak is observed in Plio-Quaternary (5.5–1.5 million years ago). If alkali undersaturated basalts and associated trachytes and phonolites are reported from the Ethiopian plateau, the whole sequence, up to present day activity, is characterised by transitional basalts associated with peralkaline rhyolites.

3. *In Afar*, where the continental rifting is followed by continental break-up (Barberi et al. 1975; Barberi and Varet 1977, 1978), a two-stage evolution model was identified:
 - A long initial stage of continental stretching and rifting initiated in early Miocene which lasted for about 20 million years, followed by
 - A stage during which continental break-up occurred and the proto-oceanic rift structures were formed (four million years ago to the present).

The continental rifting stages can be studied along Afar margins where Miocene rocks outcrop, showing the early stage characterised by phases of volcanic paroxysms occurring 25–16 million years ago (Adolei flood basalts), 14–10 million years ago (Mabla rhyolites) and 8–6 million years ago the Dalha basalts, overlying the faulted and eroded Mabla rhyolite. These peaks of activity apparently correlate with those observed in the Kenyan and Ethiopian Rifts (Barberi et al. 1982).

The Pliocene to present stage (four million years ago to present) is characterised by massive flood basalt emissions with a tectonic and magmatic behaviour radically different from the rest of the EARV. It starts with the emission of flood basalts of the “stratoid series” emitted in the period four to one million years ago along fissures trending from NNW (in the north) to WNW (in the south) direction (Red Sea and Aden), differing from the NNE trending EARV. Scarce rhyolites occur in the upper part of the series, associated with lavas of intermediate composition mostly related to central volcanoes. These complex stratovolcanoes occur at the intersection of different fracture trends. Basalts are of dominantly transitional nature with rare tendencies for undersaturated (alkali basalts) or oversaturated (tholeiites) magmas. This was interpreted as an early embryonic stage of oceanic rifting in which spreading axes are not yet well stabilised (Barberi and Varet 1977).

In the last one million years, Afar has been characterised by the development of well-defined accreting plate boundaries. Units called “axial ranges” are active volcanic structures built up by recurrent dikeing of basalt along a single central graben with symmetrical flows on both sides, the age of which increases away from the active graben axis. Those ranges are oriented parallel to the regional oceanic regional

trends (i.e. NNW to WNW from north to south, corresponding, respectively, to the Red Sea and Gulf of Aden). Characterised by low K transitional basalts, eventually very similar to oceanic tholeiites, the composition of the lava may evolve when the shield volcano develops towards iron-titanium-rich lavas. Where rifting is slowing, magmas may evolve towards rhyolites, forming cumulo-volcanoes. Slight differences are observed in the initial magma composition from one range to another, or from a volcano to another in a given range. They were shown to result from different degrees of partial melting of the asthenosphere (Treuil and Varet 1973), also reflecting chemical heterogeneities of the primary source (Barberi et al. 1979).

The nature of the magma also depends on the tectonic system to which it relates. Volcanism associated with rift faulting differs from the more alkaline magmatic units developed along transverse structures, as also observed in oceanic environments (Barberi et al. 1974). In northern Afar, these transverse ranges are located in areas offset from the continental margin of the rift, and correspond to offsets of the axial ranges. This means that old structure prevailing in the basement have determined the geometry of the rifting up to the present.

As a whole, along the East Africa Rift Valley we observe a similar situation in both the Kenyan and Ethiopian Rift, even if this is more pronounced in the former. We also note similar timing of the volcanic activity peaking, and a bimodal type of volcanic products.

A striking feature is the magmatic affinity of the basic and salic products in any place in the EARV. Strongly undersaturated phonolites occur in close association with nephelinites and basanites, and the same for trachytes with alkali basalts or peralkaline rhyolites with transitional basalts, and finally sub-alkaline rhyolites with basalts of tholeiitic affinity. The first two occur only in the southern slow spreading rifts, and the last only in Afar. One note that the salic products always correspond to the liquid that would be derived from the initial magma by crystal fractionation. It is striking to note that this also holds in central volcanoes where a complete suite of rocks is found, such as in rift segments in which a bimodal distribution is observed. This speaks for a close genetic relation of these extreme magma types all along the EARV.

Baker et al. (1972) have shown that the time compositional evolution from nephelinites to mildly alkali basalts is explained by an increase in the degree of partial melting of uprising asthenosphere. According to their model, magmas rested in shallow reservoirs formed by dilatation and injection of the crust where they underwent low pressure fractionation, resulting in the huge volumes of salic magmas erupted at the surface. Barberi et al. (1982) extended this model to the whole EARV, showing that block tilting

developed in continental rifts creates elongated traps beneath the rift floor, where basaltic magma differentiates by fractionation, producing residual liquids that are erupted at the surface along fissures created by the following tectonic phase. The silicic liquids may up-rise simply because of their lower density, but the chronology of the events all along the rift speaks in favour of a tectonic origin.

The genetic model of crustal anatexis, presented by some authors to explain the rhyolites in Afar as well as in Ethiopian and Kenyan EARV, is contradicted by the available petrological and geochemical data and fails when considered for the entire area. Of course, processes of contamination by crustal components may occur locally in all continental rifts, as suggested by isotopic data. However, they were shown to be relatively limited and overlapping the dominant crystal fractionation process. Similarly, the hypothesis of partial melting of earlier magmas injected into the crust hits against some difficulties. Of course, if the heat flow is high enough to melt basalts, it would melt the continental silicic crust even more easily, producing silicic magmas in important sectors of continental rifts.

The relation between the volume of erupted magmas and their composition can also be discussed in relation to variations in rate of extension and associated asthenosphere up-rise dynamics. According to this view, the Ethiopian dome was affected right from the beginning by a faster rate of asthenosphere up-rising, inducing a faster rate of extension with the emission of huge amounts of fissural transitional basalts. The lower rate of extension in the Kenya dome and rift links with a slower asthenosphere up-rise, producing strongly alkaline lavas through a lesser degree of partial melting. Further local up-rises of asthenosphere produced volcanic pulses with basalts of lower alkalinity produced by a greater degree of partial melting.

The sequence, observed in Afar (as well as along the EARV, although less complete), represents a progression from incipient melting deep in the upper mantle associated with early uplift, through pervasive shallow partial melting produced by the uplift of the heated zone. The formation of rift fractures controls magmatism, the volume and composition of the initial magma being determined by the opening rates. At rates of less than 1 mm/year there is little or no volcanism (as shown by the western rift). At 1–5 mm/year alkali basalts appear accompanied by large volumes of phonolites. Rates of 5–10 mm/year correlate with large volumes of transitional basalts with peralkaline silicic differentiates. Finally, at rates of 1–2 cm/year, transitional to tholeiitic basalts characterise the Afar floor-spreading axis.

This simple model, where rate of uplift of the asthenosphere and rate of spreading are sufficient to explain all the observed magmatic variations, is consistent with the geophysical data. If broadly efficient to explain the major variations in magmas observed at the surface, it needs to be

confronted with conclusions drawn from geochemical data. Treuil and Varet (1973) showed that the variations observed in the initial basalts of Afar could be explained by a simple variation of degree of melting of an homogeneous asthenosphere source, even if these data and, even more, the isotopic approach show the existence of heterogeneities within the mantle source. Therefore, besides the geodynamic influence of the asthenosphere rise and of the rate of spreading, the heterogeneities of the mantle itself needs to be better understood. That is an approach that the isotopic ratio of radiogenic trace elements such as Pb, Nd and Sr or He can improve.

References

- Avigad B, Gvirtzman Z (2009) Late Neoproterozoic rise and fall of the northern Arabian–Nubian shield: the role of lithospheric mantle delamination and subsequent thermal subsidence. *Tectonophysics* 477(3):217–228
- Ayalew D, Yirgu G (2003) Crustal contribution to the genesis of Ethiopian plateau rhyolitic ignimbrites: basalt and rhyolite geochemical provinciality. *J Geol Soc Lond* 160:47–56
- Baker BH, Mohr PA, Williams LAJ (1972) *Geology of the Eastern Rift System of Africa: Geological Society of America Special Paper* 136, 67p
- Barberi F, Ferrara G, Santacroce R, Treuil M, Varet J (1975) A transitional basalt-pantellerite sequence of fractional crystallisation, the Boina centre (Afar rift, Ethiopia). *J Petrol* 16:22–56
- Barberi F, Santacroce R, Varet J (1974) Peralkaline silicic volcanic rocks of the Afar Depression. *Bull Volcan* 38:755–790
- Barberi F, Santacroce R, Varet J (1982) Chemical aspects of rift magmatism. In: Palmason G (ed) *Continental and oceanic rifts. Geodynamics Ser.8*, pp 223–258
- Barberi F, Varet J (1977) Volcanism in Afar: small-scale plate tectonic implications. *Bull Geol Soc Amer* 88:1251–1266
- Barberi F, Varet J (1978) The Afar rift junction. In: Neuman, Ramberg (eds) *Petrology and geochemistry of continental rifts*, pp 55–69
- Barberi F, Civetta L, Varet J (1979) Sr isotopic composition of Afar volcanics and its implication to mantle evolution. *Earth Planet Sci Lett*
- Bastow ID (2012) Relative arrival-time upper-mantle tomography and the elusive background mean. *Geoph J Internat* 190:1271–1278
- Bastow ID, Keir D (2011) The protracted development of the continent-ocean transition in Afar. *Nat Geosci* 4:248–250
- Bastow ID, Nyblade AA, Stuart GW, Rooney TO, Benoit MH (2008) Upper mantle seismic structure beneath the Ethiopian hot spot: rifting at the edge of the African low-velocity anomaly. *Geochem Geophys Geosyst* 9:12
- Beccaluva L, Bianchini G, Natali C, Siena F (2009) Continental flood basalts and mantle plumes: a case study of the Northern Ethiopia Plateau. www.mantleplumes.org
- Bosworth W, Huchon P, McClay K (2005) The Red Sea and Gulf of Aden Basins. *J African Earth Sci* 43:334–378
- Calais E, Ebinger C, Harnady C, Nocquet JM (2006) Kinematics of the East African rift from GPS and earthquake slip vector data. In: Yirgu G, Ebinger CJ, Maguire PKH (eds) *The Afar Volcanic Province within the East African Rift System. Geol Soc. Spec. Publ* 259:9–22
- Calais E (2016) Le Rift Est Africain, laboratoire de la rupture continentale. *Géosci* 21:36–43

- Chorowicz J (2005) The East African rift system. *J Afr Earth Sci* 43:379–410
- Courtillot V, Jaupart C, Manighetti I, Tapponnier P, Besse J (1999) On causal links between flood basalts and continental breakup. *Earth Planet Sci Lett* 166:177–195
- Davidson A, Rex D (1980) Age of volcanism and rifting in Southwestern Ethiopia. *Nature* 283:657–658
- Davis P, Slack P (2002) The uppermost mantle beneath the Kenya dome and relation to melting, rifting and uplift in East Africa. *Geophys Res Lett* 29(7). doi:10.1029/2001GL013676
- Demissie G (2010) Mantle influence, rifting and magmatism in the East African Rift System (EARS): a regional view of the controls on hydrothermal activity. In: Proceedings world geothermal congress, Bali, Indonesia. pp 25–29 April 2010
- Dirks PHGM, Blenkinsop TG, Jelsma HA (2003) The geological evolution of Africa. *Geology IV. Encyclopedia of the life support system (EOLSS ed. UNESCO)*
- Ebinger C, Sleep N (1998) Cenozoic magmatism throughout East Africa resulting from impact of a single plume. *Nature* 395:788
- Ebinger CJ, Yemane T, WoldeGabriel G, Aronson JL, Walter R C (1993) Late eocene-recent volcanism and faulting in the southern main Ethiopian rift. *J geol Soc Lond* 150:99–108
- Furman T, Bryce JG, Karson J, Iotti A (2004) East African Rift System (EARS) Plume structure: Insights from quaternary mafic lavas of Turkana, Kenya. *J Petrol* 45(5):1069–1088
- Furman T, Bryce J, Rooney T, Hanan B, Yirgu G, Ayalew D (2006) Heads and tails: 30 million years of the Afar plume. In: Yirgu G, Ebinger C, Maguire PKH (eds.), *The Afar volcanic province within the East African Rift System: Geol. Soc. Spec. Publ.*, 259, pp. 95–119
- Gani NDS, Gani MR, Abdelsalam MG (2007) Blue Nile incision on the Ethiopian Plateau: pulsed plateau growth, uplift, and hominid evolution. *GSA Today* 17(9):4–11
- George R, Rogers N (2002) Plume dynamics beneath the African plate inferred from geochemistry of the tertiary basalts of southern Ethiopia. *Contr Mineral Petrol* 144:286–304
- George R, Rogers N, Kelley S (1998) Earliest magmatism in Ethiopia: evidence for two mantle plumes in one flood basalt province. *Geology* 26:923–926
- Hofman C, Courtillot V, Feraud G, Rochette P, Yirgu G, Ketefo E, Pik R (1997) Timing of the Ethiopian flood basalt event and implications for plume birth and global change. *Nature* 389:838–841
- Kieffer B et al (2004) Flood and shield basalts from Ethiopia: magmas from the African Superswell. *J Petrol* 45:793–834
- Lemaux J, Gordon RG, Royer J-Y (2002) The location of the Nubia—Somalia boundary along the Southwest Indian Ridge. *Geology* 30:339–342
- Lippard SJ, Truckle PH (1978) Spatial and temporal variations in basalt geochemistry in the N. Kenya rift. In: Neumann, Ramberg (eds) *Petrology and geochemistry of continental rifts*, D. Reidel Publ. Co, Dordrecht, pp 123–131
- Manighetti I, Tapponnier P, Courtillot V, Gallet Y, Jacques E, Gillot Y (2001) Strain transfer between disconnected, propagating rifts in Afar. *J Geophys Res* 106:13,613–13, 665
- Marty B, Appora I, Barrat JA, Deniel C, Velutini P, Vidal P (1993) He, Ar, Sr, Nd and Pb isotopes in volcanic rocks: evidence for a primitive mantle component constraints on magmatic sources from Afar. *Geochem J* 27:219–228
- McKenzie DP, Morgan WJ (1969) Evolution of triple junctions. *Nature* 224:125–133
- McKenzie DP, Davies D, Molnar P (1972) Plate tectonics of the Red Sea and East Africa. *Nature* 224:125–133
- Moore H, Davidson A (1978) Rift structure in southern Ethiopia. *Tectonophysics* 46:159–173
- Nocquet JM, Willis P, Garcia S (2006) Plate kinematics of Nubia-Somalia using combined DORIS and GPS solutions. *J Geol*
- Pik R, Deniel C, Coulon C, Yirgu G, Hofman C, Ayalew D (1998) The northwestern Ethiopian Plateau flood basalts: classification and spatial distribution of magma types. *J Volc Geoth Res* 81:91–111
- Pik R, Marty B (1999) Isotopic and trace element signatures of Ethiopian flood basalts; evidence for plume-lithosphere interactions. *Geoch Cosmoch Acta* 63:2263–2279
- Pik R, Marty B, Hilton DR (2006) How many mantle plumes in Africa? The geochemical point of view. *Chem Geol* 226:100–114
- Pik R, Marty B, Carignan J, Yirgu G, Ayalew T (2008) Timing of East African rift development in southern Ethiopia: Implication for mantle plume activity and evolution of topography. *Geology* 36(2):167–170
- Richard O, Varet J (1979) Study of the transition from deep oceanic to emerged rift zone: gulf of Tadjoura (Republic of Djibouti). *Int Symp Geodyn Evols, Afro-Arabian System, Roma*
- Ritsema J, Nyblade AA, Owens TJ, Langston CA (1998) Upper mantle seismic velocity structure beneath Tanzania, east Africa: Implications for the stability of cratonic lithosphere. *J Geophys Res* 103:21201–21213
- Ritsema J, van Heijst HJ, Woodhouse JH (1999) Complex shear wave velocity structure beneath Africa and Iceland. *Science* 286:1925–1928
- Rogers N, Macdonald R, Fitton JG, George R, Smith M, Barreiro B (2000) Two mantle plumes beneath the East African rift system: Sr, Nd and Pb isotope evidence from Kenya Rift basalts. *Earth Planet Sci Lett* 176:387–400
- Rooney T, Furman T, Bastow I, Ayalew D, Yirgu G (2007) Lithospheric modification during crustal extension in the main Ethiopian Rift. *J Geophys Res* 112(b10):B10201
- Rychert CA, Hammond JOS, Harmon N, Kendall JM, Ayele A, Belachew M, Stuart G (2012) Volcanism in the Afar Rift sustained by decompression melting with minimal plume influence. *Nat Geosci*
- Schilling J-G (1973) Afar mantle plume: rare earth evidence. *Nature* 242:2–5
- Treuil M, Varet J (1973) Critères volcanologiques, pétrologiques et géochimiques de la genèse et de la différenciation des magmas basaltiques exemple de l'Afar. *Bull Soc Géol France* 7(15):506–540
- Ukstins IA, Renne PR, Wolfenden E, Baker J, Ayalew D, Menzies M (2002) Matching conjugate volcanic rifted margins: $^{40}\text{Ar}/^{39}\text{Ar}$ chronostratigraphy of pre- and syn-rift bimodal flood volcanism in Ethiopia and Yemen. *Earth Planet Sci Lett* 198:289–306
- Varet J (2013) The Afar system and carbonates. *Cocarde workshop (abstract), Sicily*, pp 48–49
- Vetel W (2005) Dynamic of intra-continental extension in magmatic rift context: Turkana Rift (Northern Kenya) from Eocene to Present. *Universite de Bretagne occidentale - Brest*
- Williams LAJ (1978) The volcanological development of the Kenya rift. In: Neumann, Ramberg (ed.) *Petrology and Geochemistry of Continental Rifts*, D. Reidel Publ. Co, Dordrecht, pp. 101–121
- Wolfenden E, Yirgu G, Ebinger C, Ayalew D, Deino A (2004) Evolution of the northern Main Ethiopian rift: birth of a triple junction. *Earth Planet Sci Lett* 224:213–228

Part II

The Early Afar Geological Formations

If the emergence at the surface of a mantle plume generated deep in the Earth's interior at the core-mantle boundary played a role in the genesis and development of the regional doming and later development of the Afar depression, a geologist cannot neglect the earlier characteristics of the lithosphere prevailing in the area.

Similarly, Afar being reported as the place of reference for a triple junction of RRR type, the field geologist has to confront this theoretical model with the geological history of the development of these three rifts in the field.

However, Afar is certainly a place of choice for studying the evolution from the plateau uplift and associated flood basalts of the initial stage to the continental rift developments up to finally the ocean spreading and oceanic crust construction.

We see, in examining the various geological features found in Afar, that we have here the opportunity to observe, through time and space, several examples of these various steps of evolution. Either we see them being developed at present under our eyes or, even better, the opportunity is there to observe them even at depth for the earlier episodes presently visible, thanks to the active nature of the area (tectonics, erosion, etc.) and its desert climate (absence of soil, good outcrops, fresh rocks, etc.).

To proceed in this analysis, we successively recall the knowledge we have of the geological history and present-day phenomena.

We examine more precisely how the early stages of doming and rifting can be depicted from the observations made available from the Afar margins where wide outcrops are present, dissected by faulting and erosion. The first phase of dominantly passive rifting is observed along the foot of the Nubian escarpment north of 12°N, in the Danakil Alps (north of the Bidu—Dubbi transverse structure) and in the Aisha—Ali-Sabieh block. In these three cases the formations are well exposed at various degrees of erosion over a width of more than 50 km and length of several hundred kilometres.

However, let us first recall the characteristics of the geology prevailing before doming and rifting.

4.1 The Afro-Arabian Plate Before Doming and Rifting

The rocks making the basement of the Afar region are exposed along the periphery of the depression. There, rocks are metasediments and intrusives of the late Precambrian orogenic belt which were assembled and metamorphosed from 800 to 650 million years ago during the East African Orogen (Stern 1994). Related to the whole Gondwana tectonic event, it lasted until 450 million years ago and is commonly referred to as the pan-African orogeny, whereas it is actually made of a series of orogenies. It is worth noting that the whole tectonic system (folding and faulting) has a meridional trend which happens to be grossly parallel to the Red Sea and Ethiopian Rifts. The idea that these lines of weakness influenced the trends of the successive tertiary rift is to be considered.

It was shown by Black et al. (1974) that an old regional NNW-SSE trending lineament is parallel to the recent northern Afar volcanic lineaments of Red Sea direction. Ghebreab (1998) and Ghebreab et al. (2002) précised that N-S trending Neoproterozoic shear zones were reactivated by Afar tectonics and Collet et al. (2000) also showed the influence of a variety of ancient structures in the basement in western Afar.

Tazieff et al. (1969) and Barberi et al. (1970) had previously shown that the disposition of the present axis of spreading in northern Afar was determined by the basement geometry, the lines of weakness of which determined the continental break-up. The parallelism between the Erta Ale, the Alayta and the Manda Harraro ranges with the basement discontinuities is a striking feature as seen in Fig. 4.1.

If the proto-Afar Rift did not arise until Mesozoic (Mohr 1975), it is clear—contrary to this author's opinion—that the

Afar early rifting pattern was strongly influenced by the geometry of the ancient basement fabrics of various ages and even by the characteristics of the pre-rift Mesozoic sedimentary cover (Bosworth et al. 2005). Regional basement fabrics dominated by N and NW trending pan-African foliation in the basement gneisses and meta-sediments, NE to ENE trending early Cambrian vertical mafic dikes and N-S fracture zones, as well as WNW to NW trending shear zones (such as the Nadj fault system) all appear to have influenced the early rifting pattern in Afar as well as the present disposition of axial volcanic zones and transverse fractures and associated volcanic units (see Chaps. 8 and 9).

As shown by Bosworth et al. (2005), the Red Sea and Afar Rift expose a variety of remnants of stretched crustal blocks, such as Zabargad Island where granitic gneisses and peridotites are exposed, or the Danakil Alps in Afar. The Affara-Dara block in central northern Afar (seen in Fig. 4.1), although only exposing tertiary magmatic units, belongs in the same category.

The Precambrian basement is covered by a Mesozoic sedimentary sequence that is well exposed along the Ethiopian and Eritrean escarpment as well as in the Danakil Alps and in Yemen. The sequence ranges from Triassic to early Cretaceous and shows a major transgressive-regressive cycle. The thickness varies considerably: it culminates at 4000 m in the Danakil Alps (Bunter et al. 1998; Sagri et al. 1998). The base of the series comprises Adigrat continental sandstones and conglomerates that reach a thickness of 1600 m. It is conformably covered by the Antalo limestone of Bathonian-Tithonian age, reaching a thickness of 2400 m. This marine sequence of shallow environment with numerous cycles of sea-level changes is overlain by fluvial sandstones of the Amba-Aradom formation, of late Jurassic early Cretaceous age, reaching a thickness of 500 m (Merla et al. 1979). The Makale graben, trending WNW, shows a spectacular sequence of this marine Jurassic limestone, now karstified, that predates this Cretaceous continental detritic event.

As shown by Black et al. (1974), the Makale graben indicates that extensive conditions prevailed in the Afro-Arabian plate at this early time. A discovery, since confirmed by several observations, notably in Arabia and Somalia (Bosellini et al. 1997; Leroy et al. 2004), showed that the plume did not induce the extension (see discussion in Sect. 3.3). The dominantly N-S trending Neoproterozoic shear zones as well as NNW-SSE lineaments referred to as Marda faults (Black et al. 1974) could have determined the trends of the tertiary rifting that reactivated the lines of weakness in the Afro-Arabian continent in north-western Afar (Ghebream 1998; Ghebream et al. 2002; Collet et al. 2000).

These late Cretaceous sandstones are eventually contemporaneous with the first basalt eruption of the plateau that

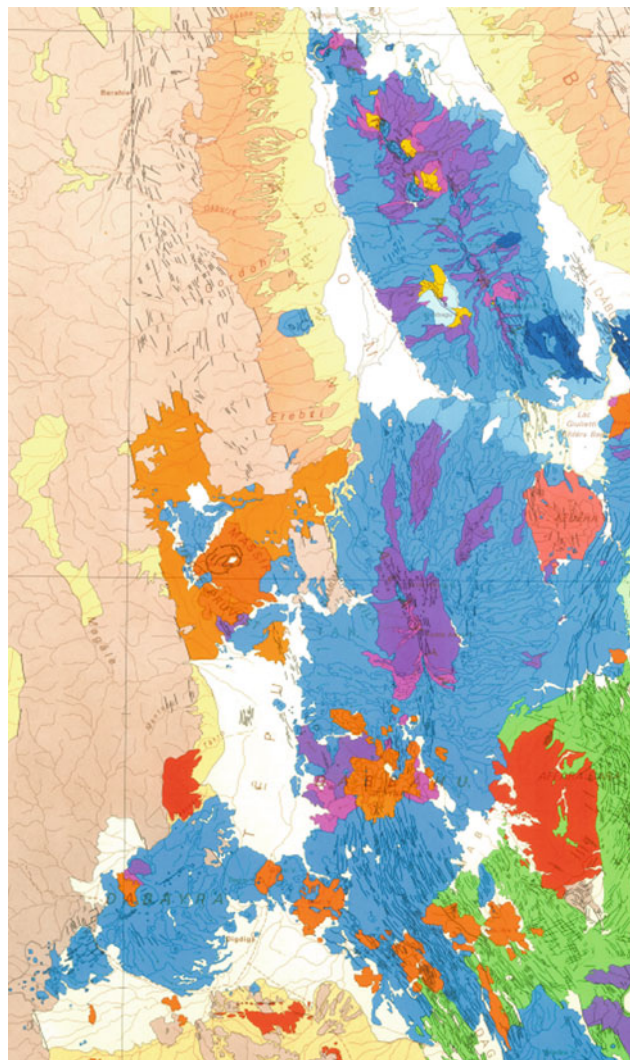


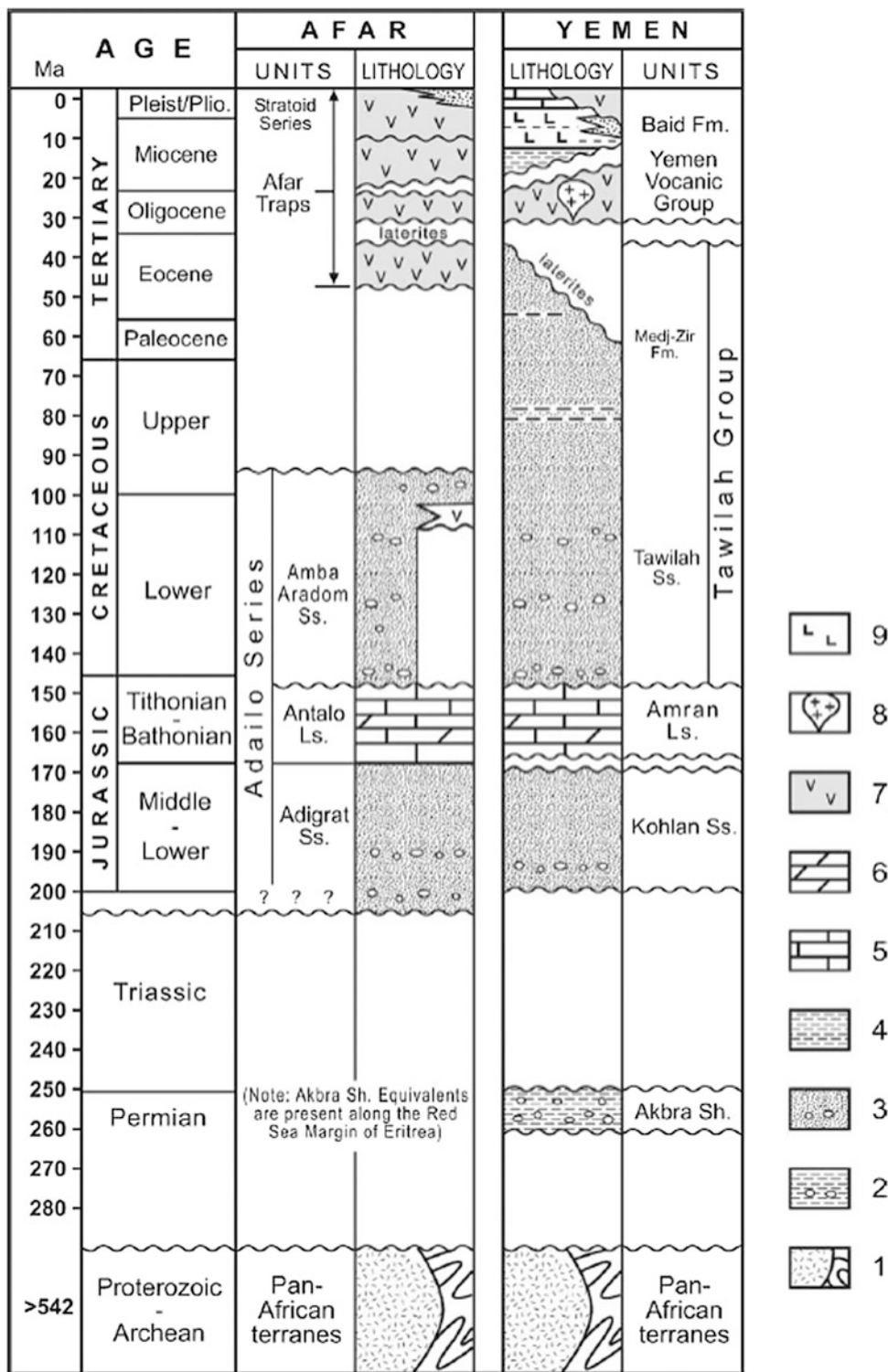
Fig. 4.1 Extract from the geological map of northern Afar (CNR-CNRS 1973) showing the lower limit of the Nubian escarpment. It displays a discontinuous pattern with dominant NNW faulting cut by NE trending transverse structures. Both correspond to directions of weakness prevailing in the basement. The axial ranges of Erta Ale, Alayta and Manda-Harraro show a disposition that clearly replicates these basements discontinuities

otherwise cover the Mesozoic sequence. Canuti et al. (1972) described alkali basalts interbedded with the Amba Aradom sandstones in the Amhar mountains on the SW margin of Afar. This can be interpreted as resulting from the fact that the whole pre-Mesozoic formations were undergoing erosion—and hence eventually the Ethiopian dome began its uplift—when the first emissions of the trap basalts of the plateaus started, and that erosion, continental sedimentation and basaltic emission were contemporaneous.

Figure 4.2 provides a generalised stratigraphy of Afar and surrounding areas including Yemen (Bosworth et al. 2005).

Makale graben presents striking analogies with similar features that are observed elsewhere in the surrounding

Fig. 4.2 Simplified stratigraphic sections of the Afar margins in Ethiopia and Eritrea and of nearby Yemen. 1 Crystalline basement (Panafrikan); 2 Pebbly mudstone (Yemen); 3 Sandstone and conglomerate; 4 Shale; 5 Late Jurassic limestone; 6 Dolomite; 7 Volcanic series; 8 Peralkaline granitic intrusives; 9 Evaporites (from Bosworth et al. 2005)



pre-Tertiary units, particularly on both sides of the Gulf of Aden and in the Nubian platform.

In the last few years, with the discovery of oil in this early distensive environment affecting the Nubian platform in Sudan, more attention has been paid to the late Mesozoic to

early Tertiary graben existing in the Afar surroundings. These are purely sedimentary grabens clearly pre-dating the Afar doming and rifting. Along the coast of the Gulf of Aden they are well expressed and clearly transverse to the rift structure. They are also well developed in Sudan.

Of Jurassic age in Aden and of Cretaceous age in Sudan and Kenya, they strikingly trend NW-SE, that is, parallel to large parts of the more recent southern Afar tectonics (Fig. 4.3).



Fig. 4.3 Schematic map of East-Africa and southern Arabia (Yemen) showing the location of the various rifts as well as oil exploration and production blocks. Permian basins (Somalian plateau and Madagascar coasts), Jurassic WNW trending grabens of N Somalia and Yemen, NW to NNW trending cretaceous oil bearing grabens in Sudan, with its

extension through Kenya. The tertiary rifts or the East African Rift Valley (western and eastern branches) are drawn in orange. Grabens presently subject to oil exploration in Ethiopia, Uganda and Kenya are drawn in dark green (*source* Africa Oil Corp 2012)

4.2 Geology of the Plateau Margins Surrounding Afar

The pre-rift geological units include the Neoproterozoic crystalline basement and its Mesozoic sedimentary cover, plus the early tertiary volcanics of the plateau. These units are exposed at the periphery of the Afar depression and in the surrounding plateau escarpments, and a more detailed description is of use to understand the early stage of Afar Rift development.

This early stage can be considered as a step of dominantly “passive rifting”, despite the fact that magmatic bodies, synchronous of this first stage of rifting, are frequently found associated with the normal faulting.

4.2.1 The Nubian Margin

We have seen that the Neoproterozoic basement consists of metamorphic units dating from 800 to 650 million years ago belonging to the Mozambique belt, as well as products of the pan-African orogeny formed until 450 million years ago. North from Afar, these show similar lithologies, well exposed along the margins of the Red Sea on both sides. In northern Afar, it consists mainly of greenstones, with various plutonic intrusions (Fig. 4.4).

This crystalline basement is covered by the Adailo sedimentary sequence ranging from Triassic to early Cretaceous. The base of the section is made of conglomerates and sandstones, dominantly continental, called Adigrat sandstones,



Fig. 4.4 Intrusion in the greenstone basement covered by the Adigrat sandstone at the bottom of the escarpment in the Makale-Dallol section (Photo Varet 2013)

locally reaching a thickness of 1600 m. The Antalo marine limestone of Bathonian to Tithonian ages reaches a maximum thickness of 2400 m there, whereas the Amba Aradom sandstones, a continental unit of early Cretaceous age, ends the sedimentary sequence.

Triassic sandstone (Figs. 4.5 and 4.6) and Jurassic limestone (Figs. 4.7 and 4.8), well exposed in the Makale basin, form the crest of the Ethiopian scarp over northern Afar, are also observed over a width of 50 km, deeply faulted and tilted, dipping westward down to the escarpment foothills in contact with the post-rift sediments of the depression.

A lateral graben is frequently present between the foot of the Ethiopian escarpment and the depression proper. These areas are suitable for agricultural development as groundwater resources fed by the short rivers eroding the plateau is found in the detrital formation filling these grabens.

Two types of extensive faulting are observed, as shown by Black et al. (Fig. 4.9). Both ensure a crustal stretching developed as the answer to the extension in the Red Sea direction.

All along the cross section—between the main escarpment fault and the Tertiary and Quaternary deposits of the depression in that 50 km-wide area which also belongs to

Afar—the dip of the faulted blocks progressively increases from west to east (Figs. 4.10 and 4.11).

At the same time, the amount of basaltic intrusions of Early Miocene age also increase while approaching the depression (Figs. 4.12 and 4.13). As a consequence, the tilted blocks may become dominantly basaltic along the lowest blocks of the Afar margin. This tendency increases from north to south along the northern part of the Nubian plate margin.

Southwards, the crystalline basement and its Mesozoic cover disappears (south of 13°N) under the basaltic cover of the trap series of the Ethiopian plateau. A major unconformity marks this important change that shows quite different characteristics in both the plateau and the Afar escarpment. This trap series could have covered a surface of at least one million km² on the Nubian plateau only, and it also extends—discontinued by more recent faulting and diking—underneath the Afar depression. Its thickness which presently reaches 2 km on the plateau may have been up to 4 km here. Although it is difficult to make quantitative measurements, it is clear that the thickness of this basaltic cover increase from north to south and from west to east along the Afar margin.



Fig. 4.5 View of the Adigrat sandstones north of Makale (Photo Varet 2013)



Fig. 4.6 Coptic church dug in the Adigrat sandstones north of Makale (Photo Varet 2013)

This trap series is mainly made of basalts, but ignimbrites and tuffs or rhyolitic compositions are observed in the upper part of the sequence. Basalts are dominantly tholeiitic to transitional in composition. On the Nubian plateau, trachyte and phonolite domes and sills are also observed intersecting the trap series in association with late alkali basaltic sequences. However, surrounding Afar, faulted plateau basalts are generally of transitional composition.

Detrital episodes were also noticed. Of Eocene and Oligocene age and called Ashangi basalts in Afar, their precise dating is still under discussion as the oldest flows are quite altered.

Whereas older ages were published, up to 45 million years ago, it appears that the main trap sequence dates back to 32 million years ago for the bottom of the exposed sequence up to 25 million years ago at the top, as reported in the Desie-Batie section by Ukstins et al. (2002).

South of 13°N, no pre-Tertiary formation is visible and only volcanic rocks are present along the Afar margin. As shown by Black et al. (1972), the tectonic style exhibits

eastwards dipping blocks separated by antithetic faults (downthrown side of faults away from the Afar depression). This zone of tilted blocks, exposed over a width that may exceed 50 km, is separated from the Ethiopian plateau to the west by a narrow but well-developed marginal graben, between 10 and 30 km across, whose floor is generally several hundreds of metres higher than the Afar floor. Bedding and normal faults intersect at angles close to 90° and bedding ranges from 25° to 40° eastward, and up to 60°. This differs from situations observed in northern and southern Afar where normal faulting with downthrown side of faults towards the depression are observed (Fig. 4.9). Both mechanisms of “bookshelf faulting”, however, are interpreted as expressions of crustal thinning (Black et al. 1972), and were later considered as typical for so-called “passive” margins tectonics, although here the abundance of magmatic intrusions and even the volcanic nature of the faulted material is rather characteristics of active margins.

There have been discussions among geologists on whether the tilting of the blocks resulted from curving fault



Fig. 4.7 View of the Jurassic limestone sequence south of Makale along the main fault scarp bordering the Danakil depression (*Photo Varet 2005*)



Fig. 4.8 Hamlet near to the escarpment, south of Makale, with “dry rock” walls built from Jurassic limestone (*Photo Varet 2005*)

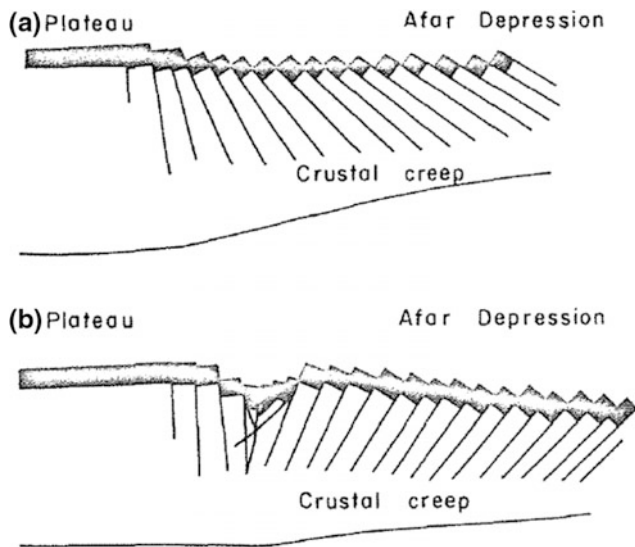


Fig. 4.9 Two models for crustal attenuation with block faulting and tilting in the upper crustal layer: **a** synthetic faulted margin; **b** antithetic faulted margin (after Black et al. 1972)

planes, the blocks sliding and rotating under the influence of gravity as lateral support was removed during crustal extension. Black et al. (1972) rather attributed the block tilting to plastic deformation of the lower crust and upper mantle associated with steep vertical fault planes dividing the upper crust into series of fault blocks that progressively tilt sideways as does a row of books on a shelf, as in crystal deformations.

4.2.2 The Arabian Margin

The Arabian margin is also marked by an important escarpment running along the coast of Yemen and Arabia over more than 1000 km. Called “the Great Escarpment”, it rises abruptly from near sea level (up to 200 m) to more than 1000 m in Arabia and more than 2000 m in Yemen, reaching 3660 m at Jebel Nabi Shuyab (Fig. 4.14). The sequence includes:



Fig. 4.10 Slightly tilted Mesozoic sediments intruded by Miocene basalts (deeply weathered) near to the foot of the main Ethiopian escarpment (Photo Varet 2014)



Fig. 4.11 At the bottom of the escarpment, while approaching the great salt plain, the basement formation and its Mesozoic cover is affected by normal faults of Red Sea direction (NNE) and blocks are tilted with the Mesozoic sedimentary sequence dipping west. The

strongly tilted block is surrounded by tertiary detrital sediments. (Photograph taken from the Makale-Dallol road, looking north by Varet 2013)

- A Neoproterozoic basement, with units similar to those found on the Nubian side of the Red Sea, including Precambrian gneisses and younger units corresponding to successive episodes of the pan-African orogeny ranging from 900 to 550 million years old (Genna et al. 2002).
- A sedimentary sequence including at the base shales and conglomerates of Permian age, not exceeding 120 m thickness, covered by the continental Kholan sandstones reaching 150 m, passing to Jurassic Amran limestones of 410–520 m thickness, and covered by a sandstone sequence 150–400 m thick called the Tawilah group, reported as late Jurassic to Eocene.

As a whole, the section appears to be quite similar to the Nubian sequence, although of lesser thickness.

Also similar to the Nubian side, the sedimentary sequence ends with a continental erosive episode, characterised by lateritic weathering, before the deposition of the overlying Oligocene trap series of Arabia (so-called “old harrats”) and Yemen. The Yemeni volcanic group includes basalts and

silicic ignimbrites dating from 31 to 26 million years ago (Ukstins et al. 2002).

At the level of Afar, the eastern part of the Great Escarpment in Yemen is characterised by intensive normal faulting and block tilting. Massive alkali granite intrusion occurs, as in Afar, outcropping along the escarpment and inland. They date from 21 million years ago (Huchon et al. 1991), that is, a little younger than their Afar equivalent.

4.2.3 The Somalian Margin

The crystalline basement exposed in the SE margin of Afar is similar to that exposed in the Nubian and Arabian margins, confirming the geological unity of the area before the plate split. These are Archean and Proterozoic units amalgamated by the Neoproterozoic pan-African orogenies. As in the other parts described above, the basement surface emerged and eroded before the Trias detrital formation (Adigrat conglomerates and sandstones) deposited. It was



Fig. 4.12 Spectacular basaltic intrusions of Miocene age (*brown*) in the Mesozoic sediments (*pale*), combining both sills and dykes, in the middle part of the stretched western Afar margin. This shows that,

southwards, the crustal extension is more and more accommodated by magma injection (*Photo* Varet 2014)

then covered by the Jurassic limestone and marls in middle to upper Jurassic. The Mesozoic sedimentary sequence also ends with fluvial sandstones lying uncomfortably on the earlier strata. This upper continental unit, similar to those found in Nubia and Arabia, passes progressively to calcareous deposits along the Gulf of Aden to the east, showing the spreading of the Indian Ocean during Cretaceous.

Near Dire Dawa, the Precambrian metamorphics are horizontally overlain by thin Mesozoic sandstones followed by about 400 m of Jurassic limestones and a variable thickness of upper sandstone locally exceeding 300 m. This sedimentary sequence is followed unconformably with basalts of the trap series, up to 1000 m thick, thinning and dying out in northern Somalia. Along the Afar margin of the Somali plateau, these are cut by normal faults striking E-W and ENE-WSW. The faulted zone affected by this normal faulting is at least 20 km wide. Blocks dip southwards at angles ranging from 10° to 30°, with a downthrown side of

faults towards the Afar depression and an increase of dip angles northwards (Fig. 4.15).

Further east, along the Gulf of Aden margins, the area was affected by late Mesozoic rifting with the formation of asymmetric grabens of WNW-ESE orientation. This phase of extension, which also corresponds to the separation of Madagascar from the African plate, is observed in many places in East-Africa (Guiraud and Bosworth 2005). It was reactivated in the late Tertiary and contributed to determining the geometry of the initial break-up of south-eastern Afar and the whole Gulf of Aden.

The age of initiation of the rifting in south-eastern Afar and the Gulf of Aden has been shown to occur in mid-Oligocene, around 30 million years ago, showing that the earliest regional extension for the Gulf of Aden continental rift segment of initial Afar breaking was N20°E, that is, oblique to the N70°E of the Gulf (Bosworth et al. 2005).



Fig. 4.13 A set of thin basaltic dikes intruded in the Mesozoic sediments along the western Afar margin (*photo* Varet 2014)

This appears as the earliest rifting stage that affected the region, pre-dating the Red Sea rifting which initiated 25 million years ago and the Ethiopian Rift Valley which initiated even later.

4.2.4 The “Danakil Alps” (or Arrata)

The “Danakil Alps”—an area called Arrata in the Afar language—extend in SE Eritrea all along the Red Sea over a width of around 100 km and from the Bure Peninsula which is the northern extremity of Afar southwards up to the transverse volcanic unit of Bidu-Nabro-Dubbi. This mountain of moderate relief (generally a few hundred metres high) consists of a continental sequence including the basement and its mesozoic sedimentary cover. Between the latitudes 13°30' and 14°30'N, the topography is more prominent and summits reach more than 1000 m above sea level. This unit is deeply faulted and eroded, and well exposed because of the arid climate. We have seen that it is in the Danakil Alps that the Mesozoic cover is the thickest, the sediments thinning towards the east on the Nubian plateau and west on the Arabian plateau. This shows that the area acted as a basin before the uplift and break-up of the Afro-Arabian continent. Towards the north, the pre-Mesozoic basement is less elevated and covered by more recent volcanic units. This is also probably the case underneath and to the south of the Bidu-Nabro-Dubbi axis, although no basement or Mesozoic sediment was ever found, neither at the surface nor as inclusion in the numerous scoria cones that carry various

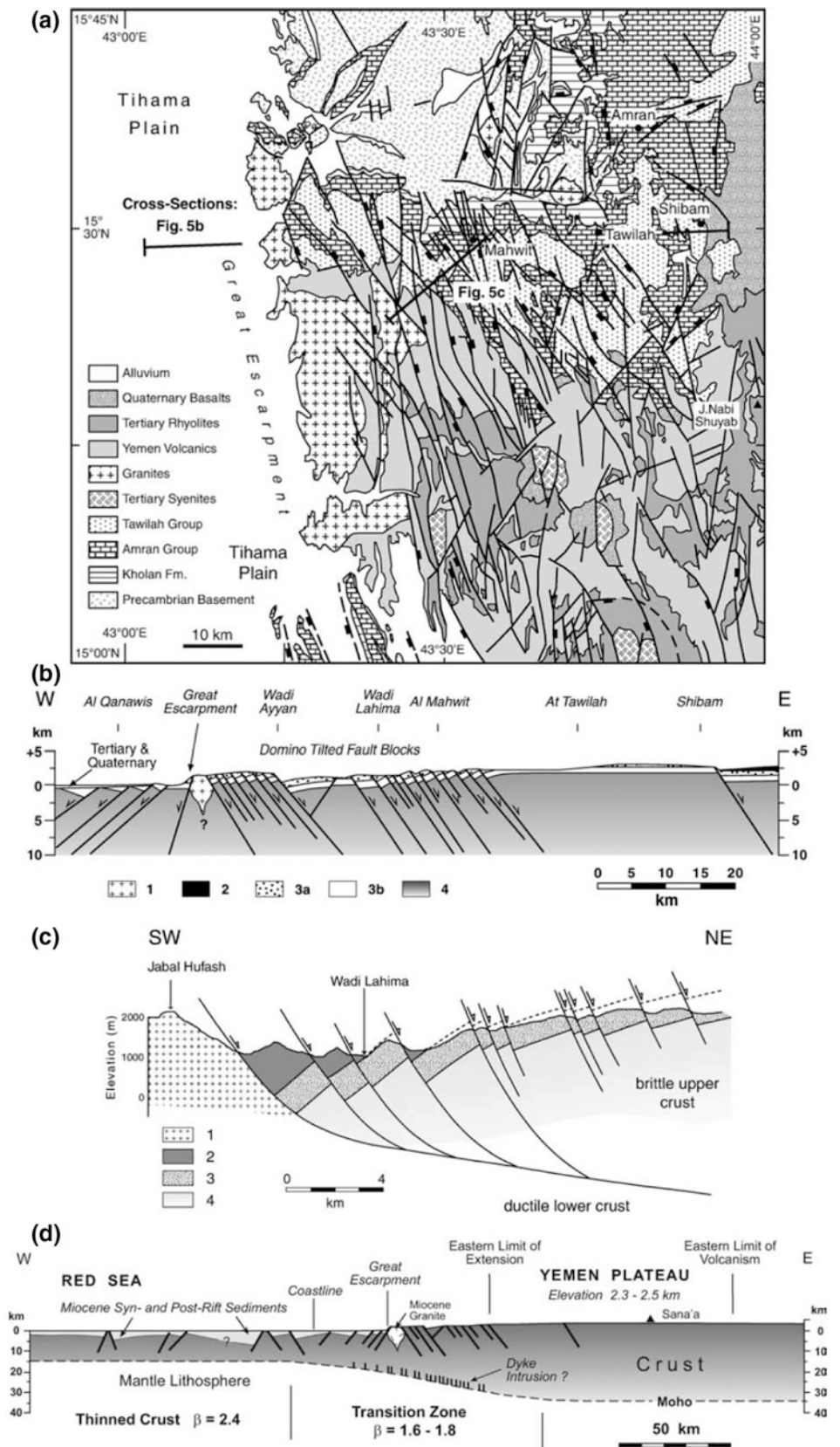
other inclusions, all of mafic or ultramafic composition in the Assab transverse alignments (De Fino et al. 1973, 1978).

Despite the fact that the area south of these transverse volcanic units is unfaulted and hence appears geographically as the southern extension of the Danakil Alps, it clearly displays a quite different geology, with volcanic products only. Therefore, contrary to most interpretations showing a rotating Danakil microplate extending south to the Gulf of Tadjourah, we do not consider that it extends south of the Dubbi-Bidu transverse structure. Judging from its extension across the Red Sea (at the level of the Hanish-Zukur Islands) and on both continents, this major transverse discontinuity appears as a fracture zone as discussed above.

The normal faulting is of NNE-SSW (Red Sea) direction with faults generally dipping towards the east, whereas the sedimentary blocks are tilted towards the west, so that the Mesozoic cover is almost comfortably covered by the Tertiary red series despite the strong erosion that prevailed as a consequence of the Afar Rift opening. These characteristics have inclined a few authors (Holwerda and Hutchinson 1968; Hutchinson and Engels 1970; Beyth 1991) to consider Afar as being a “half-graben” when the Red Sea was a real one (Fig. 4.16).

However, in cross section, the Danakil Alps appear asymmetric, cut by intense normal faulting on the Afar side with its gentler slope facing the Red Sea (Fig. 4.17). The whole tectonic unit appears to have undergone an eastwards tilting, which is clearly expressed in the geomorphological features, in particular the water drainage. Whereas the divide between the Red Sea and the Afar endoreic basin runs

Fig. 4.14 Geological map and section of the Arabian border of Afar (SW Yemen). 1 Miocene granite; 2 Oligocene volcanics; 3a Cretaceous Tawilah sandstones; 3b Jurassic limestones and sandstones; 4 Crystalline basement from Bosworth et al. (2005)



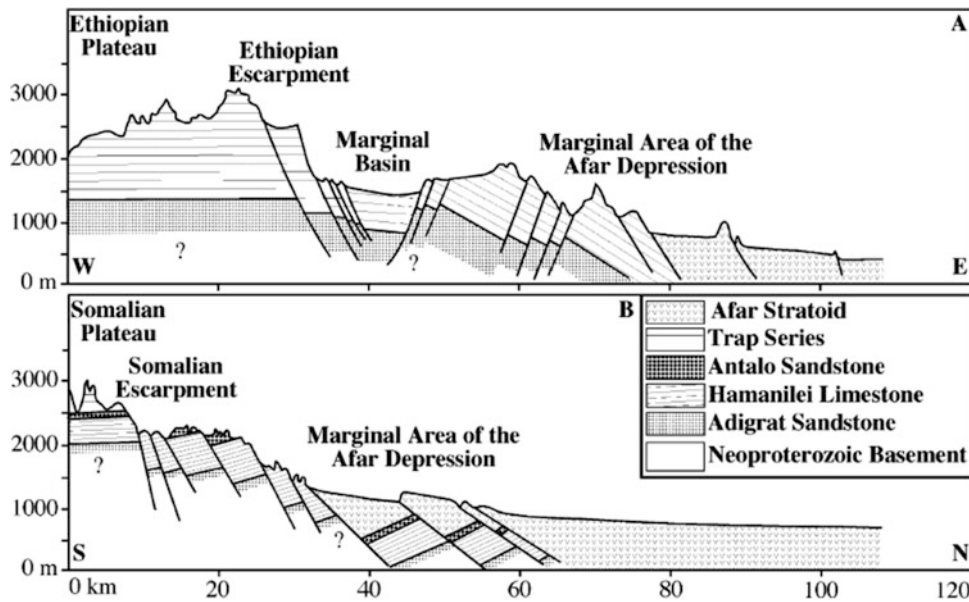


Fig. 4.15 Stylized geological sections illustrating the two kind of tectonics along the Nubian (*upper section*) and Somalian (*lower section*) escarpments, according to Beyene and Abdelsalam (2005). Note that if marginal graben are frequently present, the tectonic style

can be rather more complex. As observed in Fig. 4.11, the faults are dipping towards the depression and the blocks are dipping towards the plateau (as in the *lower figure*) in the lowest compartments along the western margin in Northern Afar

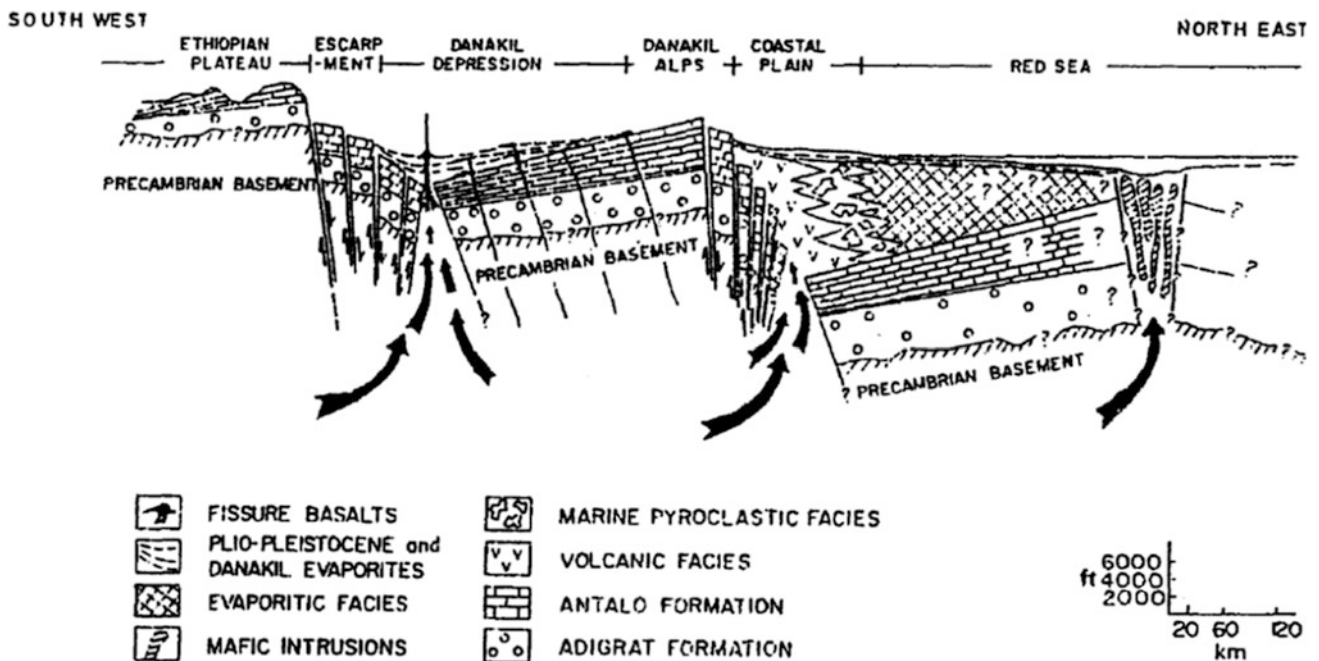


Fig. 4.16 Cross section of the Danakil Alps according to Holwerda and Hutchinson (1968) and Hutchinson and Engels (1970). According to this interpretation, Afar is a marginal half-graben of the Red Sea Rift

parallel to the direction of the range, careful examination shows that the divide migrated eastwards as a result of capture of the western drainage net. Rivers of the eastern slope show extensive alluvial deposits close to their heads, resulting from the beheading by the western hydrographic

net. The more active tectonic behaviour of the Afar side of the Danakil Alps is also expressed by the straight fault-line scarp contrasting with its sinuous limit along the Red Sea coastal plain (see Fig. 4.17). The erosion features, with steep valley walls on the depression side developed at the expense

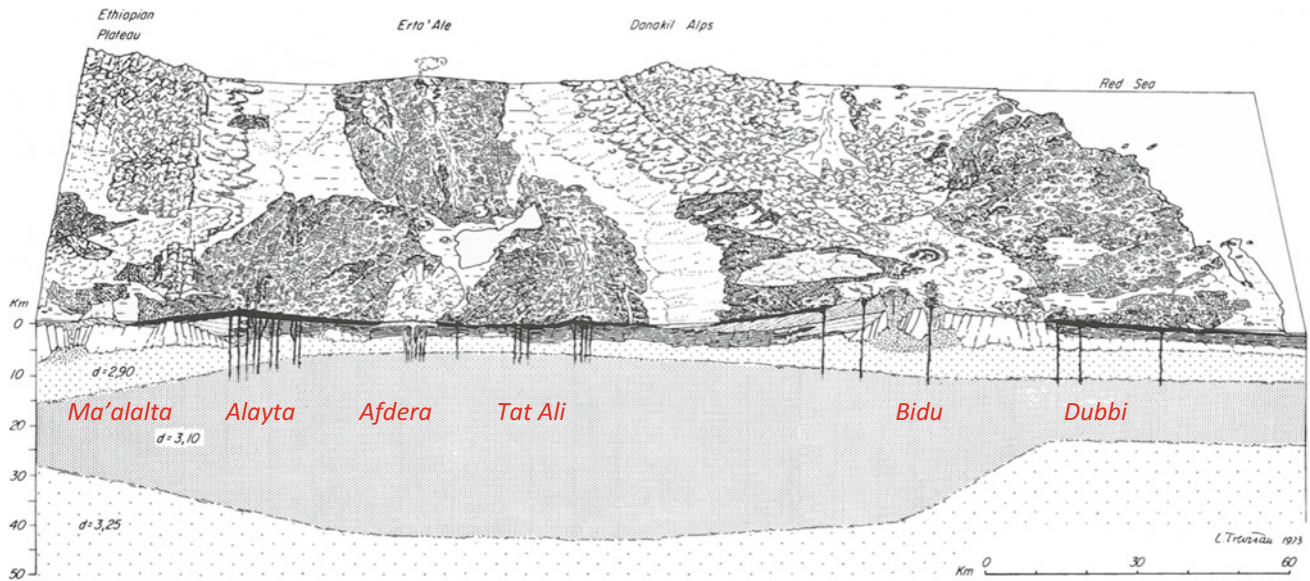


Fig. 4.17 Geological block diagram of northern Afar with a cross section at the southern extremity of the Danakil Alps (Barberi et al. 1973). The two co-existing and active axial ranges of Alayta and Tat Ali lie to the south of Erta Ale range. Both cover the earlier lavas of Afdera volcano topping the strataoid series, now extinct. This is also the level at which the western (Nubian) escarpment is shifted leaving the

place for M'alalta lateral volcanic centre, whereas the Danakil block is cut by a series of silicic central volcanic centres and associated transverse fissural basalts of Bidu-Dubbi linking the Afar Rift with the Red Sea Rift through the Hanish Island transverse structure. (In CNR-CNRS 1973, drawing by C. Trevisan)

of the eastern ones, also show the active nature of the Afar Rift contrasting with a rather inactive Red Sea rift.

In this interpretation, the Danakil Alps and the foot of the Ethiopian escarpment are both areas where the initial stages of continental stretching can be symmetrically studied. In both cases one can observe that if normal block faulting and tilting of the basement accommodated most of the extension in the north, the amount of magma injection increases towards south, with dominantly basaltic dikes and sills. Peralkaline granite intrusions are observed around 13°N in a transition zone where crystalline basement and its Mesozoic cover disappear and the only outcropping formations are basalt. Hence, the initial rifting displays contrasting behaviour from rather "passive" north of 13°N to "active" in central and southern Afar.

4.2.5 The Aisha—Ali-Sabieh Block

The Aisha Ali-Sabieh region is considered to be the south-eastern limit of the Afar depression. With an average altitude of 600 m, it marks the divide between the Gulf of Aden and the Afar depression. It is also the political boundary between Ethiopia, Djibouti and Somalia, where higher altitudes are reached (Mt. Arrey, 1289 m and Mt. Degweyn, 1025 m). This area, called "Aisha horst" from its Somali name, is made of outcropping Precambrian basement, intensively faulted, together with its Mesozoic

sedimentary cover (limestones and sandstones), themselves covered by trap basalts. In the southern part, the trap basalts are covered by rhyolite flows and welded tuffs. The metamorphic basement is outcropping in the southern part in Ethiopia and Somalia, but is not visible to the north in Djibouti.

It is quite similar to what is observed to the west of it, at the foot of the Afar Somali escarpment, with block tilting at angles of 20–40°, except that the normal faulting is trending NNW and N-S with bedding tilted to the west. Throws may reach 1000 m locally. Between the Aisha area and the western Afar Somali escarpment, a left lateral wrench fault striking NE locally causes dragging for distances up to 3 km from the fault plane (Fig. 4.18). To the north in the Ali-Sabieh area (Djibouti Republic), the normal faulting is also well expressed with similar direction (NNW to N-S), and downthrows are usually westerly with fault blocks dipping 20–50° eastwards. These normal faults, perpendicular to bedding, occur at intervals of 0.5–2 km and often have rather similar throws, up to a few hundred metres, reaching locally 1000 m. As a consequence, the same stratigraphic succession tends to be repeated in successive tilted blocks. Around Dire Dawa the succession basement-Jurassic limestone is repeated whereas in Ali-Sabieh and Dawanle the repetition of limestone-upper sandstone is observed, with sandstones representing 80% of the surface. Both block faulting and tilting clearly result from extension tectonics (Black et al. 1972).

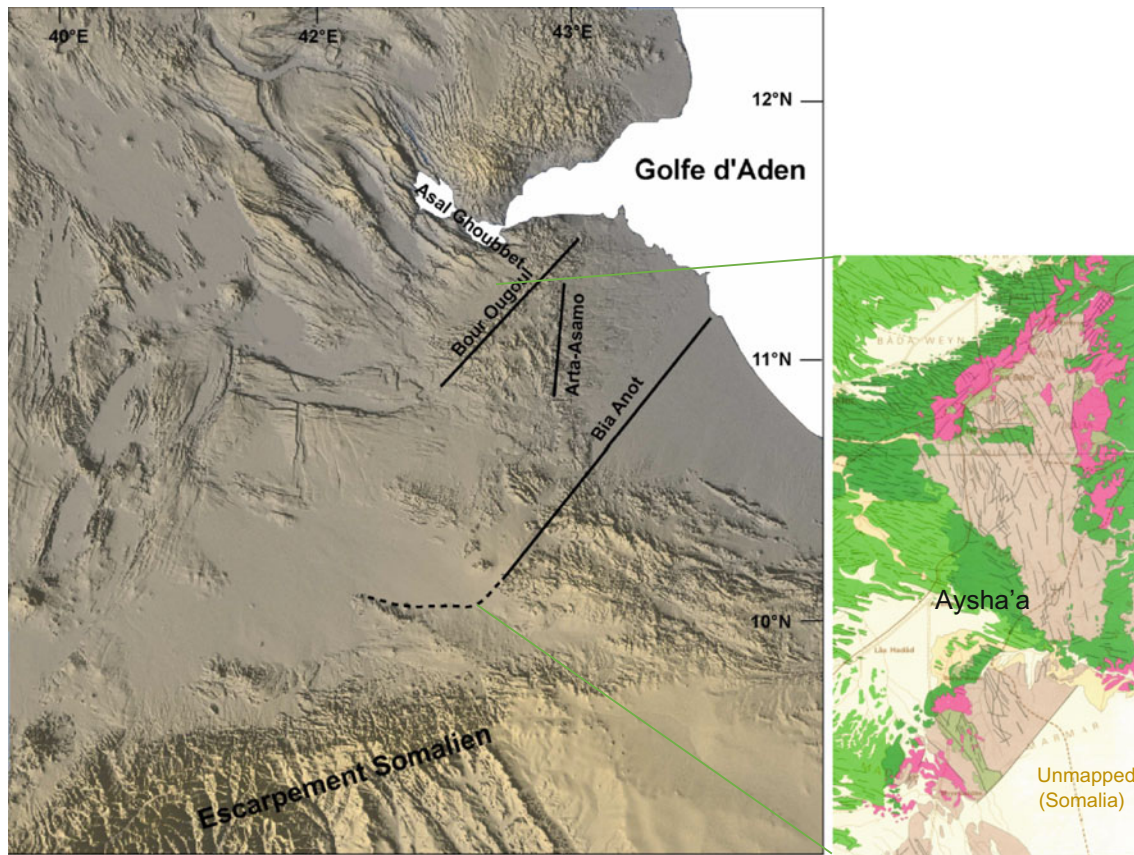


Fig. 4.18 The Aysha'a area marking the south-eastern limit of the Afar depression, seen from satellite imagery (from Daoud 2008, with geology from Varet 1978). Pre-rift formations (metamorphic basement, Mesozoic sedimentary cover and trap basalts of the plateaus) in *pale brown* are deeply faulted in a N-S to NNW direction and are partly

covered by rhyolites (*red*) and basalts (*green*). Basalts are unfaulted to the east (northern Somalia), whereas to the west (Afar) they are affected by E-W to WNW-ESE normal faults parallel to the Gulf of Tadjourah. Sharp discontinuities trending NE-SW observed north and south are interpreted as southern extensions of fracture zones of the Gulf of Aden

The NE-striking wrench fault runs parallel to the transform faults in the Gulf of Aden, which is also the case for the lineament marking the north-western limit of the block, which could also be regarded as the southern continuation of a similar transform structure in the Gulf of Tadjourah.

The block faulting and tilting of the pre-Tertiary units (Fig. 4.19) were followed by basaltic and rhyolitic injections of Miocene age with dikes running parallel with the same extensive tectonic direction (NNW to N-S).

These volcanic products include dikes, flows, domes, ignimbrites and tuffs of peralkaline rhyolitic compositions, frequently aphanitic. They are themselves faulted and tilted by NNW-trending faults, and are eventually covered to the north by later basaltic flows after a period of erosion.

This Miocene volcanic sequence displays analogies with what is observed south on the Somali escarpment and also north of the Gulf of Tadjourah, with the major difference that in the north neither the Mesozoic sedimentary sequence nor the metamorphic basement are ever observed.

As a consequence, as shown by Black et al. (1972), far from being a more or less rigid horst of unbroken crustal material, this region should be interpreted as a zone of attenuated sialic crust, which represents the early stage of spreading of the Afar Rift system, representative of parts of the early Afar floor. It shows analogies with the Danakil Alps, but the gap in between (absence of sialic crust outcrop over a distance of 300 km) is still unexplained.

The sedimentary sequence was studied in detail (BRGM and ORSTOM mapping for ISERST 1986; Daoud for CERD 2008) in the Ali-Sabieh area (Djibouti Republic, Fig. 4.20) and includes:

- Jurassic limestones:
 - Massive pyrite-rich limestone (90 m thick at least; Oxfordian?)
 - Massive fossiliferous limestone with ammonites (middle Kimmeridgian) reaching 200 m thick



Fig. 4.19 View of the Mesozoic limestones and sandstones in Ali Sabieh area. These units are deeply faulted, tilted and intruded by basalt and rhyolite dikes (Photo Varet 2014)

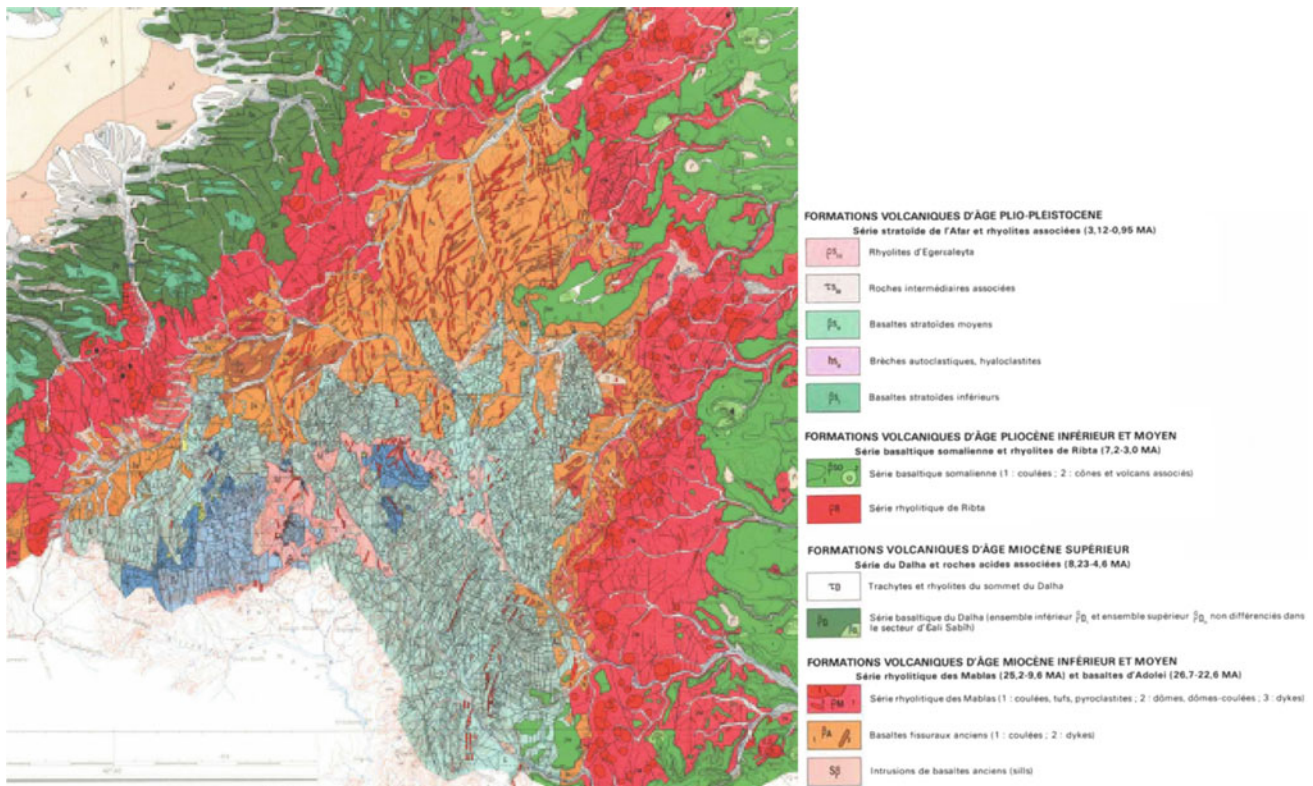


Fig. 4.20 Detailed geological map of the Ali Sabieh region (Republic of Djibouti, 1/100,000 scale, ORSTOM, 1986) showing the densely faulted (dominantly NNW) Mesozoic sandstones (blue) and limestones (grey) in a “window” of Miocene rhyolites. The eastern limit, covered

by the Somali basalts is trending N-S whereas the NW limit is marked by a NW discontinuity that is in continuation with the transform faults of the Gulf of Tadjourah

- Compact limestones representative of a marine platform (120 m)
- Calcareous marls, gypsiferous marls and dolomites, with a marine fauna (190 m)
- Sandstones:
 - Covering the gypsiferous marls a sequence of sandstones is observed, containing sandstone intercalations, 40 m thick
 - The Ali-Sabieh sandstones, covering most of the surface along the ethio-djibouti boundary; they are of continental fluvialite, contain mainly quartz, and, despite being azoic, are considered as marking the limit jurassic-cretaceous
 - As the limestones, the sandstones are injected by numerous basaltic dikes

4.3 The Miocene Peralkaline Granite Intrusions of Afar

Strikingly, three outcrops of tertiary peralkaline granites (Fig. 4.21) have been described (Bannert et al. 1970; Barberi et al. 1972) on both sides of the Afar depression along the Nubian lowest margin (the Limmo massif; Fig. 4.22), in the Danakil Alps (the Dioita massif) and in central Afar (the Affara Dara massif). These granites display clear intrusive contacts with the Precambrian basement (Limmo), the Jurassic limestones (Dioita at Asa Ali and Iddamo) or the old trap basalt (Affara Dara), with metamorphic contacts showing calcium silicate hornfels. At Dioita, this granite (dated 21.8 million years ago) is itself cut by NNW trending normal faults and intruded by dikes dated 19 million years ago (De Fino et al. 1978).

The structural pattern of these units would require further specific studies to understand their relation eventually (where they were initially part of the same geological unit, later dismantled by rifting?). At Affara Dara (Figs. 4.23 and 4.24) they are affected by early WNW-ESE and NNE-SSW tectonics. Would this indicate a MER and Gulf of Aden influence predating the Red Sea early rifting? The WNW trend also corresponds to the Cretaceous rifting (see Sect. 4.1 and Fig. 4.3).

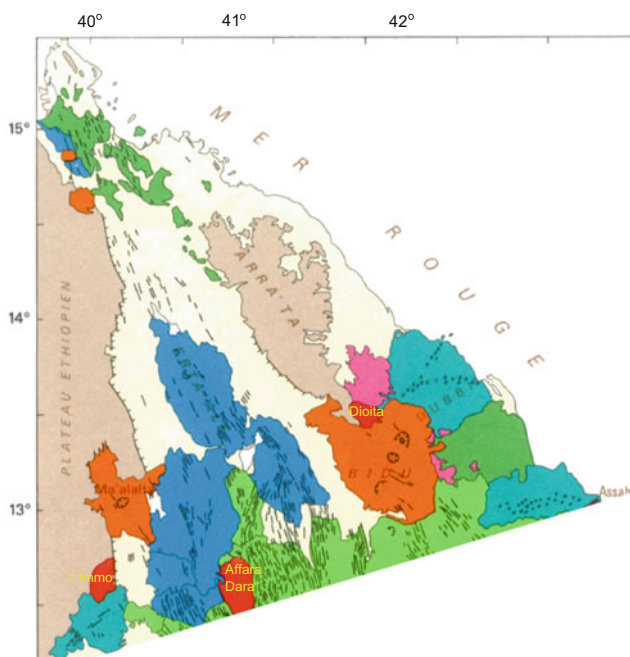


Fig. 4.21 Geological sketch map of northern Afar showing the location of the major Miocene peralkaline granitic bodies (in red). Pre-Miocene basement in grey, axial ranges in bright blue, stratoid series in green, lateral rhyolitic centres (in orange) and transverse basaltic ranges (in pale blue). Mabla rhyolites (pink) and Dalha basalts (dark green) are also shown

Although displaying an apparent alignment transverse to the rift, they are all affected by later NNW-SSE normal faulting. All display very similar ages, ranging from 26 to 22 million years, and have been considered by Barberi et al. (1972) as the first magmatic event clearly related to the initiation of the Afar Rift. More generally, peralkaline granite is known to occur at the initial stage of continental spreading (Black et al. 1972).

Other smaller bodies occur further south along the Nubian scarp at Sallu Adu, Watalis and Asa Magidayto, associated with microgranites, quartz porphyritic rhyolites or aplites. They are well developed at Iddamo and Watalis where three dikes of ENE direction intruded the old trap basalts. Chessex et al. (1975) also reported microgranites and aplites further south in the Aisha area (Somalia), dated to 22–18 million years ago.

The disposition of these intrusions at the same level across the Afar floor as well as the direction of some of the dikes indicate a genesis along lines of weakness transverse to the direction of rifting, that is, an association with fracture zones at their initial stage of development. However, although granitic, these intrusions should not be regarded as of sialic crustal origin. Their petrology indicates that they originate from basaltic magmas of mantle source, as confirmed by their geochemistry, in particular their low Sr isotopic ratio (Barberi et al. 1974).

They can be considered as the eroded, near-surface expression of important magma chambers that developed at the initial stage of doming and rifting, where basalts would differentiate producing these intrusions at the apex of very large plutonic bodies (or body?). Expressions of the deeper part, such magma bodies may be found in the peridotite and gabbroic inclusions expelled along the transverse basaltic ranges along the Afar borders (such as Ado Ale range near Assab; see Sect. 5.4.2).

The relationship between these various plutonic events and their geodynamic significance still need to be elucidated. Could they testify to the effect of an early Afar mantle plume?

On the basis of these observations, Barberi et al. (1972) proposed a Miocene age for the initiation of the Afar Rift, that is, 22–25 million years ago, as it corresponds to both the age of the top of the trap series as well as that same age obtained for these three intrusions of alkali granites. In the Affara-Dara massif the deeply faulted and weathered trap basalts of the plateau are clearly intruded by the peralkaline granite (Fig. 4.23). This outcrop appears as a relict block dismantled from an earlier magmatic unit that preceded the drift and rotation of the Danakil Alps. The tectonic pattern—both concentric and radial—of the normal faulting surrounding Affara Dara supports this interpretation (Fig. 4.24).

Let us state here that the position of these granitic bodies also corresponds to a change in the geological characteristics



Fig. 4.22 The Limmo granite intruded in the tilted plateau basalts seen from its western side along a road being built to link Yalo and Abala along the lower part of the Nubian escarpment (*Photo Varet 2016*)

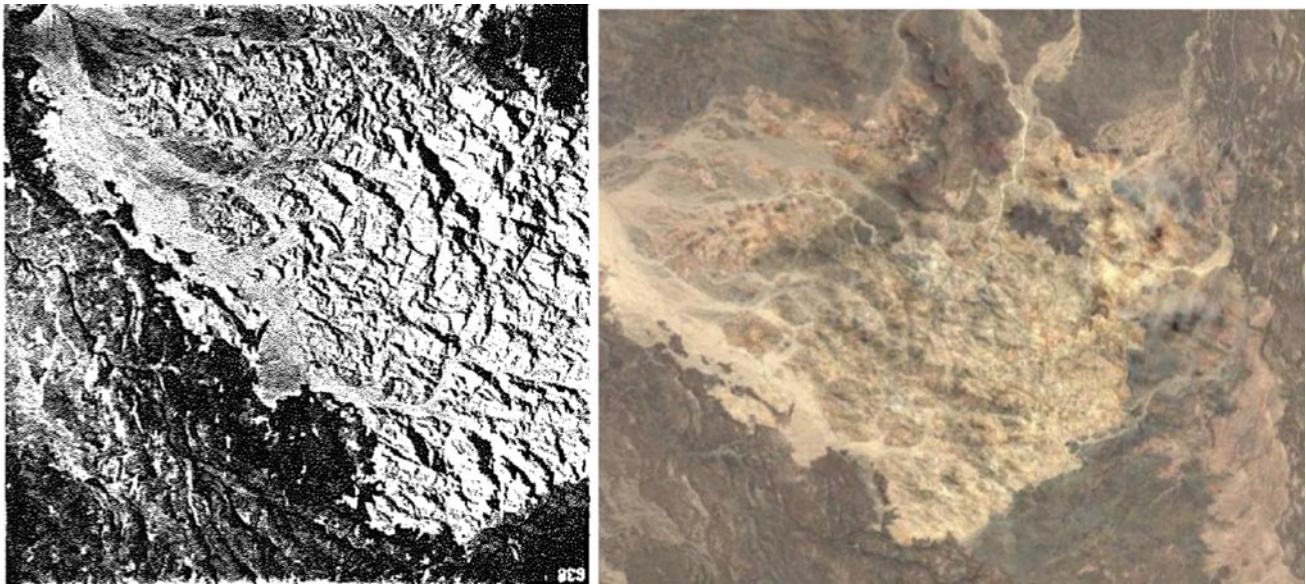


Fig. 4.23 Air photograph showing details of the Affara Dara granitic body (*white*) affected by WNW-ESE and NNE-SSW tectonics, intruded in older trap basalts and covered in discordance by the faulted stratoid series

of the Afar depression around 13°N , both in the central part and along the margins. In the Afar floor it marks the development over a large width of the stratoid series, which is less developed northwards. Along the margins it also corresponds on both sides with the disappearance of the pre-Mesozoic units, replaced by the faulted magmatic products of the Nubian plateau.

It should be noted that the pattern of the silicic centres of the upper part of the stratoid series—particularly well developed in the surroundings of Affara Dara—apparently reflect at least a structural relation and eventually even a genetic relation between the older deep magma body and the development of these fairly recent silicic centres (Fig. 4.24).

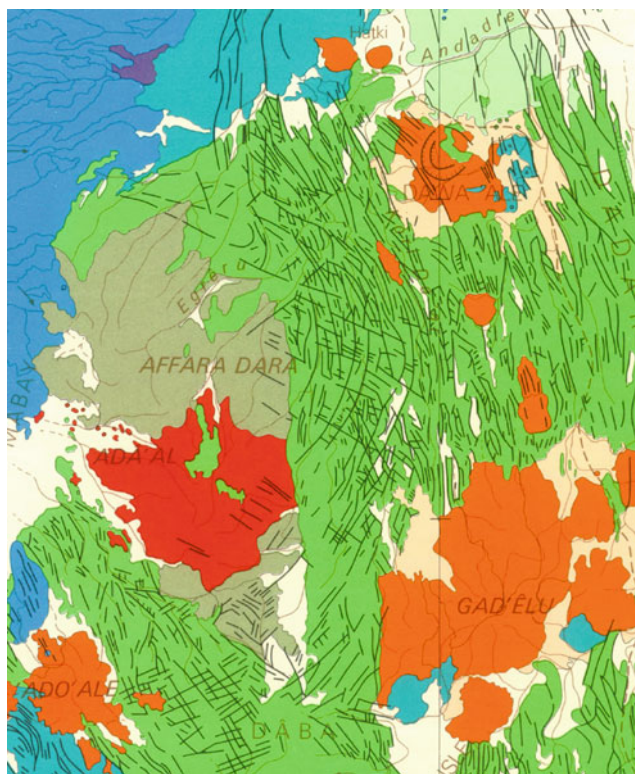


Fig. 4.24 Geological map of the Affara Dara massif in central Afar, south of the Alayta and Afdera basaltic lava fields. It appears as a relict made of trap basalts of the plateau (*grey-green*) deeply faulted, weathered and intruded by a peralkaline granite massif dating from 25 million years ago. Observe the fault pattern around the massif that indicates a mole that resisted the continuous extensive tectonics affecting the stratoid series (in *bright green*). The location of the silicic centres of the top of the stratoid series (*orange*) apparently relates to this peripheral tectonics

Even the Red Sea margin expresses this change around 13°N. The area located 70–100 km inland in Africa along the Red Sea, and marking the eastern border of Afar south of the Danakil Alps (south of Bidu-Dubbi and Assab transverse volcanic ranges), is considered by most authors (since Mckenzie et al. 1972) to be part of the “Danakil block”, and is drawn on most plate tectonic schemes as a single lithospheric unit (Danakil rotating microplate or “biolette” for Sichel 1980). However, it was shown by Marinelli and Varet (1973) that the geology and significance of this area differ greatly from the Danakil Alps. Affected by intense magmatic activity 20–8 million years ago, but stabilised since, it rather appears at present as a westernmost accretion of the Arabic plate.

4.4 The Mio-Pliocene “Polychromatic Formation”

The pre-Miocene units—metamorphic basement, Mesozoic sedimentary cover and trap basalts of the plateaus—have been intensively dissected by erosion since the early stages of rifting that marked the formation of the Afar depression 24 million years ago. As a result, a huge amount of detrital sediment accumulated in the Afar margins and floor over the whole history of the development of the Afar Rift. The process, continuing today, is a complex sequence of erosion, sedimentation and faulting that is now observed along the bottom of the escarpments, all around Afar and more precisely along the eastern foot of the Nubian plateau, the northern foot of the Somalian plateaus as well as along the western foot of the Danakil Alps. This unit is called the “red series”.

It should be noted that if this units outcrops along these Afar margins, it certainly extends at depth within the depression beneath the more recent sedimentary and volcanic cover. We can also infer that beneath the Afar floor the thinnest particles (clays, carbonates, etc.) as well as the marine, lacustrine and evaporitic interbedded sequences replace the more clastic and coarse layers currently observed along the escarpment foothills.

The polychromatic formation of the Mio-Pliocene age form a 20 km-wide band that outcrops symmetrically over 250 km in northern Afar, bordering the base of the Ethiopian escarpment as well as the periphery of the Danakil Alps. This series is transgressive on the faulted, tilted and eroded Mesozoic limestones and sandstones, their basaltic cover when present and Precambrian epi-metamorphic basement. This dominantly detrital formation seems rather complex as it was affected by several tectonic episodes, with normal faults generally looking towards the depression, and tilting of the blocks with dips increasing with depth, reaching up to 25° (Fig. 4.25).

As a whole, the formation is seen on a thickness of several hundred metres, and may even be several thousand metres thick when hidden under the recent dominantly evaporitic cover in northern Afar. It is made essentially of detrital sediments, with alternating coarse and thin sandstones, sands, red-green or polychromatic clays, with intercalations and intrusions of generally altered basalts (mainly submarine, with hyaloclastites and pillow-lavas) and some silicic volcanics. Gypsum is also observed in some of the clays and sands layers, which confirm the evaporitic context of these continental deposits.



Fig. 4.25 View of the polychromatic formation on the western flank of the northern Afar depression, at the foot of the Ethiopian escarpment (visible in the background). It is clearly made of several sub-units, successively faulted and eroded (*Photo* Varet 2003)

No fossil was found in this geological unit, the whole sequence of which—variable from north to south along the rift margin as shown by CNR-CNRS Afar Team (1973)—could not be subdivided in the map. Some of the volcanic products deliver unaltered lavas or minerals allowing for radiometric age determinations. Bannert et al. (1970) obtained ages ranging from lower Miocene to lower Pliocene from intercalated basalt flows, but a clear picture of the major events having determined this—probably discontinuous—sequence is still lacking at present. The oldest age obtained for a basaltic flow at the bottom of the series east of Lake Afrera (southern foot of the Danakil Alps) is 24 million years (Bannert et al. 1970), which constrains the age of the initiation of the Afar Rift in the 22–25 million years interval, as it also corresponds with the ages of the basalts of the plateaus and the ages of the intrusive peralkaline granites.

The rather symmetrical disposition of this geological unit on both sides of the northern part of the Afar depression (as shown in Fig. 4.26), with the recent axial volcanic ranges along the line of symmetry, indicates that the rifting process was rather simple and regular in this part of Afar, with a long phase of continental rifting lasting from Miocene to Pleistocene and a rather recent phase of an oceanic type of rifting (less than one million years ago).

It should be noted that this polychromatic formation is quite similar to what is described—to the north of Afar—as the “Red Series” on both sides of the Red Sea. However, we observe that south of the Buri peninsula (13°30'N), it is present on the Afar side of the Danakil Alps and not on the Red Sea side. This shows that northern Afar has really been

part of the Red Sea rift system ever since the earliest phase of opening of the Red Sea rift, even if the marine invasion apparently only developed in the Pleistocene as shown by K/Ar ages obtained in the deepest reached potash deposits (88,000 years according to Hutchinson, reported in CNR-CNRS 1973), as well as the marine reefs deposits (200,000–80,000 years ago).

We should emphasise that, further south, in central or southern Afar, this polychromatic formation is not observed, showing a different early history in the other parts of Afar. This difference is certainly linked to the fact that volcanic activity dominated all over the area in the same period, hiding—and eventually replacing—this continental erosion and sedimentation event.

However, because of the lack of outcrop or deep drilling, if we have no evidence for similar occurrences of intense continental erosion followed by marine invasion in Afar south from 12°30', we cannot exclude the possibility that events occurred that are now masked by more recent volcanic products and sedimentary fillings.

4.5 The Adolei Basalts

This unit was defined in the North-Tajurah area by Marinelli and Varet (1973) and Barberi et al. (1975). It is also found in eastern Afar (Civetta et al. 1974) and in the Aisha—Ali-Sabieh area (Chessex et al. 1975; Black et al. 1974) where it was called Galile or “BI” formation. This term refers to the 1/2,000,000 geological map of Ethiopia (Ethiopian Geological Survey, Kasmin, 1974). The term of

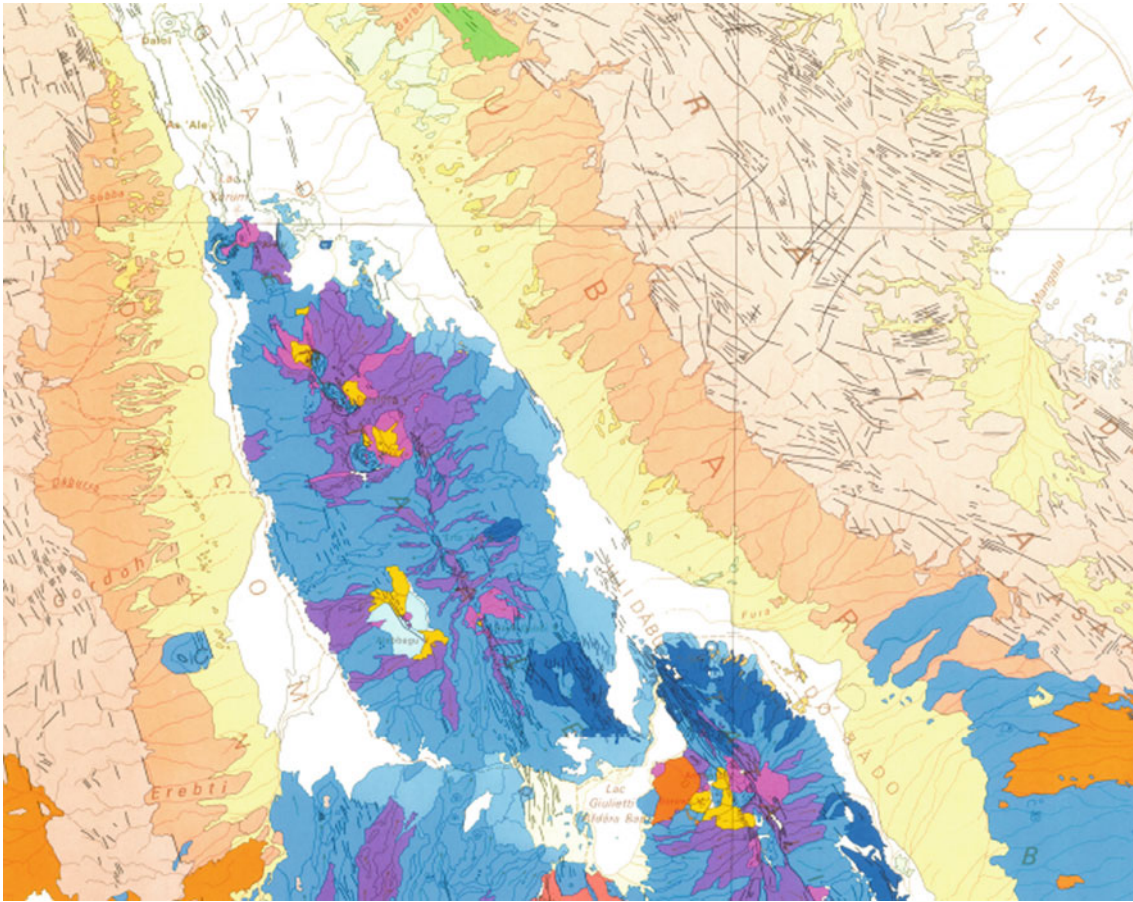


Fig. 4.26 The symmetrical disposition of the polychromatic detrital formation (*pale orange*) bordering the pre-Mesozoic basement (*beige*) on both sides of the Afar depression north of 13°N. These terraces are reworked by Pleistocene piedmont formations (*pale yellow*) made of

thin clays in the lower part where they interbed with the salt deposits (*white*). Marine coralliferous limestones of middle Pleistocene age (200,000–80,000 years ago) also outcrop on both sides (*bright yellow*)

Adolei basalts was taken as reference for the 1/500,000 geological map of Afar (Varet 1978) and the various geological maps (1/100,000 scale) of the Djibouti Republic published by BRGM and ORSTOM in the 1980s. These basaltic flows are generally strongly tectonised, eroded and altered and therefore difficult to date, but the few ages obtained vary from 22 to 15 million years.

They appear to have a grey-greenish colour, with fissures and vacuoles filled with calcite, silica, zeolite and chlorite. To the north of the Gulf of Tadjourah these basalts lie beneath the Mabla rhyolites but the bottom of the formation is not observed. The thickness, which may reach several hundreds of metres, cannot be determined. In the Aisha Ali-Sabieh area these basalts are found in contact with the Mesozoic sandstones, and numerous feeding dikes are observed cutting through the sedimentary sequence.

Two questions arise here:

1. Are these basalts distinct from the flood basalts of the Nubian and Somalian plateaus?

2. In the north Tadjourah area, is the pre-Tertiary basement present beneath these volcanic units?

Few petrological and geochemical analyses are available for these basalts, but from the scarce data available they appear to be slightly alkali tholeiites, a composition that does not allow one to discriminate between them and other pre-rift or syn-rift basalts.

Not only is no outcrop of basement observed in the whole area located between the Gulf of Tadjourah and the Assab range but also inclusion of the Precambrian basement or Mesozoic sediment was never found, neither in these basalts nor in the associated rhyolites, or more recent volcanic units, despite searching for such indices in the flows as well as in the pyroclastic or reworked layers. In particular, several transverse structure (Assab and Sept Frères volcanic alignments) that could be good candidates for such indices appear to be devoid of any such traces, despite the fact that peridotite and gabbro inclusions may be found.

Therefore nothing suggests that the north Tadjourah area belongs to the Danakil continental microplate as assigned by several authors, even in the most recent plate tectonic reconstructions (Sichler 1980; Manighetti et al. 2001; Eagles et al. 2002; Hofstetter and Beyth 2003; Wolfenden et al. 2004; Muluneh et al. 2013).

4.6 The Mabla Rhyolites

The area located north of the Gulf of Tadjourah, extending over the Republic of Djibouti along the western coast of the Bab El Mandeb strait, is characterised by a wide dominantly rhyolitic landscape where important domes and thick flows alternate with less abundant pyroclastics (ignimbrites, welded tuffs and cinerites) of pale colour (pink, yellow, to white). It is not rare to see sequences of tuffs with associated perlites and ignimbrites, covered by rhyolite flows (up to 30 m thick) that are cut by faults, tilted and intruded by

dikes and domes aligned in the same tectonic direction (Fig. 4.27). This impressive silicic unit that reaches measurable thicknesses of 600 m may reach up to 1000 m in height and creates a mountainous relief intensively dissected by erosion. The dominant N-S to NNW (Red Sea direction) trend is determined by dikes, alignment of fissural vents as well as normal faults. When the strata are visible, the lava flows, tuffs and ignimbrites appear to be generally tilted as a result of faulting.

This silicic episode covers the Adolei basalts that are eventually found at the bottom of the fault scarps, generally faulted and tilted, deeply weathered and eroded before the rhyolites were emitted. The unit originally covered an area of at least 10,000 km² and is partly covered to the east (along the Red Sea margin where it is most deeply eroded) by continental detrital and marine coral sediments and to the west by flood basalts of the Dalha unit. Many outcrops in the contact area show that the rhyolites, faulted and eroded, were progressively invaded by the basalt flows, first in the grabens



Fig. 4.27 View of the faulted Mabla rhyolites (*white and red*) in the north Tadjourah massif, covered by the horizontally lying Dalha trap basalts (Photo Varet 2013)

and valleys and progressively piling up in nearly horizontal strata (Figs. 4.28 and 4.29).

These rhyolites are generally aphyric, with eventually small anorthoclase phenocrysts, but very rarely with magmatic quartz in a glassy or thin microcrystalline groundmass. As well as dominant anorthoclase, late egyptine and aenigmatite are observed in the groundmass together with sodic amphiboles (arfelsonite, katophorite) frequently displaying plumose-like or aster-like arrangements.

The chemical analysis obtained from fresh samples (rather rare) confirms the alkaline to peralkaline composition. These are mainly comendites up to, eventually, pantellerites. Their age range from 15 to 10 million years (Barberi et al. 1975). Rocks are generally altered by late hydrothermal circulations, and frequently silicified and kaolinitised. As a consequence, the original magmatic composition is difficult to determine for any chemical, geochemical or isotopic study.

North of the important Wadi Sadai, the 140°N faulting is well developed with blocks tilted towards the east along the eastern (Red Sea) margin and towards the west along the western (Afar) margin. Nearer to the Gulf of Tadjourah, N-S and even 20°N to 40°N faults are also observed that predate

the Dalha basalts. Younger faults postdating the Dalha basalts are also well developed there (see Sect. 4.7).

It should be noted that large outcrops of rhyolites are also observed along the foot of the Nubian escarpment in central-southern Afar (Fig. 4.30). Called the Alaji rhyolitic formation (Tefera et al. 1996), this unit appears as quite similar to the Mabla rhyolites, representing a major geological event characterising central Afar before it was split apart by the consecutive dominantly basaltic active rifting. They display similar ages, volcanological and petrological characteristics despite the fact that their ages may extend over a wider period (up to 25 million years according to Wolfenden et al. 2005).

Further south, sections at around 10°N (where the NNW trending Afar escarpment passes to the NNE trending Ethiopian Rift escarpment) show the Aliyu Amba ignimbrite dating from 11 million years ago, which is contemporaneous with the upper Mabla rhyolites. They are considered by Wolfenden et al. (2005) to be representative of the early stages of formation of the East African Rift.

It should also be noted that Barberi et al. (1975) reported an age of 11.1 million years for a rhyolite flow sampled near Gad Elu, south from Affara Dara, an area where a Miocene peralkaline granite uplifted the Afar floor. This would give

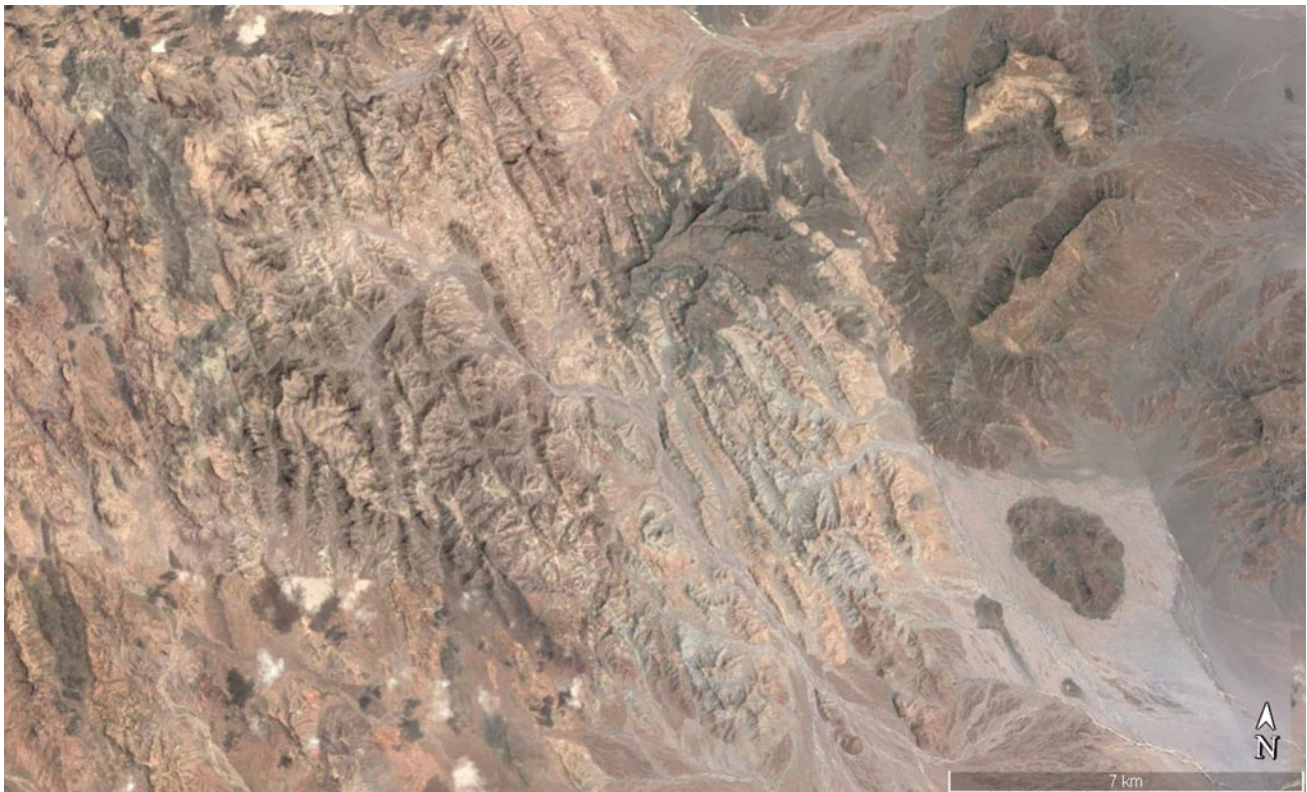


Fig. 4.28 Satellite image view of the Mabla rhyolites in the central part of the North Tadjourah block, Djibouti Republic. Observe the dominantly NNW trending faults and domes that were deeply eroded

before being invaded by the Dalha basalts, an inselberg of which is observed on the eastern side of the image (copied from Google map)



Fig. 4.29 Typical dissected landscape of the Mabla rhyolites, deeply eroded and partly covered by the Dalha flood basalts contrasting with a flat-lying surface marking the horizon to the NW (and slightly dipping in that direction). Source <http://est-afar-inedits-geologie.e-monsite.com/>



Fig. 4.30 Mabla rhyolite flows and domes, faulted, tilted and eroded, covered by Dalha basalts at the foot of the Nubian escarpment SW of Digdiga (Sullu Adu massif). Photo Varet 2015

coherence to the idea that an active continental rift system developed both in the Red Sea and Ethiopian rift through Afar in that period (Varet 1973).

A similar rhyolitic event is observed in the Aisha–Ali-Sabieh area, as the pre-Mesozoic units are covered in discordance and in fact surrounded by silicic formations that have been considered as belonging to the same Mabla unit, with radiometric ages ranging from 14 to 10 million years (Chessex et al. 1975), that is, the same age. However, more recent data published by Audin et al. (2004) report ages of 17 and 20 million years for rhyolites in Ali-Sabieh area. As basalts have also been reported to be older there, these may

also result from another earlier silicic event (from pre-rift flood basalts and rhyolites of the plateaus).

Scarce outcrops of rhyolites belonging to the same Mabla event have been reported in other places south of the Gulf of Tadjourah, such as in the Bour Ougoul massif where rhyolites associated with ignimbrites were dated from 11.9 million years ago and in the lower part of the dominantly basaltic Arta dome. The uplift in that area following the Gulf of Tadjourah opening allowed for these underlying strata to outcrop. K/Ar age determination ranged from 14 to 10 million years, consistent with the ages from the north, despite the fact that one age of 16.6 million years was

obtained for one of these lower rhyolite flows (Fournier et al. 1983).

Whatever their location in Afar, these Mabila rhyolites are intensively faulted. These faults predate the overlying Dalha basalts. Two dominant trends are observed: 160–180°N and 40–60°N, with blocks tilted towards SW and eventually NE. From field tectonic studies, Gaulier and Huchon (1991) showed that they were emplaced in a left lateral strike-slip regime with E-W extension along NNE (Ethiopian Rift regime) faults.

The fissural nature of the emissions, whether domes and flows or ignimbrites and tuffs (Gadalia and Varet 1983), indicate that they were not differentiated in classical volcanic magma chambers. In fact no trace of caldera was reported. However, the composition of these magma clearly relates to the slightly alkaline nature of the basalts that predate them. Despite the apparent lack of intermediate products, this bimodal type of association is considered as resulting from differentiation processes in elongated tectonic traps resulting from block faulting, a process rather typical of continental rift magmatism. This was interpreted by Marinelli and Varet (1973) as indicative of the development of a continental rift

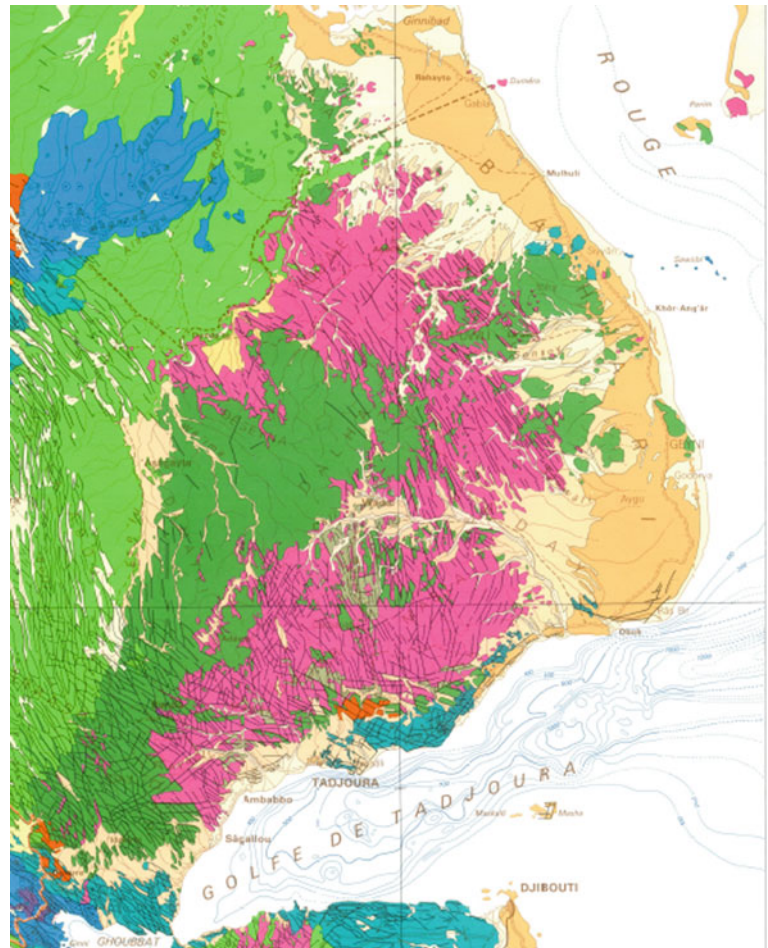
type of extension which developed in the Southern Red Sea area in that mid-Miocene (14–10 million years ago) period.

It should also be noted that the Mabila rhyolitic episode corresponds in age with the initial collision of Arabia with Eurasia (Hempton 1987; Woodruff and Savin 1989; Burke 1996). That major change in regional plate kinematics (Le Pichon and Gaulier 1988) clearly influenced the spreading pattern in the Red Sea rift, and may be the cause of this major Afar event (however ill-expressed in northern Afar).

4.7 The Dalha Basalts

The Dalha basalts unit was defined by Marinelli and Varet (1973). It is a prominent geographic and geologic feature of the area located in eastern Afar, north of the Gulf of Tadjourah, where it constitutes a wide and generally elevated flat-lying plateau that gently dips towards NW with the highest altitude (1799 m) reached in the Day Forest area only a few kilometres north of the Ghoubbet pass (Fig. 4.31). It is made of pile of flows, 5–10 m thick, with rare intercalations of ignimbrites or detritic sediments

Fig. 4.31 Geological map showing the extension of the Dalha basalts (*dark green*) covering the faulted Mabila rhyolites (*dark pink*) and themselves covered to the west and north by the basalts of the Afar stratoid series (*pale green*), and to the south by the basalts of the gulf (*turquoise blue*) on both sides of the gulf of Tadjourah. The earlier Adolei basalts are mapped in *grey*



towards the summit. Even if eroded, this unit appears to thicken towards the south and west where it reaches more than 1000 m, whereas along the Red Sea the thickness (well measurable despite erosion as original surfaces are preserved) does not exceed a few tens of metres.

This sequence made of transitional basalts (mildly alkali tholeiites, ranging from picritic to iron-rich basalts but without marked chronologic evolution) is rather homogeneous in geological behaviour (flat-lying succession of lava flows) and in composition (Figs. 4.32, 4.33 and 4.34). K/Ar age determinations by Barberi et al. (1975) range from 8 to 4 million years, an upper Miocene—lower Pliocene interval that was confirmed by Audin et al. (2004) with new determinations ranging from 7.7 to 4.8 million years ago.

An important point is that the Dalha—differing radically from the underlying Mabila rhyolites covered in discordance after faulting and erosion—is essentially unfaulted in the north and east part; that is, a 100 km surface along the Red Sea shore. This feature was taken by most authors as an indication for a wide extension of the Danakil microplate from the northern Afar apex to the Gulf of Tadjourah—misleading interpretation in our view.

The southern part of the outcrop is intensively faulted, with normal faulting of dominantly E-W direction, themselves crossed by NNW faults developed to the west and NE faults to the SE. This complex fault pattern is of recent age and clearly relates to the effect of the development of the Gulf of Tadjourah oceanic ridge.

To the west of the north Tadjourah block, the Dalha unit was eroded prior to being covered by the more recent basaltic unit of the Afar stratoid series. Between Dada'to and Asagayla a well-expressed detrital sedimentary valley now occupied by the Wadi Ese'Lu developed in an area that should constitute an aquifer of quality as it extends north

beneath the stratoid series. In the area located south from Assab (southern Eritrea), several inselbergs of the Mabila unit appear to be surrounded and included by the more recent flood basalts of the stratoid series.

To the east, from inselbergs and small plateaus remnants of later erosion, one can observe that the extension of the Dalha basalts was originally much wider, covering the whole area including the Bab-El-Mandeb segment of the Red Sea (see map in Fig. 4.31). In fact, as observed on the map, basalts of the same age and characteristics are observed a few kilometres away in the Perim Island and along the coast of South Yemen. Huchon et al. (1991) describe horizontally lying basalts near the town of Al Mokha dating from 10 million years ago, covering uncomfortably faulted and tilted rhyolites dating from 18 million years ago, both units clearly belonging to the Dalha and Mabila formations. This observation allowed Marinelli and Varet (1973) to consider the whole area as belonging to the same early continental rifting episode of the Southern Red Sea and, being sealed by the Dalha basalts, part of the Arabian plate. This means that 10 million years ago the rifting ceased in the Southern Red Sea and was totally transferred inside central Afar. This correlates with a major difference between northern Afar, where one passes directly from Mio-Pliocene continental crustal thinning to Pleistocene oceanic rifting, and central-southern Afar, where a continental type of rifting episode 14–10 million years ago predates the development of an ocean floor building process which initiated 8 million years ago and developed since 4 million years ago (Figs. 4.32, 4.33, and 4.34).

In western Afar, Barberi et al. (1975) identified a large basaltic outcrop (from Sullu Adu to Mille) along the foot of the Nubian escarpment (the pre-Mesozoic units disappear under the basalts along the Afar margin in that area) assigned



Fig. 4.32 The Dalha trap basalts overlying the faulted, tilted and eroded Mabila rhyolites north-west from Tadjourah (Photo Varet 2003)



Fig. 4.33 The Dalha basaltic unit as seen at Randa (N. Tadjourah). *Photo* Varet 2003

to the Dalha unit after an age determination of 7.4 million years. These basalts also cover the older faulted Mabla rhyolites described above (Fig. 4.35).

At 10°30'N, the normal faults of the Nubian escarpment pass from NNW (Red Sea direction) to NNE (Ethiopian Rift direction). Wolfenden et al. (2005) established a correlation between the units observed there between 9°45'N and 11°N. In the northernmost sections ages range from 26 to 25 million years, clearly belonging to the plateau basalts. Further south, in the Ankober area, lower-mid-Miocene rhyolites blanket this formation to the east, with silicic units dated 10.9 million years at Megezez, 10.7 million years at Baso-Wenera (Ukstins et al. 2002) and 10.5 million years at Mezezo (George et al. 1998), which allows them to be assigned to the Mabla Unit. Called the Aliyu Amba formation, it is covered to the east by a basaltic unit that is considered as belonging to the Dalha formation (seven to eight million years old). This step (called “step 3” in their model, Fig. 4.36) is considered by Wolfenden et al. (2005) as the first step of oceanisation in western Afar. This interpretation is consistent with the interpretation by Marinelli and Varet (1973) and Barberi et al. (1975), according to which the

Dalha basalts represent the transition phase between continental rifting and the development of the oceanic floor expressed by the stratoid series. It should be noted that this coincides in time with the rapid propagation of oceanic spreading throughout the central-western Gulf of Aden.

The Dalha basalts are also found to the south of the Gulf of Tadjourah, in less spectacular outcrops as these are limited to windows beneath the more recent units of the Afar stratoid series, the basalts of the gulf or the Somali basalts to the east (Fig. 4.37). They are, however, largely visible around the Aisha block where they appear as overlying the Mabla rhyolites. All along the NW limit of the Aisha block, the Dalha basalts are present at the contact with the rhyolites to the east and disappearing to the west under the sedimentary plains of Grand Barra and Petit Barra; as they are faulted and tilted towards Afar (see Fig. 4.37).

Although E-W and WNW faulting dominate at the surface, the whole unit appears to be mainly cut by a major NE trending discontinuity that marks the limit of the Aisha—Ali-Sabieh block. This Bour-Ougoul discontinuity (see Fig. 4.36) is located in the continuation of leaky transform faults in the Gulf of Tadjourah and hence appears as a major



Fig. 4.34 The Dalha basalt series, down-faulted to the south towards the Ghoubbet marine gulf (western extremity of the Gulf of Tadjourah)



Fig. 4.35 Flat-lying, faulted and eroded Dalha basalts, south Sullu Adu Range, Mille river basin (Photo Varet 2016)

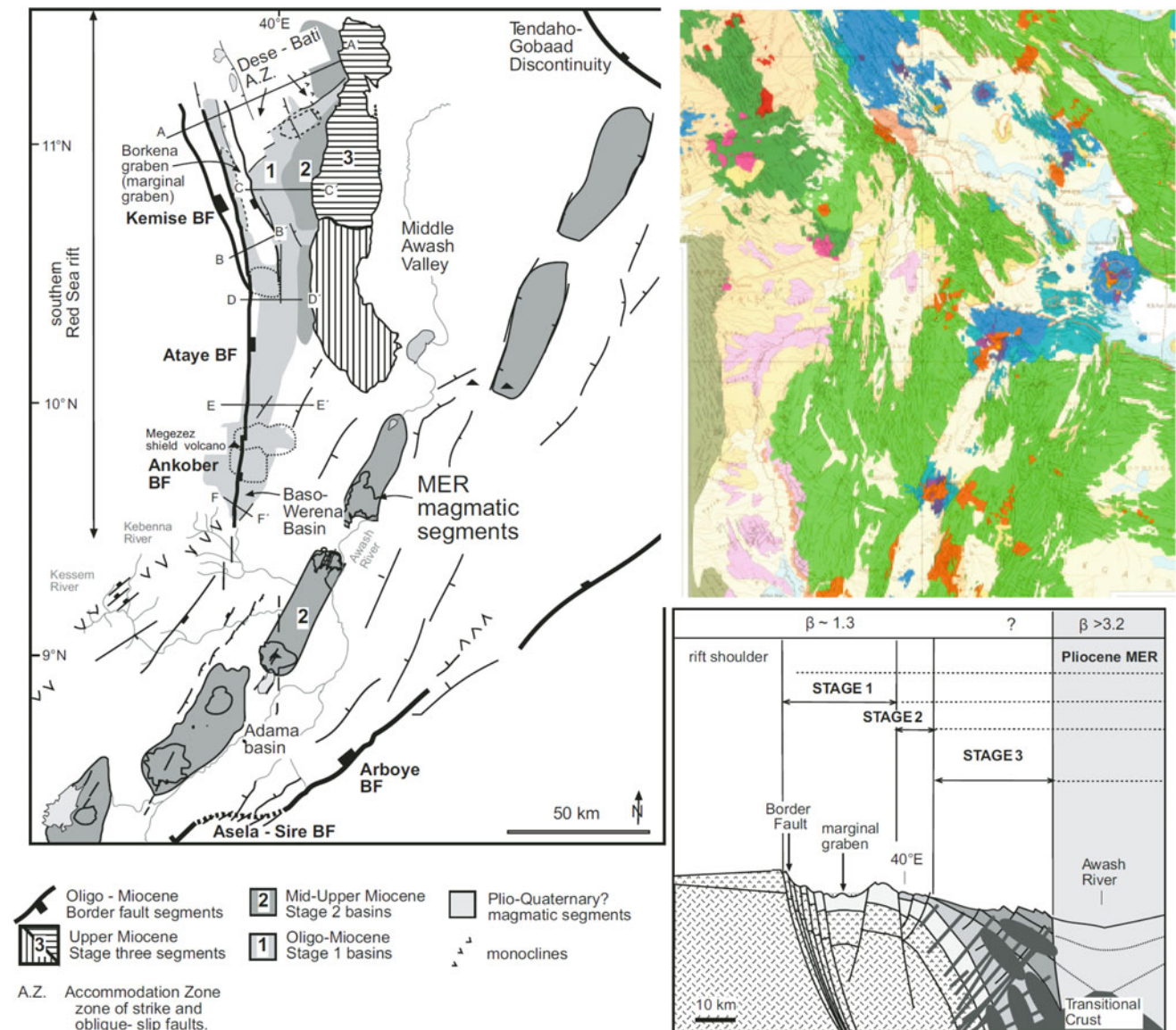


Fig. 4.36 Tectono-stratigraphic relations scheme (Wolfenden et al. 2005) and geological map (Varet 1975) in south-western Afar where the Main Ethiopian Rift (MER) reaches the Red Sea Rift (tendaho-Gobaad discontinuity). The schematic cross section illustrates the magmatic margin development at 10°50'N with vertical

exaggeration 4:1. Stage 1 border faults developed between 29 and 26 million years ago. By 15 million years ago stepped eastward to localized zones of magmatic construction (Stage 2). Further East, by 7–8 million years ago another jump occurred with riftward dipping wedge of the Dalha series (Wolfenden et al. 2005)

fracture. It was interpreted by several authors as a transform fault that allowed the Gulf of Aden oceanic spreading to link to earlier spreading in southern Afar, where magnetic anomalies are observed trending WNW to E-W.

Dalha basalts also outcrop in several places, such as in the Arta plateau and further west at Unda Hemed and Dat Ali and further south in the Adda'do graben. In this southern area, the initiation of the sequence appears to be slightly older, with K/Ar ages up to 8.9 million years at Magali and 8.7 million years at Adaeli Daba (Boucarut et al. 1980). It should be noted that in the Hemed, lacustrine limestones are observed interbedded in the upper part of the Dahla unit.

Basalts of similar age and characteristics are also present to the south of the Danakil Alps, south from Bidu-Dubbi (including Nabro) transverse volcanic range in Beylul region where no basement outcrops. The sequence was sampled at various levels and provided ages ranging from 7.6 to 6.5 million years (Barberi et al. 1975). In a few places, rhyolites are found in the uppermost part of the sequence, as observed at Ribta (3.5 million years) north of the Gulf and at Wêha to the south.

If a clear discontinuity is observed in many places to the north and to the south in eastern Afar, between the Dalha basalts and the stratoid series (equally basaltic) of Afar, the

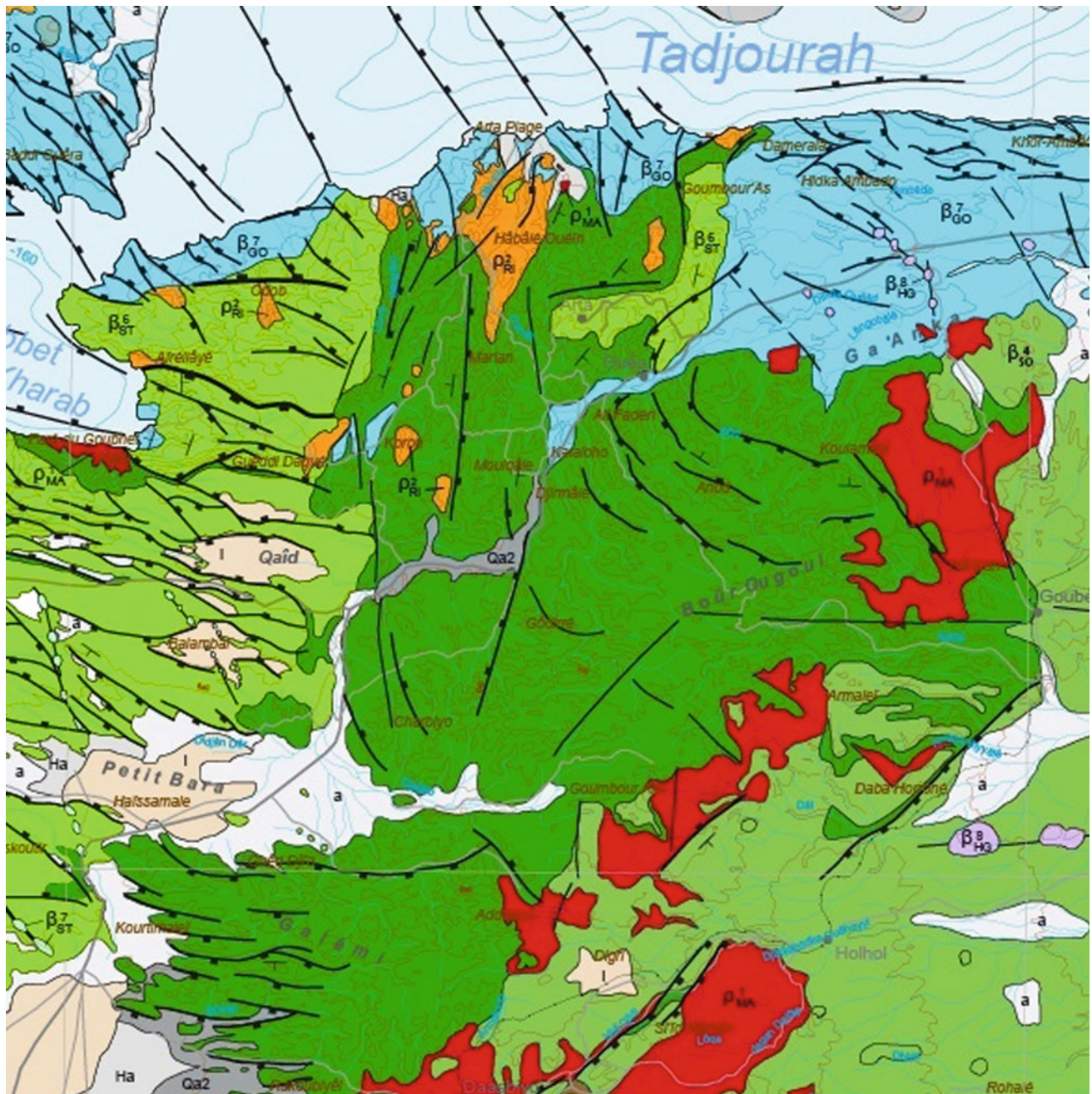


Fig. 4.37 The Dalha basalt formation (deep green) south of Gulf of Tadjourah, covered by the basalts of the stratoid series (pale green) to the west the Gulf basalts to the north (pale blue) both units less than

3 million years old and deeply faulted, and by the unfaulted Somali basalts to the East (Extract from the geological map of the Djibouti Republic, 2016)

distinction is not easy to make between the two units, which appear as rather continuous in the central part (Mararassou area, north of Asal) where the two units, deeply faulted, are in conformity. In fact, as we see below, the oldest ages found for the Afar stratoid series (3.5 million years) are only very slightly younger than the last flows of the Dalha basalts (4 million years) for the uppermost flows in the Day massif (Barberi et al. 1975).

The Dalha basalts are therefore now commonly interpreted as the first step of the transition from continental to oceanic rifting in Afar, as it clearly overlies a continental rifting episode (represented by the Mabla unit) and predates the stratoid series that show clearer analogies with an oceanic floor.

As a whole, judging from the variation in thickness of this unit, and from the relative scarcity of observed feeding

dikes, it appears that the area of emission of these basalts was most probably located in central Afar. The relation of the Dalha basalts to the Gulf of Tadjourah opening is also shown by the tectonic pattern studied by Gaulier and Huchon (1991) which shows a direction of extension passing from 160°N (oblique by 60° to the Gulf of Tadjourah) to 20° N in their period of the emplacement (Fig. 4.38).

This does not mean, however, that the Dalha basalts do not underlie the Afar stratoid series at depth. Despite systematic dating by Barberi et al. (1975), which did not allow ages older than 3.5 million years to be established, even in deeply faulted and weathered basalts found at the bottom of the main faults (such as Gamari Fault, over 1000-m section), and as new basaltic crust was since created in this central area, it is most probable that the Dalha basalts underlie the stratoid series, at least along the eastern and western Afar margins and as revealed around Affara Dara. The geothermal wells located SW from the Asal rift axis, for instance, intersected the Dalha basalts at a depth of about 1000 m.

It should be noted that where the outcropping Dalha basalt pile is the thickest (Day mountain in Djibouti), this is also the place where the uplift of the northern side of the Gulf of Tadjourah is the highest, the area behaving as a doming preceding the Tadjourah opening. In a way this is the younger, smaller-sized, equivalent to the earlier Ethio-Arabian doming which preceded the Red Sea rift. To the south and west, the Dalha unit is intensively faulted as it disappears under the stratoid series.

Le Gall et al. (2011) interpreted the area as the surface expression of a crustal downwarping representing a flexural response to the differential isostatic loading of the basaltic magma accumulation of the Afar crust (Fig. 4.39). Besides the fact that the area mapped in red is not a sialic crustal block but a mid-upper-Miocene Red Sea rift zone, we rather consider that uplift as the result of the development of the Pliocene Tadjourah Oceanic Rift. Despite the difference in age and magmatic sequence, the resulting figure expresses some similitude (a symmetrical figure) with the one

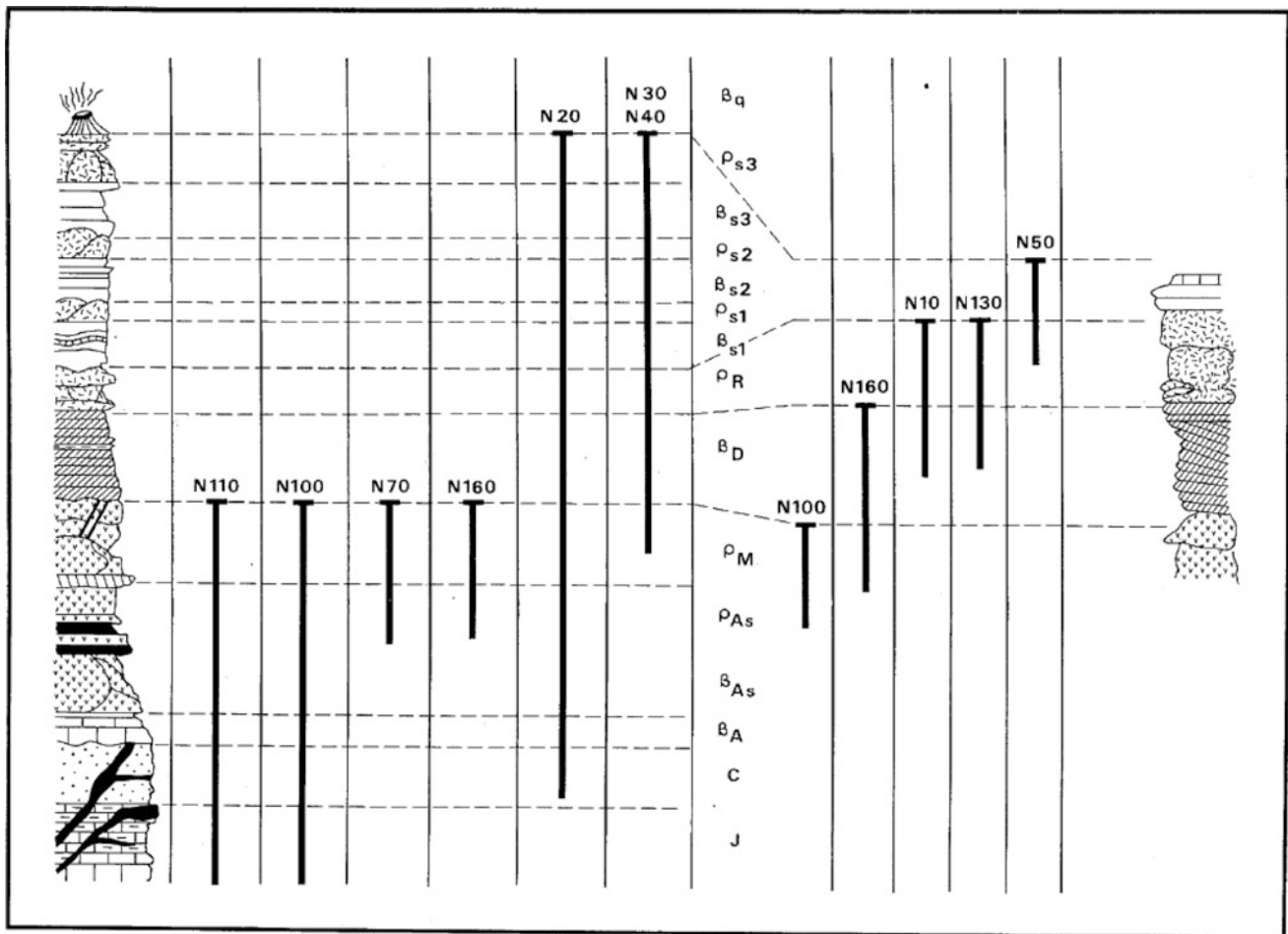


Fig. 4.38 Synthetic diagram from Gaulier and Huchon (1991) showing the distribution of the observed directions of extension within eastern Afar (Republic of Djibouti) stratigraphic column (right Arta

area, left general section reconstituted for other places). The numbers in each column are the direction of extension. J Jurassic limestones; C Cretaceous sandstones

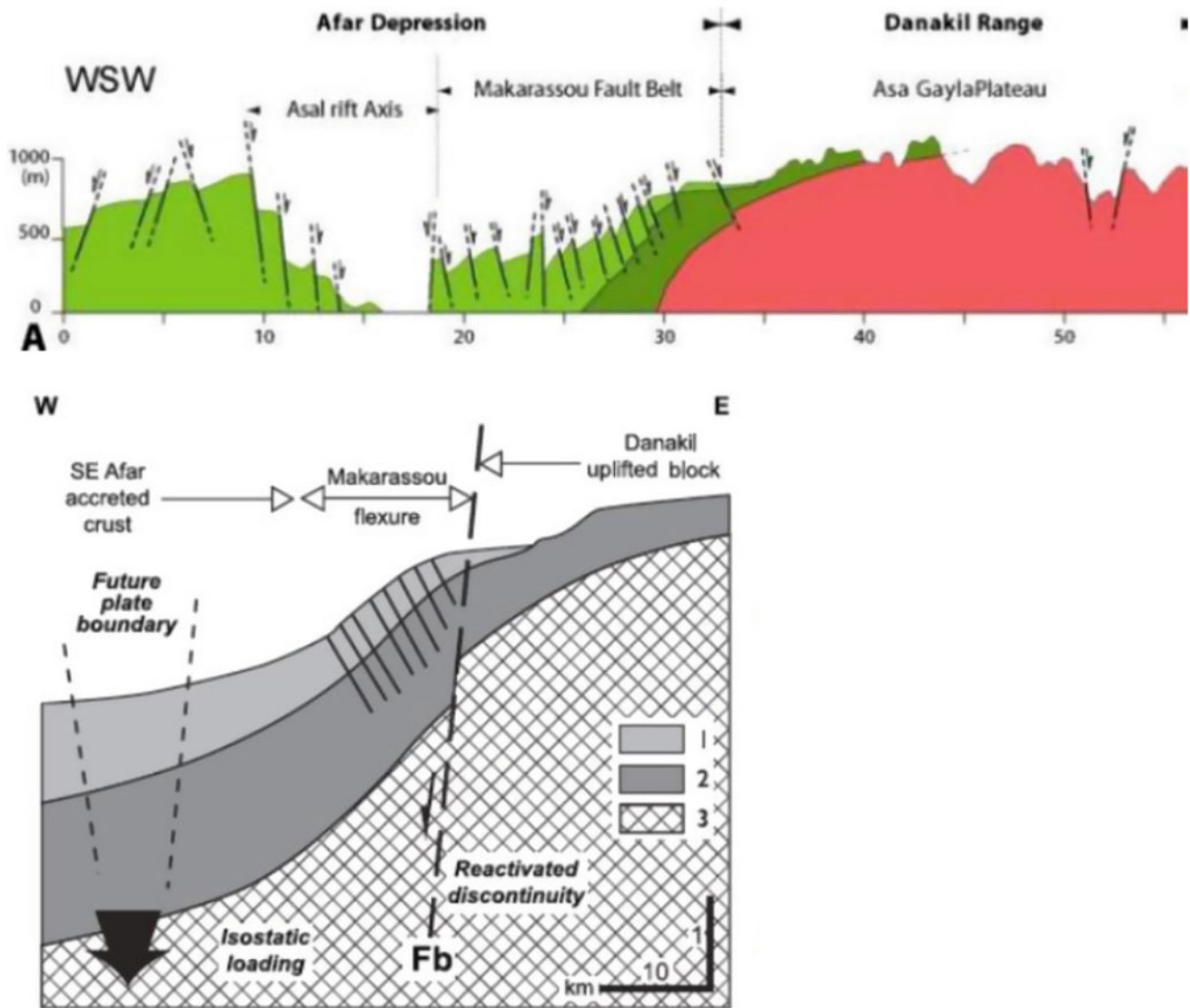


Fig. 4.39 Downwrapping model proposed by Le Gall et al. (2011) for the area of junction between the Afar Stratoid series (1) and the Dalha basalts (2) covering the Mabla rhyolites (3)

proposed by Wolfenden et al. (2005) along the Afar margin on the other side (see Fig. 4.36).

As a whole, it is clear that the Dalha event, following the Mabla event, marks a major discontinuity in the Afar geodynamic regime:

- From continental rift type to oceanic rift
- From East African and Red Sea rift environment to Aden ridge environment
- With a rotation of the extension from nearly E-W to nearly N-S
- Allowing for the oceanic floor to develop in Afar (and in the Red Sea north of Hanish Island).

4.8 The Hadar Formation (Central Western Afar, Awash Basin), a Treasure in Human Palaeontology

In central and southern Afar, the Nubian escarpment is characterised by younger geological units. The pre-Miocene basement sequence found in northern Afar is not observed despite intense and still active faulting and erosion. We have seen that the volcanic events of the plateau are more recent, with the development of central volcanoes, particularly near the Afar margin (Gani et al. 2007). Ages of 14.9 and 8.6 million years have been reported by Yemane (1997) and even 3.2 million years by Ukstins et al. (2002) for basalts of the plateau found along the Afar margin.

The earliest sedimentary formation found at the foot of the escarpment is of Pliocene age, and relates to the Awash basin, with important sedimentary inflows from the south (MER), hence differing in age and characteristics from the northern Afar foothills. Called the Hadar formation, it is characterised by a thick sequence of detrital, volcanic, volcano-sedimentary and lacustrine deposits which outcrop only in its upper sequence and are dated at five million years ago for the oldest.

This unit has been extensively studied during the last 50 years, as it displays important fossil sequences (fauna, flora) of major interest for human palaeontology. Following Taïeb first discoveries in 1968 of important mammals bones (hippo, elephant, rhinoceros, etc.) in the gullies of the Hadar wadies (western tributaries of Awash River Taïeb et al. 1976) allowed the identification of the species *Australopithecus afarensis*, dating from 3.2 million years ago, called “Lucy” by the US members of the team (referring to the popular song of the Beatles) and “Dinkenesh” by Ethiopian counterparts.

Afar then became well known worldwide as the “birthplace of mankind”, although this has since been disputed by other places in Africa (Bruxelles 2006).

On the western flank of the central Afar Rift, these sedimentary formations were intensively studied by a multi-disciplinary team around 11°N at Hadar and south of it at Gona. In this location, Quade et al. (2008) described a sequence ranging from more than 6.4 million years ago to the present, including the early Ada-Asa (6.5–5.4 million years) and Sangatole (5.2–3.9 million years) volcanic units with associated fluvio-lacustrine formations where *Ardipithecus kabbada* and *Ardipithecus ramidus* were identified,



Fig. 4.40 The Hadar formation (Photo Arizona State University). <https://shesc.asu.edu/research/research-topic/geoinformatics-based-data-integration-study-pliocene-fossil-bearing-strata>

underlying the Hadar formation *stricto sensu*. where *Australopithecus afarensis* was earlier found. *Homo erectus* was also discovered in the upper fluvial formation called Basidima (2.7 million years ago to present).

This Hadar formation, studied for the last 40 years (Aronson et al. 1977, 1981, 1996; Tiercelin 1986; Walter 1981; Walter and Aronson 1982, 1993; Yemane 1997), consists of laminated shale intervals rich in fossil mollusc and fish representing at least three transgressions dated at 3.5–2.9 million years ago. The lacustrine units are interbedded with fluvial-deltaic sands and siltstones with palaeo-sols occurrences. Walter et al. (1987) described an interesting occurrence of peralkaline rhyolite—transitional basalt mixing of same magmatic origin in the Cindery tuff interbedded in the Adar formation. The University of Arizona established a database for the study of Pliocene-bearing strata (Fig. 4.40).

References

- Aronson LJ, Taïeb M (1981) Geology and paleogeography of the Hadar Hominid Site, Ethiopia. In: Rapp G, Vondra C (eds) Hominid Sites and their Geological Settings. AAAS Sel Symp 63(1981): 165–195
- Aronson JL, Schmitt TJ, Walter RC, Taïeb M, Tiercelin JJ, Johanson DC, Naeser CW, Nairn AEM (1977) New geochronologic and paleomagnetic data for the hominid-bearing Hadar Formation of Ethiopia. *Nature* 267:323–327
- Aronson J, Vondra C, Yemane T, Walter R (1996) Characteristics of the disconformity in the upper part of the Hadar Formation. *Geol Soc Amer Abstr* 28(6): 28
- Audin L, Quidelleur X, Coulié E, Courtillot V, Gilder S, Manighetti I, Gillot P-Y, Tapponnier P, Kidane T (2004) Paleomagnetism and K–Ar and ⁴⁰Ar/³⁹Ar ages in the Ali Sabieh area (Republic of Djibouti and Ethiopia): constraints on the mechanism of Aden ridge propagation into southeastern Afar during the last 10 Myr. *Geoph J Int* 158:327–345
- Bannert D, Brinckmann J, Kading Ch. K et al (1970) Zur Geologie der danakil-Senke (Nördliches Afar Gebiet, NE-Aethiopien. *Geol Rundsch* 59(2):409–443
- Barberi F, Borsi S, Ferrara G, Marinelli G, Varet J (1970) Relations between tectonics and magmatology in the northern Danakil Depression (Ethiopia). *Philos Trans R Soc Lond A* 267:293–311
- Barberi F, Tazieff H, Varet J (1972) Volcanism in the Afar depression: its tectonic and magmatic significance. *Tectonophysics* 15:19–29
- Barberi F, Chemine’e JL, Varet J (1973) Long-lived lava lakes of Erta Ale volcano. *Rev Geogr Phys Geol Dyn* 15:347–352
- Barberi F, Santacroce R, Varet J (1974) Peralkaline silicic volcanic rocks of the Afar Depression. *Bull Volcan* 38:755–790
- Barberi F, Ferrara G, Santacroce R, Treuil M, Varet J (1975) A transitional basalt-pantellerite sequence of fractional crystallisation, the Boina centre (Afar rift, Ethiopia). *J Petrol* 16:22–56
- Beyene A, Abdelsalam M (2005) Tectonics of the Afar depression: a review and synthesis. *J Afr Earth Sci* 41:41–59
- Beyth M (1991) ‘Smooth’ and ‘rough’ propagation of spreading Southern Red Sea-Afar Depression. *J Afr Earth Sci* 13:157–171
- Black R, Morton WH, Varet J (1972) New data on Afar tectonics. *Nat Phys Sci* 240:170–173
- Black R, Morton WH, Hailu T (1974) Early structure around the Afar triple junction. *Nature* 248:496–497

- Bosworth W, Huchon P, McClay K (2005) The Red Sea and Gulf of Aden Basins. *J Afr Earth Sci* 43:334–378
- Boucarut M, Chessex R, Clin Delavoye M (1980) Données géochronologiques K-Ar de roches volcaniques de l'Afar, partie Nord de la République de Djibouti. *Schweiz Mineral Petrogr Mitt* 60:263–269
- Bruxelles L (2006) A la recherche d'une nouvelle pièce du berceau de l'humanité en Afrique Australe. *Géosciences*. 21:44-49
- Bunter MAG, Debretson T, Woldegiorgis L (1998) New developments in the pre-rift prospectivity of the Eritrean Red Sea. *J Petro Geol* 21:373–400
- Burke K (1996) The African plate. *S Afr J Geol* 99:341–409
- Canuti P, Gregnanin A, Piccirillo EM, Sagri M, Tacconi P (1972) Volcanic intercalation in the Mesozoic sediments of the Kulubi area (Harrar, Ethiopia). *Boll Soc Geol Italiana* 91:603–614
- Chessex R, Delavoye M, Muller J, Weidmann M (1975) Evolution of the volcanic region of Ali Sabieh (T.F.A.I.) in the light of K–Ar age determination. In: Pilger A, Rösler A (eds) *Afar Depression of Ethiopia, Proceedings of an International Symposium on the Afar Region and Related Rift Problems*, Bad Bergzabern, F.R. Germany, 1–6 Apr 1974, vol. 1. E. Schweizerbart'sche Verlagsbuchhandlung, Stuttgart, pp 220–227
- Civetta L, De Fino M, La Volpe L, Lirer L (1974) Geochemical trends in the alkali basaltic suite of the Assab range (Ethiopia). *Chem Geol* 13:149–162
- CNR-CNRS Afar team (1973). *Geology of northern Afar (Ethiopia)*. *Rev Geogr Phys Geol Dyn* 15:443–490
- Collet B, Taud H, Parrot JF, Bonavia F, Chorowicz J (2000) A new kinematic approach for the Danakil block using a Digital Elevation Model representation. *Tectonophysics* 316:343–357
- De Fino M, La Volpe L, Lirer L, Varet J (1973) Geology and petrology of Manda-Inakir range and Moussa Alli volcano, central eastern Afar (Ethiopia and T.F.A.I.). *Rev Geogr Phys Géol Dyn* 15:373–386
- De Fino M, La Volpe L, Lirer L (1978) Geology and volcanology of the Edd-Bahar Assoli area (Ethiopia). *Bull Volc* 41(1):32–42
- Eagles G, Gloaguen R, Ebinger C (2002) A model for the creation of a microplate: kinematics of the Danakil microplate. *Earth Planet Sci Lett* 203:607–620
- Fournier M, Gasse F, Richard O, Ruegg JC (1983) Notice explicative: Carte géologique de la République de Djibouti à 1 :100 000: Djibouti. ISERST—Ministère français de la Coopération éd. ORSTOM Paris, 70p
- Fournier M, Bellahsen N, Fabbri O, Gunnell Y (2004) Oblique rifting and segmentation of the NE Gulf of Aden passive margin. *Geochemistry, Geophysics, Geosystems* 5(11)
- Gadalia A, Varet J (1983) Le rhyolites miocènes de l'Est de l'Afar. *Bull Soc Geol Fr* 7, XXV:139–153
- Gani NDS, Gani MR, Abdelsalam MG (2007) Blue Nile incision on the Ethiopian Plateau: pulsed plateau growth, uplift, and hominid evolution. *GSA Today* 17(9):4–11
- Gaulier JM, Huchon Ph (1991) Tectonic evolution of Afar triple junction. *Bull Soc Geol Fr* 162(3):451–464
- Genna A, Nehlig P, Le Goff E, Guerrot C, Shanti M (2002) Proterozoic tectonism of the Arabian Shield. *Precam Res* 117:21–40
- George R, Rogers N, Kelley S (1998) Earliest magmatism in Ethiopia: Evidence for two mantle plumes in one flood basalt province. *Geology* 26:923–926
- Ghebreab W (1998) Tectonics of the Red Sea reassessed. *Earth Sci Rev* 45:1–44
- Ghebreab W, Carter A, Hurford AJ, Talbot CJ (2002) Constraints for timing of extensional tectonics in the western margin of the Red Sea in Eritrea. *Earth Planet Sci Lett* 200:107–119
- Guiraud R, Bosworth W (2005) Phanerozoic geological evolution of Northern and Central Africa: an overview. *J Afr Earth Sci* 43(1): 83–143
- Hempton MR (1987) Constraints on Arabian Plate motion and extensional history of the Red Sea. *Tectonics* 6:687–705
- Hofstetter R, Beyth M (2003) The Afar Depression: interpretation of the 1960–2000 earthquakes. *Geophys J Int* 155:715–732
- Holwerda JG, Hutchinson RW (1968) Potash bearing deposits in the Danakil area, Ethiopia. *Econ Geol* 63:124–150
- Huchon P, Jestin F, Cantagrel JM, Gaulier JM, Al Khirbash S, Gafaneh A (1991) Extensional deformations in Yemen since Oligocene and the Afar triple junction. *Ann Tectonicae* 5:141–163
- Hutchinson RW, Engels GC (1970) Tectonic significance of regional geology evaporate lithofacies in Northern Ethiopia. *Phil Trans Roy Soc London A* 267(1181):313–329
- Le Gall B, Daoud DA, Rolet J, Egueh NM (2011) Large-scale flexuring and antithetic extensional faulting along a nascent plate boundary in the SE Afar rift. *Terra Nova*, Wiley 23(6):416–420
- Le Pichon X, Gaulier J-M (1988) The rotation of Arabia and the Levant fault system. *Tectonophysics* 153:271–294
- Leroy S, Gente P, Fournier M, d'Acremont E, Patriat P, Beslier M-O, Bellahsen N, Maia M, Blais A, Perrot J, Al-Kathiri A, Merkouriev S, Fleury J-M, Ruellan P-Y, Lepvrier C, Huchon P (2004) From rifting to spreading in the eastern Gulf of Aden: a geophysical survey of a young oceanic basin from margin to margin. *Terra Nova* 16:185–192
- Manighetti I, King GCP, Gaudemer Y, Scholtz CH, Doubre C (2001) Slip accumulation and lateral propagation of active normal faults in Afar. *J Geophys Res* 106:13667–13696
- Marinelli G, Varet J (1973) Structure et évolution du Sud du “horst Danakil” (TFAI et Ethiopie). *CR Acad Sci (D)* 276:1119–1122
- McKenzie DP, Davies D, Molnar P (1972) Plate tectonics of the Red Sea and East Africa. *Nature* 224:125–133
- Merla G, Abbate E, Azzaroli A, Bruni P, Fazzuoli M, Sagri M, Tacconi P (1979) *A Geological Map of Ethiopia and Somalia*: Comment. Pergamon, 95 pp
- Mohr PA (1975) Structural setting and evolution of Afar. In: Pilger A, Rosler A (eds) *Afar depression of Ethiopia, proceedings of an international symposium on the Afar region and rift related problems*, Bad Bergzabren, Germany, 1974, vol 1, E. Schweizerbart'sche Verlagsbuchhandlung, Stuttgart, Germany, pp 27–37
- Muluneh AA, Kidane T, Rowland J, Bach-Tads V (2013) Counterclockwise block rotation linked to southward propagation and overlap of sub-aerial Red Sea Rift segments, Afar Depression: Insight from paleomagnetism. *Tectonophysics*
- Quade J, Levin NE, Simpson SW, Butler R, McIntosh WC, Semaw S, Kleinsasser L, Dupont-Nivet G, Renne P, Dunbar N (2008) The geology of Gona, Afar, Ethiopia. In: Quade J, Wynn JG (eds) *The Geology of Early Humans in the Horn of Africa*, *Geol Soc Am Spec Pap* 446:1–31
- Sagri M, Abbate E et al (1998) New data on the Jurassic and Neogene sedimentation in the Danakil Horst and Northern Afar Depression, Eritrea. *Peri-Tethys Memoir* 3. Paris 177:193–214
- Sichler B (1980) La bielle danakile: un modèle pour l'évolution géodynamique de l'Afar. *Bull Soc Geol Fr* XXII(6):925–933
- Stern RJ (1994) Arc assembly and continental collision in the Neoproterozoic East African Orogen—implication for the consolidation of Gondwanaland. *Ann Rev Earth Planet Sci* 22:319–351
- Taieb M, Johanson DC, Coppens Y, Aronson JL (1976) Geological and paleontological background of Hadar hominid site, Afar, Ethiopia. *Nature* 260:289–293
- Tazieff H, Marinelli G et Barberi F, Varet J (1969) Géologie de l'Afar septentrional Symposium Ass Interna Volcanologie; Canaries Bull Volc t XXXIII(4):1039–1072
- Tefera M, Chernet T, Haro W (1996) *Geological Map of Ethiopia*: Ethiopian Institute of Geological Surveys, scale 1:2,000,000, 1p

- Tiercelin JJ (1986) The Pliocene Hadar Formation, Afar Depression of Ethiopia, in *Sedimentology in the African Rifts*. Frostick, L.E. et al. (eds) *Geol Soc Sp Publ* 25:221–240
- Ukstins IA, Renne PR, Wolfenden E, Baker J, Ayalew D, Menzies M (2002) Matching conjugate volcanic rifted margins: $^{40}\text{Ar}/^{39}\text{Ar}$ chronostratigraphy of pre- and syn-rift bimodal flood volcanism in Ethiopia and Yemen. *Earth Planet Sci Lett* 198:289–306
- Varet J (1973) Critères pétrologiques, géochimiques et structuraux de la genèse et de la différenciation des magmas basaltiques: exemple de l'Afar. Thèse Doctorat d'État, univ. Paris-sud, 491p
- Varet J (1975) L'Afar, un "point chaud" de la géophysique. *La Recherche* 62:1018–1026
- Varet J (1978) Geology of central and southern Afar (Ethiopia and Djibouti Republic), map and 124p. report, Centre Natl. de la Rec. Sci., Paris
- Varet J (2013) The Afar system and carbonates. *Cocarde workshop* (abstract), Sicily, pp 48–49
- Walter RC (1981) The volcanic history of the Hadar early man site and the surrounding Afar region of Ethiopia. Ph.D. dissertation, Case Western Reserve University, USA
- Walter RC, Aronson JL (1982) Revisions of K/Ar ages for the Hadar hominid site, Ethiopia. *Nature* 296:122–127
- Walter RC, Aronson JL (1993) Age and sources of the Sidi Hakoma Tuff, Hadar Formation, Ethiopia. *J Hum Evol* 25:229–240
- Walter RC, Hart WK, Wesgate JA (1987) Petrogenesis of a basalt-rhyolite tephra from West-Central Afar, Ethiopia. *Contr Mineral Petrol* 96:462–480
- Wolfenden E, Yirgu G, Ebinger C, Ayalew D, Deino A (2004) Evolution of the northern Main Ethiopian rift: birth of a triple junction. *Earth Planet Sci Lett* 224:213–228
- Wolfenden E, Ebinger C, Yirgu G, Renne P, Kelley SP (2005) Evolution of the southern Red Sea rift: birth of a magmatic margin. *Bull Geol Soc Amer* 117:846–864
- Woodruff F, Savin SM (1989) Miocene deepwater oceanography. *Paleoceanography* 4:87–140
- Yemane T (1997) Stratigraphy and Sedimentology of the Hadar Formation, Afar, Ethiopia (Ph.D. thesis), Ames, Iowa State University, 182 p

Between 10°N and 13°N, Afar is mostly floored by a dominantly basaltic formation covering two-thirds of the surface called the stratoid series by Barberi et al. (1973, 1975). It is made of flat lying piles of flows of fissural origin, with no identified emission centres, except for silicic, frequently products found in the uppermost part of the series (Fig. 5.1). These relate to central volcanoes generally developed at the intersection of the dominantly NNW direction of normal faulting with other fault direction, either clearly transverse or linked with local features, such as around the Affara Dara massif.

It should be stressed that, north of 13°N, the stratoid series is absent and the axial ranges (less than one million years ago) appear as the first visible magmatic products of the Afar floor, showing a later, but more abrupt, oceanisation process. The coincidence of the age of the stratoid series with the penetration of the Aden ridge in Afar through the Gulf of Tadjourah on one side, and the identification of the axial through in the Red Sea should be noted. This is not just a coincidence, as it appears that this major step in the evolution of the Afar floor, in which spreading segments are not yet well defined, allowed establishment of the link between the Red Sea and the Aden oceanic spreading through Afar.

5.1 The Basaltic Fissural Piles (Afar Stratoid Series *Stricto Sensu*)

The stratoid series is affected on the whole Afar floor—except for along the Red Sea side on a 70–100 km-wide area—by an important extensive tectonics of dominantly NNW (Red Sea) direction, which probably also corresponds to the direction of the feeding dikes, as the absence of dikes observed in the numerous faults practically rules out the existence of any other feeding direction other than the Red Sea one for the whole outcropping series.

The young fault scarps affecting this unit following its emplacement exhibit up to 1500 m high sections, generally

without any break or unconformity, the actual base being hidden, and the surface frequently still showing the flow patterns, such as Aa-type basalt surfaces (e.g. Maska area) or blistered ignimbrites (e.g. south of Gad Elu). A few late feeding fissure—less than one million years old—show NNW trends as observed here and there by alignment of scoria cones on the most recent stratoid series surfaces.

To the south, it appears less intensively faulted than in central Afar. Faulting and block tilting have been continuous during the emplacement of the stratoid series as indicated in several fault scarps by the increase of the dip towards the bases. In several cases, the dip in the lower part of the section—as well as the level of alteration of the lava flow—is so important that it could be mistaken for another older unit.

Nearly 50 age determination have been carried out on this unit by Barberi et al. (1972), Civetta et al. (1975), Chessex et al. (1975) and Barberi et al. (1975), as well as more authors in the last 40 years working on this and surrounding units (Berhe et al. 1987; WoldeGabriel et al. 1990a, b; Ebinger et al. 1993; Tefera et al. 1996; Chernet et al. 1998; Renne et al. 1999; Utskins et al. 2002; Wolfenden et al. 2004, 2005, etc.). These show that the stratoid series ranges in age from 4.4 to 0.4 million years (Fig. 5.2). Despite these repeated searches, no older age could be obtained.

It should be noted that a few sedimentary episode, lacustrine or detritic, are observed in the uppermost section of the stratoid series, particularly in southern and eastern Afar. Hyaloclastites are also observed in some sections of central-eastern Afar (Demange et al. 1980). These observations show that tectonic basins existed on the Afar stratoid surface before the presently visible horst and graben structures developed.

The stratoid series developed since the Gulf of Aden ridge penetrated Afar through the Gulf of Tadjourah, ensuring a link with the newly developed oceanic rift of the Red Sea axial trough. It was interpreted by Treuil and Varet (1973), Barberi et al. (1975) and Barberi and Varet (1977) as



Fig. 5.1 View of one of the numerous fault scarps affecting the stratoid series in central Afar (south–western fault of the Gaggade graben, Djibouti Republic). Rhyolite flows issued from the Baba Alou rhyolitic centre are observed towards the top of the unit (*Photo J. Varet 2014*)

the surface expression of oceanic type of floor, despite the fact that the evidence for accretion confined to single axis of spreading is lacking before the emplacement of the axial ranges in the last one million years.

5.2 The Silicic Centres Associated with the Stratoid Series

Silicic centres are well visible in the Afar floor landscape as they constitute the few most elevated mountains that can be observed in the depression. It is also because they developed generally in the latest phase of the stratoid series and belong to the youngest volcanic events, although more recent basaltic flows are frequently observed in their immediate surroundings (Fig. 5.3).

As shown by Barberi et al. (1972), these central units developed at the intersection of the regional Red Sea (NNW) and Aden (NW) directions of spreading with transverse faults (Fig. 5.4). These either result from earlier fracture zones or from the development of shear zones or embryonic transform faulting. The Baba Alou massif (see Fig. 5.5), however, appears in the middle-upper level of the unit. This is also the case for the thick rhyolite flows surrounding Dahwi – Adda’Do graben, these two units being the largest (20 km in diameter) and for a smaller silicic dome displaying a nice “onion type” of structure that is observed at Asa Yager south of the Djibouti-Ethiopia border (Fig. 5.6).

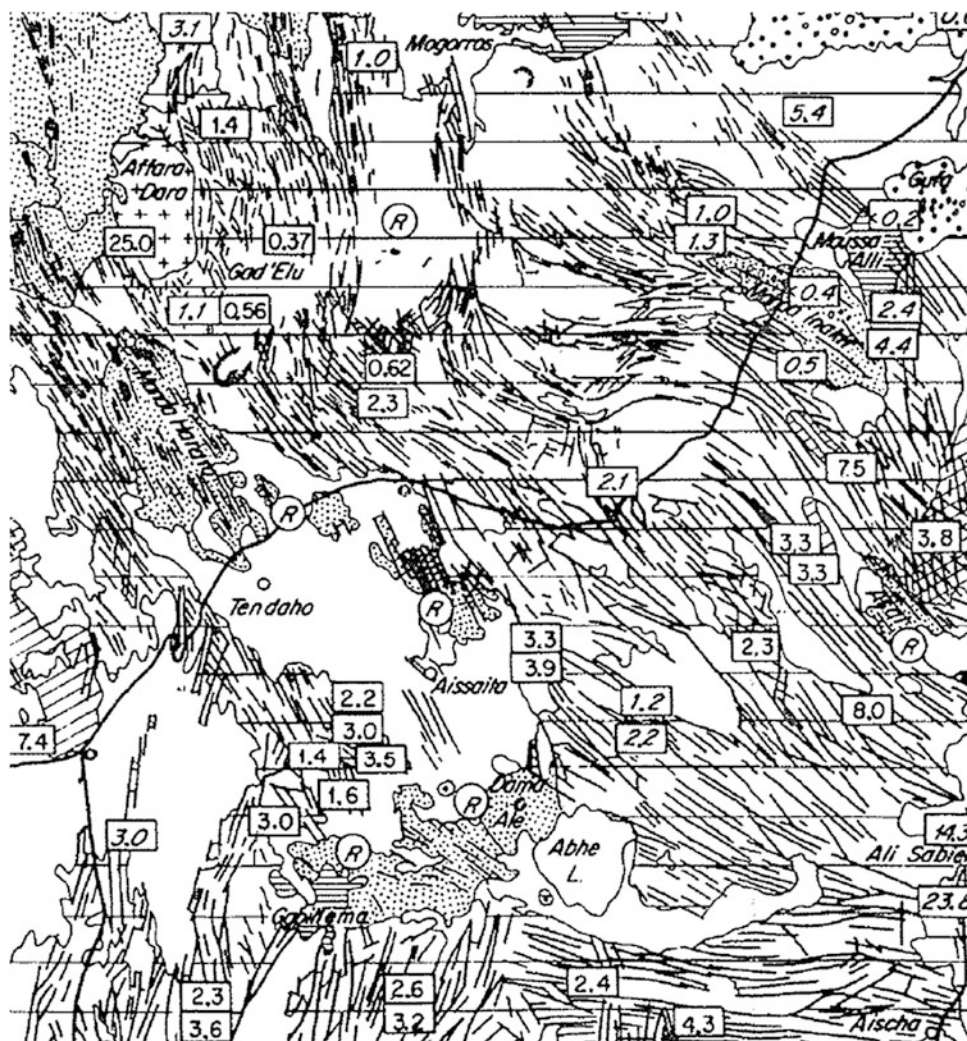
At least two tectonic directions intersect at the location of these central volcanoes: NW and NE at Baba Alou, NNW and NNE at Dahwi – Adda’Do, and NW and NNW at Asa Yager.

These silicic centres are of two types: either simple enormous domes displaying variations in crystallinity and vesicularity of the erupted lava as at Asa Yager and in the volcanoes located east from Affara Dara or complex strato-volcanoes with intercalations of glows, domes, ignimbrites and tuffs, frequently cut by numerous dikes as in ‘Ela. Calderas are sometimes observed as in Musle, Dawa Ale and Oyma, but most are built without any visible sink. The rocks range from microcrystalline to vitreous and obsidian as at Gad’Elu. Obsidians were frequently used as a source for tools and paleolithic emplacements of workshops are frequently found on flat surfaces at the top of obsidian domes where “unsold” products accumulated.

Dykes feeding these piles are sometimes observable, as in Dawa Ala and Oyma. They are very similar in composition and texture to the peralkaline microgranite facies at Affara Dara. This could mean that hypovolcanic granitic bodies—similar to the one observed at the surface at Affara Dara but younger—may exist beneath the stratoid series.

Despite the lack of sufficiently detailed analysis, no apparent relation exist between the silicic centres and the stratoid series. The rhyolite sits on the basalt trap and spatter cones and associated basaltic flows are frequently found postdating these rhyolitic volcanoes, as observed in Ali Mela

Fig. 5.2 Age determinations obtained in central Afar by Barberi et al. (1975) showing that the inner Afar floor is occupied by volcanic units (Afar stratoid series and associated rhyolite centres) ranging in ages from 5.3 to 0.56 million years



Ale, Didoli, Egersuwa or Ado Ale. These silicic units do not appear to result from a volcanological evolution of the stratoid series, and no chronological evolution could be related to petrography from the dominantly basaltic stratoid series towards the silicic volcanoes. On the contrary, basaltic flows of similar compositions are indiscriminately found below as well as over the silicic products. The petrology of the stratoid series, made of transitional basalts geographically associated with rhyolitic volcanoes of mostly peralkaline composition, however, seems to indicate a genetic link between the two volcanic units, and the global proportion of basalts—largely dominant over the rhyolites—would be compatible with a medium-depth-seated magmatic differentiation, also illustrated by the overall evolution of the rocks sampled from the two categories of units (Fig. 5.7), despite the scarcity of intermediate products. Such phenomena may occur in magma chambers trapped according to the intersecting extensive tectonic direction.

In general, the most evolved products in the rhyolitic centres show a comenditic affinity. Variations are, however,

observed from one centre to another. Some are more potassium rich, as at Gad Elu, whereas Ela is made of non-peralkaline soda rhyolites. As a general rule, however, it appears that meta-aluminous rhyolites are found in the axial part of Afar, when peralkaline and eventually more potassic magmas are found towards the margins and southern Afar. This also relates to slightly more alkali basalts in the stratoid series. Pantelleritic trachytes are found in eastern centres (Oyma, for instance) and pantellerites in southern Afar only (Gabilema, for instance). This regional variation observed in the basalts and rhyolites within Afar is also reflected in the strontium isotopic ratios as observed by Civetta et al. (1975).

A particular example of a central volcano associated with the stratoid series is the Afdera volcano (Fig. 5.8), located in a central position of the depression at the northern extremity of the stratoid series outcrops. It is a central steep cone of rhyolite flows in which pyroclastic products are absent. It also displays late terminal volcanic activity with basaltic cones and rhyolites domes aligned along a N–S direction at its southern foot, which appear to be too young to be dated

Fig. 5.3 View of basaltic scoria covering the southern foot of the Bad'I rhyolitic centre, western Afar (*Photo J. Varet 2015*)



by K/Ar methods (Barberi et al. 1972). As a whole, a complete series of volcanic products is found there from tholeiitic basalts to rhyolites, which do not show any per-alkaline tendency (Fig. 5.9).

This volcano appears to be located at the intersection of the regional NNW (Red Sea) extensive trend with a NNE distensive tectonics observed at its SE limit, which extends further north on the floor of Lake Afrera (Bonatti et al. 1977). The development of this remarkable volcano is clearly linked with this tectonic intersection which favoured the development of a magma chamber, allowing for this clear sequence of differentiation.

The NNE faults observed south of Afdera could represent the surface expression of a transform fault of NE direction, ensuring the connection between the Manda Harraro single rift segment and the twin rifts of Alayta and Tat'Ali. Along the main spreading segment, this extends down to Dabbahu volcano sitting between the two Alayta and Manda Harraro spreading segments (see Sect. 6.4).

5.3 The Recent Basaltic Flows of the Upper Part of the Stratoid Series

Whereas in the last million years the volcanic activity concentrated in specific volcanic units, which is presented in next chapter, in various places, mainly around the rhyolitic centres

but also independently from them, such as south from Afdera, in Maska, Bakila, or Rosa (see indigo blue units in Fig. 5.4), basaltic flows are emitted that postdate the stratoid series and the major tectonic activity that affected it. In some cases, such as at Eli Da'ar, an interval of erosion and detritic—or even lacustrine—sedimentation occurred between the stratoid series and the emission of the flow of this unit. These units are easily distinguished from the stratoid series because of their well-preserved contours, flow surface and emission centres (scoria and spatter cones). They appear generally of slightly more alkaline nature than the underlying basalts of the stratoid series. This distinction is, however, not always easy, as it may also appear that the surface of the stratoid series itself may display such young-looking volcanic figures, despite being heavily tectonised (Fig. 5.10). Moreover, as noticed above, the tectonic activity was continuous during the emplacement of the stratoid series and sediment intercalations are found here and there. Events similar to those distinguished on the map (in indigo blue, Fig. 10.6) have therefore occurred previously. Post-tectonic basalts displaying a cartographic discordance are clearly observed in the stratoid series south from Eli Da'ar and Afofle, north of Asela. Near Ballto, the discordance is well marked by detritic sediments. In mapping this unit we therefore simply distinguished the last phase of the volcanic activity of the stratoid series, that is fissural flows not clearly related to the well-defined axial units. The most recent is observed in the Maska area, where a

Fig. 5.5 Detail view of a typical rhyolite flow from central Afar acidic centre, several 10 m thick (SW Baba Alou; J. Varet 2013)



Fig. 5.6 Asa Yager silicic centre revealing an “onion structure”. Of reddish colour, it is surrounded by “ring dykes”; white areas at the periphery and across reflect zones affected by epithermal activity (Google Earth image)



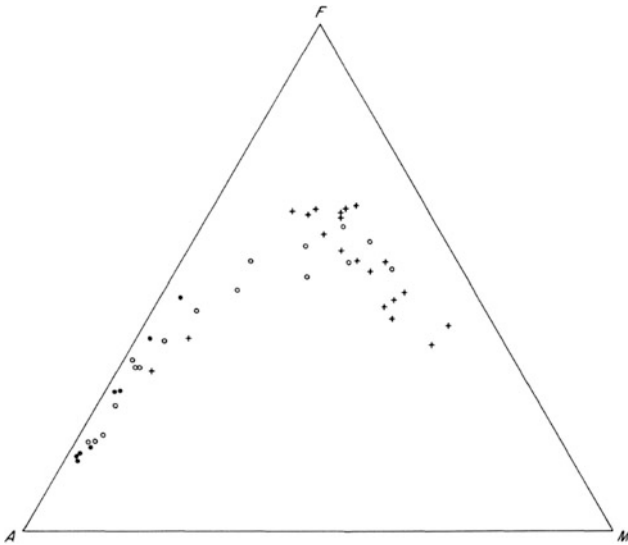


Fig. 5.7 AFM diagram showing the range of variation of the composition of the volcanic products from the stratoid series (*crosses*) and silicic centres (*circles*), filled when peralkaline (Barberi et al. 1973)

5.4 Spectacular Grabens Delimited by the Faulting Affecting the Stratoid Series in Southern Afar

Important grabens are observed, cutting through the stratoid series, all over Afar. In eastern Afar, the tectonically active Dobi (see, for instance, the 1989 event described by Jacques et al. 1999) and the curvilinear Immuno graben (Fig. 5.11) observed in Ethiopia on the road to Assab extends in Djibouti Republic through the Alol and Sakalol grabens

Fig. 5.8 Afdera central silicic volcano as observed on the northernmost extremity of the Afar stratoid series outcrop, seen from the eastern shore of lake Afdera (Photo: collection G. Marinelli, Pisa)



(Fig. 5.12). Hydrothermal manifestations are abundant in these active areas, both in the grabens and in the horsts between them (as in Alida'ar).

Pagli et al. (2014) could demonstrate, from velocity fields obtained from INSAR and GPS data, that, besides rift segments that have been evolving through repeated magma intrusions along axial ranges, extension is also accommodated by faulting in these grabens, through widespread strain accommodation area across them. These grabens hence testify that different modes of strain accommodation develop in the same time in Afar along the magmatic axial ranges in the tectonic grabens.

In the Djibouti Republic (SE Afar), the important extensive faulting affecting the stratoid series results in a particularly spectacular succession of horst and graben, the last progressively filled by sediments, first detrital, then lacustrine (with several Plio-Pleistocene variations analysed by Gass 1975) and finally evaporitic. It appears that the age of the formation of the graben is tending to become younger from south to north (Fig. 5.13). This appears from the radiometric age determinations obtained from the basalts collected along the fault scarps from bottom to top (Barberi et al. 1975) as well as from those found at the top.

It was shown by K/Ar dating of rhyolites that ages of the silicic domes vary considerably. The age of the Gobaad graben (including Lake Abhe) dates back to 2.7 million years ago, whereas Hanlé graben is 2.5 million years old, Gaggadé 2.0 million years old and Asal 1 million years old (Gasse et al. 1980). The emerging picture is that the axis of spreading producing the stratoid series progressively migrated from south to north. This migration also effected the later extensive faulting determining the horst and graben.

Fig. 5.9 Variation diagram for the lava flows from Afdera volcano (Barberi et al. 1973)

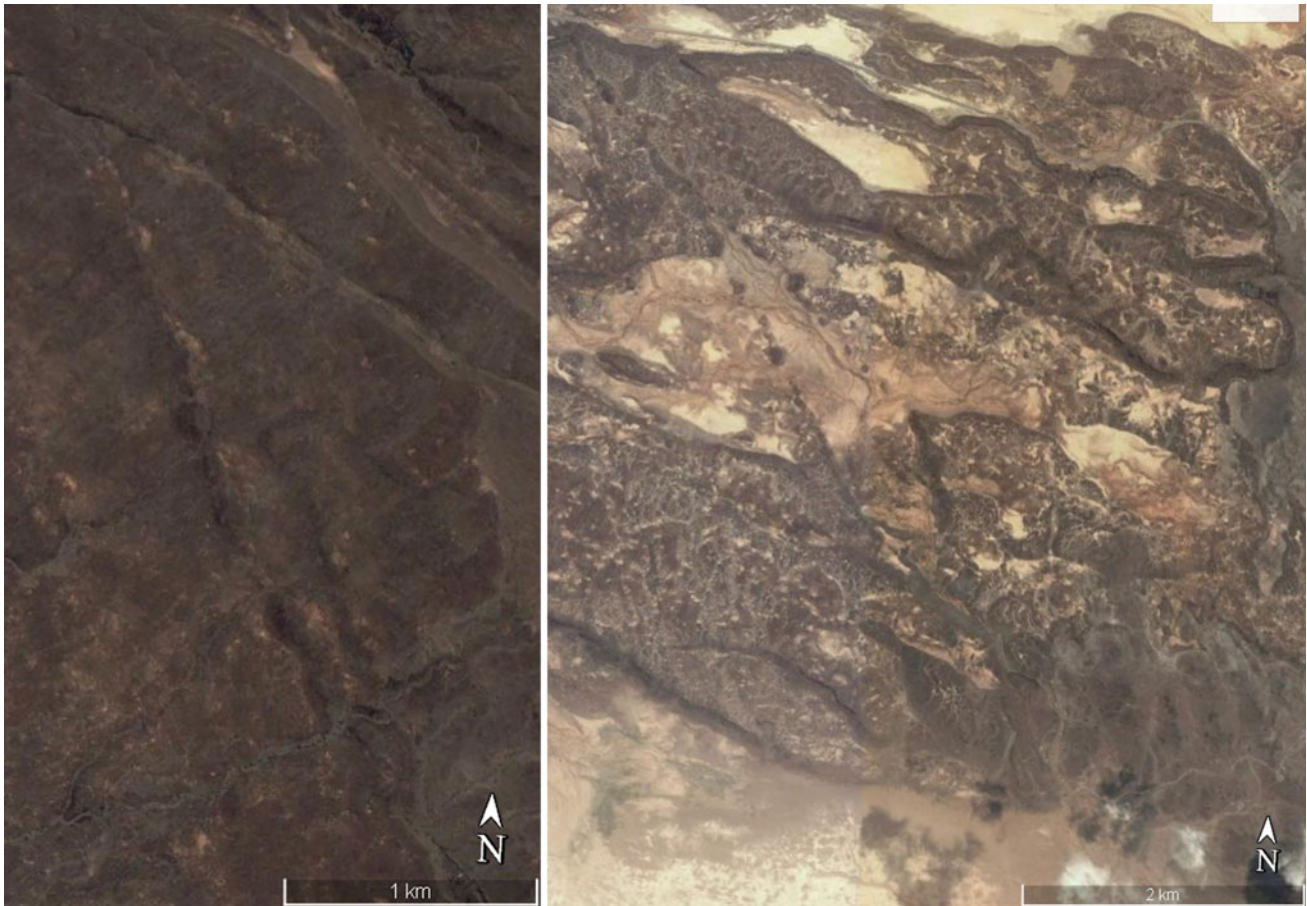
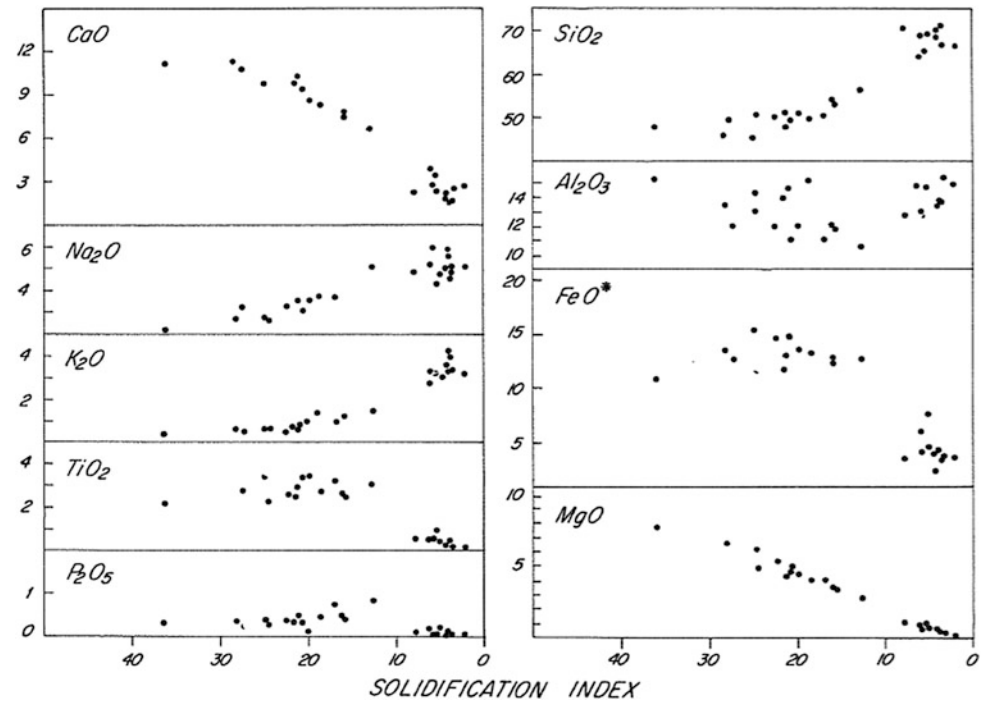


Fig. 5.10 Alignments of basaltic spatter cones along emissive fissures of NNW direction visible at the surface of the stratoid series, south from Ghoubbet (Google Earth image)

Fig. 5.11 Gum'a Graben (Ethiopia), between Immino (N) and Dobi (S) grabens, as seen along the road to Assab from southern fault scarp, looking NW (Photo J. Varet 2015)



Fig. 5.12 The Alol and Sakalol graben as seen from the northern fault scarp (looking SE); green areas are wet zones thanks to hot springs. The floor is filled with eolian, lacustrine and evaporitic sediments. Basaltic blocks offer a typical view of the surface of the stratoid series (Photo J. Varet 2012)



This movement can be tentatively related (Fig. 5.14) to the progressive migration of the Gulf of Tadjourah apex which penetrated in the same period from east to west towards Afar (Richard and Varet 1979; see Sect. 6.8).

Hence the NW–SE line bordering the Aisha block appears to have first played the role of a right lateral transform fault 2.7 million years ago over a width of 75 km, which progressively reduced with time, reaching its present

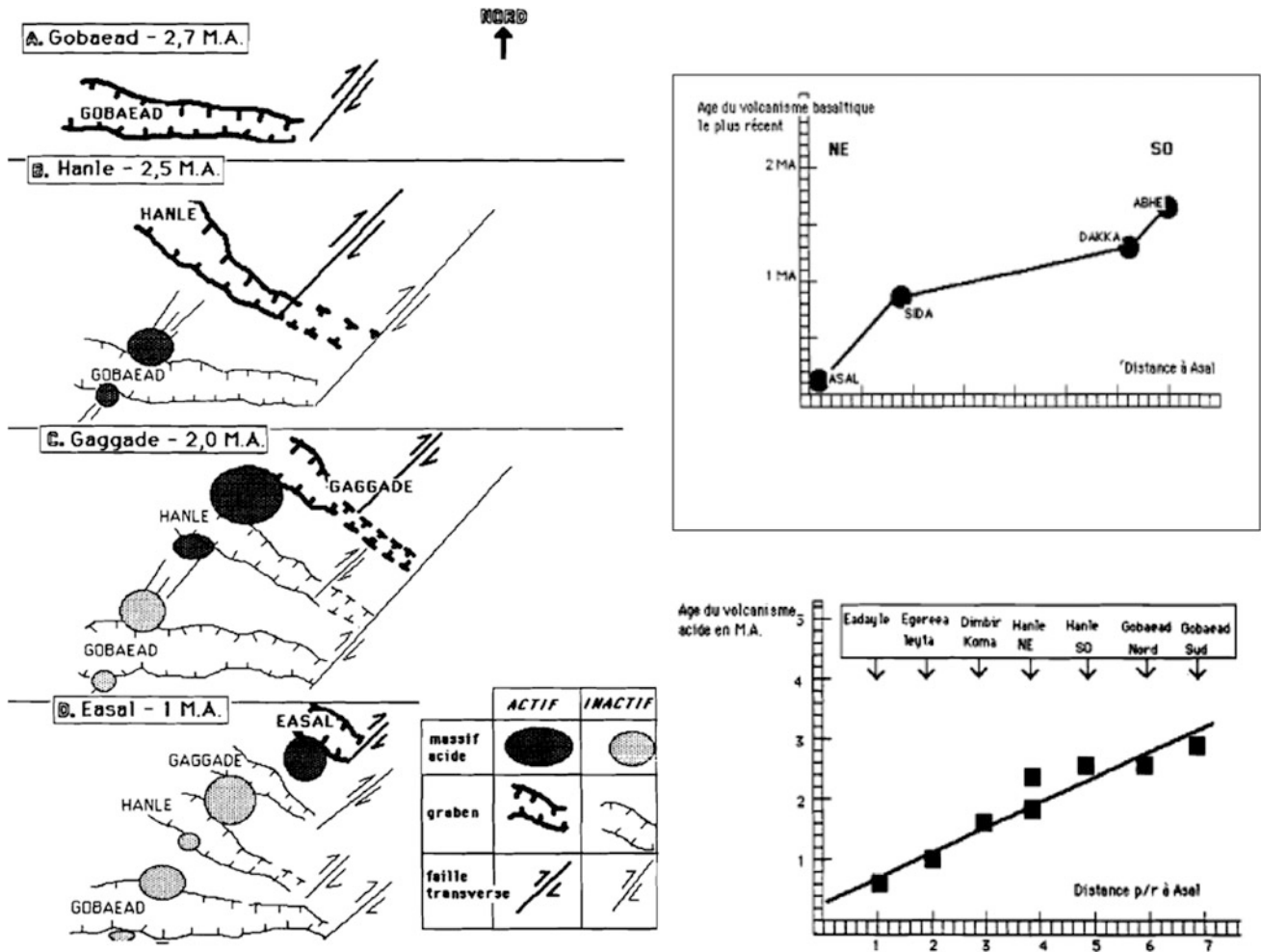


Fig. 5.13 Decreasing age of the grabens and of the most recent volcanic formations that were emitted before the episode of major faulting. From south (Goba'ad) to north (Asal) as shown by the geological notice of Dikhil (Gasse et al. 1980)

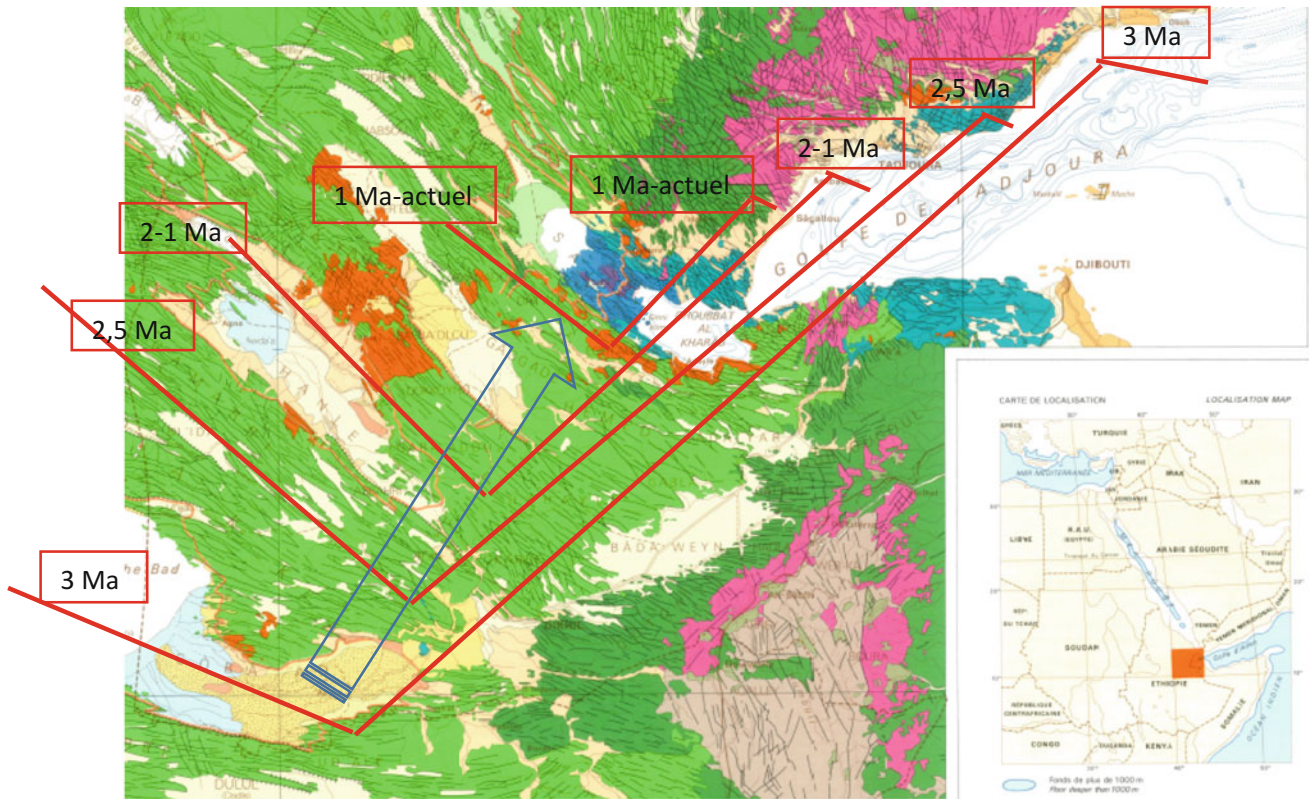


Fig. 5.14 Possible migration from SE to NW of the spreading axis in Afar in the last three million years (*blue empty arrow*), linked with the progressive penetration of the Gulf of Aden ridge from east to west within Afar. The border of the Aisha'a block, trending SW-NE,

appears to have played the role of a transform fault during that period (see Bour-Ougoul fault line in Fig. 4.18). Observe that the extensional direction in Afar turned from WNW-ESE to NW-SE during the same period

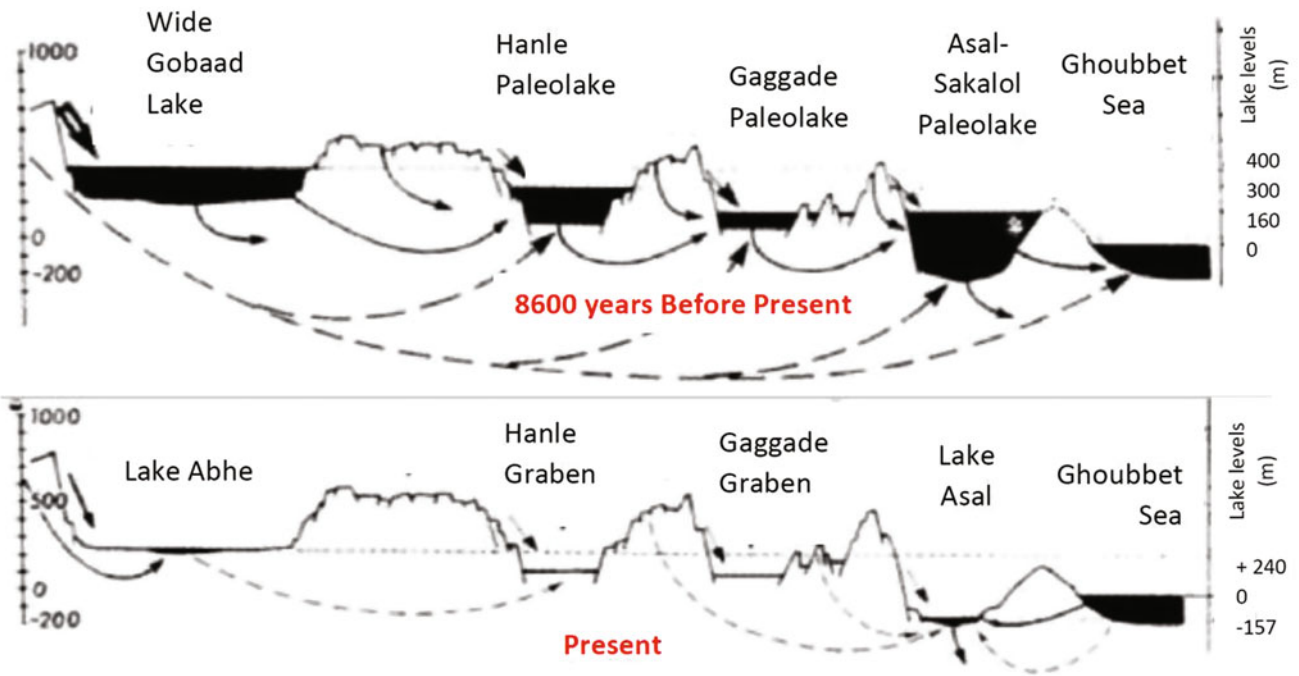


Fig. 5.15 The past 8500 years taken to present water levels, surface and subsurface circulations from EW to NE in the graben of western Afar

status 1 million years ago when the Asal-Ghoubbet rift formed and developed a real spreading segment of oceanic type through the much shorter Arta transform fault.

It also appears that, as the stratoid series was clearly built from and then affected by the extensive tectonics of Red Sea – Gulf of Aden direction, a progressive rotation of the dispersive system affecting Afar in that area is observed from the E–W direction (Goba'ad) to NW–SE in Asal.

The grabens, once formed, have been progressively filled by sedimentary deposits, detrital and lacustrine. From Plio-Pleistocene to the recent Pleistocene, most grabens were occupied by lakes, fluctuating in size and composition with climates that left deposits along the borders (see Sect. 10.1). Their thickness reaches several hundred metres, which means that the underlying basaltic basement is locally at depth below sea level. The sedimentary filling of these grabens was studied along the Awash River (for human prehistory) and the Tendaho and Hanlé grabens were surveyed at depth by geophysics and drilled for geothermal exploration. Whereas Tendaho provided interesting results that justified further investigations, no interesting geothermal gradient was encountered at Hanlé and this was interpreted as resulting from SW–NE groundwater movements across the graben structures from Gobaad (and the Awash River lower basin) towards Asal (Fig. 5.15).

References

- Barberi F, Borsi S, Ferrara G, Marinelli G, Santacroce R, Tazief H, Varet J (1972) Evolution of the Danakil Depression (Afar Ethiopia) in light of radiometric age determination, *J Geology* 80:720–729
- Barberi F, Tazief H, Varet J (1972) Volcanism in the Afar depression: its tectonic and magmatic significance, *Tectonophysics*, 15:19–29
- Barberi F, Chemine'e JL, Varet J (1973) Long-lived lava lakes of Erta Ale volcano. *Rev Geogr Phys Geol Dyn* 15:347–352
- Barberi F, Ferrara G, Santacroce R, Varet J (1975) Structural evolution of the Afar triple junction. In: Pilger A, Rösler A (eds) *Afar Depression of Ethiopia*, Stuttgart (Schweizerbart), 38–54
- Barberi F, Varet J (1977) Volcanism in Afar: small-scale plate tectonic implications. *Bull Geol Soc Amer* 88:1251–1266
- Berhe SM, Desta B, Nicoletti M, Teferra M (1987) Geology, geochronology and geodynamic implications of Cenozoic magmatic province in W and SE Ethiopia. *J Geol Soc London* 144:213–226
- Bonatti E, Gasperini E, Viglotti L, Lupi L, Vaselli O, Polonia A, Gasperini L (1977) Lake Afrera, a structural depression in the North far Rift (Red Sea) Heliyon, 3
- Chernet T, Hart WK, Aronson JL, Walter RC (1998) New age constraints on the timing of volcanism and tectonism in the northern Main Ethiopian Rift—Southern Afar transition zone (Ethiopia). *J Volcanol Geothermal Res* 80:267–280
- Chessex R, Delaloye M, Muller J, Weidmann M, (1975) Evolution of the volcanic region of Ali Sabieh (T.F.A.I.) in the light of K–Ar age determination. In: Pilger A, Rösler A (eds) *Afar Depression of Ethiopia, Proceedings of an International Symposium on the Afar Region and Related Rift Problems*, Bad Bergzabern, F.R. Germany, April 1–6, 1974, vol. 1. E. Schweizerbartsche Verlagsbuchhandlung, Stuttgart, pp 220–227
- Civetta L, DeFino M, Gasparini P, Ghiara MR, LaVolpe L, Lirer L (1975) Geology of central-eastern Afar (Ethiopia). In: Pilger A, Rosler A (eds) *Afar depression of Ethiopia, proceedings of an international symposium on the Afar region and rift related problems*, Bad Bergzabren, Germany, 1974, vol. 1, E. Schweizerbart'sche Verlagsbuchhandlung, Stuttgart, Germany, pp 259–277
- Demange J, Stieltjes L, Varet J (1980) L'éruption d'Asal de novembre 1978. *Bull Soc Géol France* 12 (6):837–843
- Ebinger CJ, Yemane T, WoldeGabriel G, Aronson JL, Walter RC (1993) Late Eocene-Recent volcanism and faulting in the southern main Ethiopian rift. *J Geol Soc London* 150:99–108
- Gass IG (1975) Magmatic and tectonic processes in the development of the Afro-Arabian Dome. In: Pilger A, Rosler A (eds) *Afar depression of Ethiopia, proceedings of an international symposium on the Afar region and rift related problems*, Bad Bergzabren, Germany, 1974, vol 1, E. Schweizerbart'sche Verlagsbuchhandlung, Stuttgart, Germany, pp 10–18
- Gasse F, Richard O, Robbe D, Rognon P, Williams MAJ (1980) Evolution tectonique et climatique de l'Afar central d'après les sédiments plio-pleistocenes. *Bull Soc Geol France* 6:987–1001
- Jacques E, Ruegg JC, Lepine JC, Tapponnier P, King GCP, Omar A (1999) Relocations of M = 2 events of the 1989 Dobi seismic sequence in Afar: evidence for earthquake migration. *Geophys J Int* 138:447–469
- Pagli C, Wang H, Wright TJ, Calais E, Lewi E (2014) Current plate boundary deformation of the Afar rift from a 3-D velocity field inversion of InSAR and GPS. *J Geoph Res* 119(11):8562–8575
- Renne PR, WoldeGabriel G, Hart WK, Heiken G, White TD (1999) Chronostratigraphy of the Miocene-Pliocene Sangantole Formation, Middle Awash Valley, Afar rift, Ethiopia: *Geol. Soc Amer Bull* 111:869–885
- Richard O, Varet J (1979) Study of the transition from deep oceanic to emerged rift zone: gulf of Tadjoura (Republic of Djibouti). *Int Symp Geodyn Evols, Afro-Arabian System*, Roma
- Tefera M, Chernet T, Haro W (1996) Geological map of Ethiopia: Ethiopian institute of Geological Surveys, scale 1:2,000,000, 1 p
- Treuil M, Varet J (1973) Critères volcanologiques, pétrologiques et géochimiques de la genèse et de la différenciation des magmas basaltiques exemple de l'Afar. *Bull Soc Géol France* 7(15):506–540
- Ukstins IA, Renne PR, Wolfenden E, Baker J, Ayalew D, Menzies M (2002) Matching conjugate volcanic rifted margins: 40Ar/39Ar chronostratigraphy of pre- and syn-rift bimodal flood volcanism in Ethiopia and Yemen: *Earth and Planetary Science Letters*, vol 198, pp 289–306
- Varet J (2004) De l'Afar à la géothermie. In: Haroun T (ed) *une vie de feu*, Glénat, pp 85–94
- WoldeGabriel G, Aronson JL, Walter RC (1990) Geology, geochronology and rift basin development in the central sector of the Main Ethiopian Rift. *Geol Soc Am Bull* 102:439–485
- Wolfenden E, Ebinger C, Yirgu G, Renne P, Kelley SP (2005) Evolution of the southern Red Sea rift: birth of a magmatic margin. *Bull Geol Soc Amer* 117:846–864
- Wolfenden E, Yirgu G, Ebinger C, Ayalew D, Deino A (2004) Evolution of the northern Main Ethiopian rift: birth of a triple junction, *Earth planet. Sci Lett* 224:213–228

Part III

**Afar Quaternary and Presently
Active Geological Units**

In this chapter we describe the volcano-tectonic units that could be distinguished since the early stages of exploration of Afar by the CNR-CNRS team (Tazieff et al. 1972; Barberi et al. 1970, 1972a). It was shown that Afar is characterised by rather different types of volcanic units, all of recent Quaternary age, displaying quite distinctive volcanological and petrological characteristics depending upon their structural location (position in the depression, tectonic control). These distinctions have not been contradicted by later observations undertaken in Afar and can be considered as still valid; understanding has been improved by most recent work.

We describe successively four types of volcanic units, and add the description of some of the most striking features of the neo-tectonics that appears to have developed at the same time as these magmatic entities. All these units are active—tectonically, volcanically and hydrothermally (fumaroles or hot grounds). The sketch map of Fig. 118 summarises the occurrence of these units within Afar. These four volcanic units are:

- The axial volcanic ranges made mainly of transitional basalts and some differentiated lavas emitted along well-defined open fissures
- The mainly silicic and pyroclastic volcanoes, with associated minor basalts, generally with calderas, located along the margins of the depression
- The transversal volcanic ranges, made of basaltic lavas and scoria cones, located along the Afar margins, mainly along the Red Sea side
- The central volcanoes, also generally with calderas, with associated fissural basalts, located in southern Afar along the northern extension of the MER

6.1 Afar Axial Ranges (Emerged MOR Analogues)

The axial ranges were named after the discovery of the Erta Ale range, which occupies an axial position between the salt plain and Lake Afrera along the northern part of the Danakil rift. With the exception of one volcano sitting on the south-western flank of the range, it was emitted along a unique open fissure along a single axis of magma injection, the lavas being emitted and flowing on both sides. This range also offers the particularity of displaying all the stages of a volcanic evolution that have encountered the volcanic sub-units, from the fissural rift, to the shield and then cumulo-volcano stages.

At the other extremity of the Afar depression, the Asal range, which extends on the continuation of the Ghoubbet submarine (oceanic) rift, also displays all the characteristics of an axial range at the early rifting stage, despite having eventually passed through a shield volcano stage. These two typical volcanic units are built along NNW (Erta Ale) or NW (Asal) directions. This is also the case for another four of them recognised within Afar: Ta'Ali, Alayta, Manda Harraro and Manda Inakir (CNR-CNRS Afar team 1973). All are quite young, with lava flows ranging from 1.2 million years ago to present. All these ranges probably encountered historic eruptions, despite the lack of scientific descriptions (Fig. 6.1).

From the petrological point of view, they are all characterised by transitional basalts, near to tholeiites as found in Mid-oceanic ridge basalts (MORB). Basalts are largely dominant over associated differentiated products that have been shown to be linked with the basalts by crystal fractionation in low-pressure, rather superficial magmatic reservoirs (Barberi et al. 1972a; Treuil and Varet 1973). In all these ranges the lava flows are dominant and pyroclastic

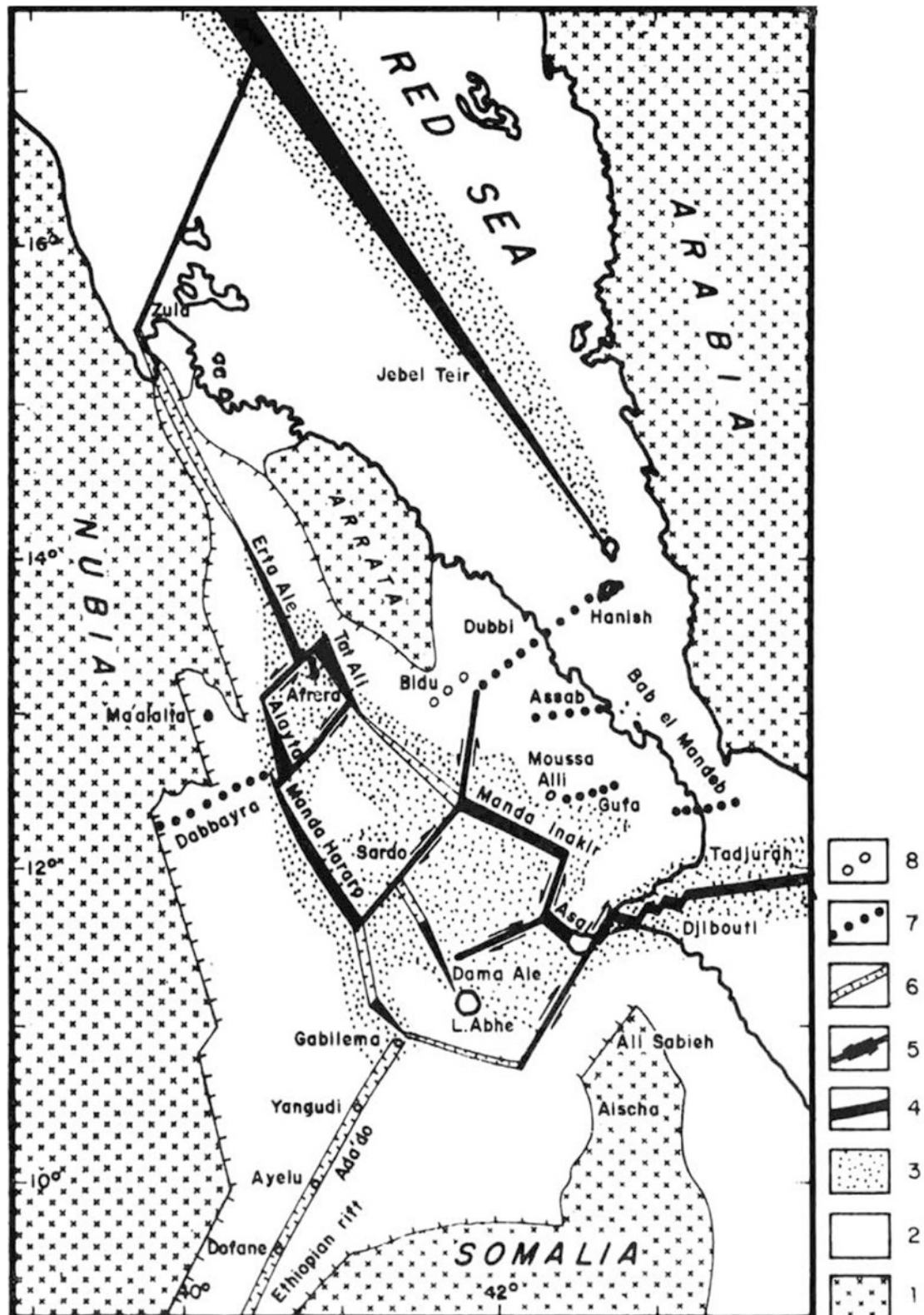


Fig. 6.1 Sketch map of the Afar recent Quaternary volcanic units in their geological context. 1 pre-mesozoic basement; 2 areas covered by volcanic formations of post-miocene pre-quaternary age (20 to 4 million years ago); 3 Afar stratoid series (3.4 to 1 million years ago); 4 Axial ranges with oceanic type of rifting; 5 zones of transform

faulting (with strike slip motions); 6 graben structures displaying characteristics of continental rifting, with indication of central volcanoes (circles); 7 transverse basaltic alignments of scoria cones and flows; 8 central silicic volcanoes with ignimbrites and calderas. From Barberi and Varet (1975), Wager prize lecture

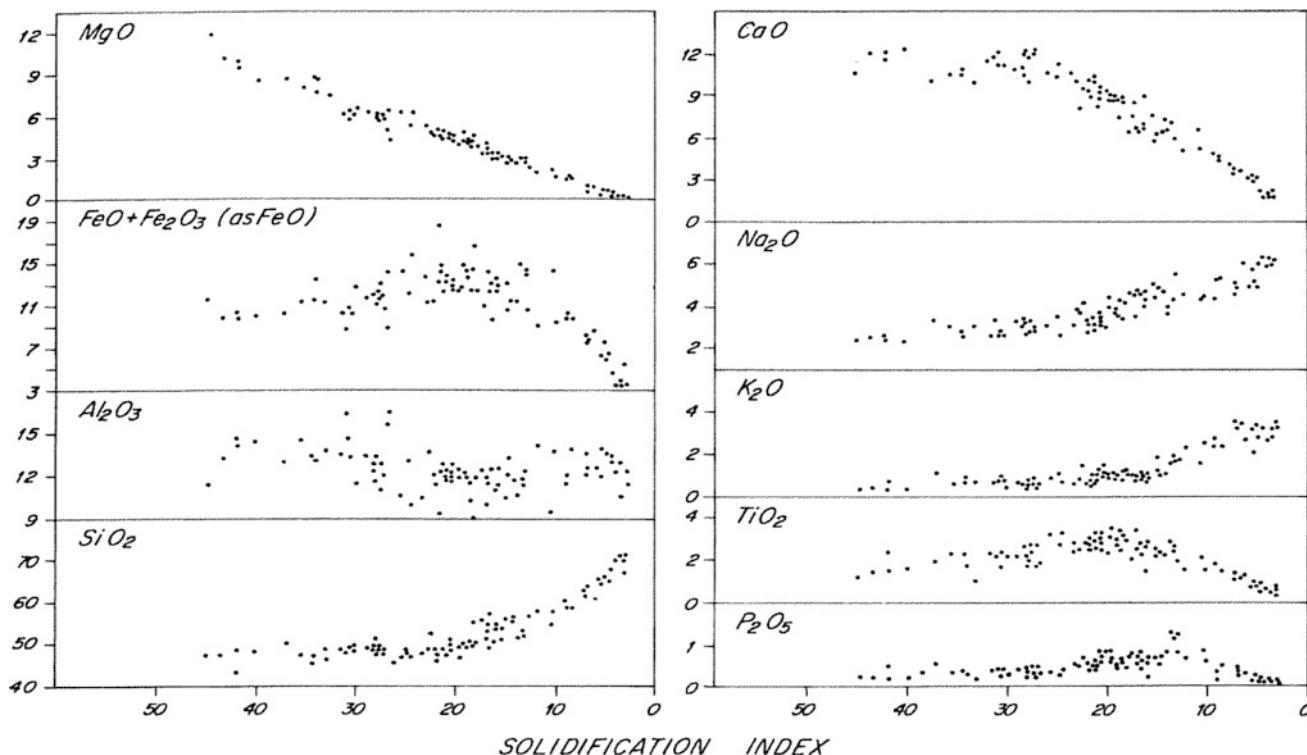


Fig. 6.2 Major elements for the rocks forming the Erta Ale range, plot against the Solidification Index ($\text{MgO} \times 100 / \text{MgO} + \text{FeO} + \text{Fe}_2\text{O}_3 + \text{Na}_2\text{O} + \text{K}_2\text{O}$). From Barberi et al. (1971)

products very rare, even for the most evolved products. In fact a similar volcanological evolution is clearly observed in all these ranges, which appears to be controlled by the volcanological evolution, with differentiated products found only in very limited quantitative proportions. They all trend from transitional basalts towards iron-rich terms, a sequence characteristic of tholeiitic sequences (Fig. 6.2). This evolution happens when the ranges evolve from fissural to shield volcano stage. In most axial ranges, the evolution does not go beyond that stage, but it may happen that cumulo-volcano development takes place in a final stage where the composition of the magma may reach silicic compositions, with compositions ranging from meta-aluminous to peralkaline rhyolites (Fig. 6.3).

We see that if each unit stem for a single parent basaltic magma produces more or less differentiated products by crystal fractionation from one unit to another, the magma changes slightly, as shown by Treuil and Varet (1973). Geochemical studies showed that if in a single unit crystal fractionation fully explains the variations encountered, the differences noted from one unit to the other could be explained by slight differences in the degree of partial melting of each initial parent basalt possibly from a single mantle source. We now describe all of them in more detail before drawing more general conclusions.

6.2 Erta Ale Axial Range

We named this emblematic unit after its most spectacular sub-unit, the Erta Ale Shield volcano, with its calderas and two active lava lakes. It extends over a length of 80 km with a variable width (of 8–42 km, generally increasing from north to south) with a visible bottom at 120 m below sea level and a maximum altitude of 613 m (Erta Ale caldera). The range is located on the axis of the northern Afar depression, at an equal distance from both Nubian and Danakil Alps escarpments (Fig. 6.4). The width of the rift increases from north to south as a result of the rotation of the Danakil Alps, and the width and volume of emitted products along the Erta Ale range also increase from north to south, apparently as a response to this increasing drift. The total surface covered by lavas is about 2.350 km².

Although the whole area was investigated by the CNR-CNRS Afar Team and mapped at the scale of 1/500,000 (Tazieff et al. 1969, 1972; Tazieff and Varet 1969; Barberi et al. 1970, 1972a, b), the Erta Ale range was more precisely described by Barberi and Varet (1972), and a detailed map was published in the same year at 1/100,000 scale, and further petrological, mineralogical and geochemical studies were conducted (Treuil et al. 1971; Treuil and Varet 1973).

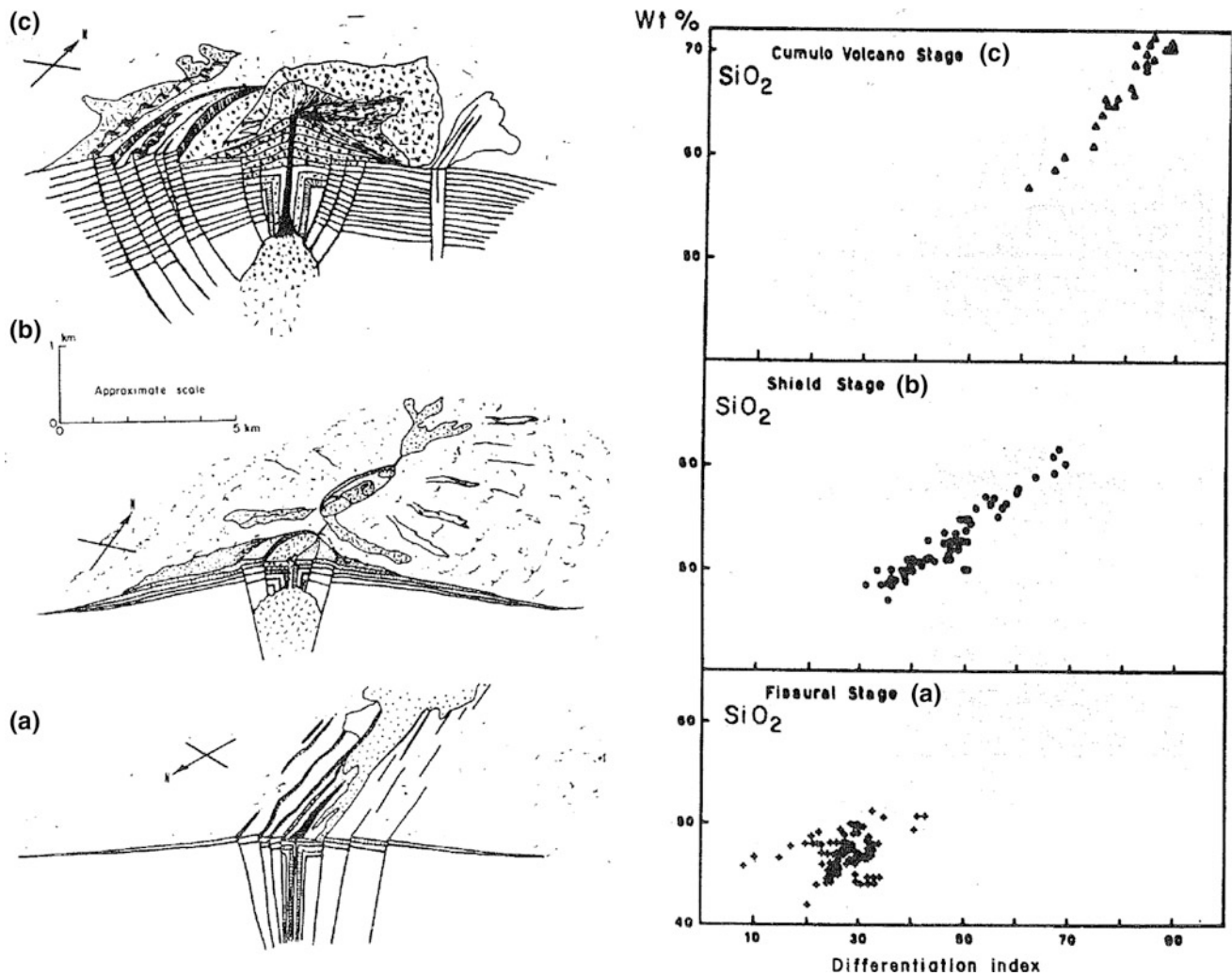


Fig. 6.3 Three stages of volcanological evolutions encountered in axial ranges in Afar: **a** fissural stage (axial rift-in-rift); **b** shield volcano stage (with shallow magma chamber, eventually at surface with lava lake) formed by accumulation of lava along the emissive axis; **c** cumulo-volcano developed at the favour of circular concentric ring

The first studies of the lava lakes were developed in the same period by Tazieff et al. (1972), Zettwoog et al. (1972), Barberi et al. (1973), Giggenbach and Le Guern (1976), Le Guern et al. (1979) and Gerlach (1989), and were followed by many other up to recently (Oppenheimer and Francis 1997, 1998; Oppenheimer et al. 2004; Acocella 2006; Field et al. 2012; Zelenski et al. 2013). As these lava lakes are permanently active and evolving with time, publications should certainly continue to describe this exceptional volcano in the future.

The earliest activity (fissural basalts found in all parts of the range) is generally submarine with characteristic “small pavement” shape (as at the surface of pillow lava), but here they are—except for the front of the flow—essentially flat-lying. Hyaloclastite rings are frequently at the emission centres, with the typical large and low

truncated shape (Tazieff et al. 1969, 1970, 1972). Seven distinct subaerial volcanic centres cover these early emissions, aligned along a single NNW–SSE line of open fissuring, showing different stages of volcanological as well as petrological evolution.

The volcanological evolution starts with fissural basalts as observed in the southernmost range called Hayli Gub from the name of the highest (and most evolved) part of this sub-unit. It reaches the shield volcano stage at Erta Ale (*sensu stricto*), where two large shields are observed elongated along the same axis. It ends with cumulo-volcanoes observed to the north of the range (Dalla Fila, Alu, Borale Ale and Gada Ale). Worthy of note is the Ale Bagu, a stratovolcano sitting aside the main range, SW from the main axis. It is also the only unit displaying a pyroclastite-hyaloclastite products (Fig. 6.5).

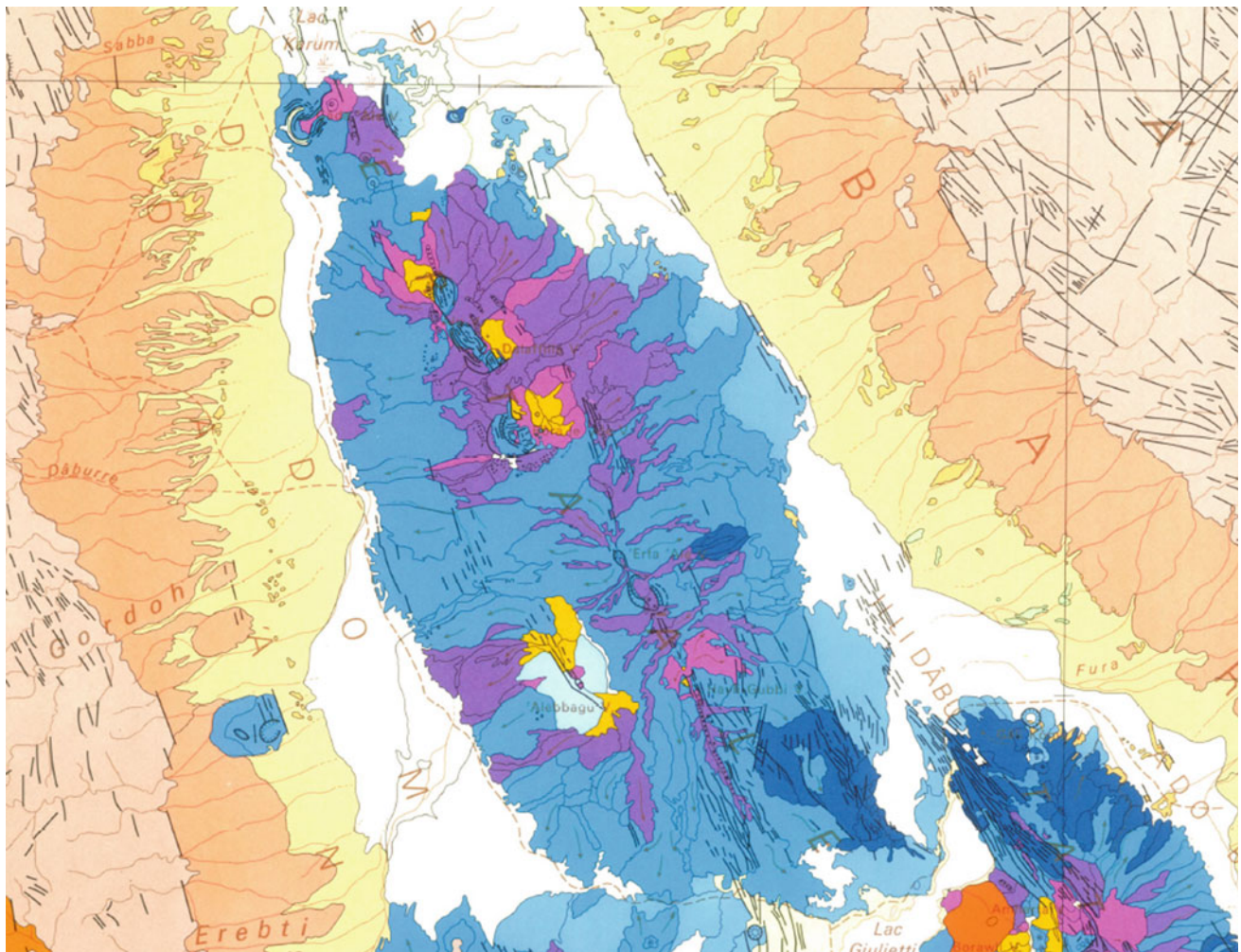


Fig. 6.4 The Erta Ale range located in its northern Afar geological context, extracted from the geological map of northern Afar at 1/500,000 scale (CNR-CNRS Afar team 1973). Whereas the faulted pre-Mesozoic basement, the polychrome tertiary detritic series and the coral reefs of the former Danakil sea (yellow) are visible on both sides,

the lava sequence of Erta Ale is made of olivine basalts (blue, deep blue when picritic), andesine basalts and ferrobasalts (violet) dark trachytes (pink), and silicic trachytes and rhyolites (yellow) in the most evolved volcanic units (to the north of the range, and also at Ale Bagu, a lateral volcano also displaying phyroclastic-hyaloclastic products (pale blue)

The fissural emissions always give basalts, generally almost aphyric with sparse olivine, some with picritic tendency (olivine-rich), whereas shield volcanoes frequently display plagioclase porphyric basalts with aphyric lavas enriched in iron. As shown in Fig. 6.3, at the cumulo-volcano and stratovolcano stages the lavas become more silica and alkali rich with trachytes and rhyolites and commendites (slightly peralkaline rhyolites).

A continuous series of petrographic terms is found in each of these single volcanic units and in the Erta Ale range as a whole (see Fig. 6.2), and divisions in terms of names are therefore quite artificial. The following terms have, however, been introduced by Barberi and Varet (1970) and have since

been followed by most workers: picritic basalts, basalts (eventually plagioclase porphyritic), andesine basalts, iron-rich basalts, dark trachytes, rhyolites and commendites. The same classification has been used for all axial ranges in Afar.

All the products of the series are explained both quantitatively and qualitatively in terms of crystal fractionation of a mildly alkaline basalt under low and falling fO_2 conditions (Treuil et al. 1971; Barberi et al. 1971). More detailed investigation, notably using geochemistry, confirms volcanologic observations (Fig. 6.4) and shows that each sub-unit did evolve in a separate magma chamber located in the uppermost part of each volcano (Fig. 6.5).

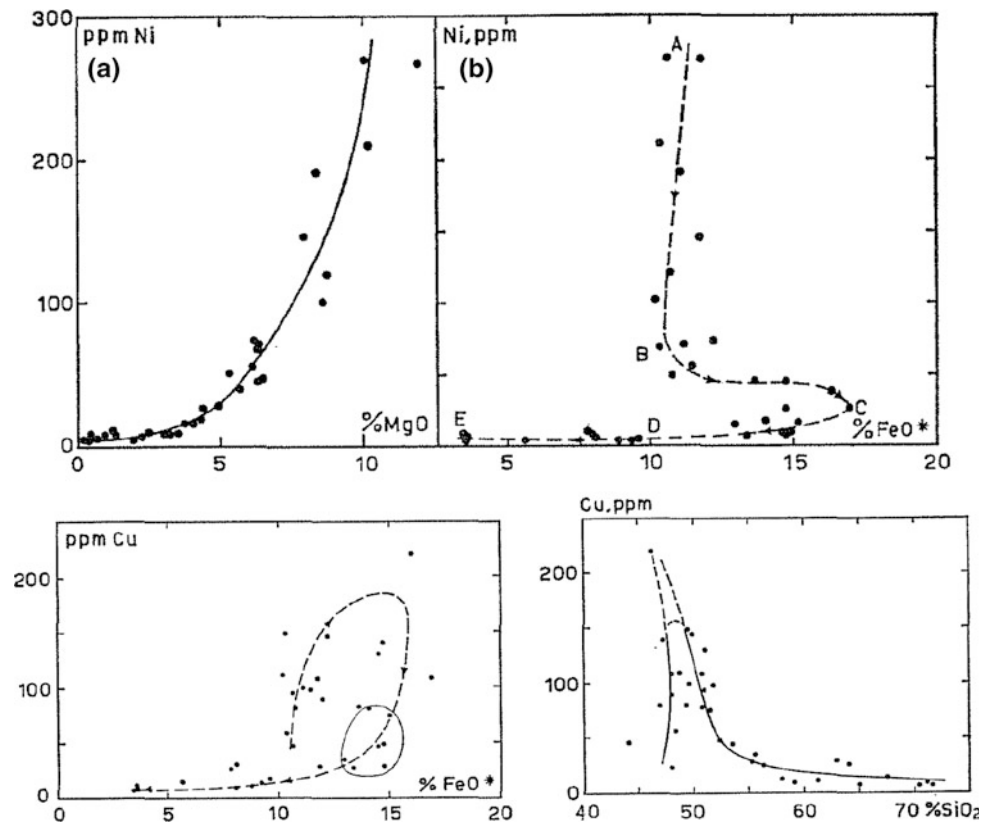


Fig. 6.5 Distribution of Ni and Cu in the process of crystal fractionation of Erta Ale range (Treuil et al. 1971)

This range is very recent and the seven volcanoes comprising it are still active—historic lava flows and lakes, solfatares, fumaroles, steam vents, etc., the most spectacular being the Erta Ale with its two lava lakes permanently active for at least 100 years (Tazieff et al. 1969, 1972; Varet 1971a, b, c, 1972a, b; Field et al. 2012; Gerlach 1989; Acocella 2006; Zelenski et al. 2013).

The initial stage of the volcanic activity is characterised by subaqueous activity observed at present all around the range. We follow the volcanological evolution and therefore describe the volcanic units of the range from south to north.

6.2.1 Submarine and Sublacustrine Initial Activity of the Rift Floor

The oldest volcanic products located along the rift axis and lying flat on the surface of the Afar floor are dating from less than one million years¹ and probably only a few hundred thousand (age of the Danakil Sea). They are observed in several sites from ash rings west of the Gulf of Zula to the

south of Lake Afrera. To the north they are abundant in the vicinity of the Alid volcano (Eritrea) and a large hyaloclastite cone is observed in the middle of the salt plain near the Ethiopia-Eritrea border called Maharo (see Sect. 7.4).

The most important submarine outcrops are visible in the vicinity of or within the Erta Ale range, in the lowest stratigraphic position. They are observed all around the range (but are more abundant on the eastern side; Fig. 6.7) and all display characteristics of subaqueous eruptions (Tazieff et al. 1969; Bonatti and Tazieff 1970), frequently covered by more recent subaerial flows. It is clear that the initial volcanic products of Erta Ale range, to be found beneath the range axis, are of the submarine type (Fig. 6.6).

Two main features are observed:

- Dozens of ash rings, made of hyaloclastites (basaltic glassy fragments), located mainly on the eastern side of the range, but also north and south of it. Seven of them are seen in the surrounding of the lakes bordering the range to the NE, clearly linked with NNW trending emissive fissures (Fig. 6.7). This includes the Catherine² volcano, a very regular hyaloclastite ring 300 m in

¹There is a lack of age determination concerning this early episode of the Danakil rift floor and Sea.

²Named by H. Tazieff after Catherine Sornein, wife of the author.

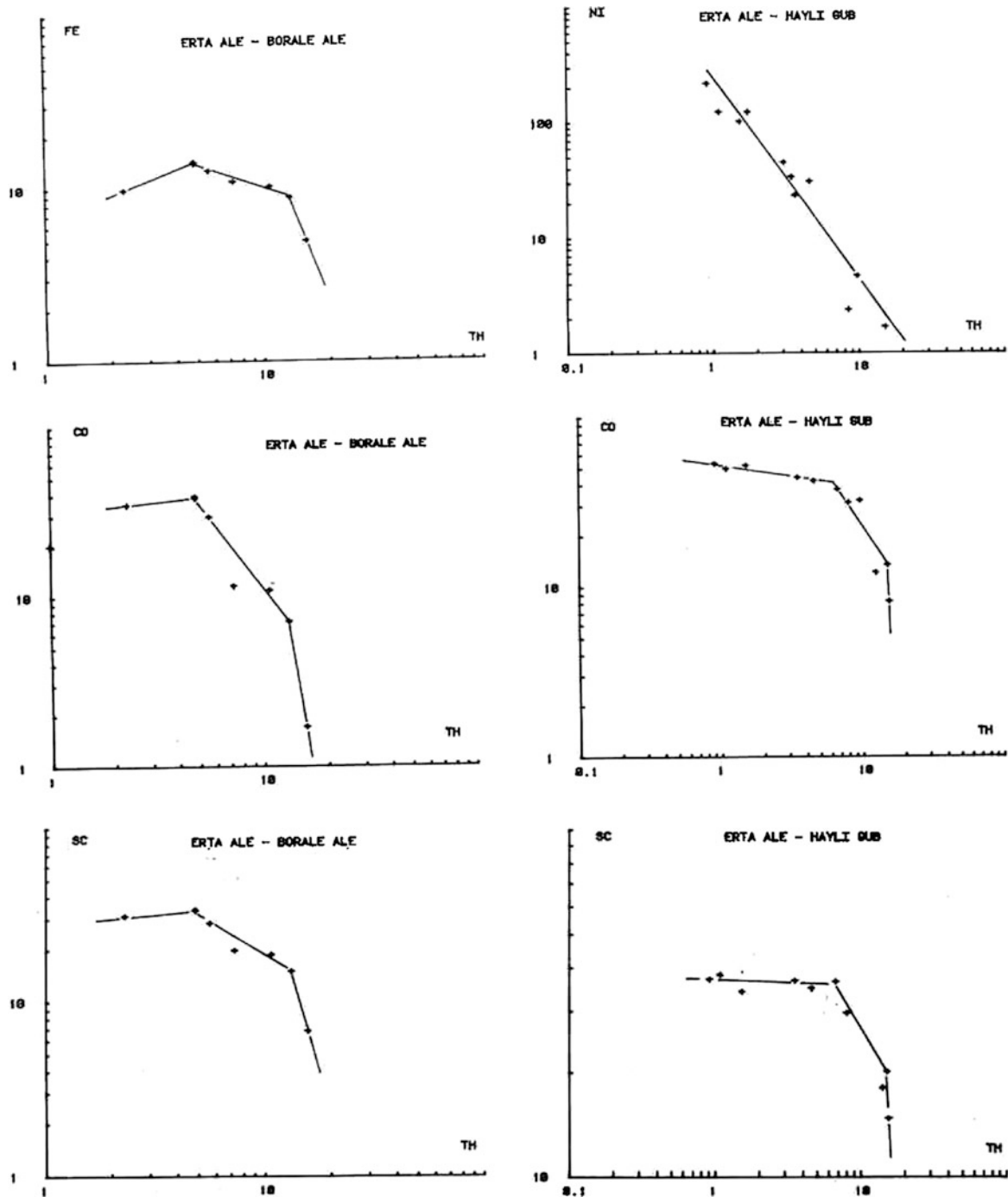


Fig. 6.6 Evolution of a few trace elements in different volcanic centres of the Erta Ale range showing distinct differentiation patterns (Treuil and Varet 1973)

diameter and 120 m high, which displays a lake fed by hot springs at its centre (Fig. 6.8). The slope of the deposits vary from 50° to the top of the ring to 10° at the bottom, indicating two different equilibriums (sub-aerial at the top and submarine at the bottom). To the south, the rim is cut by a NNW open fissure feeding a basaltic dike which emitted a small subaerial scoria cone

associated with a short lava flow. To the South of Erta Ale range, one of these cones is easily visible and accessible in the vicinity of Lake Afrera, clearly cut by more recent open fissures of NNW direction (Fig. 6.9). Numerous other hyaloclastite rings are observed around Tat'Ali, in the Sodonta plain and further south in the Saha plain. One of them displays the characteristics of

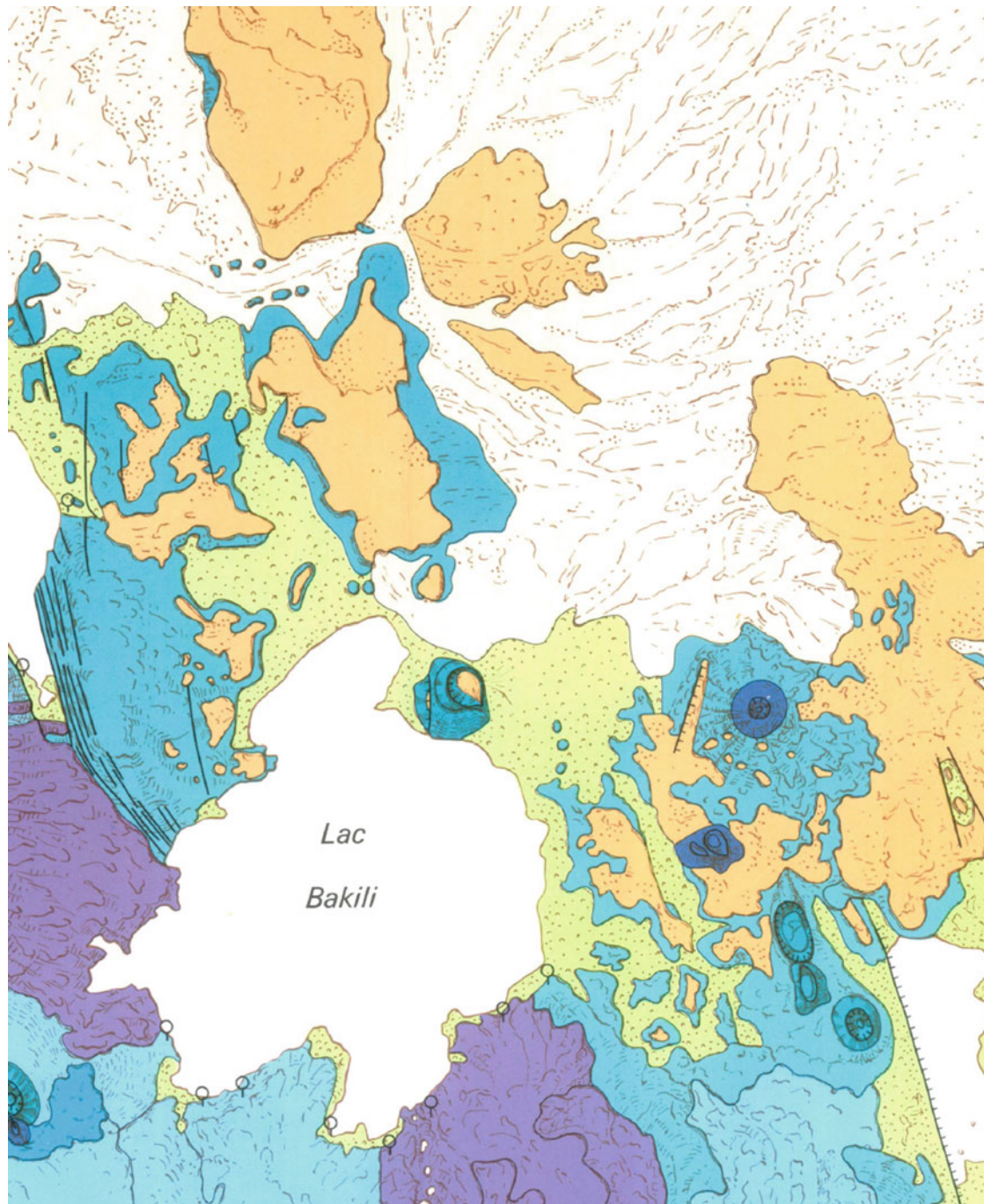


Fig. 6.7 Submarine activity exposed on the NE side of Erta Ale range, with subaqueous flat lying lava flow (covered by later marine and evaporitic sediments) and hyaloclastite cones (from 1/100,000 scale map of Erta Ale range, Barberi and Varet 1972)

an atoll (Fig. 6.10), with a coral ring described by Bonatti et al. (1971).

- “Paving stone” lava flows, characterised by a surface made of small (around 10 cm) prisms of hexagonal shape which developed at contact with the sea (or lacustrine) water. These look similar to the surface frequently observed at the outer part of pillow lava but, differing from pillows, these are flat lying surfaces (Fig. 6.11).

It should be noted that these subaqueous eruptions all resulted from fissures of NNW direction and are affected by faults of the same direction also affecting the surrounding formations, including the salt plain. This is, for instance, the case of the faults limiting lake Karum, north of the range, or the numerous recent normal faults developed to the SE of the range and bordering Lake Afrera to the NE.

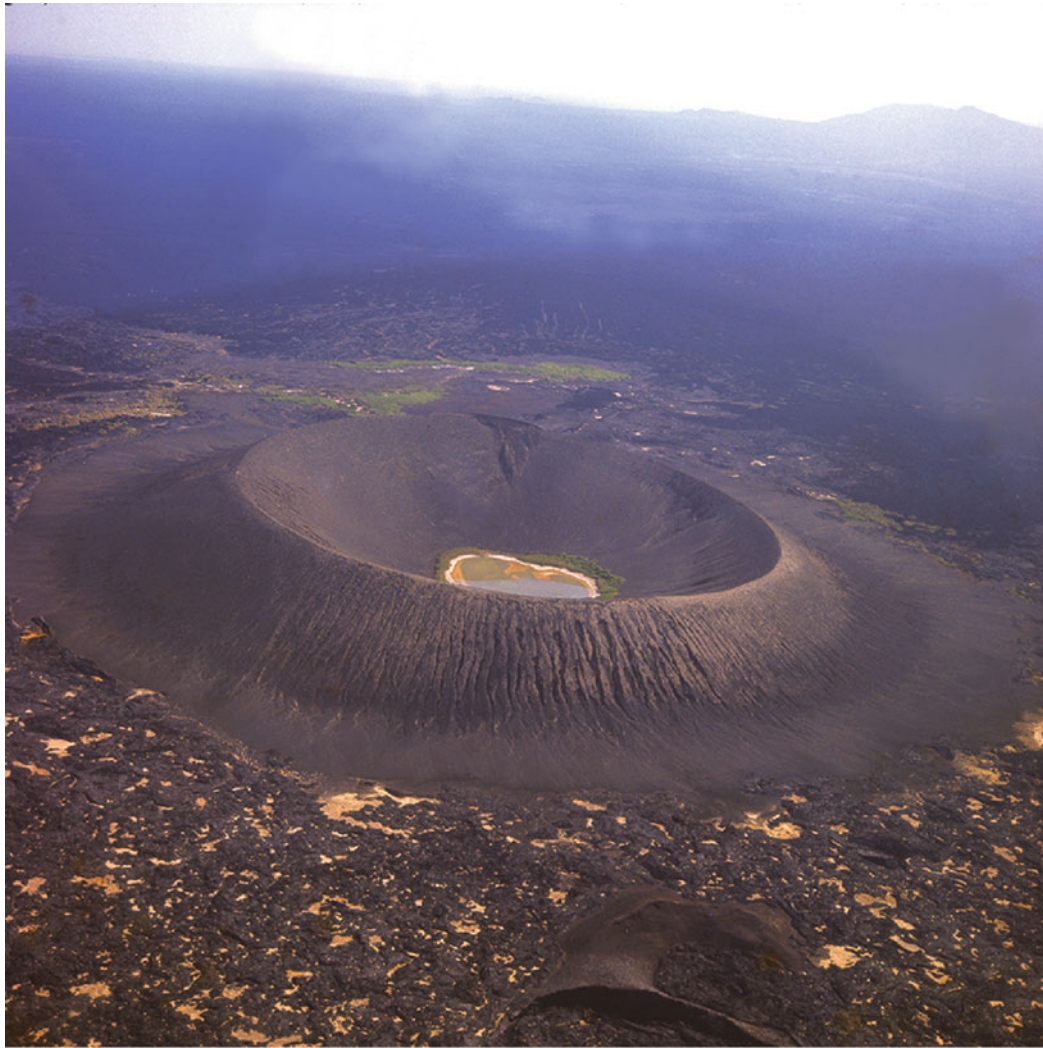


Fig. 6.8 Aerial view of Catherine volcano seen from north. The hyaloclastite cone is affected by a NNW trending open fissure that emitted a subaerial scoria cone on its southern flank. The lake is filled by hot springs (Photo G. Marinelli, Pisa University)



Fig. 6.9 Hyaloclastite cone SW of Erta Ale range, in the Lake Afrera lacustrine basin, seen from South, dissected in the middle by NNW–SSE trending faults (dominantly open fissures). *Photo Varet (2013)*



Fig. 6.10 Former atoll now emerged made of a hyaloclastite cone N to the SE of Erta Ale range partly covered by coral reefs and late evaporites (from Barberi and Varet 1970)



Fig. 6.11 Paving stone basaltic lava flow submarine surface, to the south of Erta Ale range in the vicinity of Lake Afrera (Photo J. Varet, 2015)

6.2.2 Hayli Gub Axial Emitting Fissures and Shield Volcano

Located in a perfectly axial position in the southern part of the range, extending over nearly 20 km, a single fissure of NNW direction is emitting basaltic flows on both sides and along an axial graben well developed to the south. Expanding in width towards the south, these flows cover the sedimentary plain north of Lake Afrera (Fig. 6.12). The last pahoehoe flow is younger than the lacustrine sediments

dated from 8200 years ago (Roubet et al. 1969). The tectonic activity that generated the volcanic activity partly predates it, but also continued afterwards: very recent open fissures that cut through this later flow also extend into the Afdera plain, affecting these sediments.

The origin of all the flows is well marked by a simple alignment of spatter and cinder coalescent cones elongated along the fissure axis. This axial fissure, frequently open on a few metres width, emits a sustained fumarolitic activity at several points (Fig. 6.13).

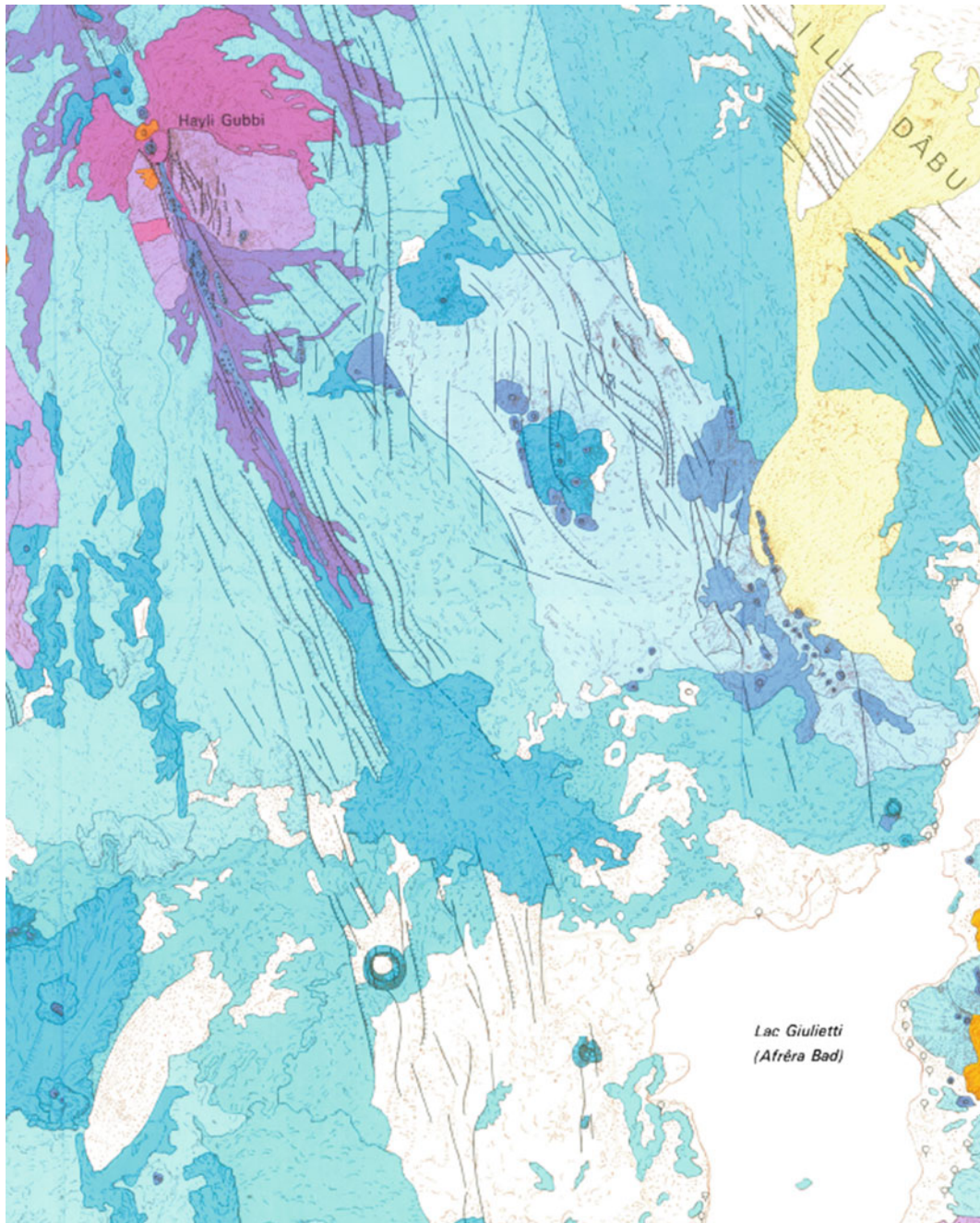


Fig. 6.12 Southern eruptive fissures emitted from the Haili Gub rift-in-rift. Observe to the north the rest of a NNW elongated shield volcano (with more evolved lavas of dark trachyte composition)

dissected by reactivation of the axial rift. Also observe the faults on the eastern flank underlining the inflation of the shield (Geological map of Erta Ale range, Barberi and Varet 1972)

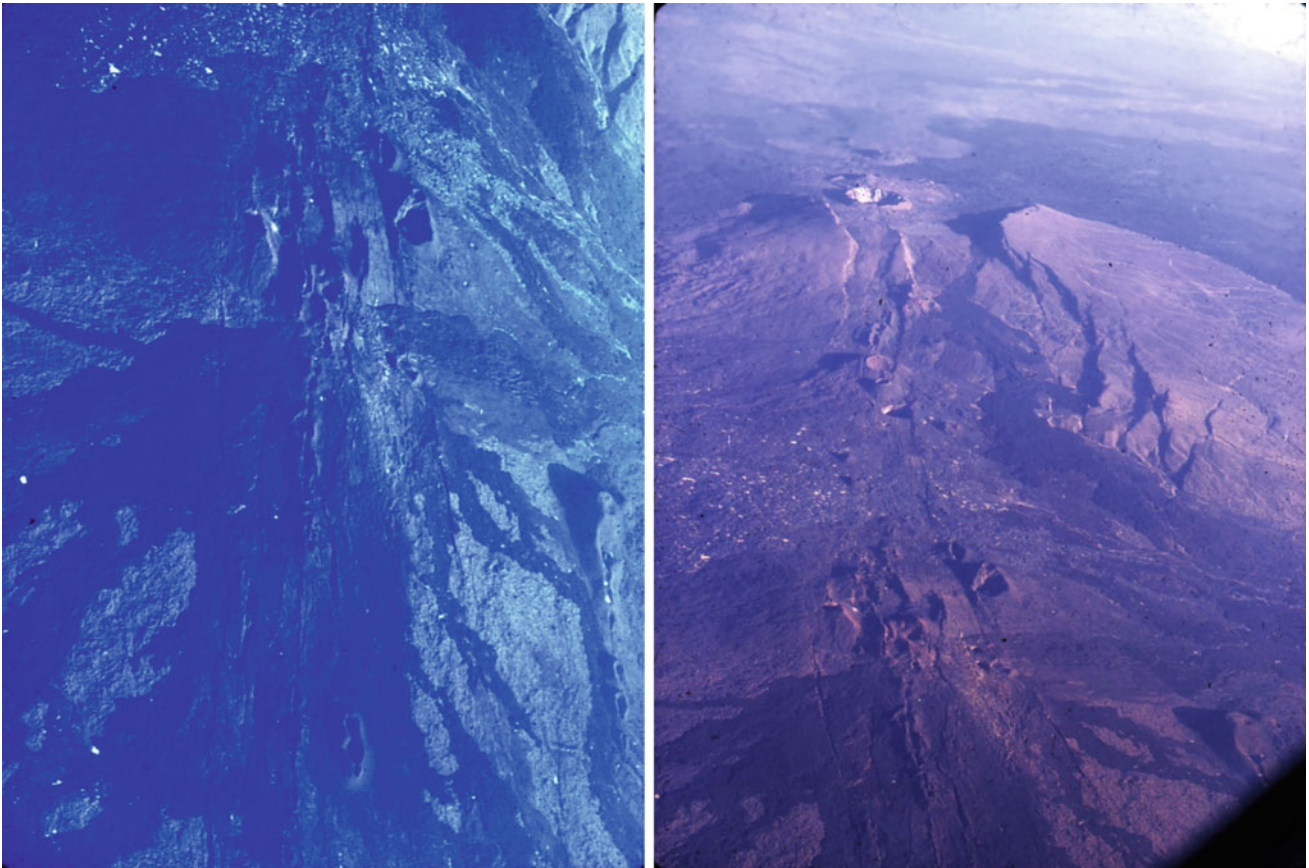


Fig. 6.13 Aerial photos of the open emissive fissures with spatter ramparts and oblique air photograph of the former shield affected by ring faults posterior to inflation and axial rift collapse, with later emission of a trachyte flow

The lava flows emitted along this fissure are all of basaltic compositions, with slight variations from picritic (olivine bearing) to plagioclase porphyritic.

On the upper (northern) part, the fissure is affecting an earlier shield volcano elongated along the same rift axis. A summit graben structure is easily visible, extending in the same NNW direction, which dissected the shield volcano (Fig. 6.14). The northern part of this shield is covered by more recent fissural basaltic lava flows in continuity with the southern extension of Erta Ale. On the flank of the shield, lava flows from an earlier eruptive cycle are visible, including a few more viscous flows of intermediate composition. The shield was in fact previously occupied by a caldera, elongated along the rift axis, at least 400 m in width, which was occupied by a lava lake that overflowed the rim. This open magma chamber allowed for a magmatic evolution up to dark trachyte, a thick Aa flow of which is observed southwards. Traces of the sink of the lava lake after the eruption are well observed along the caldera wall where pellicular lava remnants are easily visible, as also observed at Erta Ale, Asal and Manda Harraro lava lakes.

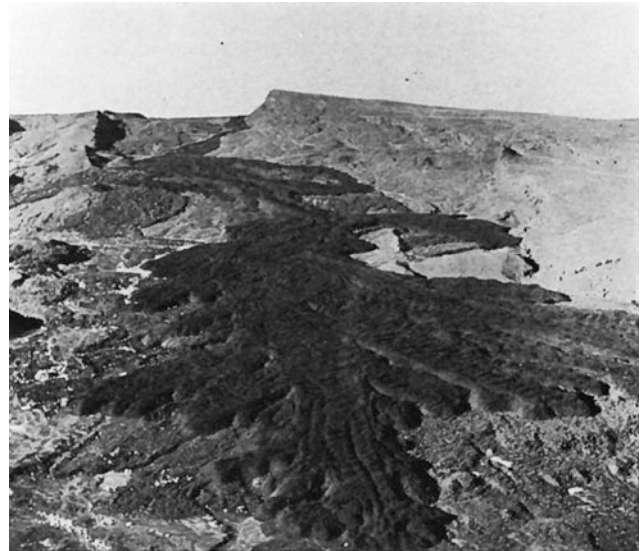


Fig. 6.14 View of viscous trachyte flowing out of the graben affecting the Haili Gub shield volcano, towards the south (from Barberi and Varet 1970)



Fig. 6.15 Views of the graben-faulted shield volcano, with the recent trachyte flow and the axial pit crater affected by fumarolic activity (coll. G. Marinelli, University of Pisa)

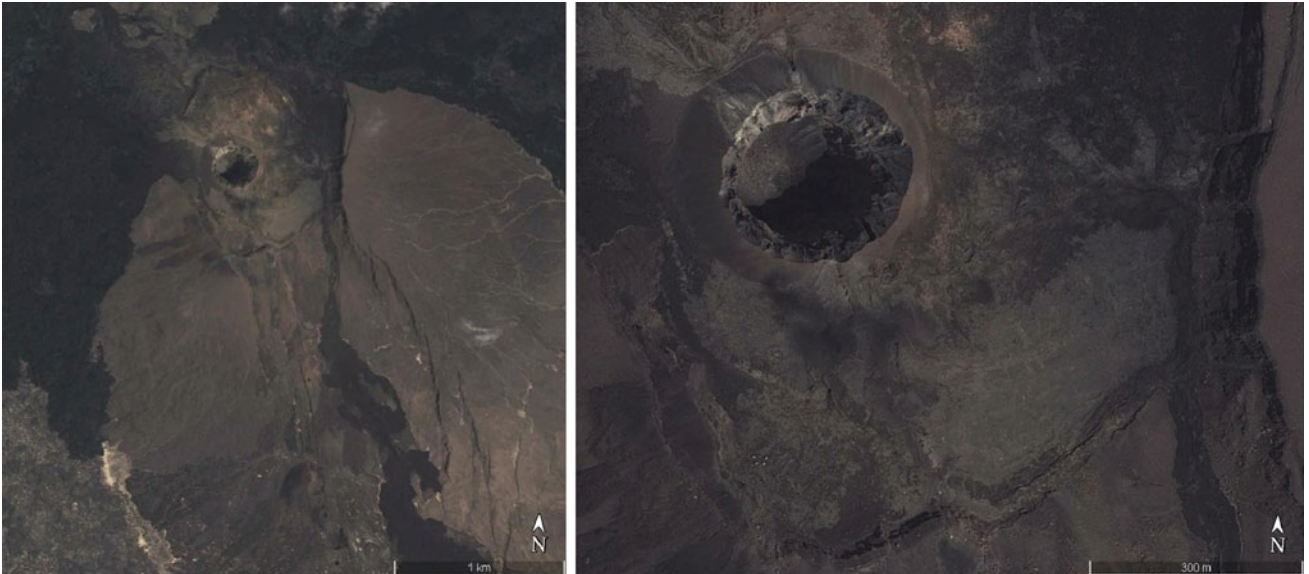


Fig. 6.16 Satellite views of the Haili Gub summit graben dissecting the former shield volcano, with detailed view of the deep axial crater affected by active fumaroles, especially on its northern flank. Note the sub-rectangular shape of the axial sink. (Images from Google Earth Pro)

Along the axis of the graben, a nice cone, 200 m in diameter, made of scoria and cinder is observed, which is affected by fumarolic activity (Figs. 6.15 and 6.16). North from this cone, a small cumulo-dome is observed, associated

with a few short viscous flows which are surrounded by the fissural basalts which largely predominate in the area.

If the tectonic activity is mainly developed along the rift axis, in a regular single NNW direction, with open fissures

along the axis and symmetrical normal faults on both sides, other transverse (NNE or N–S), frequently curvilinear faults are observed along the eastern flank of the shield volcano. Locally, small eruptive centres occur at the intersection of these faults with the regional NNW trending fissures (see map in Fig. 6.12 above). Although these may result from the influence of a transverse tectonics even more visible further south at the level of Afdera volcano, these faults and fissures may also be interpreted as volcano-tectonic features resulting from the incidence of the shield volcano structure on the regional tectonics.

As a whole, if Haili Gub reached in its northern part a phase of shield volcano, with a well-developed magma chamber and lava lake allowing for an evolution up to trachytes, it was later affected by an extensive tectonics rejuvenation with emission of basalts during a typical rift event of oceanic type, giving to the Erta Ale range this characteristic feature of Afar axial ranges (Barberi and Varet 1975).

6.2.3 Erta Ale Shield Volcano

Erta Ale volcano, which occupies a central position in the range, is the most active volcano in the region as it has

displayed permanent lava lakes for at least 48 years (Tazieff et al. 1969; Barberi et al. 1970; Varet 1971c; Tazieff 1973), and probably since the beginning of the century (Pastori 1906, unpublished oral communication; Barberi and Varet 1970). The temperature of the lava was shown to be 1150 °C by both direct (thermocouples and pyrometers) and indirect (mineral-liquid thermometers) measurements (Field et al. 2012). This indicates both a rather stable tectonic environment and quite a regular high heat flow in this axial part of the range. The volcano is 50 km in diameter and 500 m high. At the level of Erta Ale the range is widest. This typical shield volcano was formed by accumulation of basaltic flows as well as dikes and sills intrusions along the meridian NNW axis of the range. Its summit is characterised by an elliptic sink elongated NNW–SSE (1600 × 700 m). This basaltic caldera, hosting the two active pit craters, is associated with the south through another larger elliptic sink (3500 × 2000 m) topping a slightly lower shield volcano, so that altogether the area affected by these summit magmatic deformations is 6 km long (Figs. 6.17, 6.18 and 6.19).

In the northern sink, three structures can be distinguished:

- The northern pit, which is the most active and changes in shape and type of activity from large active lava lake to



Fig. 6.17 View from the north of the Erta Ale calderas, as seen in 1975. The two active lava lakes are visible in the front caldera, as well as the flat surface of the southern one. The wide elliptical sink is also visible as well as the Haili Gub shield and axial graben. All are aligned

along the same NNW rift axis (Photo J. Varet). It is along the NNW-SSE axis of this elliptic sink that important activity developed in 2017, producing large basaltic lava flows and craters, one of them with a new active lava lake



Fig. 6.18 The two active lava lakes of Erta Ale, seen from the south in 1968 (Photo J. Varet)

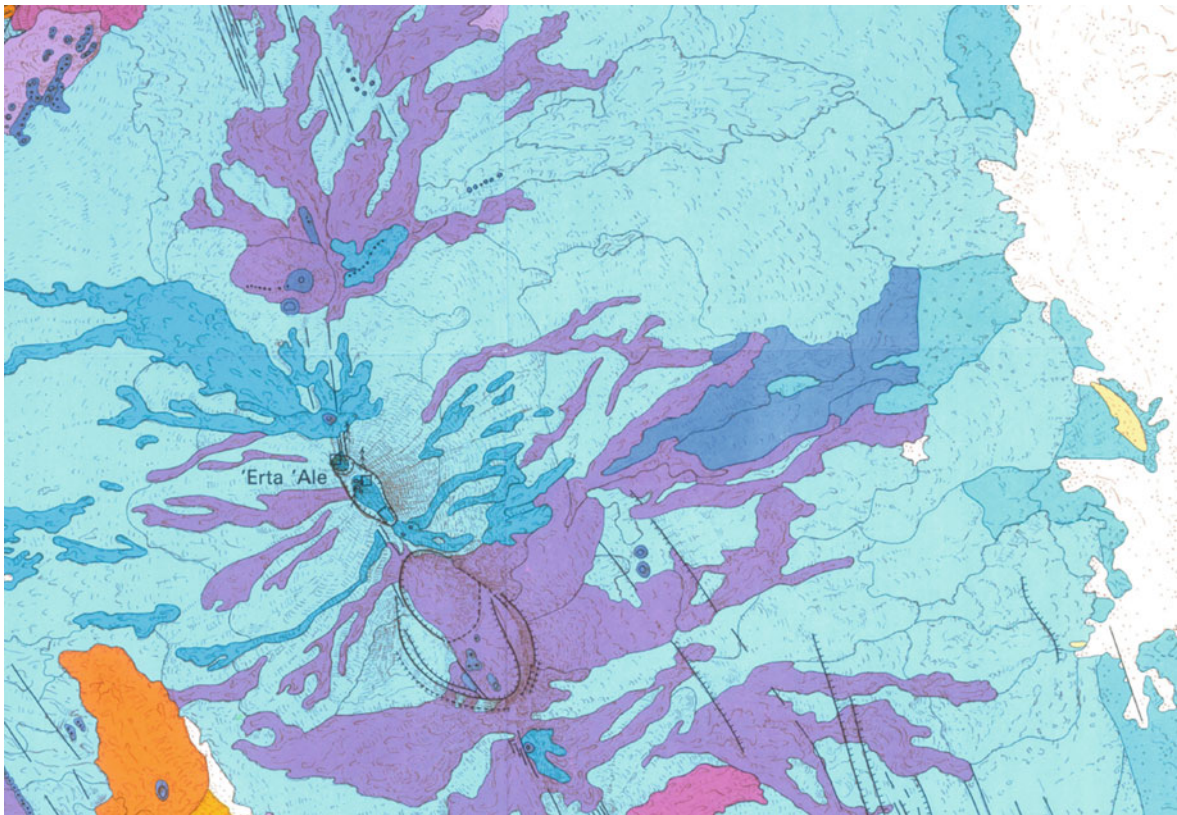


Fig. 6.19 Map of the Erta Ale shield volcano, with the two summital calderas elongated NNW along the direction of spreading of the range, the southern one being much larger than the northern one containing the

active lava lakes (extracted from 1/100.000 map of Erta Ale range, Barberi and Varet 1972)



Fig. 6.20 The northern pit, which was the most active in 1967, covering the whole diameter of the northern part of the caldera, later restricted to a smaller lava lake surrounded by a flat spatter cone in 1972 (Photo J. Varet)

smaller embedded pit or even single hornitos as observed in 2012³ (Figs. 6.20 and 6.21).

- The central pit, which has always displayed a basaltic lava lake (Fig. 6.22), the level of which varies with time, with periodic overflows, as observed in 1972, 1973 and 2010 (Varet 1972a, b; Tazieff 1973; Field et al. 2012). The activity remains continuous, with intense emission of Pelée’s hairs that carpet the rims of the crater, particularly on the western side (Fig. 6.23).
- The southern pit, which is filled by lava flows emitted from the central pit, but was an active lava lake in earlier times.

During the last few years basalts were emitted from the pits and the surface of the caldera floor was regularly

modified (Fig. 6.24). Several phases of outflows succeeded in sinking to the level of the lava in the pits.

In addition to these intra-caldera eruptions, lava flows also erupt from open fissures of a N direction, affecting both the sink interior and its flanks. Hornitos are found aligned along these fissures (Fig. 6.25).

Several open fissures trending nearly N–S in a local direction differing from that of the caldera wall (regional direction) as stressed by Aconella (2006) are affecting the northern flank of the shield. For the last 50 years at least these have been generating both an intense fumarolic activity as well as sporadic basaltic emissions on the northern slope of the caldera. As a result of this hydrothermal alteration, this part of the caldera wall became very fragile. The lava flows building this wall were transformed into soft clays that were easily overflowed by the uprising northern pit in 2013 (Figs. 6.26 and 6.27).

Barberi and Varet noted in 1970 that the southern pit was filled by a lava flow which produced a flat nearly horizontal surface that sits 2 m below the southern threshold, with indications of the former level of the lake observed on the caldera walls all around the crater (Fig. 6.28). This shows

³We use here the term hornitos, despite the fact that this was shown to be inappropriate by Barberi and Varet (1970) as they are located on the emissive fissure, therefore differing from the rootless eventually moving emission points located on flows described by MacDonald (1968). In the present case, these hornitos are built by the accumulation of very small (decametric in diameter) lava flows forming small accumulating lava tubes. The viscosity of the lava is eventually explained by the abundance of plagioclase phenocrysts.



Fig. 6.21 The northern crater is frequently changing in shape from active lava lake, as observed in 1970–1990 imbedded in a larger solidified surface, to a fountaining lava tube progressively covering the

whole former lake surface, as observed in January 2013. Observe the caldera wal, deeply changed into soft clay by fumarolic activity on its northern rim, the first part on this photo (J. Varet)



Fig. 6.22 The central lava lake as seen in 1975 (Photos J. Varet) emerged at the surface with periodic overflows in the caldera, and in 2013, 10 m below the surface of the crater, which was elevated by a



few tens of metres by successive intracaldera eruptions, as observed in 2010 by the NERC team



Fig. 6.23 Blond Pelée's hair (basaltic fiberglass) covering recent pahoehoe lava surfaces on the western flank of the central pit (*Photo* J. Varet, January 2013)

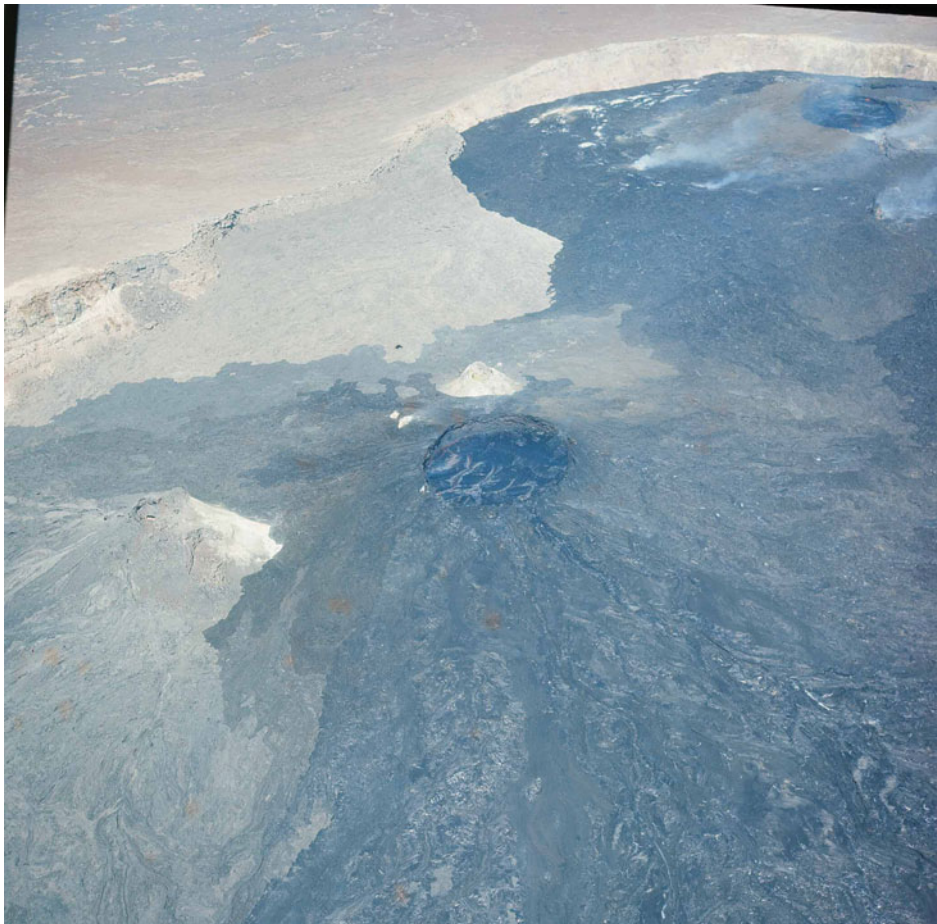


Fig. 6.24 Aerial view of the overflows that occurred in 1975 from both pit craters (*Photo* coll. G. Marinelli, Pisa University)

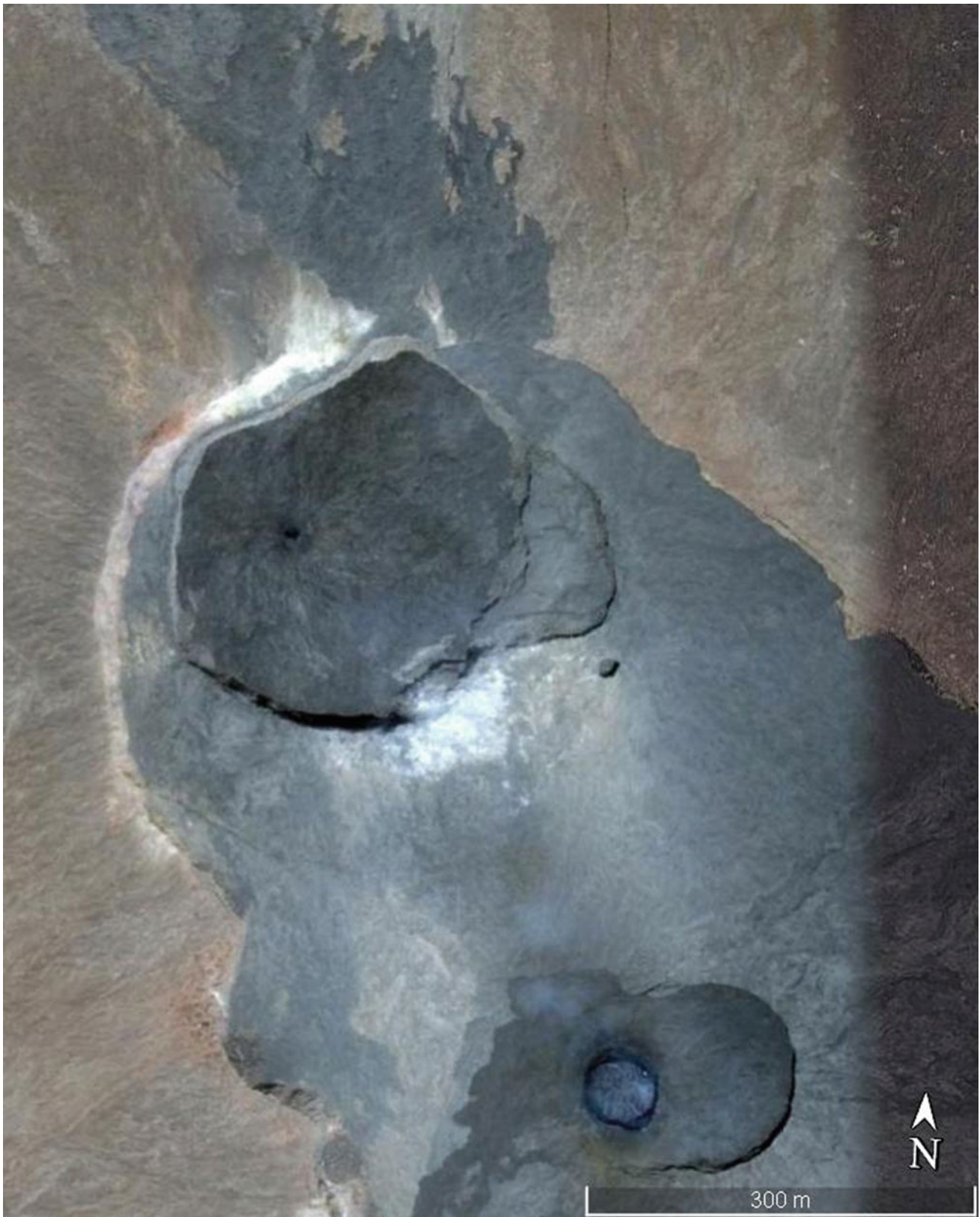


Fig. 6.25 The two active craters of Erta Ale as seen in 2016, with an active hornitos north and the lava lake overflowing the central (now double-rimmed) pit. On the northern side of the caldera, lateral eruptions from open fissures of N–S direction affected the flank of the

shield, allowing for earlier collapse of the lava lake. More recent (2013?) overflows affected the deeply altered northern extremity of the caldera wall in a high lava period. (Images from Google Earth Pro)



Fig. 6.26 Details of the open fissures of N-S direction emitting fluid basalt flow from emptying the lava lake (Image from Google Earth Pro)

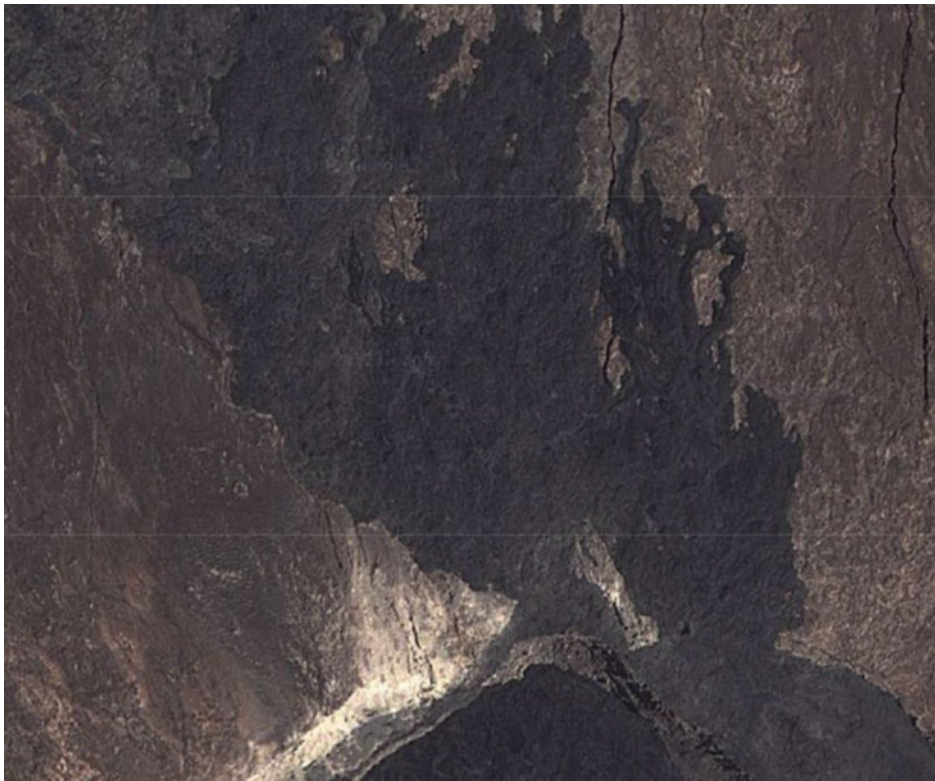


Fig. 6.27 Details of the overflow affecting the northern fumarolized wall of the caldera in 2015



Fig. 6.28 Pahoehoe flow filling the southern crater in 1979. Former level of the lava lake is observed as traces of former lava lake level are observed stuck along the wall of the caldera, 4 m higher than the present surface (Photo coll. G. Marinelli, Pisa University)

that the lava lake surface sank after the lava was emitted, either because of degassing or, most probably, to an emission through a lateral fissure as observed on the south-western slope of the volcano (Fig. 6.29). If the southern pit was active in the past, there is no evidence remaining that a lava lake once occupied this crater.

Photographs from 1992 show that the southern crater was covered by a large eruption from the central pit crater that overflowed the caldera wall, generating new extensive lava fields to the south (Fig. 6.30).

The composition of the gases emitted by the lava lakes was analysed by Tazieff et al. (1972), Le Guern et al. (1979) and Gerlach (1989). It shows the dominant H₂O (70–77%), with CO₂ (12–20%), SO₂ (5–9%), H₂ (1.6–2.4%), CO (0.5–1.6%), H₂S (0.4–1.0%) and HCl (0.4%), similar to tholeiites from oceanic spreading zones. SO₂ fluxes were measured at 1.3 kg/s for the whole volcano by Oppenheim et al. (2004). New measurements in 2005 (Sawyer et al. 2008) indicate a higher water content (93%) with a similar sequence for other gases except for H₂, which was not measured.

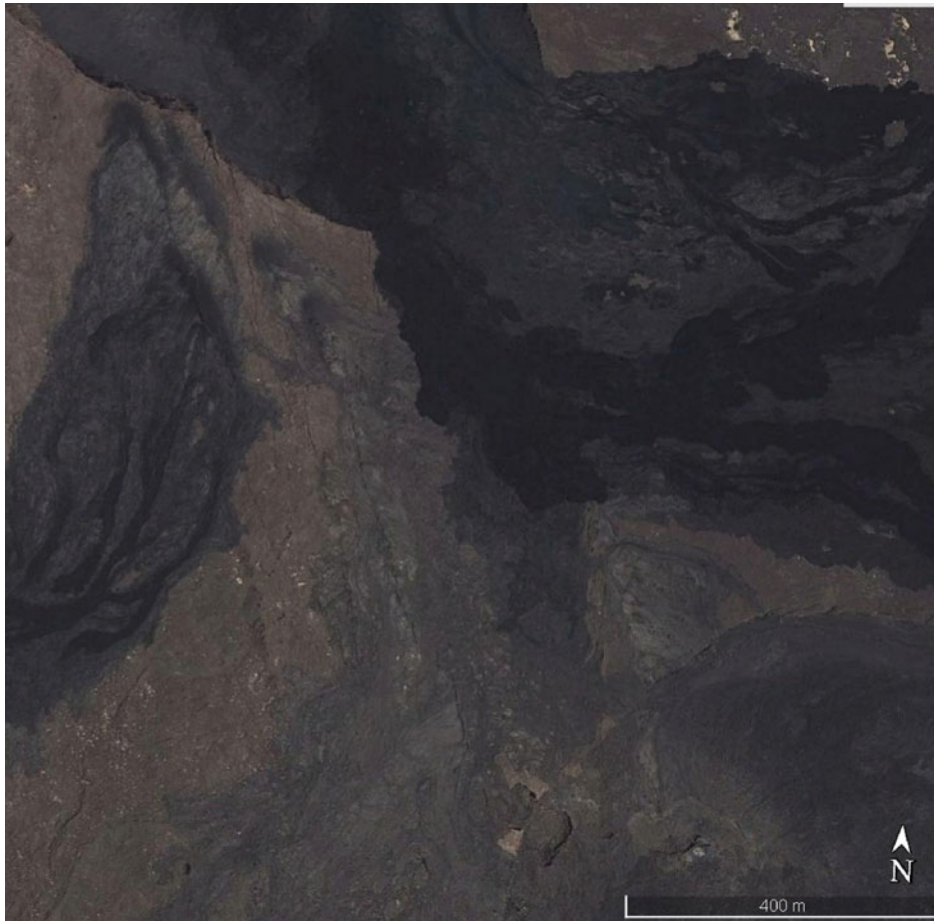


Fig. 6.29 Satellite image of lava flows emitted through NNW fissures affecting the southern flank of Erta Ale caldera, eventually responsible for the sinking of the surface of the southern lava lake as observed on the walls of the calderas (Fig. 6.135)



Fig. 6.30 The recent overflow from the central pit crater, over the whole caldera including the S pit, is shown to have been a major eruption as observed on this photo from Cantamessa (1992)

It was estimated that the heat flux was of the order of 100–400 MW over at least 30 years (Francis et al. 1993) and that a magma influx of around 500 kg/s was necessary in order to account for the SO₂ degassing from the lava pond, which is much less than the amount of magma erupted in the 1968–1999 period (around 10 kg/s) as estimated by Oppenheim and Francis (1997, 1998) from compilation of satellite images since 1974, indicating that the volcano grows largely by intrusion of dikes and sills and formation of cumulates, consistent with and probably promoted by the extension of the north Afar crust.

All around the calderas the divergent courses of the lava flows show they were emitted from Erta Ale craters. Some of them issued from lateral fissures either at a NNW direction or radial to the crater. Such emissive centres are marked by the presence of hornitos (Figs. 6.31 and 6.32). On the pahoehoe surfaces of these shield-forming flows, angular blocks of lava several decimetres in width are observed that clearly fall at high speed as they break through the surface, leaving spectacular holes (Figs. 6.33 and 6.34). A hornito 5 m high was even cut in half by such a projectile (Fig. 6.35).

To the south, the largest elliptic caldera—itsself divided into two concentric ellipses—shows that the upper part of the southern shield volcano was intruded by kilometres-wide basaltic sills that created a sequence of shallow magma chambers that later collapsed when the basalt finally erupted. As a result, both inflation and deflation structures are observed along the outside rims of this caldera, with signs of recent lateral overflows themselves also affected by these shallow underground magmatic events (Figs. 6.36 and 6.37).

While this book was being edited, a new major event occurred at Erta Ale, with an important rise of the level of the lava in the central pit in December 2016 and early January 2017, with the development of a small shield in the

caldera floor, and with new overflows to the south. This magmatic phase was followed by a tectonic event, with the opening of a 4 km-long fissure along the axis of the southern large oval sink seen in Fig. 6.17. This event produced important Aa flows inside this southern caldera, with overflows over the rim of the caldera mainly to the east and to the west. The eruption was still active on January 26, 2017 (Fig. 6.38). This event was apparently followed by a collapse of the level of the lava lake in the central pit.

The lavas constituting the Erta Ale shield volcano vary in composition from olivine magnesian basalts to ferrobasalts (up to 20% total iron oxide) with well-developed plagioclase (from Bitownite to Labrador) porphyritic lavas as intermediate products. The whole sequence shows the role of crystal fractionation under low pressure, low oxygen fugacities, in a shallow magma chamber. Plagioclase-rich lava may result from a process of flotation (Barberi and Varet 1970; Bizouard et al. 1980).

6.2.4 Borale Ale Cumulo-Volcano

Borale Ale is another distinct volcanic unit, although rather complex, sitting in the median part of the Erta Ale range. Two distinct phenomena coexist there, both evidently active in recent (historic) times and resulting from the same NNW feeding fissures of the Erta Ale range axis: the complex cumulo-volcano to the west and the fissural basaltic lava field to the east observed at 4 km distance from the central apparatus, dominant in the landscape, which gave the unit its name (Fig. 6.39).

As for other parts of the range, the activity started with submarine basaltic flows, now better exposed at the oriental foot of the range. Besides the characteristic “pavement”



Fig. 6.31 Alignment of fixed hornitos along an emissive fissure on the southern flank of Erta Ale volcano (Photo Varet 2004)



Fig. 6.32 Detailed view of one of the fixed hornito, site of emission of basaltic lava tubes, on the southern flank of Erta Ale volcano (*Photo Varet 2004*)



Fig. 6.33 Singular blocks projected by Erta Ale crater having smashed the surface of the lava flows on the western flank (*Photos Varet 2004*)



Fig. 6.34 Singular blocks projected by Erta Ale crater having smashed the surface of the lava flows on the western flank (*Photos Varet 2004*)



Fig. 6.35 Hornito cut by half by the fall of a large block emitted from Erta Ale crater, showing the empty organ like interior of the emissive vent (Photo Varet 2004)

surface, these lava flows are frequently covered by coral reef deposits of Quaternary age, deposits that are eventually covered by more recent subaerial basaltic flows emitted from the range axis. Although the recent lava flows are apparently more abundant on the western slope, the emission axis appears to have remained rather constant during the whole building process of the edifices.

The successive emission of these flows along the NNW feeding fissures led to the building of a shield volcano, the top of which is now visible in the central part, where it was affected by a later bulge, the camber of which is finally greater than the initial shield because of magma injection at a shallow depth. This bulge was followed by the emission of the cumulo-volcano, made of viscous, silica-rich lavas,

ranging from trachytes to peralkaline rhyolites. This conic central volcano sits on top of the former shield in a slightly ex-central position to the east of the major camber.

The bulge is affected by numerous faults, mostly curvilinear and related to the dominant NNW tectonic direction, but clearly deviated by the volcanic structure in elliptic shapes that seems to relate to cone sheets at depth. They frequently display a flow towards the centre that may reach 100 m and surround a small summit graben. This graben was effected by later volcanic activity, with a now deeply fumarolised (although quite recent) silicic dome and related small viscous flow covering the graben floor.

The volcano-tectonic nature of these faults is shown by the association of volcanic emission centres with several of them.



Fig. 6.36 View of the south-western part of the wide ovale sink observed in the southern part of Erta Ale shield volcano. The topography of the caldera wall clearly shows the shallow inflation

produced by sill injection before the roof of the shield finally collapsed and was partly invaded by younger basalt flows, themselves affected by later caldera collapses (*Photo G. Marinelli*)

This is particularly visible along the main nearly circular fault, 3 km in diameter, limiting the former shield to the west, as scoria cones are aligned all along its length (Fig. 6.40).

Another concentric curvilinear structure is clearly visible, tracing an outside envelope 6 km in diameter all around the outcropping former shield. Numerous scoria and cinder cones are ordinated along curvilinear structures shaping concentric arcs. These were emitted relatively recently, and now totally cover the former shield in that area. They

emphasise the presence of feeding fissures related to the same central volcanic unit and fed by a single magma chamber. It appears that these curvilinear structures responded to both uplifted and downthrown motions related to magma inflation and deflation produced by surface emissions dikes/sills injections. The small plains observed between the two outmost rims underlie the sink that followed the latest eruptions. The shape and the slope of these volcano-tectonic features clearly indicate a shallow magma chamber (Fig. 6.41).

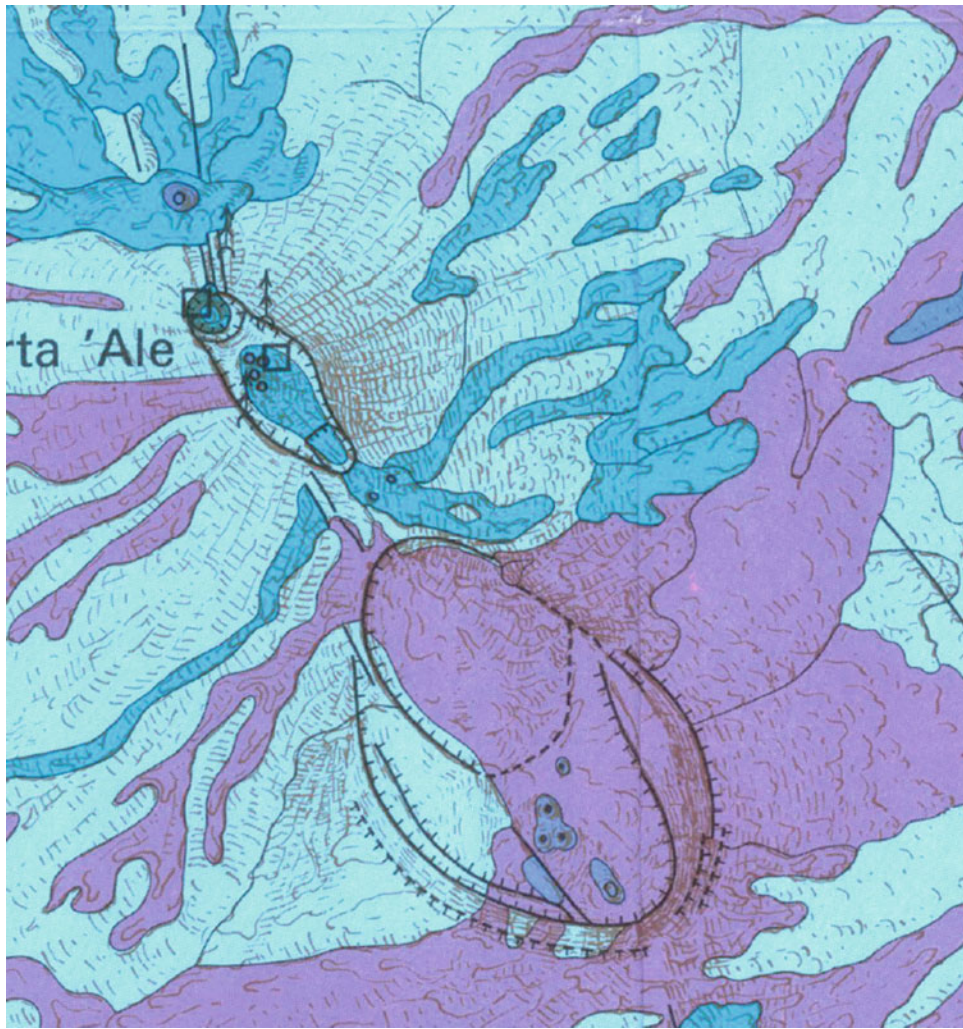


Fig. 6.37 Detailed map of the two Erta Ale calderas (Barberi and Varet 1972). The shield was inflated by successive diverging flows, but also dikes and sills of NNW direction. This is particularly evident in

the southern part where the summit sink was preceded by a wide inflation of oval shape slightly wider than the collapse, as observed in Figs. 6.17 and 6.36

In the upper part of the former shield, where it is most uplifted by the central bulge, short faults of transverse (E–W to ENE) direction are observed, shaping a summit graben along which the cumulo-volcano is located. This is volumetrically the most important acidic unit of the Erta Ale range, built by accumulation of viscous dominantly blocky lava flows from a single vent and reaching an altitude of 688 m (i.e. 800 m above the visible bottom located at circa 120 m below sea level). These flows reach a length of 5 km with an average slope of 25°. If this volcano appears to be sitting above the older deformed shield, it clearly appears to be a direct continuation of this earlier dominantly basaltic volcanic stage. The first set of viscous flows emitted from this centre is affected by the same type of faults—curvilinear, transverse and axial—affecting the shield. A thin layer of rhyolitic ash and pumice of grey-rose to green colours is interlayered between these early and later rhyolite flows. This is one of the

rare acidic pyroclastic layers observed in the Erta Ale range. A circular depression, 300 m wide, is observed on the summit part of the volcano which corresponds to a late collapse of the top part, affected by intense fumarolic activity easily visible in the early morning hours. If the shape of the silicic volcano appears to be slightly asymmetric and more developed on the eastern flank, this is linked to the fact that the flows towards the west were limited by the bulged shield. However, a few flows penetrated along some of the graben and some of the transverse faults.

To the east of the cumulo-volcano, a recent basalt field developed along a set of well-marked open fissures of NNW direction. These faults are in continuity with the Erta Ale recent faulting through a N-S trending relay (see Fig. 6.42 from Acocella 2006). They show that the regional spreading at the level of Borale Ale still continues despite the fact that the central volcano—originally built on the Erta Ale

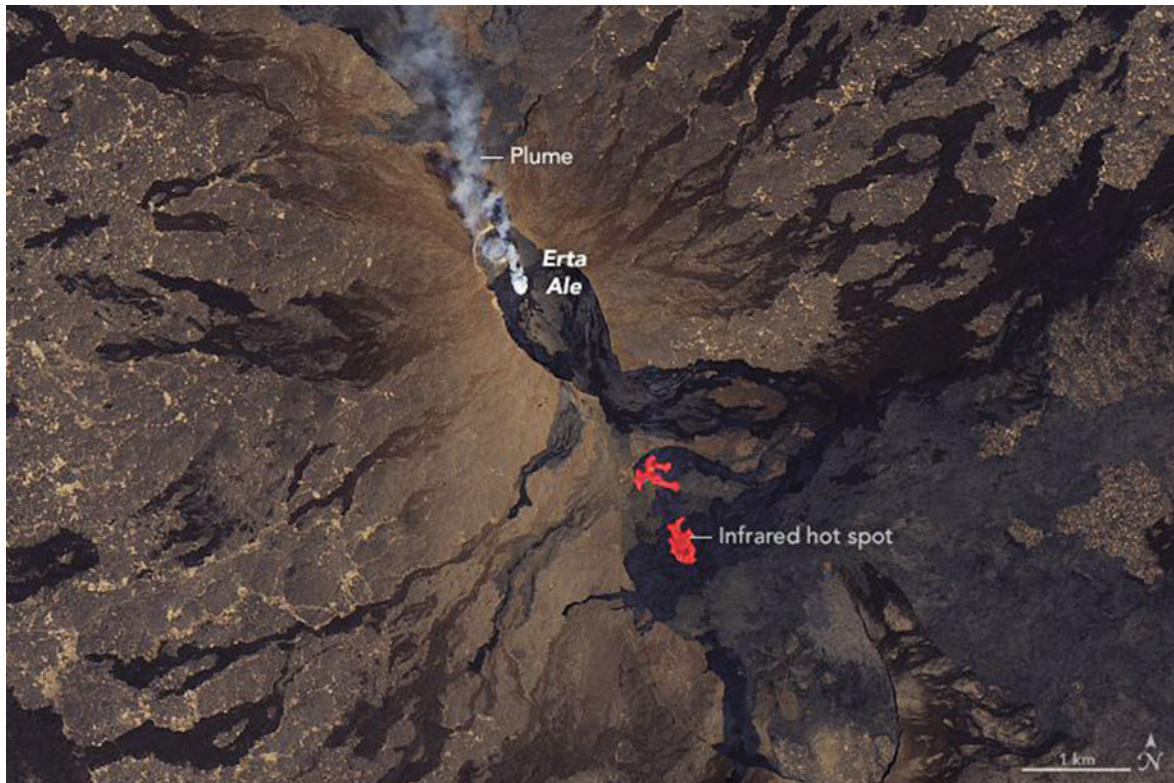


Fig. 6.38 New NNE-SSW emissive fissures opened up in January 2017, about 7 kilometers south from the summit Erta Ale caldera, spilling large amounts of lava. Meanwhile, at least one of the lava lakes has experienced large changes in the level of its lava leading to overflows and intense spattering. Image from Operational Land Imager (OLI) sensor on Landsat 8 of January 26, 2017. Composite of natural

color (OLI bands 4-3-2) and shortwave infrared (OLI band 7). Infrared hot spots representing two distinct lava flows are visible, and other images confirmed since the development of a new active lava lake in the centre of the large elliptic sink. Plumes of volcanic gases and steam (in white) drift from the lava lakes. Source <https://landsat.visibleearth.nasa.gov/view.php?id=89544>

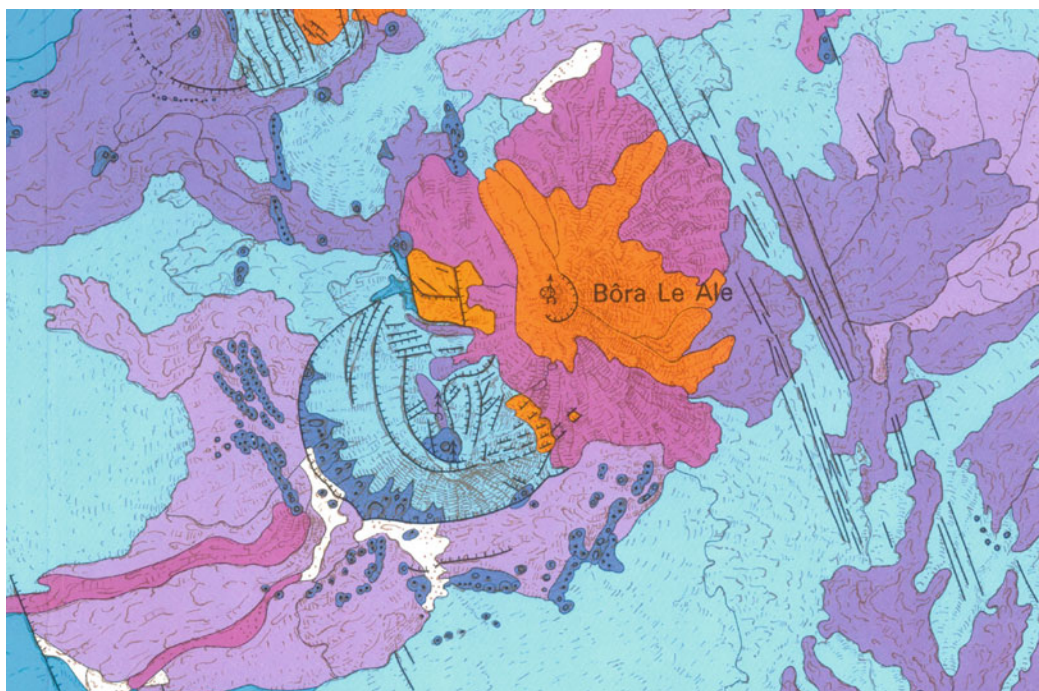


Fig. 6.39 Geological map of the Borale Ale volcano (extract from the 1/100,000 map of Erta Ale range by Barberi and Varet 1972; same legend)



Fig. 6.40 Curvilinear faulting affecting the Borale Ale shield volcano; observe also spatter cones along a similar outer concentric pattern (*Photo coll. G. Marinelli, Pisa University*)

spreading axis—appears to have stabilised with a well-developed and quite evolved magma chamber in a relatively stable very slow spreading environment.

From a petrographic point of view, the lavas of Borale Ale are mostly made of basalts constituting the fissural lava fields as well as the shield. The first flows found at the bottom of the series, particularly the submarine ones, are made of olivine basalts, whereas andesine basalts dominate in the shield. Both plagioclase porphyritic and aphyric lavas are observed there, with a marked iron enrichment for the most recent, up to dark trachytes in composition. The cumulo-volcano is made of silicic products, ranging from silicic trachytes to peralkaline rhyolites. As a whole, a complete, continuous sequence from olivine basalts to comendites could be sampled in this unit. The discontinuity in the trends from iron enrichment to silica enrichment fits well with the volcanological discontinuity observed from the shield volcano stage (from the initial olivine basalts to the andesine ferrobasalts and dark trachytes

emitted through the curvilinear faults of the bulged area) to the cumulo-volcano stage, where only the silicic lava are found (from initial silicic trachyte also affected by the curvilinear and transverse tectonics to final peralkaline rhyolites).

Contrasting with this perfect chronological and petrological evolution, the recent fissural flows emitted east of the volcanic centre are made of undifferentiated basalts characterizing the initial stages of axial rift formation elsewhere in Afar. Some of these fissures even cut through the bottom part of the silicic flows issued from the cumulo-volcano, clearly showing the contracting volcanic cycle (Fig. 6.43).

Therefore two volcano-tectonic systems topping the earlier shield volcano co-exist very closely at a few kilometres distance: a rhyolitic cumulo-volcano related to a shallow magma chamber where magma evolved along a single line of crystal fractionation and a nearby fissural basaltic system directly fed by deep inflow from the upper mantle in response to renewed spreading events of the Erta Ale rift segment.

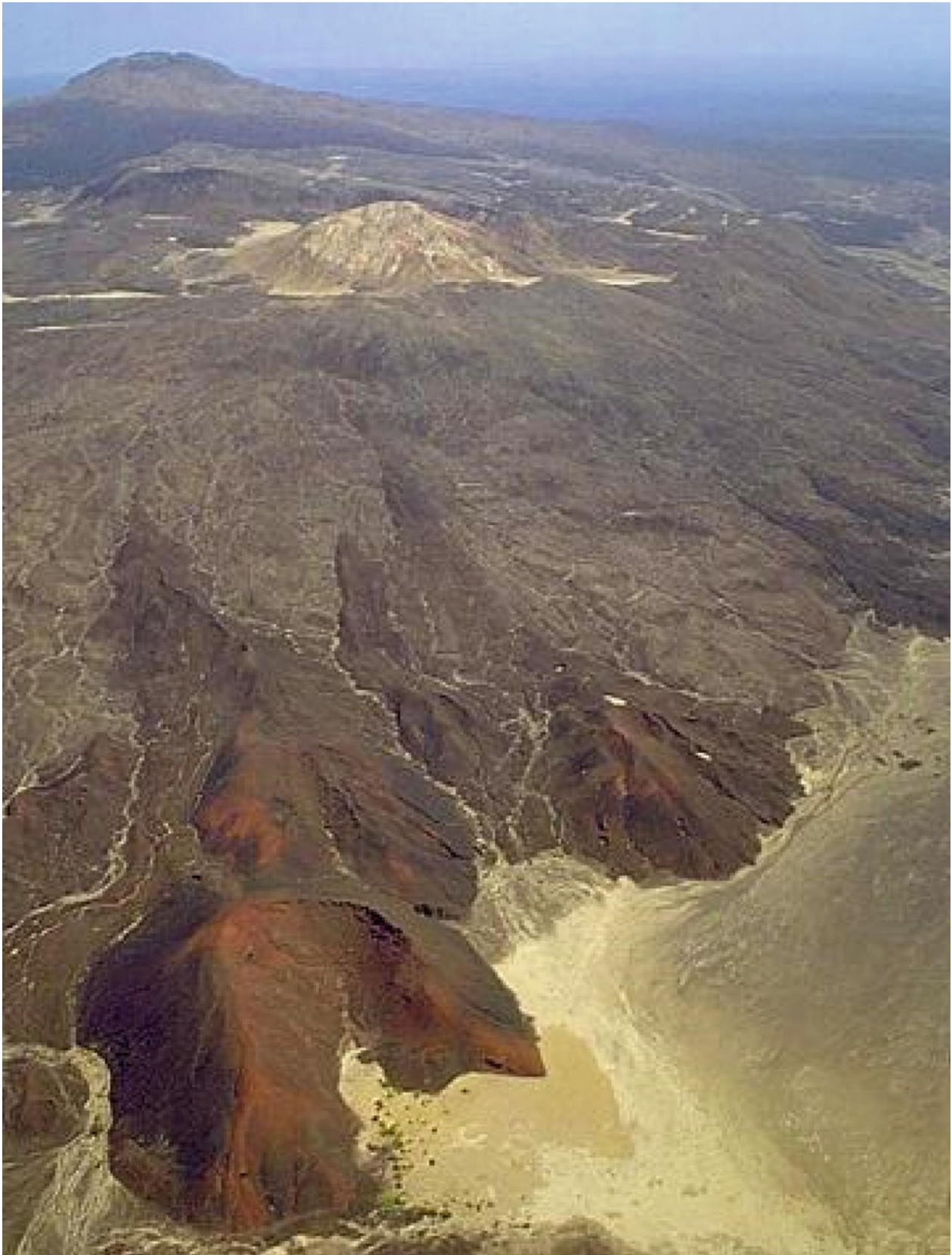


Fig. 6.41 The summit of Borale Ale (688 m, *upper left*) consists of a silicic cumulo-volcano (the largest of the Erta Ale range). Spatter cones along fissures are seen in the foreground, as well as a fumarolized lava dome and shallow magma chamber generating faults affecting the older

shield volcano. Important fumarolic activity develops within the 300 m-wide summit crater (*Photo* Smithsonian Institution, Global Volcanism Program)

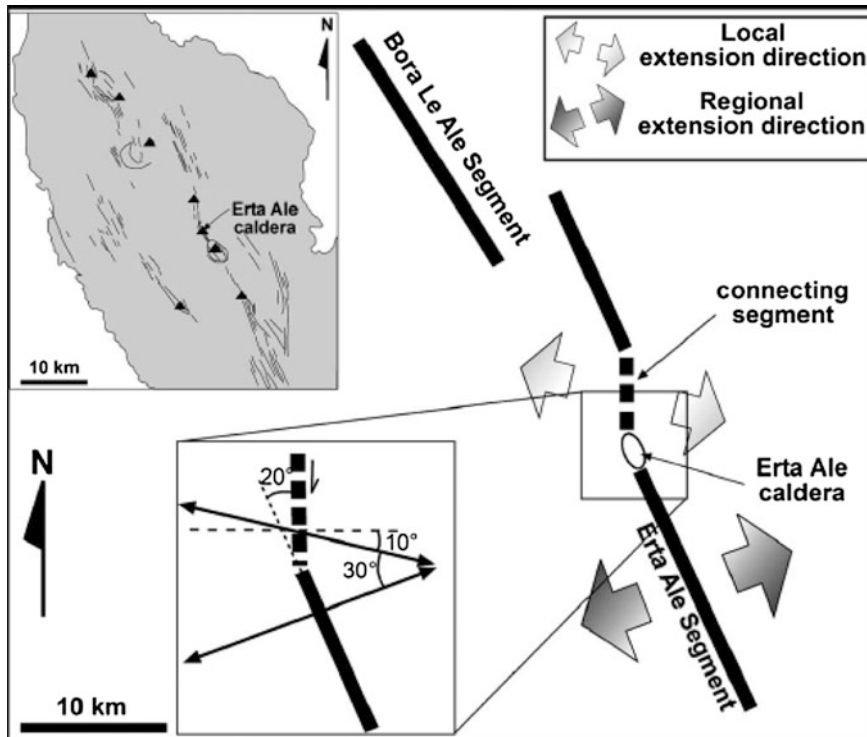


Fig. 6.42 N-S segment of open fissures connecting the Erta Ale spreading segment to the presently most active segment located at the eastern foot of Borale Ale volcano (sketch from Acocella 2006)



Fig. 6.43 Basalt flows issued from NNW trending fissures affecting the eastern flank of Borale Ale central volcano, marking the rejuvenation of the spreading along Erta Ale range axis (from Barberi and Varet 1970)

As a whole, looking at the volcanological sequence observed in the Erta Ale range from south to north with Hailigub at initial fissural stage, Erta Ale at shield stage and Borale Ale at cumulo-volcano stage, with a parallel evolution of the magma emitted from olivine basalts to peralkaline rhyolites (see Figs. 6.2 and 6.3) we observe that the Erta Ale range is a nice example of volcano-tectonic evolution of a spreading segment with successive steps observed from south to north, which can be explained by slower and slowing spreading. However, we also observe that, in each of these units, rejuvenation takes place with new superimposed spreading events involving undifferentiated fissural basalts that cut through the pre-existing evolving magmatic sequence. At Hailigub and Erta Ale this happens just along the initial spreading axis, whereas at Borale Ale, where the volcano is more evolved with a larger and better defined magma chamber, this occurs on the side of it, as if the volcanic edifice had been sealed, despite its still “soft” character.

6.2.5 Alu and Dala Filla Cumulo-Volcanoes

The Alu and Dala Filla volcanoes are prominent figures of the northern part of the Erta Ale range (Fig. 6.44). Dala Filla

in particular stands out in this generally rather low relief environment with its rather steep conic shape, reaching an altitude of 600 m (i.e. 720 m above the surrounding plains). The area is also characterised by important fumarolitic activity with a rather large steaming zone, which has apparently increased during the last few years with respect to the 1967–1970 first observations (Barberi and Varet 1970).

The Erta Ale range is of lesser width (25 km) compared to the central part (50 km). In surface, the area is mainly covered by flat lying basalts of fissural origin, apparently mostly emitted from the same axial fissure with rather mild slopes. The earliest events, of submarine type, are observed to the east in the surrounding of Lake Bakili. Large hyaloclastic cones, 700–800 m across and 100 m high, are associated with submarine flows partly covered by coral reef marine deposits with abundant flat urchins. They were emitted from a fissure located 10 km east of the present spreading axis. All are of olivine basalt composition. Contemporaneous lavas emitted from the range axis are also submarine and of similar composition, but most of the flows building this unit are sub-aerial basalts, with either Aa or Pahoe-hoe surfaces.

A wide shield volcano was built through continuous basaltic activity, and curvilinear emissive fissures associated with scoria cones, shaping an 8 km-wide and 10 km-long



Fig. 6.44 Dalafilla cumulo-volcano seen from west. The small transverse graven affecting the older shield volcano is visible as well as the ring fissures emissive of coria cones and spatter ramparts (photo Smithsonian Institution, global volcanism program)

elliptic structure, still mark the surface of this previous shield. These curvilinear fissures emitted iron-rich andesine basalts as well as thicker dark trachyte flows. Embedded in this large volcano-tectonic structure, other sets of scoria ramparts, also emitting flows of intermediate compositions, are observed. They form narrower ellipses that are also marked by faults (up to 100 m) with throw towards the outside of the range. As a whole, this induced an elongated axial horst-like structure that clearly relates to a magmatic rather than a tectonic origin.

Looking more closely, we observe that the axial part of this volcanic system is rather complex, with two distinct units—the northernmost 2-km Alu and the southernmost 4-km Dala Filla. Both consist of two distinct elements:

- The uplifted surface of the initial shield volcano, consisting of a pile of basaltic flows, intensively faulted and

affected by open fissures in a dominant NNW direction, with associated complex patterns of short transverse and curvilinear faults, also clearly extensional (Fig. 6.44).

- A silicic central volcano, located west of the horst at Alu and east of the Horst at Dala Filla. Both of these cumulo-volcanoes consist of piles of thick and short flows, each clearly genetically related to the nearby volcano-tectonic structure (Fig. 6.45).
 - In the case of Alu, the rhyolite flows are emitted from a curvilinear fissure surrounding the horst, during which lavas of intermediate compositions were emitted towards the south from similarly aligned spatter ramparts. These flows could extend west and not east as they hit against the fault scarp of the nearby horst.
 - In the case of Dala Filla, this is a perfect cone built by accumulation of viscous silica-rich lava. The upper

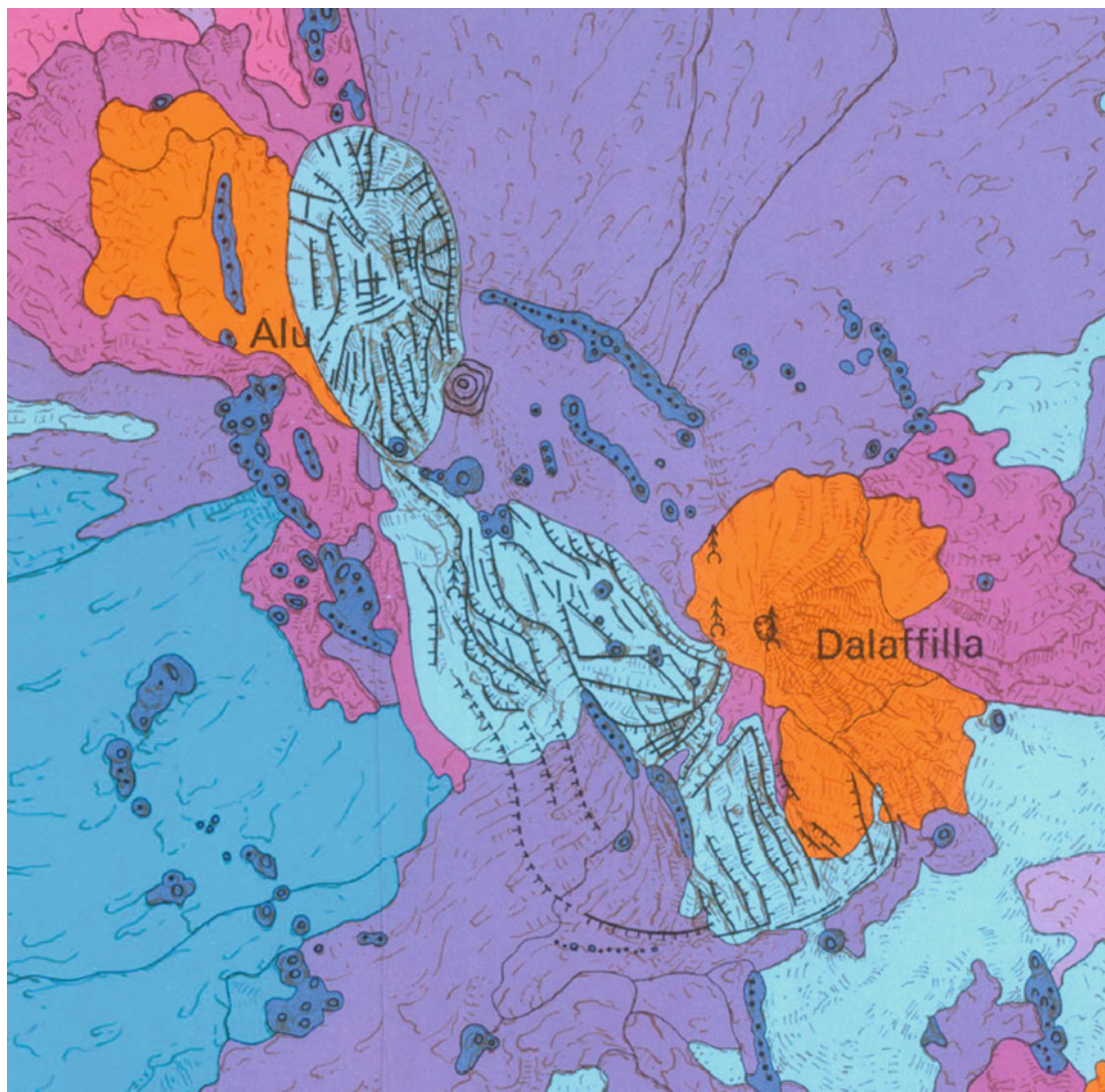


Fig. 6.45 Zoom of map of Alu and Dala Filla volcanic centres showing the deformation encountered by the underlying shield volcano as a result of the development of shallow magma chambers—inflation and deflation—controlling the development of the silicic cumulo-volcanoes

flows, which are the most viscous, reach a steepness of 35° . A crater 100 m wide is observed at the fumarolised top of the volcano (Fig. 6.44). The flows extend more widely to the east and south, as to the west they were stopped by the nearby faulted ancient shield volcano, with the exception of the small central transverse graben (aligned with the silicic volcanic centre) where the early blocky lavas from this cumulo-volcano could flow.

All these units are affected by an intense fumarolic activity. These are particularly well developed along faults bordering the Alu and Dala Filla horsts (Fig. 6.46) as well as in the silicic volcanoes themselves (Fig. 6.47). Temperatures ranging from 135 to 221°C were measured in February 1968, the chemical analysis of the gases revealing important concentrations of boric, hydrofluoric and hydrochloric acids with deposits of sulphur and NH_4Cl . At Alu, the mineral sublimates were also studied by Martini (1969), showing the



Fig. 6.46 A wide hydrothermal alteration zone developed along a NNW trending fault affecting the Alu area. It seems that an increase in this activity has been observed since the 2008 eruption (*Photo coll. G. Marinelli, Pisa University*)



Fig. 6.47 The Dalafilla volcano, formed by accumulation of viscous rhyolitic lava flows and deeply altered by high temperature fumarolic activity (Photo coll. G. Marinelli, Pisa University)

presence of coquimbite $\text{Fe}_2(\text{SO}_4) \cdot 3.9\text{H}_2\text{O}$ and sassolite $\text{B}(\text{OH})_3$.

The petrographic succession displays some similitude with the Borale Ale sequence of crystal fractionation, despite clearly independent magma chambers (Barberi and Varet 1970; Treuil et al. 1971; Bizouard et al. 1980). The earliest fissural lavas are made of olivine basalts, evolving towards andesine basalts in the shield volcano, eventually enriched in iron (up to 20% total iron). These are found in particular in

the bulged parts of the shields displaying horst-like structures. Plagioclase porphyritic basalts are also common in this environment, showing the important role played by plagioclases in the fractionation process. Dark trachytes are mainly found in the thick blocky flows issued from the curvilinear emissive fissures, and all types of intermediate products can be sampled in these lava fields of the upper part of the shield, whether anterior or posterior to the bulges. The thick, viscous lava flows of Alu and Dala Filla volcanoes are made of

vitreous silicic trachytes and rhyolites, showing a comenditic affinity for the most evolved. The Dala Filla cone is made of feldspar porphyritic obsidians.

As a whole, a continuous series of lavas is observed from the initial olivine basalts to the uppermost comendites. However, if the petrographic sequence is continuous, and the proportion of the lavas emitted in adequation with what should be expected from a process of differentiation by crystal fractionation in a shallow magma chamber, the temporal and geographic sequence is not so simple. Lavas of various compositions were emitted, even recently, in similar periods of time, from different volcano-tectonic environments. Despite the complexity of the area, the relation between magmatic compositions and volcanic origin is obvious: fissural basalts from NNW open fissures, flows of intermediate compositions issued from curvilinear fissures affecting the shield and peralkaline silicic obsidians building the cumulo-volcanoes.

It is of interest to note that the Alu—Dala Filla area was affected by significant volcanic activity in the year 2008 between October 30 and November 6 (Fig. 6.48). It started

with continuous swarms of earthquakes of local magnitude interpreted as surface faulting above propagating dykes that led to the eruption on November 3. These were deduced from tele-seismic records and satellite observations (ASTER thermal infrared from NASA's Terra Satellite; see Fig. 6.49) and OMI sulphur dioxide and MODIS thermal images showing the position of the eruptive fissure and of the flow, and the behaviour of the volcanic plume (Pagli et al. 2012). Despite the lack of direct field observations by scientists, it was possible to show that the volcanic activity peaked over a few hours and then waned and stopped on the night of November 6.

Using interferograms obtained from radar images acquired by the ENVISAT and ALOS satellites, it was possible to map the deformations preceding and accompanying the volcanic event. Pre-eruptive reconstitutions showed a 3 cm per month uplift from July to September 2008. This deformation stopped on October 17. No deformation was observed elsewhere before the eruption. Co-eruptive interferograms show an elongated subsidence along the Alu Dala filla axis, with a maximum of 1.9 m at



Fig. 6.48 Alu and Dallafilla volcanic units showing the fresh basalt lava eruption that erupted in 2008 (*black and grey*) from the 2008 ring fissure (shown in *continuous red*)—the older ring fissures are in *dotted*

red; observe the three active hydrothermal sites (in *white and yellow*). From Smithsonian/NASA Earth Observatory/FORMOSAT, December 2008

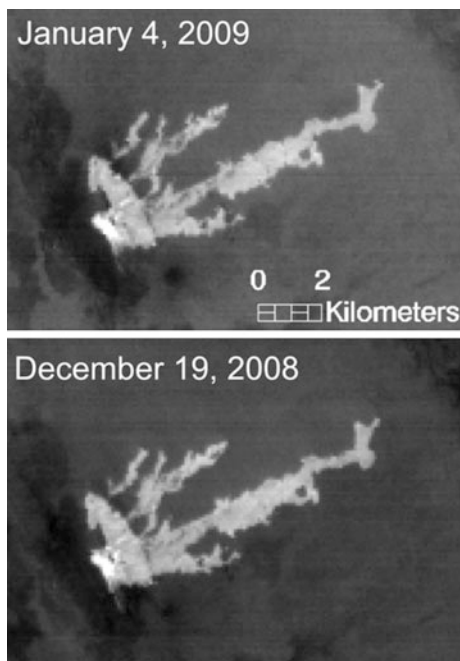


Fig. 6.49 Satellite ASTER images over Dallafila and Alu volcanoes on December 19, 2008 and January 4, 2009 (night-time thermal images, band 14, 11-micron wavelength) showing flow to the NE from fissure system north of Dallafila (Smithsonian Institution, global volcanism program)

Alu. This was followed by sequences of uplifts and subsidences during the eruption.

The data showed that three types of magmatic sources played a role during the eruption: a shallow sill at 1 km depth beneath Alu horst, a dyke at the location of the eruptive fissure and a deflating magma chamber beneath Dala Filla horst. It is interesting to note that these deformations recorded by satellite interferometry fit quite well with our previous field observations of the intensively deformed horst structures previously affected by several phases of bulge and sink.

The lava flow, of unknown composition (we speculate it is an intermediate lava), covers an area of 16 km²; the maximum dyke opening was 4.6 m with a total volume of 5.1×10^6 m³ and the total volume of the sill and the magma chamber were 30.5×10^6 m³. These volumes would fit with a flow with an average thickness of 1.6 m. Pagli et al. (2012) also interpret the phenomena as resulting from the presence of a pre-existing magma at shallow level, which fits the hypothesis of permanent shallow magma chambers (Fig. 6.50). This is consistent with the recurrent surface deformations of the shield volcano and related eruptions as deduced from the volcanological evolution observed by Barberi and Varet in 1970.

If we superpose the map of the 2008 eruption on the geological map established earlier (Barberi and Varet

1970), it appears that these new feeding fissures are superimposed onto the pre-existing curvilinear fissures linking Dala Filla and Alu. The 2008 eruption can be looked at as a rejuvenation of pre-existing lines of weakness affecting the shallow magma chamber. The composition of the flow, once analysed, may therefore prove to be a product of crystal fractionation of intermediate composition.

6.2.6 Gada Ale Volcano

The northernmost volcanic unit of the range is a small central volcano 2 km in diameter sitting above the lakes Karum and Bakili in the lowest part of the salt plain (126 m below sea level at the lakes surface; their depth is not known). This is the narrowest part of the range (13 km). The area mainly consist of flat-lying basalts that have covered the salt plain, with a surface at the latitude of 40–20 m below sea level, issued from fissures of NNW directions. Lake Karum itself is bounded by faults of this direction, building a graben on both sides. Gada Ale volcano (+260 m, i.e. 386 m above the salt plain), emissive fissures located south of it and marked by rectilinear ramparts made of coalescent scoria cones and two other volcanic centres are all aligned along the axis of this graben (Fig. 6.51).

Gada Ale volcano is made of relatively viscous lava flows, interbedded with a few hyaloclastites and pyroclastites that accumulated around a single vent where a 500 m-wide crater is observed. The rocks at the summit are deeply altered by a still intense fumarolic activity, and are transformed in soft boiling clays. The crater is occupied by a lake made of boiling mud (95 °C). Sulphur is the main sublimate. It seems from the volcanic structure that Gada Ale volcano was affected by at least two concentric uplifts, easily visible on its NW foot as well as near to the summit, particularly on the NE side of the crater.

Before the emission of the viscous lavas, the volcano was mainly built along an axial fissure that is well marked to the south with a recent basaltic activity producing diverging flows and the set of aligned scoria cones and craters mentioned above. Two cones are particularly visible: a subaerial scoria cone open to the south and Catherine volcano.

Catherine volcano is a remarkable hyaloclastite cone 300 m in diameter at the top and 120 m high. A small lake occupies this crater, which is fed by hot springs allowing for a ring of vegetation to develop in this arid environment. To the south, the rim is cut by a fault through which a basaltic dyke 1 m thick fed a small subaerial scoria cone. This submarine volcano is older than the surrounding subaerial lavas.

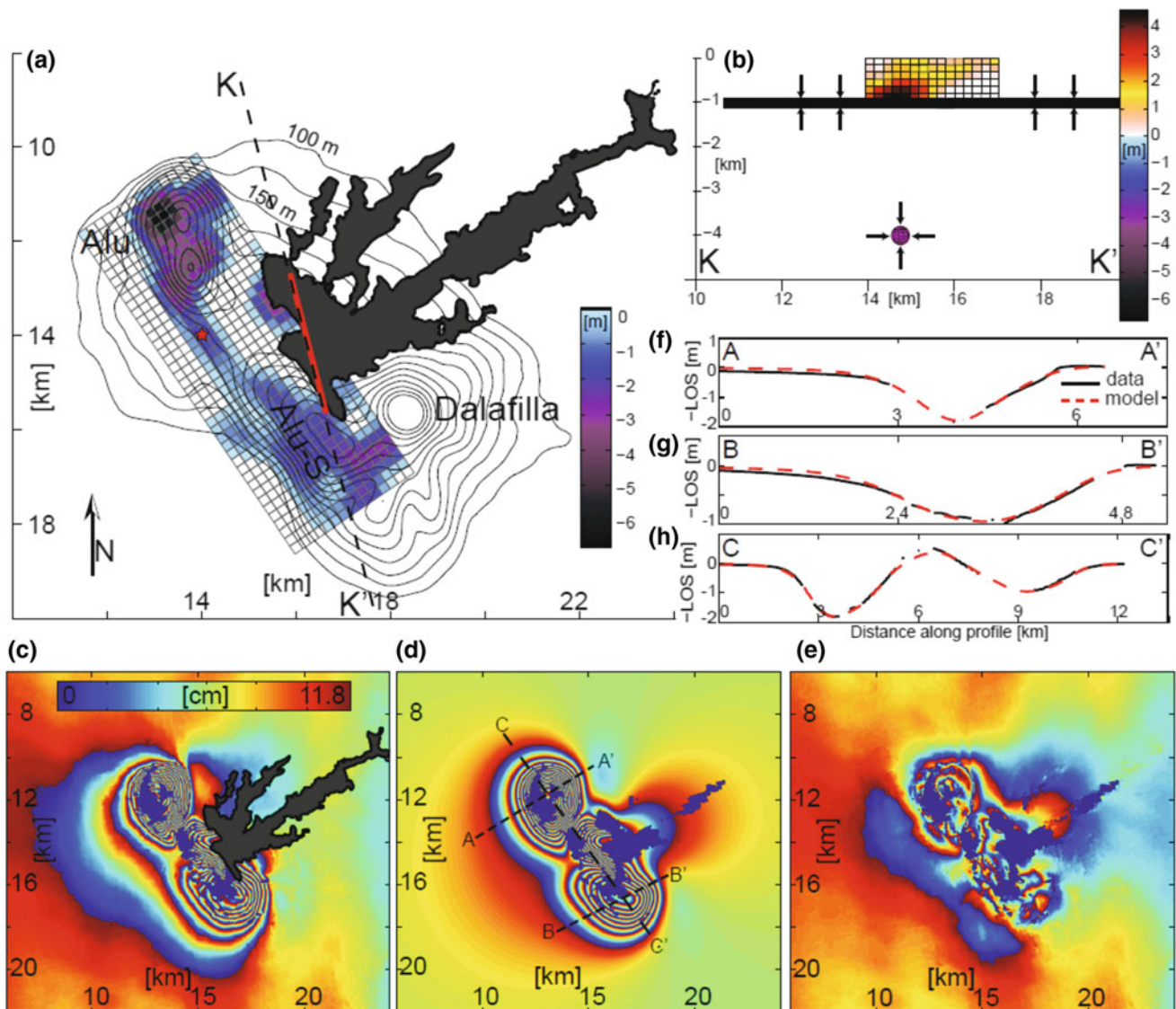


Fig. 6.50 Co-eruptive InSAR data and models. **a** Plan view of the co-eruptive distributed sill contraction, overlaid by topographic contours and the lava flow. The red line represents the dike; **b** cross section of the distributed dyke opening along line K-K'; **c** ALOS

ascending co-eruptive interferogram; **d** model interferogram; **e** residual. One colour cycle represents 11.8 cm of displacement in the satellite line of sight; **f-h** observed and modelled displacements along cross sections shown in **d** (Pagli et al. 2012)

To the west of Gada Ale volcano, a salt dome is observed that lifted up for at least 100 m all the basaltic surface covering the salt plain (Fig. 6.52). This forms a nearly circular structure of around 2 km in diameter. It appears to be linked with Gada Ale volcano by a transverse structure that appears as a small transverse horst (trending ENE). Therefore both structures are clearly related, and if both were considered as sharing a similar origin (of salt dome) by Barberi and Varet (1970), another magmatic origin can also be envisaged.

This uplifted structure allows one to observe the succession of the early basaltic lava flows and their relation to the

salt. It also allows one to observe, on the NW side, high temperature hydrothermal deposits along some of the bordering faults of NNW direction. Rose and pale green apatite crystals reaching several centimetres, preceded the crystallisation of magnetite, displaying nice octahedral forms. This relatively important mineral deposit is of interest for three reasons:

- It shows that this may not be simply a salt dome resulting from the rise of evaporites, but it is linked with magmatic processes.

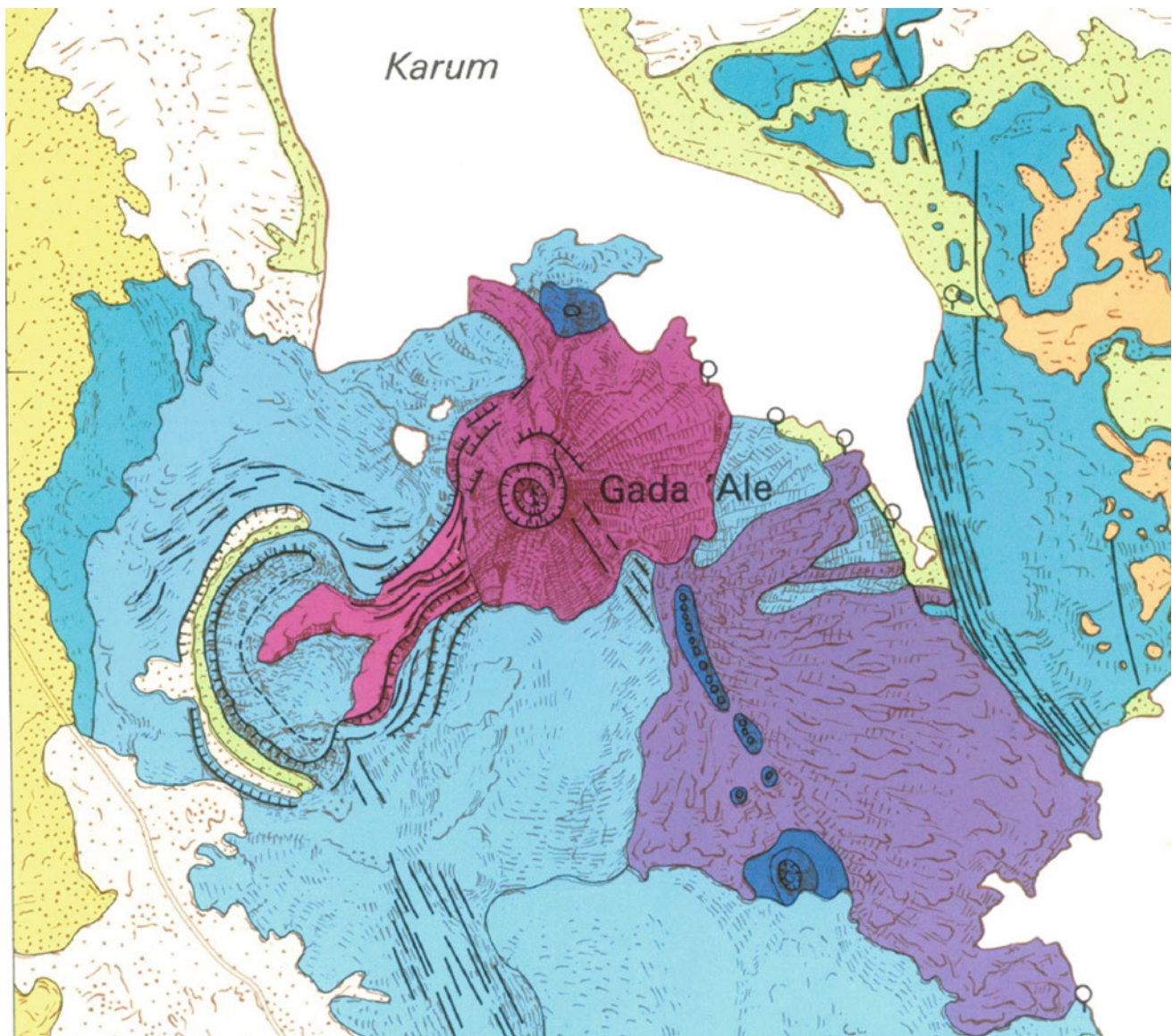


Fig. 6.51 Geological map of Gada Ale volcano (from 1/100,000 map of Erta Ale range, Barberi and Varet 1972) showing the volcano itself, located along the axial spreading axis, and a “salt dome” (of probable magmatic origin) located to the west of it

- The magmatic sequence characterising Erta Ale range (as well as other axial ranges in Afar) implies the separation, at a key intermediate stage of fractionation, of iron oxides and apatite from iron-rich basalts, allowing for the sequence to evolve towards silica-rich trachytes and rhyolites. The deposition of magnetite and apatite along fissures in the vicinity of the magma chamber may be the way these minerals are separated.
- This processes may lead to the formation of mineral deposits, eventually of economic interest if tools are developed for locating and measuring them.

Proceeding with the study of interferograms obtained from SAR images captured in the period June 1993 to October 1997, Amelung et al. (2000) could identify a deformation located at the western foot of Gada Ale volcano along the southern rim of Lake Karum, which may correspond to a 12-cm subsidence, for a magmatic event that occurred in the said period. This does not correspond to any clear feature observed at the surface until then, although this area bordering the lake is characterised by the presence of numerous hot springs. However, if the deformation process is confirmed by further data, this may indicate an extension



Fig. 6.52 Gada Ale volcano (seen from the uplifted “salt dome”) to the west. Lake Karum is seen in the background. Observe the *yellow–white* hydrothermal alteration of the top. Smithsonian Institution, Global Volcanism Program N°221050)

towards east of the transverse tectono-magmatic and hydrothermal feature along the salt dome–Gada Ale alignment. In such a case, it is probable that the hypomagmatic feature observed on the shore extends beneath the round part of the lake; this location would fit with the small graben that border the southern extremity of Karum Lake (Figs. 6.53 and 6.54).

6.2.7 Ale Bagu Strato-Volcano

Ale Bagu is a stratovolcano 1031 m high located to the south-east of the Rorom plain (50 m below sea level). Its basaltic base covers an area of around 25×15 km. This is the only volcano of the Erta Ale range not located along the same axial fissure as the others described above. It is located on a fissure of the same NNW direction located 10 km west from the axial one (Fig. 6.55). The eastern flanks of the volcano are surrounded by the basaltic flows issued from the Haili Gub—Erta Ale axis. It is therefore dissymmetrical with more flows visible on its western flank, and made accessible

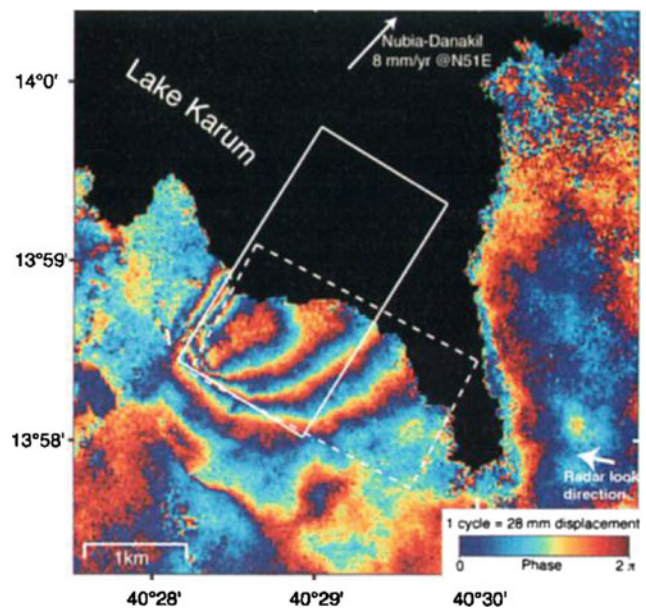


Fig. 6.53 June 1993–October 1997 interferogram for Gada Ale area. One cycle of phase correspond to a 2.8 cm change in ground-to-radar distance (from Amelung et al. 2000)

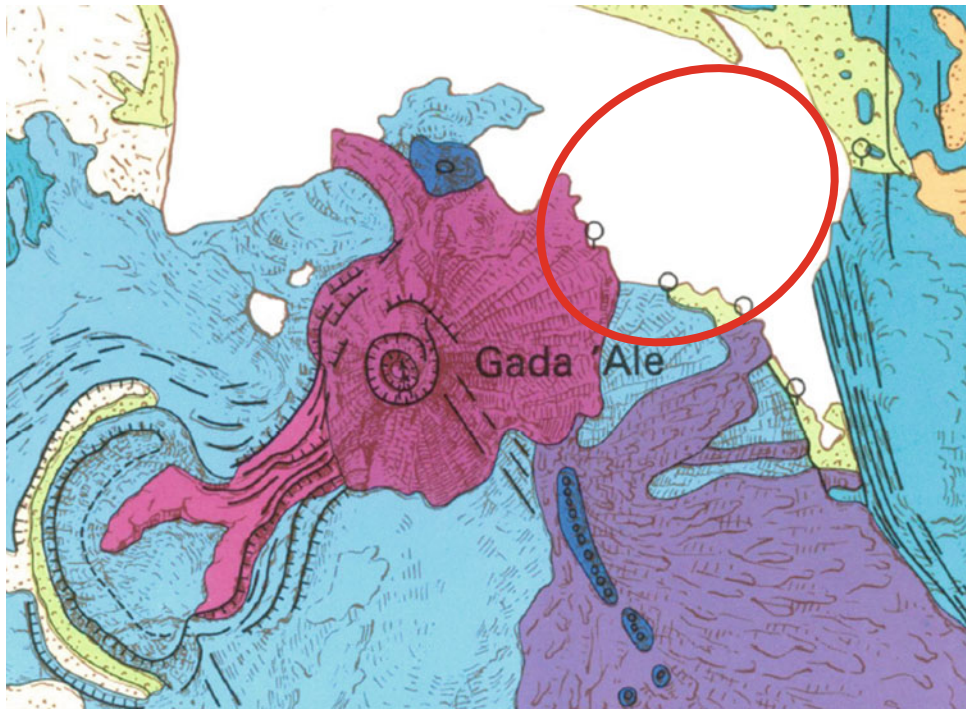


Fig. 6.54 Possible interpretation: hypothetical location of a third hypo-volcanic body located along the transverse alignment of Gada Ale at the point where it crosses the northern extension of the small rift

forming the south of Lake Karum (author's interpretation on the 1/100,000 map of Erta Ale range, Barberi and Varet 1972)

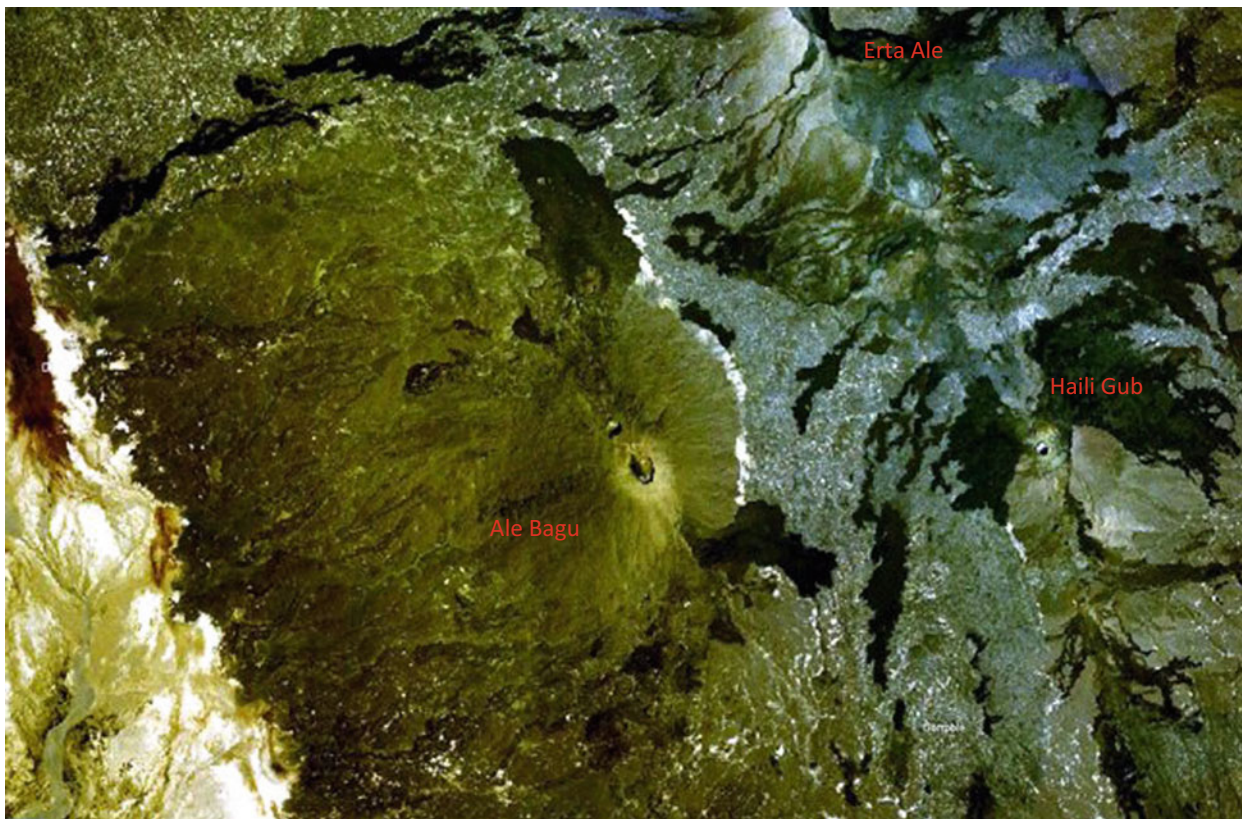


Fig. 6.55 Ale Bagu volcano emitted on a NNW fissure located 10 km west from the Haili Gub—Erta Ale rift axis, also seen on this satellite image (Smithsonian Institution/NASA Lansat 7 image)

from the Rorom plain where the ancient track follows the lava fields.

To the south, the lava fields from Ale Bagu meet with the northernmost extension of the flows from Alayta. As for the other units of the range, the initial activity was characterised by basaltic flows issued from NNW trending fissures. The southernmost lava field is characterised by a strange feature. A small graben, 2 km long and 100 m wide affect a pahoehoe flow on the flank of the volcano with a depth of a few tens of metres. This probably corresponds to the collapse of the lava surface along an open fissure that occurred while the flow was emitted, as suggested by the direction of the graben, although it is not aligned with the main volcanic axis of Ale Bagu.

The summit of the volcano is covered by dominantly basic pyroclastic products, forming alternating layers of

ashes, lapilli and scoria. The nature of the lapilli is rather heterogeneous: white pumice, obsidian fragments, more or less altered plagioclase and olivine cumulates mixed with compact and scoriaceous basalts. Among these fragments, blocks of large sizes, reaching 1 m, are found. Their composition varies from basalts to intermediate products and their structure from lavas to semi-intrusive facies. In some places interstratified figures are observed. Most craters are located along the summit of the volcano, aligned along a single NNW median trending fissure. On both extremities this fissure gives birth to recent viscous block flows covering the pyroclasts and the basaltic lava fields. In the lower part of the volcano, these flows lie over a thin base surge formation, which apparently relates to the pyroclastic event (Fig. 6.56).

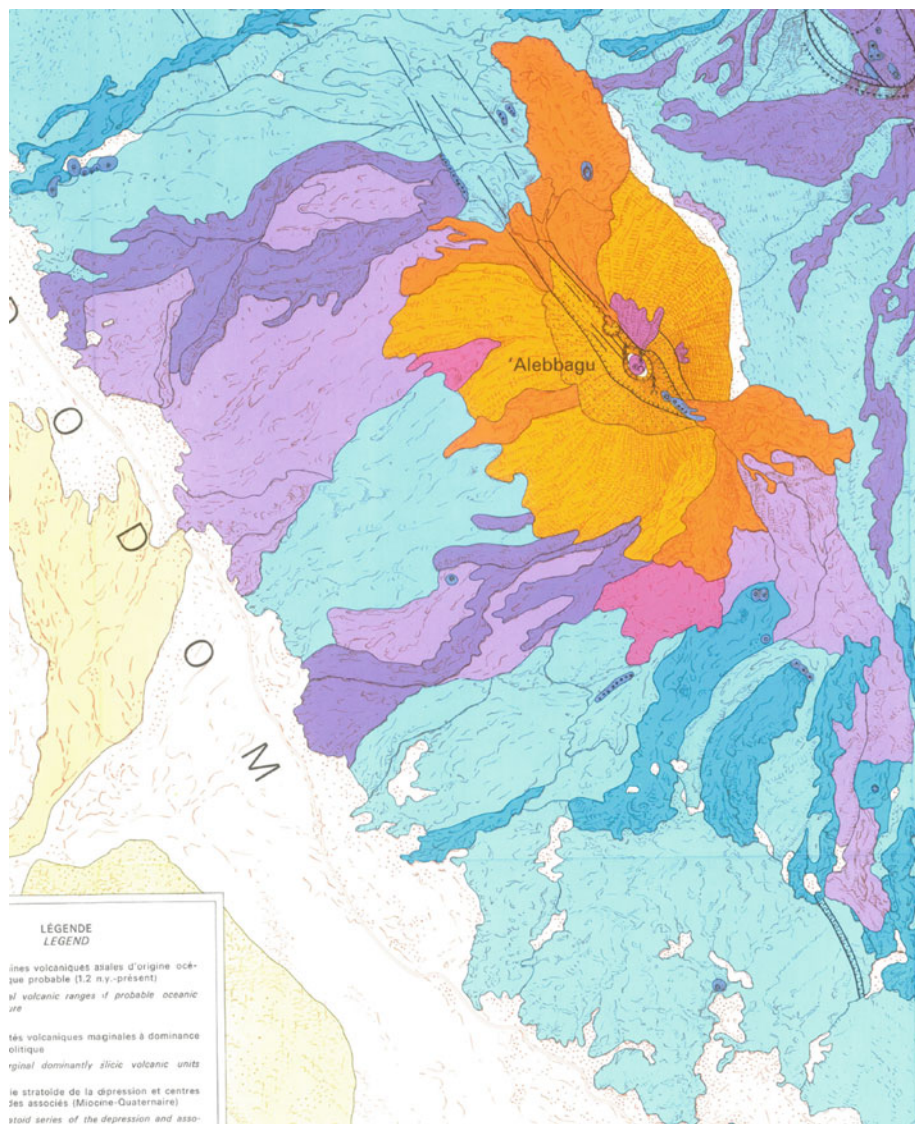


Fig. 6.56 Geological map of Ale Bagu stratovolcano, extracted from the 1/100,000 scale map of Erta Ale range (Barberi and Varet 1970). In dotted ping the pyroclastic layer covering the upper part of the

volcano. Later trachytes, rhyolites and mugearites were emitted outside and inside the crater

The fact that the only off-axis volcano of the Erta Ale range displays a different volcanological character to this well-developed pyroclastic layer is striking. It may relate to the influence of the nearby Rorom plain, where a groundflow of water issued from the Nubian plateau is being lost beneath the Ale Bagu lava fields. As a consequence, the presence of groundwater inflow may have interfered with the shallow magma chamber underlying the volcano in producing the phreato-magmatic event that generated these pyroclastic products.

The main crater is composite, formed by the coalescence of a large elliptic crater with a smaller sub-circular crater at its NNW extremity. As a result, the shape of the crater, 750×450 m, is not perfectly elliptic. The internal wall of the crater is more than 100 m high, allowing one to observe the volcanic products underlying the 30-m thick superficial pyroclasts. Observation shows that these are essentially lava flows of intermediate composition. A small cone produced

by the accumulation of lava occupies the crater floor. Slightly excentric, it is associated with a recent viscous trachytic flow (Fig. 6.57). Fumaroles are observed on the summit of the cone and at the base of this recent flow. Steaming vents are also observed in several places along the crater walls. A set of smaller pit craters, aligned along the main emissive fissure occupy the northern part of the volcano axis. Their diameters decrease with the distance from the centre (Figs. 6.58 and 6.59). The largest pit is 80 m deep, with a nearly circular shape, and is 250 m in diameter. It is partly destroyed to the north by a more recent crater covering its flank. A very viscous trachyte flow did flow along the crater rim but remained stuck against the wall, never reaching the crater bottom.

Very thick silica-saturated alkali trachytes flowed to the south and to the north along the rather steep slopes of Ale Bagu volcano, forming impressive, impassable blocky surfaces several metres high (Fig. 6.60).



Fig. 6.57 Ale Bagu crater: a pyroclastic layer (30 m thick at crater rim) covers the lava flows observed on the crater walls, and the crater floor covered by later viscous trachyte flows emitted from a dome now fumarolized (*Photo coll. G. Marinelli, Pisa University*)

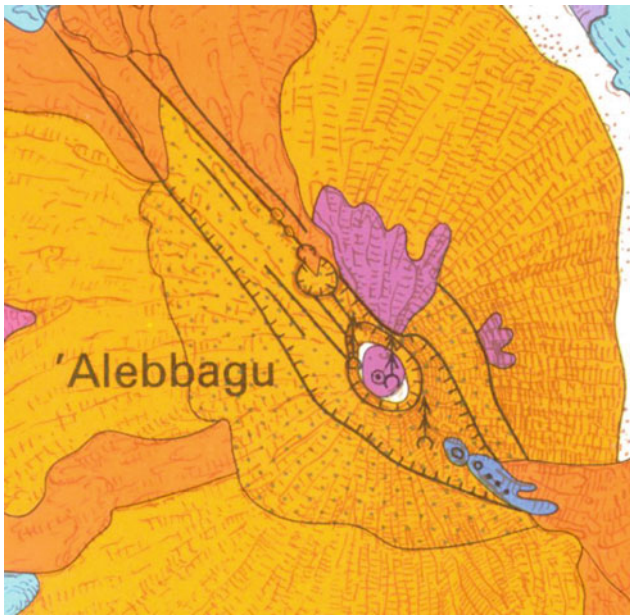


Fig. 6.58 Detailed views (satellite image and geological map) of the central part of the axis of Ale Bagu volcano displaying—along the NNW axis of spreading with a well-marked graben—a set of pit craters of decreasing size from the central pit to the north. Another emissive fissure is observed on the western side of this alignment



Fig. 6.59 Detailed views (satellite image and geological map) of the central part of the axis of Ale Bagu volcano displaying—along the NNW axis of spreading with a well-marked graben—a set of pit craters of decreasing size from the central pit to the north. Another emissive fissure is observed on the western side of this alignment



Fig. 6.60 Front of the thick, blocky trachyte lava flow emitted from Ale Bagu volcano towards the north where it meets with the basalts emitted from Erta Ale shield

From a tectonic point of view, let us confirm that this lateral fissure with respect to the axis of the Erta Ale range fed the whole activity of the Ale Bagu volcano, meaning a rather stable dual expansion along the southern part of the range. A particularity developed even more, further south, with the presence of two parallel axial ranges: Tat'Ali and Alayta.

In addition, observe that this volcano is marked by a well-expressed axial graben of NNW direction that affects the whole pyroclastic layer and results in emitting fissures on both the northern and southern side where the graben tends to close in a single fissure.

As a whole, Ale Bagu displays a few distinctive features besides its position: relative abundance of pyroclastic products and deep and large summit craters. Besides this, although the composition of each volcano differs slightly from the others despite the same sequence from olivine basalts to differentiated products to comendites, Ale Bagu is the only unit in which the final products are not peralkaline. The magma sequence is also slightly more potassic than those of the axial volcanoes of the range.

6.3 Tat'Ali–Mat'Ala Axial Range

To the south of Erta Ale range, the Afar depression is becoming larger because of two phenomena:

- To the east, the rotation of the Danakil Alps induces an increasing opening of the rift southwards
- To the west, the Nubian escarpment is subject to a right lateral *en échelon* offset, which displace the fault scarp further west

To fill the gap, two axial ranges co-exist at that level, in addition to the older Afdera volcano and stratoid substratum. The coexistence of two active axial ranges at this level is a striking feature of the Afar Rift system (see Fig. 4.17).

Tat'Ali–Mat'Ala axial range sits on the eastern side of Lake Afrera, and is located at the foot of the escarpment of the Danakil Alps, on a sedimentary floor made of marine coral reefs and evaporites covered by more recent lacustrine deposits that also extend south of the range. Fed as other axial ranges by fissures emitted from a single NNW trending line, it is quite a complex structure in which several volcanic units can be distinguished (Fig. 6.61):

- Tat'Ali fissural lava field to the north, which developed at the same latitude as the Haili Gub axis, at a distance of 20 km

- This extends towards south in the Tat'Ali volcano, characterised by an elongated summit caldera built along the axial graben of this rift
- Further south, to the Mat'Ala shield volcano at the northern extremity of the lacustrine Sodonta plain
- On the western flank of the Tat'Ali axis, sits the Borawli volcano that contribute to the shape of Lake Afrera as it borders to the south its northern lobe

As for Erta Ale range, the activity starts with submarine (to the north and east) and sublacustrine (to the south and west) activity with hyaloclastite cone observed to the north and the typical pavement surface of the fissural basalts observed in early flows all around the range.

The fissural flows observed to the north of the range are deeply faulted, with sometimes important fault scarps, despite the fact that the affected lava flows are quite recent. One of the fault scarps marks the limit of Lake Afrera to the NE. All these lavas have been emitted along open fissures that are parallel to the faults (NNW trend) and the tectonic and volcanic activity appear to have been contemporaneous over several phases, up to very recent (historic) periods (Fig. 6.62). Only basaltic materials are found, ranging from picrites—with typical olivine cumulates and xenocrysts—to aphyric basalts. A phreato-magmatic explosion crater erupted numerous mafic and ultramafic blocks that allow one to sample earlier activity; it is also a geothermal index of interest.

The main Tat'Ali volcano is built on the southern extension of these fissures, but whereas these appear as a ridge, a well-developed axial graben, building a rectangular caldera, 3 km wide and at least 10 km long, extends towards the south in line with the Mat'Ala crater.

If the shield volcano is mainly made of basalts, the lavas, emitted from the latest fissures bordering the sink walls on both sides, are mainly andesine ferrobasalts and dark trachytes on the eastern flank and silicic trachytes and peralkaline rhyolites (pantellerites) on the western flank (Figs. 6.63 and 6.64). Field observations show that the faults bordering the caldera were partly contemporaneous with the silicic eruption, showing inflation and deflation from a shallow magma chamber, also giving rise to post-caldera pantellerite domes and flows (the latest well visible to the west of the ring wall of the caldera; Fig. 6.65).

Postdating the caldera sequence, a recent basalt flow emitted near the southern rim of the caldera partly covers the floor of the central sink (Fig. 6.66).

In the NW part of the range, Borawli is a simple cumulo-volcano of typical conical shape. It is made of silica-saturated trachytes covering older faulted basalts. It is surrounded by a few other rhyolitic domes, one of which emitted fairly recent pantelleritic obsidian associated with

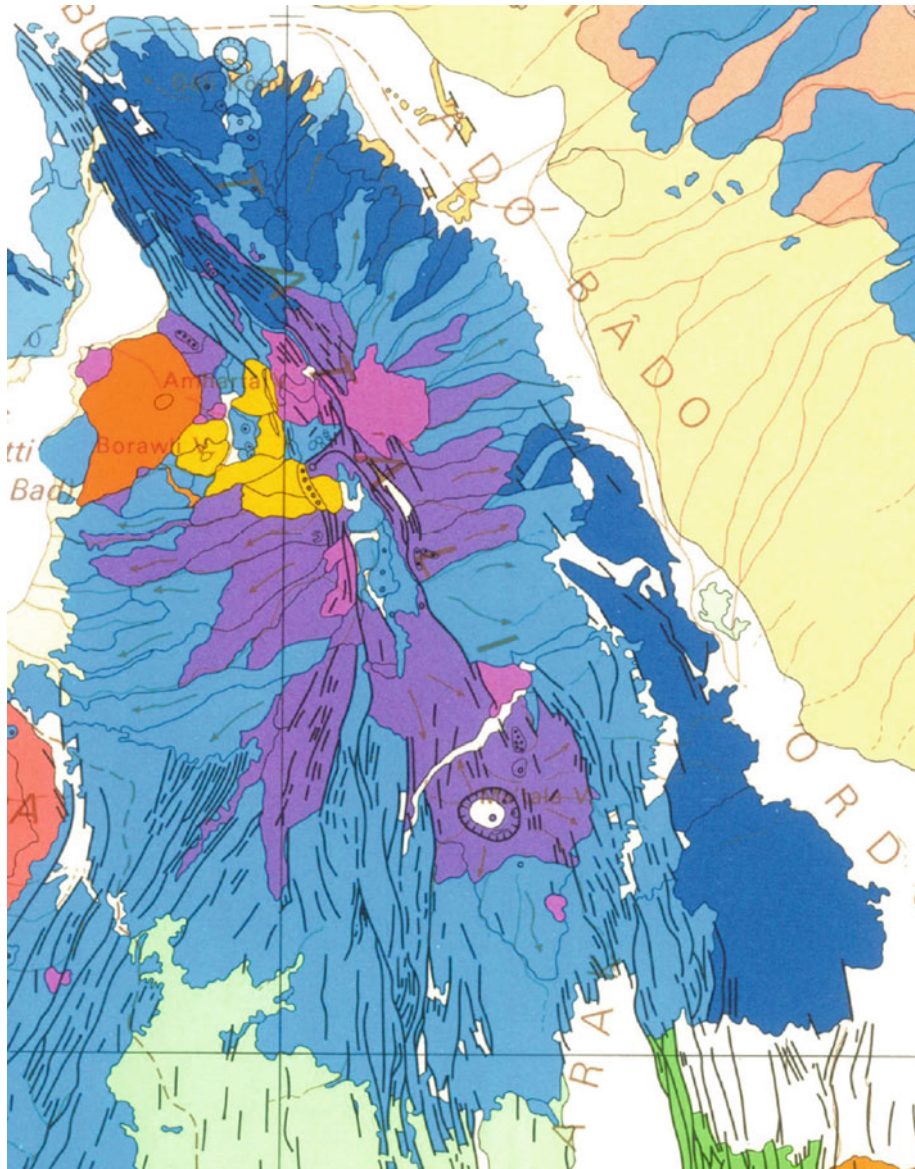


Fig. 6.61 Geological map of the Tat'Ali–Mat'Ala axial range, extracted from the 1/500,000 scale map of northern Afar (CNR-CNRS 1973). Observe the northern fissural, intensively faulted basaltic lava field, the complex central volcano with elongated caldera along axial

rift, the southern Mat'Ala shield with its large crater and the densely faulted and fed by fissural emissions SE side affected by transverse (NNE–SSW) tectonics. All units are hydrothermally active

pumice, probably the source of rounded pumice fragments found all around Lake Afrera (Barberi et al. 1973).

Mat'Ala is a flat shield volcano with a large summit crater 3.5×2.5 km diameter and approximately 300 m deep, slightly elongated in a transverse direction (Fig. 6.67). It is located along the axis of the Tat'Ali rift, and close to it to the south. Note that this volcano sits along the axis of an important graben that extends south for over 50 km along

Dadak, and may have ensured a direct link, now aborted, between Tat'Ali–Mat'Ala range and Inakir range, located 150 km SE, through Maska lava field and Ab'a graben (see Fig. 6.117 and Sect. 6.6).

Faults in a NNE direction, well developed at the foot of Afdera volcano, reach the Tat'Ali–Mat'Ala rift axis and have influenced both the closing of the Tat'Ali caldera to the south and the location of the Mat'Ala crater, finally

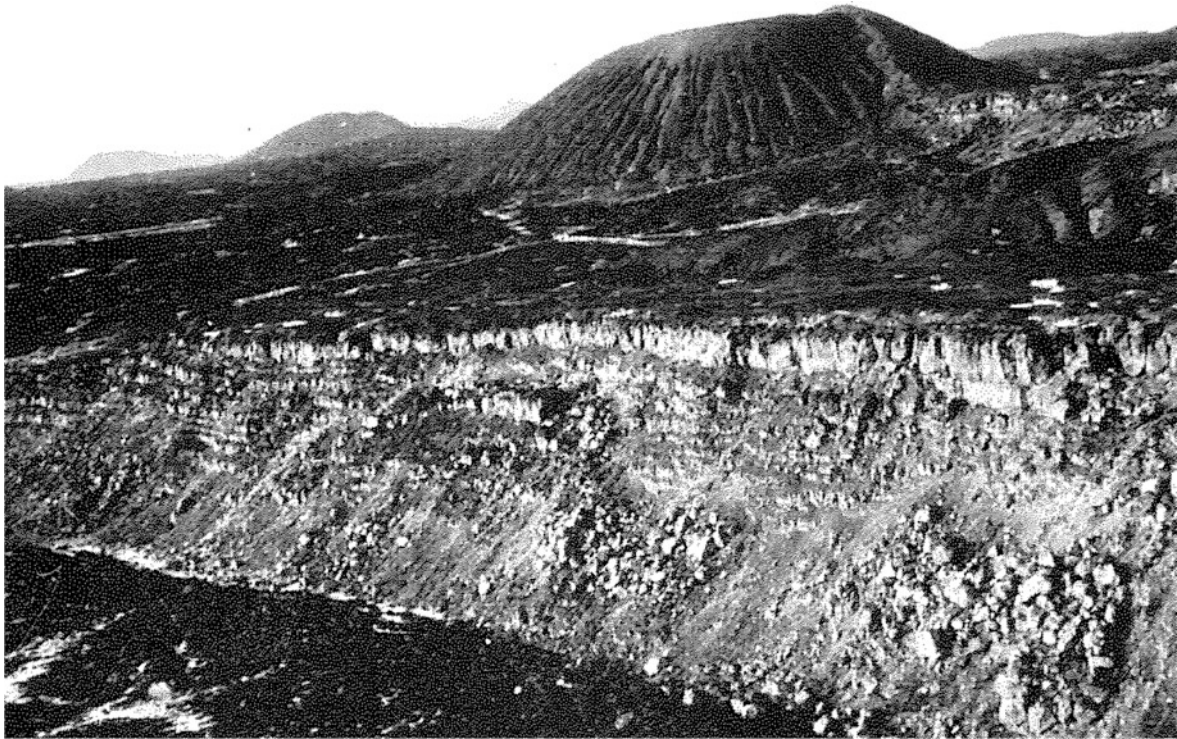


Fig. 6.62 The northern lava field of Tat Ali range is marked by an important tectonic (open fissures and normal faults) and volcanic (basaltic fissural) activity, including present day faulting affecting even the young scoria cones

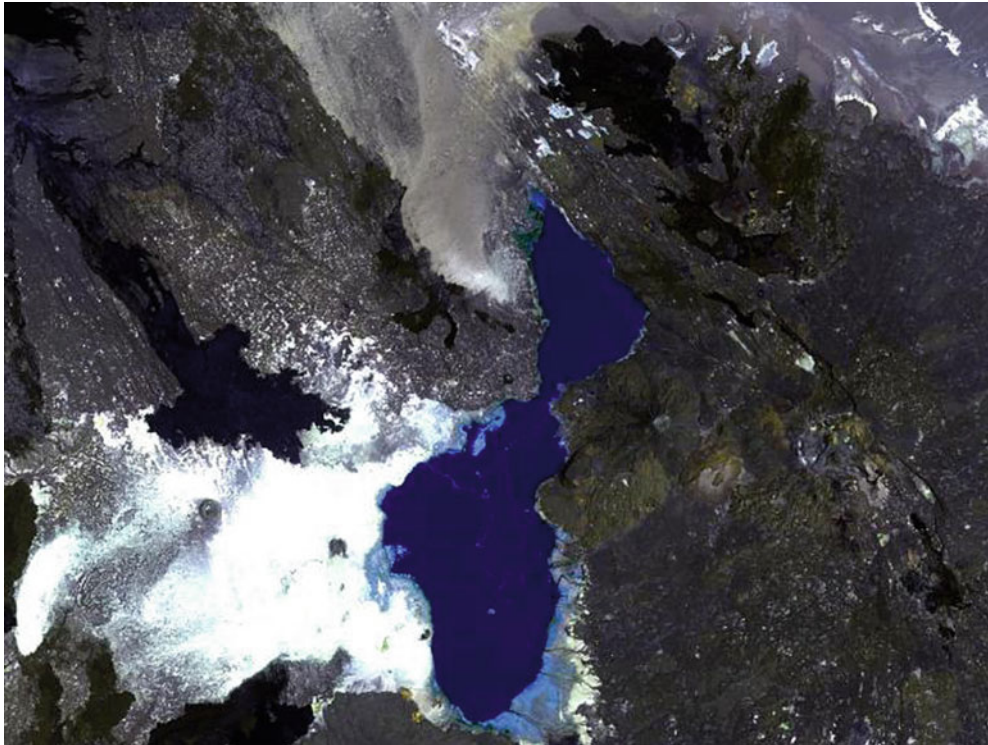


Fig. 6.63 NASA Landsat image (1999, Smithsonian) of the NW part of the Tat Ali range. The elongated axial depression affects the shield volcano if covered by recent basaltic flow. The youngest Aa flows of the northern fissural basaltic highly faulted lava field are of dense

black colour. Borawli central volcano lies near to Lake Afrera. Lava flows at the *upper left* are from Hayli Gub axial graben (S end of Ertale range), whereas the N edge of the Alayta lava field is seen at *lower left*



Fig. 6.64 Satellite image of the Tat Ali axial zone showing the NNW elongated sink (faults underlined in *red*) which developed contemporaneously with the emission of alkali-silica trachytes and pantellerites topping the elongated shield volcano



Fig. 6.65 Detailed view of the alkali-silica trachytes (*right*) flowing from the NW rim of the caldera walls and of the fairly recent pantellerite twin domes-flows on the flank of the shield



Fig. 6.66 Oblique air photograph of the twin pantelleritic dome-flows erupted on the flank of Tat'Ali shield, with Borale stratovolcano dominating Lake Afrera on the *back*. The NNW faulted limit of the Lake is clearly visible at the horizon (*Photo coll.* G. Marinelli, University of Pisa)

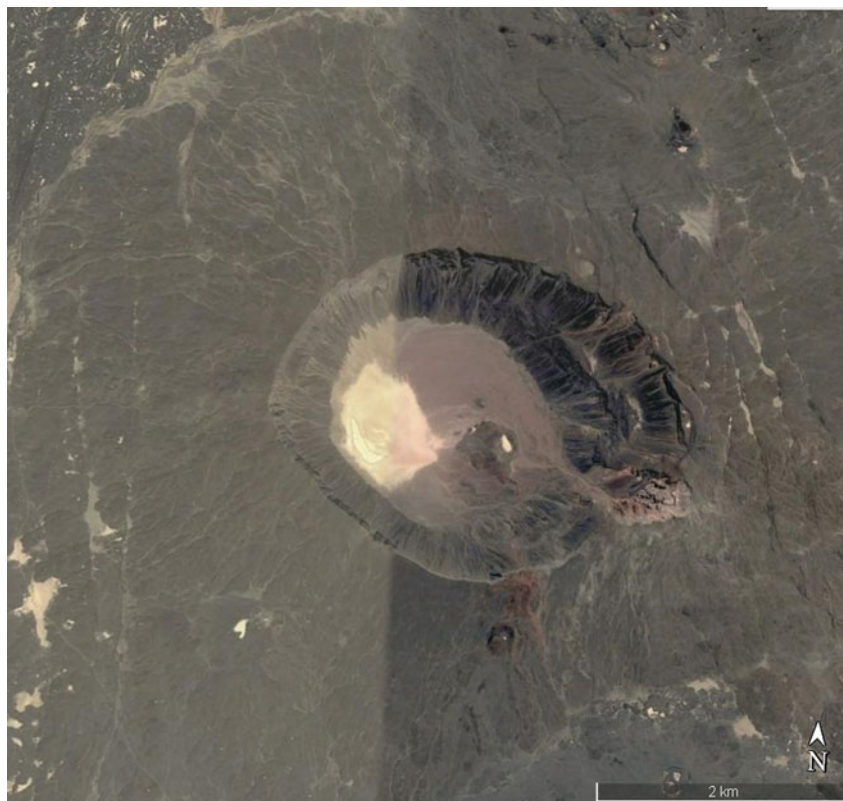


Fig. 6.67 Satellite image of the Mat'Ala crater

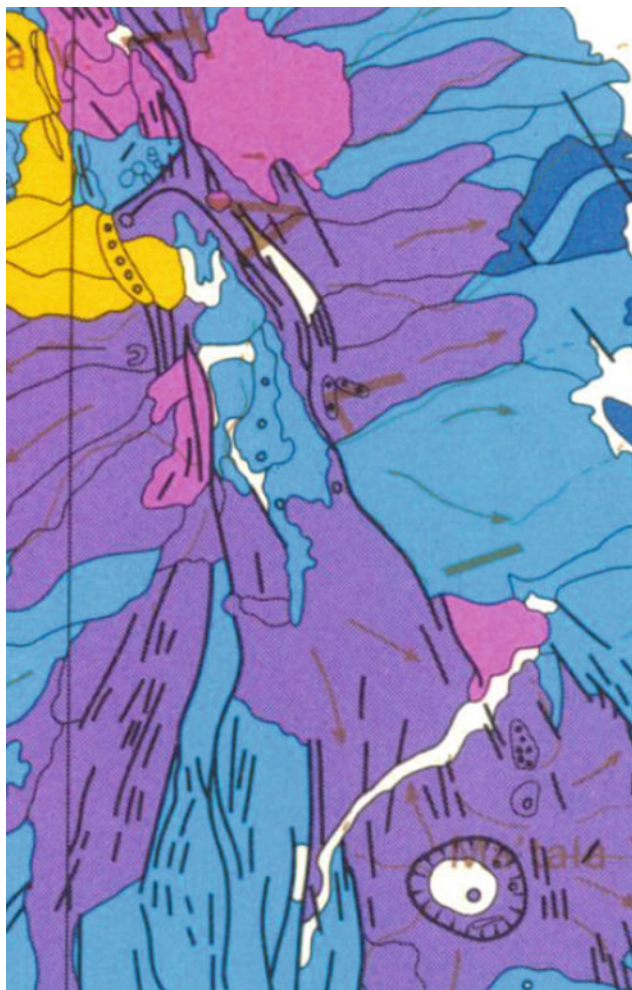


Fig. 6.68 Zoom on the axis of the Tat'Ali–Mat'Ala range with the large crater of the southern shield volcano closing the axial graben from which most evolved products were emitted. Hydrothermal activity is still persistent along these emissive border faults. Later basalts emitted from an axial fissure carpet the floor of the sink

stopping the southern extension of the range. South of the crater, open faulting develops in a fan shape with all intermediate directions between NNW and NNE. This allows for the development of a 12 km-wide active graben extending over 50 km south of the range in the Sodonta and Haral plains controlled by normal faults of dominantly N–S direction.

Altogether, from a magma genetic point of view, the Tat'Ali–Mat'Ala range is characterised by a continuous series ranging from picritic basalts to pantellerites, with all intermediate materials (Figs. 6.68 and 6.69), showing that a persistent magma elongated chamber allowed several cycles of crystal fractionation to develop until recent times.

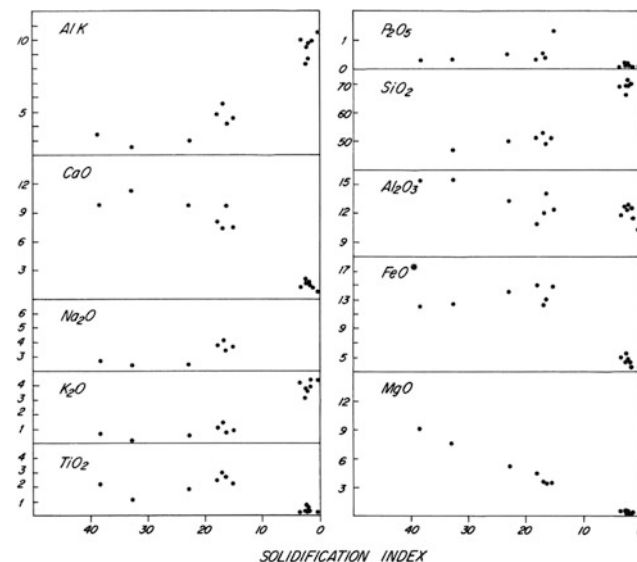


Fig. 6.69 Magmatic evolution in the Tat'Ali–Mat'Ala axial range, from picritic basalts to pantellerites observed from major elements plotted against the Solidification Index (from Barberi et al. 1973)

However, the Tat'Ali–Mat'Ala, similar to the Erta Ale range, is not a dying axis of spreading. Despite the development of an elongated shallow magma chamber, allowing for the evolution of initial basaltic magma by crystal fractionation up to the most evolved peralkaline end products, the range is also affected, mainly in its northern extremity but also along its whole axis, by recent tectonics and basalt emissions showing that the spreading is still active.

To the south, Mat'Ala shield has played an important role in the past but is no longer active. The most recent sub-historic volcanic activity has developed along the NNE–SSW trending graben that was interpreted by Barberi and Varet (1977) as the surface expression of a leaky transform fault connecting Tat'Ali range to Manda Harraro through Dabbahu.

Besides volcanic and tectonic activity, hydrothermal manifestations are well expressed in several places in this range. A fumarolic activity is well developed along the faults limiting the elongated Tat'Ali caldera as well as on the top of Borawli volcano and on the south-west fissured wall of Mat'Ala volcano. Together with the hot springs located at the foot of the range along the Afrera Lake shores and the phreatic activity, this allows one to consider the area as a target of geothermal interest.

Looking at the most recent seismic monitoring (red square on Fig. 6.70), the Tat'Ali range also appears to be one of the most active parts of northern Afar, at present—at least in the 2007–2008 interval!—more active than the parallel segment of Alayta.

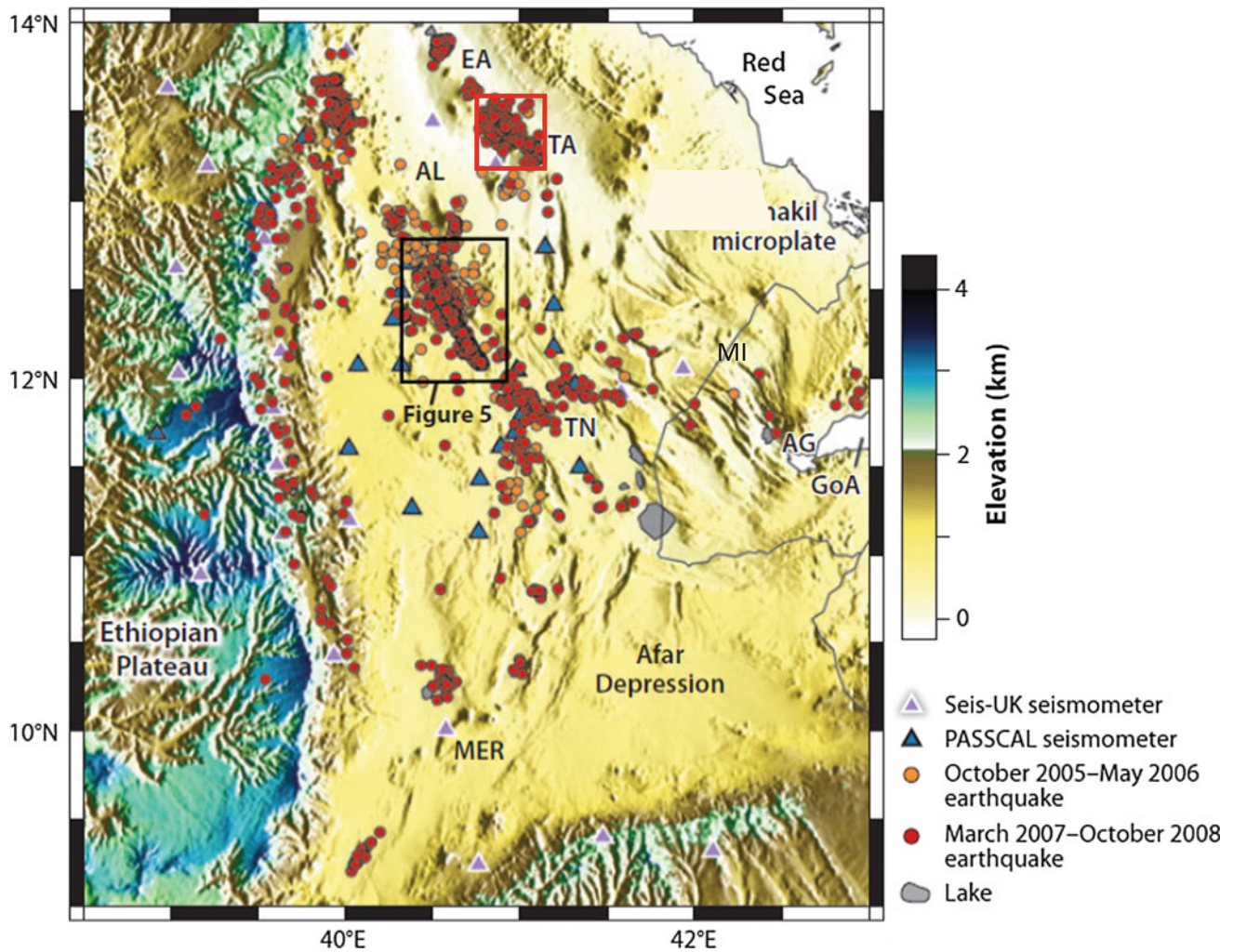


Fig. 6.70 Regional compilation of seismicity recorded on four or more seismometers from October 19, 2005, to November 2009. *Black box* encloses Dabbahu-Manda Hararo segment, whereas *red box* encloses the Tat Ali segment. Incipient seafloor spreading segments

along axial ranges reported are: AG for Asal-Ghoubbet; EA for Erta; TA for Tat Ali; AL for Alayta; MI for Manda Inakir (after Ebinger et al. 2010). Note that if earthquakes are rare there, stations are equally rare in Eastern Afar

6.4 Alayta Axial Range

This axial range, located south from Erta Ale on the Afar floor in a similar position with respect to the Nubian escarpment (displaying a dextral en echelon pattern), is the largest (2660 km²) with an impressive width (60 km) and is the highest (1100 m) of the Afar axial ranges. It consists of two units: an elevated volcano to the west and a flat-lying more recent fissural lava fields to the east (Fig. 6.71).

The first is a typical shield volcano, elongated in a NNW direction, formed from continuous emissions of basalts along a single fissure, at least 40 km long, with basaltic flows directing on both sides and progressively building the shield (Fig. 6.72). An axial graben in the same direction crosses through the summit of shield, along which craters and scoria cones are aligned. On the top of the shield, a

double-rimmed caldera emitted viscous trachyte flows on the western slope before sinking. The floor of the youngest is covered by post-caldera lava with fumarolic activity (Fig. 6.73). On the northern and southern slopes, viscous flows made of dark trachytes were emitted rather recently and found a longer extension to the south (Fig. 6.74). Intermediate lava flows, andesine basalts in particular, frequently plagioclase porphyritic, are abundant on the shield surface. To the NW the Alayta flows hit against the tertiary granitic massif of the Damuma horst, limiting their extension to the west; instead they extended north towards the Dodom plain and to the SW in the Teru plain.

The watershed flowing from this horst are channelled along the contact, collecting several tributaries, including wadi Erepti that brings outflowing waters from an important lateral graben along the downfaulted part of the Nubian

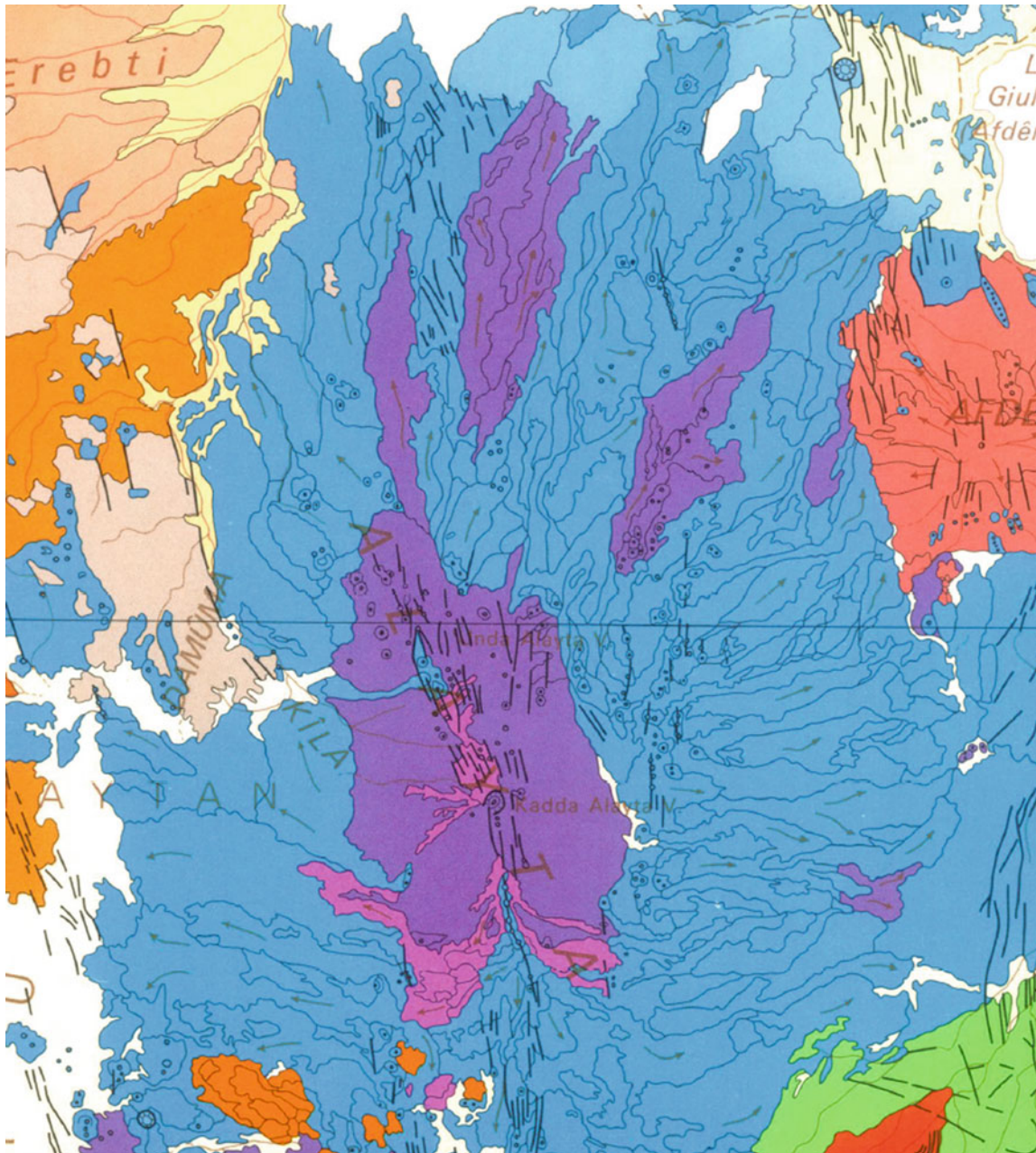


Fig. 6.71 Geological map of the Alayta range extracted from the 1/500,000 map of northern Afar (CNR-CNRS 1973). The elongated shield volcano build on fissures on NNW direction emitted lava flows

of intermediate composition in the later stages. The fissural basaltic lava field, fed by fissures on N–S direction, is made of undifferentiated basalts

escarpment. This wide network feeds the endoreic inflow of the green Dodom plain.

Similarly, the tributaries flowing from the Nubian escarpment further south—including the large wadi Magâle that is also fed by a marginal graben—funnel out in the Teru plain and hit against the lowest flows from Alayta, resulting in a wide plain where important vegetation develops (Fig. 6.75).

As shown by Tazieff et al. (1969), the design of the Erta Ala and Alayta axial ranges that are arranged en echelon

with axis distance of the order of 20 km duplicate the pattern of the Ethiopian escarpment, the bottom line of which is also arranged en echelon, with the major offset of Ma'alalta (13° N), also 20 km wide. The pattern of the present spreading axis is therefore determined by the initial cut of the Ethio-Arabian dome in Miocene times.

The second unit is an extensive basaltic lava field, made of subaerial, recent and partly historic Aa and pahoehoe lavas (Fig. 6.76). The most recent, rather large flow dates back to 1907. It was reported by Tancredi who erroneously



Fig. 6.72 Alayta shield volcano, seen from south. In front, the basaltic lava fields are affected by open fissures, clearly visible on both sides of the image. The axial graben is detached on the horizon, with recent basaltic flows emitted along the NNW rift axis (*Photo coll. G. Marinelli, University of Pisa*)



Fig. 6.73 Detailed satellite images (USGS Earth Explorer) of the main Alayta craters topping the shield and located in the axial graben, itself affected by more recent emissive fissures. The graben was partly filled by lava flows emitted from the crater, with outflows to the west. Both imbedded craters are affected by fumarolic activity

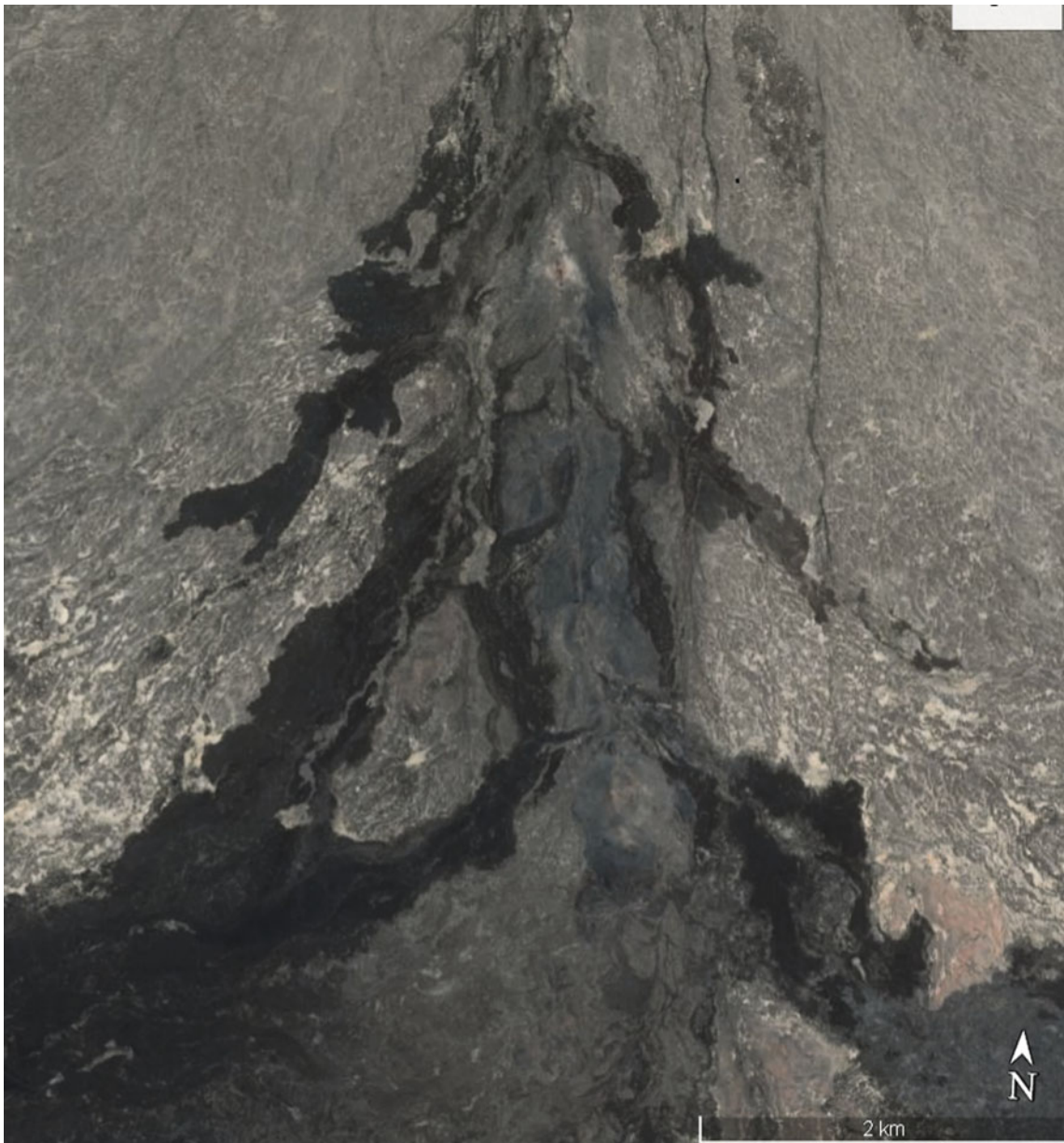


Fig. 6.74 Detailed view of the lava flows (of intermediate up to trachyte compositions, covered by more recent basalts; see map, Fig. 6.80) emitted along the southern part of the Alayta shield volcano axial graben. Flowing inside the graben, they overflow on both sides, expanding south. Observe that the tectonic activity is largely

synchronous with the volcanic eruptions, both pre-dating and post-dating the flows. This shows the link between the magma genesis, its differentiation in shallow elongated magma chambers and related inflations and sinks of the shield surface. (Satellite image from USGS Earth explorer)

assigned it to Afdera (Tazieff et al. 1969). This impressive basaltic eruption was certainly one of the most important that affected Afar in the past. The flows were emitted by a N–S trending set of fissures that developed along the eastern side of the shield. Together with open fissures, many small craters, scoria cones and linear cinder accumulations mark the feeding fissures. From these fissures, the flows extended northwards in the Dodom and Afdera plains and towards the east along the flank of Afreda volcano. To the south-east, the Alayta flows reach the northern

foot of the Affara Dara tertiary granitic massif, whereas to the south-west, they meet the lava of Boina (Dabbahu) peralkaline silicic volcano.

The recent fissural lava field is quite homogeneous—olivine basalt—in composition. In contrast, the Alayta shield displays a wide variety of lavas, ranging from basalts to silica-saturated trachytes, but reaching neither rhyolitic nor peralkaline compositions (Fig. 6.77). Intermediate products are particularly rich in iron (20% FeO) and titanium (5% TiO₂), a trend that characterises the tholeiitic magmas.



Fig. 6.75 The Teru plain in 1970; difficulty for F. Barberi and J. Varet to find a way through the abundant vegetation at the western foot of Alayta range

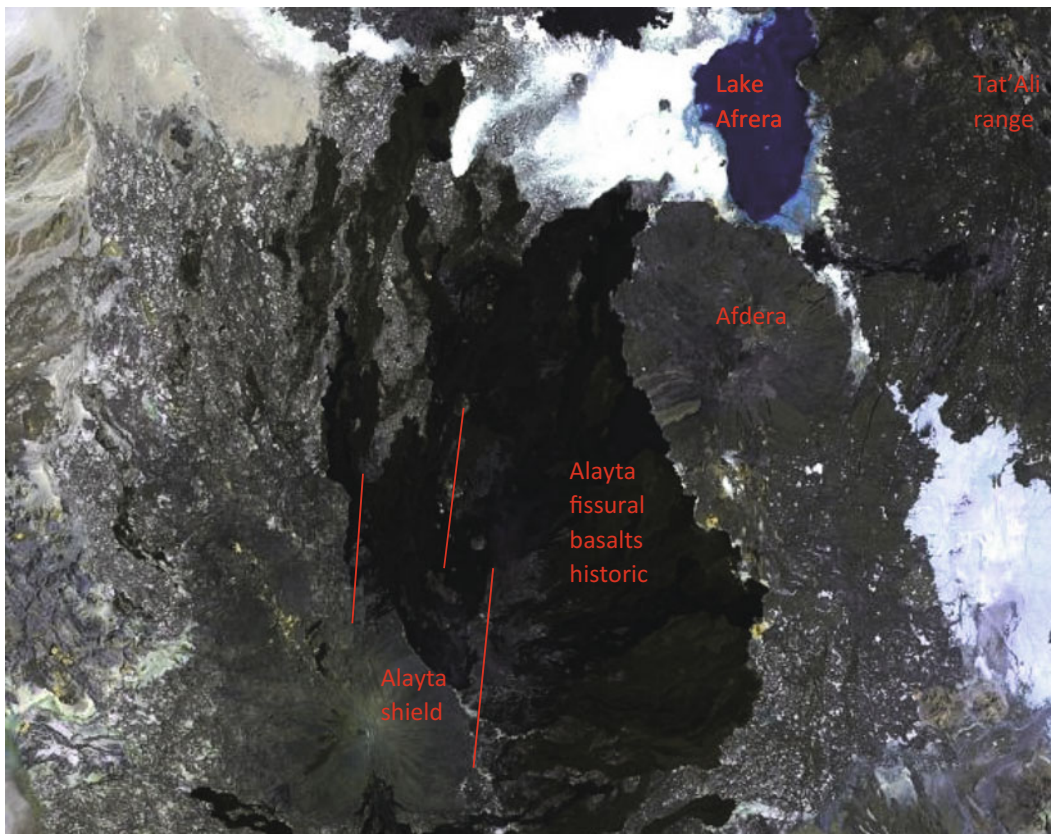


Fig. 6.76 Alayta shield volcano (greenish colour, SW side), with series of very recent craters aligned along the NNW-trending axis of the basaltic-to-trachytic shield. Very fresh lava flows (dark black) resulting from a partly historic eruption emitted from sub-N-S-trending

fissures along the east side (*central* part of the image) laps up against the western flank of Afdera volcano, immediately south of Lake Afrera. (Smithsonian Inst. NASA Landsat image, 1999)

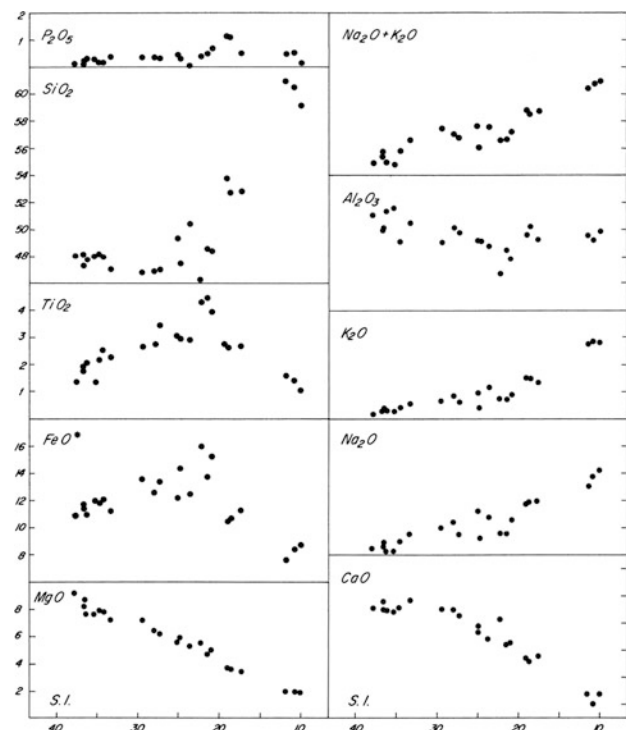


Fig. 6.77 The differentiation trend (major elements against Solidification Index) observed in the Alayta range from basalts to silica saturated trachytes with strong iron and titanium enrichment in intermediate stages (Tazieff 1973)

As a whole, the Alayta lava sequence is rather similar to that found in the Erta Ale range at the level of Hailigub and Erta Ale volcanoes. The development of recent fissural lava fields to the east of the shield volcano is also observed in the Erta Ale range.

It is worth emphasising that the recent—and probably historic—basaltic flows constituting the lava fields East of Alayta shield volcano were emitted through sub-N-S trending fissures oblique to the Alayta shield axis. They appear to establish a direct link between the two en echelon axial ranges. It could prefigure a future more direct pattern of opening of the axial ranges in this area, competing with the Tat'Ali spreading segment, which incidentally appears to be more active at present (Ebinger et al. 2010; see Fig. 6.70).

6.5 Dabbahu Volcanic Centre⁴

Dabbahu is a recent volcanic centre emerging from basaltic lava fields between the Alayta and the Manda Harraro axial ranges. It was assigned to axial ranges by Barberi et al.

⁴It was also called “Boina”, but it appeared that this Afar name result from the well-developed fumarolic activity, Dabbahu referring to the mountain appears more appropriate.

(1975a, b) who studied this magmatic unit in great detail using volcanological, petrological, mineralogical and geochemical analysis. This unit became known more recently because of the historical eruption occurring there in September 2005, with a seismic event starting on September 9 with the largest shocks (magnitude 5 or above) recorded in the period of September 20 to October 4, with a major shock on September 26, contemporaneous with the onset of an explosive volcanic eruption (Ayele et al. 2006). The eruption occurred at the Da'Ure site south of the main edifice and produced rhyolitic ash on both sides of an open fissure of N–S direction. A minor ash fall was recorded up to 35 km from the vent, but the main event was in fact the opening of a fissure over more than 75 km, with injection of basaltic magma into a dyke that lasted for several years.

We should emphasise that the location of Dabbahu is in fact peculiar, as this central volcanic unit—differing from axial ranges—is located in the area where the two axial ranges of Alayta and Handa Harraro display a dextral en échelon pattern with a distance of around 25 km between the axis of these two subparallel-spreading segments. Dabbahu volcanic centre is also aligned with the Dabayra transverse volcano-tectonic unit (trending WSW–ENE, located at the foothill), where the Nubian escarpment encounters a major left lateral offset (70 km) while passing from Teru to Boda (Mille River basin) plains. Incidentally, Dabbahu peralkaline volcanic centre is also located at a mid-distance between the two Miocene equally peralkaline granitic bodies of Limmo and Affara Dara (Fig. 6.78).

To the east, Dabbahu also appears to be eventually connected to the southern extremity of the Tat'Ali axial range through a set of NNE–SSW trending faults and emissive fissures that extend south of Afdera volcano and was considered as the surface expression of a NE–SW trending transform fault by Barberi and Varet (1977).

Dabbahu should therefore be considered to be the surface expression of a major leaky fracture zone and transform fault, between axial ranges rather than an axial range in itself.

The volcanic unit is 25 km wide, reaches an altitude of 1400 m and covers a surface of around 750 km². It was initially built on basaltic fissural lavas found all around the volcano that evolved into a shield. The successive feeding of basalts along a set of fissures of N–S direction permitted the progressive identification of magma chamber(s), allowing the composition of magmas to evolve into andesine basalts, ferrobasalts and dark trachytes found at the surface of the shield (Fig. 6.79). The volcano was topped by fairly recent rhyolite domes aligned along several (up to seven) parallel N–S trending emission fissures, extending east until the Alayta axis. Their compositions vary, with pantellerites dominant at Dabbahu, whereas comendites prevail south of Alayta, showing different magmatic sources (Barberi et al.

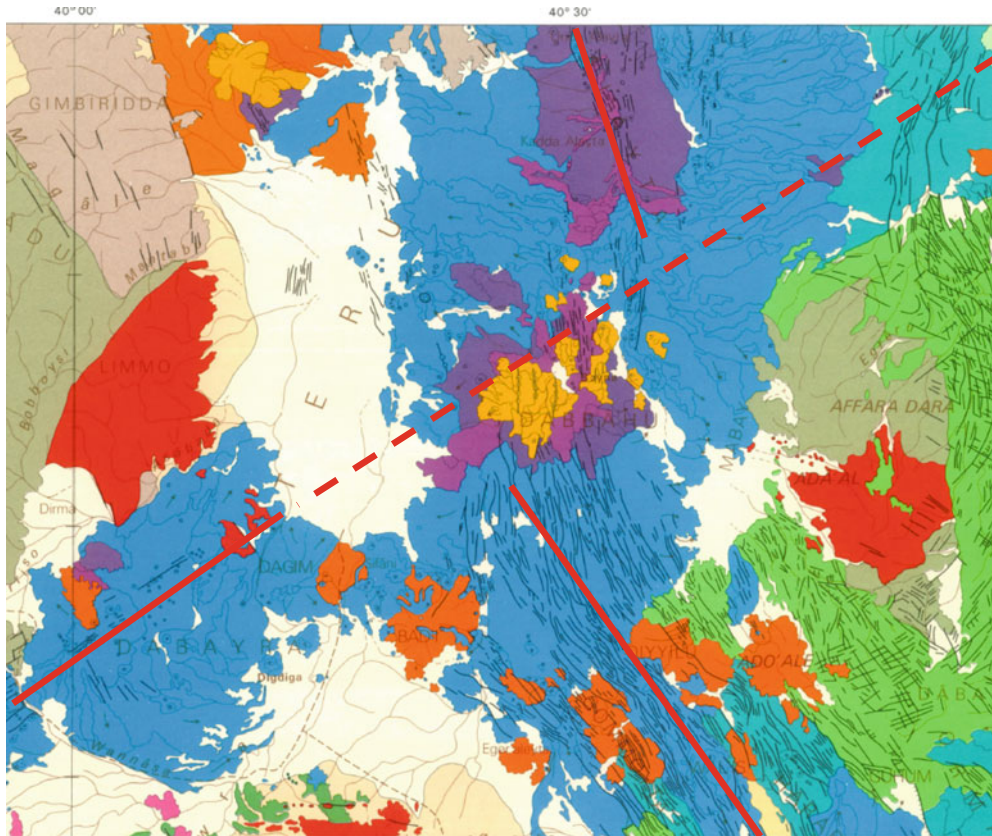


Fig. 6.78 Location of the Dabbahu volcanic centre, to the south of Alayta, and to the north of another wide axial range, called Manda Harraro from the name of the major lava fields extending in its southern half. This right lateral offset of the axial ranges also correspond with the offset of the Nubian escarpment. Dabbahu is also

located in line with the ENE-WSW axis of the Dabayra dominantly basaltic transverse volcanic unit, that also extends to tat'Ali through NNE-SSW surface expression of the same NE-SW trending transform fault and fracture zone. This discontinuity cuts also mid-way between the two peralkaline granites of Limmo and Affara Dara

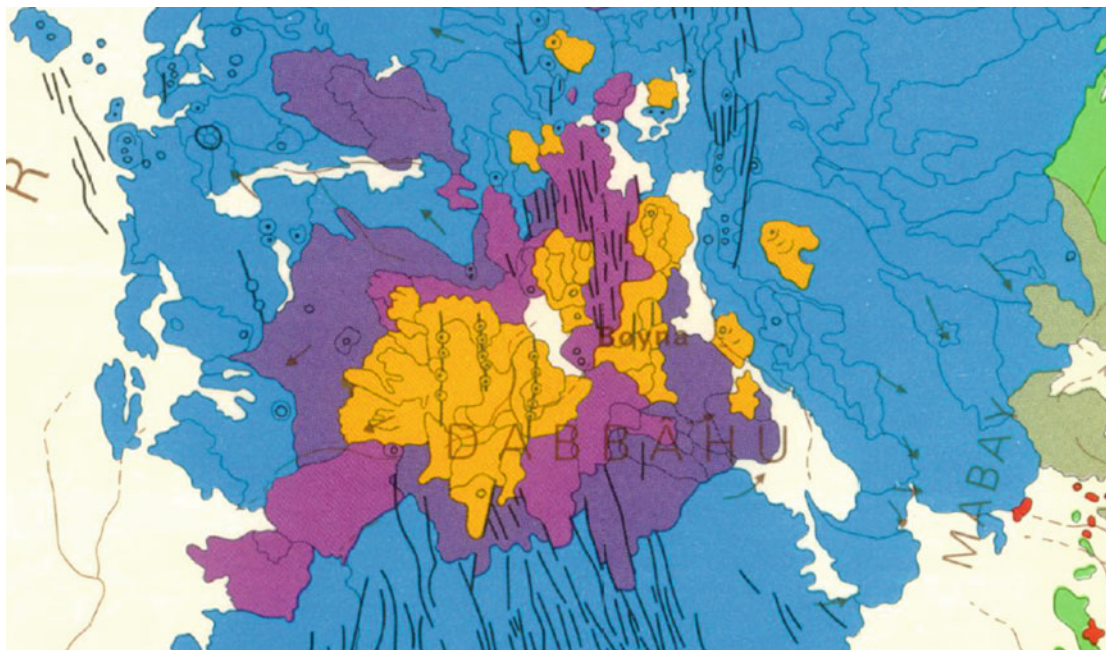


Fig. 6.79 Map of Dabbahu volcanic centre, showing the succession of the lavas from initial fissural basalts to andesine basalts and dark trachytes building a shield volcano with late peralkaline rhyolite domes

covering the top. All lavas emitted along N-S trending fissures, whereas N and S from Dabbahu, the NNW direction predominates in both Alayta and Manda Harraro axial ranges (from Varet 1978)

1975a, b). As a whole, the width along which the domes are dispersed is impressive (22 km) and, despite a relative dispersion and emission from N–S fissures, trends in the ENE–WSW direction of the nearby Dabbayra transverse marginal volcanic unit.

Among the silicic products, crystalline domes, obsidian flows, and subordinate pumice and pyroclastics are present. Ages were measured at 44–10 thousand years by Barberi et al. (1972a, b) for two obsidians. Field et al. (2012) provided ages of 64 thousand years for andesine basalts from the shield volcano, whereas younger andesine basalts were dated from 33 thousand years ago, comendites from 30 thousand years ago and pantelleritic obsidians were younger than 7.8 thousand years old, showing a regular activity from at least 64 thousand years ago to the present day. The length of the emissive fissures never exceed 8 km and their precise and limited structural position indicate that they are closely related to the magmatic evolution of the underlying stratovolcano. However, no clear volcano-tectonic evidence points to the existence of a unique low-depth magma chamber, as no caldera nor summit sink is observed. In addition to the several N–S short axes, the

existence at depth of an elongated transverse line of weakness can be inferred from the distribution of the silicic emission centres.

As shown by Barberi et al. (1975a, b), the volcano displays a complete sequence of rocks and mineral solid solutions, from olivine basalts to andesine basalts, ferrobasalts, dark trachytes, silica-saturated trachytes, comendites and pantellerites. This continuous evolution was demonstrated by mineralogical, petrological and geochemical data. The linear correlation of hygromagmatophile elements allowed quantification of the fractionation (Fig. 6.80) and Europium variations to measure the evolution of the oxygen fugacity during the whole process. Each lava sample could be determined as a function of the residual liquid fraction (Fig. 6.81). The whole magma sequence was explained by successive fractionation of olivine, plagioclase, clinopyroxene of evolving composition, iron oxide, apatite and, finally, anorthoclase in the peralkaline liquids from a single transitional basalt source (Fig. 6.82). The plagioclase effect was shown to explain the initial iron enrichment in the shield volcano stage and the genesis of hyperalkaline liquids (Figs. 6.83 and 6.84).

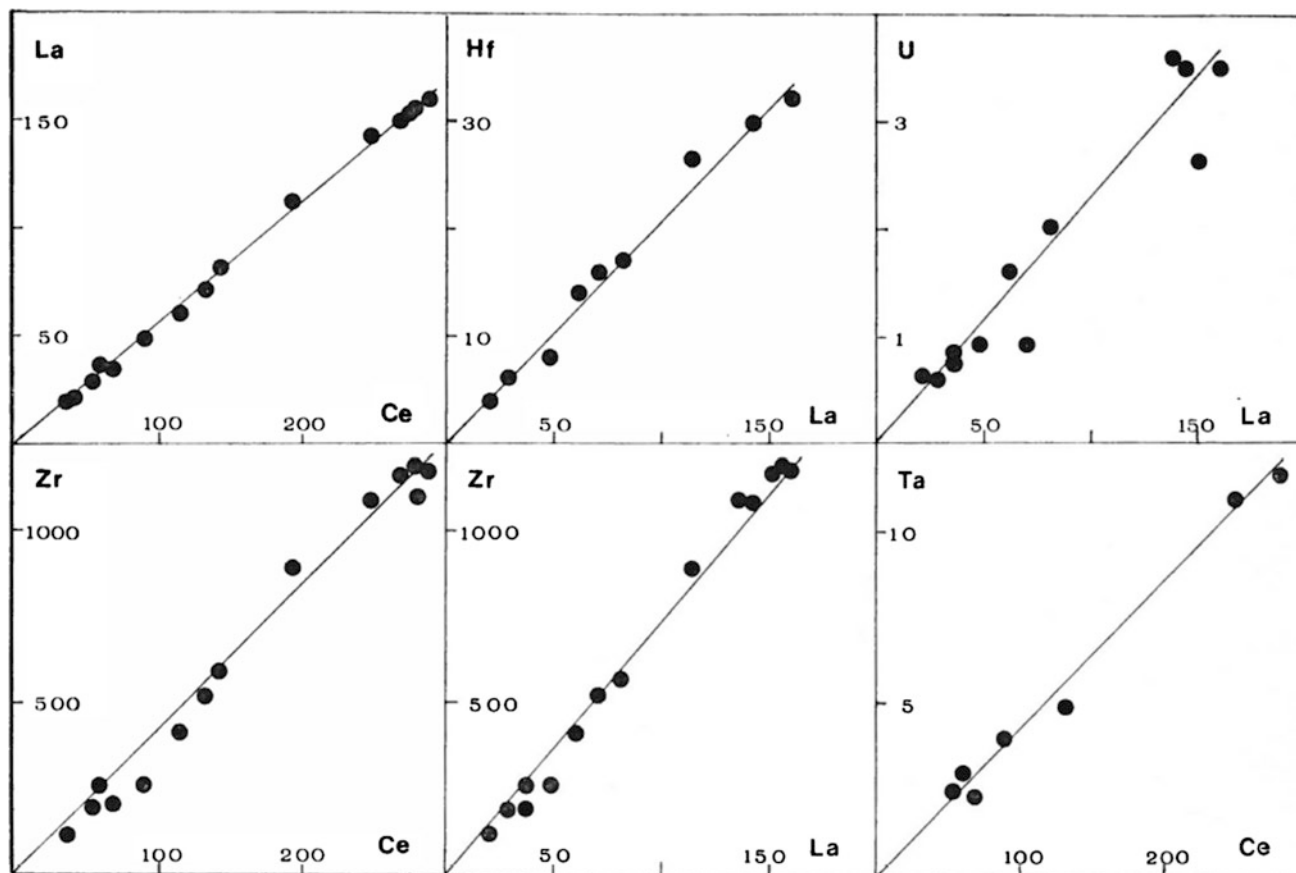


Fig. 6.80 Linear correlation for pairs of hygromagmatophile elements in the whole Dabbahu rock series showing the crystal fractionation process from a single magmatic source (Barberi et al. 1975a, b)

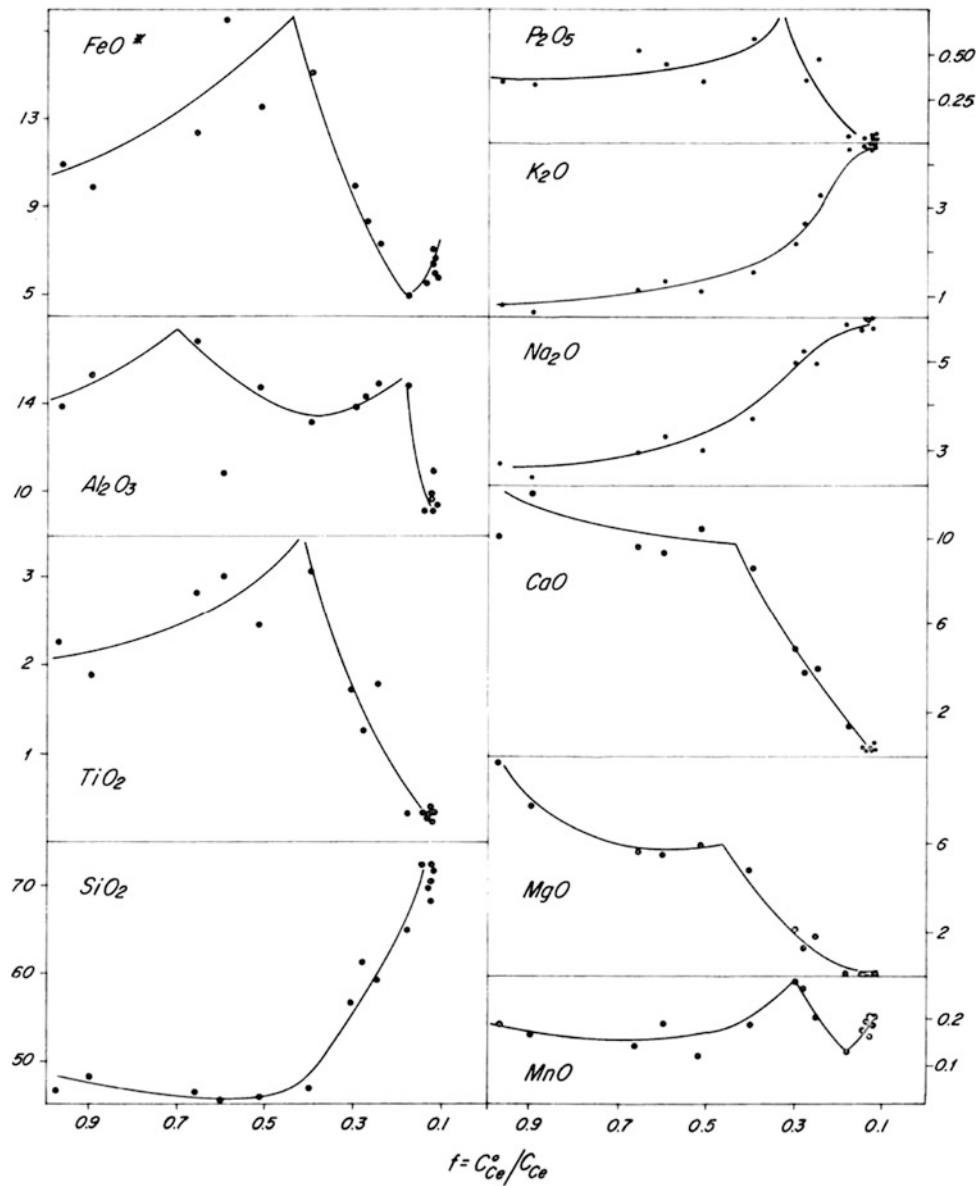


Fig. 6.81 Evolution of major elements as a function of the residual liquid fraction (Barberi et al. 1975a, b)

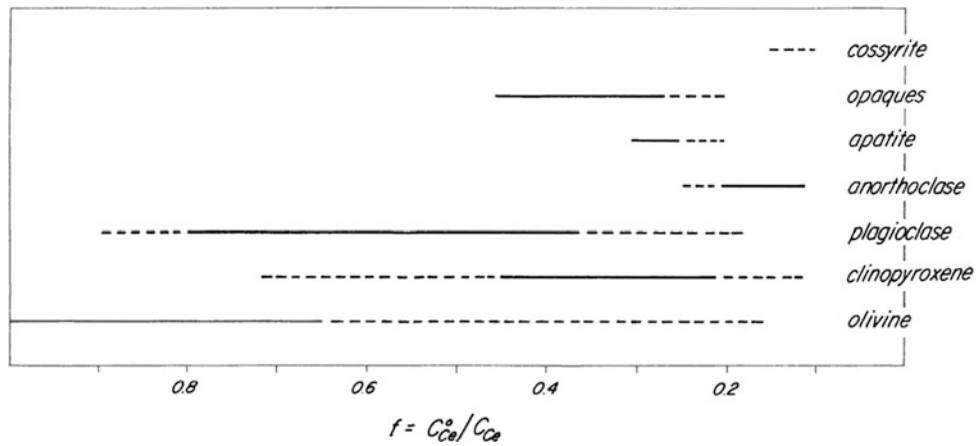


Fig. 6.82 Sequence of fractionating minerals as a function of residual liquid fraction (Barberi et al. 1975a, b)

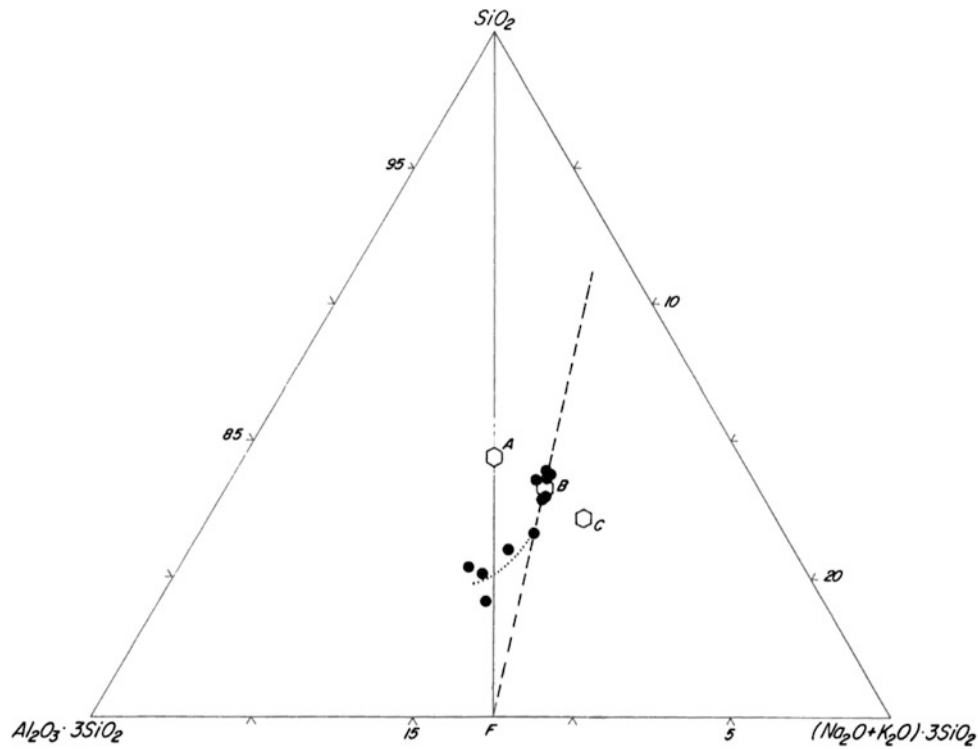


Fig. 6.83 SiO_2 - Al_2O_3 - $\text{Na}_2\text{O}+\text{K}_2\text{O}$ molecular diagram. F represent stoichiometric alkali feldspar. A, B and C are experimental minima for increasing peralkalinity (Carmichael and MacKenzie 1963). Dotted line marks the transition to the peralkaline field by plagioclase effect. Dashed line marks the alkali feldspar fractionation trend for the most peralkaline samples (from Barberi et al. 1975a, b)

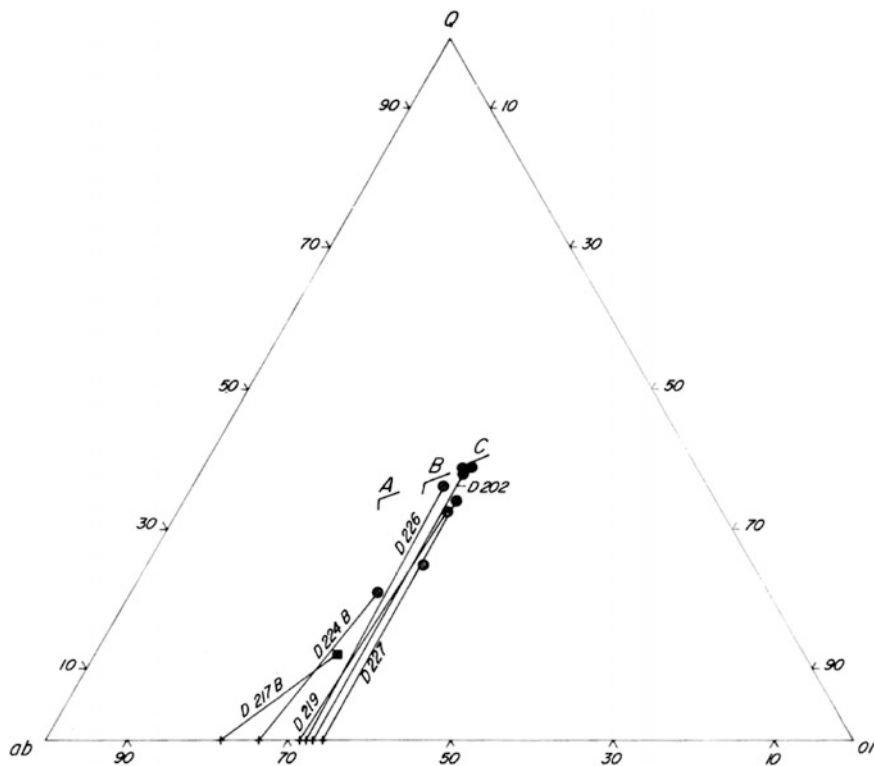


Fig. 6.84 Couples of Feldspar phenocrysts versus glass compositions for trachytes and rhyolites of Dabbahu volcano plotted in the quartz-albite-orthoclase normative triangular diagram (with same minima as in Fig. 6.83)

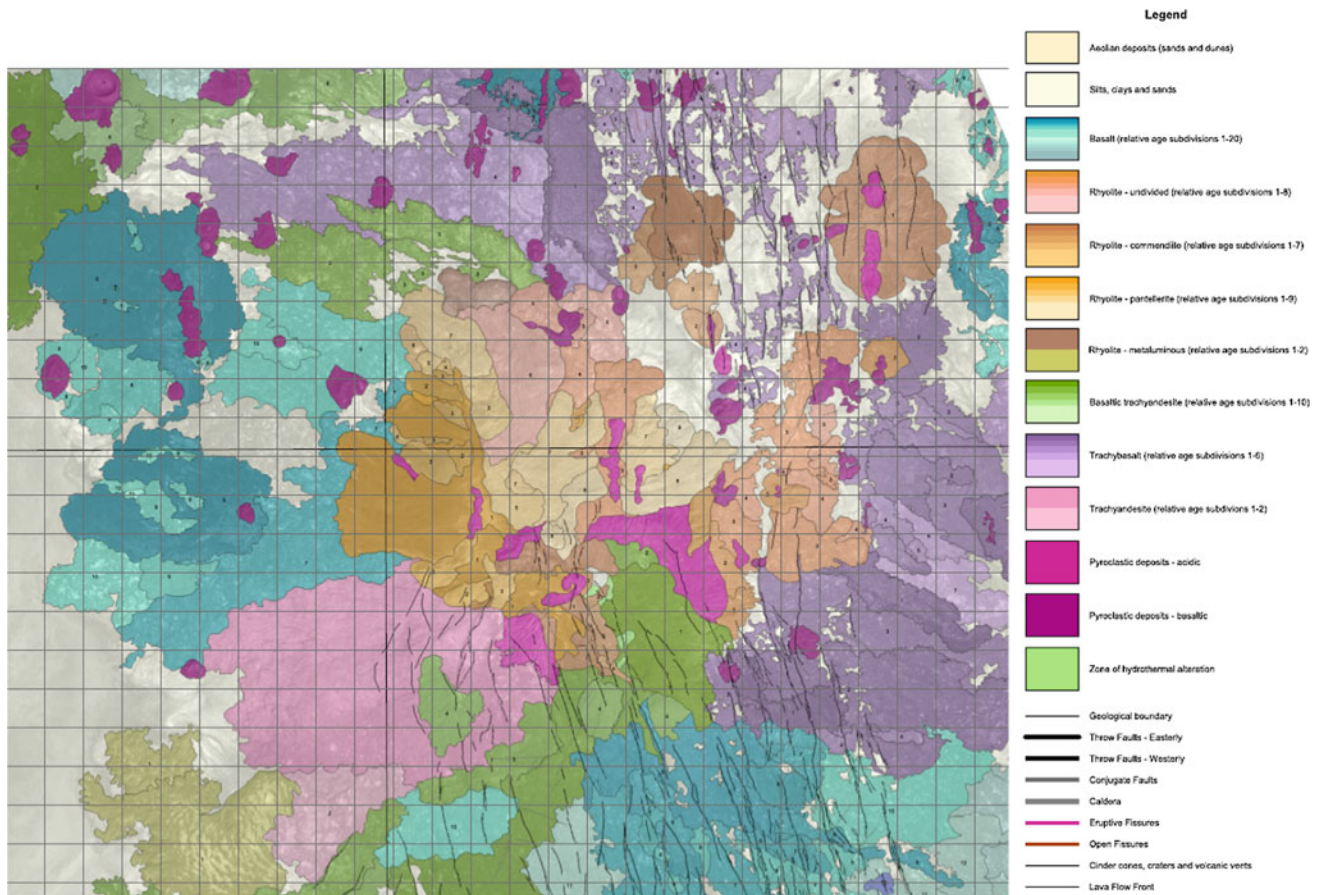


Fig. 6.85 Detailed map of Dabbahu (original at 1/50,000 scale; kilometric squares, area mapped by Field, BGS, 2013)

New data by Field et al. (2012) (Fig. 6.85) provided precise measurements of the temperature (1200–680 °C) and depth (10–15 km) ranges where this crystal fractionation process occurred, with an important H₂O enrichment (up to 5.8 wt%) in the final liquid. From these and other data from seismology and geodesy obtained during and after the 2005 eruptive event, Field et al. (2012) could deduce:

- A depth of 2–6 km for the magma storage region from the aseismic zone observed in the 2005–2006 earthquake data at the vertical of the 2005 eruption site, whereas abundant earthquakes above 2 km suggest a fractured roof above the magma chamber
- A careful examination of InSAR modelling of interferograms obtained since the 2005 event allowed identification of an uplift signal of 50 cm that could be interpreted as a point source at a depth of 3 km inflated by 0.022 km³, but a better fit was obtained from multiple stacked sills at a depth of 3–4.5 km

The authors conclude that the final steps of differentiation at Dabbahu occurred at shallow depths in small bodies, such as stacked sills or closely-spaced dykes, located at shallow depth in a magma storage system that has maintained a stable geometry over the past few thousand years.

6.6 Manda Harraro Axial Range

6.6.1 Geological Description

Located south of Dabbahu, between 11°45'N and 12°50'N, and north of Dubte in the Tendaho graben, this range is 105 km long and 20–30 km wide (Fig. 6.86), but is not as visible as the northernmost ranges as it never exceeds 400 m above the surrounding plains. It is disposed in a dextral en echelon pattern that characterises the three axial ranges of Erta Ale, Alayta and Manda Hararo, each spreading segments corresponding to a parallel discontinuity in the

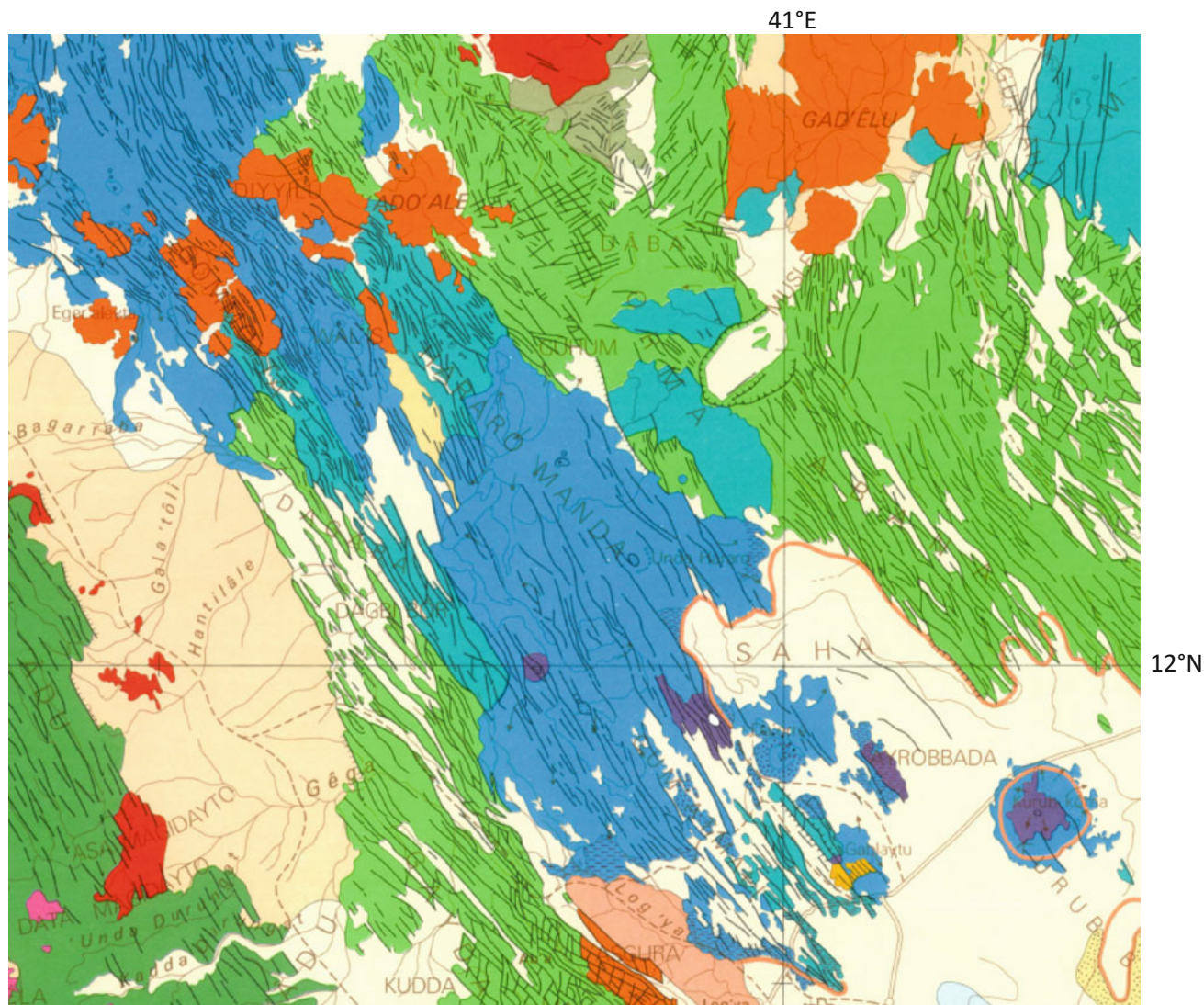


Fig. 6.86 The Manda Harraro basaltic axial range (*blue*) cutting through the stratoid series (3.5 to one million years ago, *pale green*) and associated rhyolitic centres (*orange*) in central Afar. The Pliocene (eight to four million years ago) volcanic series of Sullu Adu—Gurräle horst (basalts in *dark green*; rhyolites in *pink*, microgranites in *red*) is seen to the west at the foot of the Nubian scarp, separated from the

stratoid series by the sedimentary plain of the Mille river basin (extracted from map by J. Varet, 1978). To the NE, the southern extremity of the Miocene Affara Dara massif is visible, probably extending south beneath the stratoid series as deduced from the surrounding tectonic features

Nubian Escarpment. Although apparently less spectacular and rather linear, essentially fissural and affected by intense distensive tectonics (open fissures and normal faults), it is a rather complex fast spreading unit, made of several components. If fissural zones dominate (Figs. 6.87 and 6.88), embryonic shield volcanoes are also present, as well as graben-shaped and bulge-faulted spreading axes.

As a whole, this axial range shows geological, volcanological, petrological and geochemical evidence for faster spreading than those encountered elsewhere in Afar, observations established since 1973 by Treuil and Varet being confirmed by recent events (see Sect. 6.5.2).

The name was given because of the wide basaltic lava field called Manda Harraro by Afar people that extends in the central and SE part of the range.

From north to south, the following units have been distinguished:

- A shield volcano, located south of Dabbahu. That is a small (7 km in diameter) volcano with a small summit crater, built on gaping fissures of sub-meridian direction. It only erupted olivine basalts. A strange feature is observed south from this volcano: a small block (100 × 100 m) made of a pile of recent lavas is faulted

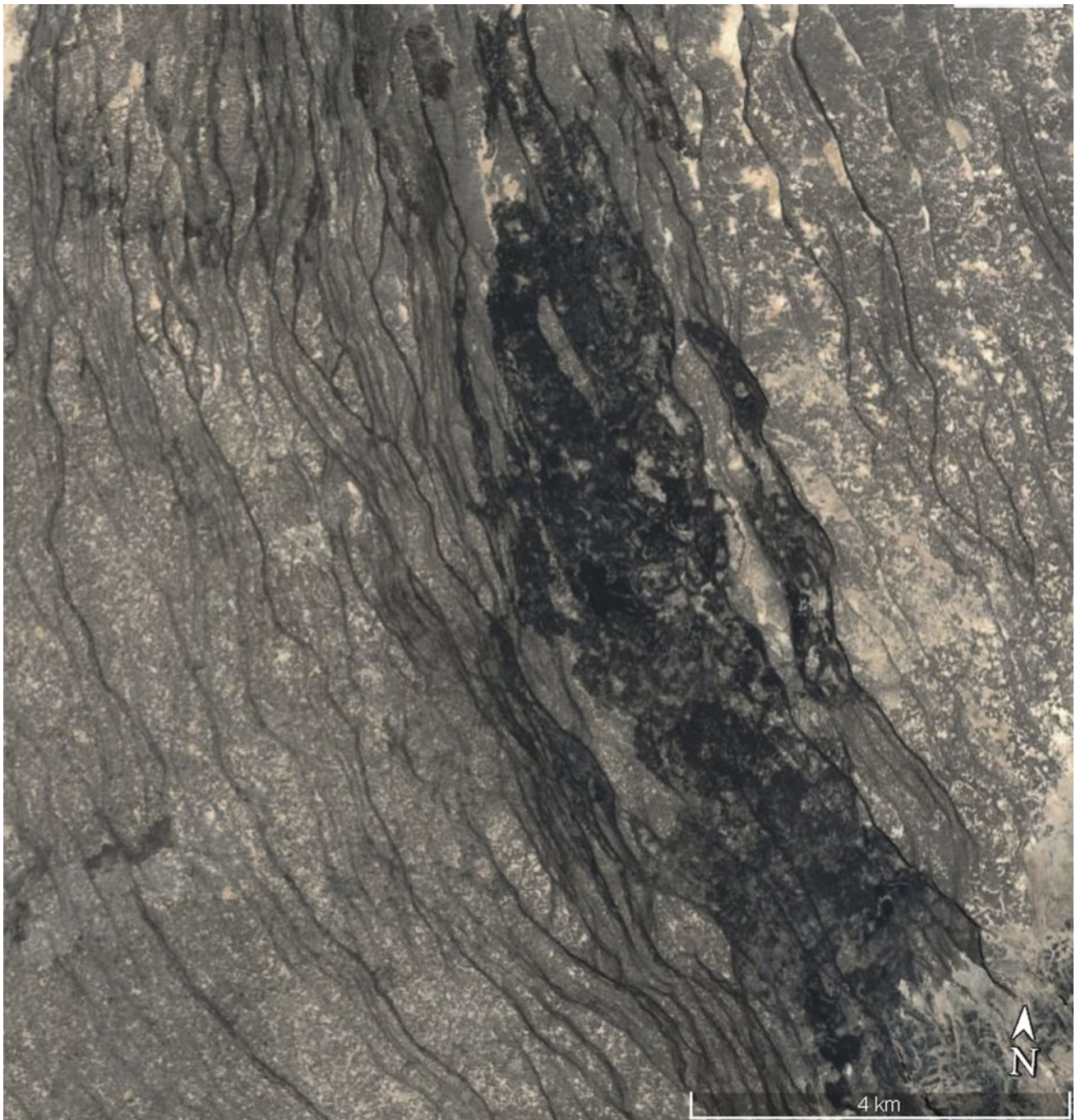


Fig. 6.87 Satellite view of the axial graben of the northern part of Manda Harraro range. Fissural basalts are emitted from open fissures, and surrounding faults affecting recent flows show an intense tectonic activity contemporaneous with basalt emissions along the same faults (satellite image from USGS Earth Explorer)

and tilted at 45° . We interpreted it as resulting from uprising magma which suddenly stopped in its ascension before reaching the surface (Fig. 6.89).

- A long fissural field extends south of this volcano, made of innumerable open and emissive fissures affecting rather recent basaltic lava fields. The flows

reached the wide Bagarraba plain to the west and the Mabay sedimentary basin to the east. All these lavas consist of apparently undifferentiated olivine basalts. This central and rather narrow part of the range is the place where the centre of the 2005–2009 diking event was located.

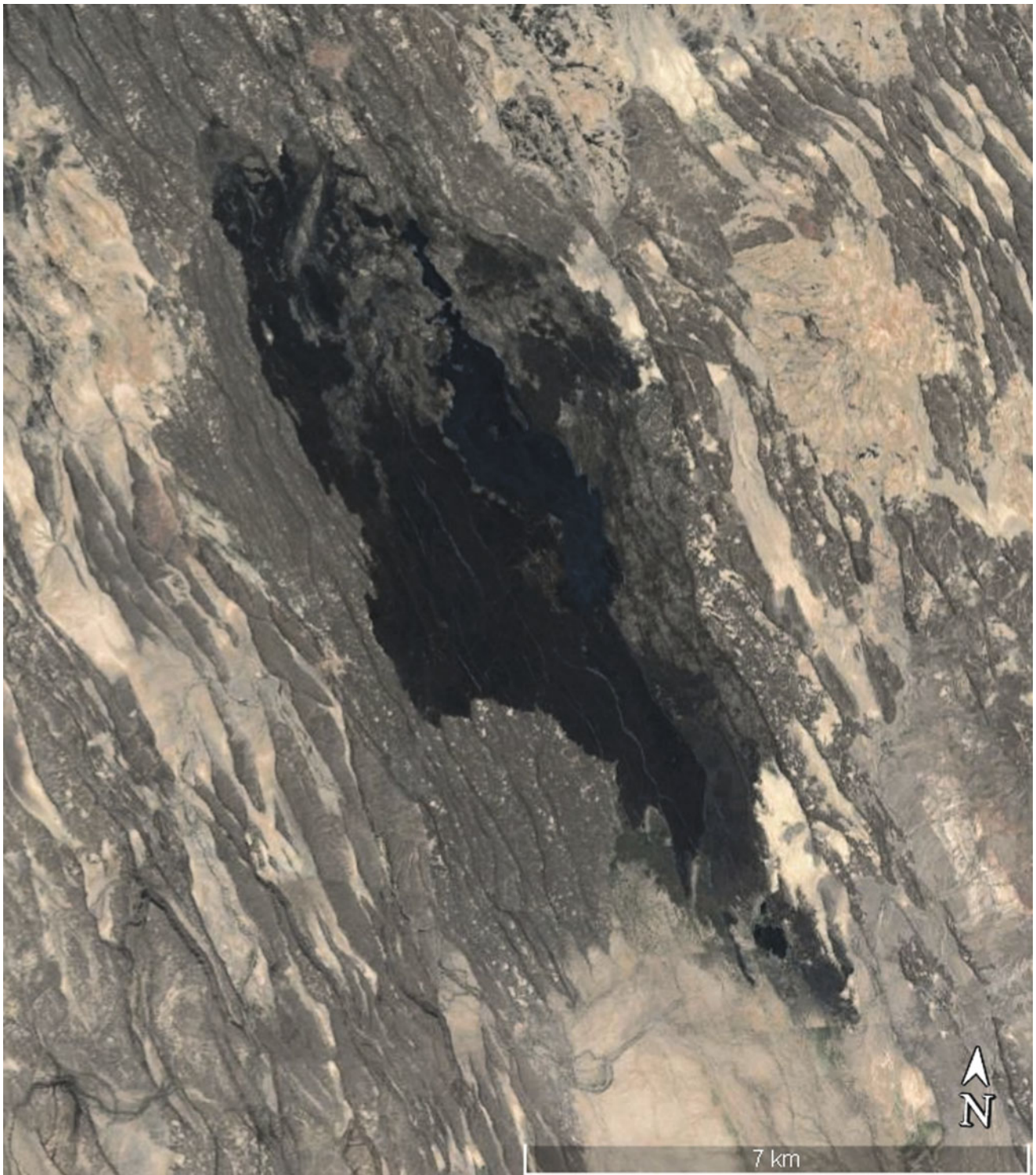


Fig. 6.88 Basaltic flows emitted from NNW axial fissures at the southern extremity of Manda Harraro range. Early dominantly subaqueous lavas are covered by more recent subaerial flows (grey

colour) near to rift axis where the most recent (dark) flows are observed (satellite image from USGS Earth Explorer)

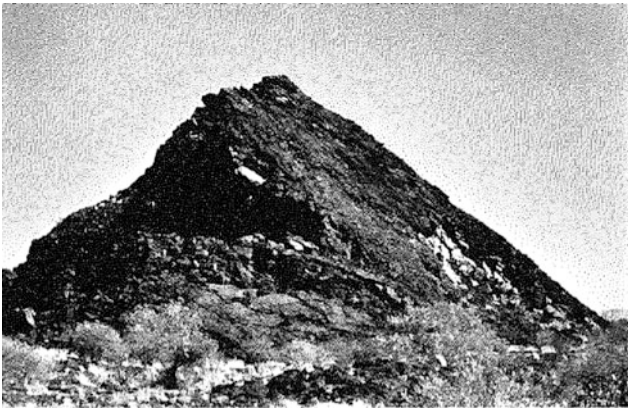


Fig. 6.89 Tilted block made of a basaltic lava pile in Manda Harraro range

- Two basaltic shield volcanoes are observed in the central part of the range. Unda Harraro is the largest, and displays a spectacular pattern easily visible on air and satellite images (Figs. 6.90 and 6.91). An 800 m-wide crater occupies the summit, surrounded by smaller elliptical craters disposed in a wide hemicycle around it. This was interpreted as resulting from the surface expression of a cone sheet which, together with ring fissures, fed basaltic flows, building the summit of the shield. A smaller shield volcano located north of Unda Harraro is also occupied by a summital crater, but this is produced by the coalescence of several small craters of rather angular shape without displaying a clear, easily understandable geometrical figure.
- The major segment of the range, called Gumatmali from its southern deeply faulted lava fields, is the most spectacular volcano-tectonic unit of Manda Harraro (Fig. 6.92). It is bordered to the west by the Mille river and the newly built Samara capital of Afar Regional State sits on its southern extremity.⁵ This is a purely fissural basaltic segment built on NNW open fissures and is dissected by intense recent faulting. Only flat-lying flows, some of which are of very large extension, are observed in the northern and southern parts.
 - The northern field is so flat and deprived of cones or craters that the exact position of emissive fissures is difficult to locate (Fig. 6.93). An extensive pahoehoe flow with a smooth surface, in which flow directions can be determined, was evidently emitted from NNW fissures, but the lava was so fluid and degassing so easily that it did not generate scoria, spatter cone or cinder alignment. The tectonic event producing this

⁵Meaning the capital of Afar Regional State was located on the most active volcano-tectonic axis of Afar, but apparently without consideration of eventual precaution construction measures.

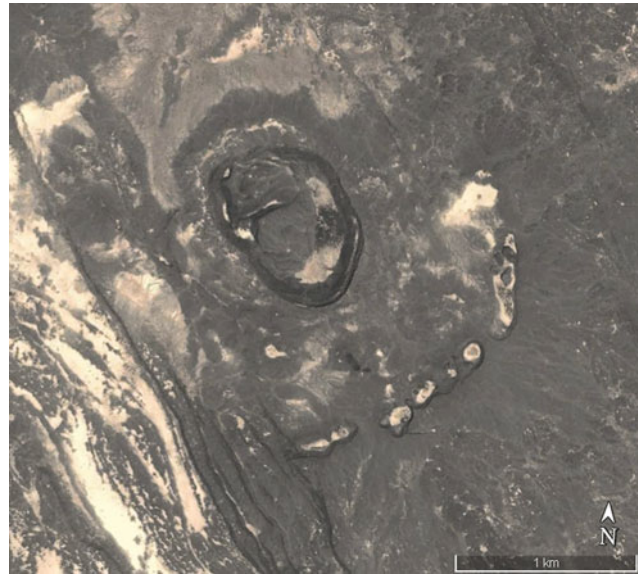


Fig. 6.90 Unda Harraro ring of pit craters surrounding a 1.2 × 0.7 km wide crater (cone sheets underlying a magma chamber?) topping a flat shield volcano of central part of Manda Harraro range (satellite image from USGS Earth Explorer)

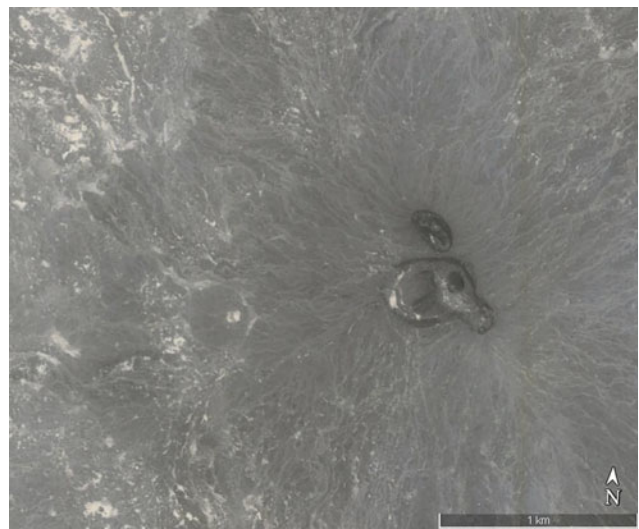


Fig. 6.91 Set of inter-fingered craters topping a flat shield volcano in the southern part of Manda Harraro range (satellite image from USGS Earth Explorer)

flow, with significant fissure opening, clearly happened simultaneously with the basaltic emission.

- The median part of this segment is slightly bulge shaped with the central part topped by a series of rectangular craters—similar features were observed on ocean floor in fast spreading ridges—aligned in the NNW direction of spreading. Their size decreases north and south, the largest being observed in the most uplifted part of the bulge (Figs. 6.94 and 6.95).

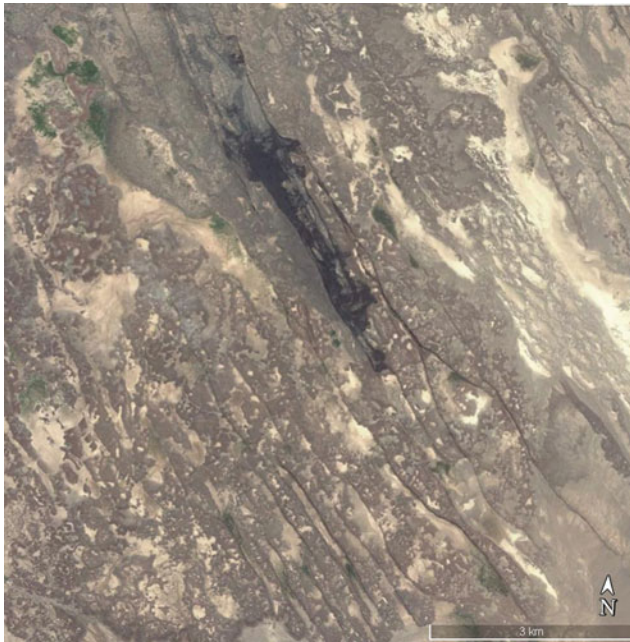


Fig. 6.92 General view of the basaltic fissural fields in the southern part of Manda Harraro range, with the youngest flows emitted along the rift axis, which display rectangular calderas to the north and axial graben to the south (satellite image from USGS Earth Explorer)



Fig. 6.93 In the central part of Manda Harraro range, a wide, fluid basaltic lava flow emitted from long fissures covers large surfaces (around 100 km²), affected by sub-contemporaneous faulting (satellite image from USGS Earth Explorer)

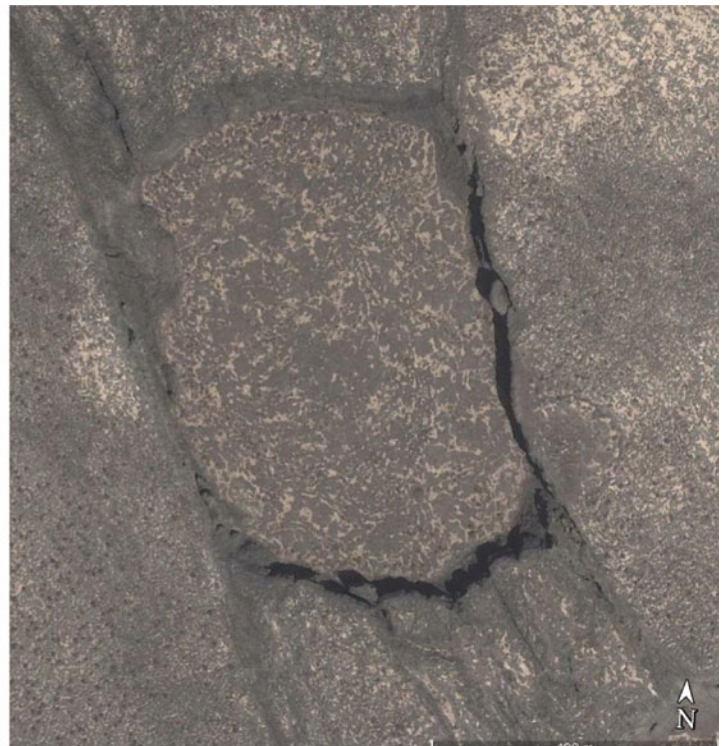


Fig. 6.94 Rectangular craters aligned along NNW rift axis in the central part of Manda Harraro range, with smaller craters and scoria cones along the same axis south (satellite image from USGS Earth Explorer)



Fig. 6.95 Oblique air photo of the same pit craters as in Fig. 6.94 showing the sunk interior of the craters covered by the same basalt lava surface as the one erupted from the craters around them. The craters sunk after the lava flows were emitted, as shown by lava stuck against the walls (*Photo coll. G. Marinelli, University of Pisa*)



Fig. 6.96 Pit crater topping a former shield volcano now dissected by intense extensive faulting postdating the eruptive phase, called Daore, in the southern extremity of Manda Harraro range. As a result, the crater is now located on a horst. The lake is fed by hot springs (satellite image from USGS Earth Explorer)

Basaltic lava lakes have occupied the two major craters. They were filled by lava which was emitted from them and fed the surrounding lava fields. Similarly to what is observed at Erta Ale southern crater, the lava level later dropped in these lakes and a thin lava coating and stalactites remained stuck to the walls of these craters. Molten lava later occupied the crater at a lower level, as attested by the solidified surface of the present crater floors. Similar features were observed at Hawaii (Swanson and Peterson 1972).

- The southern extremity of the Gumatmali axis is occupied by a well-defined axial graben where the most recent (sub-historic) basaltic eruptions concentrate (see Fig. 6.92), whereas earlier flows are observed on both sides (Fig. 6.88).
- Parallel to the Gumatmali axis, but at a distance of 8 km to the east, another emissive tectonic axis is observed, essentially older, but still quite recent (pre-historic), which borders the Saha sedimentary plain.
 - To the north, the Da'ore crater—of oval shape, reaching 1 km in length along the horst axis—marks an important emission centre (Fig. 6.96). It displays

the particularity of being occupied by a lake fed by hot springs merging from NNW fissures affecting the crater walls. A possible interpretation of this rather young horst is that it resulted from the collapse of the surrounding lava fields because of a phase of extensive regional spreading along an axis that apparently remained uplifted as it was consolidated by earlier dikeing, producing this 27 km-long, 800 m-wide wall.

- A small shield volcano called Gablaytu occupies the southernmost extremity of this axis. It sits on a thin horst, 800 m wide and 27 km long along which other magmatic emission centres are aligned. The area was intensively dissected by late extension tectonics that affected this SE extremity of Manda Harraro range. The bulged Gablaytu shield was affected by successive extension tectonic steps that pre- and post-dated the successive volcanic eruptions. This is similar to what was observed in the northern part of Erta Ale range (Borale Ale and Alu-Dala Filla), but with a more rectilinear tectonic pattern reflecting a more intense rifting. A complete series of magmatic evolution is observed in this shield volcano, from initial fissural basalts to andesine basalts, ferrobasalts and dark trachytes, up to rhyolites constituting a thick

dome-flow that was lately open by an axial graben in the presently downthrown upper part of the volcano (Figs. 6.97 and 6.98). The whole structure reflects the effect of a local presence of a shallow magma chamber affected by a “cigar-shaped” ellipsoidal source along a horizontal axis cutting the volcano through the middle.

- To the east of this Gablaytu volcano, other small volcanic units are observed in the Saha plain. The main outcrop constitutes the Ayrobbada subaqueous basaltic lava field,

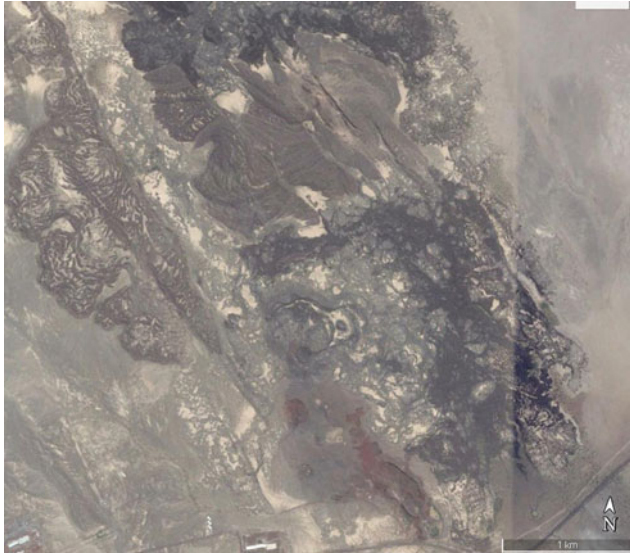


Fig. 6.97 Gablaytu faulted shield volcano to the south-eastern extremity of Manda Harraro range. The shield is affected by later rift faulting along its axis (satellite image from Google Earth Pro)

which is surrounded by several hyaloclastite cones. Three of them are aligned along a NNW fissure, including the spectacular ash ring to the north, where several craters are embedded, including later subaerial craters and basaltic flow (Fig. 6.99), and another two of decreasing size towards the south. These subaqueous eruptive centres are aligned with subaerial scoria cones along the same emissive fissure.

- The small Kurub shield volcano is observed south of the Addis to Djibouti road that crosses the south extremity of the Manda Harraro range in an E–W direction (Fig. 6.100). This basaltic shield is partly subaerial whereas the earliest phase outcropping at the foot was subaqueous. We could not observe the fumarolic activity described by Cortani and Bianchi (1941).

If the volcanic activity started earlier than 8000 years ago, when the whole area of the lower Awash basin was covered by a very large lake (Gasse 1978), most of the Manda Harraro range was built later, showing a quite intense, essentially basaltic, volcanicity.

Despite the presence of several spreading sub-segments, displaying a variety of volcanic features including dominantly fissural lava fields and a few embryonic shields, the whole range appears to be produced by a fast-spreading rift. This is also reflected in the petrology and geochemistry as shown by Treuil and Varet (1973). The basalts of Manda Harraro are the poorest in K in the whole Afar and display a REE chondritic pattern characteristic of oceanic tholeiites.

Numerous fumaroles and hot grounds (with the typical “fiale” grass) are observed in the Manda axial zone, in Gumatmali and along the southern prolongation of the



Fig. 6.98 Profile of the Gablaytu shield volcano affected by an axial rift as seen from the Addis-Djibouti road (Photo taken from the Semera-Sardo road, J.Varet, 2015)

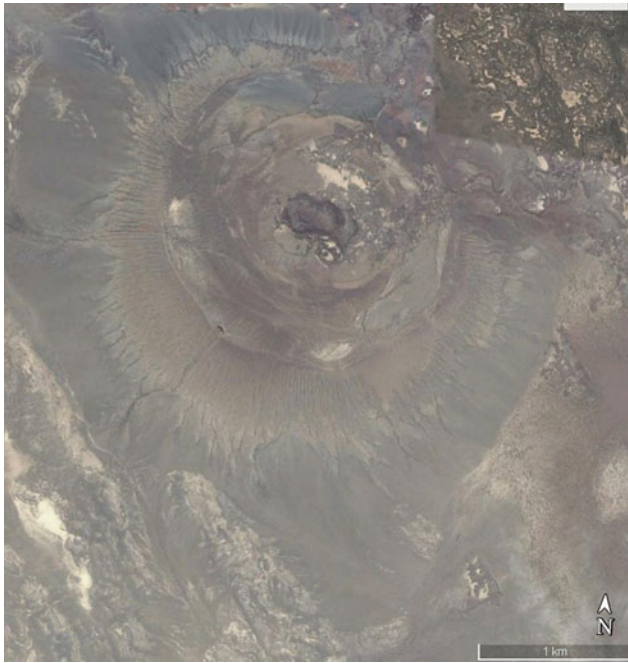


Fig. 6.99 The main unit of the aligned hyaloclastite cones bordering the Saha plain on the eastern side of Manda Harraro range. A subaerial basaltic crater and flow followed the sublacustrine event. The size of the craters decreases from north to south along this axis (satellite image from USGS Earth Explorer)

Manda and Gablaytu axial fissures in the Kalo plain (Dubte area). Hot springs and fumaroles are also observed at Da'ore crater lake. Such thermal manifestations are also abundant in Ayrobbada and surrounding plains.

As a result, the area was chosen as a target for geothermal exploration by Aquater (1996) that engaged in a feasibility study in the Tendaho graben, with a productive well in Dubte. The geothermal exploration is now (2015) under progress in the area under the Ethiopian Geological Survey, with the financial support of AFD and ICEIDA. From MT geophysical data, Didana et al. (2015) deduced the presence of a magma chamber at 5 km depth beneath the southern extremity of the Manda Harraro range. A 70-MWe (mega-watt electric) geothermal plant is envisaged by EEPCo.

6.6.2 The 2005 Dabahu–Manda Harraro 2005–2010 Rifting Episode

A major rifting episode occurred in the period 2005–2010, affecting the Manda Harraro range up to the Dabbahu volcano which induced a large number of new earth sciences studies and publications—Yirgu et al. (2006a), Wright et al. (2006), Rowland et al. (2007), Ebinger et al. (2008, 2010), Barisin et al. (2009), Ayele et al. (2009), Grandin et al. (2009), Keir et al. (2009), Hamling et al. (2009); Beutel et al. (2010), Ferguson et al. (2010, 2013)—and the event



Fig. 6.100 Kurud small isolated basaltic shield volcano sitting in the middle of the Saha plain the lower part of the volcano is sub-aquatic and affected by an axial graben, whereas the upper part is subaerial (above the surface of the former lake covering the whole lower Awash basin)

continues to generate data and interpretations now and for years to come.

Following the initial seismic and explosive volcanic event of September 2005 at Dabbahu (see Fig. 2.31), 13 successive intrusions of magma were recorded until June 2009 along Manda Harraro, affecting the range over a length of 75 km and a width of 8 km, with an intense crustal deformation (up to 9 m cumulative opening) and a volume of injected basaltic magma of over 3 km³, despite the small volume of lava erupted at the surface during two short events on August 13, 2007 and June 29, 2009. The epicentres of the events registered during this period (Ebinger et al. 2010) are mapped in Fig. 6.101.

The succession of the events is as follows:

- *Period 1 (September 2005):* 4.5 and 5.0 magnitude earthquakes on September 4 and 14, with seismic activity restarting on September 20 and continuing until October 4, peaking September 24–26, with a *silicic pyroclatite eruption* along a 500 m-long, 60 m-deep, N–S oriented vent, with sporadic tremors and longwave signals 7 km NE of Dabbahu (Yirgu et al. 2006). The 120 × 25 km seismic zone and the volcanic eruption pointed to a segment-wide magma intrusion event. The pattern of vertical crustal movements matched *faulted dike intrusion* models: parallel zones of uplift flanking a faulted graben above the dike intrusion (Fig. 6.102). The combination of SAR and correlations with SPOT images show roughly circular zones of subsidence, indicating pressure release

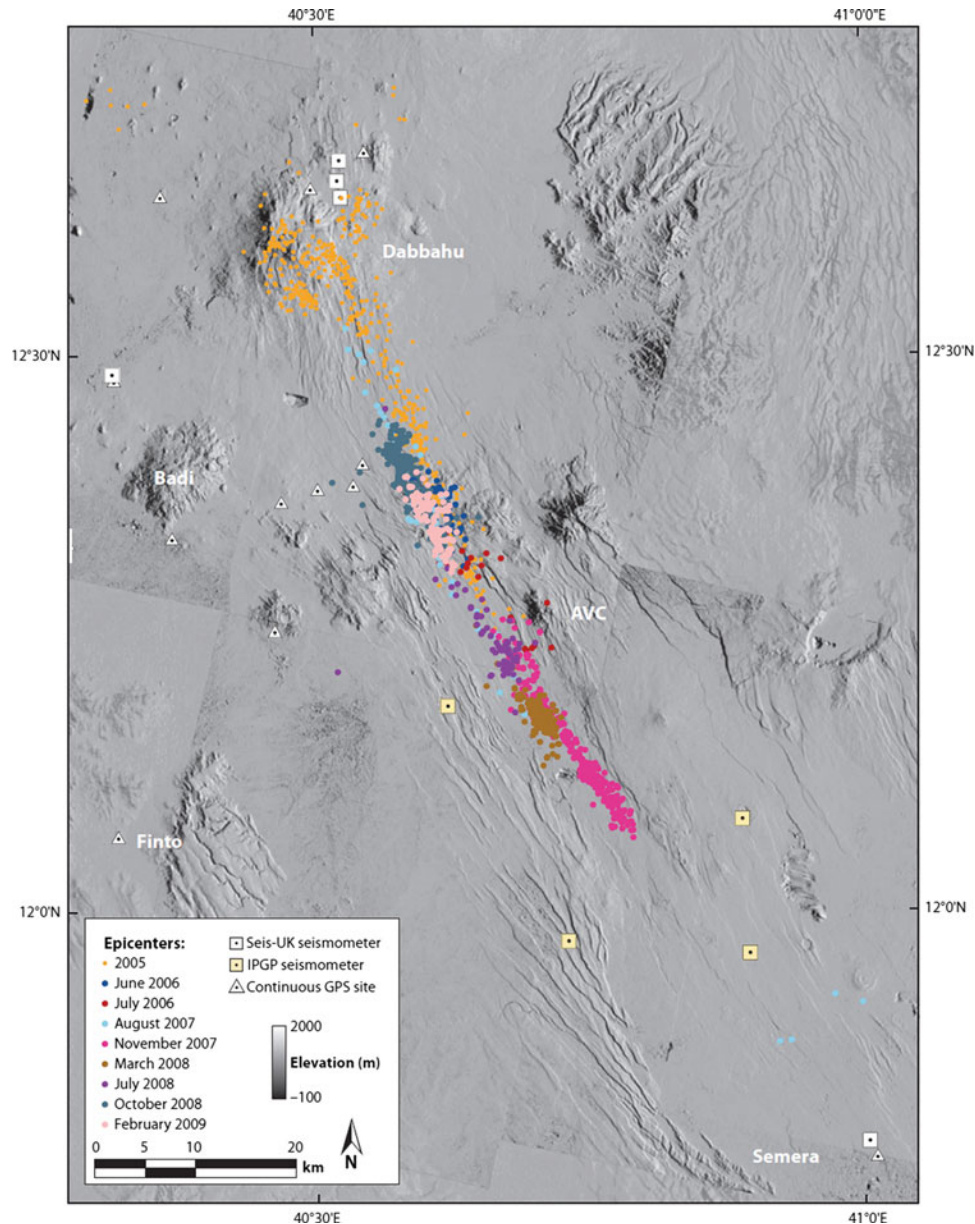


Fig. 6.101 Map of the epicentres of Dabbahu Manda Harraro segment from 2005 to 2010. Same colour code as Fig. 6.105. Composite digital elevation model constructed from SPOT 5 imagery. From Ebinger et al. (2010)

and/or volume changes in the magma chambers beneath Dabbahu and Gab'ho volcanoes. The along-axis variations suggest horizontal openings of 3–10 m along the length of the rift with dike intrusions to within 2.5 km subsurface and fault slips above the dikes, nearly all the strain during the rifting episode being accommodated aseismically by the intrusion of multiple dikes (Wright et al. 2006; Grandin et al. 2009; Ayele et al. 2009).

- *Period 2 (October 2005–June 2006)*: Earthquake hypocentres lie at a depth of 10 km along the length of the segment, showing *rift-normal opening*. Deformation

identified in the InSAR data (Fig. 6.102) suggests magma movement at two levels: 8–10 km and ~ 2 km (Ebinger et al. 2008).

Period 3 (June–July 2006): 8 km long, 2 m wide on June 17, and 10 km long, 1 m wide on July 25 dikes intruded the upper 10 km. Both earthquake clusters are characterised by 4–5 h long migration of seismicity along the dike length. Magma intrusion accounts for the vast majority of deformation, with no subsidence, suggesting a relatively deep (≥ 10 km) magma chamber (Keir et al. 2009).

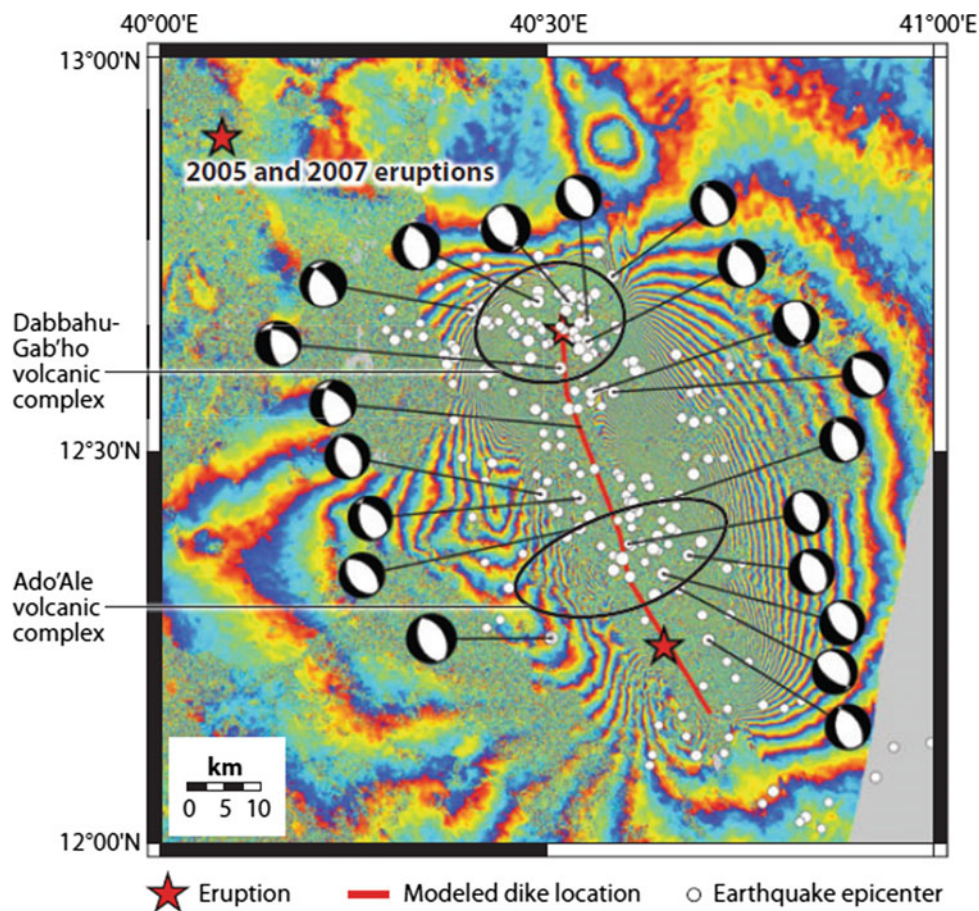


Fig. 6.102 Fault plane solutions (lower hemisphere projections) of earthquakes that occurred during the onset of the rifting cycle in the Dabbahu-Manda Harraro segment during the period September 4–October 4, 2005. Solutions are superposed on the descending track 49 interferogram formed by differencing satellite radar images acquired on

May 6 and October 28, 2005. Each repeated colour fringe corresponds to 2.6-cm deformation. *Red stars* indicate sites of the 2005 silicic eruption (north) and the 2007–2009 fissural basalt eruptions (south-center). From Ebinger et al. (2010)

– *Periods 4–6 (September 2006–January 2007)*: Following a swarm of 14 earthquakes, interferograms indicate a *dike intrusion*. *Event 5 (December 2006)*: A 7–8 km-long dike intruded the central rift sector. Normal faults slipped by 0.9 m (Hamling et al. 2009).

Period 7 (August 2007): A seismic swarm started August 11 with an earthquake near the centre of the rift segment. A sudden, southward-propagating cracking noise was heard prior to the onset of *fire fountaining* on August 13 (Ebinger et al. 2010) followed by *lava flow for four days* (Fig. 6.103a). As a result, numerous small spatter and scoria cones were arranged along N10W striking en échelon fissures; fault scarps with fresh breaks and rock falls bordered the new Aa and pahoehoe lava flow (Yirgu et al. 2006b). Interferograms indicate a dike intrusion accompanied the earthquake swarm preceding the curtain of fire episode up to 5 km south. Surface deformation suggests a dike opening of 2.4 m and a normal fault slip of 0.7 m. *Eruption was only 3% of the total intruded volume* (Hamling et al. 2009).

– *Periods 8–12 (November 2007–February 2009)*: Initiated with a tectonic earthquake along the fault system bounding the eastern flank of the rift. Radar interferometry and GPS data indicate a large volume, implying two separate intrusions (N°8 and 9) with opening between 5 and 9 km deep. Earthquakes associated with Dike Event 10 initiated at the segment centre and propagated southwards to the termination of Dike 9, whereas Dikes 11 and 12 also started near the segment centre but propagated northward.

– *Period 13 (29 June 2009)*: NASA’s EOS-Aura satellite detected a large SO₂ cloud which resulted in *plagioclase porphyritic Aa basalt flow* (Fig. 6.103b), sourced from fissures 4–5 km long, lined by scoria ramparts 30–50 m high with largely *aseismic dike intrusion*.

The timeframe, geographic location and characteristics of these successive tectonic and magmatic events is reported in Fig. 6.104 (from Grandin et al. 2009) whereas the depths and volumes are reported in Ebinger et al. (2010), with

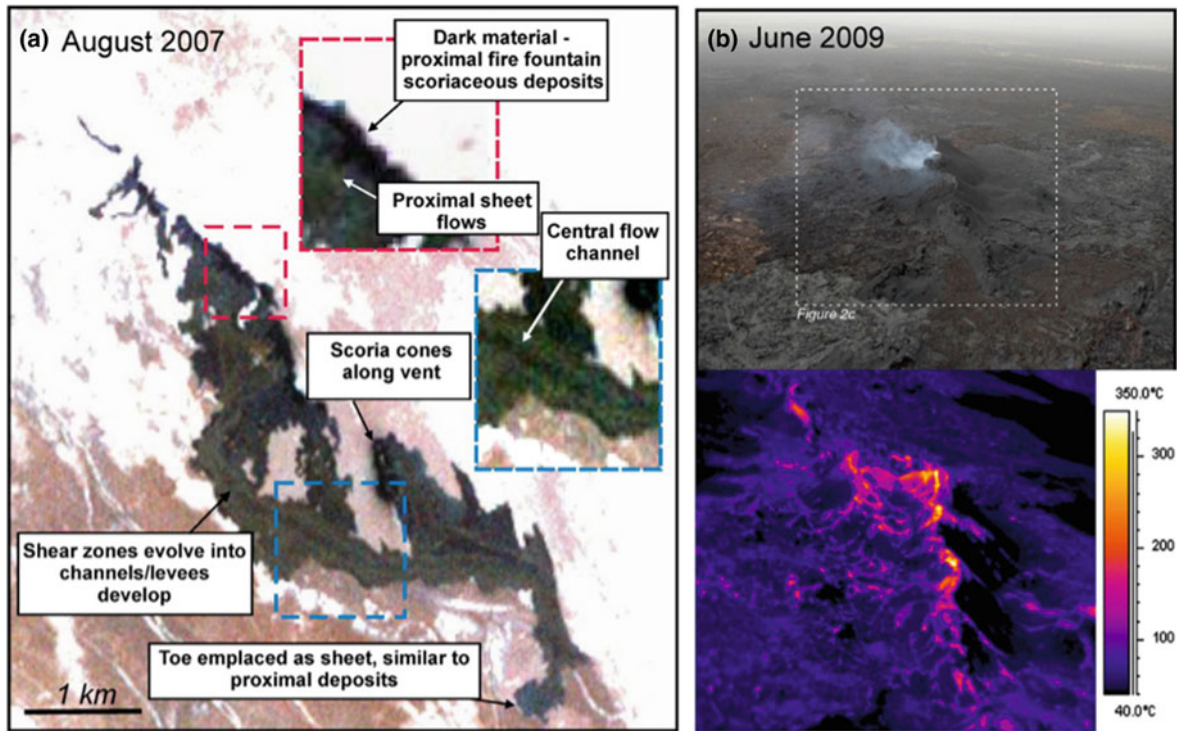


Fig. 6.103 Images of major Manda Harraro eruptive events: Aster image of the 2007 eruption lava flow field, and oblique aerial photograph and aerial thermal image of the 2009 fissure vent (Ferguson et al. 2010)

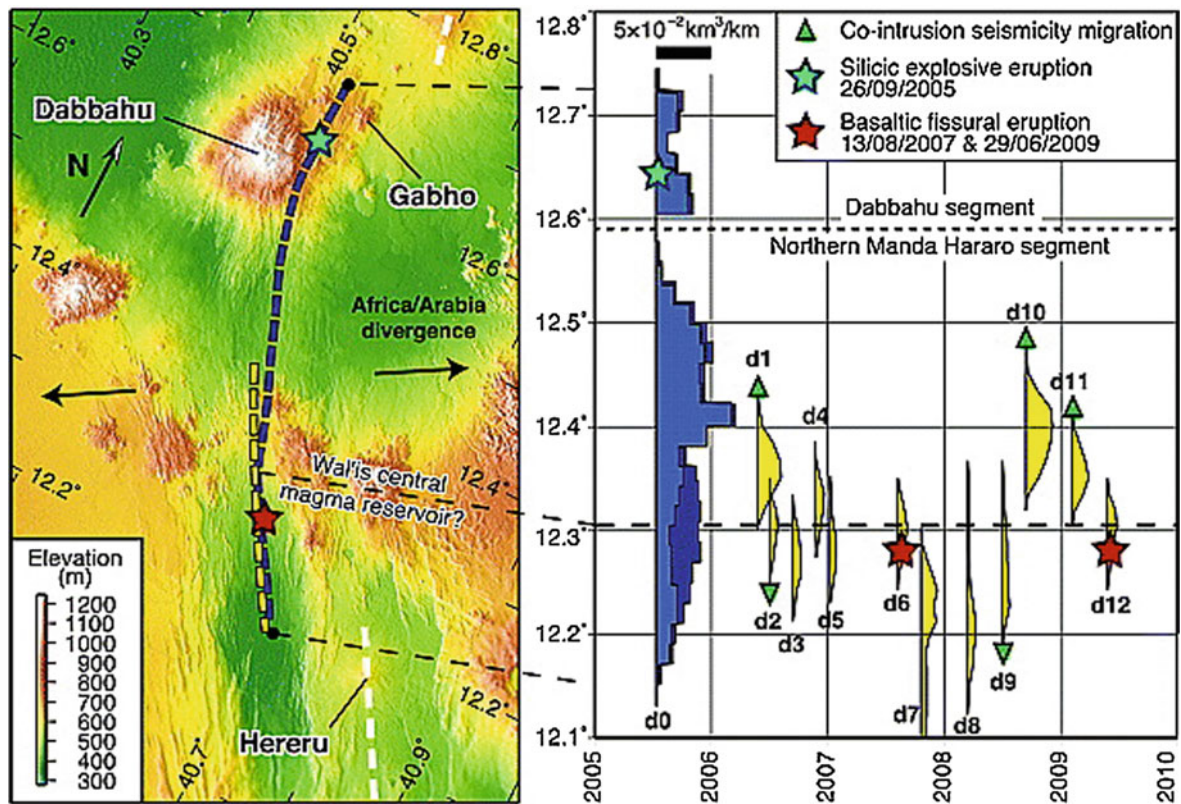


Fig. 6.104 Digital elevation model (DEM) of the Manda Harraro–Dabbahu rift (map, right). Thick dashed lines indicate the location of dike intrusions (blue, September 2005 mega-dike; yellow, 2006–2009 dikes); white dashed lines show the location of neighbouring Alayta and Southern Manda Harraro axial ranges. Distribution of dike

intrusions as a function of time and latitude; thickness of the coloured curves indicates dike volume per unit distance along the dike. Green triangles show the direction of the migration of seismicity coeval to dike injection. Stars indicate eruptions

respect to location along the axis of the Manda Harraro range, in Fig. 6.105, showing the importance of the initial magma injection.

As a whole, the 13 rifting events that occurred from September 2005 to June 2009 in the Manda Harraro rift illuminate the process of dike intrusion at a divergent plate

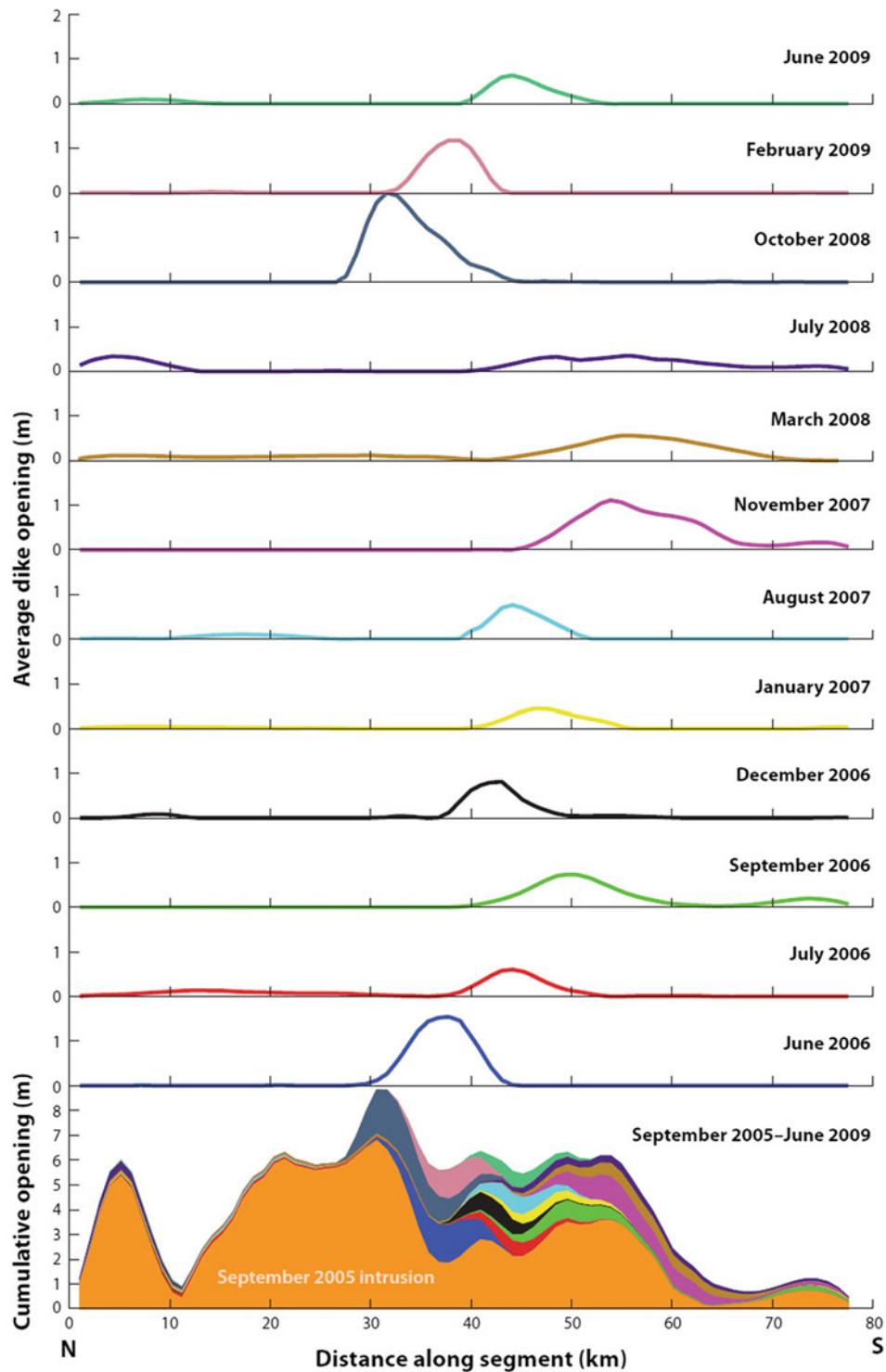


Fig. 6.105 Depth-averaged dike opening for the top 10 km of the crust beneath the Dabbahu-Manda Harraro segment plotted against distance along the segment from N to S. Zero is N flank of Dabbahu volcano. Lines represent the average opening for each of the dike

intrusions. Solid graph (bottom) shows the cumulative opening for all the dikes in the same colours as each of the individual graphs, in addition to the September 2005 intrusion (orange). From Ebinger et al. (2010)

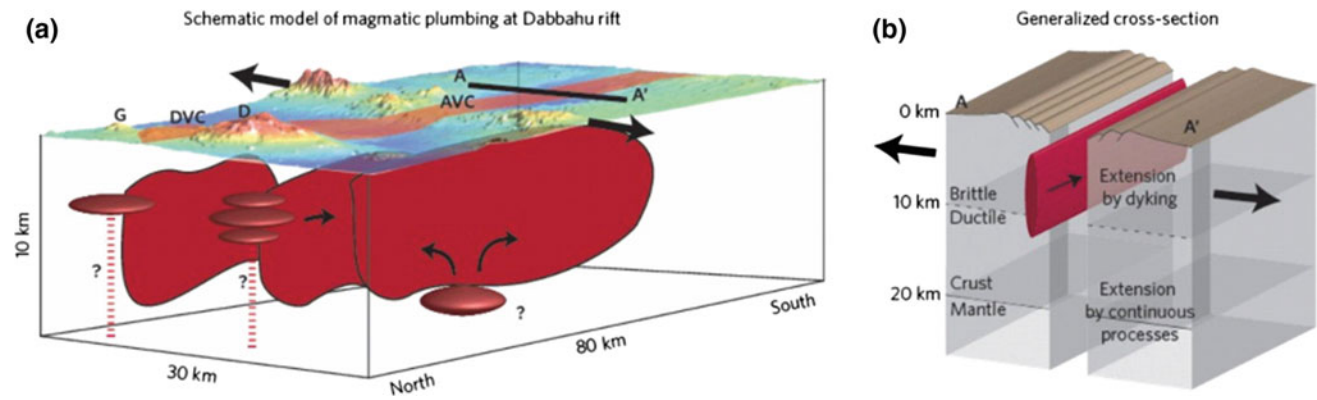


Fig. 6.106 Model of the dyke and magma chambers beneath the Dabbahu-Manda Hararo magmatic segment; extract from Wright et al. (2012)

boundary (Wright et al. 2006) (Fig. 6.106). Inversion of InSAR data shows that dikes were emplaced at between 0 and 12 km depth, with a volume of $>1 \text{ km}^3$ magma intruded in a 12 m-wide over 65 km-long dike for the September 2005 initial event, followed by later smaller diking events, 0.8–3.5 m wide over lengths of 10–15 km, with volumes of $0.04\text{--}0.2 \text{ km}^3$. Dikes are intruded north, south or above a magma reservoir inferred in the middle of the segment. Cumulative opening distributions of the dikes suggest a thinner (4–6 km) lithosphere at the latitude of the magma reservoir rather than towards segment ends (10–12 km). Groups of successive dike intrusions are clustered in space and time, suggesting that dikes interact, breaking sections of the plate boundary that had already been opened by the September 2005 event. Only two dikes propagated to the south in regions that had only moderately opened in 2005, and they were followed by events that extended the rupture area to the south, beyond the limits of the 2005 megadike.

6.6.3 Manda Harraro in the Context of Afar Volcanic Ranges

Replacing these data in the geological context, the 2005–2010 event could be interpreted as resulting from the unlocking of the Manda Harraro rift segment at the level of the Dabbahu strike-slip transform zone linking the Alayta rift segment to the north with the Manda Harraro segment to the south. Incidentally, this first basaltic diking interacted at depth with one of the shallow magma chambers that are known to have developed in this area along the MNW-ENE Dabbayra transverse structure (see Fig. 6.78).

As a result of this unlocking at the northern extremity of the range, diking and associated basalt injection could develop along the Manda Hararo range, with a wider opening to the north and propagation towards the south.

However, the propagation did not extend along the whole length of the Manda Harraro axial range, the southernmost part

of the range being unaffected, despite the fact (or because of the fact?) that it was shown to be the most active in the recent past.

The fact that Manda Harraro range—as shown by its exceptional length and diversified geology—is made of a set of fissural basaltic lava field and embryonic shield volcanoes implies that the successive diking events do not affect the whole length of the range at once. As in 2005–2010, several of these sub-segments were found to be spreading along the range down south to the Gumatmali area. Such segmented diking and fissure eruption will characterise Manda Harraro activity in the future as in the past.

From a petrological and geochemical point of view, the Manda Marraro range is characterised by transitional basalts of generally “primitive”, rather undifferentiated compositions (Treuil and Varet 1973; Barberi and Varet 1977). Plagioclase porphyritic basalts and ferrobasalts, however, show that it is fractionation processes developed in shallow magma chamber feeding the dikes and flows that characterise the range. In the few shield volcanoes, the magmatic evolution may reach dark trachyte compositions and, exceptionally, silica-saturated trachytes or even rhyolites, as observed in Gablaytu.

The petrology of the basalts erupted in 2007, in particular the plagioclase porphyritic lavas, as well as their geochemical signatures, indicate that some component evolved at depths of 5–7.5 km, confirming the scheme implying multiple magma reservoirs beneath the Manda Harraro range (Ferguson et al. 2010).

From a geochemical point of view, it was shown by Treuil and Varet (1973) that the Manda Harraro range displays the basalts that are the nearest to MORB in the whole Afar, as shown by REE ratios (Figs. 6.107 and 6.137 below). This is in agreement with the position of this range with respect to its plate tectonics environment. Whereas the Erta Ale range lies on the northern apex of Afar where the rotation of the Arrata block implies slower spreading rates, and the faster spreading south is accommodated by two segments (Alayta and Tat’Ali), Manda Harraro—a unique spreading segment at this latitude—represents the area of fastest spreading.

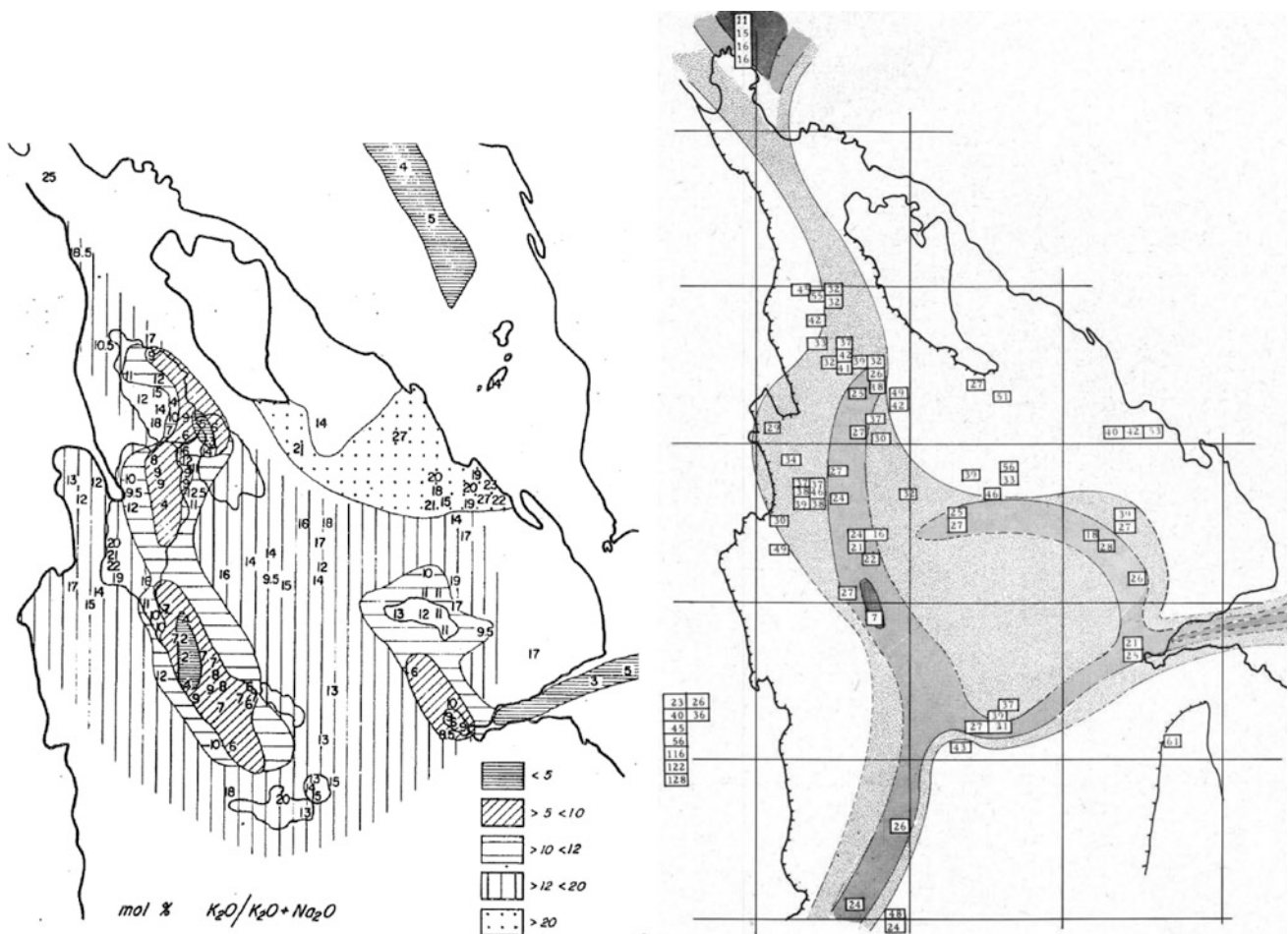


Fig. 6.107 Ratio $\text{Na}_2\text{O}/\text{Na}_2\text{O}+\text{K}_2\text{O}$ (molecular ratio, from Barberi and Varet 1978) and La/Tb (from Treuil and Varet 1973) for the basalts from Afar. Manda Harraro appear as the nearest in composition to nearby Red Sea and Gulf of Aden MORB

6.7 Manda Inakir Axial Range

Along the NNW-SSE Afar axis, around 12°N (Fig. 6.108), the next axial range found after Manda Harraro, called Manda Inakir, is shifted by 150 km to the NE. Together with Manda Hararo, they ensure the link between the Red Sea spreading segments of N and E Afar and the Gulf of Tadjourah—Aden oceanic ridges through the Asal axial range.

The Manda Inakir range lies along the boundary between the Federal Republic of Ethiopia (Afar Regional State) and the Republic of Djibouti. It covers the stratoid series and displays all the characteristics of the axial ranges, that is, it concentrates in that part of Afar most of the recent Quaternary (less than one million years old) volcanic activity, with continuous emission of basalts along a narrow set of fissures in the regional Gulf of Aden—Red Sea direction. This “rift in rift” is built—as are other axial ranges—of transitional basalts with a few differentiated products, ferrobasalts or dark trachytes (Fig. 6.109).

The age of the Manda Inakir range is from 0.4 million years (Civetta et al. 1975) to recent, and quoted as historical by Audin et al. (1990), who showed that the latest eruption dates back to 1928–1929, a year or two before the

coronation of Emperor Haile Selassie I in Ethiopia. The eruption was accompanied by a strong earthquake and remained in the Afar people’s memories as *Dijdira Karma*, meaning “the year of the earthquake”. A seismic sequence was recorded on 18 May 1929 at Addis observatory which would clarify the date of the eruption (Gouin 1979; Audin et al. 1990; Manighetti et al. 1998). The event was reported to have modified the drainage system and created fault walls in the nearby Andabba Plain (Fig. 6.110).

The Manda Inakir range was shown by De Fino et al. (1973) to be made of two distinct units: the Inakir shield volcano and the Manda rift:

- The earlier Inakir shield volcano is 25 km long and 16 km wide and extends in a NW–SE direction, parallel to the Asal-Ghoubbet rift (Aden ridge direction). The continuous activity of these basaltic fissures covered the stratoid series and one of its late actions topped the Andabbi Ale rhyolitic centre (dating from 872 thousand years ago) on the SW slope of the range. Between 350 and 190 thousand years ago an elongated shield volcano was built by the piling of lava flows up through andesine

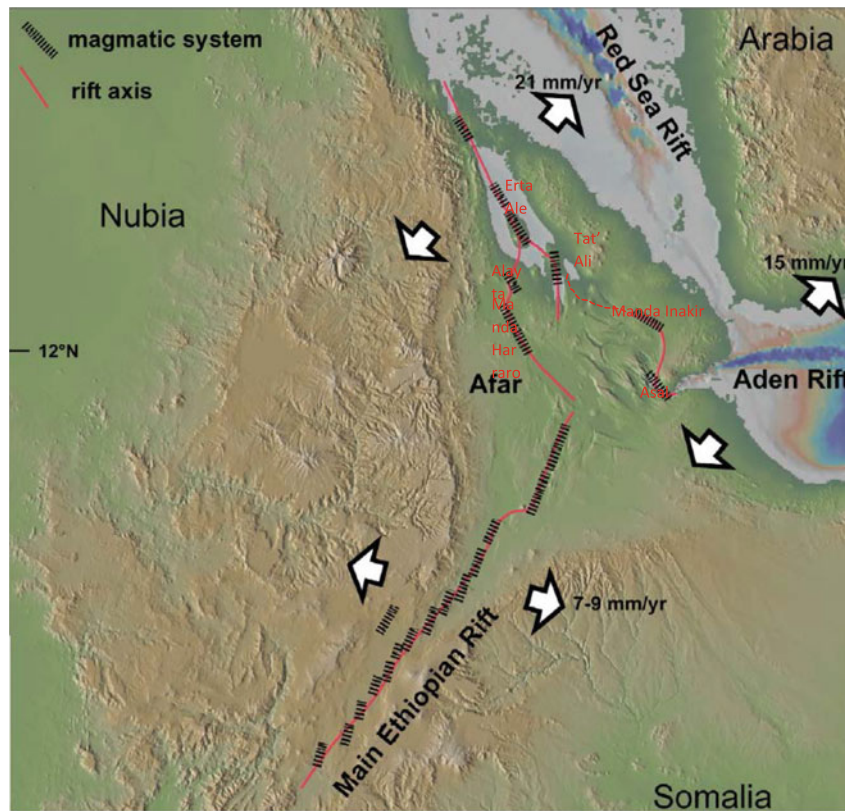


Fig. 6.108 Axial volcanic ranges in Afar (in red) and MER rift segments showing the 150 km-wide shift from Manda Harraro to Manda Inakir in central Afar. A dotted line linking Manda Inakir to

Tat'Ali was drawn showing the hypothetical aborted link between Mat'Ala and Inakir considered in Sect. 6.2. (Modified from Acocella et al. 2014)

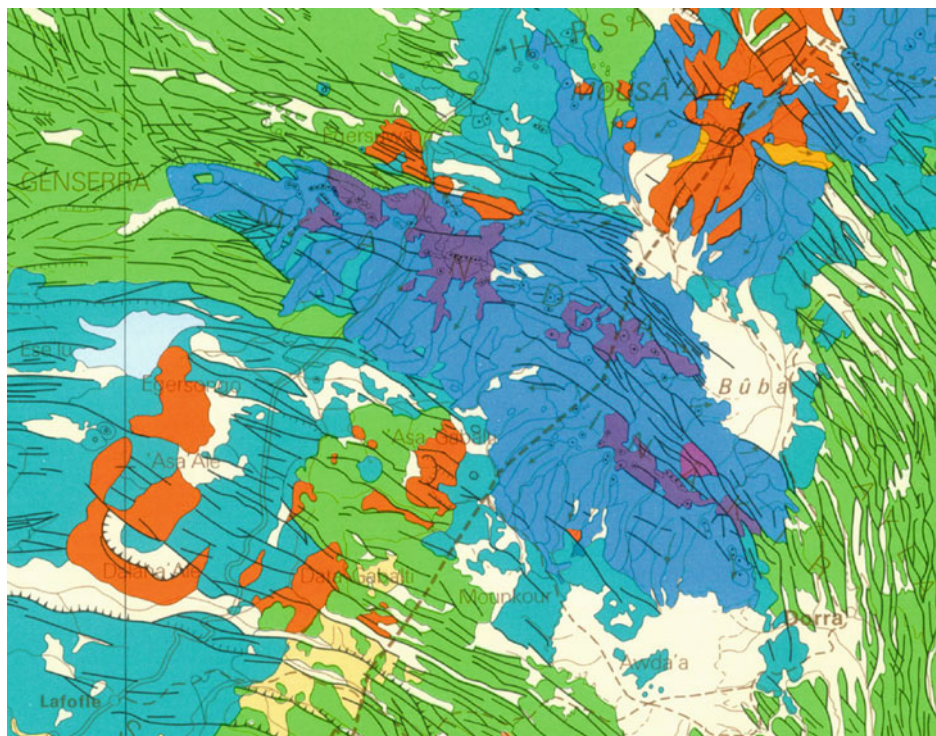


Fig. 6.109 Geological map of Manda Inakir axial range (from 1/500,000 map of central Afar, J. Varet 1975; same legend). Dotted line shows the Ethio-Djibouti boundary and the Assab-Kambolcha road crossing through the western part of the range. Mousa Ali volcano is visible in the NE

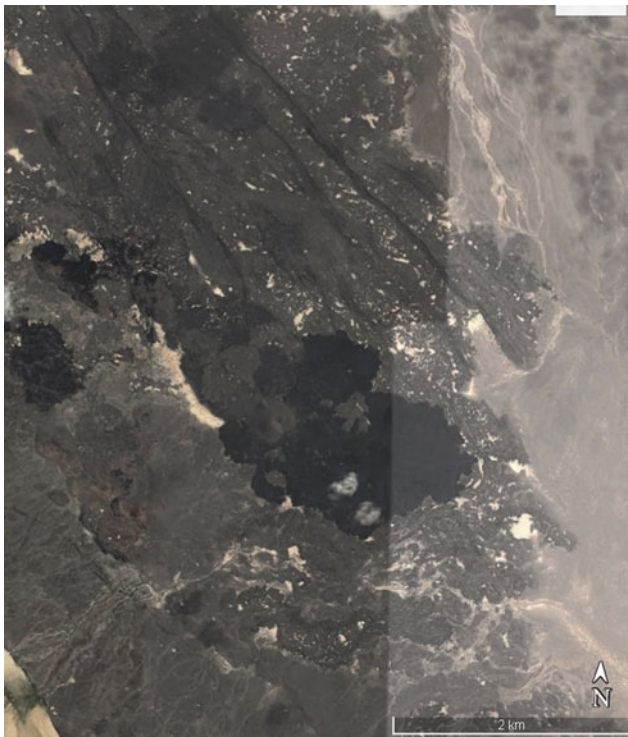


Fig. 6.110 Satellite view (USGS Earth Explorer) of the 1929 Aa flow (*black*) and scoria cones on the SW extremity of Manda

plagioclase porphyritic basalts to ferrobasalts and dark trachytes, with one outcrop of silicic alkali trachyte in a small dome in the central part of the shield. A slightly asymmetric (faults mostly dipping SW) graben structure—10 km long and 3 km wide—can be observed along the axis of the volcano. The most recent activity in this

part of the range is limited to that axis, where numerous spatter cones are aligned.

- Manda is located on the northern flank of Inakir. It is a much younger range, elongated along 40 km with a width of 15–20 km (Fig. 6.111). Manda is clearly built on slightly different trending open fissures and faults oriented WNW–ESE. Rift in rift structures are observed, with older flows now on the sides and younger flows and emission centres along the axis (Fig. 6.112). Manda is exclusively made of basalts, with minor hawaiites and mugearites, but no detectable difference is found between the parent magma of the two units.

As a whole, a shift is noticed, the most recent volcanic activity having migrated from the south at Inakir shield to the north at the Manda range, where the historical basaltic eruptions occurred. Open fissures affecting the most recent basaltic flows and nearby sediments in the rift direction and light coloured scarplets show that the extensional phenomena and normal faulting is still active. The three subrifts of Inakir, Manda and Dirko Koma were interpreted by Manighetti et al. (1998) as resulting from the propagation of the rift north-westwards, Dirko Koma representing “the northern tip of the propagation of the Aden ridge in Afar” (Fig. 6.113).

Another possible interpretation is that Inakir developed NW–SE when a direct link was established with Mat’Ala through the grabens observed between these units, as hypothesised in Sect. 6.2, along the dotted line of Fig. 6.108 and the BC segment of Fig. 6.116.

Concerning the shift in the volcanic activity, one should remember similar observations made in the northern half of the Erta Ale range and in Alayta, where an evolved volcanic



Fig. 6.111 Satellite image showing the more recent nature (*black* Aa flows) of the northern half of the range (Manda) with respect to Inakir now extinct shield (Source USGS, Earth Explorer)

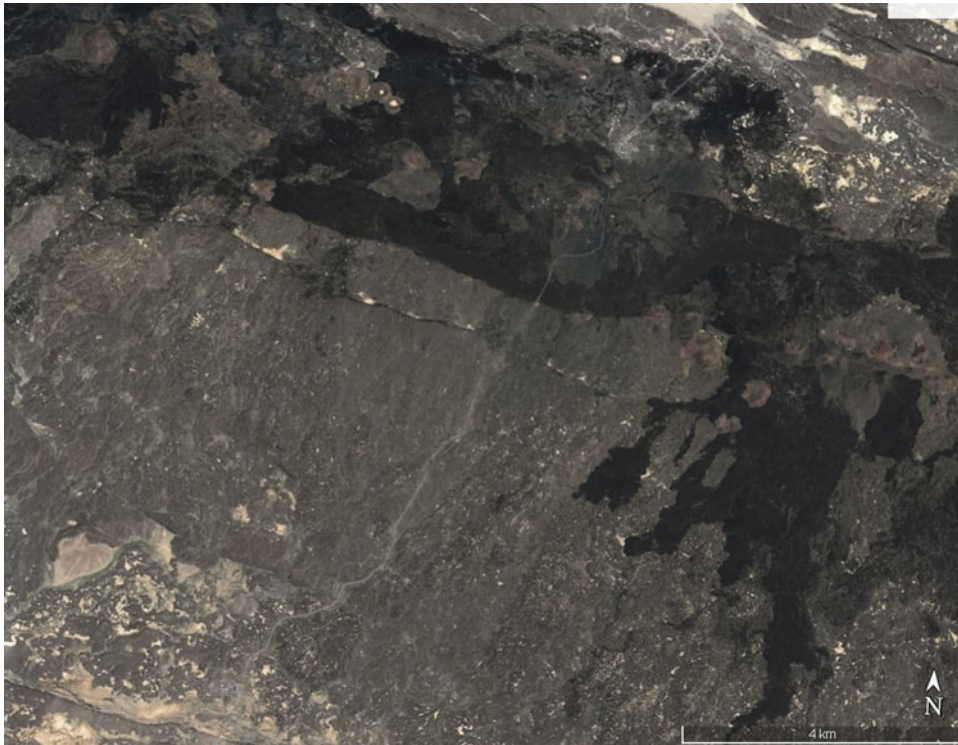


Fig. 6.112 Satellite view (USGS Earth Explorer) of the axial graben of Manda along the RN1 Assab-Kambolcha (road built in 1936). A symmetrical graben occupies the axis of the range containing the most recent basalts emitted through fissures along the axis. Open emissive fissures do not necessarily show craters and cones, but are bordered by continuous spatter ramparts (former “wall” of fire”)

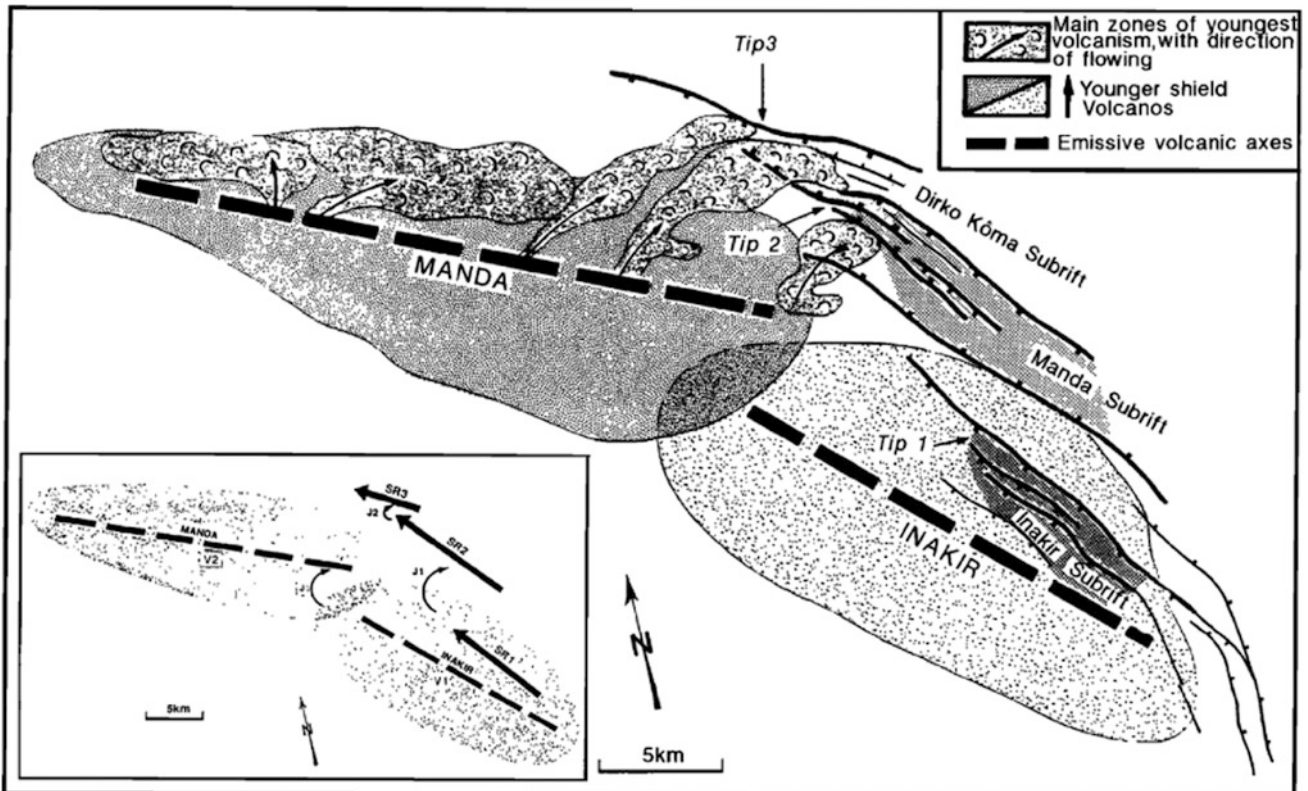


Fig. 6.113 Structural interpretation by Manighetti et al. (1998) of the Manda Inakir rift and sub-rift system

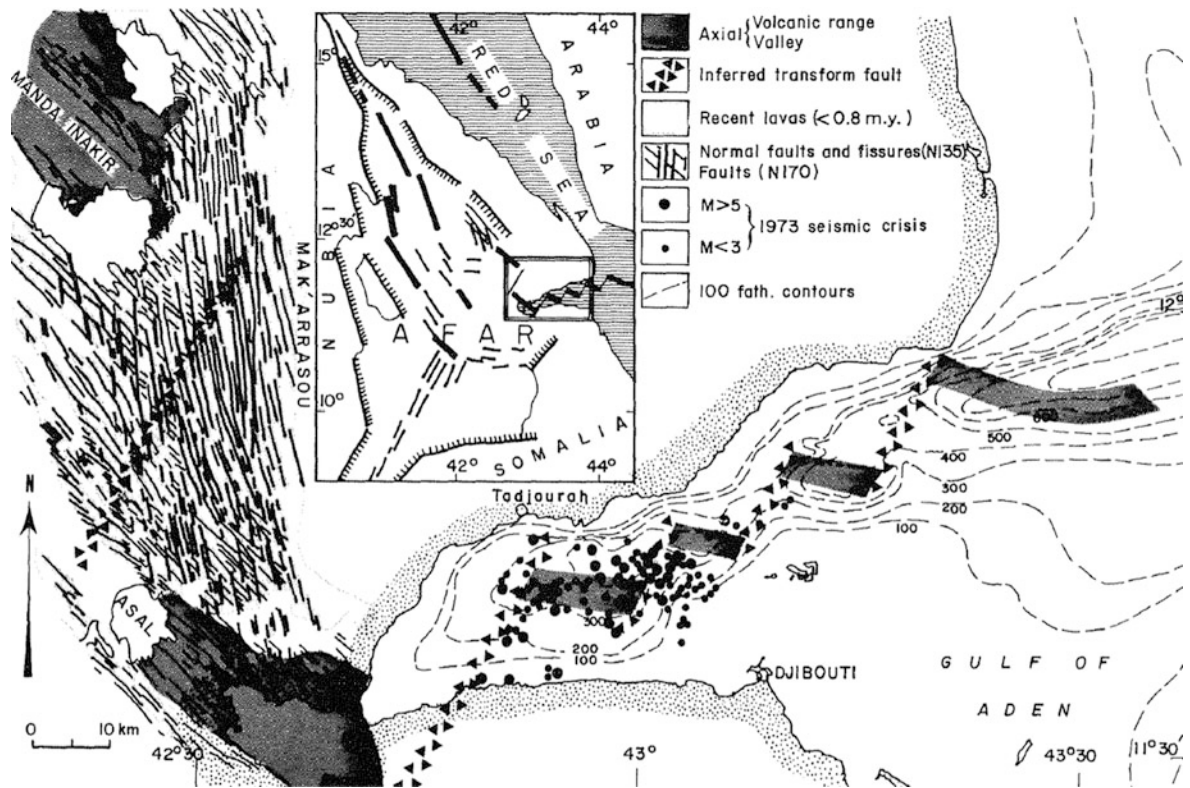


Fig. 6.114 Sketch map of the axes of spreading and transform faults in the gulf of Tajourah and its continuation in eastern Afar. The Makarrasou transform fault is shown to fit with the transforms to the Gulf (Courtillot et al. 1974)

unit is replaced laterally by a younger fissural lava field, a trend also observed at Asal (see below).

It is of interest to observe how the Manda Inakir ends on both sides:

- To the SE, the NW trending faults progressively merge with the N–S trending linear faults of Mararrasou that link the Manda Inakir rift with the Asal rift. It was shown by Tapponier and Varet (1974) to represent the surface expression of a transform fault (Fig. 6.114).
- To the NW, the fault behavior is equally significant. As observed in Fig. 6.115, the fault system develops a divergent pattern. To the north, the faulting develops with two conjugated directions (WNW and NNW) intersecting each other and delimiting diamond-shaped blocks, whereas to the south, large NE faulting predominates, crossing through the nearly E–W rift pattern there, shaping diamond-shaped blocks of opposite orientations.
- These patterns were interpreted by Barberi and Varet (1977) as showing the surface expression of two transform zones, one (D) connecting Manda Inakir to the north with the Red Sea Rift through the Bidu-Dubbi-Hanish Islands transverse megastructure, and the other (C) connecting Manda Inakir to Manda Harraro through the major transverse graben that affect this wide area covered by an intensively faulted stratoid series (Fig. 6.116).

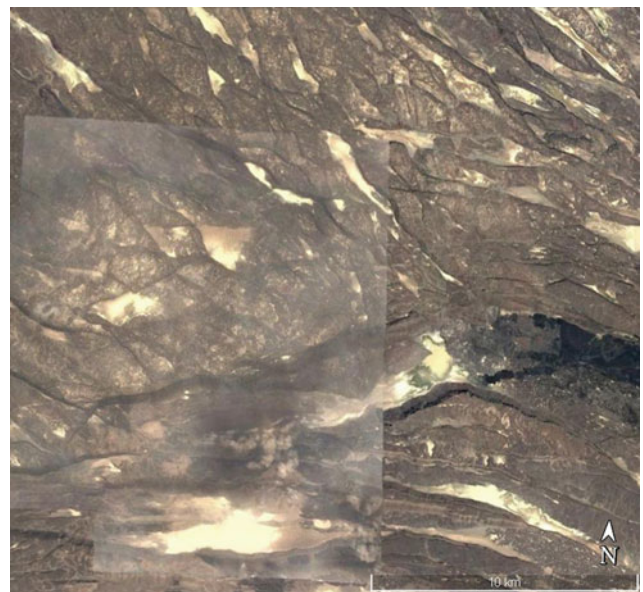


Fig. 6.115 Western tip of the Manda Inakir range where it merges in two divergent direction with diamond shaped blocks of opposite orientation: NNW/WNW to the north, where the fault system tends to link Manda Inakir rift segment to the Red Sea through Bidu-Dubbi-Hanish transverse megastructure and NE/E–W to the south where the major transverse graben underline the transform zone linking Manda Inakir to Manda Harraro

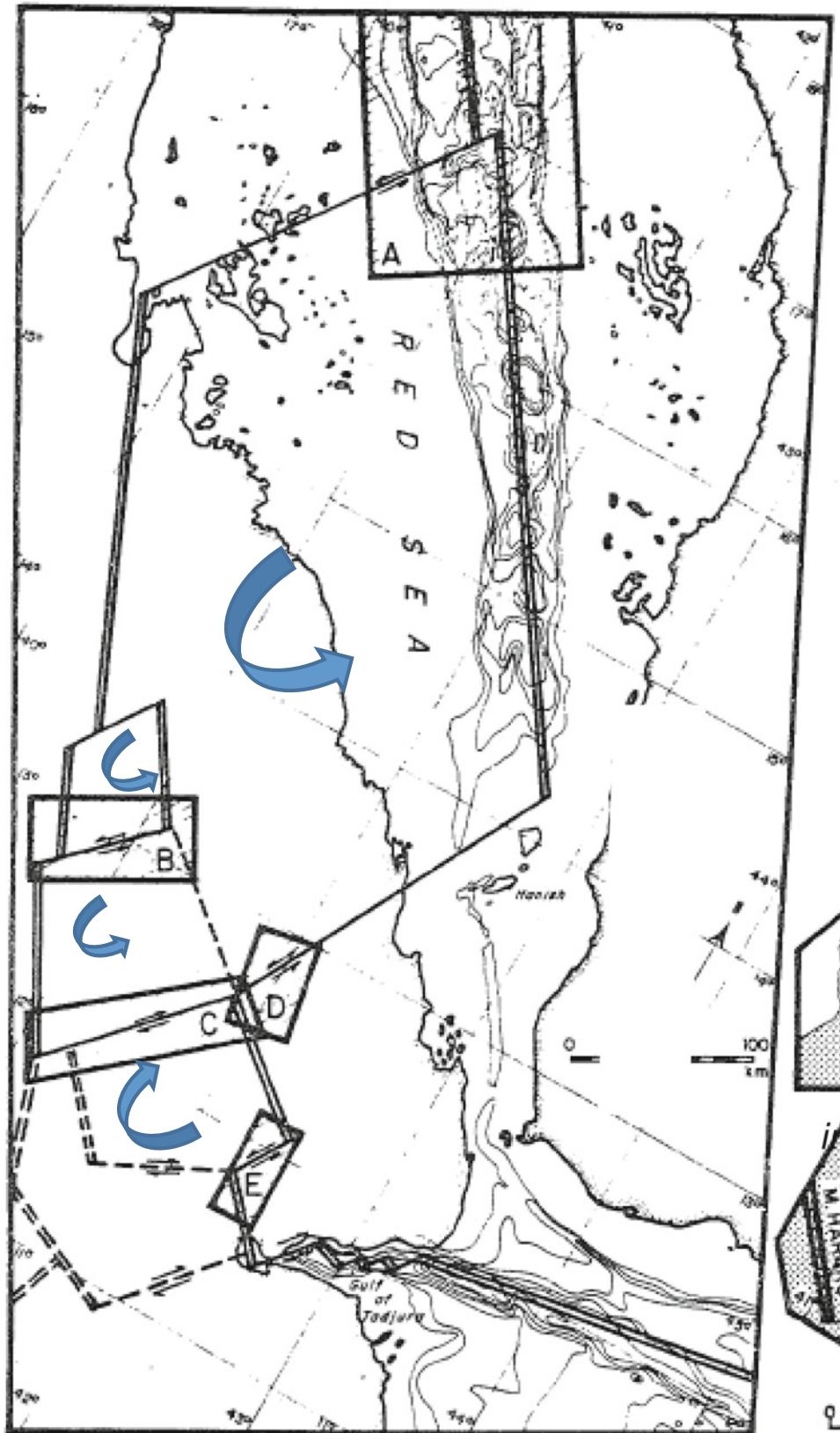


Fig. 6.116 Drawing of the plate boundaries within Afar (Barberi and Varet 1977). The Red Sea rift is progressively replaced in its southern part by the Danakil (north-western Afar) rift, and finally dies at the level of Hanish Islands and is replaced by the eastern Afar rift which

links with the Aden ridge through the Gulf of Tadjourah. Rectangles A, B, C, D indicate the areas of major transform faulting deformation. The rotation of the blocks is shown

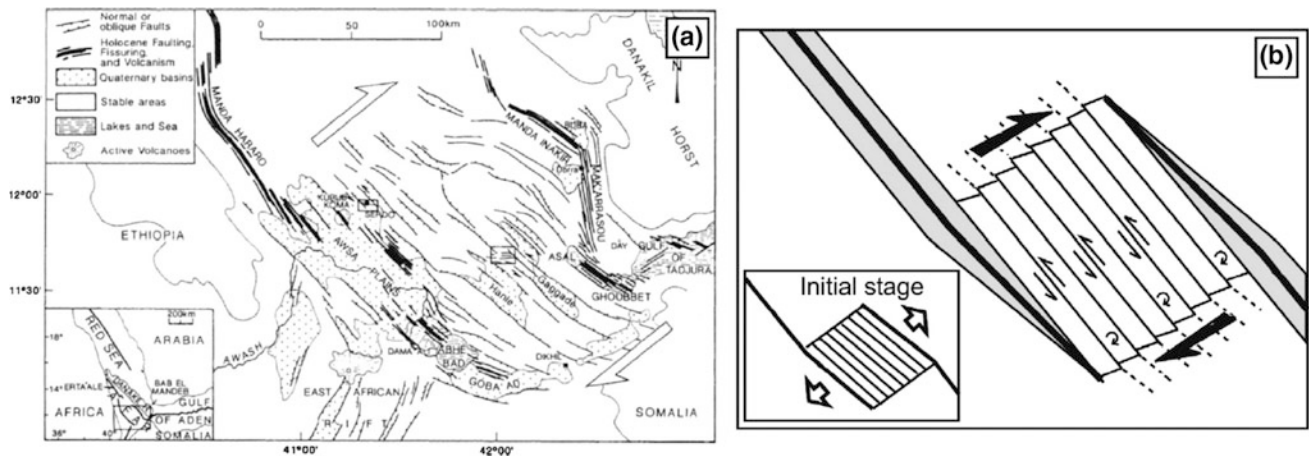


Fig. 6.117 Deformation of the area of central Afar located between the southern dying extension of Manda Harraro axial range and the Manda Inakir range, with the resulting rotation and bookshelf faulting

- In the wide area located between the southern extension of the Manda Harraro range (Tendaho graben with sparse volcanic units ending at Dama Ale and Lake Abhe) and the Manda Inakir—Makarassou—Asal Ghoubbet plate boundary of SE Arabia, intense deformation occurs, caused by the rotation of the resulting microplate, with induced bookshelf faulting identified by Tapponnier et al. (1990); see Fig. 6.117.

The GPS speed measured in the whole north Tadjourah block, including Assab, Manda, Tadjourah and north Ghoubbet, with a NE orientation was 15 mm/year and evolves within the Arabian plate, confirming our view that this area should be regarded as the accretion of the southernmost Danakil block to the Arabian plate (McClusky et al. 2010; Déprez 2015). However, seismicity and GPS data also show that the Manda Inakir segment and the Makarassou accommodation (or transform fault) zone have not been particularly active in the last 15 years, the activity being spread over the whole area located west of Makarassou (Fig. 6.118).

This does not mean in our view that the Manda Inakir segment is no longer active. It could just be that the periodicity of the activity in this axial range is discontinuous, with events concentrated in periods of 10–20 years (as observed in Manda Harraro and Asal), occurring in secular cycles. It may also be that the lack of seismic stations in the Manda-Inakir and Mousa Ali area partly explains the relative lack of activity registered.

6.8 Asal Axial Range

Asal was identified early on as one of the most typical axial ranges in Afar. Despite the fact that the concept was derived from the observations made in northern Afar, with the Erta

identified by Tapponnier et al. (1990). Figure from Acocella et al. (2014) after Tapponnier et al. (1990)

Ale range (Tazieff et al. 1969), in parallel with the exploration of northern Afar, attention was placed on Asal which appeared to be one of the most typical analogues to mid-ocean rifts. It was shown (Tazieff et al. 1972; Barberi et al. 1970) that Asal was one of the most spectacular axial basaltic ranges, showing a symmetrical volcanic rift, where the present spreading mechanism concentrates (Fig. 6.119).

6.8.1 Geology of the Asal Volcanic Range

In parallel with geological mapping, the first geodetic measurements across the Asal rift and the emplacement of a seismic network linked with the geophysical observatory at Arta (Ruegg et al. 1979, 1993), a geothermal exploration program was engaged in Djibouti by BRGM (1970, 1973) under the supervision of G. Marinelli. This quickly led to the identification of the Asal rift as a target of major interest for geothermal exploration. Detailed geological, petrological and tectonic studies by Stieltjes as well as hydrogeology and fluid geochemistry by Lopoukhine, followed by geophysical surveys, allowed a geothermal model to be proposed for the Asal rift (Fig. 6.120).

The active nature of the Asal volcanic and tectonic range, displaying a continuous basaltic activity in the recent Quaternary period, with a magmatic evolution by crystal fractionation (Stieltjes et al. 1976) and a typical rift in rift structure location of the present activity along the axis, indicated the presence of a magmatic heat source at shallow depth, the last expression of which was found in the lava lake at Fialé.

We should stress here that the Asal rift is the NW, emerged extension of the Asal-Ghoubbet rift, which is in fact mostly a submarine oceanic rift structure that ensures the link with the Gulf of Aden mid-oceanic ridge (MOR) through the Gulf of Tadjourah (Fig. 6.121).

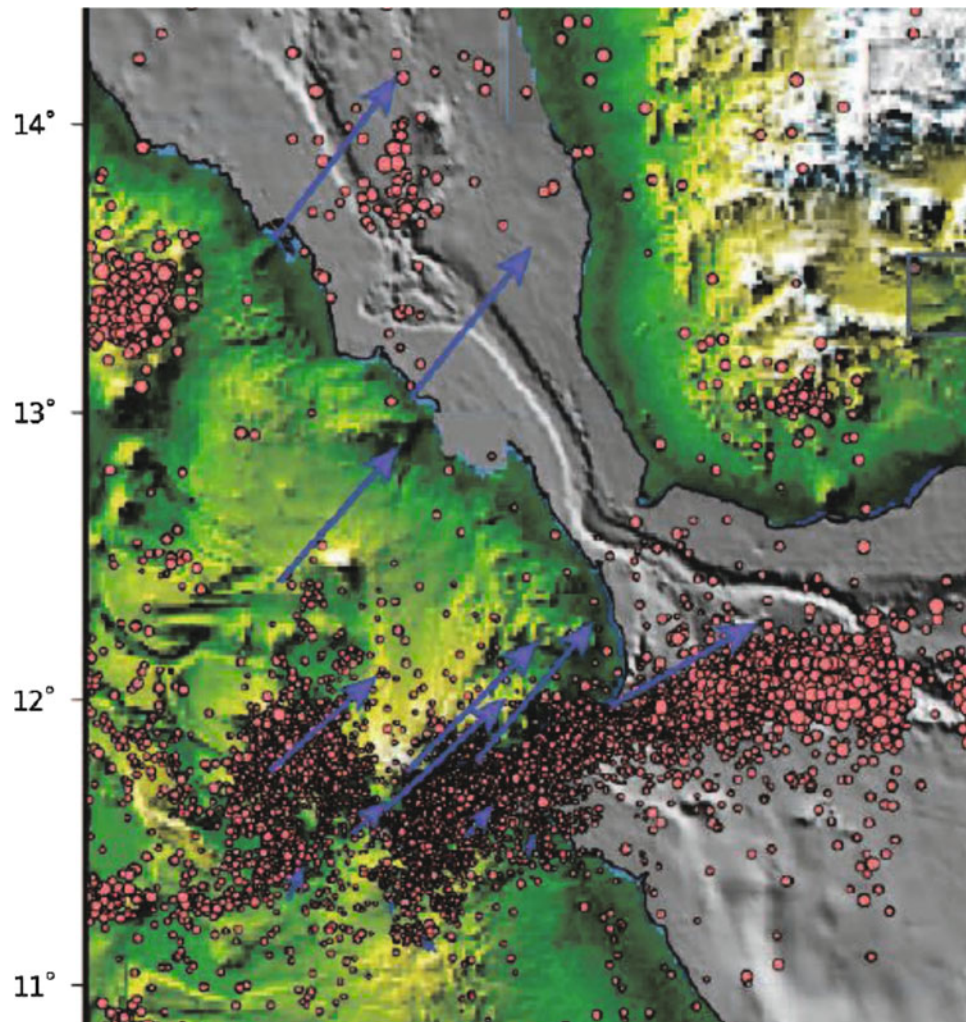


Fig. 6.118 Seismicity registered by the Arta observatory (AGO, Djibouti Republic) in the period 2001–2012. *Blue arrows* indicate GPS orientation and speed. From Déprez (2015)



Fig. 6.119 The symmetrical rift structure of Asal volcanic range, as seen from Lake Asal (154 m below sea level)

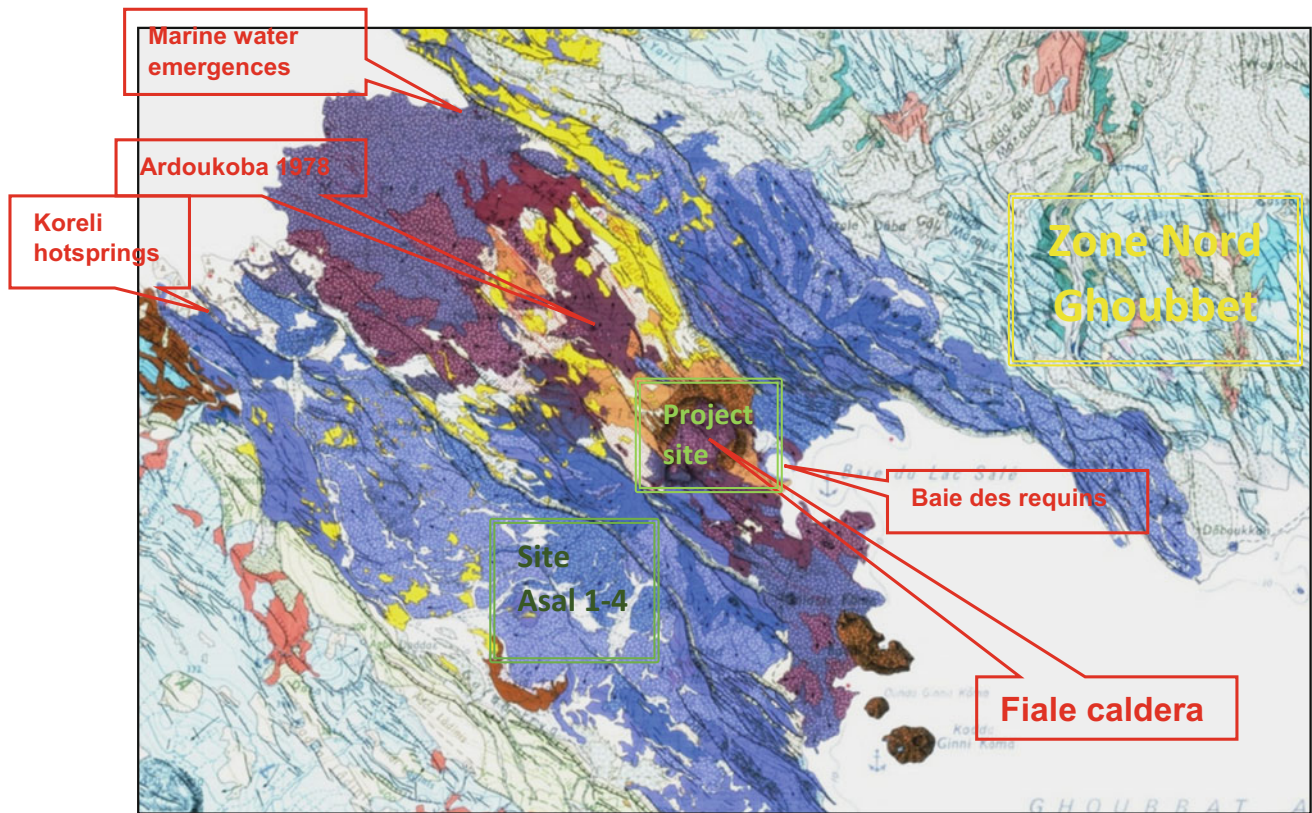


Fig. 6.120 Geological map of the Asal rift (Stieltjes, ed. BRGM 1978); hyaloclastites are in *orange*, recent basalts in *deep blue* and *violet* whereas early rift basalts (300,000–100,000 years ago) are in

pale blue; the stratoid series (3–1 million years ago) is in *very pale blue* colour. Lacustrine deposits (diatomite) in *yellow*

Detailed field works and age determinations showed that the Asal shield volcano formed 300,000 years ago and was subject to successive rifting episodes with an equilibrium established between extensions of 17–29 mm/year in a 40°N direction and magma injections (De Chabaliere and Avouac 1994); see Fig. 6.122.

6.8.2 The Ardoukoba Simo-Volcanic Event, 1978

Whereas a precision levelling of 200 benchmarks was established in 1973 along a 100 km traverse across the rift, no deformation was observed until the 1978 tectono-volcanic event (Figs. 6.123 and 6.124), a seismic crisis including strong faulting and the eruption of the Ardoukoba volcano along the axis of the rift (Demange et al. 1980). The lava emitted was a transitional basalt, slightly olivine and plagioclase (bytownite) porphyritic, quite similar to the recent lava sequence of the Asal rift axis (Stieltjes et al. 1976). A set of scoria cones and a few short lava flows appeared in a few days on the north-eastern flank of the shield, erupted from an open fissure that continued to open after the eruption, as presently seen in the field (Figs. 6.125 and 6.126). The amount of magma erupted was small



Fig. 6.121 The Ghoubbet rift seen from Asal western margin; observe the NE bordering faults and the hyaloclastite cones along the axis (Photo coll. G. Marinelli, University of Pisa)

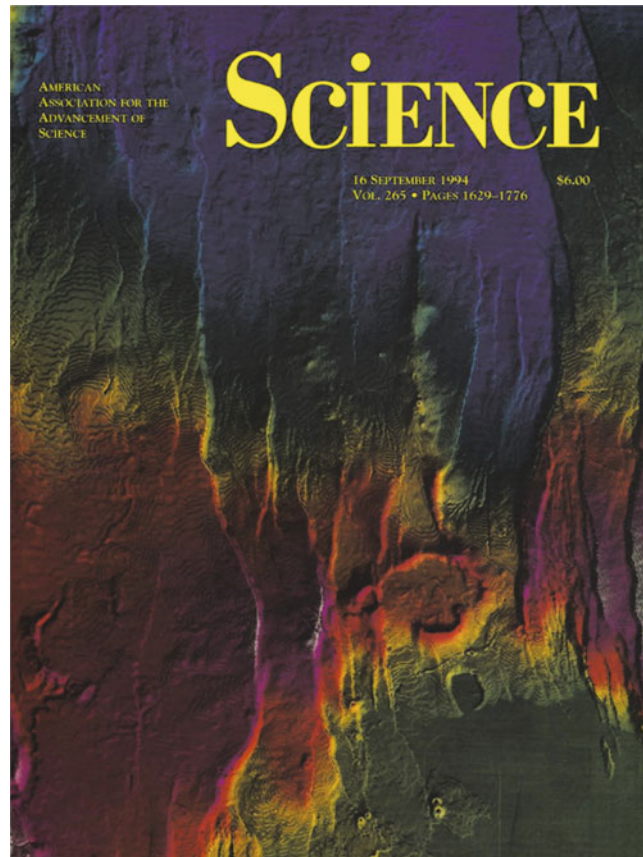


Fig. 6.122 Shaded topography of the 12 km-long (emerged part) Asal rift. Colors indicate elevations, from -150 m below sea level (dark blue) to +350 m above sea level (purple). The topography results from the dismemberment over the past 100,000 years of a large shield volcano formed stride the rift zone 300,000 to 100,000 years ago.

Reconstruction of the volcano by Chabalier and Avouac (1994) indicates a spreading rate across the rift of 17–29 mm/year. Cover page of Science. The Fiale caldera and the Baie des Requins crater are clearly visible, as well as the axial ridge of Ardoukoba 1978 eruption

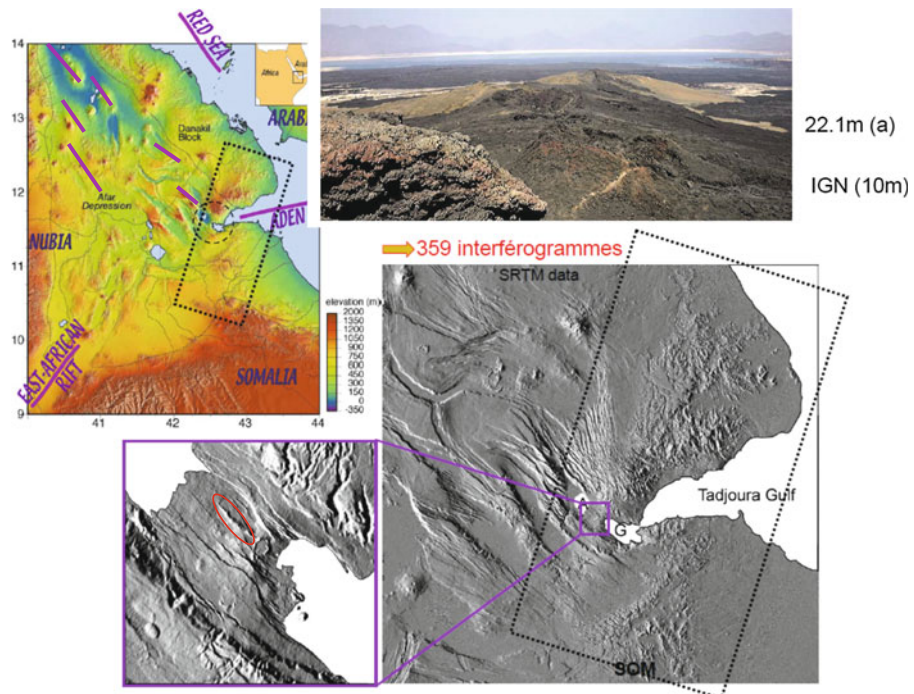


Fig. 6.123 Location of Ardoukoba volcanic eruption (surrounded by a red oval) along the axis of the Asal axial range, which is the first emerged rift segment in SE Afar. That is where the Afar emerged rift

axis (axial volcanic ranges, in violet) meet the Aden ridge through the Gulf of Tadjourah and the Ghoubbet Bay (G). Photo the Ardoukoba crater line and fissure eruption (from Doubre et al. 2007a, b)

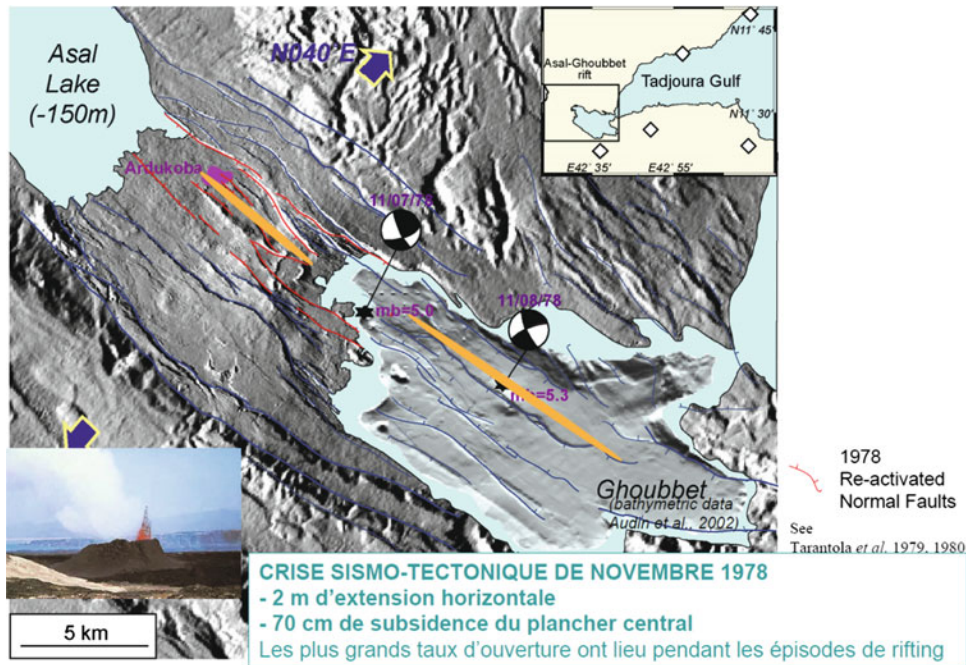


Fig. 6.124 The seismo-tectonic crisis of November 1978: 2 m of horizontal extension occurred along the Asal emerged rift segment as well as along the Ghoubbet gulf (shown in yellow). Fissures and faults along the inner rift (in red) were reactivated (after Doubre pers. comm.)



Fig. 6.125 General view of the Ardukoba eruptive fissure along the axis of Asal rift seen from the south. The faults bordering the inner graben are seen in the back. Observe the lava covering the 500 year-old lacustrine deposits, frequently faulted



Fig. 6.126 The northern extremity of the Ardoukoba rift axis, as presently observed from the main Ardoukoba crater (Photo ODDEG, December 2016)

compared to the volume injected in the dike. The central part of the traverse was measured again in 1979 just after this event, and showed an opening of 1.9 m in the inner part of the Asal graben (Ruegg et al. 1979).

In the winter of 1984–1985, new sets of geodetic measurements were obtained (Ruegg and Kasser 1987) which showed that continuous extension occurred at a rate of 6 cm/year during the following decade. Further measurements showed that since 1987 the rift-opening speed drastically decreased to 1 cm/year (Fig. 6.127).

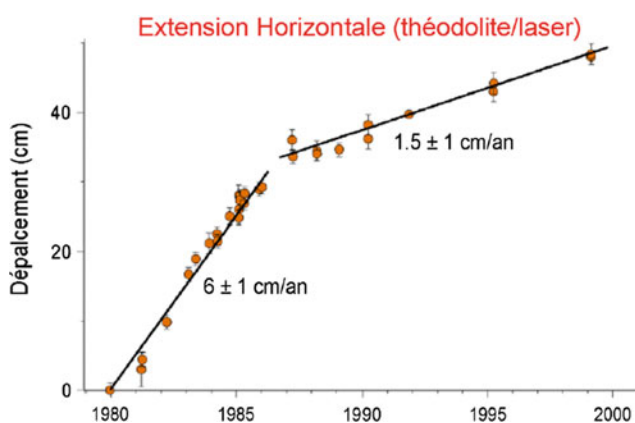


Fig. 6.127 Change in the rate of horizontal extension across the rift occurring in 1988–2000 compared to 1980–1987, that is in the 10 years following the Ardoukoba event, as shown by successive theodolite/laser measurements across the rift axis (Vigny et al. 2006a, b). In the period 2000–2010 a slight decrease in the speed is observed (Déprez 2015)

GPS measurements were also obtained which confirmed these field data and defined the deformation occurring in the rift, with an uplift of the rift northern shoulder at a rate of 5–7 mm/year (Vigny et al. 2006a, b); see Fig. 6.128. Within the rift floor, contrasting behaviour was observed with:

- Sinking at a rate of 2–4 mm/year, located in the “petit rift”, that is, the tectonic axis north of the volcanic axis
- The central part of the volcanic axis mid-distance between Lake Asal and the Ghoubbet was shown to inflate at a rate of 8 mm/year

It was also shown by Ballu et al. (2003) that the gravitational acceleration decreased in the central part of the rift axis between 1985 and 1999. This can be interpreted either as resulting from an uplift of the bedrock or as the result of a decrease of the density caused by magma up-rise, and most probably for both reasons.

These observations were confirmed by further radar interferometry studies using RADARSAT imagery covering the period 1997–2005 (Doubre et al. 2007a, b). The processing of these images showed the uplift of the northern shoulder of the rift and downthrows of the normal faults that limit the inner rift floor. The inner part of the rift appears relatively stable except on the Fialé caldera western margin, where an uplift movement is visible (Fig. 6.129).

This can be related to the seismic data which confirm the activity of the faults north of Fialé and show a spectacular concentration in the caldera itself in the period 1987–2001, whereas very few events were recorded in the 10 previous years following the Ardoukoba eruption (Fig. 6.130).

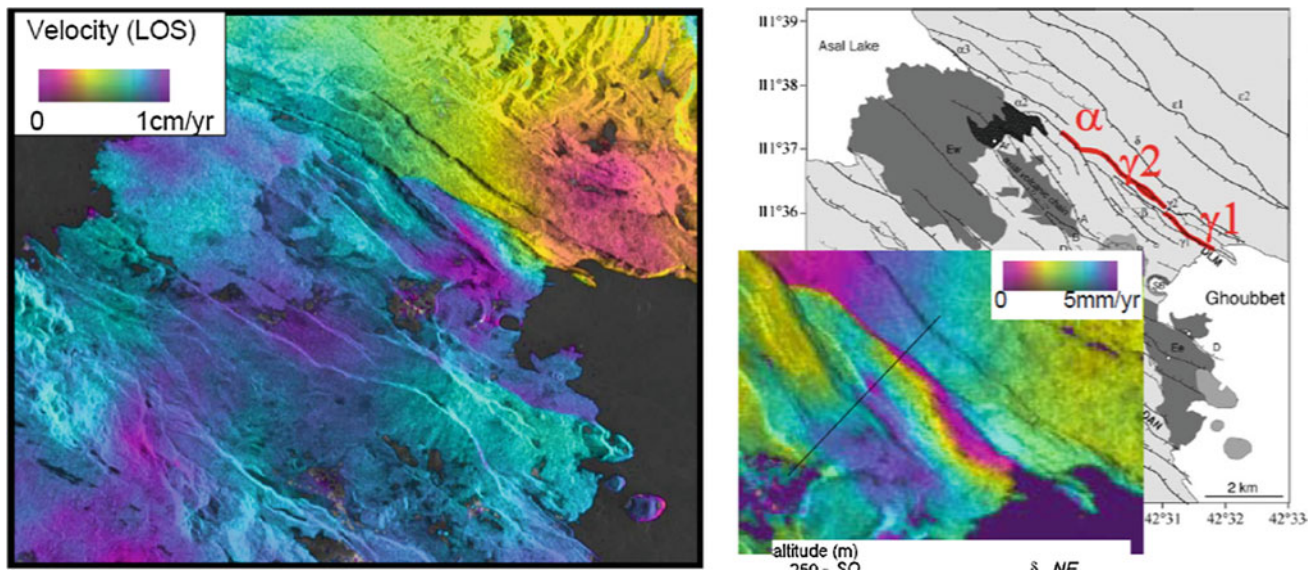


Fig. 6.128 Cumulative displacement measured by interferometry in the period 1997–2005 using RadarSat data (90 images). Observe the uplift of the northern block, the sinking of the central floor (on the left) and the measured displacements on “petit rift” fault NE of volcanic axis (after Doubre pers. comm.)

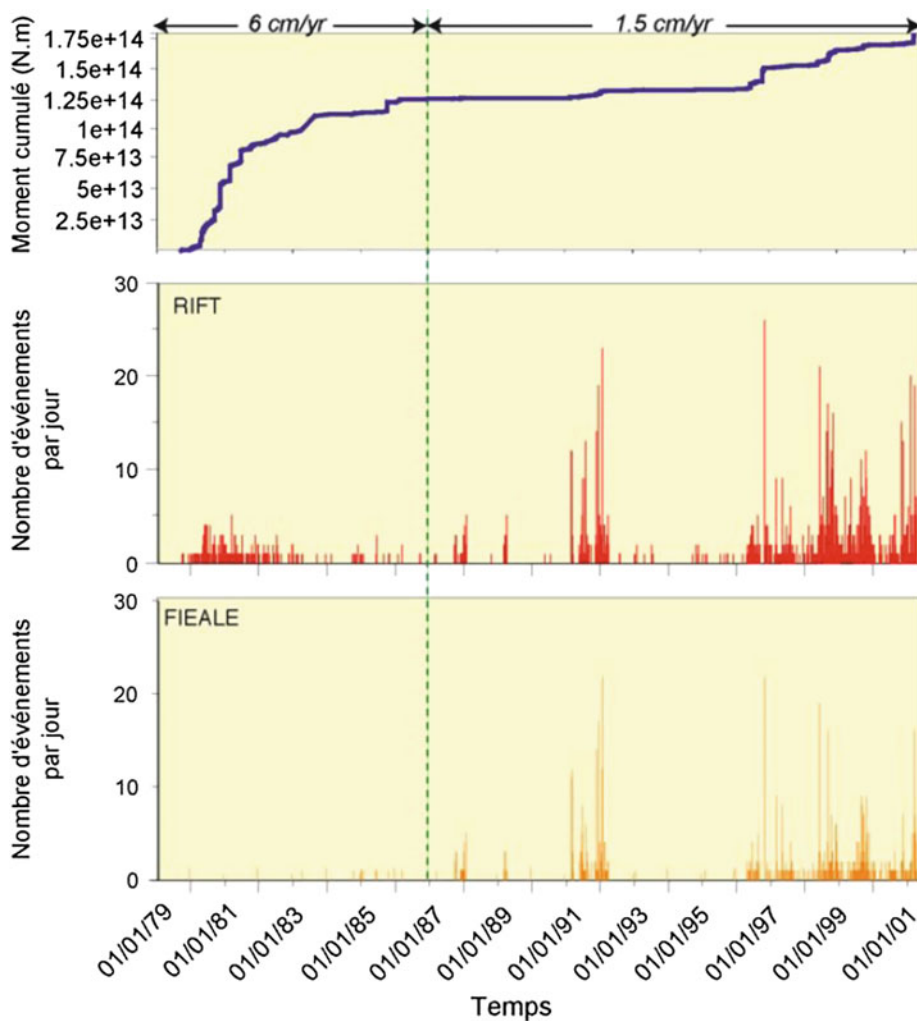


Fig. 6.129 Record of the seismic activity in the Asal rift in the period 1979–2001 following the 1978 seismo-tectono-volcanic crisis. Note that the change of seismic behaviour in 1987 corresponds with the change in the spreading rate (or cumulative moment) measured (Doubre et al. 2007a)

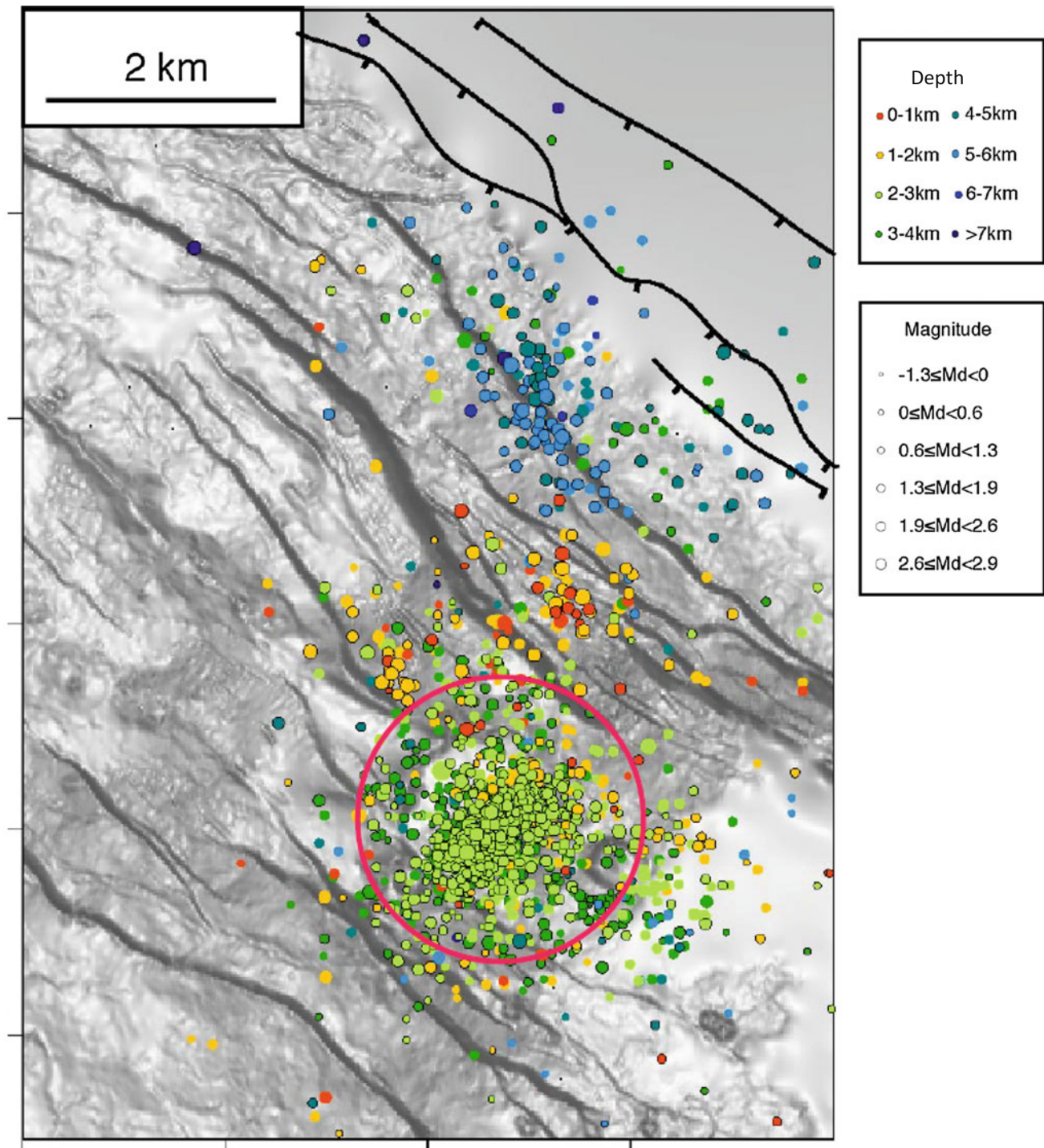


Fig. 6.130 Seismic activity observed in the Asal rift in the period 1987–2001. Whereas in the period 1978–1987, that is during the 10 years following the Ardoukoba event, very limited seismic activity was observed in the Fialé caldera, this recent axial volcanic unit shows important activity in the next 12 years. Very few events are recorded at shallow depth (0–2 km) in the caldera centre where intense activity is measured in the 2–3 km depth interval. The depth of the events appear to be deeper (3–4 km) along the caldera walls and margins. Shallow

events occurred N and E of the caldera. The absence of deep events below 3 km in the inner part of the caldera can be interpreted as resulting from the presence of a magma chamber below that depth. (Note that a distinct deeper set of events is observed along the fault bounding the rift margin where important vertical displacements are observed; differing from Fialé, this area has been continuously active since 1978)

One should examine here the two distinctive events which affected the Asal inner floor and more precisely the Fialé site during the last 40 years, and their consequences in terms of water circulation and heat release, of interest in view of geothermal applications:

- The first period includes the Ardoukoba event and the following 10-year period (1978–1987):
 - It allowed for a modest basaltic eruption near the NW extremity of the rift opening, showing a basaltic magmatic diking along the rift axis
 - It mainly allowed for the brutal opening of the rift axis up to 2 m in width at the level of the caldera
 - This distensive tectonic event continued during the following 10 years at a rate of 6 cm/year, allowing for more fissures to open
 - As a consequence, the axial part of the rift floor, notably between the “petit rift” and the Ardoukoba-Fialé-Baie des Requins volcanic axis, was continuously filled by an accelerated flow of cold seawater descending from the gulf of Ghoubbet towards Asal Lake 155 m below
- The second period is the Fialé caldera seismic event:
 - It occurred progressively in a distinct period, lasting 14 years, between 1987 and 2001
 - It can be interpreted as resulting from the new infilling of magma beneath the “lava lake” of the caldera
 - It allowed for a renewed magmatic heat source to become available at shallow depth

Let us now specify the characteristics of this rather shallow seismic activity as observed in Fig. 6.131. It can be interpreted as resulting from the influx of seawater on

contact with hot (around 1200 °C) basaltic magma. Several elements support this interpretation:

- No seismic activity is recorded more than 3 km below the “lava lake”, the recent surface volcanic feature which occupies the caldera floor.
- The depth of this aseismic roof tends to increase along the caldera walls and the caldera margins.
- The seismic activity is confined in a 1–2 km deep interval, which can be interpreted as a zone of direct interaction between the hot rising magma and a faulted layer intruded by seawater.
- No seismic activity is recorded at shallow depth (less than 1 km), eventually indicating a plastic (clay zone) hydrothermal cap. When the chronology of the seismic events is more precisely observed (Fig. 6.131) it is possible to deduce that the brittle roof of the ductile aseismic mass migrated as a consequence of five events that can be interpreted as resulting from the displacement of the magma in the chamber. This correspond to a step-by-step up-rise of the basaltic magma, successively hitting the lower part of the seawater table that flowed strongly through the newly opened fissures of the rift axis during the first—dominantly tectonic—1978 to 1987 period.
- The first of these events occurred in 1991 and affected an area located in the central part of the caldera at a depth of 3.5–2.5 km and hit and migrated up the caldera SW wall.
- The next (1996) event was located at a similar depth but affected and migrated up the NE side of the caldera.
- The 1998 event was located at the same depth in the central part of the caldera.
- In 1999, the brittle zone migrated upwards, at a depth ranging from 2.2 to 3 km maximum only.

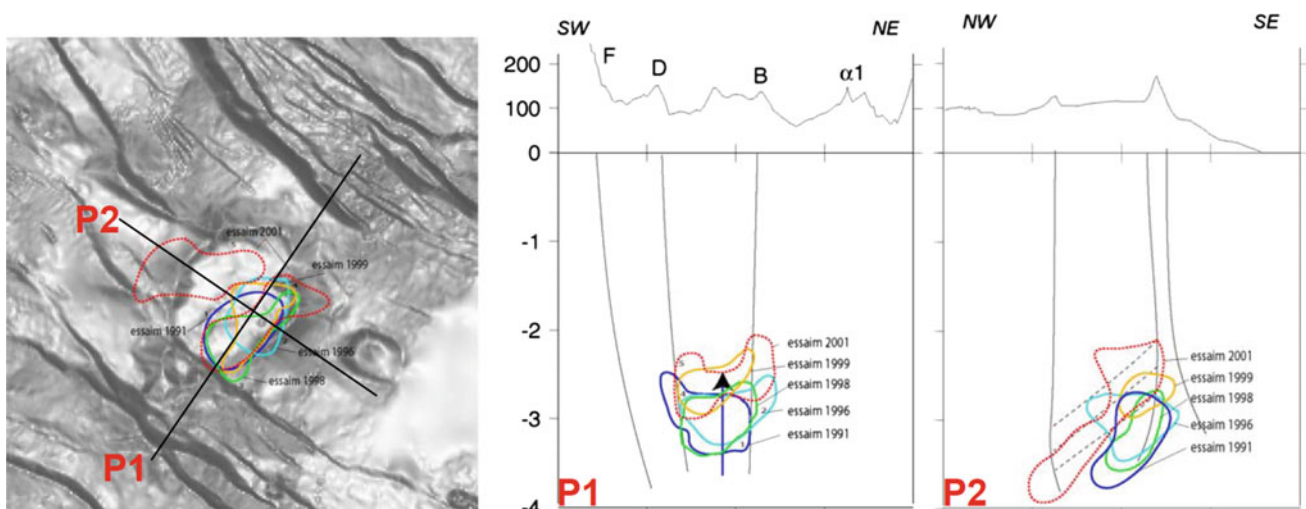


Fig. 6.131 Detailed mapping of the chronology of the main seismic events that occurred at Fialé caldera in the period 1991–2001 showing a general movement of rise of the seismic activity, which can be interpreted as a rise of the magma chamber, the upper part of which

migrated from 3.5 to 2.0 km depth with a displacement of the events towards NW where the uplift was also observed from radar interferometry (Doubré et al. 2007a, b)

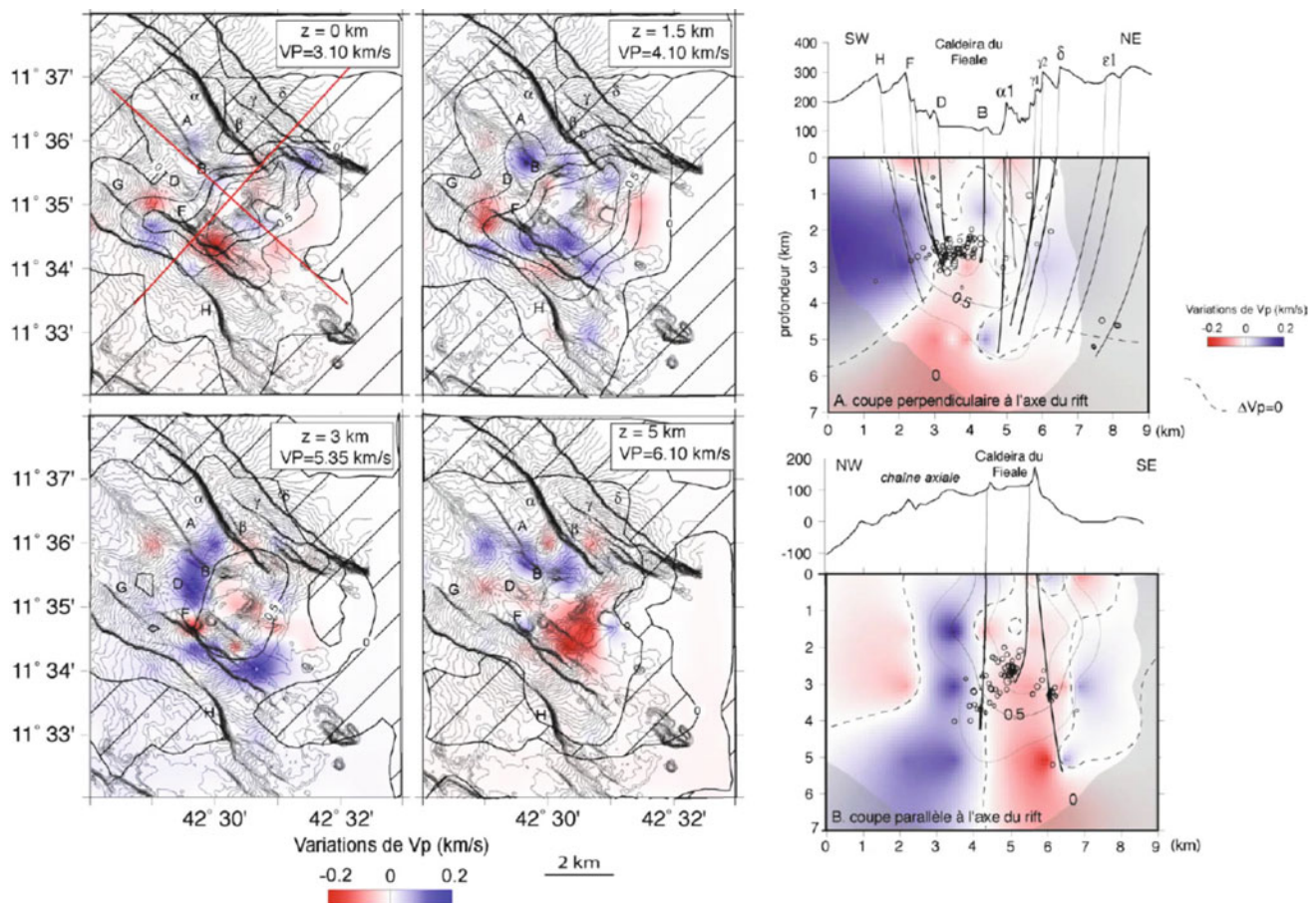


Fig. 6.132 Seismic tomography of the Asal-Fialé (Dobre et al. 2007a, b)

- The last event recorded in 2001 showed both a shallower depth (less than 2 km) along the SE wall of the caldera and beyond towards Baie des Requins, as well as deeper events on the NW margin on the caldera and beyond in the A5 area.

The seismic tomography developed by Dobre et al. (2007a, b) also provides a clear picture of the Fialé Caldera in which a low velocity zone is developed in the caldera interior, compatible with the presence of a liquid magma chamber, whereas the sides of it, particularly to the west and south, underline the presence of more rigid walls, probably ring dikes (Fig. 6.132).

On a broader scale, Vigny et al. (2007) showed from the study of GPS stations around Asal-Ghoubbet that this rift system accommodates 16 ± 1 mm/year of opening perpendicular to its axis. Stations lying in the Danakil block have almost the same velocity as the Arabian plate, which confirms our geological observations, according to which the opening is null along the southern tip of the Red Sea and is accommodated in the Afar depression.

Inside the rift, the deformation appears to be very limited on the SW side but significant on the NE side, showing a strong asymmetry, with the most seismically active part located in the “petit rift” rather than on the Ardoukoba-Fialé magmatic axis. Along the rift axis, the rate decreases to the NW, which may confirm propagation in that direction.

It should be noted that the rate measured in this recent period is slightly higher than the large-scale Arabia-Somalia motion (13 ± 1 mm/year), suggesting transient variations associated with relaxation processes following the Asal-Ghoubbet 1978 seismovolcanic event.

6.8.3 Geothermal Exploration and Undergoing Developments at Asal

On the basis of the geological context, and of specific mapping, particularly geophysical surveys, showing both the presence of a heat source and of normal faults and fissures, allowing for the formation of geothermal reservoir(s), Asal was considered as a geothermal target in 1970. A geothermal

exploration programme was then engaged by BRGM, followed by several studies which are still continuing at present, with a new project aiming at drilling deep in the Fialé caldera led by the World Bank, whereas the newly established ODDEG is exploring the superficial reservoir. (see Sect. 12.7).

6.9 The Gulf of Tadjourah Oceanic Spreading Segments

A striking feature of the western Afar region is the penetration of the Aden ridge into the African continent through the Gulf of Tadjourah. It consists of an active ridge trending generally in an E–W direction but made of NW–SE rift segments and NE–SW transform faults, emerging at the Asal-Ghoubbet, the westernmost segment. While looking at the bathymetric or seismicity maps of the area, a striking feature appears: the active ridge is not located in the middle of the Gulf of Tadjourah, but on the northern side, very close to the coast, which itself appears as paralleling the ridge (see Fig. 6.133).

Besides the surface geology studied earlier (Marinelli and Varet 1973; Richard and Varet 1979), the marine side was studied by at least two oceanographic cruises, SUDMEROUAD (Choukroune et al. 1986) and TADOURADEN (Hebert et al. 2001), generating further studies and interpretations (Courtilot 1980; Courtilot et al. 1987; Manighetti et al. 1998; Audin et al. 2001, 2004).

On both sides, the geological formations present along the Gulf are all of rather recent age (recent Pleistocene) and clearly postdate and cover in discordance the normally faulted earlier units. Important contrasts are observed, as the northern side of the gulf has undergone an important uplift (up to 1000 m) in the last four million years ago (as it postdates the emission of the Dalha basalts), whereas the southern side remained comparatively stable (despite a local uplift at Arta). Postdating the normal faults and their erosion products, basalts piles, clearly emitted along the former Gulf axis, were identified and called “Gulf Basalts”.

On the northern side, the visible thickness of the Gulf Basalts volcanic pile is around 350 m, made of subaerial

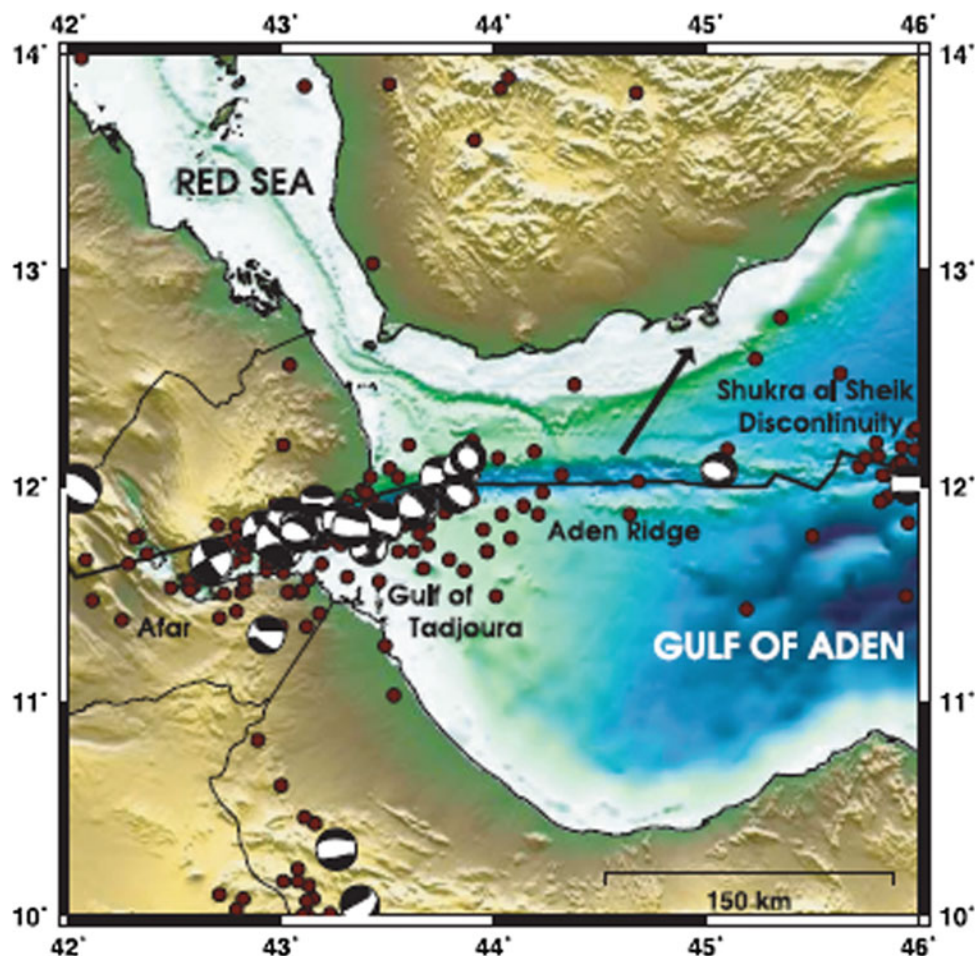


Fig. 6.133 Seismicity map of western Afar region and surroundings showing the activity concentrated in the northern side of the Gulf of Tadjourah, compiled by Shuler and Nettles (2012). Maroon dots mark

the locations of earthquakes in the NEIC catalogue (1973–2010). Focal mechanisms are from the Global CMT catalogue (1976–2010)

lava flows averaging 10 m thick. A few submarine lava flows are also observed on the bottom visible part of the sequence. The presence of a few vertical mafic dykes in the tilted lava successions confirms the fissural origin.

In the NE part of this area, the outcropping coralliferous plateau of Obock (orange on the map) was dated 100,000 to 150,000 years old. It extends up to 4 km inland. This carbonate formation is well developed and underlies the town. This recent plateau was first uplifted (up to 120 m high), meaning an uplift of the order of 1 mm/year (which lasted for the last one million years at least), and later intensively affected by normal faults along the coast of the gulf.

To the south, along the Gulf of Tadjourah, the whole series (Mabla and Dalha) are also affected by normal faulting along E–W and SW–NE directions that amplifies—although less important than to the north—while approaching the coast. This still active faulting affects the volcanic as well as the sedimentary formations of Quaternary age located along the gulf coasts. On the south-eastern side (Djibouti plain) the

Gulf Basalts outcrop along a 10 × 20-km coastal faulted plateau which up rises southwards until it hits a northerly tilted surface of the 7.2–3.6 million years old Somali basalts (Daoud et al. 2011). To the west they abut against the NS-oriented eastern edge of the Arta reliefs, locally filling the Wea palaeo-valley. The pile reaches a thickness of 220 m (as observed at PK20 boreholes).

Geological observations show a divergent direction of the flows from the gulf axis on both sides. As shown by Richard (1979) and Bizouard and Richard (1980), the compositions of these initial basalts of the gulf systematically overlap on both sides. The initial basalts of the gulf (covered by the coral reef deposits or partly inter-bedded with detrital sediments) were dated back three to one million years, depending on their position, with a global decrease of the age towards the west (Richard and Varet 1979), interpreted as a progressive penetration of the Aden ridge into Afar along the Gulf of Tadjourah (Courtilot et al. 1980; Manighetti et al. 1998, 2001; Audin et al. 2004). Although

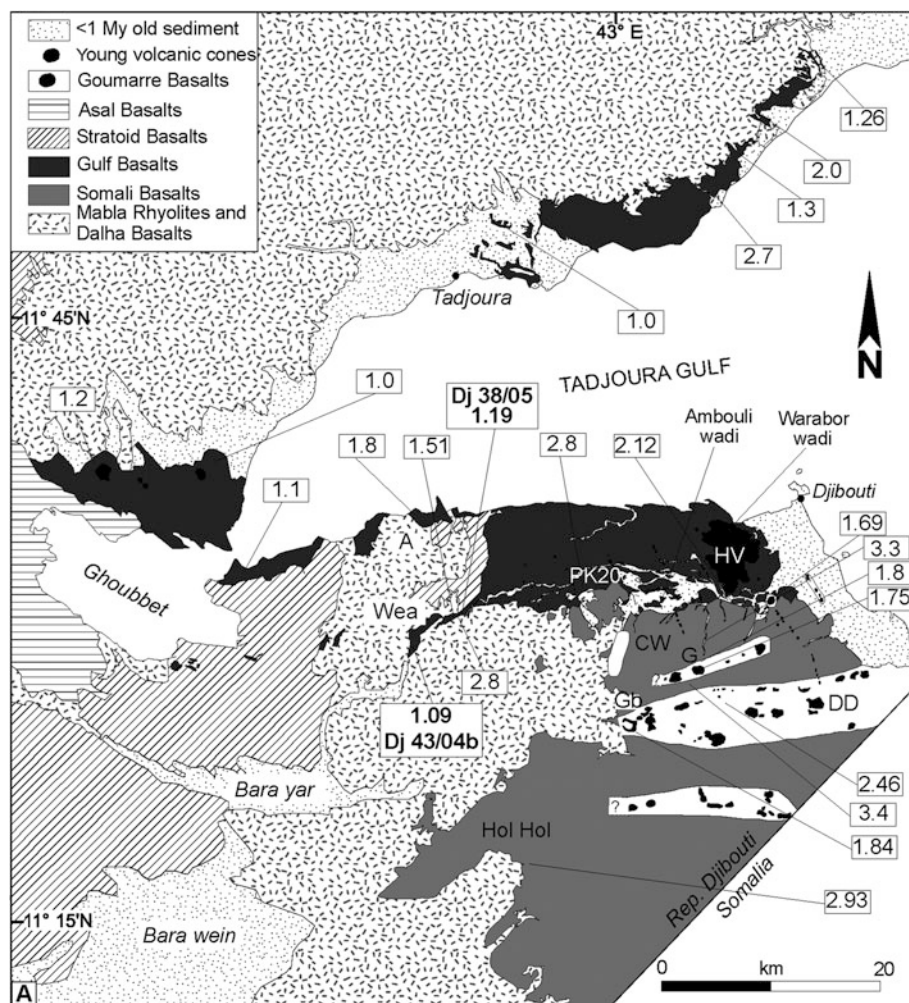


Fig. 6.134 K/Ar ages of the Gulf basalts on both sides of the gulf of Tadjourah (from Daoud et al. 2011)

discussed by Daoud et al. (2011) on the basis of new age determinations, the progressive westerly younging of the Gulf Basalts remains a valid observation. If younger ages were added on the eastern side for recent volcanic manifestations (Fig. 6.134), it remains that the first erupted basalts in the piles provide older ages to the east (up to 2.8 million years) whereas ages not older than 1.1 million years are found west, in the vicinity of Ghoubbet

Along the Gulf active axis, several troughs are bordered by symmetrical faulting in NE–SW and WNW–ESE directions; near to Obock, three such rifts trending WNW–ESE are separated by transform faults of SW–NE direction. The most important is the Obock trough, 1500 m deep. Basaltic volcanoes are aligned along the axis of these axial valleys. A total of 375 craters could be counted, 50 of them with calderas, and an 8 km diameter shield volcano was identified south of Obock where the dominantly coralline coastline, uplifted and affected by E–W faults, is very close to the ridge itself. Similarly, the transform fault linking that rift to the next one located SW (north of Dalhac islands) extends north and determine the shape of the coast towards the Red Sea and Bab-El-Mandeb strait. From these studies (Dauteuil et al. 2001), it was shown that the direction of spreading is

oblique with respect to the rift as well as to the transform faults, and that hence both have an opening component. It means that a shallow, hot, anomalous and magma-generating mantle is also present along transverse structures. This geophysical interpretation corroborates the field observations, such as in Rouéli where both WNW and NE faults appear extensional. This has, in turn, interesting geothermal consequences (see Sect. 12.1).

As the active troughs are located north of the gulf, the question of the link of the active spreading segments with the Asal-Ghoubbet rift is posed. Lépine et al. (1976) presented the results of geological field investigations in the short Arta corridor, SW of the gulf where they identified strike-slip faults in a NNE–SSW direction, interpreted as the surface expression of a transform fault linking the Ghoubbet rift to the Tadjourah spreading segment. This observation was confirmed by Artaud et al. (1980). This fault zone appears clearly on the digital elevation model of the area (green arrows in Fig. 6.135). However, the present day seismic activity does not show this fault as presently active, the recent (limited to the period 2001–2012) microseismic activity concentrating along ENE trends, ensuring a direct link through the Ghoubbet strait (Fig. 6.136).

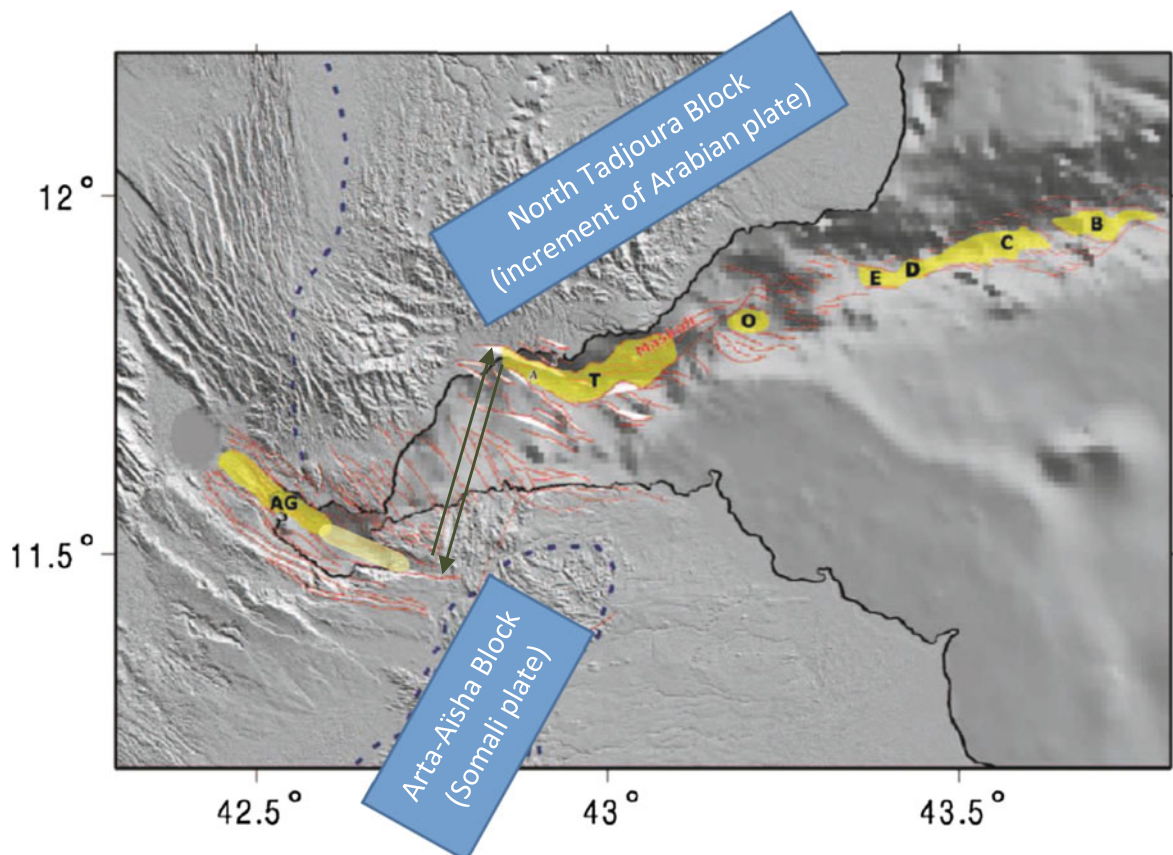


Fig. 6.135 Map showing the axial through of the Gulf of Tadjourah and the Asal Ghoubbet rift (in yellow) and (in red) the faults mapped by Audin (2009), showing the location of the Arta corridor identified by Lépine et al. (1976) and Artaud et al. (1980) as a transform fault

zone (green arrows) linking the easternmost extremity of the Ghoubbet rift (AG on the map, extending SE with a well-defined graben) with the Tadjourah through (T). Modified from Déprez (2015)

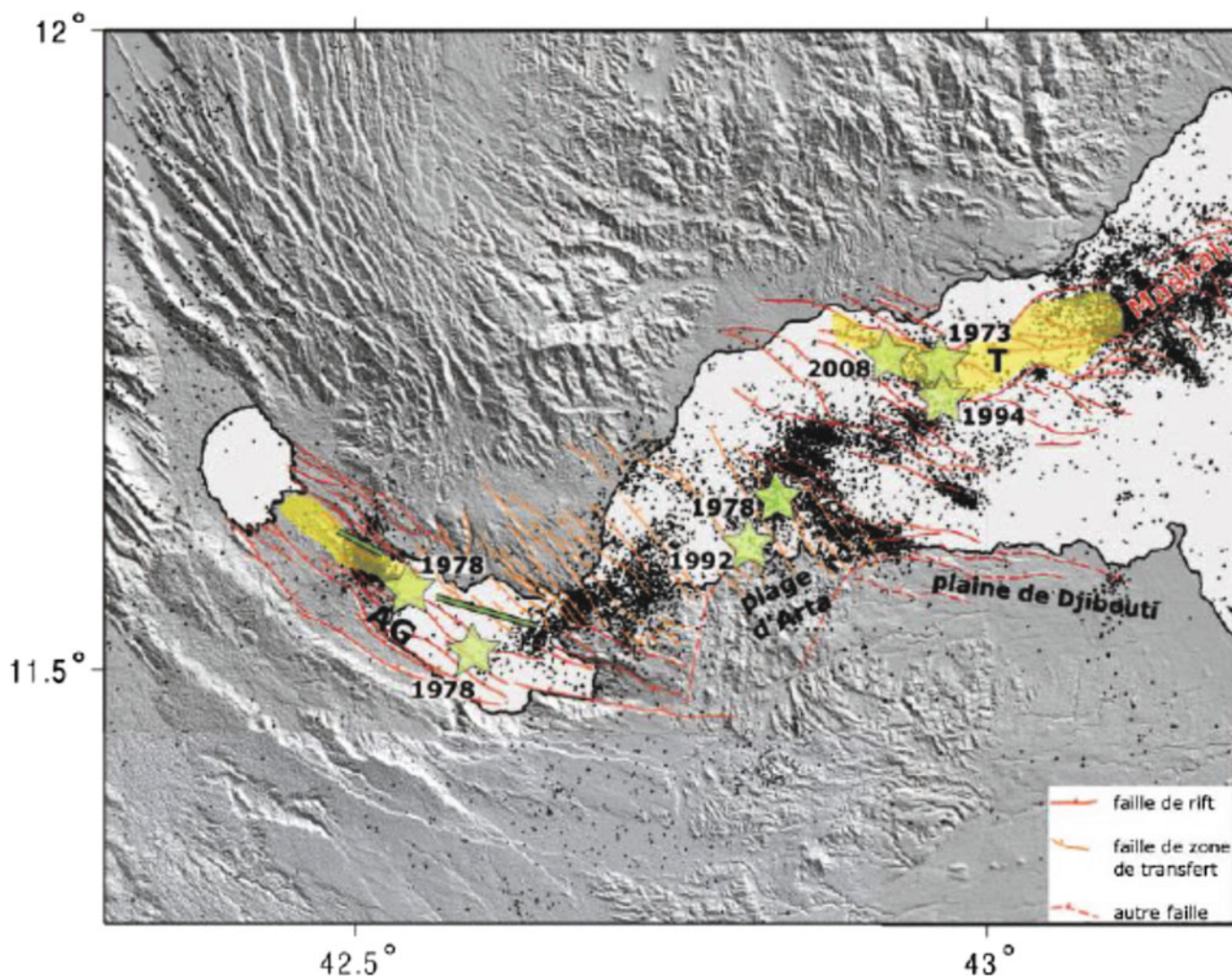


Fig. 6.136 The 2001–2012 seismicity (*black dots*) in the Asal-Ghoubbet—Tadjourah through the transfer zone, with the main dated previous events shown as *green stars*. From Déprez (2015)

6.10 Discussion: The Significance of the Axial Ranges

As a whole, the axial ranges of Afar are the sites of the presently active spreading axis within Afar, ensuring the link between the Red Sea oceanic ridge located along the axial trough and the Aden Ridge trough near the Gulf of Tadjourah. Their tectonic orientations, ranging from NNW–SSE to the north and west to NW–SE to the south and west, are in good agreement with those known to occur in the Red Sea and Aden oceanic ridges.

Their structure, with typical rift-in-rift settings, the age of the volcanic products getting younger towards the rift axis is a good expression of oceanic spreading segments. The axes are always tectonically active, with open fissures giving rise to magmatic (fissure) eruptions through a dike filling the spreading axis, as well as more permanent thermal convective activity (fumaroles and steam vents).

If the dominant volcanic feature is fissure flows, the succession of eruptions may give rise to a shield volcano frequently affected by consecutive rifting. However, periods of tectonic quiescence permitting, the shield may develop into a cumulo-volcano, with a parallel evolution of the magma that passes from initial basalts to iron-rich intermediate products (ferro-mugearites and dark trachytes), and eventually up to rhyolites as end products. In all axial ranges it was shown from petrological, mineralogical and geochemical studies that the differentiation could be explained by crystal fractionation under low pressure and oxygen fugacity conditions, that is, in shallow magma chambers. This interpretation fitted well with the volcanotectonic deformations observed at the surface (Barberi and Varet 1970) and could be confirmed and quantified using radar interferometry studies in the case of Alu-DalaFilla.

Petrological and geochemical studies also revealed changes in composition of the initial basalt (and hence of the

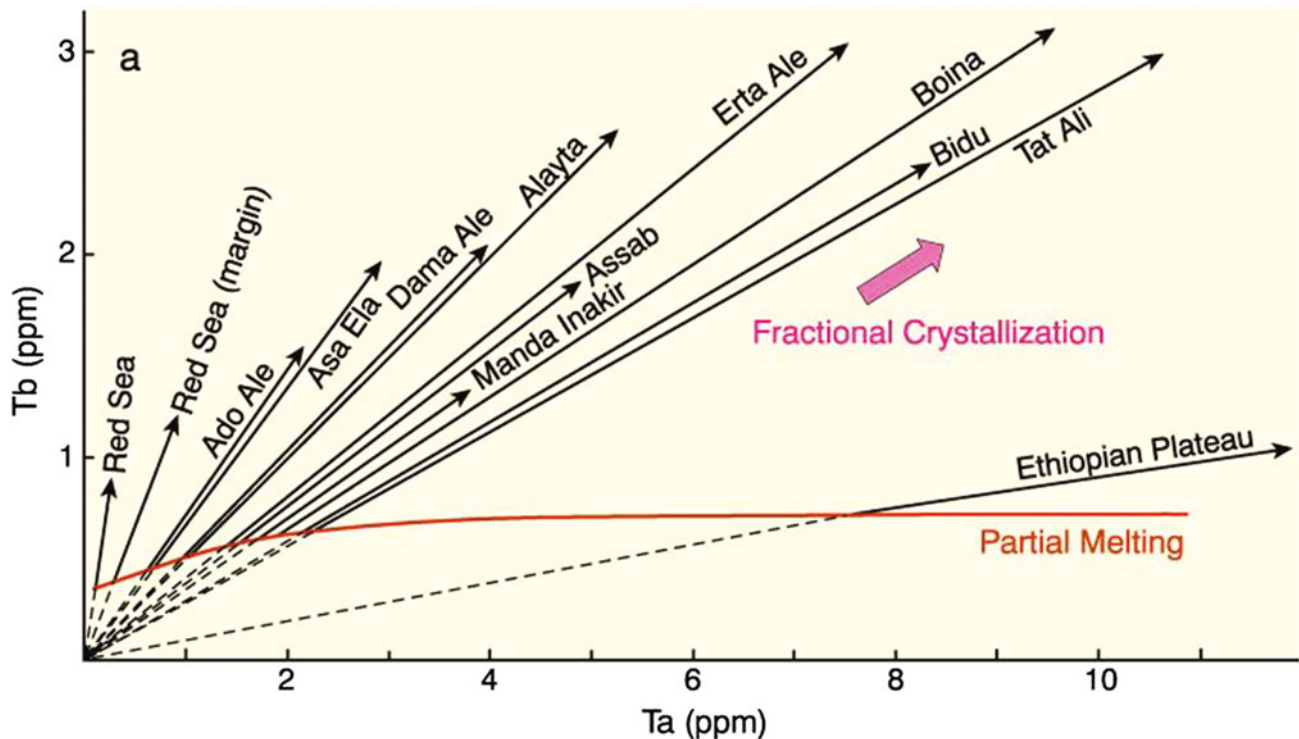


Fig. 6.137 Tantalum-terbium diagram for the volcanic rocks from Afar axial ranges and surroundings (including the Nubian plateau basalts). These elements were chosen as being the most “hygromagmatophile”, that is, entering the magmatic liquid and not the crystalline phases (Treuil and Varet 1973). Rock samples from each axial range appear to fit along a single line passing through the origin, showing a pure crystal fractionation process. The ratio, which characterises each unit, also varies from unit to unit and the envelope of the less evolved products (basalts issued primary liquids) appears to fit along a curve

that corresponds to a partial melting. The degree of partial melting was considered to relate to the spreading rate, with lower Tb/Ta ratios for oceanic tholeiites (samples from the Red Sea and Gulf of Aden axis) showing higher spreading rates, whereas the basalts from the Nubian plateau show the highest values, and axial ranges from Afar display values quite similar to mid-ocean ridges as Manda Harraro or Asal (high spreading rates) whereas other express slower conditions (Tat’Ali, Manda Inakir or Erta Ale), fitting with the geodynamic model (microplates) proposed by Barberi and Varet (1978)

whole differentiation series) from an axial range to another, from transitional basalts to nearly tholeiitic on one side, and to mildly alkaline on the other. This variation was even more accurately determined using hygromagmatophile elements ratios such as tantalum and terbium (Fig. 6.137). Besides linear variation resulting from crystal fractionation in each axial range, a curve could be drawn linking the initial basaltic magmas of all ranges that could be interpreted as resulting from different degrees of partial melting from a single mantle source. Manda Harraro and Asal ranges were shown to display more tholeiitic composition and higher degrees of partial melting, whereas Manda Inakir or Tata’Ali were shown to result from lower degrees of partial melting.

Considering that the degree of partial melting of the mantle would relate to the spreading rate, this geochemical index was shown to fit well with a microplate tectonic interpretation of Afar (Barberi and Varet 1978). In this the axial ranges of Asal and Manda Harraro—which are single

spreading axes, in the part of Afar that is directly controlled by the motion of the Arabic plate (at around 2 cm/year)—display the fastest rates, whereas at the level of Manda Inakir, Tat’Ali and Alayta two spreading segments act in parallel, and the spreading with respect to the southernmost Red Sea axis as the rotating Arrata block (Danakil alps microplate) separates the two parallel spreading axis, therefore reduced in each. Erta Ale is in a similar situation to the rotating Arrata block (Danakil Alps) which separates the The Red Sea spreading axis is progressively dying south at the level of Hanish Islands whereas spreading increase from north to South in the Erta Ale segment. Even within Erta Ale, the north to south variations observed in both degree of fractionation (and volcano-structural evolution) and degree of partial melting of the initial basalts fit that geodynamic interpretation.

As a whole, the location, structure, composition of the initial magmas and differentiation processes in the axial ranges appear to meet a rather clear pattern.

References

- Acocella V (2006) Regional and local tectonics at Erta Ale caldera, Afar (Ethiopia). *J Struct Geol* 28:1808–1820
- Acocella V, Abebe B, Korme T, Barberi F (2014) Structure of Tendaho Graben and Manda Hararo Rift: Implications for the evolution of the southern Red Sea propagator in Central Afar, *Tectonics*, 27, TC4016. doi:10.1029/2007TC002236
- Amelung F, Oppenheimer C, Segall P, Zebker H (2000) Ground deformation near Gada 'Ale Volcano, Afar, observed by radar interferometry. *Geophys Res Lett* 27(2000):3093–3096
- AQUATER (1996). Tendaho geothermal project, final report. MME, EIGS—Gov. of Italy, Ministry of Foreign Affairs, San Lorenzo in Campo
- Arthaud F, Choukroune P, Robineau B (1980) Evolution structurale de la zone transformante d'Arta (République de Djibouti). *Bull Soc Geol Fr* 22:909–915
- Audin J, Vellutini PJ, Coulon C, Pigué P, Vincent J (1990) The 1928–1929 eruption of Kammourta volcano—evidence of tectonomagmatic activity in the Manda-Inakir rift and comparison with the Asal Rift, Afar depression, Republic of Djibouti. *Bull Volcanol* 52:551–561
- Audin L, Manighetti I, Tapponnier P, Métivier F, Jacques E, Huchon P (2001) Fault propagation and climatic control of sedimentation on the Ghoubbet Rift Floor: insights from the Tadjouraden cruise in the western Gulf of Aden. *Geophys J Int* 144:391–413
- Audin L, Quidelleur X, Coulié E, Courtillot V, Gilder S, Manighetti I, Gillot P-Y, Tapponnier P, Kidane T (2004) Paleomagnetism and K–Ar and ⁴⁰Ar/³⁹Ar ages in the Ali Sabieh area (Republic of Djibouti and Ethiopia): constraints on the mechanism of Aden ridge propagation into southeastern Afar during the last 10 Myr. *Geoph J Internat* 158:327–345
- Ayele A, Stuart GW, Bastow ID, Keir D (2006) The August 2002 earthquake sequence in north Afar: Insights into the neotectonics of the Danakil microplate. *J Afr Earth Sci*
- Ayele A, Keir D, Ebinger C, Wright TJ, Stuart GW, Buck WR, Jacques E, Ogubazghi G, Sholan J (2009) September 2005 mega-dike emplacement in the Manda-Harraro nascent oceanic rift (Afar depression) (PDF file). *Geophys Res Lett* 36
- Ballu V, Diament M, Briole P, Ruegg J-C (2003) 1985–1999 gravity field variations across the Asal Rift: Insights on vertical movements and mass transfer. *Earth Planet Sci Lett* 208:41–49
- Barberi F, Varet J (1970) The Erta 'Ale volcanic range. *Bull Volc* 34:848–917
- Barberi F, Varet J (1972) Carte volcanologique et pétrologique de la chaîne de l'Erta 'Ale (Afar, Ethiopie) au 1/100.000 *Géotechnip, La Celle-Saint-Cloud*
- Barberi F, Varet J (1975) Volcanological research in Afar (L. R. Wager prize summary lecture). *Bull Volc* 39(2):166–174
- Barberi F, Varet J (1977) Volcanism in Afar: small-scale plate tectonic implications. *Bull Geol Soc Amer* 88:1251–1266
- Barberi F, Varet J (1978) The Afar rift junction. In: Neuman E, Ramberg B (eds) *Petrology and geochemistry of continental rifts*, pp 55–69
- Barberi F, Borsi S, Ferrara G, Marinelli G, Varet J (1970). Relations between tectonics and magmatology in the northern Danakil Depression (Ethiopia). *Philosophical Trans Royal Soc London* A267:293–311
- Barberi F, Bizouard H, Varet J (1971) Nature of the clinopyroxenes and iron enrichment in alkalic and transitional basaltic magmas. *Contr Mineral Petrol* 33:93–107
- Barberi F, Tazieff H, Varet J (1972a) Volcanism in the Afar depression: its tectonic and magmatic significance. *Tectonophysics* 15:19–29
- Barberi F, Borsi S, Ferrara G, Marinelli G, Santacroce R, Tazieff H, Varet J (1972b) Evolution of the Danakil Depression (Afar Ethiopia) in light of radiometric age determination. *J Geol* 80:720–729
- Barberi F, Chemine'e JL, Varet J (1973) Long-lived lava lakes of Erta Ale volcano. *Rev Geogr Phys Geol Dyn* 15:347–352
- Barberi F, Ferrara G, Santacroce R, Treuil M, Varet J (1975a) A transitional basalt-pantellerite sequence of fractional crystallisation, the Boina centre (Afar rift, Ethiopia). *J Petrol* 16:22–56
- Barberi F, Ferrara G, Santacroce R, Varet J (1975b) Structural evolution of the Afar triple junction. In: Pilger A, Rösler A (eds) *Afar Depression of Ethiopia*, Stuttgart (Schweizerbart), pp 38–54
- Baris I, Leprince S, Parsons B, Wright T (2009) Surface displacements in the September 2005 Afar rifting event from satellite image matching: asymmetric uplift and faulting. *Geoph Res Lett* 36(7)
- Beutel E, van Wijk J, Ebinger C, Keir D, Agostini A (2010) Formation and stability of magmatic segments in the main Ethiopian and Afar rifts. *Earth Planet Sci Lett* 298:225–235
- Bizouard H, Richard O (1980) Etude de la transition dorsale océanique/rift émergé: Golfe de Tadjoura, Asal, Afar central. Approche pétrographique et minéralogique. *Bull Soc Geol Fr* 22:935–943
- Bonatti E, Tazieff H (1970) Submarine volcanoes in the Afar rift. *AGU Trans Amer Geoph Un Gen Meeting*
- Bonatti E, Emiliani C, Ostlund G, Rydell H (1971) Final dissection of the Afar Rift, Ethiopia. *Science* 172:468–469
- BRGM (1970) Reconnaissance géothermique du TFAI. Rapport BRGM/70-SGN-GTM, 59p
- BRGM (1973) Etude géothermique de la région du lac Asal, campagne 1972–1973. Rapport BRGM/73-SGN-144-GTH, 22p
- Carmichael ISE, MacKenzie WS (1963) *Amer Journ Sci*, vol 261, p 382
- Choukroune P et al. (1986) Tectonics of the westernmost: Gulf of Aden and the Gulf of Tadjoura from submersible observations. *Nature* 319:396–399
- Civetta L, DeFino M, Gasparini P, Ghiara MR, LaVolpe L, Lirer L (1975) Geology of central-eastern Afar (Ethiopia). In: Pilger A, Rosler A (eds) *Afar depression of Ethiopia, proceedings of an international symposium on the Afar region and rift related problems*, Bad Bergzabren, Germany, 1974, vol 1. E. Schweizerbart'sche Verlagsbuchhandlung, Stuttgart, Germany, pp 259–277
- CNR–CNRS Afar team (1973) Geology of Northern Afar (Ethiopia). *Rev Geogr Phys Geol Dyn* 15:443–490
- Cortani and Bianchi (1941) Carta della Danalia meridionale e degli altipiani hararini. *Scalal1/500.000 Acad Ital Centro Studi AOI*
- Courtillot VE (1980) Opening of the Gulf of Aden and Afar by progressive tearing. *Phys Earth Planet Inter* 21:343–350
- Courtillot V, Tapponnier P, Varet J (1974) Evolution of the surface expression of transform faults. *Tectonophysics* 24:317–329
- Courtillot V, Galdeano A, Le Mouél J-L (1980) Propagation of an accreting plate boundary: a discussion of new aeromagnetic data in the Gulf of Tadjurah and southern Afar. *Earth Planet Sci Lett* 47:144–160
- Courtillot V, Armijo R, Tapponnier P (1987) Kinematics of the Sinai triple junction and a two-phase model of Arabia-Africa rifting. In: Coward MP, Dewey JF, Hancock PL (eds) *Continental extensional tectonics*, vol 28, pp 559–573. Geological Society, London, Special Publications
- Daoud MA, Le Gall B, Maury RC, Rolet J, Huchon P, Guillou H (2011) Young rift kinematics in the Tadjoura rift, western Gulf of Aden, Republic of Djibouti. *Tectonics* 30, TC1002
- Dauteuil O, Huchon P, Quemener F, Souriot T (2001) Propagation of an oblique spreading center; the western Gulf of Aden. *Tectonophysics* 332:423–442
- De Chabaliér J-B, Avouac J-P (1994) Kinematics of the Asal Rift (Djibouti) determined from the deformation of Fieale Volcano. *Science* 265:1677–1681

- De Fino M, La Volpe L, Lirer L, Varet J (1973) Geology and petrology of Manda-Inakir range and Moussa Alli volcano, central eastern Afar (Ethiopia and T.F.A.I.). *Rev Geog Phys Géol Dyn* 15(2):373–386
- Demange J, Stieltjes L, Varet J (1980) L'éruption d'Asal de novembre 1978. *Bull Soc Géol France* 12 (6):837–843
- Déprez A (2015) Apport de la géodésie à l'étude de la jonction triple de l'Afar. Thèse, Université de Strasbourg—IPGS, 193p
- Didana YL, Thiel S, Heinson G (2015) Magnetotelluric Imaging at Tendaho High Temperature Geothermal Field in North East Ethiopia. Proceedings World Geothermal Congress Melbourne, 19–25 April 2015
- Dobre C, Manighetti I, Dorbath C, Dorbath L, Jacques E, Delmond J-C (2007a) Crustal structure and magmato-tectonic processes in an active rift (Asal-Ghoubbet, Afar, East Africa): 1. Insights from a 5-month seismological experiment. *J Geophys Res* 112
- Dobre C, Manighetti I, Dorbath L, Dorbath C, Bertil D, Delmond J-C (2007b) Crustal structure and magmato-tectonic processes in an active rift (Asal-Ghoubbet, Afar, East Africa): 2. Insights from a the 23 year recording of seismicity since the last rifting event. *J Geophys Res* 112
- Ebinger CJ, Keir D, Ayele A, Calais E, Wright TJ, Belachew M, Hammond JOS, Campbell E, Buck WR (2008) Capturing magma intrusion and faulting processes during continental rupture: seismicity of the Dabbahu (Afar) rift. *Geoph J Int*
- Ebinger C, Ayele A, Keir D, Rowland J, Yirgu G, Wright T, Belachew M, Hamling I (2010) Insights into extensional processes during magma assisted rifting: evidence from aligned scoria cones. *Ann Rev Earth Planet Sc* 38:437–64
- Ferguson DJ, Barnie TD, Pyle DM, Oppenheimer C, Yirgu G, Lewi E, Kidane T, Carn S, Hamling IJ (2010) Recent rift-related volcanism in Afar, Ethiopia. *Earth Planet Sci Lett*
- Ferguson DJ, Maclenman J, Bastow ID, Pyle DM, Jones SM, Keir D, Blundy JD, Plank T, Yirgu G (2013) Melting during late-stage rifting in Afar is hot and deep. *Nature* 499:70–73
- Field L, Barnie T, Blundy J, Brooker RA, Keir D, Lewi E, Saunders K (2012) Integrated field, satellite and petrological observations of the November 2010 eruption of Erta Ale. *Bull Volcanol* 74(10):2251–2271
- Francis PW, Oppenheimer C, Stevenson DS (1993) Endogenous growth of persistently active volcanoes. *Nature* 366:544–557
- Gasse F, Street A (1978) Late Quaternary lake-level fluctuations and environments of the northern Rift Valley and Afar region (Ethiopia and Djibouti). *Palaeogeogr Palaeoclimatol Palaeoecol* 24:279–325
- Gerlach TM (1989) Degassing of carbon dioxide from basaltic magma at spreading centers: I. Afar transitional basalts. *J Volc Geoth Res* 39:211–219
- Giggenbach WF, Le Guern F (1976) The chemistry of magmatic gases from Erta'Ale, Ethiopia. *Geochim Cosmochim Acta*, 40:25–30
- Gouin P (1979) Earthquake History of Ethiopia and the Horn of Africa. *Int Dev Res Centre Ottawa Ont*, 258 pp
- Grandin R, De Chabelier J-B, Socquet A, Binet R (2009) Evènement en frontière de plaque: le cas du Manda Hararo (Ethiopie). *Géosciences* 9:20
- Hamling I, Ayele A, Bennati L, Calais E, Ebinger CJ, Keir D, Lewi E, Wright TJ, Yirgu G (2009) Geodetic observations of the ongoing Dabbahu rifting episode: new dyke intrusions in 2006 and 2007. *Geoph J Int*
- Hébert H, Deplus C, Huchon P, Khanbari K (2001) Lithospheric structure of a nascent spreading ridge inferred from gravity data: the western Gulf of Aden. *J Geophys Res* 106:26,345–26,364
- Keir D, Hamling IJ, Ayele A, Calais E, Ebinger C, Wright TJ, Jacques E, Mohamed K, Hammond JOS, Belachew M, Baker E, Rowland JV, Lewi E, Bennati L (2009) Evidence for focused magmatic accretion at segment centers from lateral dike injections captured beneath the Red Sea rift in Afar. *Geology* 37:59–62
- Le Guern F, Carbonelle J, Tazieff H (1979) Erta `Ale lava lake: heat and gas transfer to the atmosphere. *J Volc Geoth Res* 6:27–48
- Lépine JC, Richard O, Ruegg JC, Treuil M, Varet J (1976) Mise en évidence d'une zone de faille transformante reliant la vallée axiale de la dorsale de Tadjoura à celle de Goubbet-Asal (T.F.A.I.). *CR Acad Sci Paris, série D* 283–1:9–12
- MacDonald GA (1968) "Composition and origin of Hawaiian lavas". *Geological Society of America Memoirs*. 116:477–522
- Manighetti I, Tapponnier P, Gillot P-Y, Jacques E, Courtillot V, Armijo R, Ruegg J-C, King G (1998) Propagation of rifting along the Arabia-Somalia plate boundary: into Afar. *J Geophys Res* 103:4947–4974
- Manighetti I, Tapponnier P, Courtillot V, Gallet Y, Jacques E, Gillot Y (2001) Strain transfer between disconnected, propagating rifts in Afar. *J Geophys Res* 106:13,613–13,665
- Marinelli G, Varet J (1973) Structure et évolution du Sud du "horst Danakil" (TFAI et Ethiopie). *CR Acad Sci* 276:1119–1122
- Martini M, (1969) Studio di Prodotti fumarolici di alcuni vulcani della catena dell'Erta Ale (Ethiopia). *Rend Soc Ital Mineral Petrol* 25: 1–16
- McClusky S, Reilinger R, Ogubazghi G, Amleson A, Healed B, Vernant P, Sholna J, Fisseha S, Asfaw L, Bendick R, Kogan L (2010) Kinematics of the southern Red Sea—Afar triple Junction and implications for plate dynamics. *Geophys Res Lett* 37(5)
- Oppenheimer C, Francis P (1997) Remote sensing of heat, lava and fumerole emissions from Erta'Ale volcano, Ethiopia. *Int J Remote Sens* 18:1661–1692
- Oppenheimer C, Francis P (1998) Implications of longeval lava lakes for geomorphological and plutonic processes at Erta `Ale volcano, Afar. *J Volc Geoth Res* 80:101–111
- Oppenheimer C, McGonigle A, Allard P, Wooster M, Tsanev V (2004) Sulfur, heat, and magma budget of Erta Ale lava lake, Ethiopia. *Geology* 32:509–512
- Pagli C, Wright TJ, Ebinger CJ, Yun S, Cann JR, Barnie T, Ayele A (2012) Shallow axial magma chamber at the slow-spreading Erta Ale Ridge. *Nat Geosci* 5:284–288
- Richard O, Varet J (1979) Study of the transition from deep oceanic to emerged rift zone: Gulf of Tadjoura (Republic of Djibouti). *Int Symp Geodyn Evols Afro-Arabian System, Roma*
- Roubet C (1969) Essai de datation absolue d'un biface hachereau paléolithique de l'Afar (Ethiopie). *L'Anthrop* 13(7–8):503–523
- Rowland JV, Baker E, Ebinger CJ, Keir D, Kidane T, Biggs J, Hayward N, Wright TJ (2007) Fault growth at a nascent slow-spreading ridge: 2005 Dabbahu rifting episode, Afar. *Geoph J Int*
- Ruegg J-C, Kasser M (1987) Deformation across the Asal-Ghoubbet Rift, Djibouti, uplift and crustal extension. *Geophys Res Lett* 14: 745–748
- Ruegg JC, Kasser M, Lépine JC, Tarantola A (1979) Geodetic measurements of rifting associated with a seismo – volcanic crisis in Afar. *Geophys Res Lett* 6:817–820
- Ruegg JC, Briole P, Feigl K, Vigny C, Abdallah A, Bellier O, Huchon S, Al Khirbash S, Laiké A, d'Oreye N, Prevot M (1993) First Epoch Geodetic GPS measurements across the Afar Palte Boundary zone. *Geoph Res Lett* 20:1899–1902
- Sawyer GM, Oppenheimer C, Tsanev VI, Yirgu G (2008) Magmatic degassing at Erta `Ale volcano, Ethiopia. *J Volcanol Geotherm Res* 178: 837–846
- Shuler A, Nettles M (2012) Seismology Earthquake source parameters for the 2010 western Gulf of Aden rifting episode. *Geophys J Int*. doi:10.1111/j.1365-246X.2012.05529.x.GJI
- Stieltjes L, Joron JL, Treuil M, Varet J (1976) Le rift d'Asal, segment de dorsale émergée discussion pétrologique et géochimique. *Bull Soc Geol France* 18(4):851–862
- Swanson DA, Peterson DW (1972) Partial draining and crustal subsidence of Alae lava lake, Kilauea Volcano, Hawaii, in

- Geological Survey research 1972: U.S. Geological Survey Professional Paper 800-C, pp C1–C14
- Tapponnier P, Varet J (1974) La zone de Mak'arrasou en Afar: un équivalent émergé des «failles transformantes» océaniques. *CR Acad Sci* 278:317–329
- Tapponnier P, Armijo R, Manighetti I, Courtillot V (1990) Bookshelf faulting and horizontal block rotations between overlapping rift zones in southern Afar. *Geophys Res Lett* 17:1–4
- Tazieff H (1973) The Erta 'Ale volcano. *Rev Geogr Phys Geol Dyn* 15:437–441
- Tazieff H, Varet J (1969) Signification tectonique et magmatique de l'Afar septentrional (Ethiopie). *Rev Géog Phys Geol Dyn* 2(11): 429–450
- Tazieff H, Marinelli G, Barberi F, Varet J (1969) Géologie de l'Afar septentrional symposium. *Ass. Interna. Volcanologie; Canaries. Bull. Volc.*, t. XXXIII-4:1039–1072
- Tazieff H, Barberi F, Borsi S, Ferrara G, Marinelli G, Varet J (1970) Relationships between tectonics and magmatology in the Northern Afar (or Danakil) depression. *Phil Trans Royal Soc London A*.267:293–311
- Tazieff H, Barberi F, Giglia G, Varet J (1972) Tectonic significance of the Afar (or Danakil) depression. *Nature* 235:144–147
- Treuil M, Varet J (1973) Critères volcanologiques, pétrologiques et géochimiques de la genèse et de la différenciation des magmas basaltiques exemple de l'Afar. *Bull Soc Géol France* 7(15):506–540
- Treuil M, Billhot M, Barberi F, Varet J (1971) Distribution of Nickel, Copper and Zinc in the volcanic chain of Erta 'Ale, Ethiopia. *Contr Mineral Petrol* t. 30: pp 84–94
- Varet J (1971a) Erta'Ale volcanic activity. Smithsonian Institution, Center for short-lived Phenomena. Event 22–71, 18/2/71, cards no 1132–1133 and 1308
- Varet J (1971b) Erta'Ale activity (Afar, Ethiopia). *Bull Geophys Obs Addis Ababa* 13:115–119
- Varet J (1971c) Sur l'activité récente de l'Erta'Ale (Dankalie, Ethiopie). *C R Ac Sci Paris* t. 272, pp 1964–1967
- Varet J (1972a) Erta Ale volcanic activity. Smithsonian Institution, Center for short-lived Phenomena. Event 16–72, 6/3/72, card No 1363
- Varet J (1972b) Erta Ale volcanic activity—Smithsonian Institution, Center for short-lived Phenomena. Event 16–72, Cards no 1390 and 1390 A
- Varet J (2004) De l'Afar à la géothermie. In «Haroun Tazieff, une vie de feu», Ed. Glénat, pp 85–94
- Varet J (2013) The Afar system and carbonates. *Cocarde workshop (abstract)*, Sicily, pp 48–49
- Vigny C, Huchon P, Ruegg JC, Khanbari K, Asfaw L (2006a) New GPS data in Yemen confirm slow Arabia plate motion. *J Geophys Res* 111:B02402
- Vigny C, Huchon P, Ruegg JC, Khanbari K, Asfaw LM (2006b) Confirmation of Arabia plate slow motion by new GPS data in Yemen. *J Geophys Res* 111:B02402
- Vigny C, de Chabalière J-B, Ruegg J-C, Huchon P, Feigl KL, Cattin R, Asfaw L, Kanbari K (2007) Twenty-five years of geodetic measurements along the Tadjoura-Asal rift system, Djibouti, East Africa. *J Geophys Res*
- Wright TJ, Ebinger C, Biggs J, Ayele A, Yirgu G, Keir D, Stork A (2006) Magma-maintained rift segmentation at continental rupture in the 2005 Afar dyking episode. *Nature* 442:291–294
- Wright TJ et al. (2012) Geophysical constraints on the dynamics of spreading centres from rifting episodes on land. *Nat Geosci* 5 (4):242–250
- Yirgu G, Ayele A, Ayalew D (2006a) Recent seismovolcanic crisis in Northern Afar, Ethiopia. *Eos* 87(33):325–336
- Yirgu G, Ebinger CJ, Maguire PKH (2006b) The Afar volcanic province within the East African Rift System: introduction. In: Yirgu G, Ebinger CJ, Maguire PKH (eds) *The Afar Volcanic Province within the East African Rift System*, Geol Soc London Spec Pub 259, pp 185–190, 1–6
- Zelenski ME, Fischer TP, de Moor JM, Marty B, Zimmermann L, Ayalew D, Nekrasov AN, Karandashev VK (2013) Trace elements in the gas emissions from the Erta-Ale volcano, Afar, Ethiopia. *Chem Geol* 357:95–116
- Zettwoog P, Le Carboneille J, Guern F, Tazieff H (1972) Mesures de transfert d'énergie et de transferts de masse au volcan Erta'Ale. *CR Acad Sci Paris* 274:1265–1268

7.1 The Danakil Sea and the Dagad Salt Plain

The northern Afar extremity, also called Danakil, extending into Ethiopia and Eritrea, is characterised by a wide lowland area, up to 250 km long and increasing in width from north to south up to 70 km, occupied along its median axis by a salt plain 120 km long and 30 km wide on average, with minimum altitudes of 120 m below sea level, corresponding to a former gulf of the Red Sea that dried out around 25,000 years ago (Tazieff et al. 1969; CNR-CNRS Afar team 1973). It extends beneath the Erta Ale range. This Quaternary unit is presently the seat of intense mining exploration (potash, previously mined by Italian and US enterprises). The remnants of the shores of the former Danakil Sea are observed all around the northern Afar depression at around zero level altitude, and include coral reefs, flat urchins and human occupation remnants.

It should be noted that marine sediments also occur in south-eastern Afar, around the Gulf of Tadjourah, which started opening with oceanic crust development and marine invasions three million years ago (Richard and Varet 1979). They are found on both sides of the Gulf, in faulted and eventually tilted blocks, where they cover the basalts emitted at the initial stage of the Afar oceanic rift opening. The outcrops are also well developed on the shore of Obock, north of the gulf, where they constitute a wide coral-reef plateau lifted up to +120 m (Varet 1975) along both the Gulf of Tadjourah and Bab-el-Mandeb strait (see Fig. 7.1).

7.1.1 Marine Limestones

A striking feature is the presence of marine limestones and corals all along the bases of the Ethiopian scarp and Danakil Alps (see Fig. 4.26). Together with later gypsum, often associated, they mould an ancient topography fairly comparable to the present one (Fig. 7.2). In certain places they

surround ancient islands or the summits of submarine volcanoes (e.g. the atoll of NE Afrera Lake) (Bonatti et al. 1971). Marine deposits outcrop over a distance of 200 km along the margin of the Danakil Alps and over a distance of 150 km along the Ethiopian escarpment. They outline the limits of an ancient gulf which extended up to 70 km wide and 250 km long to the SE of the present day Gulf of Zula. The bottom of the depression, filled with alluvial and volcanic flows, rises progressively and marine deposits disappear southwards.

Further south, gypsum is present in the Soddonta plain, together with lacustrine limestones, but south of parallel 12° 45' no marine deposit is observed. The thickness of marine limestone outcrops rarely exceed 20 m. The width of outcrops varies from a few metres to several kilometres. The altitude of the marine deposits ranges from -30 to +90 m. The same horizon may sometimes be followed over several kilometres, its altitude changing by a few tens of metres.

Marine limestones are fairly often overlain by continental conglomerates (with a Mousterian industry) which may be 5–10 m thick. Frequently, they are eroded and cut by gullies up to 20 m deep. Two marine cycles have been distinguished, each being more or less complete according to the place. A complete cycle, from bottom upwards, consists of:

1. *Conglomerates*: Pebbles consist of various escarpment rocks. Some Jurassic pebbles show perforations caused by marine organisms.
2. *Clays and bedded ashes*: These beds are locally intercalated at the base of the calcarenite; they contain brackish gastropods and are finely bedded or varved.
3. *Calcarenites*: This important lithological unit thins out and disappears upstream and thickens downstream where it may reach 10 m thick. Massive indurated calcareous biogenic sand, highly fossiliferous, white or reddish, contains abundant flat urchins *Laganum depressum* in the recent cycle, whereas older cycle contains numerous small oysters. Towards the top, calcareous oolites may

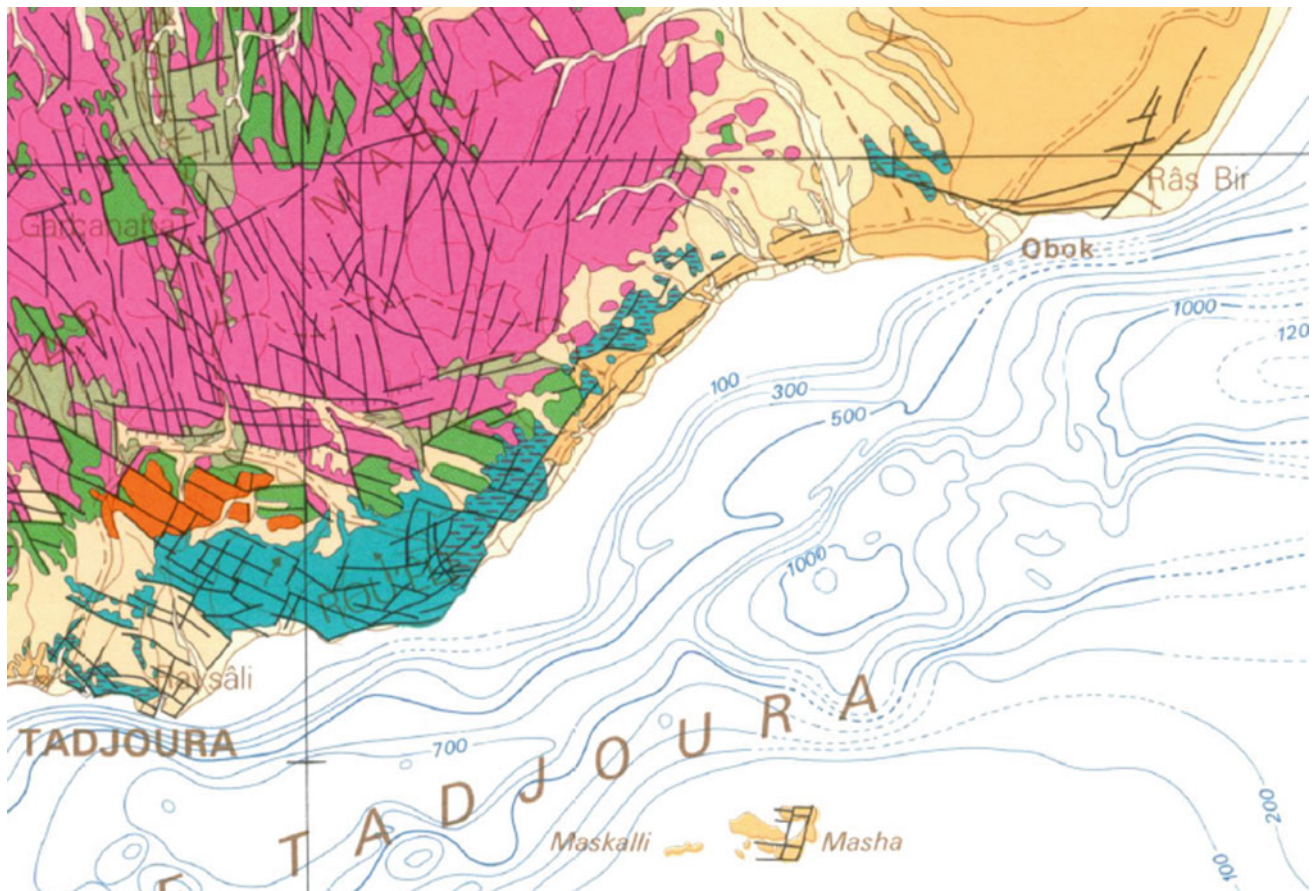


Fig. 7.1 Uplifted coral reefs on the northern shore of Gulf of Tadjourah, as seen (*pale orange colour*) on the CNR-CNRS geological map of central Afar (Varet 1975)

Fig. 7.2 Marine limestone outcrops stuck along the eroded polychromatic formation along the foot of the Nubian escarpment around the 0 m altitude (*Photo Varet 2004*)



develop. At En Kaddala the base of the calcarenites locally contains accumulations of manganese oxides which have been exploited (Bonatti et al. 1971).

4. *Coral bioherms*: These are madreporite herms (Fig. 7.3) in their original position, only developed in favourable topographical conditions, as isolated domes and elongated flat-top banks contouring a pre-existing topography. The flat top probably corresponds to the average sea level.
5. *Oolitic limestones*: This lithological unit, very constant, is characteristic of the end of marine cycles. It occurs before the precipitation of massive gypsum. The very fine textured calcareous ooliths form fairly regular white indurated beds with beige or reddish weathering surfaces. The thickness of the beds is several decimetres to 1 m. The total thickness of the stratified ooliths rarely exceeds several metres and diminishes towards the shore. It is a very shallow water deposit. Locally, particularly at the bottom of the ancient bays, the beach ooliths have been reworked by wind to form dunes, now indurated. The thickness of these eolian deposits may exceed 15 m. At the mouth of the ancient wadi, boulder and gravel beds are intercalated in the oolitic limestones (Fig. 7.4). In some areas (En Kaflala mines, Dallol western butes) oolitic beds are replaced by bedded limestones displaying abundant moulds of small lamellibranchs and gastropods. A perfectly preserved Acheulean biface has been found in this facies (Roubet 1969). The oolitic beds generally overlie the calcarenites (3) and can overlie the coral bioherms (4) as well. Downstream, they may be overlain by varved gypsum. Lastly, conglomeratic

terraces containing Mousterian industries cover both ooliths and gypsum. The five units (1–5), followed by the gypsum and salt units, form the complete marine evaporite sedimentary cycle of the Danakil Gulf.

The transition from normal marine to hypersaline settings that result from the closure of the connection to the Red Sea at the level of the Gulf of Zula or Alid is characterised by the deposition of fibrous aragonite crusts, as well as fibrous aragonite build-ups and spherules. On top of the oldest reef units, crusts are covering and filling cavities (up to 30 cm) with red algal bioherms and bivalve coquinas. The youngest coralgal bioherms are topped by aragonitic crusts and build-ups. Bivalves and serpulids are often actively involved in the formation of the build-ups (Jaramillo-Vogel et al. 2016).

Besides the presence of Acheulean artefacts which indicate a mid-Pleistocene age for the older marine cycle, 18 radiometric age determinations by uranium disequilibrium methods have been carried out (Lalou et al. 1970) on corals, *Tridacna* and ooliths being carefully located in detailed sections. Results from selected non-recrystallised specimens are grouped around two ages, around 200,000 and 80,000 years ago.

Four ^{14}C determinations on corals have given apparent ages between 24,405 and 34,470 years ago (Bannert et al. 1970; Bonatti et al. 1971). These probably correspond to a slight rejuvenation of specimens whose age is too ancient for this method. It may be noted that a verification using the U/Th method on a non-recrystallised specimen gives nearly twice the age—54,000 years ago (Bonatti et al. 1971).

Fig. 7.3 Corals and oysters abundant in the bioherms exposed in the medium part of the marine sequence along the shore of the Danakil Sea (Photo Varet 2014)





Fig. 7.4 Detail of an outcrop of oolitic limestone from the upper sequence of the marine littoral belt surrounding the Danakil Sea (Photo Varet 2014)

7.1.2 Gypsum Deposits

The evaporite sequence, well developed on the floor of the Danakil depression, corresponds to stages of partial isolation of ancient marine gulfs which evaporated in the tectonic basin. Gypsum forms deposits, accumulation, and incrustation very regularly distributed around the edges of the salt plain at an altitude ranging between a few metres above and 100 m below sea level. They are often covered by upper-Pleistocene conglomerates and later Holocene sediments which may fill 5–20-m deep ravines in the gypsum. Gypsum and anhydrite display the following facies:

- *Stratified or bedded gypsum*: This corresponds to a primary deposit by precipitation of gypsum from a saturated solution. Gypsum may alternate with ashes and volcanic tuffs, producing a varved appearance. Locally they may overlie calcareous oolites. Its thickness is 2–10 m.
- *Massive non-bedded gypsum*: Forms the incrustations covering the marine formations of stratified gypsum. They may occur with accumulations at a higher altitude than the coral deposits. They are often redissolved and recrystallised eolian gypsum deposits, located on the slopes and borders of the depression. Their thickness is generally 1–4 m.
- *Lower bedded gypsum*: Scattered outcrops are in a lower position, sometimes far away from the above types. They represent either synchronous deposition under deeper water or a slightly later deposit during the drying up of the gulf preceding salt deposition. In some cases, one is dealing with secondary reprecipitations.

Gypsum deposits are frequently associated with marine deposits (Fig. 7.5), and are even found interlayered at the end of the last marine cycle. They may be older than the oolites (80,000 years old) and younger than the

Fig. 7.5 Eroded marine limestones deposits topped by gypsum layers covering the polychromatic formation at the foot of the Nubian escarpment (Photo Varet 2014)



conglomeratic terraces containing Mousterian industries. However, gypsum deposits, frequently varved, are mostly younger and top the marine cycle of the Danakil Sea. They also outcrop at lower levels (below present sea level), between the marine and the salt outcrops of the floor of the depression.

On the CNR-CNRS geological map of northern Afar, the gypsum along the eastern and western borders of the depression have not been distinguished from the marine limestones at the base of which they only form a narrow fringe. However, the large outcrop of gypsum on the floor of the depression (800 km²) and in the Soddonta plain to the south 1250 km² have been distinguished from marine limestones.

7.1.3 Salt Deposits

Salt (halite) forms the floor of the Danakil depression in the Dallol-Assale region, beneath part of the Erta Ale range (Martini 1969). The surface of the salt plain (120 m below sea level) collects annual flood waters from wadis rushing down the escarpments. These waters are rapidly saturated by dissolving the upper layers and salt is reprecipitated by the following evaporation. Thus the upper decimetres at the surface are constantly reworked (Fig. 7.6). The upper layers are exploited by cutting regular rectangular salt sheets which are transported by caravans all over the country (Figs. 7.6, 7.7, 7.8, 7.9 and 7.10).

The deeper horizons outcrop in the salt domes (Dallol, Gada Ale) and in phreatic explosion craters in the salt plain

(see Fig. 7.16). They display a varved aspect (Fig. 7.11). Salt layers with an average thickness of 3.5 cm are separated by thin films of clay. Individual salt layers are thought to represent an annual cycle of evaporation (Fig. 7.12). Deposition would have occurred in an arid climate comparable to the present one from evaporating over-saturated seawater. Several horizons of potassium salts occur and have been exploited near Dallol-Mousseyle (Fig. 7.16). Boreholes have cut through a thickness of salt greater than 1000 m, with at least three horizons of potassic salts at 73,210 and 610 m (Holwerda and Hutchinson 1968). The total thickness of evaporites cut by petroleum boreholes or indicated by geophysics along the coast of the Red Sea is of the order of 5000 m in near Dahlac, north of the Afar.

The age of the salt determined by K/Ar (Hutchinson and Engels 1970) is 76,000 years at a depth of 73 m, 88,000 years at 137 m and perhaps 125,000 years at 610 m (Hutchinson, pers. comm.). These figures seem to be in fair agreement with the rate of salt deposition which would be of the order of 1–1.2 cm/year. This rate also agrees with actual evaporation of brines, as measured at Dallol. The latter leads to a precipitation of several centimetres per year. If one extrapolates the average rate of salt precipitation of the entire evaporite deposits to 5500 m (Tazieff et al. 1970) it may be concluded that the base of the salt may still be of Quaternary age. The base of the evaporites of the Red Sea, however, is generally considered to be of Miocene age. Taking into account the average calculated rate of salt precipitation (1.2 cm/year) the drying up of the Danakil Gulf must have been practically complete around 70,000–65,000 years ago, that is, before the low world sea level (60,000–55,000 years

Fig. 7.6 View of the salt plain; along the horizon, caravans of camels carrying the salt to Makalé salt market on the plateau. The surface is particularly fresh, being recrystallized every year after the rainy season had dissolved the surface, regenerated by deposition because of intense evaporation along the otherwise all-year-long arid climate (Photo Varet 2013)



Fig. 7.7 The salt is exploited manually by digging along the hexagonal contraction fissures and detaching a salt slate along a weaker, slightly clayed horizon (Photo Varet 2013)



Fig. 7.8 Yearly seasonal variations induce layers of different salt crystals compaction and purity, allowing for slates to be detached (Photo Varet 2015)

ago) during which the gulf was certainly isolated from the sea. It seems therefore very likely that the separation of the Danakil depression from the Red Sea (Gulf of Zula) occurred 70,000–60,000 years ago, the probable age of the last salt deposits.

At the northern extremity the salt plain narrows, and is finally at the level of the Alid volcano, south of the Gulf of Zula which belongs to the same structural unit (northern visible end of the Danakil rift).

7.1.4 Loams and Silts of the Plains

When not covered by salt deposits, the depressions and particularly the floor of the grabens and the rifts-in-rifts are filled with pale coloured loams. These fine-grained materials have several origins. They consist partly of muds transported to the heart of the plains by wadi during the flood periods. In some areas (near to the silicic centres of the margins) they appear to be composed mainly of ashes and slightly altered



Fig. 7.9 The salt slates are then cut in regular rectangles, cleaned by peeling the clayed surfaces, and piled with the right shape for commercial use (Photos Varet 2015)



Fig. 7.10 The salt slates are then packed for transport by camels or donkeys (Photos Varet 2015)

acid volcanic dust. This may include pumice spread out over the plains, up to several decimetres thick. This deposition corresponds to ash falls reworked by waters. In the depressions, which are still invaded by seasonal floods, argillaceous silts may engender dark coloured vertisols. These loams can be deeply ravined as a result of recent volcanism and tectonism. In several places, open fissures of NNW-SSE direction cut these deposits. Prehistoric artefacts are frequently found (obsidian splinters).

7.2 Volcanoes of the Gulf of Zula (Eritrea)

The northernmost limit of the Afar triangle—in Eritrea—is affected by several volcanic units aligned on the NNW rift axis, along a graben quite narrow in this area. In the Gulf of Zula, a large central volcanotectonic depression is open to the sea (Fig. 7.13). This volcano called Jalua is mainly built by lava flows and pyroclasts of peralkaline silica nature. It shows fumarolic activity on its western flank. The Irafaille volcanic centre, situated at the northern limit of this silicic stratovolcano, is a rhyolite hyaloclastite with a small round ash ring included in a larger elliptic one. Hot springs issue from its eastern flank and flow to the Red Sea at the Gulf of Zula (Mesfin and Yohannes 2014).

7.3 Alid Volcanoes (Eritrea)

Alid, the main volcanic unit in this northern extremity of Afar, is located south of the Gulf of Zula and north of the salt plain, in an area where the rift is narrowest (15 km). It is probably the unit that closed the Danakil Sea to the north and caused its evaporation with the formation of the salt plain. The rift is rather asymmetrical. The western escarpment is affected by east dipping normal faults with elevations of the Precambrian basement ranging from 2500 m on the plateau down to 300 m at the foot of the depression. The eastern boundary is marked by a 300-m high west dipping normal fault, with Precambrian rocks locally exposed at the base of the scarp, uncomfortably overlain by post-Miocene detrital and evaporitic sediments and volcanic products. The top of the Precambrian section is therefore at least 2000 m lower than west of the graben (Clynne et al. 1996).

Alid is made of two recent flat-lying basaltic lava fields developed at the northern and southern flanks of a central mountain displaying apparent aspects of a stratovolcano (Fig. 7.14).

The volcanic centre observed at the middle (Fig. 7.15) was considered by Barberi et al. (1973) to be a stratovolcano from air photograph interpretation as access was impossible at that time for safety reasons. Detailed investigations undertaken since by USGS have shown it to be in reality an elliptical structural dome (Fig. 7.16) caused by shallow intrusion of rhyolitic magma, some of which erupted (Clynne et al. 1996) as pumice and lava dome. A variety of rocks are found cropping out on the dome: Precambrian quartz–mica and kyanite schists are found at Sillalo canyon that drain the east

Fig. 7.11 Layered salt deposits covered by gypsum, uplifted at Dallol dome, showing a section of the salt deposit in the Danakil salt plain (*Photo Varet 2015*)



Fig. 7.12 Detailed view of layered halite-sylvite deposits, as observed on eroded cliffs in the SW part of the dome (*Photo Varet 2015*)



side of the mountain, as well as large outcrops of the polychrome sedimentary sequence, with siltstone sandstone and sands, anhydrite beds and fossiliferous limestone, and also pillow as well as subaerial basalts and andesine basalts lava flows. These formations are intensively faulted and deformed and may dip locally as steep as 65° .

A wide sink is observed on the upper part of the dome, probably resulting from a collapse following the pumice

eruption (Fig. 7.15). Another sink is observed on the eastern flank, apparently linked with a rhyolite lateral dome-flow (see map in Fig. 7.16).

Clinopyroxene-bearing rhyolite lavas, dated at $33,500 \pm 4400$ years old, were erupted subsequent to the initiation of structural doming. Similar rhyolite was erupted as pyroclastic flows from the summit region and today forms blankets of tephra up to 15 m thick in the summit basin and



Fig. 7.13 The volcano-tectonic structures observed on the south and western shore of the Gulf of Zula, as seen from satellite image (USGS Earth Vision). A set of volcanic centres are aligned along a NNW (Red Sea) direction, with successive collapse structures developed from SE to NW, the most recent being two imbedded hyaloclastite cones along the western coast of the gulf

the west flank of Alid. The final phase of this eruption, a lava dome, dated at $23,500 \pm 1900$ years (Duffield et al. 1997), also brought to the surface fragments of granitic blocks. These show typical micrographic textures—the term of granophyre is preferred by Lowenstern et al. (1997, 1999) who studied them in detail. Vermicular to cuneiform

feldspars radiate off and are in optical continuity with pre-existing feldspar phenocrysts, implying a rapid and simultaneous crystallisation of quartz and feldspar from a melt. Note that this age fits with the determination from sedimentary sequences of the time of evaporation of the Danakil Sea.

In depth study of the granophyre blocks found within the pyroclastic ejecta showed them to be the intrusive equivalent of pumice from the pyroclastic flow. Their phenocryst compositions and geochemical characteristics are virtually identical. Silicate melt inclusions and other geochemical and geological considerations developed by Lowenstern et al. (1999) revealed that the rhyolitic magma with ~ 2.6 wt% dissolved H_2O and a temperature near $870^\circ C$ was intruded at a shallow depth—within 2–4 km of the surface—causing deformation and structural doming of pre-existing geological strata. According to this interpretation, the eruptions of crystal-poor rhyolite from this shallow magma chamber caused degassing, forcing undercooling and consequent granophyric crystallisation of some of the magma remaining in the intrusion. The crystallised granitic wall of the magma chamber was excavated as clasts at the surface by the most recent eruption.

Detailed studies of the hydrothermal manifestations in and around the dome (Fig. 7.17) showed that a geothermal reservoir at a temperature of $225^\circ C$ developed in the Alid volcano-tectonic system, whereas geophysical surveys are in progress, together with detailed structural mapping (see fracture density map in Fig. 7.18) to locate targets for geothermal exploration drillings (Yohannes 2015).

The geothermal potential of Alid is discussed in Sect. 12.2.

As a whole, besides showing a magmatic unit of quite particular nature, being both a young shallow plutonic dome

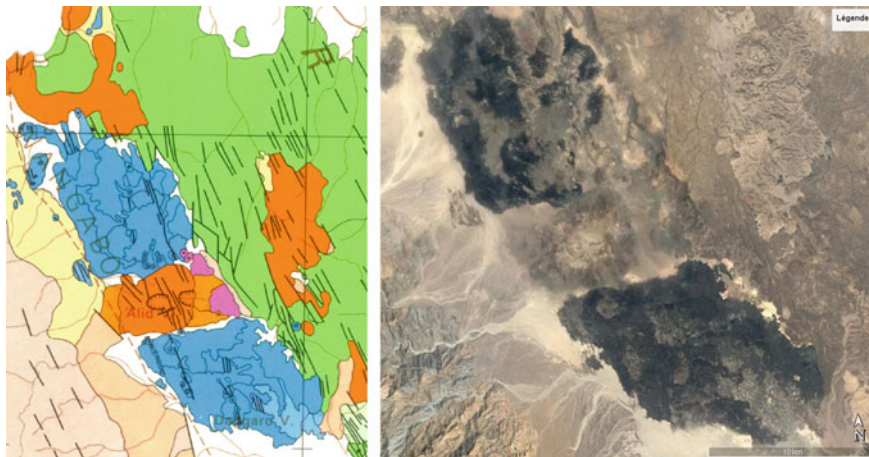


Fig. 7.14 The Alid volcanic system is composed of two fissural basaltic lava fields separated by an elliptical bulge affected by summital sinks astride the structural axis of the graben, which is 7 km along the ENE direction and 5 km along the NNW direction of the graben. It rises

roughly 700 m above the basalts that appear to lap against the northern and southern flanks of the mountain (extract from the CNR-CNRS map of northern Afar, 1973 right and satellite image from Google Earth Pro, left)

Fig. 7.15 Central part of Alid volcano, a rhyolite dome that uplifted the pre-existing geological formations (*Photo Lowenstern*)



Fig. 7.16 View of the central sink at the top of the dome. Pumice layers are visible on the upper part of the cliff (photo by Lowenstern)



and an embryonic volcano, and therefore a site of geothermal interest, Alid also shows the active expression of similar features observed elsewhere in Afar. These are the peralkaline granite bodies, observed along the foot of the Ethiopian scarp, in the Danakil Alps and in the middle of Afar in the Affara Dara massif, all dated at a similar (22–25 million years) Miocene age (see Sect. 4.3).

It is worth noting that the same tectono-magmatic phenomena, having affected central Afar 25 million years ago at the time of its initial opening, were still active only 25 thousand years ago at Alid. Alid can therefore be considered as expressing now the same geodynamic step of initial

opening that occurred earlier in the central Afar Rift, where it has now reached the stage of oceanic rifting.

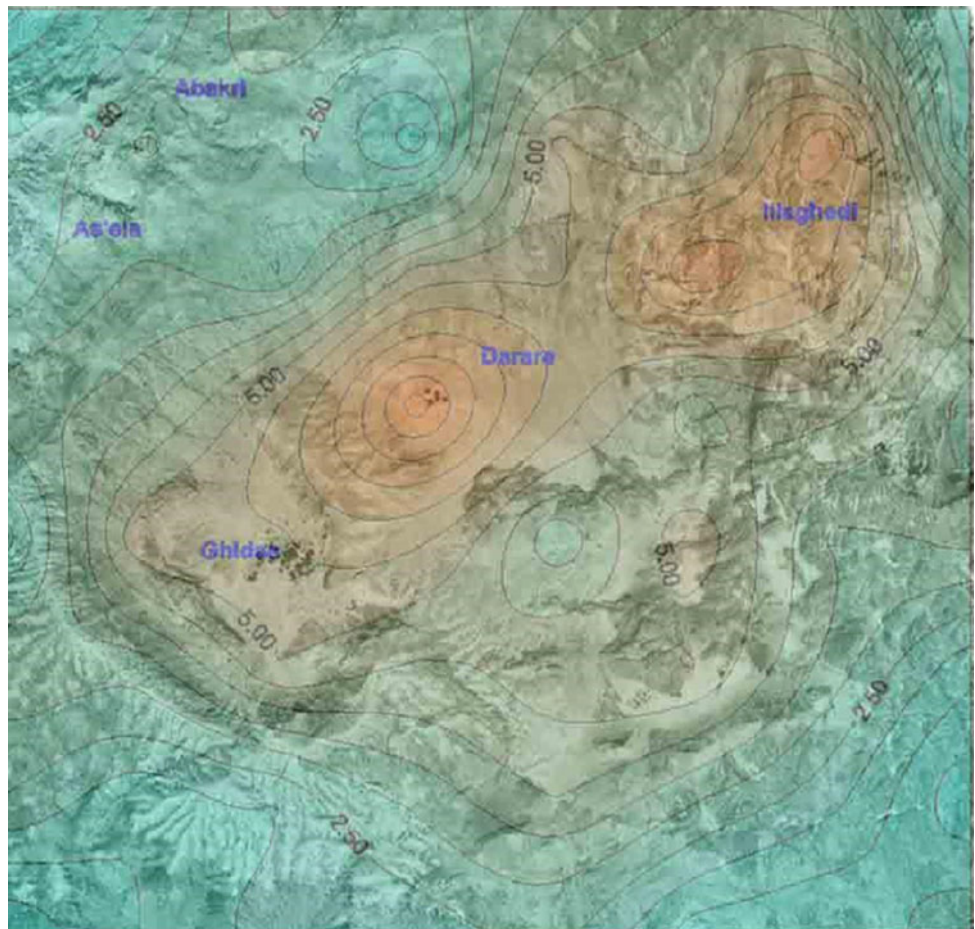
7.4 Maraho Submarine Volcano in the Dagad Salt Plain

A wide hyaloclastite cone (1 km wide and 150 m high) sits in the middle of the Dagad salt plain (120 m below sea level), near the Ethio-Eritrean boundary, called Maraho (see map in Fig. 7.22). This submarine volcano is cut by faults and feeding dikes in a NNW direction and covered by subaerial

Fig. 7.17 Fumaroles, with sulphur deposits at Illegedi on the flank of the Alid dome (Yohannes 2015)



Fig. 7.18 Detailed topographic map of the summit sink of the Alid dome, with indication of the density of fractures (Yohannes 2015)



olivine basalts, the same that made the hyaloclastite cone (Fig. 7.19).

This volcano produced a large amount of deposits all around the emission centre. Corresponding strata should be

found in the surrounding marine and evaporitic sequence. Hyaloclastite layers, several metres thick (Fig. 7.20), are observed along the lower flank of the Nubian escarpment up to a distance of 10 km from Maraho (Fig. 7.21).



Fig. 7.19 Maraho hyaloclatite cone seen from the western side of the rift (*Photo Varet 2015*)



Fig. 7.20 Hyaloclatite deposits emitted from Maraho submarine volcano, as observed at the foot of the Nubian escarpment (*Photo Varet 2015*)



Fig. 7.21 The yellow deposits of hyaloclastites are observed over several kilometres, stuck against the Nubian scarp lowest foothills, as observed up to 10 km south of Maraho volcano (*Photo Varet 2015*)

The Maraho volcano was not dated but was emitted in the period of extension of the Danakil Sea, that is, between 200,000 and 65,000 years ago. Although isolated, it shows that basalt diking has occurred along the axis of the northern Afar depression north of the Erta Ale range, an observation that is also confirmed in Dallol, although no volcanic outcrop is visible there.

7.5 Dallol Hydrothermal Dome in the Dagad Salt Plain

The Dallol site is located in the middle of the vast Dagad Salt Plain at 14°15'N (Fig. 7.22). It is a former potash mining site (Holwerda and Hutchinson 1968; ELMICO 1984) (Fig. 7.23) and also a tourist destination because of the multi-coloured salt concretions that have developed as a result of spectacular hydrothermal activity. Hot water and fumaroles (the temperature of which may reach 120 °C) deposit sodium, potassium and magnesium chloride as well as elemental sulphurs, creating a wide range of colours at the emission sites, from black and green under reduced conditions, to yellow, red and brown after oxidation (Fig. 7.24). Springs and fumaroles are clearly aligned along NNW trending fissures, certainly linked to the opening of fissures on the rift axis. Vent locations change with time, as salt deposits plug old vents, whereas new vents appear nearby along new fissures. This confirms that Dallol is also located on the active Afar Rift axis. In the Black Mountain site, an MgCl₂-saturated brine (128 °C) bubbles at the surface (Tazieff et al. 1969; Barberi et al. 1973).

The Dallol elliptically-shaped updomed structure rises some 50 m above the surrounding salt plain with a long axis striking ENE-WSW. Rather than a real salt dome, it is a vertical uplift probably initiated by a deep magmatic intrusion. The regularly horizontal strata exposed in Dallol's eroded hills confirm this hypothesis. The top layer is an anhydrite which forms a reliable marker horizon (Fig. 7.25) and served as a protective cover against erosion from precipitation. It may indicate that the updoming occurred when anhydrite formed the top layer of the saltplane. The age of the updoming hence is assumed to be younger than the last Danakil Sea, some 30,000 years old. Mineralogical sampling show—in addition to halite—anhydrite, gypsum, carnalite, jarosite, bischofite, sylvite and thenardite. The iron oxides are mainly haematite and some magnetite, but no sulphides such as pyrite was found. Native sulphur is also commonly found. A similar uplift feature is observed in the northern tip of the Erta Ale range, in the Gada Ale area (see Sect. 6.2).

Geophysical data (magnetic and gravimetric) indicate that a magmatic body (most probably basaltic), a few kilometres deep, might underlie the sediments, although no volcanic products are found in Dallol. The magnetic data show a

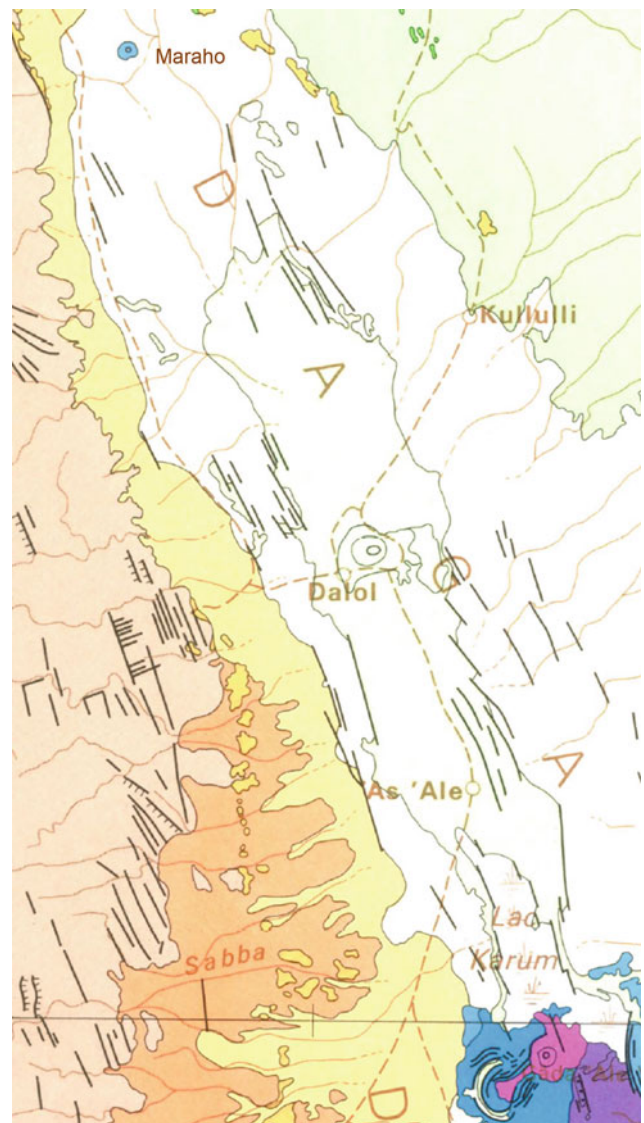


Fig. 7.22 Geological map of the Dagad salt plain with Maraho hyaloclastite volcano to the north, the Dallol dome at the centre, As'Ale phreatic explosion crater and the "salt dome" of Gada Ale at the northern extremity of the Erta Ale range (see Sect. 6.2). Extract from CNR-CNRS geological map of northern Afar (CNR-CNRS 1973)

sharp positive anomaly close to Black Mountain and another somewhat broader at Mount Dallol. The gravity data poorly reported is, however, inconclusive. With its location in the middle of the rift, right on the NNW alignment with the Erta Ale range, the presence of an active magmatic heat source is quite plausible.

As well as its transverse elongation, geophysical data also show E-W anomalies that can be interpreted as being the result of transverse faults. As a whole, Dallol represents the surface expression of a particularly active geothermal system (see Sect. 12.1), which eventually extends further south beneath the salt plain.



Fig. 7.23 Rests of the former salt mine on the Dallol hill-top (Photo Varet 2015)

7.6 As Ale Phreatic Explosion Crater in the Dagad Salt Plain

South of Dallol and north of the Erta Ale range, in the middle of the salt plain, 55 m wide, As Ale is the expression of a former phreatic explosion (Fig. 7.26). The force of the eruption that produced the crater is reflected by salt boulders up to 1 m in diameter embedded in the crater wall (Fig. 7.27). This indicates the presence of a high-pressure, high-temperature (above 180 °C) geothermal reservoir currently active beneath this part of the salt plain.

7.7 Lake Afdera and Sodonta Plain

7.7.1 Lacustrine Limestones and Diatomites

Lacustrine deposits are found mainly around Lake Afrera and in Soddonta plain, and consist of a white, very light, unbedded pulverulent limestone containing less than 5 wt% of diatoms. A grey layer less than 1 cm thick of acid volcanic ashes occurs within the limestones. This formation is well developed around the northern and western foot of the older Afrera volcanic centre, while the recent, probably historic, Alayta flows cover the limestone and limit the outcrop to the west (Fig. 7.28). Elsewhere (southern Erta'Ale range, northern

Tat'Ali range and Borawli volcano) it provides a very useful marker bed when intercalated in basalts (Barberi et al. 1972). Basalts covered by these deposits show typical subaqueous features (Barberi and Varet 1970). Eolian erosion of this light material has led to the disappearance of about 20% of the deposit around the lake.

Boreholes in connection with salt prospecting have shown that, at depth, basalt flows alternate with Pleistocene lacustrine deposits. Quantitative and qualitative studies of the diatoms of the lacustrine deposits (Gasse and Street 1978) allow one to follow the evolution of the lacustrine environment between 10,000 and 7000 years ago. After this date, it seems that the level of the lake fell considerably, evaporation giving rise to calcareous pisoliths and incrustations, as well as to gypsiferous and carbonate impregnations which are characteristics of the present borders of the lake. It is therefore considered as a saline relict (Martini 1969) of a larger Holocene lake that probably also extended south, contouring the Tat'Ali-Mat'Ala range, in the Sodonta plain.

The high levels of the lake are marked by algolimestones which incrust basaltic boulders. Other high level occurrences, perhaps produced by tectonics, allow one to locate high levels of the lakes several tens of metres above the present water level. Existence of these lacustrine deposits is related to a humid period dating from the beginning of the Holocene, well known in the whole region.



Fig. 7.24 View of some of the thermal springs at Dallol. Hot water and gas percolate through the dome and deposit slat with metallic sulphides (*black and green* in color) that progressively oxidise with the development of *yellow to red and brown* colors (Photo Varet 2015)

7.7.2 Lake Afdera

At present, Lake Afdera has a surface area of 115 km². Bathymetric mapping evidence (Bonatti, pers. com.) shows that the maximum depth of the lake is at least 73 m. When the wind blows, thick white foam is formed on the lake shore as a result of biogenic activity (Fig. 7.29). Numerous hot springs surround the lake; along the western shore they average 50 °C with carbonate composition, and deposit travertine (Fig. 7.30). At the limit between the springs and the hyper-salty lake, when water is neither too hot nor too salty, numerous fish are to be found.

These springs are often associated with carbonate build-ups—and travertine chimneys develop up to 4 m high above the plain, probably resulting from earlier sublacustrine deposits from the still active fissures feeding the thermal springs (Fig. 7.31). Although less spectacular, it represents a case analogous to the travertine observed west of Abhe Lake (Djibouti Republic).

Gypsum actively precipitates along the lakeshore, forming gypsum crusts and concretions around plant roots.

Preliminary water measurements, CTD profiling and camera footage reveal a high content of green algae in the



Fig. 7.25 View of the evaporitic formations lifted up and eroded on the SW part of Dallol dome (*Photo Varet 2015*)



Fig. 7.26 The As'Ale phreatic explosion crater, in the middle of the salt plain between Dallol and Gada Ale (northern extremity of Erta Ale range) (photo coll. G. Marinelli, Pisa University)



Fig. 7.27 The products of the explosion in the walls of As'Ale crater, with metric blocks, showing the stratification of the salt at depth, imbedded in the walls (*Photo Varet 2015*)

upper part of the water column and anoxic water conditions in the deeper part of the lake. There, the sediments are mostly composed of flocculated dead algae, volcanoclastic particles and fine silt. A study of the hot springs surrounding the lake is also under way by Jaramillo-Vogel et al. with the intention of giving more insight into the non-climatic parameters controlling the lake level and the sediment factory in this hypersaline system.

During the last 10 years a salt extractive industry has developed along the western shore of the lake, pumping the brine into artificial ponds for evaporation and subsequent precipitation (Figs. 7.32 and 7.33). A small town is growing in size along the newly asphalted Makalé to Semara (and Djibouti) road.

7.8 Comments on the Danakil Sea and Other Sedimentary Areas

The Danakil Sea had an important influence on the whole northern Afar, as it generated thick sediment layers and deeply impacted the volcanic and thermal activity up to present times. If we are able to describe and understand eventually the most recent sedimentary and volcano-tectonic features (for the last few hundred thousand years), the early

phases (earlier than one million years ago) are more difficult to depict.

Although the development of the escarpments, the crustal thinning in the foot-hills and Danakil Alps, the deepening of the axial trough and associated erosion and sedimentation date back to Miocene, geological indices are lacking in the five to one million year period, for which we have no evidence for either marine or volcanic events.

It remains that in Afar and surroundings, four areas are eventually characterised by thick sedimentary units that would deserve better knowledge and specific exploration works:

- The Danakil Sea area from the Gulf of Zula to the north to the Sodonta plain to the south
- The Asash endoreic basin covering central Afar where thick detritic and lacustrine units developed during the last four million years at least
- The southern Afar area, between the foot of the Somalian escarpment and the central Afar volcanic units, where recent detrital and evaporitic deposits obliterate any possible observation of earlier geological units
- The Bab-El-Mandeb area which has been stable for the last four (and eventually eight) million years and accumulated sediments of unknown—and probably important—thicknesses

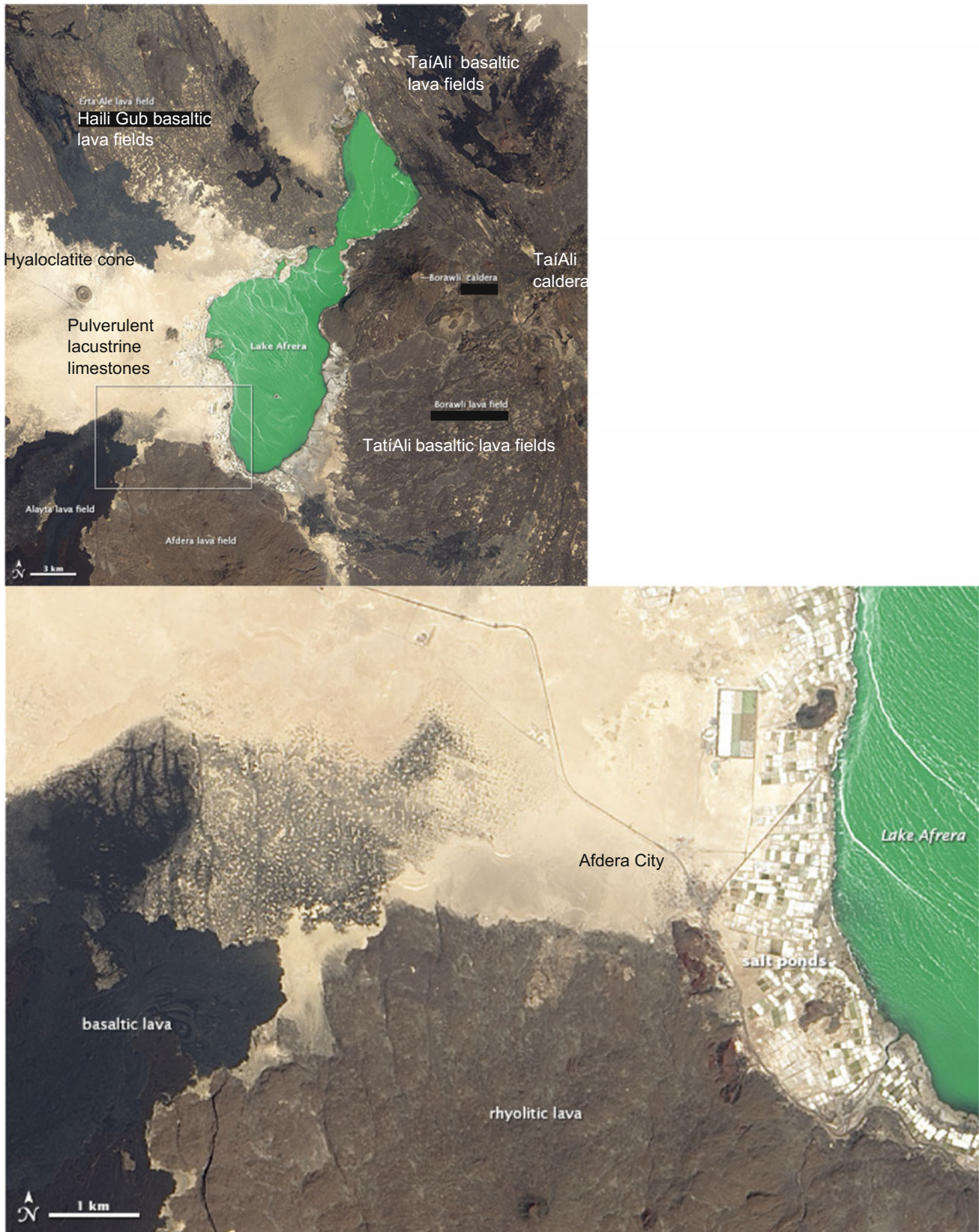


Fig. 7.28 Satellite images of Lake Afrera (NASA Earth Observatory, Jan. 2014) which extends in a NW-ES (transverse) direction between the Erta Ale range to the north and the two coupled axial ranges of Alayta and Tat'Ali to the south. Surrounded by earlier lava fields, it is abruptly limited to the NE by the intense normal faulting and associated fissural basaltic eruptions of the Tat'Ali range. The older lava fields of Afdera rhyolitic volcano, mark the SW limit, and the lava fields of the

Erta Ale and Tat'Ali ranges of more recent age limit the northern and the SE side. The historic basaltic flow of Alayta (on the west) and the recent flow of the axial graben of Haili Gub (Erta Ale range) cover the lacustrine sediments that are well developed in the plain west of the lake. A hyaloclatite cone was formed in this sublacustrine environment. The *bottom* image is a blow out of the rectangle figures on the *upper* image



Fig. 7.29 Biogenic foam deposited on the western shore line after a windy period (*Photo* Varet 2013)

Fig. 7.30 Hotspring along the western shore of lake Afrera, algae developing on carbonaceous travertine (*Photo* Varet 2013)





Fig. 7.31 Travertine chimneys built from carbonate deposits on former hot springs conduits, developed when the lake was at a higher altitude. With the expansion of the town, these edifices are progressively incorporated in housing (*Photo* Varet 2015)



Fig. 7.32 Salt evaporation ponds built around Lake Afrera. The saline water of the lake is pumped up into these ponds where the salt precipitates. In the background is a subaqueous hyaloclastite cone (*Photo* Varet 2015)



Fig. 7.33 Workers on duty extracting the salt from a pond along the Lake Afrera shoreline. Observe the palm trees that developed along the shoreline in the hot spring environment, now victims of the salinisation

of the water table caused by the development of these salt ponds (Photo Varet 2015)

References

- Bannert D, Brinckmann J, Kading KC et al (1970) Zur Geologie der danakil-Senke (Nördliches Afar Gebiet, NE-Aethiopien). *Geol Rundsch* 59(2):409–443
- Barberi F, Varet J (1970) The Erta `Ale volcanic range. *Bull Volc* 34:848–917
- Barberi F, Borsi S, Ferrara G, Marinelli G, Santcroce R, Tazief H, Varet J (1972) Evolution of the Danakil depression (Afar Ethiopia) in light of radiometric age determination. *J Geol* 80:720–729
- Barberi F, Chemine`e JL, Varet J (1973) Long-lived lava lakes of Erta Ale volcano. *Rev Geogr Phys Geol Dyn* 15:347–352
- Bonatti E, Emiliani C, Ostlund G, Rydell H (1971) Final dissection of the Afar Rift, Ethiopia. *Science* 172:468–469
- Clynne MA, Duffield WA, Fournier RO, Weldegiorgis L, Janik CJ, Kahsai G, Lowenstern J, Weldemariam K, Tesfai T (1996) Geothermal potential of the Alid Volcanic Center, Danakil depression, Eritrea. US Geological Survey, Final report to U.S. Agency for International Development under the terms of PASA No. AOT-0002-P-00-5033-00, 46 pp
- CNR—CNRS Afar team (1973) Geology of northern Afar (Ethiopia). *Rev Geogr Phys Geol Dyn* 15: 443–490
- Duffield WA, Bullen TD, Clynne MA, Fournier RO, Janik CJ, Lanphere MA, Lowenstern J, Smith JG, Giorgis L, Kahsai G, Mariam K, Tesfai T (1997) Geothermal potential of the alid volcanic center, Danakil depression, Eritrea. US Geological Survey Open File Report 97-291
- ELMICO (1984) Dallol Potash project. PEC Ingenierie, Mulhouse, France, 2 vol, 280 p
- Gasse F, Street A (1978) Late Quaternary lake-level fluctuations and environments of the northern Rift Valley and Afar region (Ethiopia and Djibouti). *Palaeogeogr Palaeoclimatol Palaeoecol* 24:279–325
- Holwerda JG, Hutchinson RW (1968) Potash bearing deposits in the Danakil area. *Ethiopia Econ Geol* 63:124–150
- Hutchinson RW and Engels GC (1970) Tectonic significance of regional geology evaporate lithofacies in Northern Ethiopia. *Phil Trans Roy Soc London A* 267, 1181:313–329
- Jaramillo-Vogel D, Foubert A, Schaegis JC, Grobety B, Atnafu B, Kidane T (2016) Pleistocene fibrous aragonite crusts and spherulites in the Danakil Depression (Afar, Ethiopia). 24th Meeting of Swiss Sedimentologists—Fribourg, February 27, 2016
- Lalou C, Nguyen HV, Faure H, Moreira L (1970) Datation par la méthode U/th des hauts niveaux de coraux de la dépression de l'Afar. *Rev Geogr Phys Geol Dyn*, 2/X11/1 3–8

- Lowenstern JB, Clynne MA, Bullen TD (1997) Comagmatic A-Type granophyre and rhyolite from the Alid Volcanic Center, Eritrea, Northeast Africa, *J Petrology* 38:1707–1721
- Lowenstern JB, Janik CJ, Fournier RO, Tesfai T, Duffield WA, Clynne MA, Smith JG, Woldegiorgis L, Weldemariam K, Kahsai G (1999) A geochemical reconnaissance of the Alid volcanic centre and geothermal system, Danakil depression, Eritrea. *Geothermics* 28:161–187
- Martini M (1969) La geochimica del Lago Giuletti. *Rend Soc Ital Mineral Petrol* 25:67–78
- Mesfin A, Yohannes E (2014) The geology of the northern Danakil depression and its geothermal significance. *Proceedings 5th African Rift geothermal Conference*. Arusha, Tanzania, 29–31 Oct 2014
- Richard O, Varet J (1979) Study of the transition from deep oceanic to emerged rift zone: gulf of Tadjoura (Republic of Djibouti). *Int Symp Geodyn Evols, Afro-Arabian System*, Roma
- Roubet C (1969) Essai de datation absolue d'un biface hachereau paléolithique de l'Afar (Ethiopie). *L'Anthrop* 13(7–8):503–523
- Tazieff, H, Varet, J. (1969) Pétrographie et tectonique de l'Afar septentrional (Ethiopie). *Colloque Géol. Africaine Clermont-Ferrand (résumé)*. *Ann Fac Sc Clermont* (41):54
- Tazieff H, Barberi F, Borsi S, Ferrara G, Marinelli G, Varet J (1970) Relationships between tectonics and magmatology in the Northern Afar (or Danakil) depression. *Phil Trans Royal Soc London A* 267:293–311
- Varet J (1975) Carte géologique de l'Afar central et méridional, CNR-CNRS, 1/500 000 Géotechnip
- Varet J (2004) De l'Afar à la géothermie. In « Haroun Tazieff, une vie de feu », Ed. Glénat, pp 85–94
- Varet J (2013) The Afar system and carbonates. In: *Cocarde Workshop (Abstract)*, Sicily, pp. 48–49
- Varet J (2014) Asal-Fialé geothermal field (Djibouti republic): a new interpretation for a geothermal reservoir in an actively spreading rift segment. In: *Proceedings 5th African Rift geothermal Conference*, Arusha, Tanzania, 29–31 Oct 2014
- Yohannes E (2015) Geothermal exploration in Eritrea – Country Update. *Proceedings 5th African Rift geothermal Conference*. Arusha, Tanzania, 29–31 Oct 2014

It was recognised early on (Barberi et al. 1970; CNR-CNRS 1973) that Afar, particularly in the northern part, displayed recent volcanic units with distinct characteristics, located along the margins of the depression. Their location and nature are clearly linked with the pre-rift surrounding discontinuities—on the western side the Ma'alalta (Pierre Pruvost) massif and on the eastern side the Biddu range including the Nabro volcano. Both sit on the deeply faulted pre-Mesozoic sequence. Differing from the units found on the Afar floor, these are stratovolcanoes with calderas and abundant pyroclastic products, such as ash flows and ignimbrites.

8.1 Ma'alalta (Pierre Pruvost)

This volcanic complex consists of a dominantly acidic central volcano with caldera surrounded by two—north and south—basaltic lava fields. The volcano is located on the southernmost extremity of the long Erebtı graben that extends along the foot of the Ethiopian escarpment, at the place where the lateral Damuma horst disappears leaving a 35 km wide right lateral offset of the escarpment (Fig. 8.1).

The stratovolcano is 15 km wide with a double-rimmed summit caldera (5×4.5 and 4×2.5 km in diameter), with additional internal collapses, elongated in an ENE (transverse) direction (Fig. 8.2). All the products are of silicic nature (oversaturated trachytes and rhyolites), with a peralkaline tendency of some end-products. They consist of intercalations of pyroclastics (pumice and ignimbrite) and lava flows with intrusions (sills and domes) of trachytes in the upper part. An extensive ignimbrite sheet emitted from the caldera covers the surrounding plains up to a distance of

more than 30 km, with large extensions in the Erebtı graben to the north and in the Dodom and Teru plains to the east and south. This ignimbrite overlies older rhyolite and basaltic flows emitted north of the caldera. The age of the oldest sampled rock of this unit is 0.55 million years (Barberi et al. 1972).

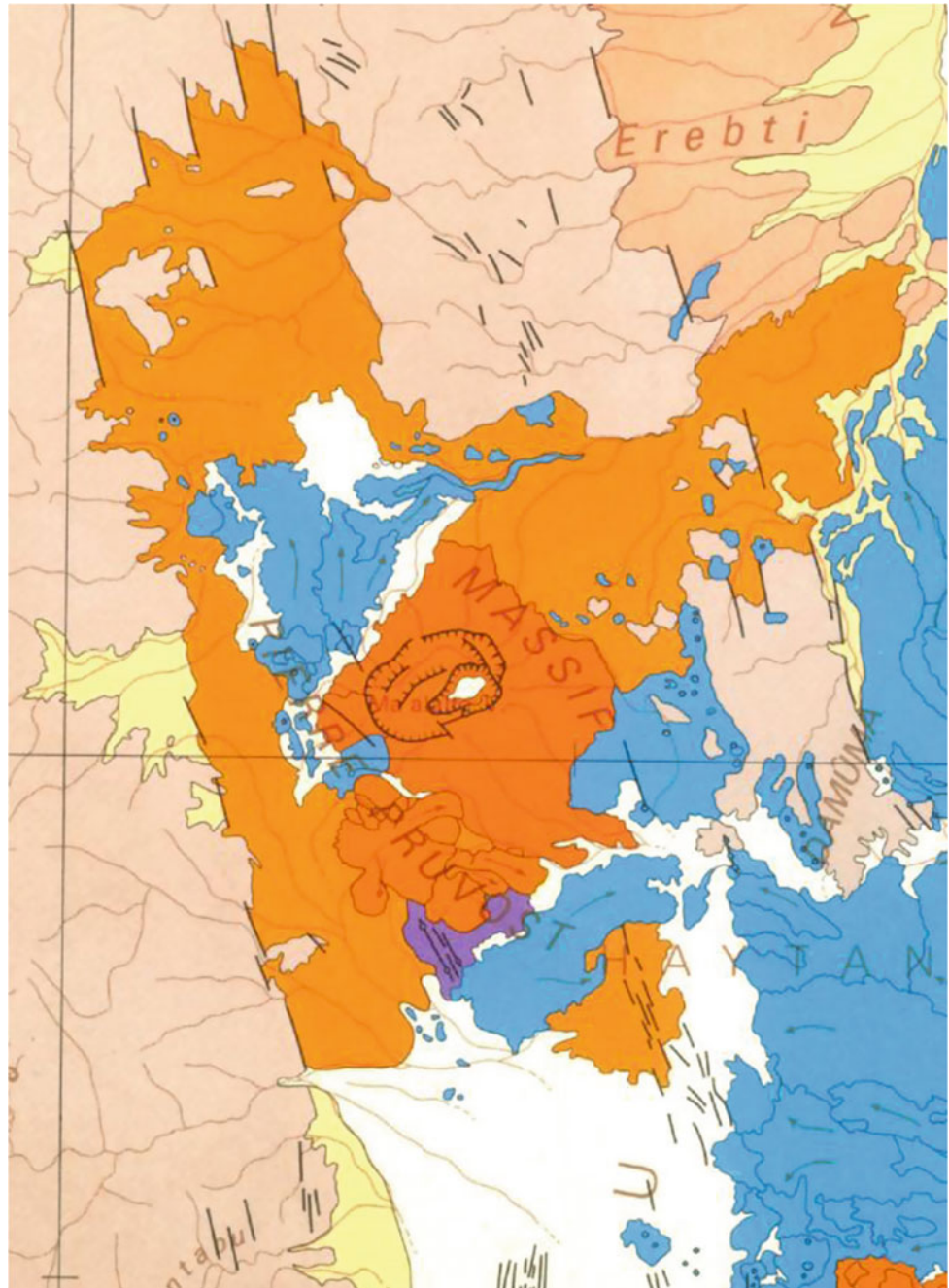
Recent silicic activity occurred off the southern foot of the volcano, where domes and short viscous flows of panteliritic obsidians are aligned along a NNW fissure. This part of the massif is the most active, as shown by fumarolitic activity also present within the caldera (Figs. 8.3 and 8.4).

Ma'alalta volcanic centre shows several hydrothermal manifestations in the caldera as well as at the foot of the stratovolcano, in the areas affected by recent volcanic and tectonic activity, which is particularly the case in the plain located SW of the centre, in the northern extremity of Teru plain. Several are exploited as a source of water by condensation by the Afar pastoralists.

Fissural lava fields north and south of the silicic centre were erupted through fissures of NNW direction off the western foot of the stratovolcano. Some small basaltic spatter cones are observed there as well as on the eastern side, overlying the basement of the Damuma horst.

As shown by Barberi et al. (1970), the petrology of this complex clearly contrasts with that of the axial ranges. Differing from the latter, silicic products are largely dominant, often produced through eruption of gas-rich magma producing important amounts of pyroclatites (pumices and ignimbrites). Potassium-richer, non-alkaline rhyolites are abundant in the stratovolcano and petrological as well as isotopic data support the idea of contamination with the sialic crust for at least some of the rhyolite products (Fig. 8.5).

Fig. 8.1 The Ma'Alalta—Pierre Pruvost stratovolcano along the foot of the Ethiopian escarpment where it is shifted west by some kilometres to the south. The western limits of the lava fields of Alayta are seen on the eastern side. (Extract from CNR-CNRS map of northern Afra, CNR-CNRS 1973)



8.2 The Bidu Transverse Alignment

Three stratovolcanoes with large calderas are aligned along a NE-SW (transverse) direction on the southern extremity of the Danakil horst. This 2500 km² volcanic unit marks a clear limit between the pre-Mesozoic deeply faulted units

outcropping to the NW along the Red Sea margin, from the volcanic formation, which remained unfaulted for the last eight million years, observed to the SE.

The most important is Nabro, located in Eritrea, which clearly lies on the basement, whereas the other two (or even three if including Oyma located on the rift floor) are located



Fig. 8.2 Ma'alata caldera double rimmed caldera, largely controlled by transverse faults (WSW-ENE). *Image Google Earth Pro*

near to the faulted western limit of the Danakil horst, their products covering the polychromatic series that disappears further south (Fig. 8.6).

Nabro is the highest volcano in northern Afar (2218 m). It is a complex stratovolcano made of dominantly silicic products: ignimbrites and pumices as well as domes and lava flows. The summit displays a double-rimmed caldera (8 and 5 km in diameter) which is closed with high walls on all sides except to the SW where post-caldera activity overflowed a less elevated rim.

Post-caldera activity produced pumice deposits, obsidian domes of silicic composition as well as basaltic spatter cones and flows inside and around the caldera, particularly on the SE and NW flanks, where they appear to result from fissures of NNW direction. Basaltic flows, some of them very recent,

were also emitted along fissures of NNW direction, that is, the Red Sea trend and not the transverse alignment.

Mallahle stratovolcano is of similar size, despite a smaller summit caldera, 6 km in diameter and perfectly circular. The caldera is partly filled by late pyroclastics, partly emitted from Nabro. Several post-caldera obsidian domes and flows are observed on the north-western slope. An alignment of domes and flows is well developed along a fissure of Red Sea direction which seems to cross through between the two volcanoes. Fumarolic activity is present in the caldera (a thick vegetation relates to hydrothermal venues) and along the flanks, particularly the western.

Bara Ale is also a stratovolcano aligned with the other two. Despite being less high, it displays a 7.5×6 km caldera which is almost completely infilled by lavas emitted



Fig. 8.3 View of some of the recent pantellerite domes and flows emitted along NNW trending fissures on the SW foot of Ma'alalta volcano. Image Google Earth Pro

from a cone located in its centre. Differing from Nabro and Mallahle, where pyroclatites dominate, this silicic unit appears to be made of lava flows of trachytes and rhyolites. This lack of gaseous components relates to its position away from the outcropping basement.

In addition to the major calderas, two other distinct volcanic units are observed in the vicinity of Nabro stratovolcano (Figs. 8.7 and 8.8):

- The Mabda rhyolitic centre made of viscous rhyolites and trachytes, partly covered by more recent basalts, along the same transverse alignment to the NE foot of Nabro.
- The Sork Ale cumulo-volcano located on the SE slope of Mallahle stratovolcano, a “typical” textbook volcano, 1500 m in diameter, 1500 m high with steep slopes and a regular summit crater 300 m deep.



Fig. 8.4 Fairly recent domes and viscous obsidian flows emitted to the south of Ma'alalta along the same fissure as observed in Fig. 8.3, postdating basalts and lavas of intermediate composition. A recent basaltic fissural lava field developed further south (as seen in a small part on the SE corner). Satellite image extracted from Google Earth Pro

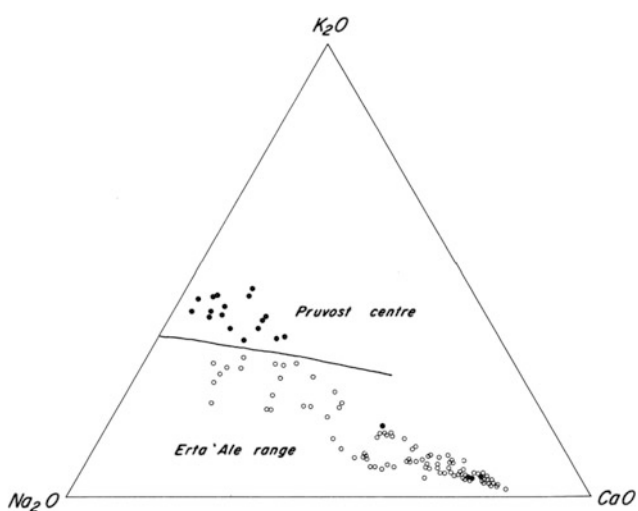
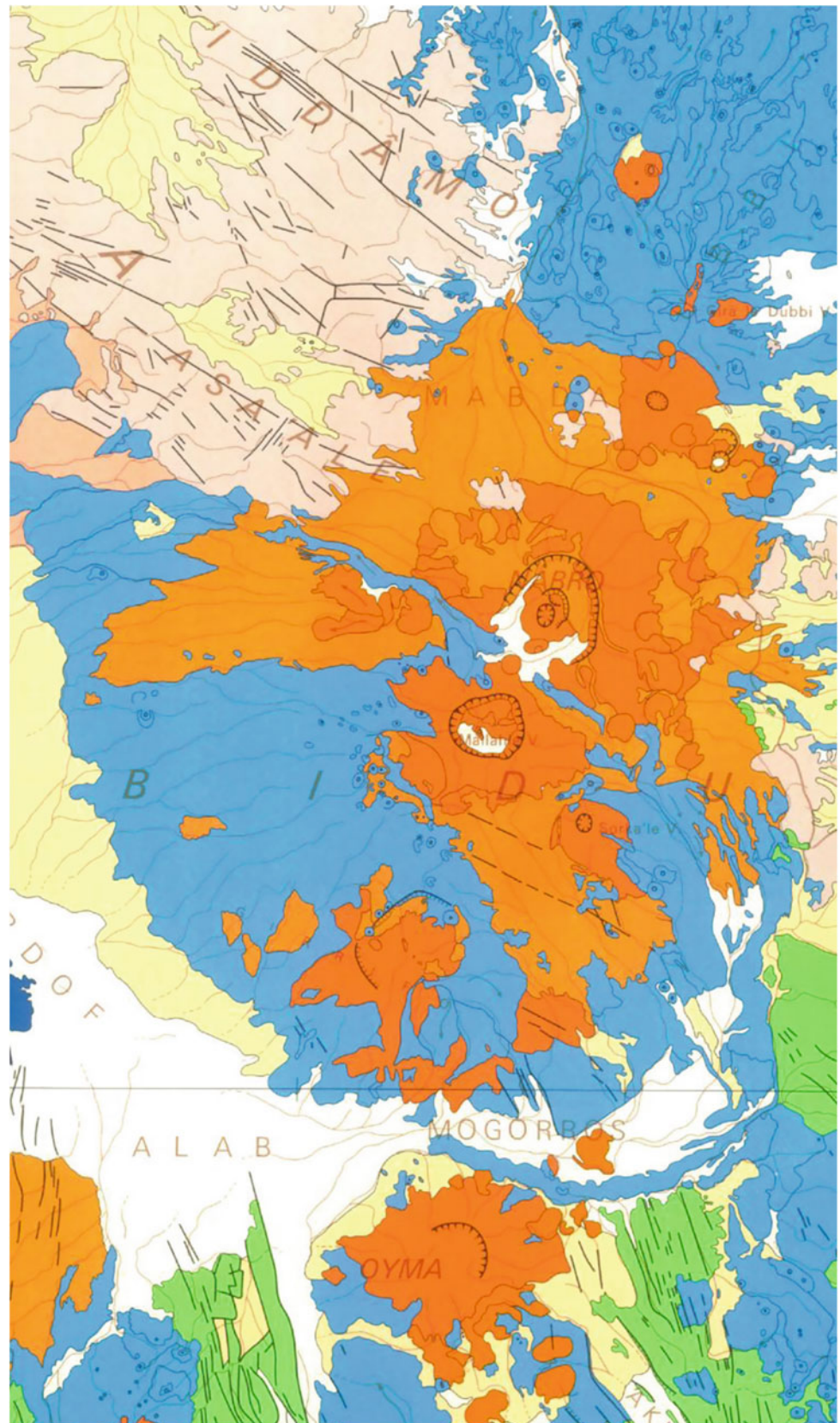


Fig. 8.5 Composition of the volcanic products of Ma'alalt—Pierre Pruvost volcanic centre (black dots) compared with those of Erta Ale range (open circles). From Barberi et al. (1970)

The Nabro volcano made itself known in 2011 with an eruption that began on 12 June 2011 after a series of earthquakes and emitted an ash plume rich in H_2O and other gases, including the highest level of SO_2 ever observed on Earth which disrupted airline traffic in the region as it reached 14,000 m high and extended for over 1000 km into Sudan (Fig. 8.9). Severe ash fall developed in the eastern Afar depression to the west of Nabro and was even felt in Mekele and Asmara. The salt exploitations in Afar had to stop because of the pollution by sulphuric acid particles. The eruption killed at least 7 people (and eventually up to 31) and directly affected the health of 5000 people in Eritrea and the food and water sources for 48,000 others in Afar (in particular in Afdera, Erebt, Elidar and Teru) as a whole. Satellite images showed a large volcanic eruption, which lasted at least from 12 to 30 June, with ash plume clearly visible on MODIS images from NASA's Aqua and TERRA satellites. Besides sulphur dioxide, water vapour, and ash emissions measured all along the period, a 15 km long lava

Fig. 8.6 Geological map of the Bid—Nabro transverse volcanic alignment of stratovolcanoes with calderas observed on the southern extremity of the Danakil Horst. Extracted from CNR-CNRS map (CNR-CNRS 1973)



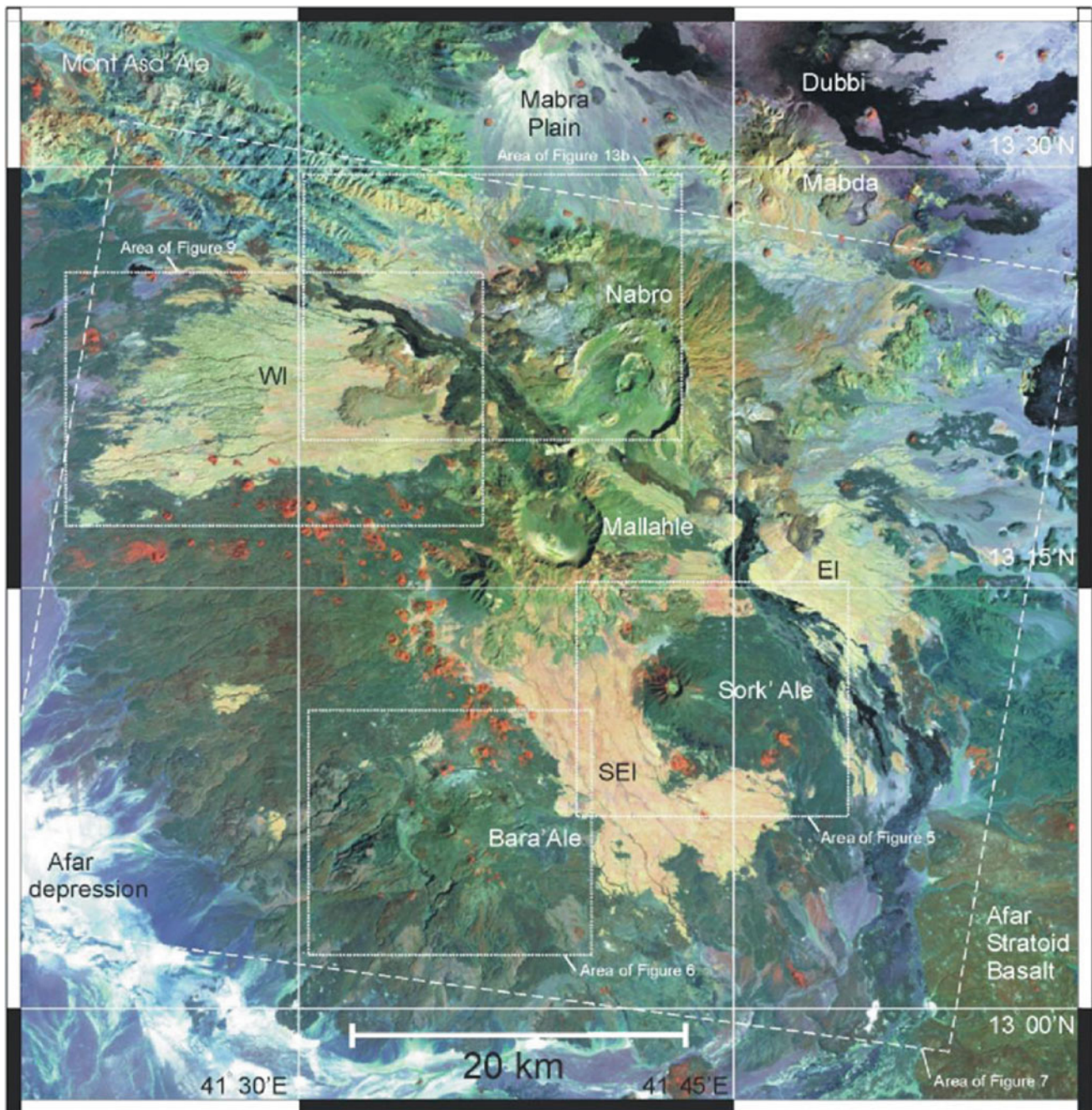


Fig. 8.7 Landsat-5 TM image showing the various volcanic units of Bidu volcanic complex (in February 1987, from Wyart and Oppenheimer 2005)

flow occurred on 19 June according to satellite images (Fig. 8.10) and the Eritrean government reported a lava flow still moving 20 m per day on 30 June. The ash and gas emission progressively weakened and were much reduced after 7 July.

However, the eruption did not totally cease as alerts were periodically emitted until June 2012.

The eruptive events were studied with the use of INSAR images between 1 July 2011 and 10 October 2012, as well as seismic records for 658 earthquakes detected in the period 21

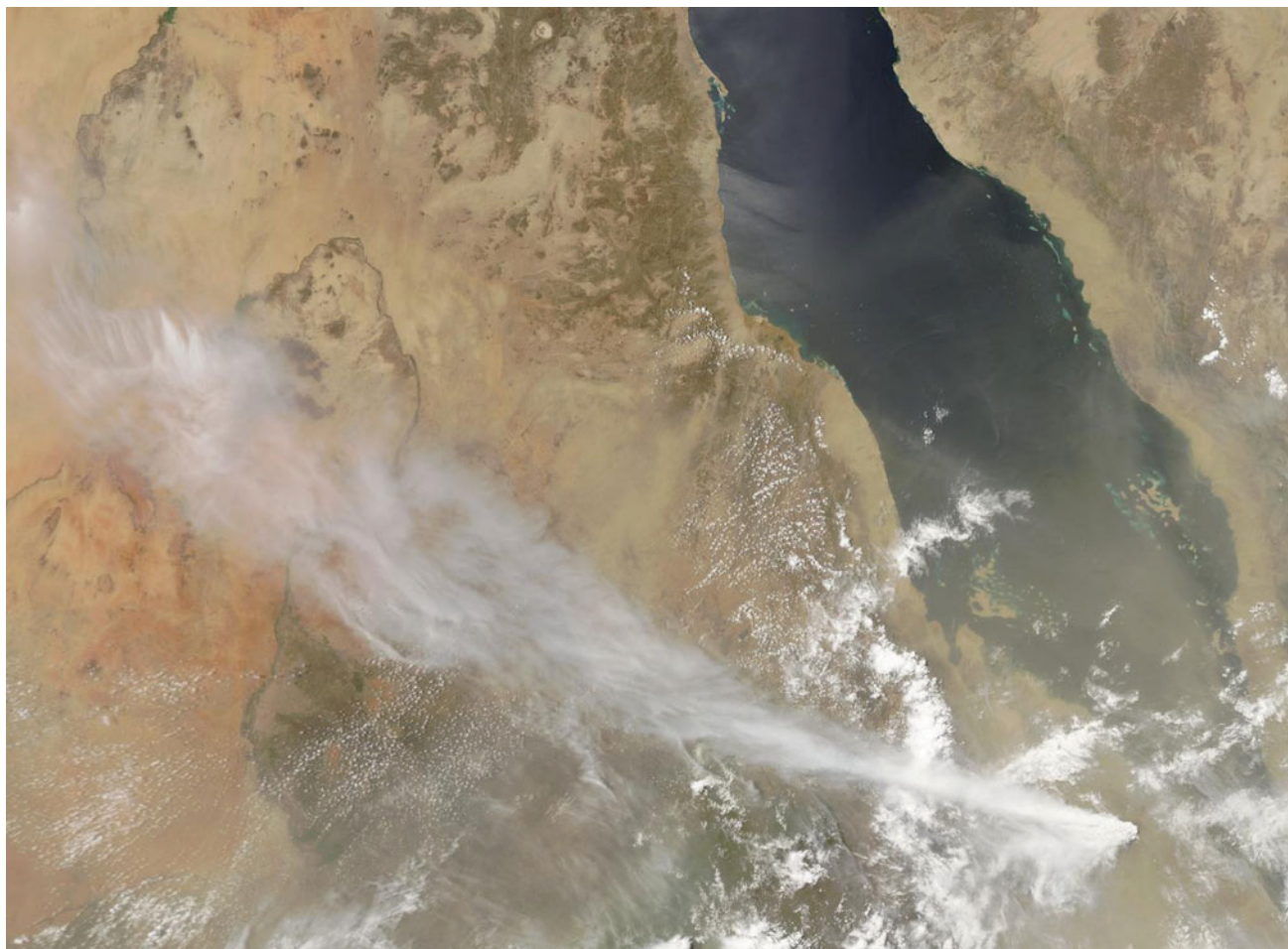


Fig. 8.8 The Nabro plume seen from NASA AQUA MODIS satellite extending NW in Eritrea, Ethiopia and Sudan

Aug to 7 October 2011, with an exhaustive synthesis published by Hamlyn et al. (2014). A set of seismic events was clearly shown beneath both Nabro and Mallahle calderas, displaying a NE-SW alignment corresponding to the Bidu axis. A post-eruptive circular subsidence signal was identified centred on the SW side of the Nabro caldera topography, but apparently the ring caldera faults were not reactivated. The depth of the magma body calculated from the surface deformation was 6.9 ± 1.1 km or 11 ± 2 km depending on the model, whereas the seismic activity indicated one 11-km source beneath both volcanoes and shallower events in the 7–4 km depth range beneath the two calderas with shallower events under Nabro crater only (Fig. 8.11).

As a whole, the seismic events recorded during this period following the major volcanic eruption, combined with

the study of the catalogue of earthquakes in the region, confirm the hypothesis proposed by Barberi et al. (1974) of a transverse structure which developed through rejuvenation of a tectonically weak zone predating the rift formation. Fault planes show a NE-SW strike which dips 45° to the SE, cross-cutting the caldera floors. The catalogues show a well-delineated NE-SW striking alignment of earthquakes that show a tensional motion with a strike slip component, which can be interpreted as resulting from a transform motion partly accommodated by magma injection. These observations are consistent with the “leaky transform fault” proposed by Barberi and Varet (1977) such as the southern plate boundary of the Danakil block (called Arrata) along this transverse structure.



Fig. 8.9 True colour image from June 19, 2011 showing area affected by pyroclastic deposits, NASA. <http://rapidfire.sci.gsfc.nasa.gov/gallery/?2011170-0619/Eritrea.A2011170.1010.250m.jpg>

8.3 Moussa Ali

Moussa Ali is a central volcano which marks the triple boundary of Eritrea, Ethiopia and Djibouti, and was described in detail by De Fino et al. (1973). With an altitude of 2021 m, it is the highest point in Djibouti Republic. The volcano is made of a pile of lava flows, with basalts dominating at the base and intermediate, trachyte and rhyolites forming the viscous lavas emitted in the summit part (Fig. 8.12).

The volcano covers the stratoid series and could be looked on as one of the numerous silicic centres found in the upper part of this trap basalts unit if it was not seated along the limit of the Afar depression, in the area where one passes from the

deeply faulted stratoid series in the SW to the quite area bordering the southern extremity of the Red Sea, unfaulted since eight million years ago. Three tectonic lines cross each other at the level of the volcano, which probably explains the development of the magma chamber that allowed for its construction and petrologic evolution (Fig. 8.13):

- The dominating NW-SE normal faulting, with downthrows mainly oriented towards the depression.
- The N-S faults of the Makarasou transform structure that hits Musa Ali floor to the north and ends there. These faults, with extensional components, result in block tilting towards the west and downthrows oriented opposite to the depression.

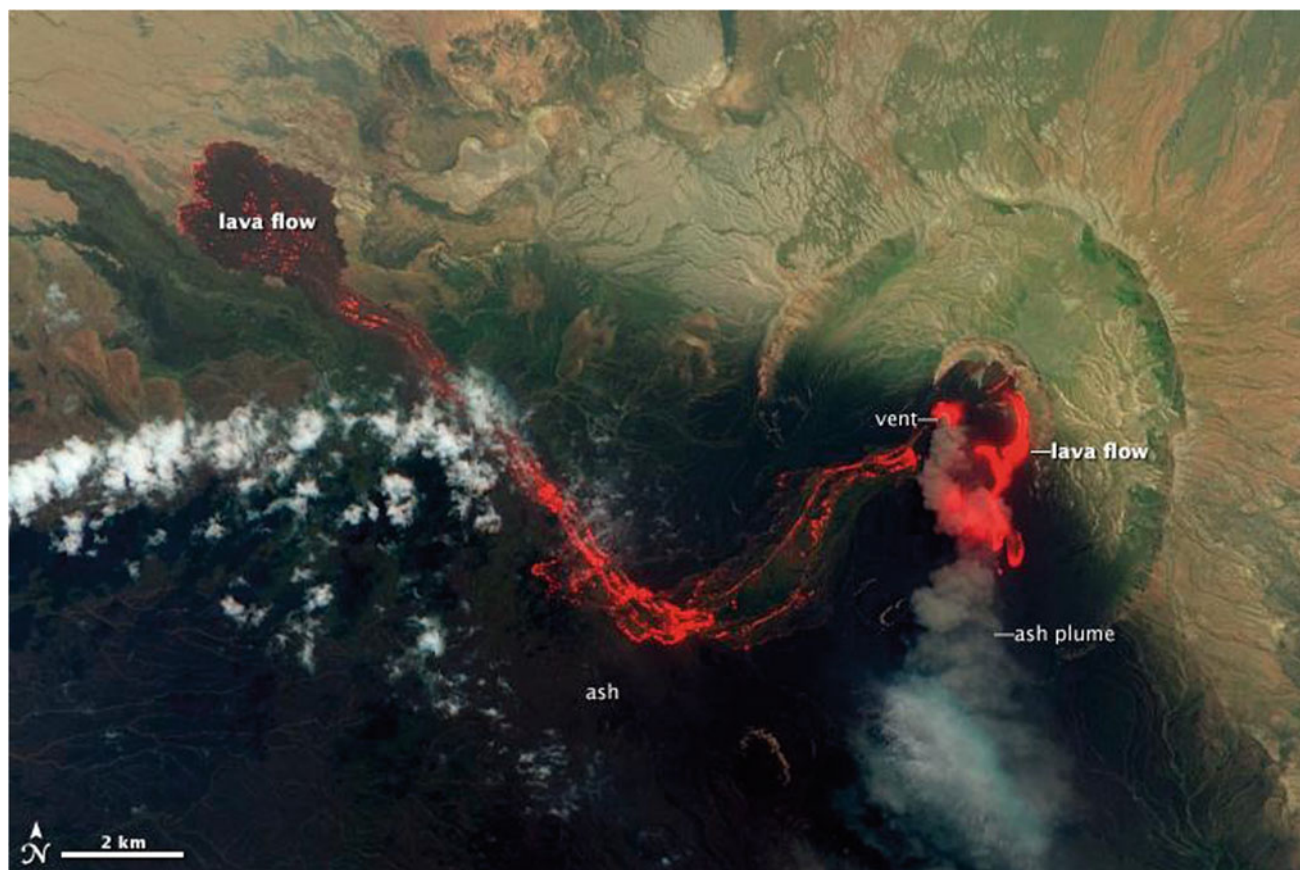


Fig. 8.10 Satellite view of Nabro by NASA showing the lava flow issued from the central crater on June 19, 2011

– A well-developed E-W line of extension, which is not much expressed in the tectonics, except for some of the faults of the caldera complex, but gave birth to an alignment of scoria cones and associated basaltic flows along two lines in an E-W direction. The Moussa Ali caldera system (4.5 km long in the E-W direction and 3 km wide, with a smaller late caldera 1 km in diameter) is rather complex, with faults controlled by this regional context plus NE-SW faults visible in the summit and northern part. The southern extension of this discontinuity corresponds to the place where the WNW-ESE Manda axial range passes to the NW-SE Inakir shield. The sequence is not unique, and if silicic lavas are more abundant in the summital part, basalts, trachytes and mugearites may be found in any sequence.

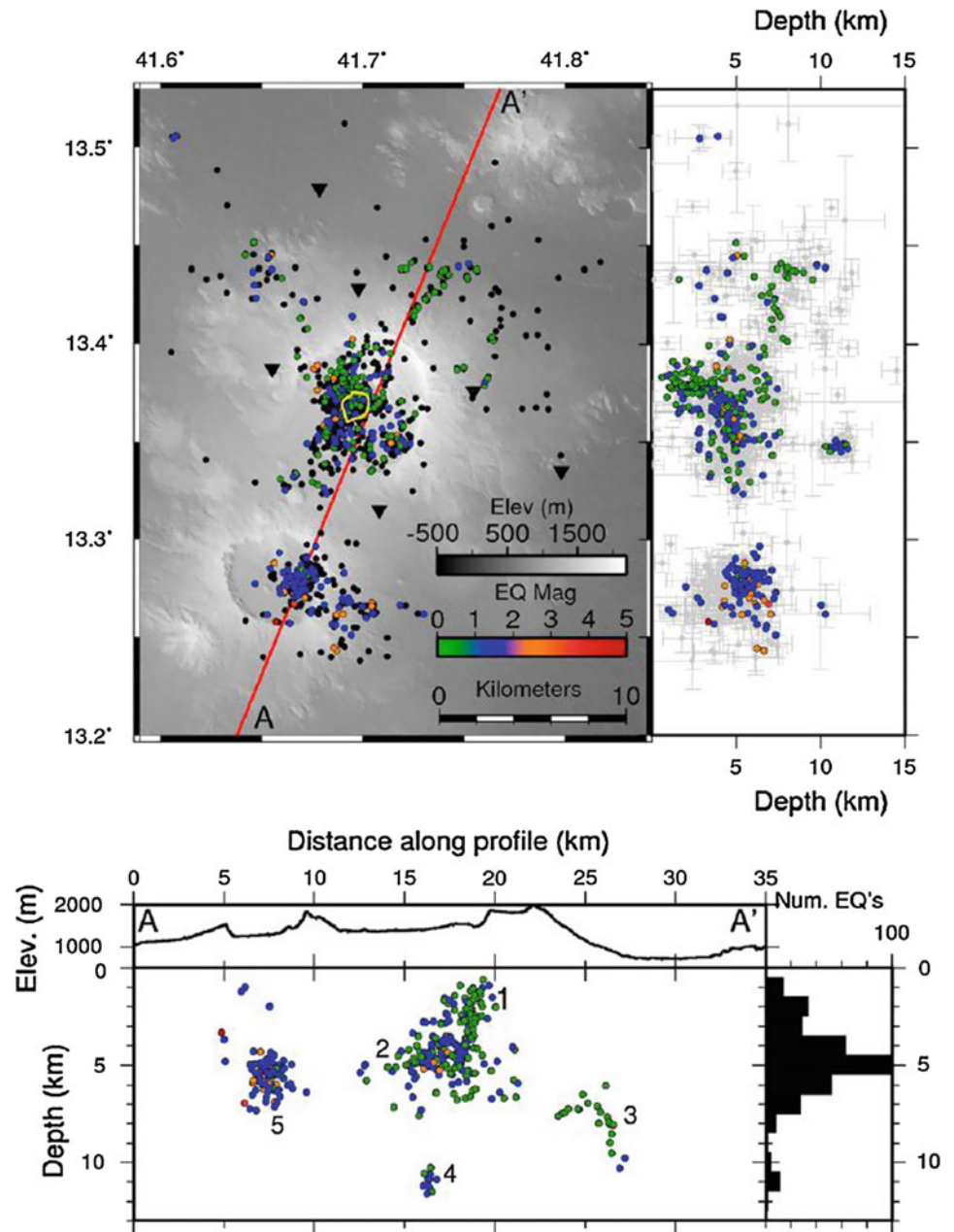
A complete series of terms ranging from alkali olivine basalts to porphyritic (fayalite and anortholase) trachytes and rhyolites has been sampled and analysed by De Fino et al. (1973). No hydroxylated minerals have been found, the

series displaying continuous sequences of olivine (Fa 13 to Fa 77) and clinopyroxenes. Chemically the whole sequence is more alkaline than the axial ranges, with higher potassium/sodium ratio. The final products are moderately saturated (13% normative quartz) and slightly peralkaline. The scarcity of pyroclastic products differs from the Ma'alalta, Nabro and Mallahle, and probably relates to the absence of a pre-Mesozoic basement. The whole sequence—which displays analogies with the Hawaii alkali trend—was considered as resulting from crystal fractionation in a well-developed magma chamber resulting from this multiple distensive tectonic crossing.

8.4 Comments About These Volcanic Centres of Afar Margins

Besides their location along the Afar margins, these centres display characteristics of interest:

Fig. 8.11 Top: Initial hypocentre locations for the 658 earthquakes detected in the period August 21 to October 7, 2011 shown as *black dots* on the map and *grey dots* with errors bars on the depth profile (bottom). A total of 456 relocated hypocenters are shown as *coloured dots*, dependent on their magnitude. *Black triangles* indicate the location of the seismic stations. Depths are given referenced to 700 m above sea level



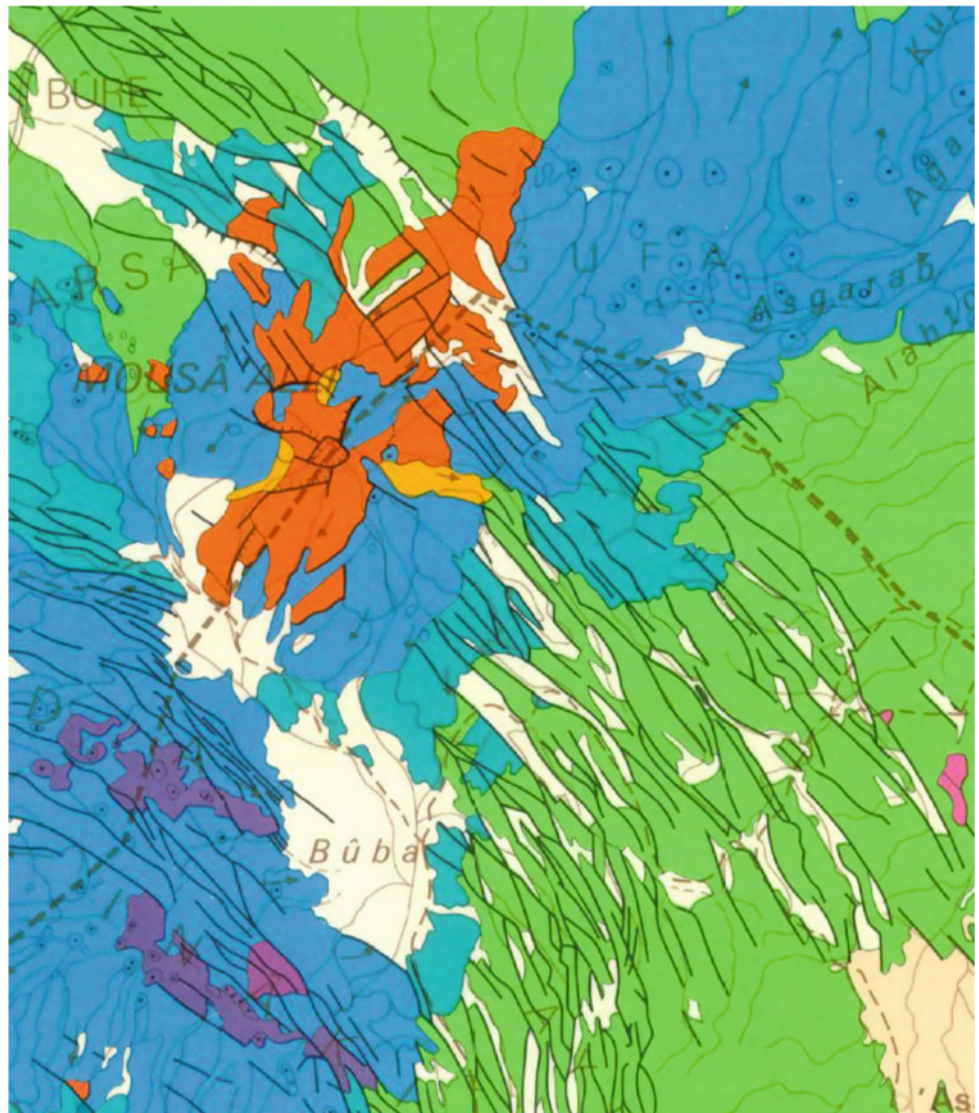
- A diversity of volcanic products, with abundant silicic terms (rhyolites) with pyroclastic products (ignimbrite, pumice, ash fall) associated with lava flows and domes.
- The presence of calderas, sometimes embryonic as in Moussa Ali or well developed and complex (successive caldera collapses) as in Ma'alalta or Bidu.
- Their location in a tectonic environment where transverse tectonic structures (E-W to NE-SW trending faults analogous to fracture zones) played a determinant role in the genesis and development of these units, including the characteristics of the volcano superstructure (the shape of the caldera in particular).
- The interaction of magmas of mantellic origin with the sialic crust of the thinned underlying basement, well documented in Ma'alalta.

As a whole, these units display quite a few analogies with the volcanic centres of the MER, and more generally of the eastern branch of the EARV. Further comparative studies would be fruitful to understand better the origin and behaviour of these typical features of the EARV. Including, in particular, the understanding of the development of their hydrothermal systems, as these units appear to be interesting targets for geothermal energy development.

Fig. 8.12 View of Moussa Ali volcano as seen from its southern foot (Photo J. Varet 2012)



Fig. 8.13 Moussa Ali volcano and its complex caldera. Observe the regional NW-SE dominant normal faulting that disappears north of the volcano, as well as the N-S Makarasou faults that also end at the level of the volcano, whereas Gufa is characterised by E-W basaltic emission fissures developed at the eastern foot in the direction of the Red Sea (from Varet 1975)



References

- Barberi F, Varet J (1977) Volcanism in Afar: small-scale plate tectonic implications. *Bull. Geol. Soc. Amer.* 88:1251–1266
- Barberi F, Bonatti E, Marinelli G, Varet J (1974) Transverse tectonics during the split of a continent data from the Afar Rift. *Tectonophysics* 23:17–29
- Barberi F, Borsi S, Ferrara G, Marinelli G, Varet J (1970) Relations between tectonics and magmatology in the northern Danakil Depression (Ethiopia). *Philosophical Trans. Royal Soc. London* A267:293–311
- Barberi F, Tazieff H, Varet J (1972) Volcanism in the Afar depression: its tectonic and magmatic significance. *Tectonophysics* 15:19–29
- CNR—CNRS Afar team (1973) Geology of northern Afar (Ethiopia). *Rev Geogr Phys Geol Dyn* 15:443–490
- De Fino M, La Volpe L, Lirer L, Varet J (1973) Geology and petrology of Manda-Inakir range and Moussa Alli volcano, central eastern Afar (Ethiopia and T.F.A.I.). *Rev Geogr Phys Géol Dyn* 15(2):373–386
- Hamlyn JE, Keir D, Wright TJ, Neuberg JW, Goitom B, Hammond JOS, Pagli C, Oppenheimer C, Kendall JM, Grandin R (2014) Seismicity and subsidence following the 2011 Nabro eruption, Eritrea: Insights into the plumbing system of an off-rift volcano. *Journ Geoph Res Solid Earth*
- Varet J (1975) L'Afar, un "point chaud" de la géophysique. *La Recherche* 62:1018–1026
- Wiat P, Oppenheimer C (2005) Large magnitude silicic volcanism in north Afar: the Nabro volcanoc range and Ma'alalta volcano. *Bull Volc* 67:99–115

Another volcanic feature characterises the Afar margins: volcanic—dominantly basaltic—alignments of scoria cones and associated lava flows issued from E–W to NE–SW, feeding fissures that frequently relate to discontinuities affecting the pre-Tertiary basement, and express deep lines of weakness in these intraplate crustal areas. These volcanic transverse structures are shown as dotted lines in the sketch map of Afar, Fig. 6.1.

9.1 Dubbi (Eritrea)

A wide recent Quaternary basaltic lava field develops on the Afar margin, along the Red Sea ($13^{\circ} 39'–14^{\circ} 45'N$), with flows emitted from the continent and reaching the sea over a length of 75 km south of Eddi, covering a width of 40 km over a total surface area of 2800 km². The scoria cones from which they erupted are scattered over a wide surface from the upper SW side on the flank of the Nabro volcano to the Red Sea where emission centres are also visible in small islets, at least two of them clearly trending SW–NE in the direction of the feeding dikes. This basaltic fissural unit globally display a WSW–ENE orientation, although with no fault visible at the surface (Fig. 9.1), and a few spatter cones are also aligned in the NNW–SSE (Red Sea) direction.

Dubbi last erupted in May 1861. Earthquakes associated with the opening phase of the eruption were felt in Yemen and the explosion heard as far away as Massawa (330 km NW). Two villages were destroyed and more than 100 local inhabitants were reported killed by the pumice eruption, showering maritime traffic in the Red Sea and plunging coastal settlements into darkness. By October the activity switched to basaltic fire-fountaining along a 4 km-long summit fissure that fed several lava flows up to 22 km length, reaching the sea. Nineteen small craters were numbered aligned along a fissure of NNW–SSE direction. The volume of lava flows, estimated at 3.5 km³, makes this the largest reported historical eruption in Africa (Wiar et al.

2000). In 1862, an anomalously cold northern hemisphere summer (recorded in tree-ring records) could have resulted from Dubbi's eruption. The black basaltic lavas of this historic eruption are clearly visible on satellite images, as well as the remnants of the pumice fall (Fig. 9.2).

Apparently, another eruption that reached the Red Sea occurred in 1400 AD. The vents were located along a NW–SE fissure system still visible in the terrain.

Several basaltic islands corresponding to emission centres are visible along the sea coast south of Eddi. Kod Ali ($13^{\circ} 57' N, 41^{\circ} 49'E$) is a single diatreme structure resulting from the erosion of a former hyaloclastite cone. It was studied by Hutchison and Gass (1971) who showed that it was made of alkali basalts containing peridotite inclusions. These peridotites are considered to be fragments of mantle material.

This volcanic unit clearly relates to the Hanish-Zukur Islands located to the west in the Red Sea. Together with Bidu volcanic units, they are considered by the author to be the southern limit of the Arrata block (“Danakil Alps” microplate). That is a major plate boundary in Afar that allows for the Red Sea oceanic rift to disappear further south and to be totally replaced by the spreading segments within Afar (Barberi and Varet 1977). The alkali basaltic nature of the products and the presence of peridotite inclusions are taken as indices for a leaky transform fault, and the fact that the characteristics of the volcanoes evolve from dominantly acidic to exclusively basaltic along the Dubi-Biddu-Hanish line is consistent with a more leaky transform to the east than to the west in order to accommodate for the rotation of the Arrata block (Fig. 9.3).

9.2 Hanish-Zukur (Red Sea Islands)

The Hanish-Zukur volcanic islands group is situated in a NE–SW direction in the middle of the Red Sea, which is transverse to the spreading axis and aligned with Dubbi unit on land. Hanish Island group was studied in detail by Gass

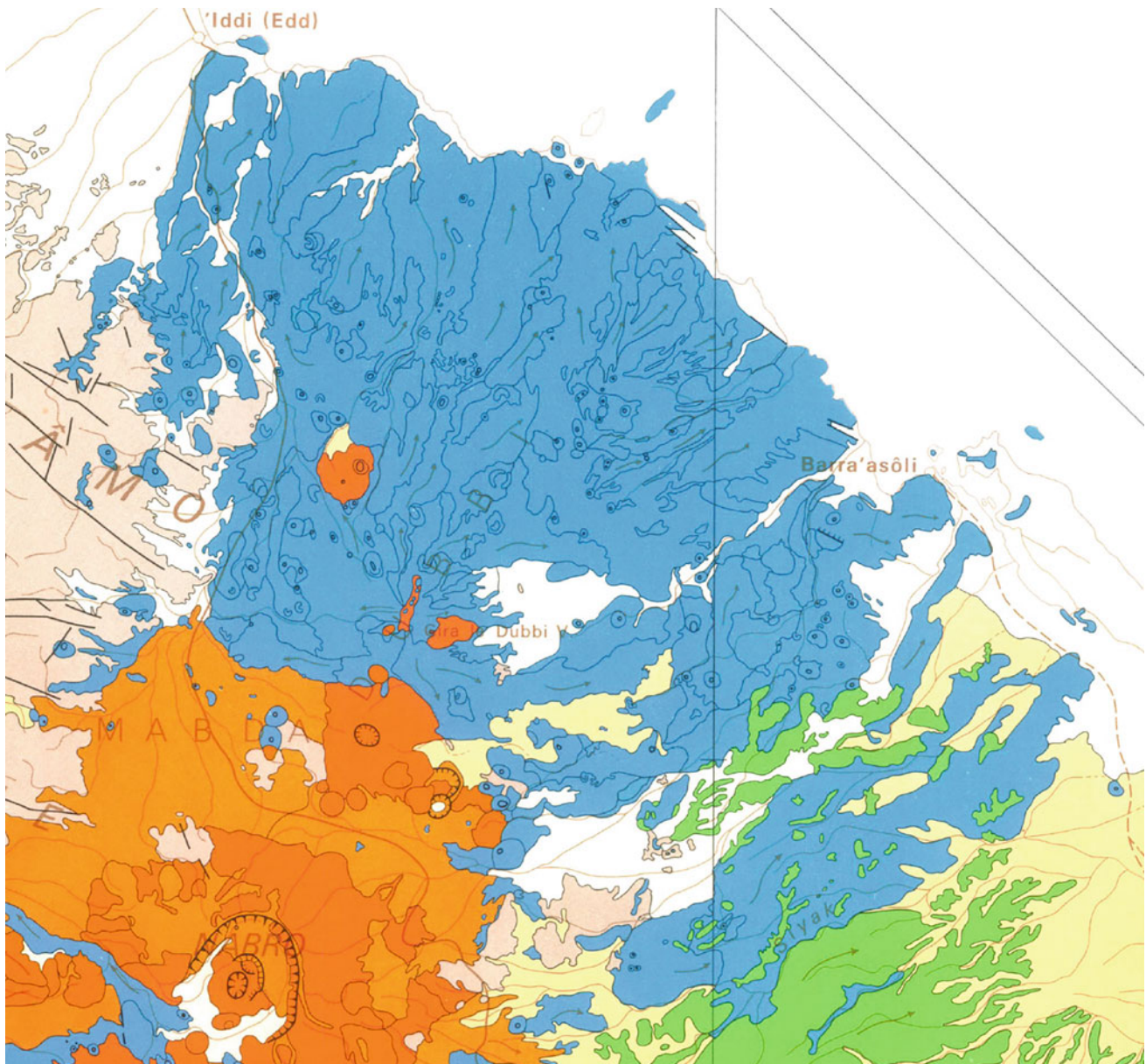


Fig. 9.1 The Dubbi basaltic lava field (*blue*) south of Edd along the Red Sea in southern Eritrea (from CNR–CNRS 1973). To the north it covers the pre-Mesozoic basement (*beige*), whereas to the south it covers the unfaulted, eroded stratoid series (*pale green*)

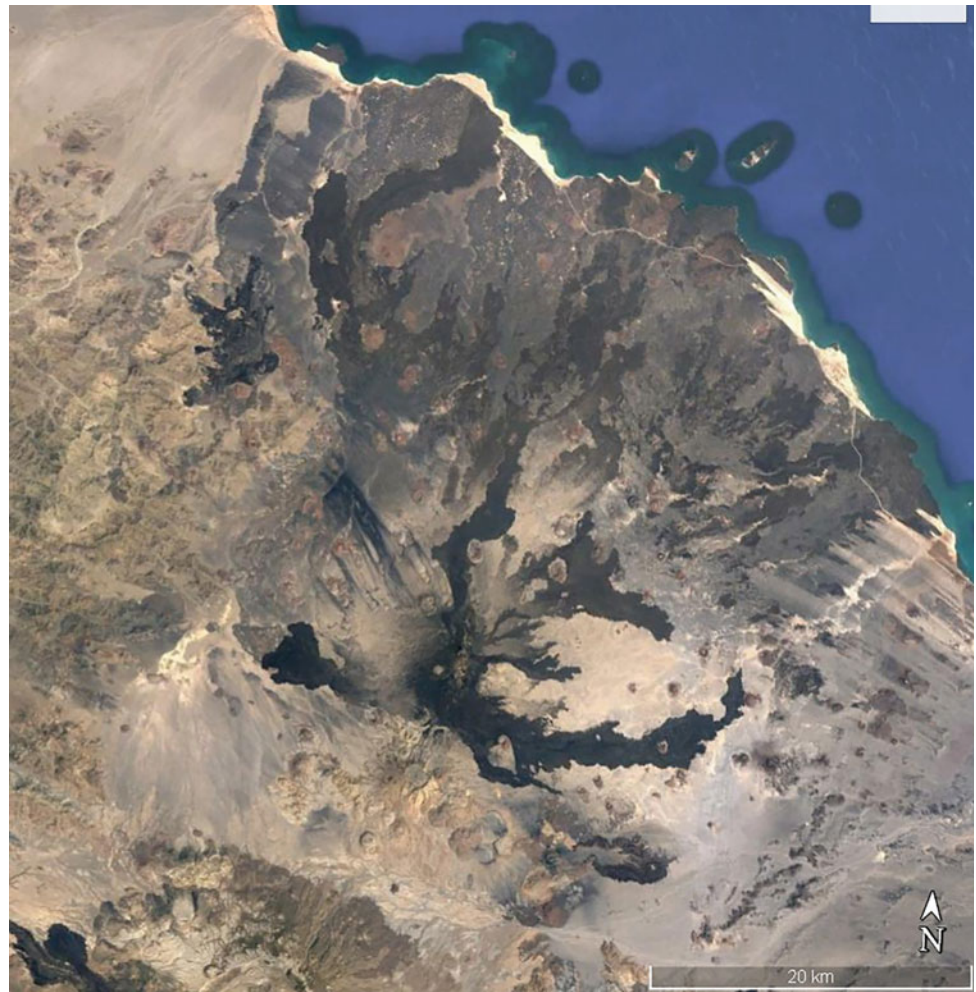
(1970), which showed that they are made of alkali olivine basalts. This contrasts with the Ramad sea mount located to the north in structural alignment with the Red Sea axis, whose lavas are made of tholeiitic basalts similar in composition to the composition of the submarine basalts dredged from the Red Sea axial valley (Schilling 1973).

Hanish Island group ($13^{\circ} 72'N$, $42^{\circ} 73'E$), 422 m above sea level at the highest point, shows a structure built along two NE–SW trending fractures (Fig. 9.4). A third emissive fracture is seen between Hanish and Zukur, expressed by a rock alignment.

Zukur Island ($14^{\circ} 02'N$, $42^{\circ} 75'E$) is also controlled by feeding dikes of the same NE–SW transverse direction along at least three distinct fissures, combined with a minor Red Sea trend observed on the NE extremity of the island (Fig. 9.5).

Note that both Hanish and Zukur remained inactive historically whereas Zubair, located 120 km north ($15^{\circ} 3'N$, $42^{\circ} 10'E$), which includes a group of 10 major volcanic islands on top of an underlying shield volcano, continued to erupt in historic times (Fig. 9.6). Differing from Hanish and Zukur, the volcano was built on a NNW–SSE rift line.

Fig. 9.2 The Dubbi volcanic lava field, as seen from satellite image south of Edd along the Eritrean Red Sea coast. The lava flows emitted during the 1861 eruption are visible in *black*, covering a pumice layer clearly visible (*pale colour*) all around the emission centre that displays a NE–SW orientation, with a late NNW–SSE emissive fissure. (Google Earth Pro image)



Eruptions occurred in 1824, and in 2011–2012 and a new island had grown by 710 m in January 2012, followed in September 2013 by a new submarine eruption southwest of the 2011–2012 site, which emerged from the ocean in late October 2013. This activity in the Southern Red Sea was studied in detail by Xu et al. (2015), showing significant increase of the seismicity since 2007, before an eruption that took place on Jebel at Tair Island. At least six seismic swarms have occurred in the past 20 years, probably resulting from separate magma intrusions. Three of them—in 2007, 2011 and 2013—were followed by eruptions within a year.

The south Red Sea islands were also studied by Volker et al. (1997) who showed the geochemical affinity of Ramad sea mount and the Zubair group with the Red Sea, whereas Hanish and Zukur are interpreted as influenced by the Afar plume.

Seismicity shows that the Southern Red Sea region, in Hanish-Zukur and Zubair area, is an active plate boundary separating the Danakil block from the Arabian plate. This has also been inferred by GPS data, which show a residual rate of opening of around 6 mm/year at the latitude of Zubair,

whereas at the same level in Afar the Erta Ale range accommodates for around 10 mm/year opening. The Red Sea spreading axis, if still active at this latitude, progressively dies out at the level of Hanish-Zukur where it hits against the leaky transform that connect through Dubbi-Bidu with the active Afar spreading segments further to the SW.

9.3 Ado Ale (Assab Range, Eritrea)

The Ado Ale transverse basaltic alignment is an important Quaternary unit at 13°N extending over 80 km (from 42° 00' to 42° 45'E) above sea level to the west of Assab which also gave the name to the range (Fig. 9.7). Numerous spatter cones emitted flows of alkali olivine basalt and associated composition (De Fino et al. 1973). Although no fault is visible at the surface except for a few NW–SE trending fissures, it seems that at least two distinct fissures of E–W direction contributed to feed this unit.

If alkali-olivine-basalts and hawaiites largely dominate, some mugearites and benmoreites are also present as well as

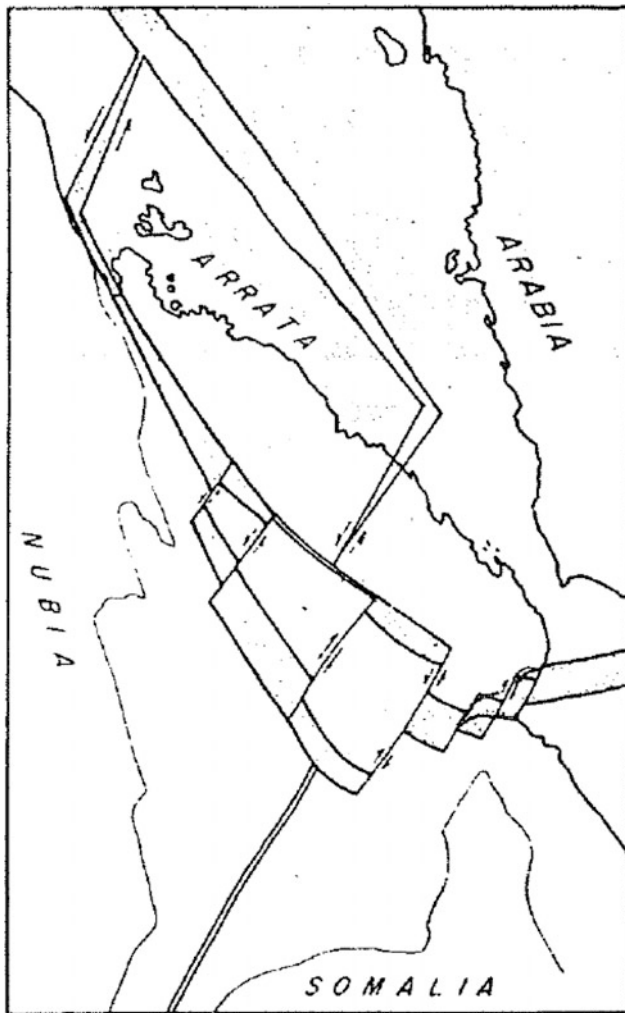


Fig. 9.3 Schematic representation of the last phase of spreading in Afar, as interpreted from volcano-structural and petrology by Barberi and Varet (1977). Stippled areas are zones of oceanic crust produced during the last 3.5 million years of spreading segments (axial ranges in Afar) or leaky transverse fractures (Bidu-Dubbi-Hanish) enlarging towards East in coherence with the well-developed basaltic fissural activity in Dubbi and Hanish Islands

a few rare occurrences of trachyte. They cover the stratoid series that outcrops unfaulted to the north and south of the range. The earliest age obtained within this unit is 0.6 million years (Civetta et al. 1975), and the activity was apparently nearly continuous until recent times. One of the flows emitting north in the middle of the range could be sub-historic (Fig. 9.8).

Several craters and flows in the range contain ultrabasic xenoliths and one of the craters called Heltagi, near Assab airport, was identified by us as particularly productive as it contains a diversity of xenoliths including dunites, hartzburgites, lherzolites, peridotites, pyroxenites, gabbros and anorthosites. Pyroxene, plagioclase and olivine

megacrysts are also found, sometimes automorphous in this and other craters of the range.

These inclusions were studied in detail by Ottonelo et al. (1978) with mineralogical, petrological and geochemical approaches. Two families of inclusions were identified: (1) mantle xenoliths made of spinel lherzolite, with minor dunites and lherzolites and (2) crustal xenoliths made of gabbros and peridotites with layered structures showing a magmatic origin.

It is worth noting that, despite the variety of rocks xenoliths carried to the surface and the number of sampling points, no trace of sialic crust was found in the range. As the same observation is valid for the other transverse units located along the Red Sea southern Afar margin (as well as in the earlier volcanic units of the area), we conclude that the thinned lithosphere identified by geophysics (Mackris et al. 1991) beneath the area rather results from earlier magmatic spreading than from continental stretching.

9.4 Gufa (South Eritrea)

As seen looking at Moussal Ali volcano (Sect. 7.3), another E–W trending (double) alignment of basaltic spatter cones of recent Quaternary age is observed north of the Eritrea-Djibouti border (Fig. 9.9) overlying the unfaulted stratoid series developed for over 35 km along the 12°35' parallel (Marinelli and Varet 1973). Basalts are alkaline in composition whereas olivine-rich facies are abundant and peridotite, gabbro, pyroxene and olivine megacrysts have been found in some of the craters. No E–W fault is visible but a dyke trending in that direction has been observed in one of the craters.

9.5 Sawâbi Islands (Sept Frères, Djibouti)

Seven hyaloclastite cones emerge in the Bab-El-Manded part of the Red Sea (Figs. 9.10 and 9.11); aligned in an E–W direction, five of them are islands, one a peninsula and the other in the coastal zone near Kor Angar (Djibouti Republic). These are made of basalts of constant alkali-olivine composition, with various types of ultramafic inclusions: peridotites, pyroxenites, and gabbros evenly layered.

9.6 Dabbayra (Western Afar)

South–west from the Teru plain, in correspondence with the shift from Alayta axial range to Manda Marraro, an important volcanic system developed on the second important right lateral offset of the Ethiopian scarp (Fig. 9.12). Despite

Fig. 9.4 Satellite image of Hanish Island group showing its clear alignments along NE–SW trending fissures transverse to the Red Sea Rift (Google Earth Pro), linking with similar volcano-tectonic trends on the western Afar margin



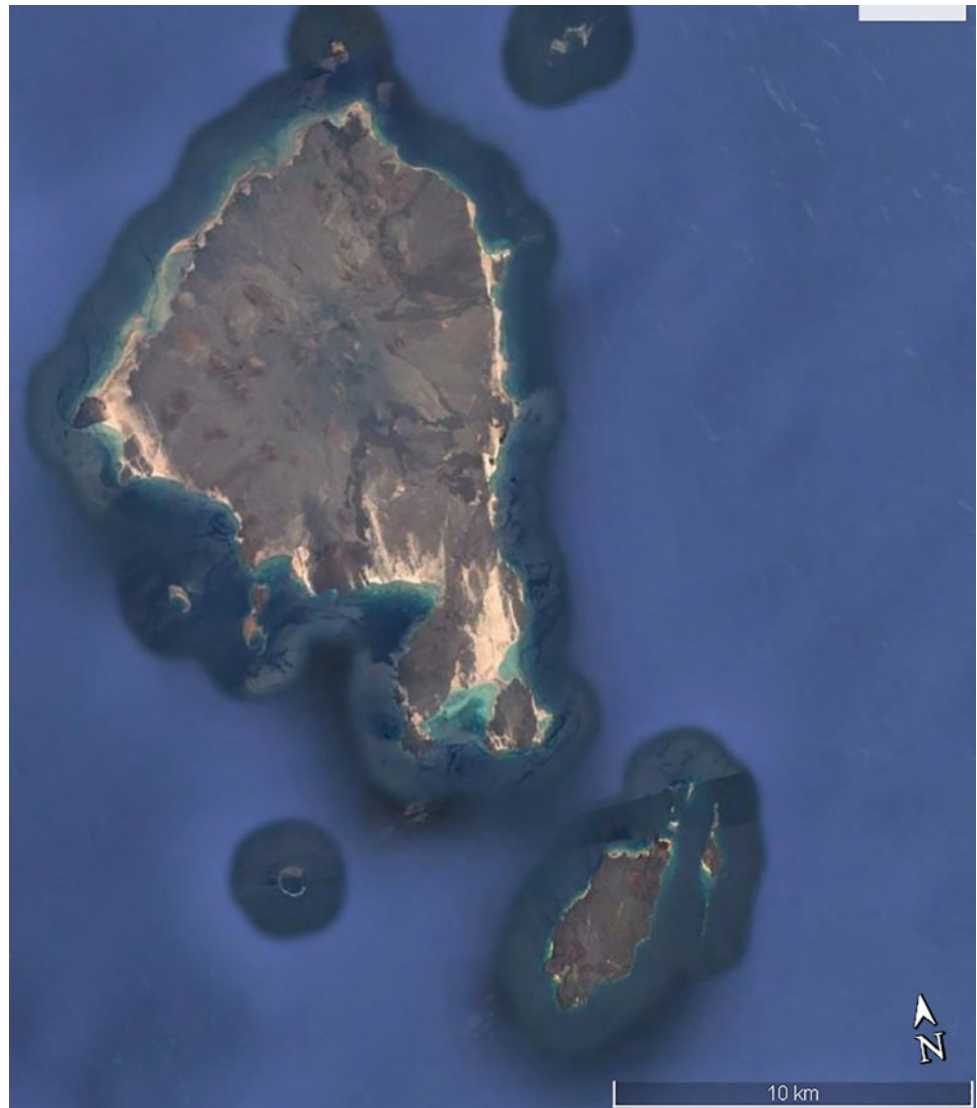
a similar location, Dabbayra differs from Ma'alalta as it is dominantly basaltic in composition, and in addition, this fissural system is deprived of caldera. As a whole, the edifice displays a shield volcano shape built along fissures of NNE–SSW (transverse) direction. Alignments of cones, domes and pyroclastics are, however, also observed along NNW trends.

This unit extends as a whole (60×30 km wide) from the Ethiopian escarpment foothills to the Teru plain where it marks the hydrogeological discontinuity between the Teru and Mille basins. It should be noted that this recent basaltic alignment extends far inside the basement foothill, marking an important fracture zone (Fig. 9.13).

9.7 Geodynamic Interpretation of These Transverse Units

All these transverse volcanic alignments display similar characteristics, with rather alkali basalt compositions compared with the transitional basalts with tholeiitic affinities of the axial ranges. They are also characterised by their fissural nature, but without any expression of rifting. Faults are generally not visible, except in Dabbayra where open fissures, apparently rather recent (and even contemporaneous with the Manda Harraro-Dabbahu event according to local sources), are observed. Ultrabasic inclusions are frequently

Fig. 9.5 Satellite image of Zukur Island, showing the combination of NE–SW and NNW–SSE feeding dikes and emissive fissures building the volcano (Google Earth Pro)



observed in these units, whereas they are apparently absent in the axial ranges and in the stratoid series.

Barberi et al. (1974) underlined the analogies of these units with the oceanic fracture zones where alkali basalts are also present, associated with ultrabasic rocks. These units were therefore considered as the possible surface expression of fracture zones. It is also a fact that these units generally occur along discontinuities of major importance. That is clearly the case for Dabbayra, which marks a major discontinuity in the escarpment. This is also the case for Dubbi that marks the southern extremity of the Arrata block

according to our interpretation.¹ We have noticed that these two discontinuities could be interpreted as a single fracture zone, an interpretation that would also explain the transform fault zone linking within Afar, Tat'Ali, Alayta and Manda Harraro through Dabbahu (see Sect. 6.4 and Fig. 6.78).

Let us emphasise that these fracture zones are clearly “leaky”, showing a component of mild N–S extension that affects the whole Afar area. Not so well expressed in the Afar floor, it happens to be more visible along the otherwise stabilised margins, such as in Ado Ale, Gufa and Sawâbi islands.

¹Most authors, even in the most recent publications, extend the Danakil block south down to the Gulf of Tadjourah.

Fig. 9.6 Satellite image of a volcanic eruption on the Zubair Island group aligned along NNW–SSE (Red Sea rift). (Smithsonian Global Volcanism program)

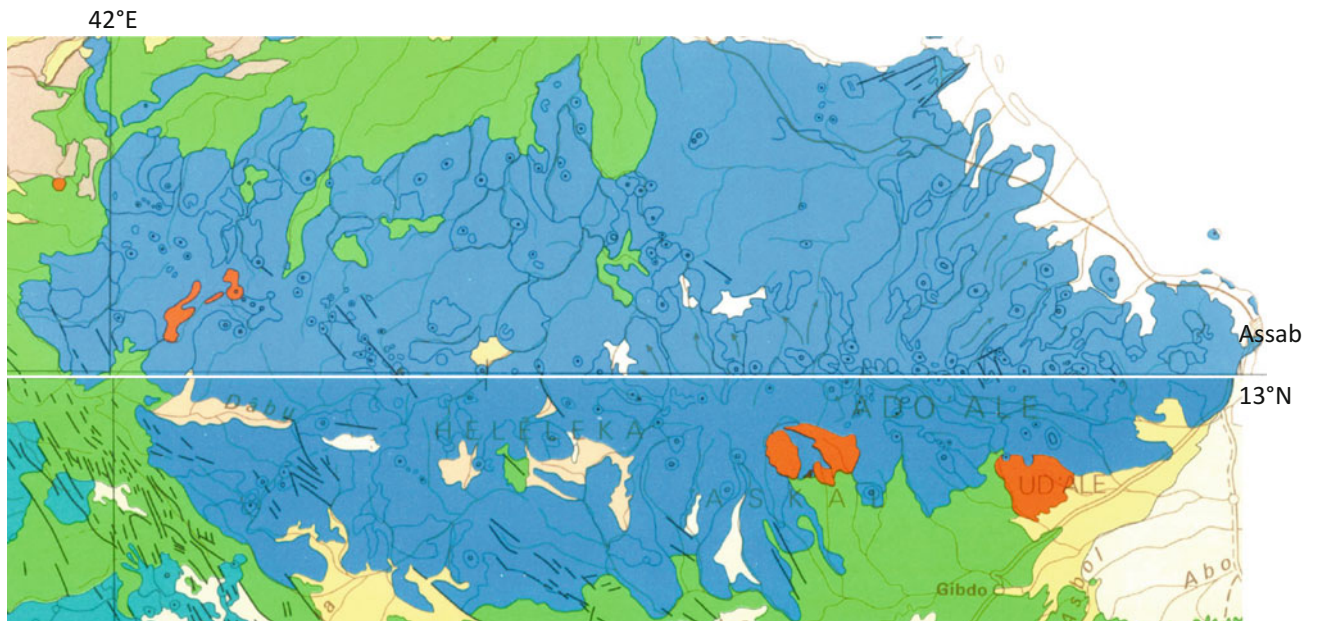
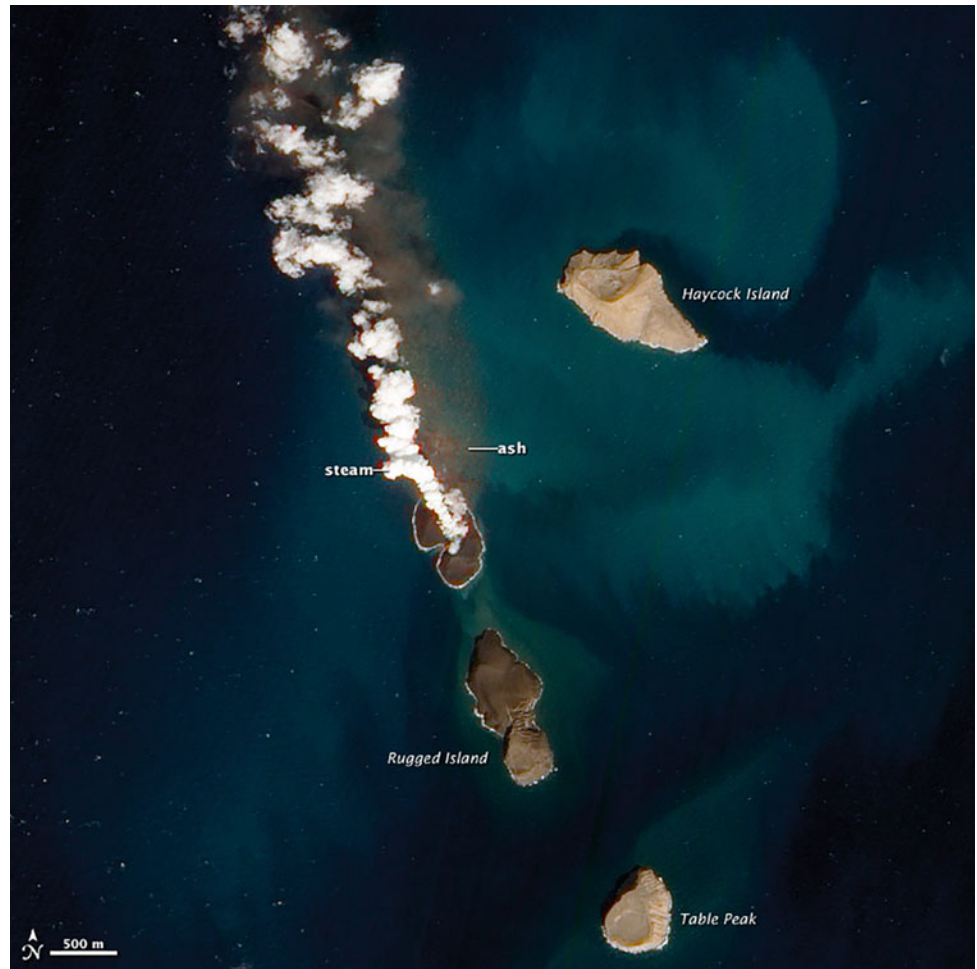


Fig. 9.7 Geological map of the Ado Ale transverse basaltic alignment located West from Assab port in Eritrea. Assembled from CNR–CNRS geological maps of Afar 1973 (north) and 1975 (south)



Fig. 9.8 Satellite image of Ado Ale range west from Assab port in Eritrea, showing a double alignment of scoria cones emitting flows on both sides of the E–W feeding fissures (from Google Earth Pro)



Fig. 9.9 Satellite image of Gufa range showing a double alignment of scoria cones emitting basaltic flows issued from E–W feeding fissures, east from Moussa Ali (from Google earth Pro)

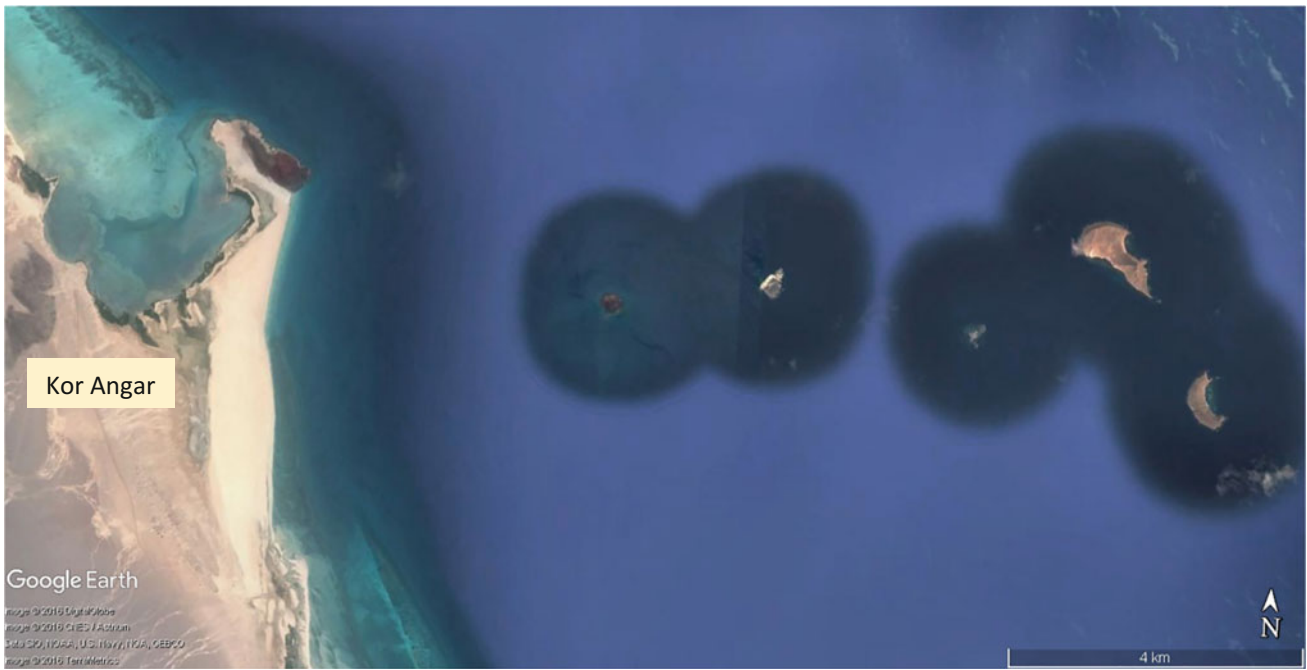


Fig. 9.10 Satellite image (composed by Google Earth Pro) of the Sawâbi (“Sept Frères”) volcanic alignment across the Bab-El Mandeb straight (Djibouti Republic)

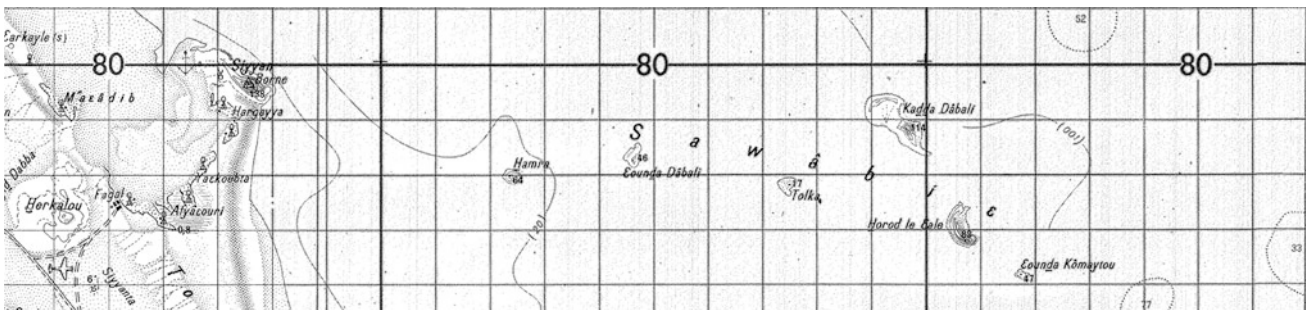


Fig. 9.11 Extract from the 1,100,000 IGN topographic map (Khor Angar sheet) showing the Sawâbi (“Sept Frères”) Islands (alkali basaltic hyaloclastite cones)

Fig. 9.12 The Dabbayra dominantly basaltic volcanic unit built on NE–SW trending fissures in an area where the pre-rift basement (dominantly volcanic—i.e., faulted trap basalts of the Nubian plateau—in this area). Extract from CNR–CNRS map by J. Varet (CNR–CNRS 1975)

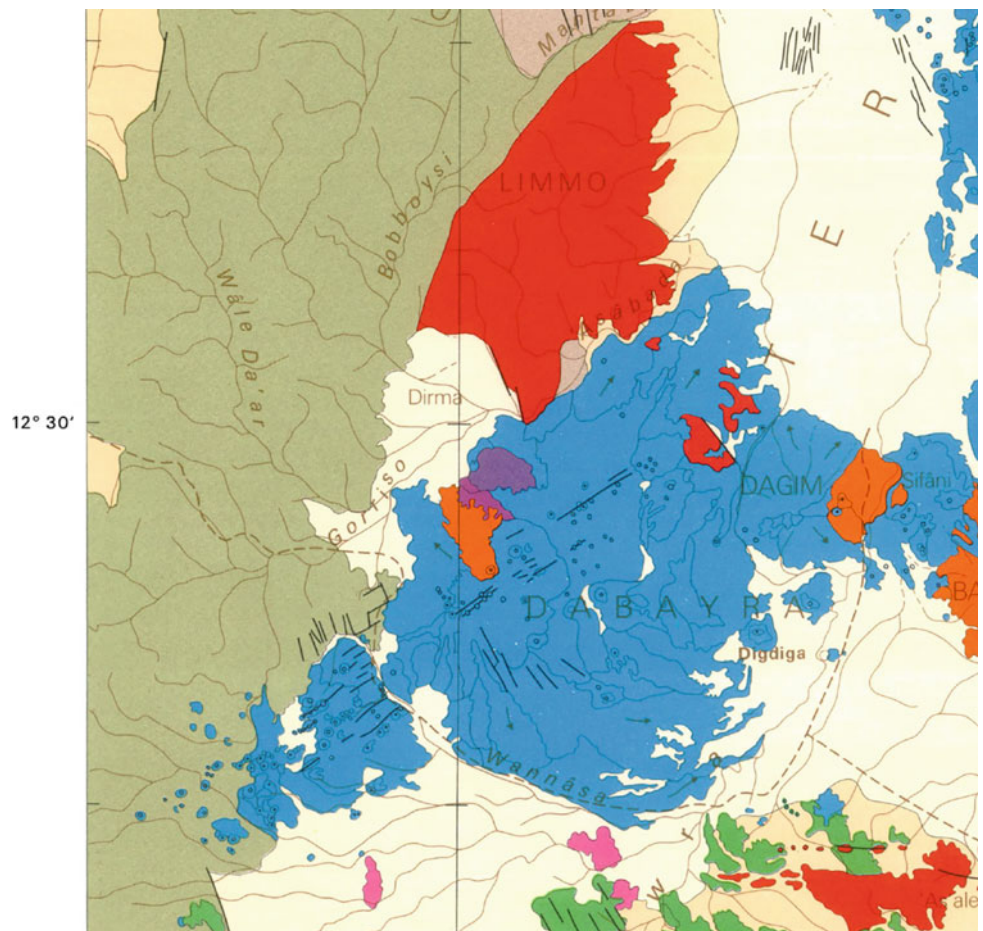




Fig. 9.13 E–W views of the alignments of basaltic scoria cones and lava flows from Dabayra unit (shield visible in the background on the upper-right), extending far inside the escarpment foothill. Seen from

the wide plain extending west of Digdiga. The lower picture extends the upper one to the west (Photos J. Varet 2016)

References

- Barberi F, Bonatti E, Marinelli G, Varet J (1974) Transverse tectonics during the split of a continent data from the Afar Rift. *Tectonophysics* 23:17–29
- Barberi F, Varet J (1977) Volcanism in Afar: small-scale plate tectonic implications. *Bull Geol Soc Amer* 88:1251–1266
- Civetta L, DeFino M, Gasparini P, Ghiara MR, LaVolpe L, Lirer L (1975) Geology of central-eastern Afar (Ethiopia). In: Pilger A, Rosler A (eds) *Afar depression of Ethiopia, proceedings of an international symposium on the Afar region and rift related problems*, vol 1. Bad Bergzabren, Germany, 1974, E. Schweizerbart'sche Verlagsbuchhandlung, Stuttgart, Germany, pp 259–277
- CNR—CNRS Afar team (1973) Geology of northern Afar (Ethiopia). *Rev Geogr Phys Geol Dyn* 15:443–490
- De Fino M, La Volpe L, Lirer L (1973) Volcanology and petrology of the Assab range (Ethiopia). *Bull Volc* 37–1:1–16
- Gass IG (1970) The evolution of volcanism in the junction area of the Red Sea, Gulf Aden and Ethiopian Rifts. *Phil Trans R Soc London* 267:369–381
- Hutchison R, Gass IG (1971) Mafic and ultramafic inclusions associated with undersaturated basalt on Kod Ali Island, Southern Red Sea *Contrib Mineral Petrol* 31(2)
- Makris J, Henke C, Egloff F, Akamaluk T (1991) The gravity field of the Red Sea and East Africa. *Tectonophysics* 198:369–381
- Marinelli G, Varet J (1973) Structure et évolution du Sud du "horst Danakil" (TFAI et Ethiopie). *C.R Acad Sci (D)* 276:1119–1122
- Ottonello G, Piccardo GB, Joron JL, Treuil M (1978) Evolution of the upper mantle under the Assab region (Ethiopia): suggestions from petrology and geochemistry of tectonic ultramafic xenoliths and host basaltic lavas. *Geol Rundsch* 67(2):547–575
- Schilling J-G (1973) Afar mantle plume: rare earth evidence. *Nature* 242:2–5
- Varet J (1975) Carte géologique de l'Afar central et méridional, CNR-CNRS, 1/500 000 Géotechnip
- Volker F, Altherr R, Jochum K-P, McCulloch MT (1997) Quaternary volcanic activity of the southern Red Sea: new data and assessment of models on magma sources and Afar plume–lithosphere interaction. *Tectonophysics* 278:15–29
- Wiat P, Oppenheimer C, Francis P (2000) Eruptive history of Dubbi volcano, Northeast Afar (Eritrea), revealed by optical and SAR image interpretation. *Int J Remote Sens* 21:911–936
- Xu W, Ruch J, Jonsson S (2015) Birth of two volcanic islands in the southern Red Sea. *Nature Comm* 6: 7104

The southern half of Afar includes two major hydrographic basins (Fig. 10.1):

- In its western part and central part, the Awash River loop, which flows from south to north along the foothills of the Nubian escarpment, from the plateau in the Addis Ababa area down to central Afar (at Mille and Semara, the capital of the Afar Regional State). The river is permanent, and receives many tributaries from the western escarpment, but the basin is endoreic. The river curves with the last part of the course flowing south in the Kalo plain, ending in a swampy area (Uddummi, Haytankōmi and Gêra Bad) and finally at Abhe Bad (meaning in Afar language “rotten lake”) in the Gobaad graben in Djibouti Republic.
- In its eastern part to the foot of the Somalian escarpment, where several rivers flow from south to north in the western part (Gega’as basin) and from WE to NW in the eastern part (Dallaymale basin), filling as a whole a large basin (200 km long and 60 km wide) with detritic, eolian and lacustrine sediments, the geology of which is little-known.

They are separated by basaltic plateaus of the Afar stratoid series, themselves cut by grabens, the major one (Adda’do, northern end of the MER) being both tectonically and volcanically active with the alignment of central volcanoes of Ayelu-Abida, Yangudi, Gabillemma and Dama Ale separating the Kalo and Gobaa’d basins.

10.1 Sedimentary Plains of Southern Afar

In this specific geological context, several distinct sedimentary basins have developed in southern Afar and are discussed in the following.

10.1.1 The Yaldi-Hadar Basin

The Yaldi basin is located between the foot of the Nubian escarpment and the recent volcanic units of Afar: the stratoid series and the recent Quaternary volcanic centres, over a width of 50–60 km. The Awash River flows along this N–S elongated plain, which largely results from the filling by sediments carried from the plateau by this important river network (see Fig. 2.2) of Awash and western tributaries, hitting against the low plateaus of the stratoid series.

This basin contains in its northern part the Hadar formation, reaching an outcropping thickness of 250 m (probably more in the deeper, eastern part of the basin), which is a dominantly detritic unit (boulders, sunstones, siltstones and mudstones), with lacustrine intercalations, including bioclastic carbonates and volcanic tuffs. The whole sequence is lying uncomfortably on late Miocene and Pliocene volcanic formations of the faulted and eroded Nubian plateau margin. It was studied in great detail for its high palaeontology interest as abundant early hominid remains were identified (Taieb et al. 1976; Aronson and Taieb 1981; Walter and Aronson 1993; Feibel 2004). The base of the unit dates from 3.4 million years ago, which corresponds with the oldest age found for the Afar stratoid series (Barberi et al. 1972). Several hundred human fossils were found—associated with a rich mammal fauna—including the well-known “Lucy” and “First Family” (13 individuals), assigned to *Australopithecus afarensis* (Taieb et al. 1976).

At least four sedimentary units have been distinguished in this sequence marked by lacustrine and volcanic tuff intercalations in dominantly detrital sediments, allowing the human fossils to be dated as ranging in age from 3.4 to 3.2 million years. Extending over a large surface in central western Afar between Gabillemma and Ayelu, the Cindey tuff, dated 3.9 million years old, found at the base of the sedi-

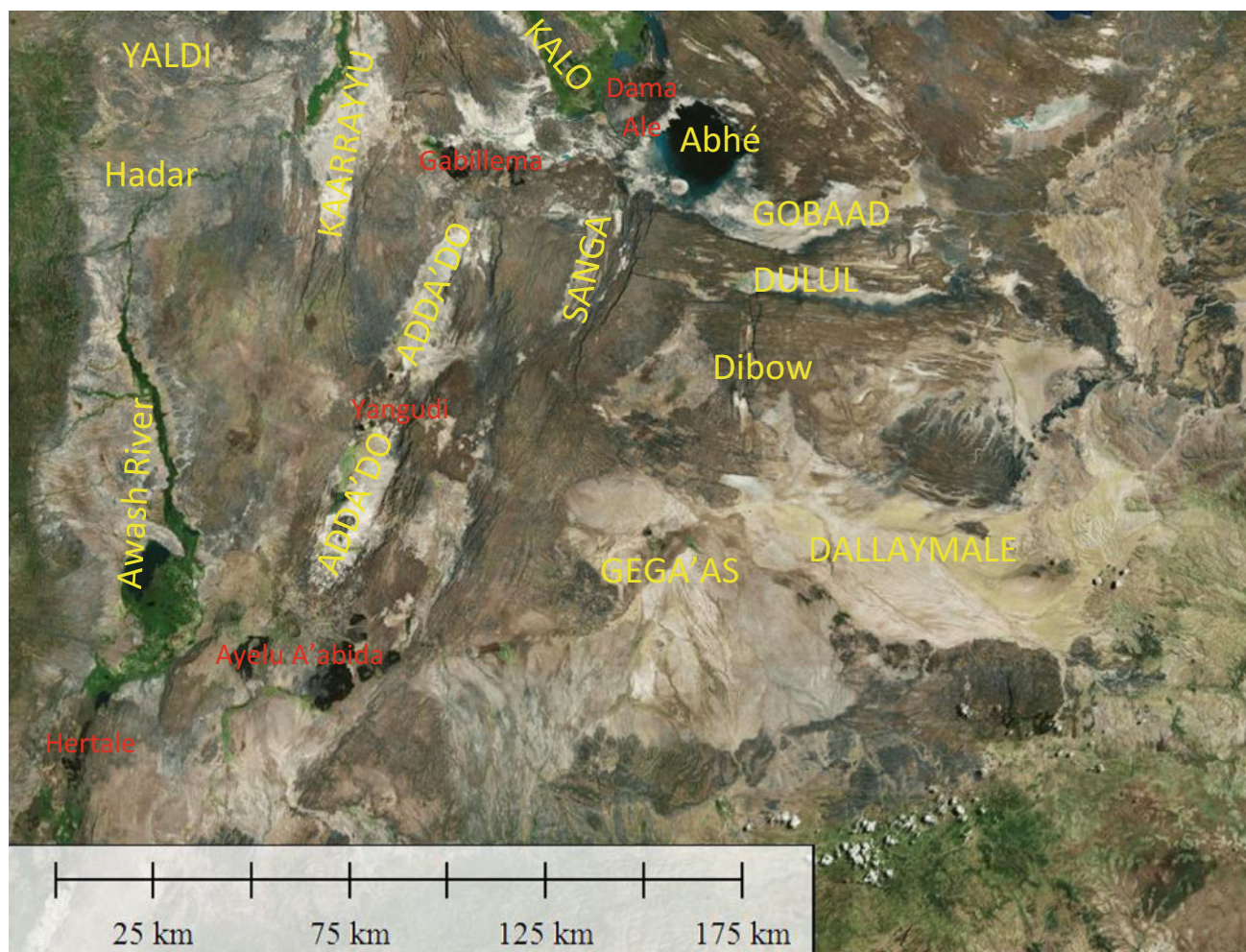


Fig. 10.1 Satellite image (from Global mapper 16) of southern Afar showing the major sedimentary basins (in *yellow*) and recent quaternary volcanoes (in *red*). Toponymy is from Chèdeville (from Varet 1975)

mentary sequence, was studied in detail by Hall et al. (1984) and Walter et al. (1987), and was shown to result from a magma mixing of a basalt and a rhyolite of the same origin (probably by intrusion of basalt in the upper differentiated part of the magma chamber). A significant change was shown to occur 2.9 million years ago, considered to be of tectonic origin (Feibel 2004), with a migration of lacustrine facies down-rift.

This Hadar sequence, however, is certainly not the oldest at the foot of the Nubian escarpment, as the MER developed around 10 million years earlier at least. Earlier sedimentary units most probably exist below these rather recent fillings of the Awash basin.

It should also be noted that more recent sedimentary units developed in the Peistocene period as a result of wide lakes that occupied the basin during the humid periods described below. Remnants of these lacustrine episodes are observed along the eastern side of the Awash River basin, such as

around Gawani, where the main road from Addis Ababa to Djibouti is built on one of the latest terrasses (see Fig. 10.23), and 10 km north, where an important diatomite deposit is observed in wadi Bunkato Basin (Fig. 10.2).

10.1.2 The Kalo (Tendaho)-Gobaad Graben

To the south, the Awash River delta filled the Kalo-Gobaad plain, 150 km long, over a width that decrease from north to south from 40 km to 20 km at the level of Lake Abhe, ending at 10 km in the Gobaad. Geologically, this is a graben limited by very large normal faults of NNE–SSW direction (Red Sea trend) to the north, virgating south to E–W direction, which corresponds with the Gulf of Aden trend. This graben is filled with sediments, the total thickness of which is unknown but may reach several thousand metres. These sediments are interbedded with tufs and hyaloclastite formations as well as



Fig. 10.2 Diatomite deposits (in white) of the Bunkato basin, on the eastern side of the Awash River basin, 10 km north of Gawani. (Satellite imagery from Google Earth Pro)

basaltic lava flows, most of them showing pavement surface and pillow lava fronts characteristic of subaqueous eruptions.

Three sedimentary sequences were distinguished by Gasse (1977), ranging from early Pleistocene to recent (Fig. 10.3), on the basis of the study of the lacustrine deposits (Figs. 10.4 and 10.5). A wide lake was occupying this central part of Afar in the humid periods 100,000 and 10,000 years ago (Fig. 10.6). Lake Abhe, today a small, shallow, hyper-alkaline waterbody, was part of a 160-m-deep freshwater water body that extended over

5000 km². The highest level (as also shown by its maximum water-dilution) was reached from 29,000 to 23,000 years ago. After 19,000 years ago, arid conditions were progressively established, with a lake-level at least as low as today from 17,000 to 10,000 years ago. A return of humid conditions was observed elsewhere in the region by 13,000–11,000 years ago, and Lake Abhe was shown to fill up rapidly 10,000 years ago, with low salinity and high stands from 9400 to 8300 years ago and 7000–6000 years ago, separated by a regression around 8000–7500 years ago. The

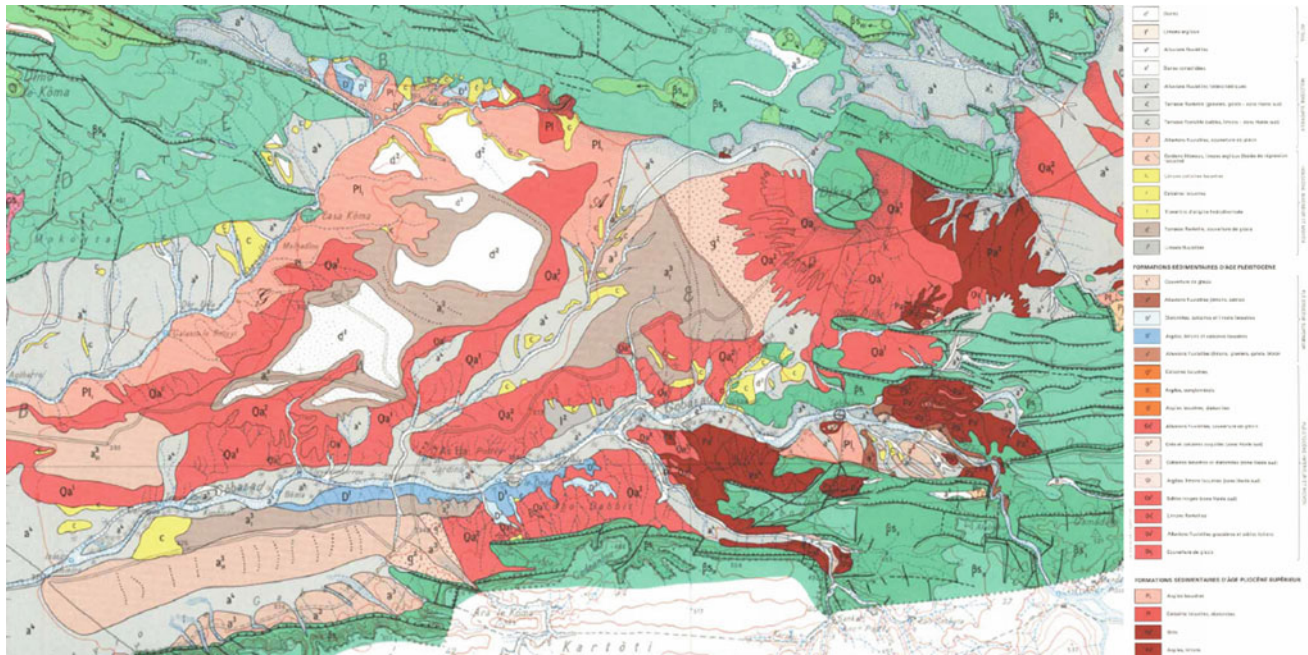


Fig. 10.3 Detailed geological map showing the extension of the sedimentary formations of Gobaad basin (east of Lac Abhé), where three sequences were distinguished by Gasse et al. (1980): early Pléistocène

(3 to 0.7 million years ago), recent Pléistocène (0.7 to 0.1 million years ago) and most recent (100,000 to 10,000 years ago)



Fig. 10.4 Lacustrine limestone deposits of Pleistocene age, Gobaad basin (Photo J. Varet 2012)



Fig. 10.5 Recent deposits (9000 years ago) of diatomites and pulverulent limestones (Gobaad, *Photo J. Varet 2012*) of the last humid episode in Afar

arid period prevailing at present appeared 4300 years ago, with oscillations of minor amplitude.

10.1.3 The Grabens of Southern Afar

If the Tendaho-Gobaad graben is dominant because of its size and volcanicity, the surrounding grabens cannot be ignored.

South from Gobaad, a narrow graben called Dulul extends in the same N–S direction. This appears to be older than Gobaad as the numerous faults trending N–S and NNE–SSW observed south only partly affect the narrow horst separating Dulul from Gobaad (Fig. 10.7).

Next to it to the west is Sanga graben, trending NNE (MER), which appears younger. It cut through the Dulul faults and created a bulged plateau on the eastern side. This distensive feature extends north through the Gobaad and appears to control the location of the Dama Ale volcano.

However, its structures shows characteristics of a “half graben”, bordering the Adda’do graben located further west.

Adda’do appears to be the youngest and most active graben in the area. It is affected by significant volcanic activity, and represent the northern extremity of the MER, with the development of the important Gabillemma volcanic centre at the crossing of Adda’do graben with the Tendaho-Gobaad southern margin.

Symmetrically to Sanga with respect to Adda’do (Fig. 10.1), the Karrayyu graben developed in a parallel NNE direction. This, however, appears as an older structure, predating the Adda’do axis. It may represent an earlier path of the MER rift at an earlier stage (more than one million years ago), as shown by the extension of the NNE tectonic trend to the north ($11^{\circ} 50'$), up to Tendaho where these MER trending faults are still visible, being cut through by more recent Red Sea trending faults, forming lozenge-shaped blocks (Fig. 10.8). The Awash River benefited from this double faulting to cross through the Tendaho graben western border.

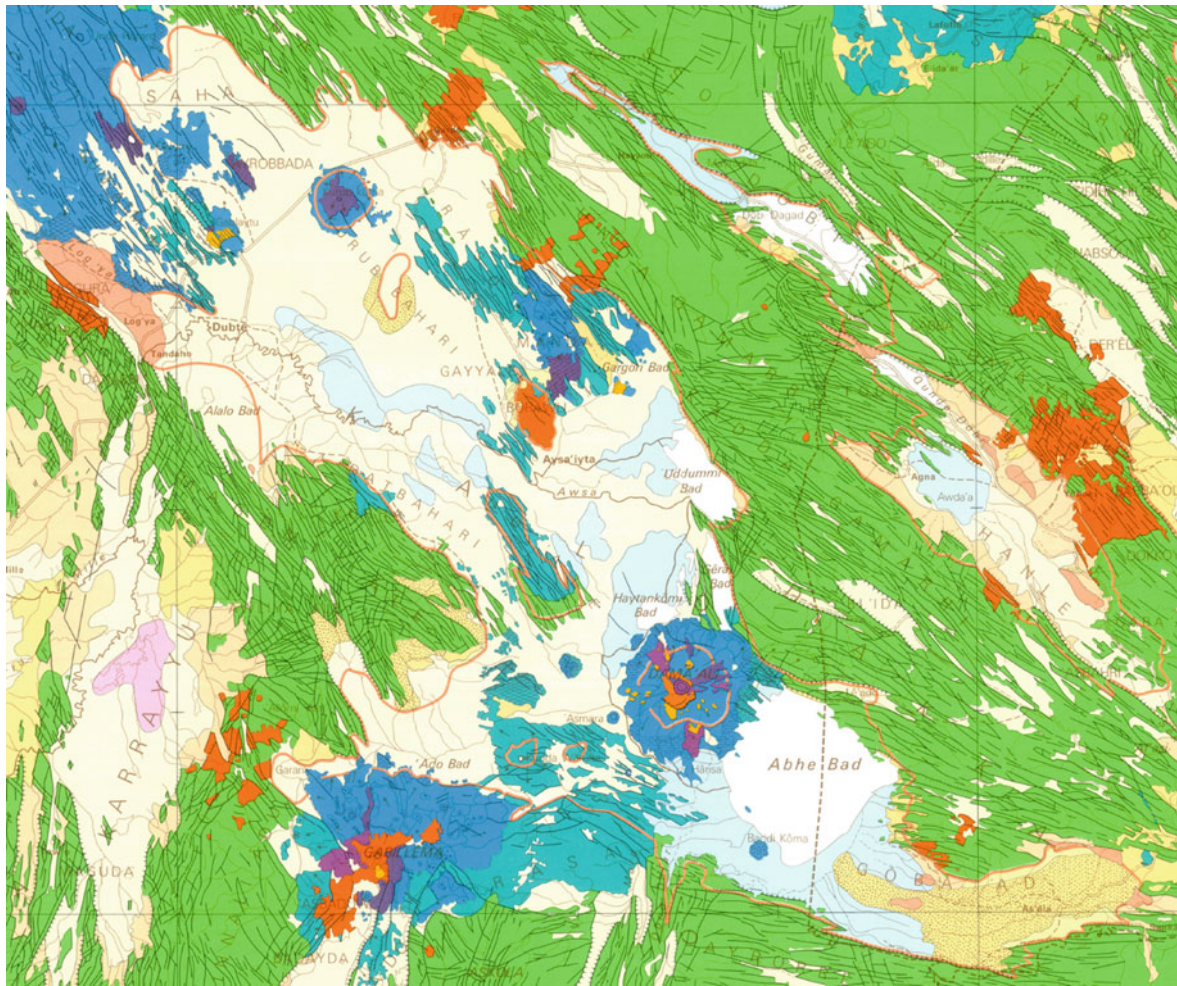


Fig. 10.6 The Kalo-Gobaad basin filling from Awash (endoreic basin). Orange curve shows the early-middle Holocene paleoshorelines drawn by F. Gasse, on J. Varet geological map of central southern Afar

(Varet 1975). This shows that the Holocene lake extended from Tendaho graben in Ethiopia to Gobaad graben, SE of Lake Abhe, in Djibouti

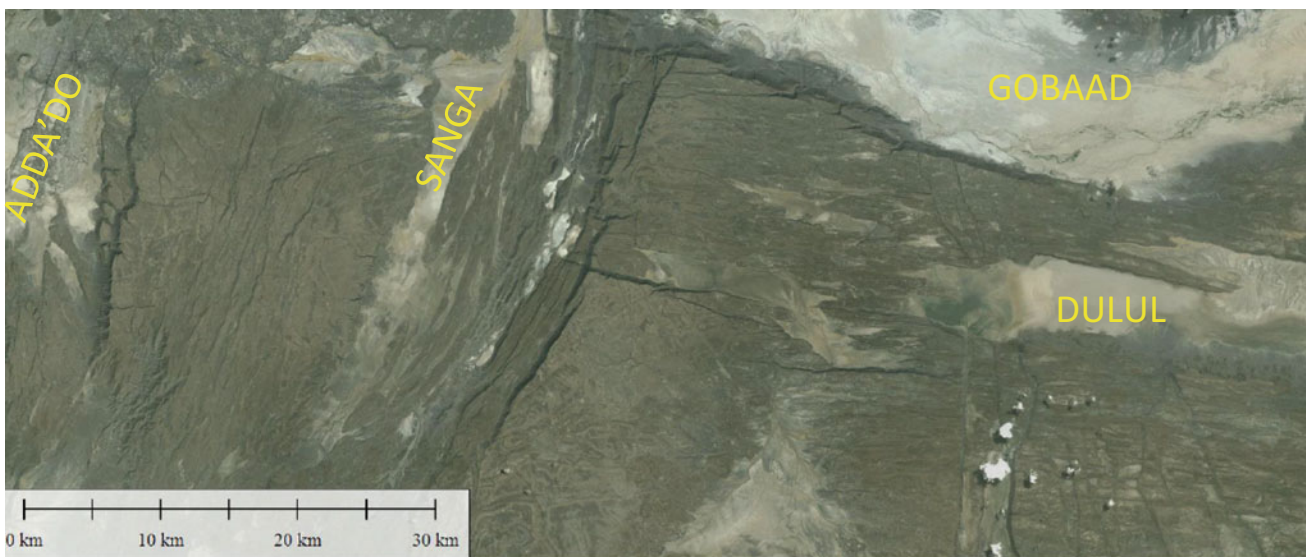


Fig. 10.7 Satellite image (from Global Mapper 16) of the grabens located south of Gobaad: Dulul, Sanga and Adda'to (present location of the MER northern extremity). NNE (Red Sea trend) earlier faults affect

the stratoid series south of Dulul, whereas the Sanga and Adda'to (MER) appear younger

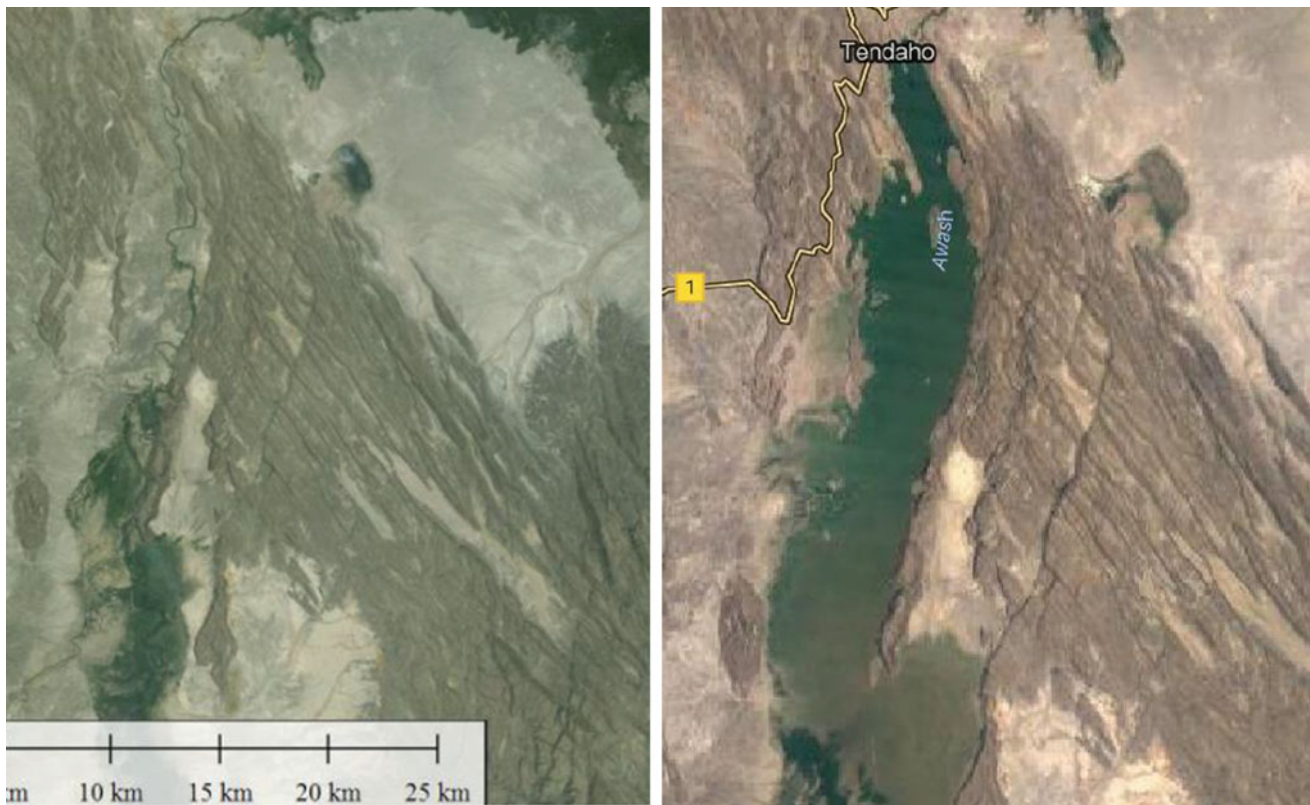


Fig. 10.8 Recent past and present satellite images showing the extension of older NNE trending faults (MER direction) cut by more recent NNW faults (Red Sea) at the level of Tendaho, where the Awash River borrowed the resulting lozenge block faulting to cross the western fault scarp of the Tendaho graben. A dam was built on this narrow pass.

Its present extension is visible on the image right (Google Earth), whereas the earlier image left (from Global Mapper 16) showing the swampy area (now covered by the lake) dates back to before the dam was built

As a whole, it appears that it is only recently—postdating the surface of the stratoid series, that is, less than one million years ago—that the MER borrows a well-defined axis, after having divagated earlier over a wider area, and ensured a direct link with the Red Sea axis further north, when at present it hits against the Red Sea-Aden rift at 11°N . Similarly, Red Sea trends developed south of Dulul, as observed in Figs. 10.1 and 10.6, down to $10^{\circ} 20'$ in southern Afar, and probably further south, a trend of extension also found in the Aisha block (Black et al. 1972).

10.2 Geodynamics of Tendaho-Gobaad Graben

10.2.1 Volcanic Features in the Tendaho-Gobaad Graben

The volcanic floor of the Tendaho-Goba'ad graben is made of faulted basalts from the stratoid series (three to one

million years ago) covered locally by recent Quaternary dominantly basaltic lava. The lowest sequence is typically sublacustrine with the characteristic small pavement surfaces with pillow lava at the front of the flows, and emission centres made of hyaloclastites (among which Asmara and Baddi Koma are the most spectacular). With its truncated shape, Asmara (750 m wide at the flat top, 350 m above the basin floor, 1250 m total diameter) was compared by Bonatti and Tazieff (1970) with a submarine “guyot” (Fig. 10.9).

We have seen that this wide plain was occupied by very large lake until recent Pleistocene as shown by the widespread lacustrine sediments, the subaqueous volcanism and the shorelines observed all around the basin. Several distinct recent volcanic units are observed. From north to south they are (Fig. 10.10):

- Kurub volcano, a small (10 km in diameter) isolated basaltic shield observed south of the Assab to Kambolcha road (see Fig. 6.109)

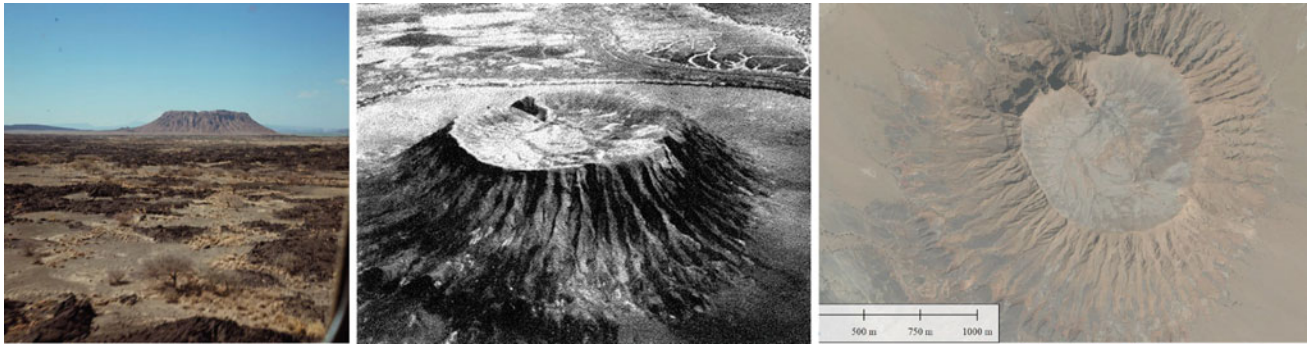


Fig. 10.9 The Asmara guyot, a sublacustrine hyaloclastite cone in the Awash lower basin, SW of Dama Ale (land and air photos coll. G. Marinelli, Pisa University and satellite image from Google Earth Pro)

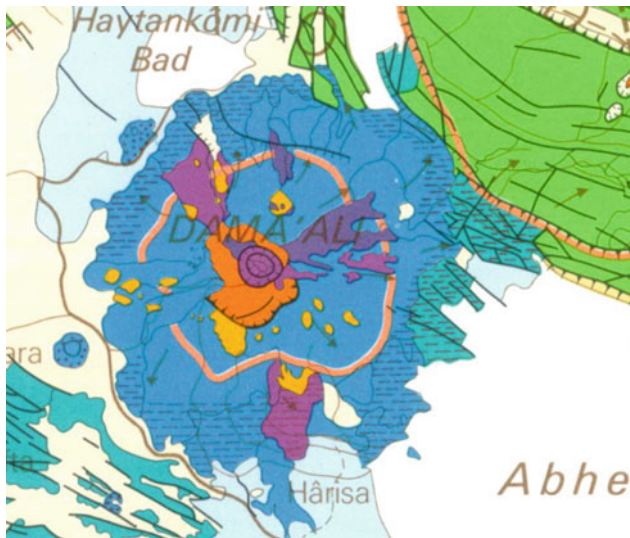


Fig. 10.10 Dama Ale shield volcano, at the intersection of NW–SE and N–S grabens (extracted from CNR-CNRS map, J. Varet, 1975). Observe that the basaltic flows partly predate and postdate the lacustrine deposit of the Holocene lake of maximum extension (orange line, 9400–8400 years ago). Dominantly basaltic it also shows intermediate iron terms and rhyolite domes in the upper part, where silicic pyroclastites also appear in relation to a former caldera

- South of it, along the same line, the Raso Manda basaltic lava fields, located north of Aysa'iyta (the traditional Afar capital), over a length of 25 km with a width of 10 km
- The slightly older Ud'Ale faulted lava field located NW from Dama Ale
- Kadda Warufta lava field located SW from Dama Ale, including the Asmara hyaloclastite guyots, these last two units being made of fissural subaqueous flood basalts
- South from Lake Abhe, the hyaloclastite cone of Baddi Koma is the last recent volcanic unit of this ensemble, dominated by NNW–SSE (Red Sea) and WNW–ESE (Aden) trending faults and feeding fissures

- It should be noted that the lava fields located at the northern foot of Gabillema, and the Rasa lava earlier field to the east are also the products of WNW–ESE trending fissures, despite the fact that Gabillema central volcano clearly belongs to the Ethiopian Rift Valley (it is in fact the northern end of it)
- Dama Ale shield volcano, the dominant volcanic centre in this wide unit that separates the Tendaho graben from the Gobaad graben, which is described in the next paragraph.

These units clearly show that the volcanic activity persisted in recent times on the floor of the Tendaho graben, but do not show the characteristics of the axial ranges, with only sporadic events not fed by a single spreading axis.

10.2.2 Dama Ale Shield Volcano

Dama Ale is a typical shield volcano, with a rather regular circular shape, 25 km in diameter. The volcano is built on a graben of NE–SW direction, well visible on its SW side (Fig. 10.10). It is located south of the wide Kalo plain, along the axis of the Tendaho-Gobaad graben. This recent Quaternary (and still active) volcanic feature differs from the axial volcanic ranges found elsewhere to the northern and eastern part of the depression.

The location and unusual circular shape of this shield volcano is clearly determined by the intersection of the Sanga graben (of NNW–SSE direction, i.e. MER) with the NNW-SSE trending Tendaho-Gobaad graben (Red Sea-Aden rift). This double extension could explain the tholeiitic nature of the initial magma.

Dama Ale determines the south-eastern final course of the Awash River ending at Abhe Bad (partly in Djibouti Republic). The river feeds several lakes and swamps north and west of the volcano before it contours it to the south, feeding the lake to the east. In this hydrogeologic context, it is not excluded that a groundwater flow crosses through the

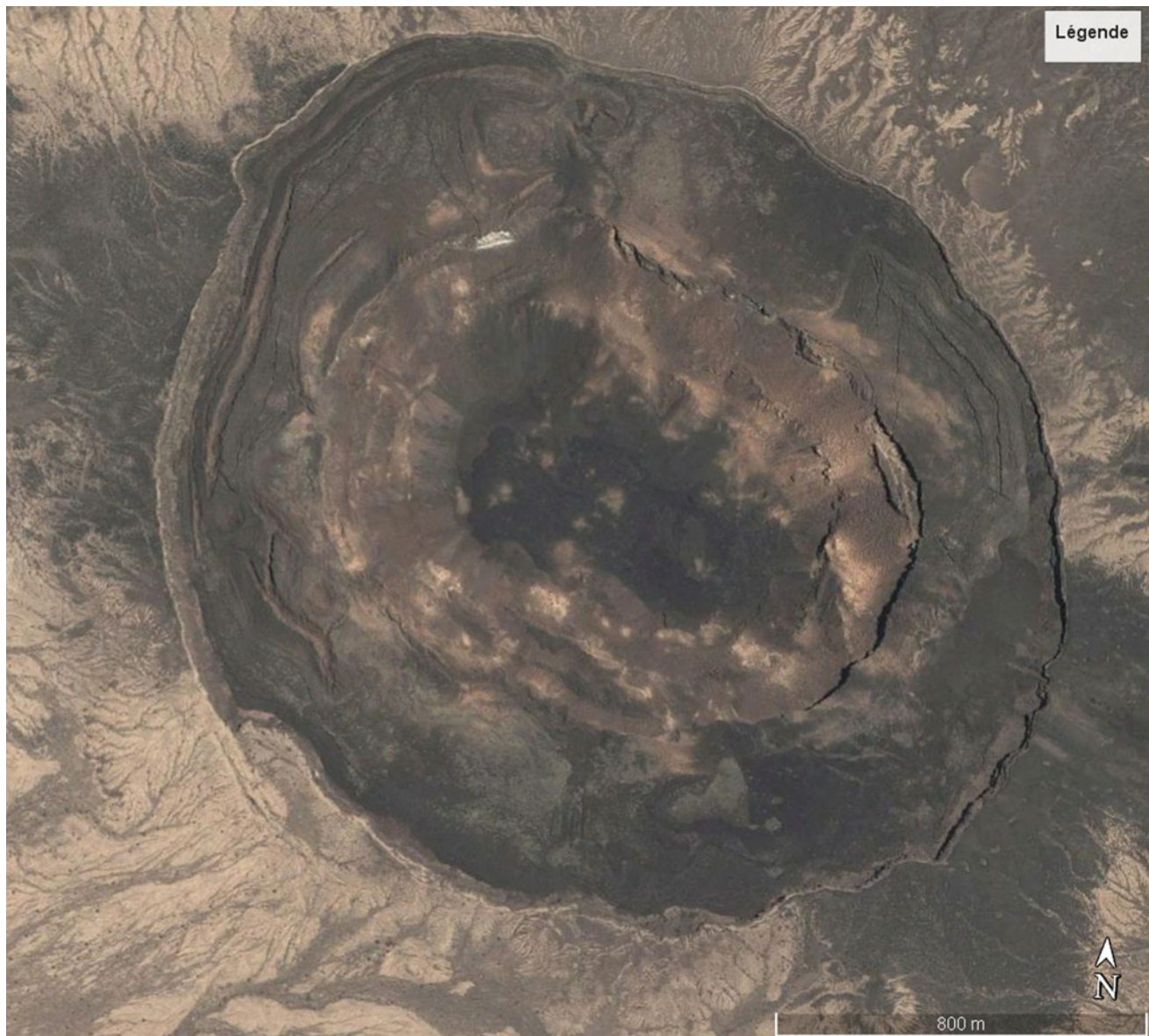


Fig. 10.11 Satellite image (Google Earth Pro) of the summit part of Dama Ale volcano, showing the double-rimmed crater, both occupied by lava lakes that partly overflowed the crater rim and consequently sunk. The floor of the crater was subject to a later event, with basaltic

lava flows and hornitos. The latest eruption was reported to occur in 1631. Fumaroles are observed in several places, in particular along the inner crater walls. Hot springs also occur at the foot of the volcano, notably along the NE-SW trending faults

NW–SE faulted stratoid series beneath the volcano, with a flow from NW to SE towards the lake.

This pretty regular shield volcano is topped by a spectacular, equally circular, double-rimmed crater, 2–2.5 km in diameter (Fig. 10.11). It is dominantly basaltic, and the earliest activity was subaqueous, as shown by well-developed pillow lavas observed all along the front of the lower flows. Intermediate terms, ferrobasalts and dark trachytes occur on the flanks, where obsidian domes are also observed. These rhyolite domes are located mid-slope around the volcano and may be the result of the combination of radial and ring dikes (cone sheets) linking to a

shallow magma chamber where these products are differentiated by crystal fractionation. They are not the most recent products, as younger flows emitted from the central crater have surrounded and partly covered them (Fig. 10.12).

Observation of the summital part shows that the rather recent double-rimmed (in fact multiple-rimmed) crater (historic?) was produced by the sinking of a wide lava lake that overflowed the rims before it collapsed (Fig. 10.13). The floor of the crater is occupied by a wide lava lake that remained active after the sink and was fed by several fissures, before it solidified during several successive periods, over several tens of metres.



Fig. 10.12 Recent basaltic lava flow emitted from the central crater surrounding a rhyolite dome emitted on the northern flank of Dama Ale shield volcano (satellite image from Google Earth Pro)



Fig. 10.13 Detailed views (from Google Earth Pro) of the northern and SE rims of Dama Ale crater showing the basaltic cover overflowing the rims before the lava lake collapsed. Major fumaroles appear in white and yellow

Dama Ale is made of a complete differentiation sequence, studied by Ferrara and Santacroce (1980) with initial basaltic flows of tholeiitic affinity up to iron-rich intermediate products topping the shield, and ending with subalkaline rhyolites found in the domes on the top part of the volcano. If the sequence is chronological and fits with the volcanic evolution, showing the expression of a shallow magma chamber, several cycles have affected the volcano, with younger basaltic lavas partly covering the silicic domes. The historic basaltic sequence observed in the craters is the last sequence of magmatic rejuvenation, showing a recurrent magma production from the mantle.

On the southern upper part of the volcano, the remnants of a large caldera (6 km wide) are observed (Fig. 10.14), associated with a few pyroclastic products, within which several blocks display fine, medium up to coarse grained crystalline structures: gabbros, diorites and granites. They

are considered as intrusive equivalents of the lava emitted at the surface, interpreted as testimony of former differentiated shallow magma chambers. Important fumarolic activity is observed around the rim of the crater, and numerous hot springs are found, both in Ethiopia and in Djibouti along the shore of Lake Abhe.

Let us stress that Dama Ale magmatic sequence appears to be of rather tholeiitic affinity, an observation also confirmed by geochemical data (Tb/Ta ratio, for instance, as shown in Fig. 6.128). This can be interpreted as resulting from the fact that this central volcano—displaying magmatic analogies with axial ranges despite its shape—results from the effect of the addition of the Red-Sea—Gulf of Aden spreading of the Tendaho-Gobaad graben (although dying at the level of this volcano) and of the MER rifting (also ending there). This double spreading effect explains the high degree of partial melting of the initial basaltic magma.



Fig. 10.14 Southern rim of the former caldera and pyroclastic products observed south from the crater of Dama Ale volcano (satellite image from USGS Earth Observer)

10.2.3 Discussion of the Geodynamic Significance of the Tendaho-Gobaad Graben

Several geodynamic schemes published in the last 20 years refer to a wide axis of spreading extending from Manda Hararo to the SE including Dama Ale, as well as the recent volcanic units observed in the lower Awash basin described above. This is interpreted as a “propagator” of the Red Sea

spreading axis within Afar (Fig. 10.15). According to this interpretation, proposed initially by Manighetti et al. (1997, 1998, 2001), the Manda-Harraro-Gobaad rift segment is propagating from NW to SE, whereas the Aden rift propagates from SE to NW through Asal and eventually Manda Inakir (Fig. 10.15). This concept of propagating the Manda-Harraro-Gobaad rift became popular and was also repeated by Hofstetter and Beith (2003), Wolfenden et al. (2004), Beyene and Abdelsalam (2005) and Muluneh et al. (2013).

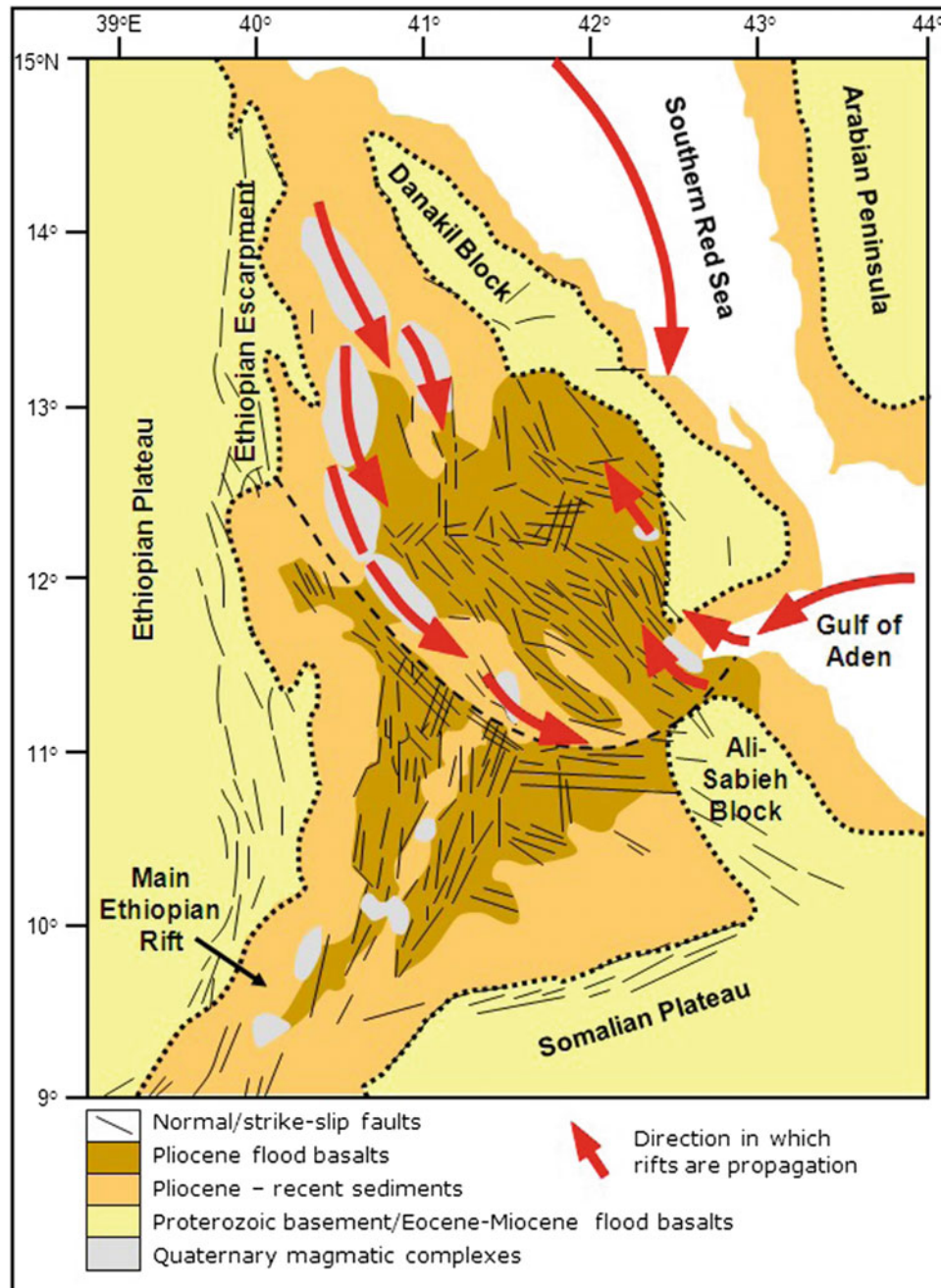


Fig. 10.15 The concept of propagating rift in Afar after Beyene and Abdelsalam (2005) following the initial model of Manighetti et al. (1997)

Our observations are not consistent with this interpretation, and would rather imply, instead of an active propagator, a progressively “dying” rift segment south from Manda Harraro. The existence of a few recent volcanic units dispersed in the southern part of the Tendaho graben could be considered as down to Dama Ale and are the surface expression of this “dying” spreading axis. Note also the influence of the Ethiopian Rift Valley that provides a supplement component of spreading to a Red Sea rift system that disappears at the level of Dama Ale and do not extend further to Gobaad.

According to our observations, it appears that the Pleistocene rifting in south-eastern central Afar developed with a migration from south to north as shown by the progressively more recent ages of the basaltic stratoid series, the rhyolite centres and the graben formation. We have seen that the Dulul graben south from Gobaad is older, whereas it was shown (Sects. 10.1.2 and 10.1.3) that the grabens located north of Gobaad (Hanle, Gaggade, and Asal) are getting younger towards the north-east. The direction of the faulting

also passed from nearly WNW–ESE in Gobaad (and E–W in Dulul) to the NW–SE trend presently observed at Asal-Ghoubbet.

We therefore propose an alternative model according to which the Gulf of Aden propagates early (3.5 million years ago) in southern Afar (Dulul followed by Gobaad) through a NE–SW transform fault located along the border of the Ali Sabieh block linking the Gulf of Aden to central Afar before the formation of the Gulf of Tadjourah, this early active rifting feeding the stratoid series. In successive steps, the spreading migrated from SW to NE, passing from Gobaad to Asal between three and one million years ago (Fig. 10.16). This period corresponds to the effusion of the stratoid series in central Afar, and the cartography of the migration of the successive spreading segments, if any existed, remains hypothetical, as diking could also have been diffused as hypothesised by Barberi et al. (1982). In this interpretation, the NW border of the Ali-Sabieh block (along Grand Bara or Bada Weyn plain) would represent a fossil transform fault zone.

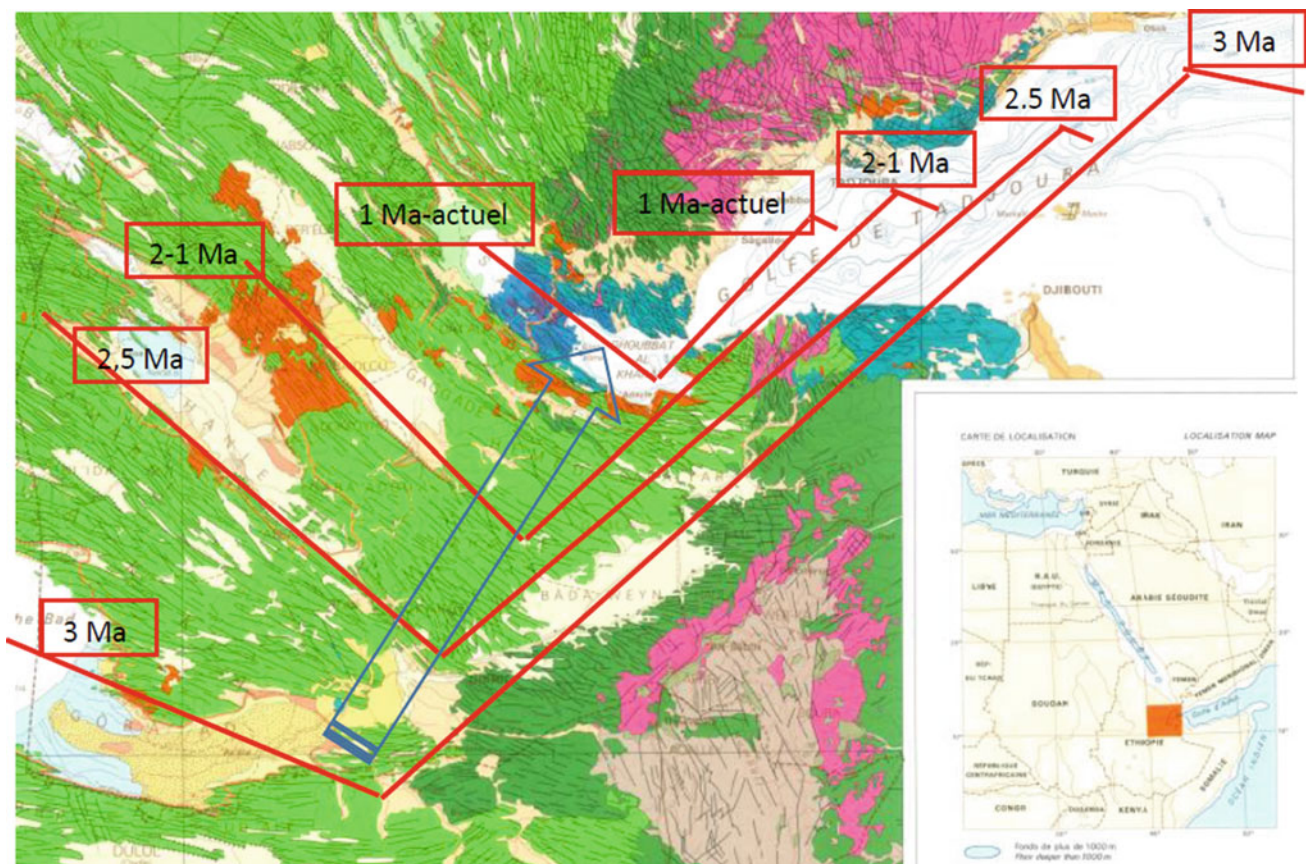


Fig. 10.16 Migration towards NE (blue arrow) of the spreading in southern Afar (with more recent volcanic sequences and consecutive graben formation from Gobaad to Hanle, Gaggade and Asal) in relation

to the progressive penetration from east to west in the Gulf of Aden rift to the Gulf of Tadjourah since three million years ago

10.3 The MER Volcanic Units of Afar

The present volcanic and tectonic activity in southern Afar is concentrated along a line trending NNE–SSW which extends from Gabillega to Fantale and corresponds to the northern extension of the MER. Differing from the MER, this affects the Afar floor and is not limited by the Nubian and Somalian plateau margins on both sides, but only the Nubian escarpment to the west.

More precisely, the Rift axis is divided in three en echelon segments that correspond with shifts in space and ages (younger from N to S) of the Nubian escarpment including, from north to south (Fig. 10.17):

- The Adda’do graben with Gabillega, Yangudi and Ayelu-Abida central volcanoes between 11° 10’N and 9° 55’N
- The Hertale-Angele-Dofan segment between 9° 55’N and 9° 20’N
- The Dofan-Fantale segment between 9° 20’N and 8° 55’N

10.3.1 Gabillega

Gabillega is a complex rhyolitic volcanic system with two major emission centres 10 km apart, aligned along the NNE (MER) trend, overlying the faulted basaltic unit of the stratoid series. The bottom of these units is built of basaltic lava flows followed by lava of intermediate composition forming two shields that were subject to NNE faults to the south and WNW faults to the north prior to the construction of the stratovolcanoes (Fig. 10.18).

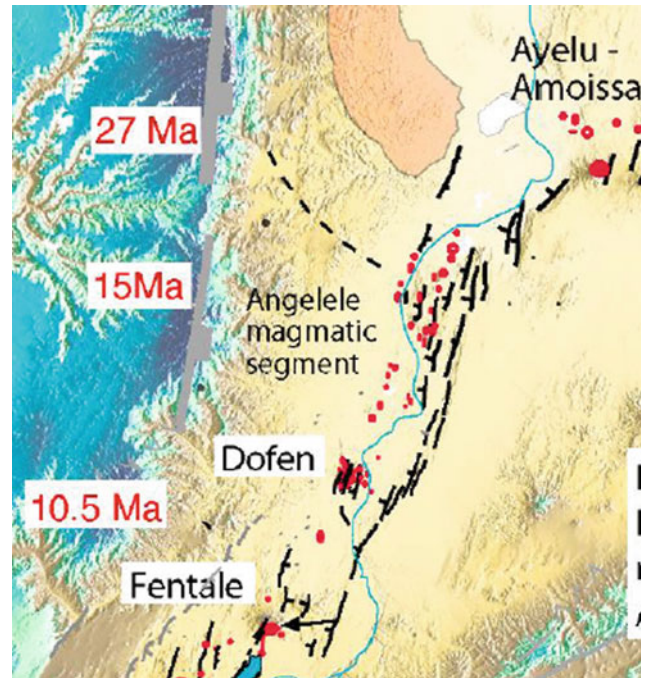


Fig. 10.17 Structural interpretation of the tectonic and magmatic rift segments in southern Afar. Active faults in black, active volcanism in red. Ages relate to the initiation of the faulting along the Nubian plateau margin. Observe the “en echelon” disposition of the successive segments of Fantale, Dofan-Angelele and Ayelu-Abida—Yangudi—Gabillega (from Keir et al. 2011)

The top of these two units consists of thick sequences of short rhyolite flows accumulated around the central vent. Pyroclatites are rare and no real caldera is observed. Recent basaltic activity postdating the major rhyolite emissions

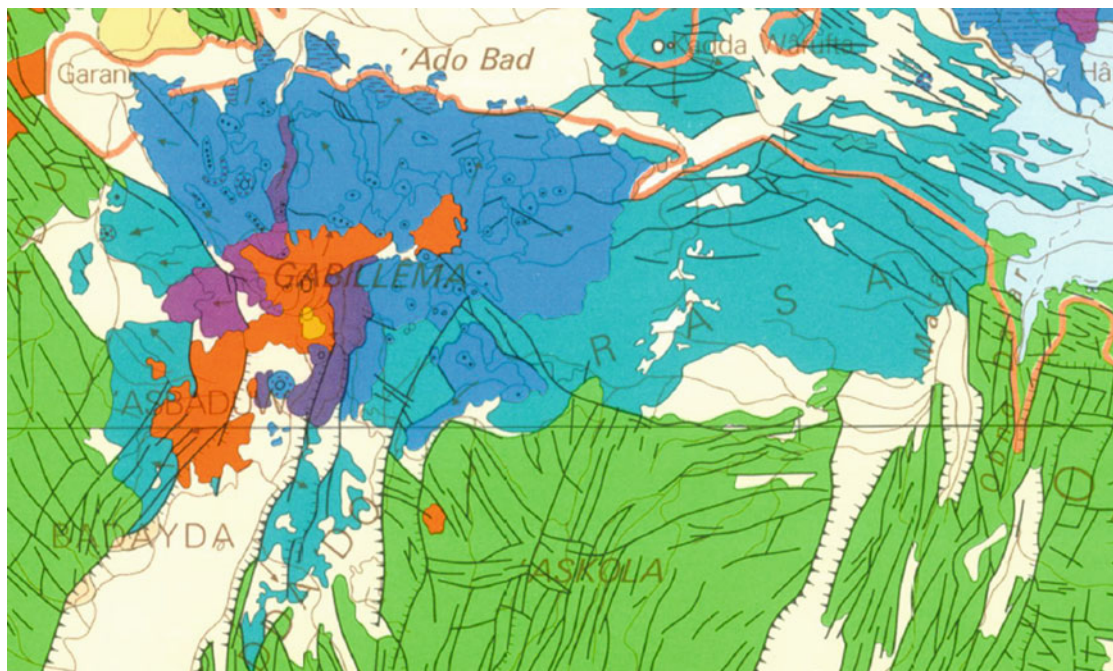


Fig. 10.18 Geological map (Varet 1975) of Gabillega volcanic complex, located at the northern extremity of the MER (NNE–SSW trending Adda’do graben), at the intersection with the NW–SE to WNW–ESE trending faulted margin of the Tendaho-Gobaad graben.

The early subaqueous Rasa and Adda’do basaltic lava fields are covered by more recent basalts emitted from the volcanic centre characterised by intermediate and silicic products in the central part

occurred by rejuvenation of the western and southern faults along fissures in an E–W direction and along the axis of the Addado graben.

In the early sequence, a large part of the emissions was subaqueous as shown by the morphology of the flows and the presence of hyaloclastite cones, one of them well-developed along the axial graben affecting the two rhyolitic centres (Fig. 10.19).

A spectacular, recent, rhyolitic dome and flow developed on the SE flank of the northern edifice (Fig. 10.20).

As a whole, a complete magmatic sequence is observed there, ranging from basalts to rhyolites, including intermediate terms, with several cycles of differentiation. This is interpreted as resulting from the development of magma chambers at the crossing of NNW–SSE and NN–SSW directions of extension.



Fig. 10.19 Detailed satellite view (Google Earth Pro) of a silicic hyaloclastite cone topping lava flows of trachytic composition in the middle part of Gabillega volcanic complex. The cone is affected by NNE–SSW (MER) faulting



Fig. 10.20 Recent rhyolite dome and flow in the central part of Gabillema volcanic massif (*Photo coll. G. Marinelli, Pisa University*)

10.3.2 Yangudi

Yangudi is a 15 km-wide volcano located in the median part of the Adda'do graben, half way (at a distance of 60 km from both) between Abida and Gabillema. It is a stratovolcano with a summit caldera, built by accumulation lava emitted from a vent along the axis of the graben (Fig. 10.21). The volcano displays a quite complete sequence of magmas from basalts to rhyolites, with all intermediate terms. As for Gabillema, the early basaltic flows partly overlie the Udukya plateau to the west, showing

that the building of the volcano was initiated before the graben collapse. An early central silicic volcano was even built there, pre-dating the axial volcano, showing that the location of the volcano corresponds to earlier lines of weakness. The volcano itself was subject to recent distensive tectonics with development of an axial graben with the most recent silicic lava accumulated in the axis. A double-rimmed elliptical caldera (elongated along the graben axis) occupies the centre of the volcano. Limited pyroclastites are observed; the stratovolcano is made of flows and breccias with the most recent crater built on the southern edge of the caldera.

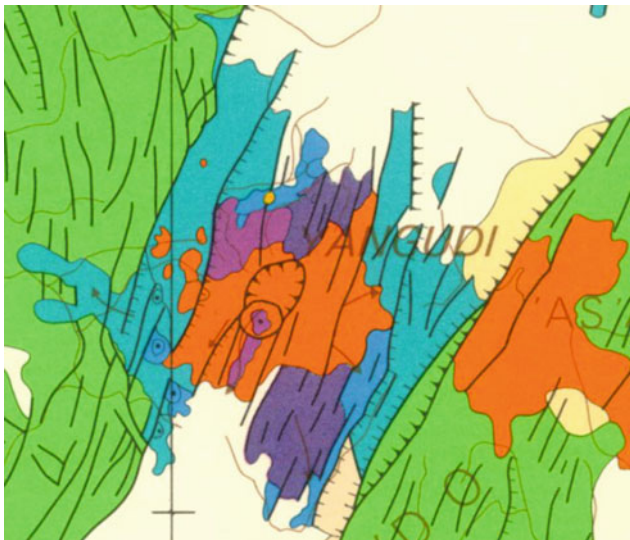


Fig. 10.21 Geological map of the Yangudi volcano located on the axis of the Addado graben (extracted from Varet 1975)

A recent volcanic activity is observed north of the centre, consisting of short basaltic flows. A post-caldera lava flow was also emitted from the most recent crater towards the

south. Fairly recent basaltic lava flows also developed along the western faults of the graben border, south of the volcanic centre. Wet zones are observed in the vicinity. Yangudi is classified as a National Park.

Although not studied with the same details, the magmatic sequence is similar to that observed in Gabilema and could be explained with the same process of crystal fractionation.

10.3.3 Ayelu-Abida (Called Amoisa in Ahmaric)

Twin volcanoes called Ayelu and Abida in Afar language (Abida also known as Amoisa in Amharic and on early US aeronautical maps) are observed along the same graben south of Yangudi and east of the town of Gawani (Fig. 10.22). Gawani, the main town in southern Afar, at an altitude of 620 m, is located along the eastern side of the Awash valley, at a mid-distance between Awash Station (150 km south) and Mille (150 km north). Mille is on the highway from Dessie to Semara (capital of the Afar Regional State, at a distance of 62 km). Gawani is also half way along the main road linking Addis Ababa and Djibouti (770 km).

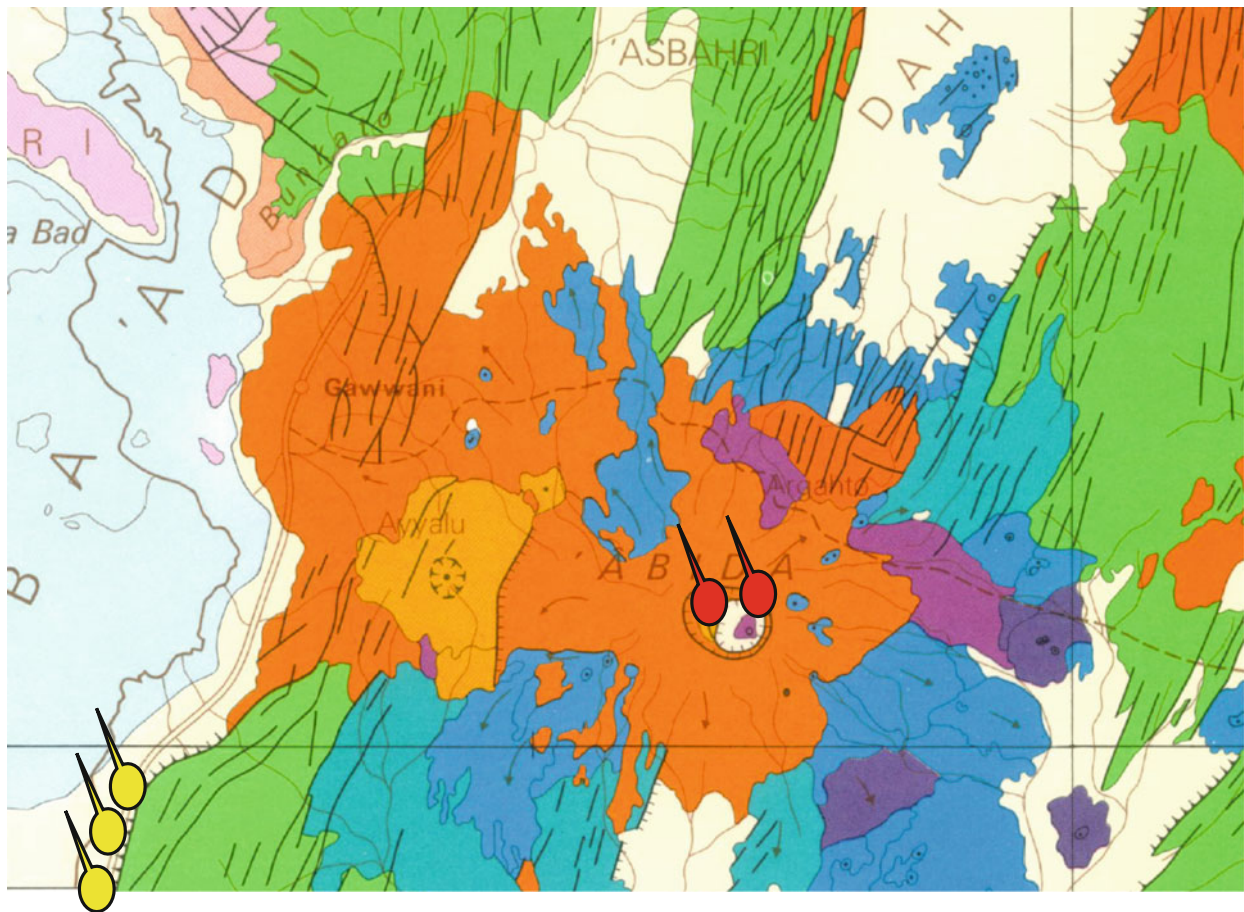


Fig. 10.22 Geological map of the Ayelu—Abida volcanic complex to the East of Gawani (Varet 1975). This complex volcanic unit appears as a potential geothermal site with fumaroles (red) at Abida caldera and hot spring outflows (yellow) at the lowest point, along the Awash border

The volcanic complex is bounded to the west by an important normal fault that put the volcanic pile in contact with the sediments of the Awash basin, covering the wide plain developing until the foot of the Nubian escarpment, located 40 km away. The main road from Addis Ababa to Djibouti traverses the area along the foot of the fault, and is built on detrital terraces where former lake deposits are observed (Fig. 10.23).

Gawani, with around 12,000 inhabitants, is located at the foot of Ayelu (or Ayyalu, 2145 m high), a steep cumulo-volcano forming a high cone by accumulation of viscous rhyolitic lava flows from a central vent. Age determinations at 500,000 years were obtained for lavas sampled at the base of the edifice. The eastern flank of Ayelu is affected by faults bounding the Addado graben and covered by ignimbrites emitted from Abida (1733 m), a rather recent, presently active volcano (fumarolic stage with historic lava flows eruptions). Abida is a typically truncated stratovolcano largely made of pyroclastites (pumice and ignimbrites) and displaying an impressive caldera (Fig. 10.24).

This summit caldera, elliptic (5 × 4 km) and elongated along a transverse WNW-ESE axis, occupies the centre of

the volcano, and was formed immediately after the eruption of the last ignimbrite eruption. A more recent, circular (2.4 km in diameter) caldera collapsed after a trachyte dome solidified inside the main caldera. The ignimbrite eruption covers a wide area: the sheet extends up to 40 km away from the centre, the pumice associated with it extending wider. This is a green ignimbrite, of pantelleritic composition, and, as in Fantale, it displays in the plain a blistered surface at a distance of 20–25 km from the caldera (Gibson 1970).

Post-caldera basaltic activity is well developed on the slopes of Abida volcano, mainly to the NW, SW and SE as well as inside the caldera, where a trachyte dome occupied the floor of the main caldera before it collapsed and the centre remains in the eastern part of the later small caldera floor.

To the south of Abida, two recent Quaternary ring structures are observed, respectively 2 km and 1.5 km across (Fig. 10.25). These appear to be very thick olivine-augite porphyritic basalts that were apparently extruded to the surface in a nearly solid state (considered as surface expression of cone sheets by Varet 1978).

From the shape of the caldera, the alignment of the two volcanoes and the transverse tectonics observed, it appears



Fig. 10.23 Faulted carbonaceous travertine and lacustrine sediments forming terrasses of a Pleistocene former lake observed S of Gawani. Interbedded silica deposits (*white layer*) result from earlier thermal activity, in the vicinity of the present thermal springs (see Sect. 12.1.9)

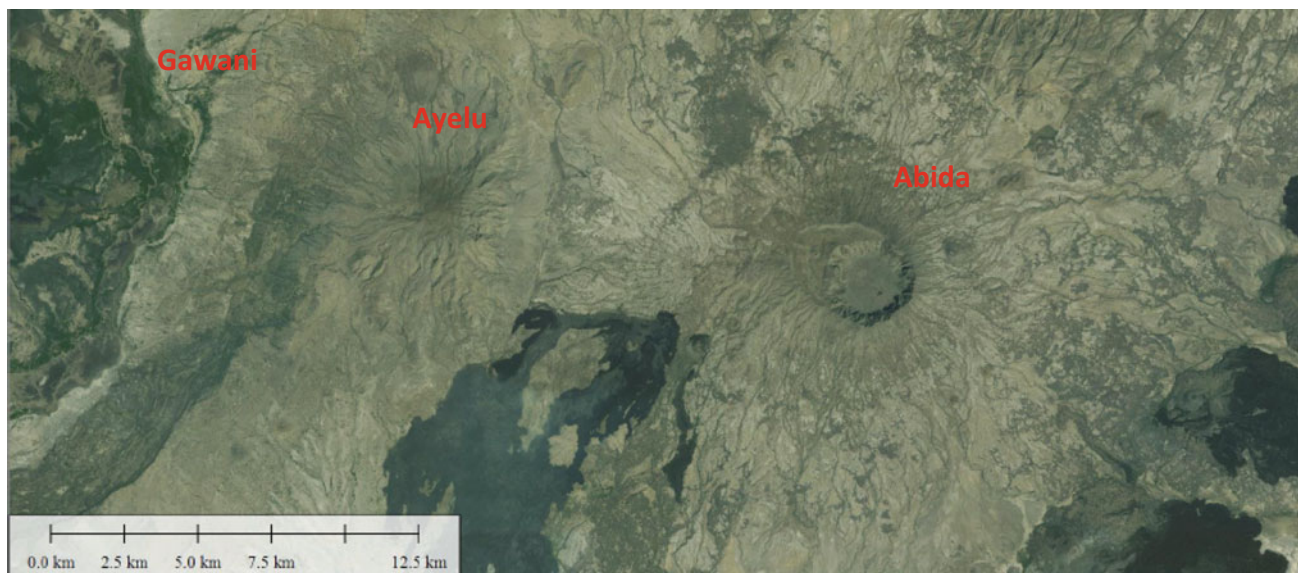


Fig. 10.24 Satellite image (Global Mapper 16) of Ayelu and Abida volcanoes, aligned E–W with the city of Gawani along the road that passes along the contact between the volcanic reliefs and the swampy (dark) Awash plain to the west. Observe the pale ignimbrite cover and the dark post-caldera lava flows around Abida calderas

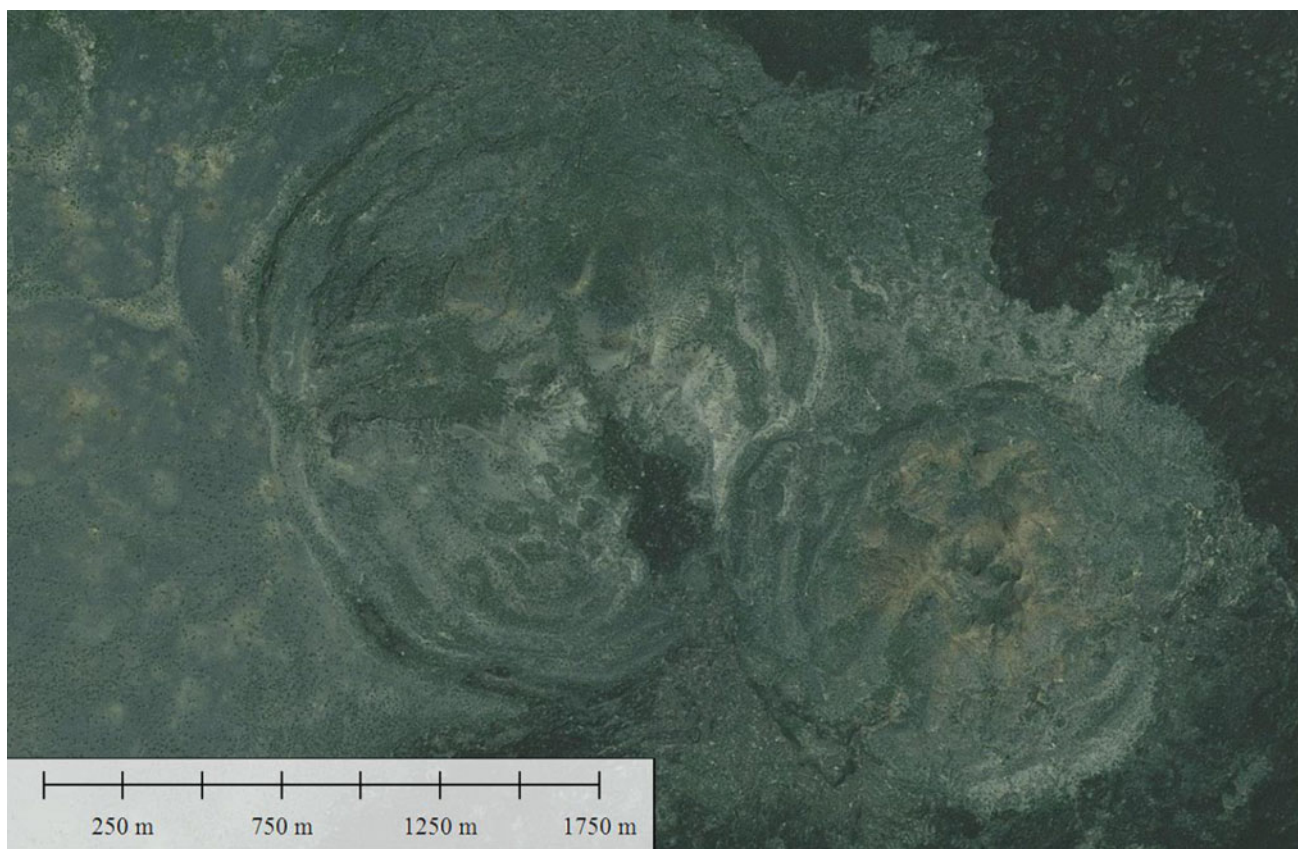


Fig. 10.25 Satellite image (Global Mapper 16) of ring structures observed south of Abida, made of viscous porphyritic basalts extruded at a nearly solid state

that this complex volcanic unit developed along a major WNW–ESE transverse structure that also corresponds with the change occurring in the Nubian basement from the NNE–SSW trending faults to the south to the NNW–SSE trending faults to the north.

With at least two sequences of fractionation (pre- and post-caldera) at Abida, postdating earlier differentiation sequences in Ayelu, we must consider the area to be a wide centre of long-lasting activity where successive supplies of magma were provided, allowing intense fractionation in successive nearby magma chambers.

South from Ayelu-Abida, the rift Afar depression extends south down to Fantale, with the active axis displaced towards the west by a few tens of kilometres, where another axis is found with the alignments of three major volcanic units: Angelele-Hertale, Dofan and Fantale (Fig. 10.26).

10.3.4 Angelele-Hertale

South from Gawani, the axis of the rift is displaced towards the west in the swamps surrounding the Awash River. There, a recent volcanic unit developed along NNE trending faults and open fissures. This spreading segment called Angelele ends to the north on Lake Hertale where hot springs occur. This unit is therefore also called Hertale in the geothermal literature.

Angelele rift segment is located on the eastern side of the Asash River, and is therefore accessible from the main Addis to Djibouti road south from Gawani. It is made of lava of dominantly basaltic composition, fairly recent, with sub-historic lava flows along the 30 km-long axis of the rift, where a well-developed, 2.5–3 km-wide, axial graben (rift-in-rift) is observed (Fig. 10.27).

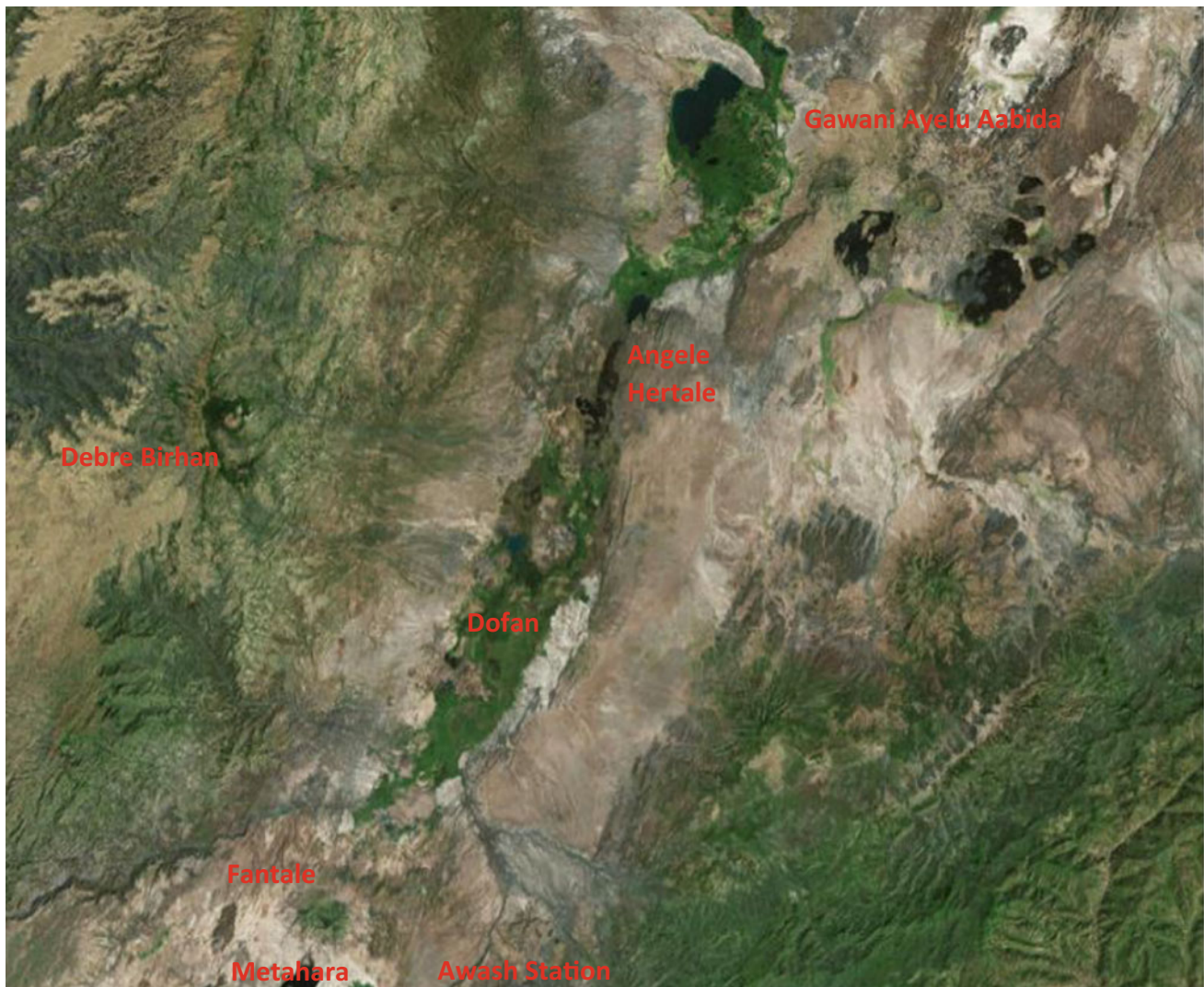


Fig. 10.26 Satellite image (Global Mapper 16) of the southern spreading segment of southern Afar, showing the location, on a satellite image, of the major volcanic units identified long the active

axis of the rift. The Awash Valley appears green along the axis of this otherwise deserts rift structure cutting NNE–SSW through the Nubian and Somalian highlands (*green*)



Fig. 10.27 Satellite image (Google Earth Pro) of the Angelele-Hertale volcanic system. The symmetrical normal faults looking towards the axis are well developed and visible, as well as the recent basaltic fissural flows filling the floor of the axial graben (*dark*).

The Awash River contours this unit on the western side. It is therefore directly accessible from the main road Addis-Djibouti visible on the right (east), but no route is built through this wild landscape

In the central part of the range, more or less developed shield volcano structures are observed, rejuvenated by extensive tectonics (Fig. 10.28). Although no petrological sampling is yet available, one can infer that the lava is dominantly basaltic with a few intermediate products, iron-rich intermediate fluid lava flows and more viscous silica-saturated trachytes. On the western flank of the rift

axis, a dome structure is observed in the median part of the range, later cut by rejuvenation of the rift axis (Fig. 10.29). These observations show that a magma chamber developed periodically in this volcanic range, providing a shallow heat source for a potential geothermal system.

On both extremities of the range, the axial graben enlarges and deepens, with more intense, fairly recent faults



Fig. 10.28 Detailed satellite imagery (Google Earth Pro) of the northern extremity of the Angelele axial range and southern shore of Lake Hertale. A shield volcano with the eastern half of a double

rimmed summit caldera is observed, dissected by normal faults downthrown in the axis and covered by more recent basaltic lava flows

and basaltic emissive fissures, allowing for the formation of the Hertale Lake to the north and of swamps and smaller lakes to the south (Fig. 10.30).

Hot springs are known to occur on the eastern and southern shores of Lake Hertale, emerging at the level of the lake from the faults. Temperatures of 40 and 44 °C were measured by the UNDP study in 1972, but no more recent study has been carried out and no chemical analysis of interest is yet available. It is not excluded that other thermal manifestations exist in the southern extremity of the range, along the sides of the swamp, for instance in the vicinity of the small lakes, or fumaroles along the axis.

As a whole, the area is of real potential geothermal interest, as it displays both a shallow magmatic heat source along the axis of the range and a hydrothermal system that could develop in the highly fractured basaltic lava pile, whereas there is no problem of water recharge in this swampy environment of the Awash valley. However, the site, despite its location on the eastern side of the Awash

River (which is not far from the Addis to Djibouti road), is at present difficult to access because of the lack of a suitable road.

From a volcanological and petrological point of view, it is worth emphasising that this volcanic unit appears as an essentially basaltic range, showing analogies with the axial ranges of NE Afar, with the absence of silicic stratovolcanoes which otherwise characterise the volcanic units of the MER. This probably results from the fact that this unit developed along a unique NNE axial trend, with no interference from other transverse faulting which elsewhere allow for the development of central volcanoes. It would be of interest to develop further petrological and geochemical studies to identify its specificities with respect to other volcanic units of the MER and Afar axial ranges.

South of this unit, another smaller (20 km-long, 7 km-wide) basaltic fissural lava field is developing on the western side of the Awash River. This appears to be just a recent lava field, which would also be worth studying.

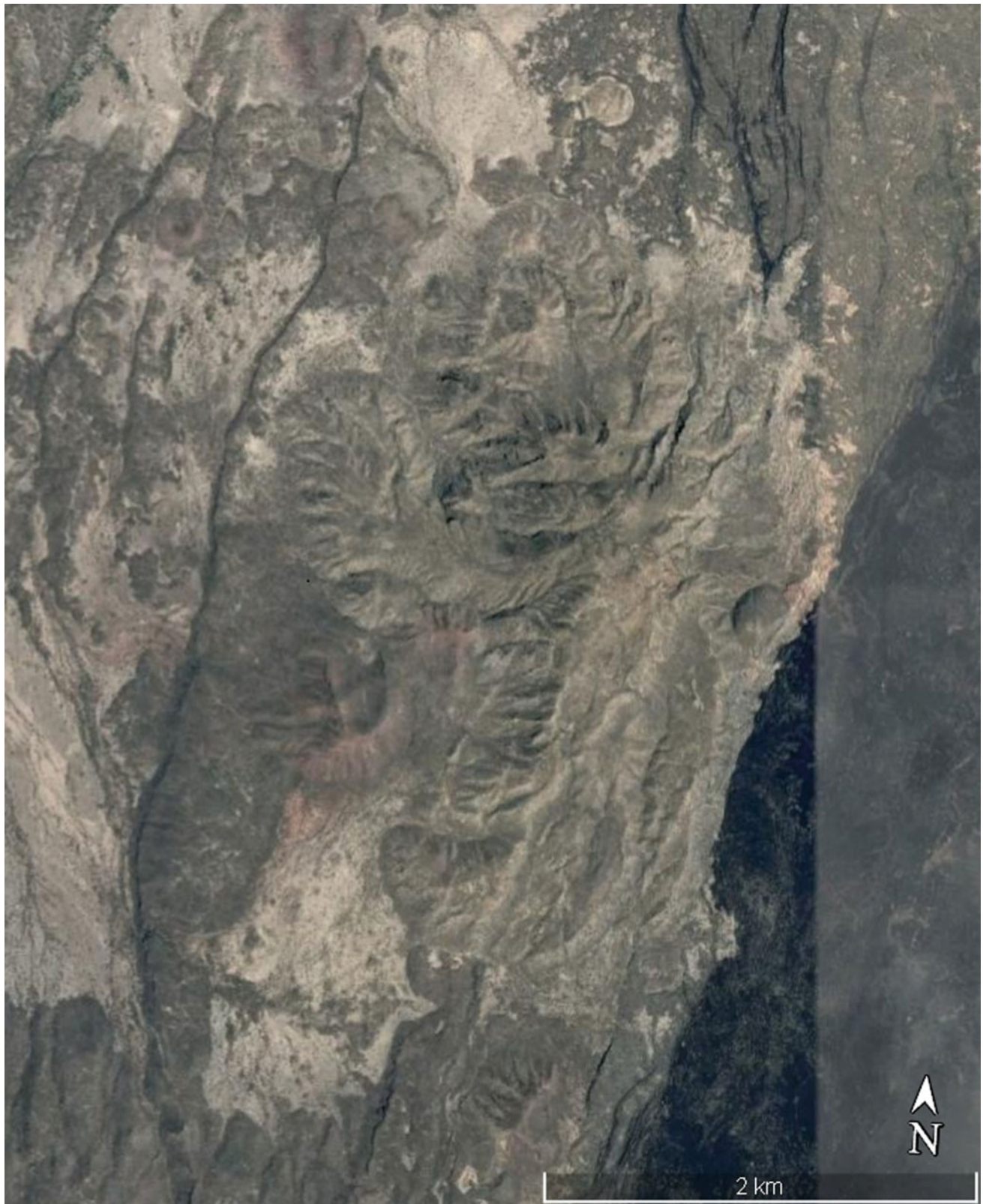


Fig. 10.29 View of a silicic dome (trachyte?) that developed in the central part of the Angelele range, now located on the western side of the spreading axis (satellite image from Google Earth Pro). The dome

—5 km long—is intensively dissected by normal faulting with apparently a dextral strike-slip component. On the right, the axis of the graben is observed, filled by black basaltic lava flows



Fig. 10.30 Detailed satellite imagery (Google Earth Pro) of the southern part of the Angele axial range showing the NNE–SSW emissive fissures along the MER rift axis (open fissure and alignment

of spatter cones). A hyaloclastite cone is observed on the NW side of the picture, showing magma–water interaction in this wet part of the Afar rift system

10.3.5 Dofan

Dofan is located along the same magmatic segment as Fantale in its northern extremity. The basaltic lava fields of both volcanic units are continuous on the floor of this southernmost Afar segment of the MER. The base of the edifice lies at an altitude of 750 m (Awash River) whereas the maximum height reaches 1151 m. The area is drained to the west by the sub-permanent creeks originating from the highland, but is dominantly drained along its N–S axis by the Awash River, as it is affected by numerous normal faults of N–S direction. The Awash River contours to the east of the volcano and large plantations (sugar, cotton, fruit) surround the edifice, providing several access road, in particular for accessing to the newly built Kesem sugar plant (Fig. 10.31).

There is therefore a need to cross the Awash River in order to reach the Dofan site from the Addis to Djibouti highway. From the newly built asphalted road accessing to the Chinese built Kesem sugar plantation, a dust road allow

to cross the massif to the south and to also reach the northern side contouring its western flank.

Dofan is a small (not exceeding 10 km wide) but complex volcanic unit. It is characterised by the occurrence of a variety of magma types, including basalts and various silicic products, among which trachytes dominate. The volcano grew in the last 500,000 years, with nearly continuous activity up to the present day. During the most recent period, the edifice has been affected by vigorous extensive tectonics (Fig. 10.32) that created a well-developed symmetrical rift structure along its axis (Fig. 10.33). Trachyte domes, some of them with developed fumarolic activity, are found along this rift-in-rift axis (Fig. 10.34). The last eruption of sub-historic age emitted a basaltic flow on the NW side of the volcanic system.

It should be noted that a sedimentary layer, 40–100 m thick, made of lacustrine-fluviatile products capped by hyaloclastites, is observed, tilted, faulted and covered by more recent volcanic, on the complete western side of the unit, and has a very wide extension. At depth it would act as a good geothermal cover.

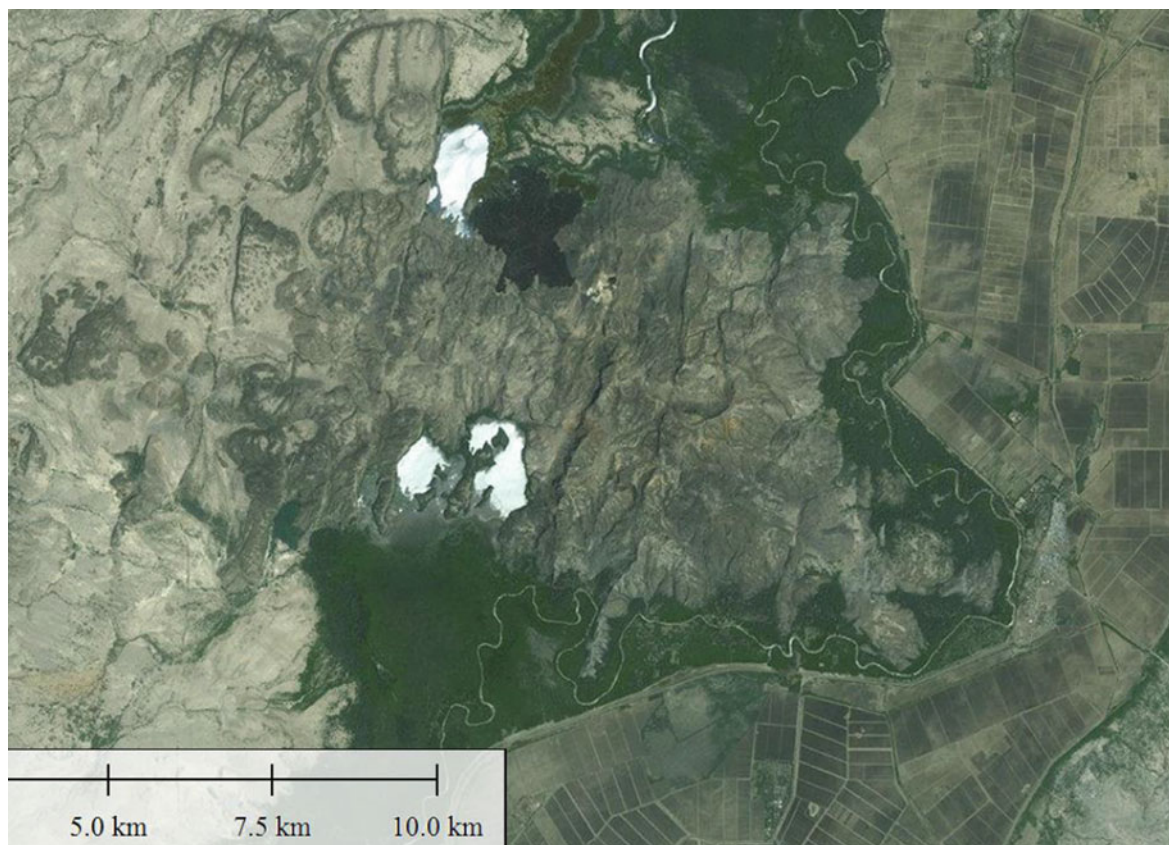


Fig. 10.31 Satellite image (Global Mapper 16) of Dofan Range, which clearly constrains the Awash River and its swampy surroundings (green) to contour the volcanic system on the eastern side. Observe the intense normal faulting, trending NNE–SSW, that cuts through the

volcanic system with the formation of an axial graben, 5 km wide. The viscous structures of the silicic domes is well visible along the sides and a sub-historic basaltic flow is observed in the north-central part



Fig. 10.32 One of the normal faults observed in the SW side of the Dofan shield volcano (Photo J. Varet 2016)



Fig. 10.33 Dofan volcano seen from the south, showing the 5 km-wide axial graben with recent domes and craters topping the edifice (*Photo J. Varet 2016*)



Fig. 10.34 View of the north-eastern part of the Dofan volcano (seen from N), showing the faulted and tilted blocks (western half of the graben) and the axial silicic domes (*Photo J. Varet 2016*)

10.3.6 Fantale

The southernmost volcanic unit of Afar is the Fantale volcanic system, a complex stratovolcano, which underwent an important sequence of lava and pyroclastic flows and a huge ignimbrite eruption, shaping the surrounding relief and all the rift floor. Made of peralkaline rhyolite, the floor lies very flat all around the volcano over long distances and is known for its “blisters” (Fig. 10.35) crossed by the Addis Ababa to Djibouti railway (Gibson 1970). The blisters resulted from

the degassing of the obsidian fiamme after the ignimbrite sheet was emitted. The magma types erupted from Fantale vary from basalts to pantellerites with all intermediate products, including peralkaline trachytes.

Culminating at 2007 m, it dominates the surrounding plains by 1000 m. Its truncated shape results from the presence of a well-expressed elliptical (3.5×2.5 km) summit caldera elongated WNW–ESE which tops the edifice. It exhibits steep walls, 200–250 m high, with a floor at 1465 m (Fig. 10.36).



Fig. 10.35 One of the numerous blisters observed along the road crossing through the southern flank of Fantale volcano, resulting from the late degassing of the peralkaline ignimbrite (Photo J. Varet 2013)



Fig. 10.36 Panoramic view of the Fantale volcano as seen from the plain, SE. The truncated morphology results from both the summit caldera and the normal faults affecting the stratovolcano (Photo J. Varet 2016)



Fig. 10.37 Satellite imagery (Google Earth Pro) of the Fantale volcanic unit. The main stratovolcano is seen in the centre-left, with its elliptic caldera elongated NNW–SSE, transverse to the MER faulting (NNE–SSW) well expressed on both sides. The older “Tinish Fantale”, dissected by faults, is seen NE of the recent stratovolcano

A smaller volcanic edifice is found NNE from the main volcano called “Tinish” (meaning small) Fantale that reaches a height of 1403 m over the plain at an average elevation of 800 m. It is older, and affected by tectonic activity (NNE–SSW trending normal faults) and erosion (Fig. 10.37).

Most of the area is included in the Awash National Park that extends north to the Awash and Kasem Rivers and south to the Metahara farms. The level of the water is regularly increasing and a lake developed west of Matahara town because of the development of irrigation, which had to displace the road and the railway north, on the flank of the volcano.

The last (historical: 1810–1830) eruptions were made of scoriaceous basalts giving rise to cones and flows at the south flank of the volcano. The presence of hyaloclastite cones proves the magma–water interaction that developed at shallow depth.

Fantale is easily reachable from Addis Ababa through the highway that connects with Djibouti, which is subjected to important traffic with heavy trucks, particularly on the way up (most are empty on the way down). Good gravel roads

allow one to reach most parts of the area, also because of the flat average ignimbrite surface, except for the steep slopes surrounding the caldera, which can be reached with a four-wheel-drive vehicle only via a trail starting from the west and reaching the northern rim of the caldera.

Variations in the composition of the last ignimbrite eruption are evidence of a zoned magma chamber, with a volume of at least 2 km³

Numerous normal faults of NNE–SSW direction and associated flows, affecting the last ignimbrite sheet, and even more recent volcanic features prove the active distensive rift axis crossing through this recent volcanic unit.

Fantale volcano was affected by a continuous hydrothermal activity in its central part. Besides fumaroles observed in the caldera, and hot springs occurring on the northern foot, andradite garnets of fumarolitic origin affecting a faulted trachyte have been described (Varet 1969).

South from Fantale, the next segment displaced en echelon to the west is the Kone volcanic unit, crossed in the middle by the Addis Ababa to Djibouti road and railway, which extends south with the wide Boseti volcanic centre.

References

- Aronson LJ, Taieb M (1981) Geology and paleogeography of the Hadar Hominid Site, Ethiopia. In: Rapp G, Vondra C (eds) *Hominid Sites and their geological settings*. AAAS Selected Symposium vol 63, pp 165–195
- Barberi F, Borsi S, Ferrara G, Marinelli G, Santacroce R, Tazief H, Varet J (1972) Evolution of the Danakil Depression (Afar Ethiopia) in light of radiometric age determination. *J Geol* 80:720–729
- Barberi F, Santacroce R, Varet J (1982) Chemical aspects of rift magmatism. In: Palmason G (ed). *Continental and Oceanic Rifts Geodynamics Ser vol 8*, pp 223–258
- Beyene A, Abdelsalam M (2005) Tectonics of the Afar Depression: a review and synthesis. *J African Earth Sci* 41:41–59
- Black R, Morton WH, Varet J (1972) New data on Afar tectonics. *Nature Phys Sci* 240:170–173
- Bonatti E, Tazieff H (1970) Submarine volcanoes in the Afar rift. *Amer Geoph Un Gen Meeting*, AGU transactions
- Feibel CS (2004) Sedimentary pattern in the Pliocene Hadar formation, Afar Rift, Ethiopia. *Denver Annual Meeting*, November 2004
- Ferrara G, Santacroce R (1980) Dama’Ale: a tholeiitic volcano in southern Afar (Ethiopia). *Atti Convegna Lincei* 47:437–453
- Gasse F (1977) Evolution of Lake Abhe (Ethiopia and TFAI), from 70,000 b.p. *Nature* 265:42–45
- Gasse F, Richard O, Robbe D, Rognon P, Williams MAJ (1980) Evolution tectonique et climatique de l’Afar Central d’après les sédiments plio-pléistocènes. *Bull Soc Géol Fr* 22:987–1001 (in French with English summary)
- Gibson IL (1970) A review of the geology, petrology and geochemistry of the volcano Fantale. *Bull Volcanol* 38(2):791–802
- Hall Walter RC, Westgate JA, Yord D (1984) Geochronology, stratigraphy and geoghemistry of Cindery Tuff in Pliocene hominid-bearing sediments of the Middle Awash, Ethiopia. *Nature* 308:26–31
- Hofstetter R, Beyth M (2003) The Afar Depression: interpretation of the 1960–2000 earthquakes. *Geophys J Int* 155:715–732
- Keir D et al (2011) Mapping the evolving strain field during continental breakup from crustal anisotropy in the Afar Depression. *Nat Comm* 2:285
- Manighetti I, Tapponnier P, Courtillot V, Gruszow S, Gillot P-Y (1997) Propagation of rifting along the Arabia-Somalia plate boundary: the gulfs of Aden and Tadjoura. *J Geophys Res* 102:2681–2710
- Manighetti I, Tapponnier P, Gillot P-Y, Jacques E, Courtillot V, Armijo R, Ruegg J-C, King G (1998) Propagation of rifting along the Arabia-Somalia plate boundary: into Afar. *J Geophys Res* 103:4947–4974
- Manighetti I, Tapponnier P, Courtillot V, Gallet Y, Jacques E, Gillot Y (2001) Strain transfer between disconnected, propagating rifts in Afar. *J Geophys Res* 106:13,613–13,665
- Mulheneh AA, Kidane T, Rowland J, Bach-Tads V (2013) Counter-clockwise block rotation linked to southward propagation and overlap of sub-aerial Red Sea Rift segments, Afar Depression: Insight from paleomagnetism. *Tectonophysics*
- Taieb M, Johanson DC, Coppens Y, Aronson JL (1976) Geological and paleontological background of Hadar hominid site, Afar, Ethiopia. *Nature* 260:289–293
- Varet J (1969) New discovery of fumarolitic garnets (Fant’Ale, Ethiopia). *Contrib Mineral Petrol* 22:185–189
- Varet J (1975) Carte géologique de l’Afar central et méridional, CNR-CNRS, 1/500 000 Géotechnip
- Varet J (1978) Geology of central and southern Afar (Ethiopia and Djibouti Republic), map and 124 pp. report, Centre Natl. de la Rec Sci, Paris
- Varet J (2013) The Afar system and carbonates. *Cocarde workshop* (abstract), Sicily, pp 48–49
- Walter RC, Aronson JL (1993) Age and sources of the Sidi Hakoma Tuff, Hadar Formation, Ethiopia. *J Hum Evol* 25:229–240
- Walter RC, Hart WK, Westgate JA (1987) Petrogenesis of a basalt-rhyolite tephra from West-Central Afar. *Ethiopia Contr Mineral Petrol* 96:462–480
- Wolfenden E, Yirgu G, Ebinger C, Ayalew D, Deino A (2004) Evolution of the northern Main Ethiopian rift: birth of a triple junction. *Earth planet Sci Lett* 224:213–228

Part IV
Conclusive Remarks

After this comprehensive description of Afar geology, another look at the geodynamic context can be proposed. Recalling that Afar appears as a unique place on planet Earth, the following would be good subjects for further investigation:

- The process of break-up of a continent in an area of triple junction.
- The way continental drift develops from continental to oceanic rifting.
- How ridges progress and microplates form, deform and rotate.
- The pertinence and limits of the mantle plume models.

At the intersection of three major Earth rift structures: the Red Sea, the Gulf of Aden and the EARV, and at the centre of an area where three plate margins (Arabia, Nubia and Somalia) gave rise to high plateaus, Afar itself is a lowland partly below sea level, gifted with a particularly arid environment. It therefore provides exceptional opportunities for the geologist to observe and eventually understand this part of the story of the Earth's evolution.

11.1 The Process of Break-up of a Continent in an Area of Triple Junction

Afar displays a geological evolution that directly relates to—and finally fits fairly well with—results from the study of the surrounding rifts: the Red Sea, the Gulf of Aden and the MER segment of the EARV. The main events are summarised below (Fig. 11.1).

The pre-existing Afro-Arabian plate was subject to early extension (essentially passive spreading with no or limited magmatic activity) in Jurassic and Cretaceous times, with the development of grabens along dominantly WNW trending faults over a wide area including Afar's present location and its surroundings (ex. Makale graben).

A first Miocene stage (around 31–24 million years ago) was characterised by crustal upwelling, emission of trap volcanics on the resulting then unique plateau, followed by the sinking of the Red Sea, Gulf of Aden and MER, northern end of the EARV, and the separation of the three Nubian, Arabic and Somali plateaus. The centre of this regional upwelling was located in what is presently central Afar, and that is probably where major dike events feeding these traps occurred. The underlying continental crust is affected by this event (diking). The period 31 million years ago marks a key step, with the production of most of the trap basalts on the three plateaus then being continuous.

In a second stage (24–15 million years ago) the three rifts were subject to crustal attenuation by dominantly passive rifting (normal faulting and crustal thinning by “bookshelf faulting”, with minor magma injections and emissions). During this period, Afar was only affected by the NNW-SSE trending Red Sea rift and NNE-SSW trending EARV, both at a continental rift stage. The influence of the Gulf of Aden (E-W trend) is expressed in the border faults of the Somalian escarpment observed in southern Afar. However, the expression of a continental rifting stage is not observed as for the Red Sea and MER rifts. The time 24 million years ago represents a key step in this period, with the development of a wide pluton (former magma chamber having fed contemporaneous eruptions), differentiating from transitional basaltic compositions to peralkaline granites in its upper part. The silicic top of this body is now observed in central Afar (Affara Dara) and at the same latitude along the Ethiopian escarpment and the southern extremity of the Danakil Alps (Arrata). Now separated by later (four million years to present) crustal spreading and magma injection along the two axial range axes (Tat'Ali and Manda Harraro), it is split into three pieces. The location of this pluton corresponds to a major transverse line of weakness. This could be interpreted as a sort of leaky fracture zone which even now represents a major discontinuity in Afar. Affara Dara pluton appears later as a rather rigid mole determinant for the later tectonic pattern, surrounding it.

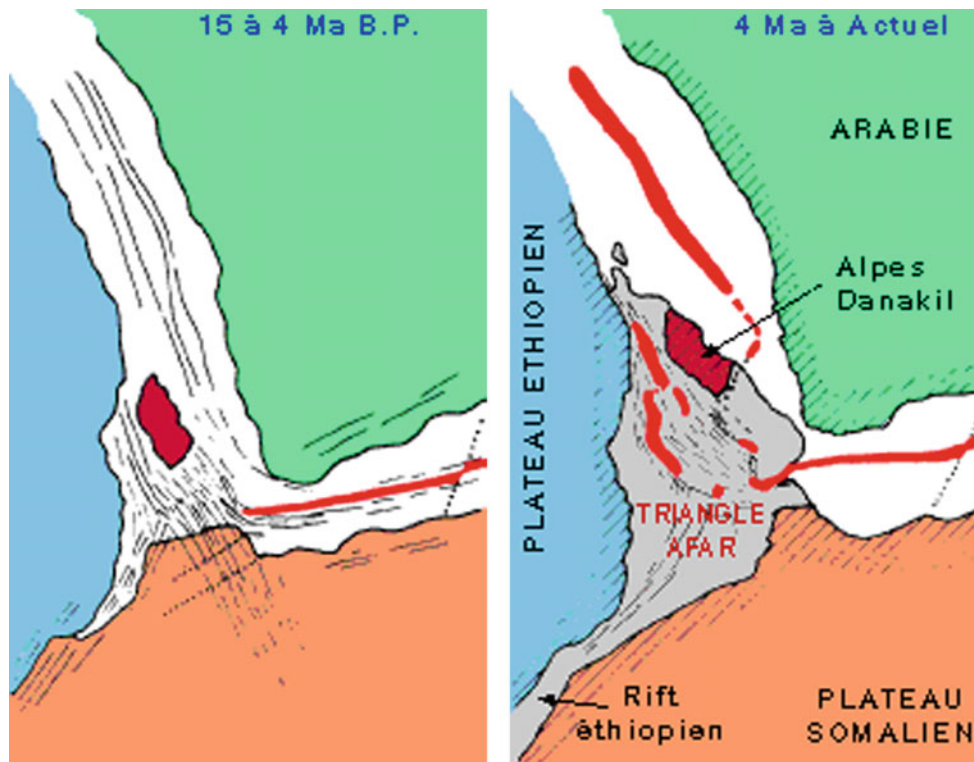


Fig. 11.1 Schematic representation of two major steps in Afar transition from continental to oceanic rifting. In a first step (from 24 to 4 million years ago) crustal attenuation by normal bookshelf faulting and magma injection develops along the Red Sea and MER, whereas the Gulf of Aden starts oceanic spreading. In a second step (from 4 million years ago to present) oceanic crust also develops in the central

part of the Red Sea, and the process progressively penetrates in southern Afar through the Gulf of Tadjourah, whereas the Danakil microplate rotates to account for the ceasing of spreading in southern Red Sea, with the development (around 1 million years ago) of spreading segment of oceanic type along the axial ranges (in red) of Central and northern Afar

In a third stage (15–8 million years ago) active continental rifting developed in central-southern Afar, ensuring the link with the Red Sea and MER continental rifts. It is characterized by the emission of abundant silicic products, emitted through linear fissures rather than central volcanoes and made of rhyolites of mildly alkaline composition. These units are intensively faulted, hydrothermally altered and eroded. This stage is particularly well expressed in the area now located on both sides of the Afar floor, in the northern half of the Djibouti Republic and at the foot of the Nubian escarpment in the Mille basin area. In this period, central-southern Afar differs from northern Afar, where this stage is not observed.

In a fourth stage (eight to four million years ago) the Gulf of Aden engaged—in its central-western part—in a process of continental crust separation, with production of oceanic crust. During this period, the south-eastern margin of Afar and Southern Red Sea became stable and acted as a western extension of the Arabian plate. A wide basaltic plateau developed in northern Djibouti Republic, thick on the Afar side and thinning towards the Red Sea, sealing this previously spreading area. Similarly, the central western Afar (along the foot of the Nubian escarpment) until then subject

to crustal extension and magmatic activity, also stabilised, with similar basalts (Dalha formation) emitted.

In a fifth stage (four to one million years ago) the Gulf of Tadjourah progressively extended westwards within Afar, the E-W trending rift cutting through the brittle crust until affected by the NNW (Red Sea) trending continental rift. Initially, in western Afar (southern Djibouti Republic), a major transform fault links the western Gulf of Aden to southern Afar basaltic spreading segments. Then the tectonic activity migrates from south (Goba'ad) to north (Asal), whereas the Aden spreading propagates west, developing the Gulf of Tadjourah. Oceanic crust is generated along the Red Sea axis north of Hanish Island but not south of it, where the area stabilises and becomes an accreting margin of the Arabian plate. North of the Gulf of Tadjourah, the newly accreted margin of the Arabian plate is progressively lifted up by 2000 m, as a result of a process similar to the one operating 25 million years earlier in the whole region. As a result, through Afar, a new junction is operated with the Red Sea and Gulf of Aden tending to develop as a single accreting plate margin, resulting in the emission of the basaltic fissural stratoid series over the whole central Afar. Continental rifting—crustal attenuation,

erosion-sedimentation and associated volcanism—continues to develop in southern Afar as well as in northern Afar, without creation of a basaltic crust.

In a sixth stage (one million years to present) active spreading segments develop in northern and central Afar along the axial ranges from Erta Ale range to the north to Asal-Ghoubbet to the east, through Tat'Ali and Alayta, Manda Harraro and Manda Inakir. This ensure the link between the Red Sea and the Gulf of Aden through real oceanic-like spreading segments with diking of oceanic type. In northern Afar, the coexistence of the Erta Ale, Tat'Ali and Alayta spreading segments with the Southern Red Sea axis north of Hanish Islands results in the rotation of the Danakil Alps (Arrata microplate). In central Afar, the spreading is concentrated in the axial ranges of Asal-Ghoubbet, Manda Inakir and Manda Harraro only, as the Southern Red Sea and western Afar appear to be a stable extension of the Arabian plate. It should be noted that, according to these observations, the Danakil microplate is much smaller than in the presently prevailing geodynamic models, and therefore its rotation is more important.

The changes occurring in the Red Sea – Aden area are considered as resulting from variations in the relative motions of the three plates involved. This is certainly the case for the change having occurred four million years ago when oceanic spreading first appeared as the Red Sea developed, whereas Gulf of Aden already had acted for long as an oceanic spreading centre. However, the hypothesis that clearly fits our observations in Afar is that the spreading rate of the Arabian plate increased significantly four million years ago.

As a whole, one clearly sees that Afar does not act as a well-identified triple junction that would impulse the development of the three surrounding rifts, as expected in the textbook model. It does not show either the influence of a single mantle plume that would have engineered the Afar construction. On the contrary, the three rifts appear to have more or less interfered with time, and as a result the junction area fluctuated with no well-defined driving centre. The pre-existing structural discontinuities in the pre-Cambrian basement have played a major role in this fabric, as well as the newly generated discontinuities resulting from the successive steps of the tectonic and magmatic evolution (such as sealing effects of granitic bodies or trap series).

11.2 From Continental to Oceanic Rifting

As a whole, Afar expresses in time and space the way that drift develops from continental to oceanic rifting.

If the two kinds of rift systems are well expressed in Afar, with a generally good contrast between the continental type in southern Afar and MER with respect to axial ranges analogues of oceanic spreading segments in northern and central Afar, some variations are also observed.

At the continental rift stage, two types of geological phenomena prevail in Afar:

- Normal faulting with crustal thinning through bookshelf faulting with associated basaltic magma injection, as observed eventually along the NW Afar margin as well as in the Danakil and Aisha blocks.
- In southern Afar, central stratovolcanoes with calderas and rather abundant pyroclastic products of peralkaline composition typically developed in association with fissural dominantly basaltic lava between centres located at a distance of 50–70 km. Also observed along Afar margins in continental crustal environment, and at least there, along Afar margins at least, these are shown to result from contamination with the underlying basement.
- The occurrence of fissural silicic eruptive material also appears at certain stages, such as in the north Tadjourah area between 15 and 8 million years ago, and eventually along the MER south of Afar, but are not documented in the Afar floor proper.

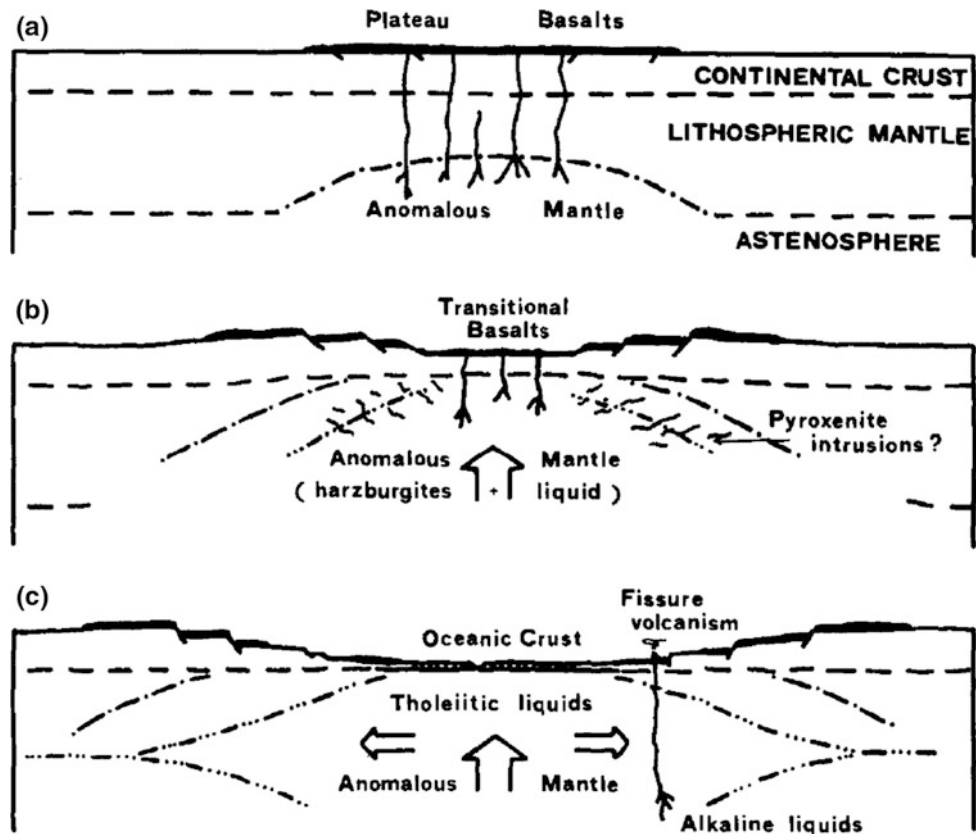
At the oceanic rift stage, the volcanic activity of basaltic (transitional to tholeiitic) composition concentrates along the axes of linear ranges. Normal faulting develops symmetrically on both sides of the spreading axis where repeated diking occurs. As a result, a symmetrical unit is formed, with older lava left on the sides and progressively more recent lavas moving towards the axis, where open fissures give rise to permanently active hydrothermal and eventually volcanic systems (lava lakes). Basalts of transitional composition dominate in these units at the fissural stage, evolving to iron-rich intermediate lavas at the shield volcano stage, by separation and flotation of plagioclase phenocrysts found in abundance in the lavas. Exceptionally, silicic lava (cumulo-volcano) occurs, topping the shield. Petrological and geochemical data show that all products result from crystal fractionation from the initial basalts in shallow (1–5 km deep) magma chambers. Note that the whole sequence develop under low oxygen fugacities, in a dry magmatic environment, with no (or very rare) pyroclastic product emitted at the surface.

It appears that from one axial range to another the composition of the initial basalt varies slightly, and this could be attributed to different degrees of partial melting of a similar mantle. The degree of partial melting appears to increase with the spreading rate. With the development of the process, the underlying mantle is progressively impoverished and magmas tend to become more tholeiitic (Fig. 11.2).

If the two types of volcanic systems are clearly distinct, some singularities can be noticed:

- In northern Afar, where axial ranges are located, marginal units are observed along both sides in places with thinned continental outcrops. These are characterised by

Fig. 11.2 Evolutive model proposed from the petrology and geochemistry of the basalts and associated ultramafic xenoliths in eastern Afar (Assab transverse range). Three successive hypothetical lithospheric sections are shown from early doming stage (A), to crustal thinning with the development of the rift producing transitional basalts (B), and the oceanic stage where tholeiites are produced along spreading segments and alkali basalts along transverse structures across the margins (C)



large stratovolcanoes with pyroclastic products and calderas and abundant silicic products.

- In southern Afar, along the MER northernmost segments, at least one unit (Angelele-Hertale) displays a volcanic structure that is very similar to axial ranges, with dominantly basaltic lava emitted along an axial graben, showing the MER northern extremity, where spreading rate is higher can display locally oceanic type accreting phenomena.

11.3 Transform Faults and Fracture Zones

In the MOR model, transform faults ensure the strike-slip connection between the successive spreading rift axes. One of the problems encountered in Afar is that the transform faults are not observed at the surface. The absence of visible transform faults was underlined since the earliest geological observations (Tazieff et al. 1970). However, a closer look allowed the identification of a few of them. To the east of the Ghoubbet, searching for the connection with the Gulf of Tadjourah spreading axis, a large fault system, trending NNE-SSW, was identified by Lepine et al. 1974 in the trench of Arta beach, with well-expressed horizontal strike-slip surfaces. Later on, the Makarassou fault system was

identified as the surface expression of a transform fault by analogy with the deformation obtained on clay models. At the initial stage of deformation it was shown that the surface expression of the transform fault was a set of en echelon faults trending at an angle of 30° with respect to the fault direction (Tapponnier and Varet 1974). The fact that this area is also an extensional flexuring margin (Le Gall et al. 2011) of the newly (five to eight million years old) accreted margin of the Arabian plate does not contradict the interpretation that Makarassou acts as the transform fault system connecting the Manda Inakir rift segment to the Asal rift segment.

In Barberi and Varet (1977), extended this approach and transverse faulting was used elsewhere to identify several incipient transform zones, leading to the proposal of a microplate model of the whole Afar in which axial ranges act as spreading segments whereas transform fault zones are expressed by oblique faults with respect to the main NNW-SSE to NW-SE (Red Sea – Gulf of Aden) pattern. Such transform structures were identified particularly south of Tat'Ali and south of Alayta, ensuring the connection with the Manda Harraro spreading segment, or at the western extremity of Manda Inakir, ensuring the connection with the Hanish-Biddu-Dubi transverse structure to the north and the southern extremity of Manda Harraro range to the south.

From this interpretation a picture emerges of Afar with several microplates located between the spreading segments

and transform fault zones, implying block rotation and intense deformation of these areas, which were shown to be subject to bookshelf faulting by Manighetti et al. (1998).

Surface equivalents of fracture zones were identified by Barberi et al. (1974) along the stabilised Afar margins, expressed in the form of transverse volcanic alignments, where the magmas differ from axial ranges, with a pronounced alkaline tendency, and the frequent presence of mafic cumulate inclusions and peridotite nodules, otherwise absent in central Afar. These transverse structures frequently correspond, inside Afar, with the discontinuities of the axial ranges, with a clear link between fracture zones (outside the Afar floor) and transform faults (inside the floor).

11.4 MOR and Oceanic Island Analogues

If Afar axial ranges display analogies with “textbook” MORs, one should also emphasise a few differences.

Besides the typical “rift in rift” structure where an axial dike of undifferentiated basalt is regularly injected along the rift axis, as observed in the Asal (1978) and Manda Hararo (2005–2010) events, axial ranges in Afar may display a few peculiarities. This relates in particular to the volcanic and magmatic evolution that is encountered in most or some of them.

Most display at certain stages of their evolution a shield volcano that contains differentiated lavas up to iron-rich intermediate liquids. The crystal fractionation process of the plagioclase (bytownite) responsible for this evolution is shown by the presence of plagioclase porphyritic basalts (eventually as crystal mesh) found in the lava flows and scoria cones or hornitos also found in abundance at this stage¹. Such a shield volcano may remain in an axial position, as observed in Asal range or in Hailigub (south Erta Ale range), and be rejuvenated by later spreading and rift in rift formation. However, it may equally be left aside with the development of a new rift zone along the NE side of the volcano as observed in Alayta or Manda Inakir. In the case of Manda Harraro and Erta Ale range, shield volcanoes are observed in parts of the range along its axis. This is in particular the case of Erta Ale (s.s.) where two shield volcanoes are observed, the northern one displaying two permanent lava lakes in the summit elliptic sink.

Exceptionally, the evolution reaches central cumulo-volcanoes made of silicic end members (trachytes and rhyolites) topping the shield. Here again, these were shown to be products of crystal fractionation in shallow

magma chambers. Such examples are well expressed in the northern half of the Erta Ale range. This volcanic evolution can be interpreted as caused by the slower spreading rate resulting from the sinistral rotation of the Danakil block. Similar products are also found in the Tat’Ali range and in the Inakir shield of the Manda Inakir range. However, despite the presence of these expressions of stable (non- or slow-spreading) volcanic forms, evidence of active rifting is expressed in the geology and the historical events at the level of these central volcanoes. At Alu-Dalafilla (one of the major silicic volcano of the northern part of Erta Ale range), the 2005 event showed the formation of a fissure eruption along the eastern side of the central volcano resulting from a new feeding event of the magma chamber.

These central volcanoes of the axial ranges display similarities to the oceanic islands observed along or close to the MOR, where sequences of lavas produced by crystal fractionation of transitional basalts are also present.

11.5 Pertinence and Limits of Mantle Plume Models

Following Morgan (1971), the mantle plume hypothesis has taken a prominent place in Earth sciences. Although accounting for less than 10% of the surface heat flow, it has been suggested that plumes profoundly influence the geologic environment, in particular in mid-plate volcanism and continental break-up. Afar was listed very early on among the major world plumes as soon as the theory was emitted.

The EARV and Afar in particular is of particular interest as the large amount of flood basalts, associated with regional uplift, initially emitted 31 million years ago, have been attributed a mantle plume (Schilling 1973; White and McKenzie 1989; Ebinger and Sleep 1998). Magmas, ranging from low-Ti to very high-Ti basalts and picrites, erupted in such a short space-time interval, and being overlain by younger alkaline basalts with peridotite xenoliths provide evidence on the nature of the mantle at this initial stage of the process, and a mantle plume has been suggested on the basis of geophysical data (Ritsema et al. 1999). However, despite numerous studies, there has been no consensus on the types and number of plumes. Seismic tomography shows a cylindrical, vertical tail through the lower mantle beneath Afar, which could merge into an “African Superplume” in the deep lower mantle (Montelli et al. 2006).

However, this model does not fit several geochemical studies supporting the existence of two distinct mantle plumes beneath East Africa (George et al. 1998; Nelson et al. 2007, 2008; Rogers et al. 2000). Furman et al. (2006) suggested that different plumes could stem from a common large mantle superplume, a hypothesis recused by Pik et al. (2006). Chang and van der Lee (2011) proposed a three

¹The same phenomena is observed at Erta Ale in Pelees hair, where plagioclase crystals drive the basaltic liquid which solidifies as yellow glass.

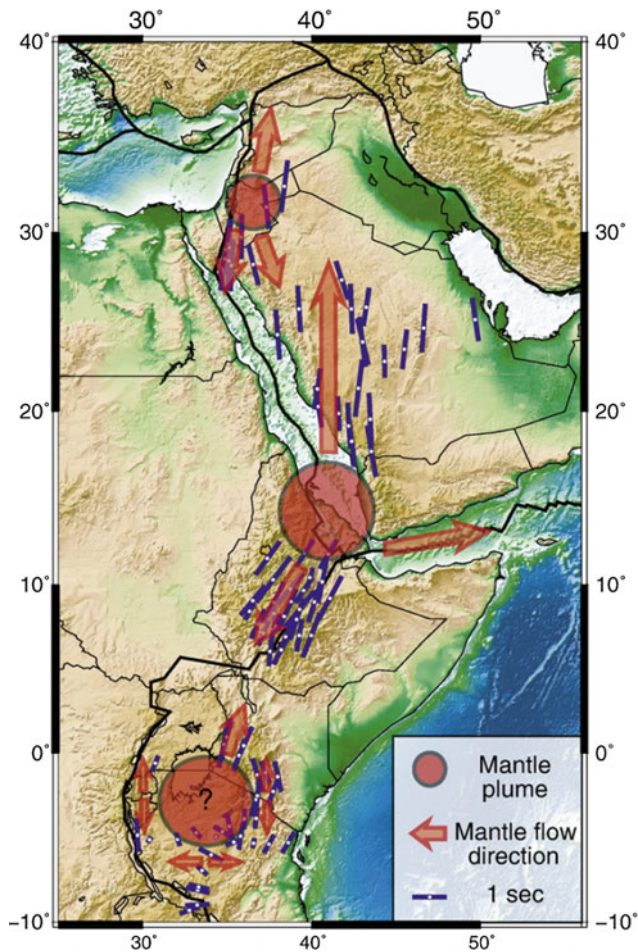


Fig. 11.3 Schematic picture showing locations of mantle plumes and mantle flow directions in Afar and surroundings. In this model, two plumes are proposed in Kenya and Jordan in addition to the Afar plume with three mantle flows along Aden, MER and the Red Sea—Arabian Harrats directions (after Chang et al. 2011). If it could account for the MER segment where spreading rates decrease from central Afar to south, it does not fit with the other two rift segments, particularly the Aden one

plumes model with channelling of the lower mantle in the three rift directions from a plume centred on Afar (Fig. 11.3). However, this model is not supported by geological observations, for instance, the westwards penetration of the Aden rift within Afar.

11.6 Proposed Interpretation of the Evolution of Spreading Within Afar

In Sect. 11.1 the process of doming of the Afro-Arabian plate and progressive break-up of the three resulting plates could be analysed. The geological observations revealed in this book also allow to determine accurately the geometry



Fig. 11.4 Active plate boundaries and other active segments in Afar and surroundings. The oceanic rifts of the Red Sea and Gulf of Aden are drawn in *thick red lines*, as well as the axial ranges of Afar. The transverse volcanic alignments and transform fault zones are drawn in *thin red lines*. The MER axis is drawn in *thick yellow*. *Dotted thick red lines* indicate spreading segments with weak volcanicity. *Dotted orange line* shows area of weakness (larger than the line) expressed by transverse faulting, seismic and fumarolic activity. Outcropping pre-Miocene formations are mapped in *pink*. Outcropping areas of mio-Pliocene continental rifting presently stabilised and accreted to the corresponding continental plates are mapped in *pale yellow*

and draw an interpretation of the evolution of the spreading within Afar. Our conclusions differ from both models prevailing presently in the literature, of either centripete “propagators” of the Aden and Red Sea rifts from outside to inside Afar (see Fig. 10.15) or the centrifuge model of the Afar plume (Fig. 11.3).

Figure 11.4 summarises the present stage of our understanding of the internal structure of Afar. The oceanic spreading segments of the Red Sea and of the Gulf of Aden are pictured in red. The Red Sea axis stops south when it hits against the Hanish Islands transverse structure, which continued on land through the Dubbi-Nabro-Bidu alignment. This ancient line of weakness also extends in the Dabbayra transverse volcanic unit that marks a major shift in the Nubian escarpment. It determines the recent shifts observed in the Afar axial ranges (the transform fault zone linking Tat’Ali and Alayta spreading segments with the Manda

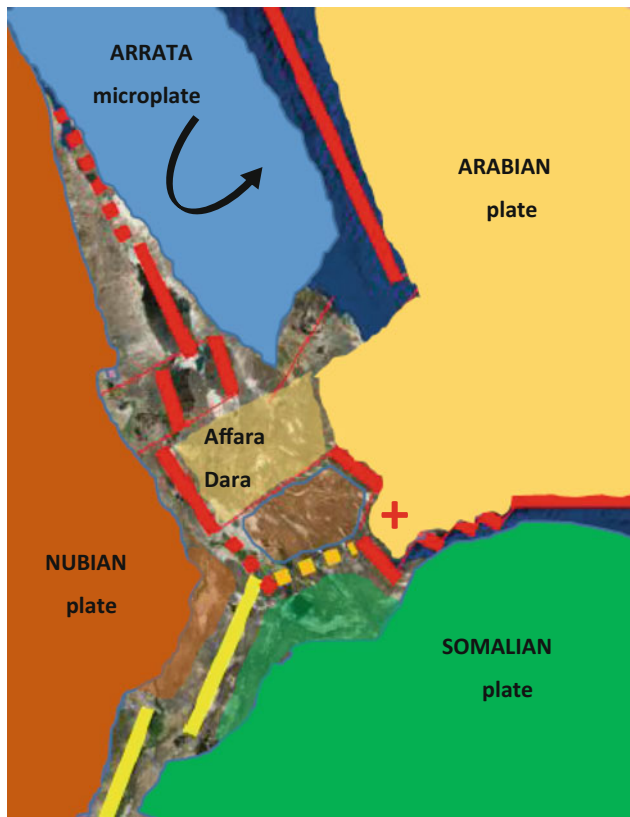


Fig. 11.5 Arabian (yellow), Nubian (maroon) and Somalian (green) plate boundary scheme resulting from our geological observations, showing the accreted margins during mio-Pliocene (zones of continental rifting stabilized in the last four million years). The Danakil Alps (Arrata block), in blue, is subject to sinistral rotation, with resulting opening from SW to NE along its southern margin. In pale colours are shown the accreting areas under progress for each of the three plates, with the Affara Dara microplate tending to become the westernmost extension of the Arabian plate. A remaining microplate in SE central Afar is subject to intense deformation because of both NNE-SSW (MER) and residual NE-SW extension not fully accommodated yet by the Manda Inakir spreading segment

Harraro segment, determining the location of the Dabbahu peralkaline silicic centre). It should be remembered that this also links the three early Miocene peralkaline granites of the Afar margins and Affara Dara (the only pre-Pleistocene outcrop found inside Afar).

Parallel to the Red Sea axis, the Erta Ale spreading segment is clear, (including the sparse magmatic bodies identified along the axis of the salt plain), an increase of the spreading from N to S, amplified south by the demultiplication of the spreading axis (Alayta and Tat'Ali axial ranges). This first transform fault zone (which can be called Afrera as the lake also results from it) in northern Afar is also controlled by the pre-existing fracture zone observed in the Nubian basement, determining the location of the Maa-lalta central silicic volcano.

The behaviour of the part of Afar floor located North of the Dabbayra-Dababhu-Dubi-Bidu-Hanish (DDDBH) fracture zone (FZ) is determined by the sinistral rotation of the Danakil Alps (or Arrata block), explaining the rapid increase of the spreading from north to south.

It should be noted that, as the DDDBH FZ marks the end of the Red Sea spreading axis, the area located south of this fracture zone should be considered to be a western accretion of the Arabian plate, and this down to the Gulf of Aden – Gulf of Tadjourah rift south of Bab-El-Mandeb strait. The other consequence is that the axial range located south of the DDDBH FZ is just the Arabian-Nubian plate boundary that accommodates the total whole spreading, which explains its particularly active characteristics as observed from the geology and the now well-documented 2005–2011 dyking and tectonic event.

The Manda Harraro axial range ends south at $11^{\circ}45'N$ at the level of Tendaho and Semara, the capital of the Afar Regional State. The active volcanic range is replaced by a rather wide, essentially sedimentary graben, filled by thick detritic and lacustrine sequence resulting from the erosion of the wide Awash River basin for the last 3.5 million years at least. A few sporadic volcanic units are found in this plain, largely emitted in sublacustrine conditions, with the noticeable exception of the Dama Ale volcano, which differs from axial ranges. It simply benefitted from the additional effect of the MER, but does not show any behaviour of an active rift. At the other extremity of the Tendaho graben (east of Dama Ale) the Gobaad graben dates back to Pliocene, showing that there is no process of propagation of the spreading segment south-eastwards, but rather a pre-existing graben that helped with the location of the axial range at its northern end.

The next spreading axis in Afar is found at a considerable distance NE, which is Manda Inakir crossing the Ethio-Djibouti border. This NW to WNW trending axial range then ensures the link with the Asal-Ghoubbet range through the Makarassou transform fault zone which connects with the Gulf of Aden through the Gulf of Tadjourah oceanic rift Zone.

The resulting picture, in terms of present plate boundaries, is reported in Fig. 11.5:

- The Arabic plate now includes the Bab-El-Mandeb strait and the north Tadjourah area up to the Assab transverse line, with two lines of E-W weakness (Sept Frères and E Mousa Ali) with recent alkali basaltic volcanism as for Assab line. The Tadjourah – Asal-Ghoubbet rift system ensures the line of accretion between the Arabic and Somalian plates. The whole new southern plate margin north of the Gulf of Tadjourah is subject to up-doming, with a particular intensity in the Day area, on the southern extremity of the Dalha basaltic plateau. This basaltic trap series emitted in the period eight to four

million years ago appears—with respect to the Tadjourah rift—as the equivalent of the Ethio-Somalian plateau basalts with respect to the Red Sea. The phenomenon is, however, clearly asymmetric here, as the northern side is uplifted much higher than the southern side (where some doming is also observed at Arta). This results from both the asymmetric spreading of the Tadjourah – Ghoubbet-Asal rift (developing near to the northern coastline) and from the geometry of the southern tip of the plate accretion stuck up between two inverse transform faults (redcross).

- The Nubian plate also enlarged at the foot of the escarpment south of Dabbayra, incorporating the now stabilised area accreted in Pliocene times, and sealed, as in the above case, after the emission of the Dalha basalts. Along the MER axis, the relative stabilisation of the Awash basin north of 10°30' (Ayelu-Abida transverse alignment) is more recent (around two million years ago).
- The rotating Arrata block (Danakil microplate) is more limited than in the currently prevailing models, and rotates between the Southern Red Sea trough and the Afar northern ranges. We are unable to define accurately its northern extremity, located in the Red Sea margin, north from Afar. Its southern extremity is more visible, in the Bidu Dubbi Hannish transverse structure, which acts as an opening from SW to NE as expressed in the evolution of the volcanism from large rhyolitic central volcanoes aligned SW-NE along the Afar internal margin to fissural basalts along the Red Sea coast (Dubbi shield) and in the Hanish Islands.
- In central Afar, despite the intense NNW-SSE normal faulting affecting the stratoid series (surface at one million years ago), the surface located south of the Dabbahu-Dubi transform fault over a width equal to the length of de Manda Harraro spreading segment and up to the western extremity of the Manda Inakir range appears as an accretion under progress of the Arabian plate within Afar.
- South of this area, the surface located between the Tendaho-Gobaad graben, Manda Inakir and the western extremity of the Asal rift appear as a microplate subject to intense deformations resulting from extension along both NNE-SSW (MER) and NW-SE (Red Sea-Aden) residual extension not yet fully accommodated by the Manda Harraro spreading segment.

Geological observations within Afar also allow attempts to reconstruct how this present scheme was acquired in the last few hundred thousand years (Fig. 11.6A–D):

- Departing from the present situation described above (Fig. 11.6A), it is possible to consider that
- One hundred thousand years earlier, the Manda part of Manda Inakir was not yet active, the axis of spreading being located in the Inakir range, which is trending NW-SE when the Manda segment is WNW-ESE (Fig. 11.6B). Similarly, the Tat'Ali range now trending N-S and even NNE-SSW in its southern extremity was not yet active and the spreading was fully accommodated by the Mat'Ala segment, trending NNW-SSE. We have observed a large graben south of Mat'Ala, and a series of other grabens and areas of recent volcanicity occurring between Mat'Ala and Inakir. From these observations it appears that a direct line of incipient spreading developed along this line (dotted line in Fig. 11.6B). In the Alayta range, the spreading was fully accommodated along the shield trending NNE-SSW whereas the historical activity occurred along a nearly N-S trending fissure. In southern Afar, the active axis was located E of the present Adda'do graben. As a whole, we observe two parallel axes along the whole Afar depression extending from Alayta-Tat'Ali (Afrera TF) to Abhe and Asal.

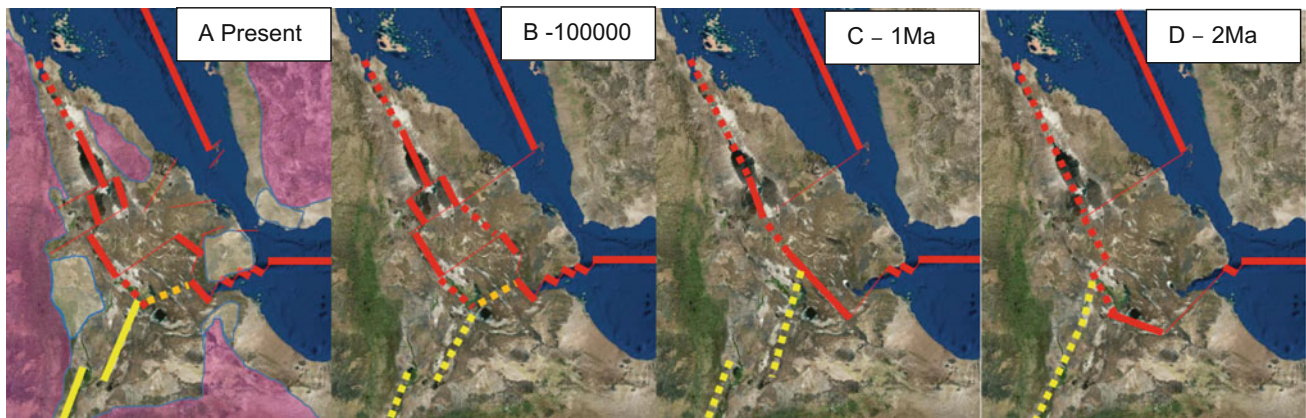


Fig. 11.6 Tentative reconstruction of the Afar major axis of spreading through time from the present to two million years ago from available geological data (comments in text)

- One million year ago, the present axial ranges were not yet active, whereas the stratoid series was emitted through fissures trending NNE-SSW dispersed over the whole Afar width. However, the important thickness of the stratoid series in central Afar may indicate a major diking along the median axis along a line trending from the present Hanlé-Gaggadé graben SE to the Affara Dara massif to the NW (Fig. 11.6C). The Gulf of Tadjourah was not yet fully open, with a direct link through the transform fault zone along the margin of the Ali-Sabieh block. The Afdera volcano marks the presence of this active axis to the north in that period. The continuity of this axis is dubious in its median part at the level of Affara Dara. This Miocene alkali-granite unit appears as a resistant nut that explains the later shift of the spreading axis to the west and to the east at present. This implies an extension of the MER axis north, which is visible in the Gamari faulting.
- From 3.5 to 2 million years ago (Fig. 11.6D), the Aden ridge did not reach Tadjourah, and the transform fault zone along the Ali-Sabieh block ensure the link with the dominant spreading segment located south of Gobaad. The volcanic activity is weak or non-existent north of the DDDGH FZ, marking a phase of passive rifting, whereas in central Afar, the stratoid basaltic series is emitted along NNW trending fissures without well-defined rift axes. The MER spreading segment is displaced to the west along the foot of the Nubian escarpment and extends north along the Karrayyou axis up to Tendaho, ensuring a direct link with the Red Sea spreading system.

As a whole, the picture emerging from this tentative reconstruction is that of an interplay of the three spreading systems, all present in the Afar floor for the last 3.5 million years (and earlier at the stage of continental rifting), and somehow competing with each other in the search for the best path, without any centripete (triple point of plume induced) or centrifuge (propagators) determinant. The path appears to be determined by pre-existing lines of weakness and the presence of resistant nuts (cf. Affara Dara), micro-plates (cf. Arrata) or stabilised accreted zones along the three major plate margins, as the best answer to the major plates divergent motions. It appears that, for both the Arabian and Nubian accreted plate borders, there is a tendency for the active rift to stick as near as possible to the plate border, leaving the Afar basaltic floor accommodating the remaining deformations.

References

- Barberi F, Varet J (1977) Volcanism in Afar: small-scale plate tectonic implications. *Bull Geol Soc Amer* 88:1251–1266
- Barberi F, Santacroce R, Varet J (1974) Peralkaline silicic volcanic rocks of the Afar Depression. *Bull. Volcan.* 38:755–790
- Chang SJ, van der Lee S (2011) *Earth Planet. Sc. Lett.* 302:448–454
- Chang S-J, Merino M, van der Lee S, Stein S, Stein C (2011) Mantle flow beneath Arabia offset from the opening Red Sea. *Geophys Res Lett*
- Ebinger C, Sleep N (1998) Cenozoic magmatism throughout East Africa resulting from impact of a single plume. *Nature* 395:788
- Furman T, Bryce J, Rooney T, Hanan B, Yirgu G, Ayalew D (2006). Heads and tails: 30 million years of the Afar plume. In: Yirgu G, Ebinger C, Maguire P.K.H. (eds.) *The Afar volcanic province within the East African Rift System: Geol. Soc. Spec. Publ.*, 259, pp. 95–119
- George R, Rogers N, Kelley S (1998) Earliest magmatism in Ethiopia: evidence for two mantle plumes in one flood basalt province. *Geology* 26:923–926
- Le Gall B, Daoud DA, Rolet J, Egueh NM (2011) Large-scale flexuring and antithetic extensional faulting along a nascent plate boundary in the SE Afar rift. *Terra Nova*, Wiley 23(6):416–420
- Manighetti I, Taponnier P, Gillot P-Y, Jacques E, Courtillot V, Armijo R, Ruegg J-C, King G (1998) Propagation of rifting along the Arabia-Somalia plate boundary: Into Afar. *J. Geophys. Res.* 103:4947–4974
- Montelli R, Nolet G, Dahlen FA, Masters G (2006), A catalogue of deep mantle plumes: New results from finite-frequency tomography. *Geochem Geophys Geosyst* 7, Q11007
- Morgan WJ (1971) Convection plumes in the lower mantle. *Nature* 230:42–43
- Nelson WR, Furman T, van Keken PE, Lin S (2007) Two plumes beneath the East African Rift System: a geochemical investigation into possible interactions in Ethiopia. *Eos. Trans. AGU* 88 (52)
- Nelson WR, Furman T, Hanan B (2008) Sr, Nd, Pb and Hf evidence for two-plume mixing beneath the East African Rift System. *Geochim Cosmochim Acta* 72:A676
- Pik R, Marty B, Hilton DR (2006) How many mantle plumes in Africa? The geochemical point of view. *Chem Geol* 226:100–114
- Ritsema J, van Heijst HJ, Woodhouse JH (1999) Complex shear wave velocity structure beneath Africa and Iceland. *Science* 286:1925–1928
- Rogers N, Macdonald R, Fitton JG, George R, Smith M, Barreiro B (2000) Two mantle plumes beneath the East African rift system: Sr, Nd and Pb isotope evidence from Kenya Rift basalts. *Earth Planet. Sci. Lett.* 176:387–400
- Schilling J-G (1973) Afar mantle plume: Rare earth evidence. *Nature* 242:2–5
- Taponnier P, Varet J (1974) La zone de Mak'arrasou en Afar: un équivalent émergé des «failles transformantes» océaniques. *CR Acad Sci* 278:317–329
- Tazieff H, Barberi F, Borsi S, Ferrara G, Marinelli G, Varet J. (1970) Relationships between tectonics and magmatology in the Northern Afar (or Danakil) depression. *Phil.Trans.Royal Soc London. A.*267(1970): 293–311
- White R, McKenzie D (1989) Magmatism at rift zones: The generation of volcanic continental margins and flood basalts. *J Geophys Res* 94:7685–7729

12.1 Thermal Manifestations, Geothermal Potential and Development Perspectives

12.1.1 Despite Arid Climate, a Gifted Region

Afar makes possible favourable geothermal conditions because of its geological context. The development of plateaus and border faults along the rift promotes the flow of meteoric water into the faulted rift floor, where crustal thinning and upwelling of the hot mantle lead to exceptionally high heat flows. Furthermore, normal and open faults along the rift axis favour the creation of convective systems. Moreover, when magma chambers develop at shallow depth (2–5 km) conditioned by central volcanic units, large high-enthalpy geothermal systems naturally arise, as all conditions are combined in these structures to favour the development of fractured reservoir and impermeable cover. Basic ingredients for “classic” high-enthalpy geothermal systems are thus available in numerous places (Omenda et al. 2014).

Although the earliest initiatives date back to the 1970s, in particular with the CNR-CNRS team¹ followed by UNDP studies in Ethiopia and Kenya and BRGM exploration in Asal (Djibouti), it is only over recent decades that geothermal energy has actually reached a convincing stage of development in Kenya. Besides the multilateral involvement by UNDP, UNEP, World Bank, OFID² and GEF³ as well as EU, programs supported by bilateral donors (BGR—Germany, ICEIDA—Iceland, USAID—United States, AFD—France etc.) and regional agencies (ArGéo, African Development Bank, etc.), allowed for developments to emerge.

¹see: <http://www.nature.com/nature/journal/v531/n7596/> <http://www.nature.com/nature/journal/v235/n5334/abs/235144a0.html>.

²OPEC Fund for International Development.

³United Nation Development and Environment Programs; Global Environmental Fund.

Compared with the resource potential, the use of geothermal energy is only in its early stages and broad areas are still open to research and innovation. If the approach is now based on large-scale systems serving the national electric grid, another form of geothermal development also needs to emerge that would answer local needs, such as community, factory, agro-industrial complex or touristic sites, with diversified applications of “direct uses”. Such systems can be developed on more diversified contexts such as convective fault-related hydrothermal systems in a-magmatic environment. The “Geothermal Village” concept (Fig. 12.1) was proposed to answer the needs of local communities using small ORC⁴ plants and cascade use of energy tapping shallow resources with low-cost access. The Afar Geothermal Development Company (AGAPI) was created to promote such community-based geothermal systems.⁵

Conditions for the development of high enthalpy geothermal fields were shown to be met in eastern Afar when the superposition of three geological features was encountered (Varet 2006). These include:

- The presence of active spreading segments, with important and recent volcanic activity developed in the axial ranges (Erta Ale, Tat’Ali, Alayta and Manda Harraro), as well as in the central volcanoes of southern Afar (Ayalu-Abida, Ertale, Dofan, Fantale), allowing for the development of significant and rather shallow heat sources.
- The development of transverse faulting crossing through the dominantly NNW-SSE normal and open faults, which frequently correspond to offsets in the scarp of the Nubian plateau as well as between axial ranges, which allow for the development of fracture permeability in geothermal reservoirs.

⁴Organic Rankin Cycle or “binary” plants.

⁵AGAPI, Afar Geothermal Development Company, a community based initiative, was created in 2015.

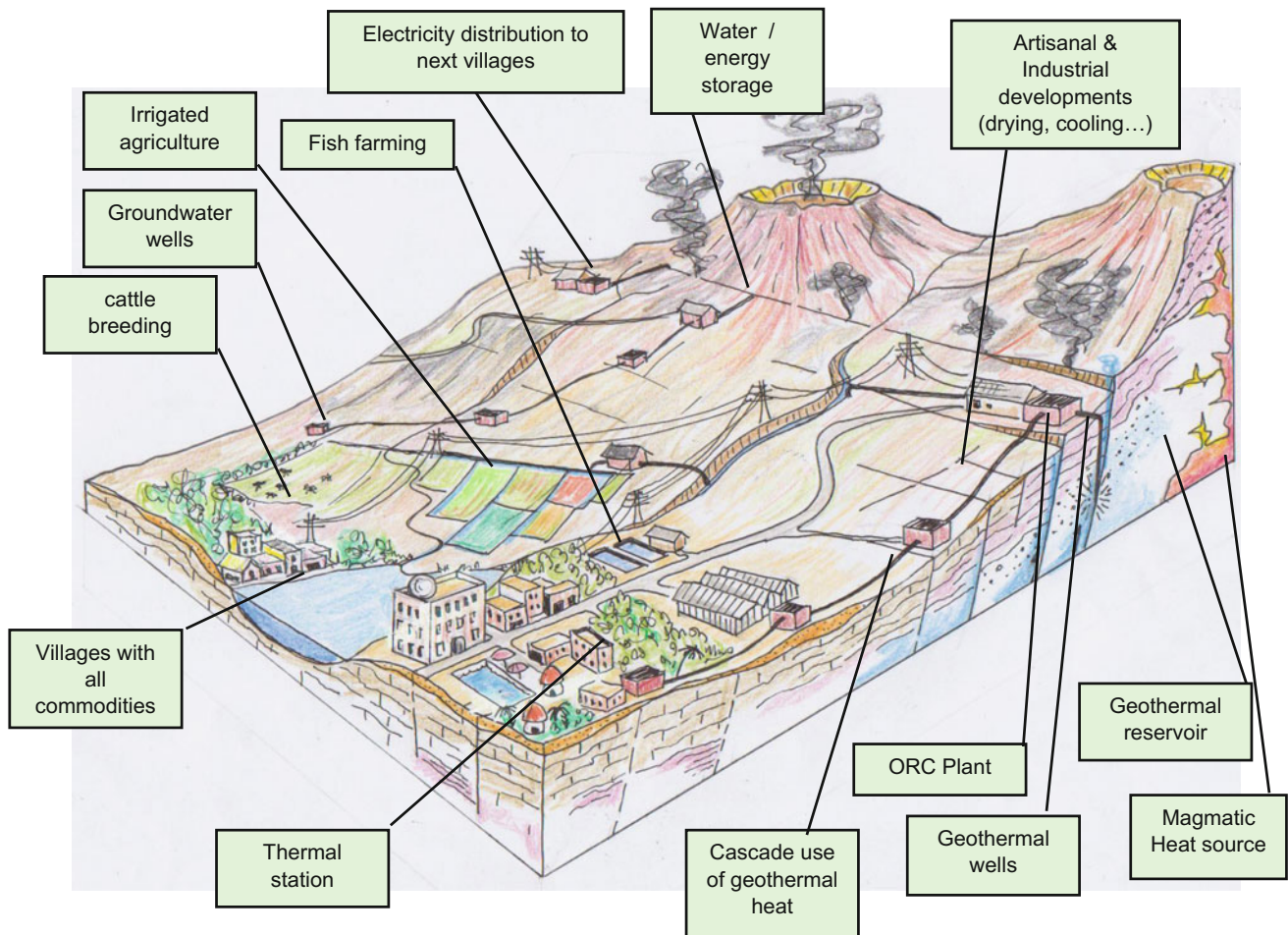


Fig. 12.1 Diagram of the geothermal village concept, tapping shallow geothermal resources for the development of local communities (Omenda et al. 2014)

- The feeding of the geothermal reservoirs from eventually wide basins developed along the intensively eroded escarpment of the Nubian Plateau, with frequent lateral grabens allowing for the infiltration of meteoric water from the wet highlands into Mesozoic sedimentary (Jurassic limestone and Cretaceous sandstone) as well as Tertiary and Quaternary detrital formations or the trap basalts from the plateau and Afar Mabl formation and stratoid series.

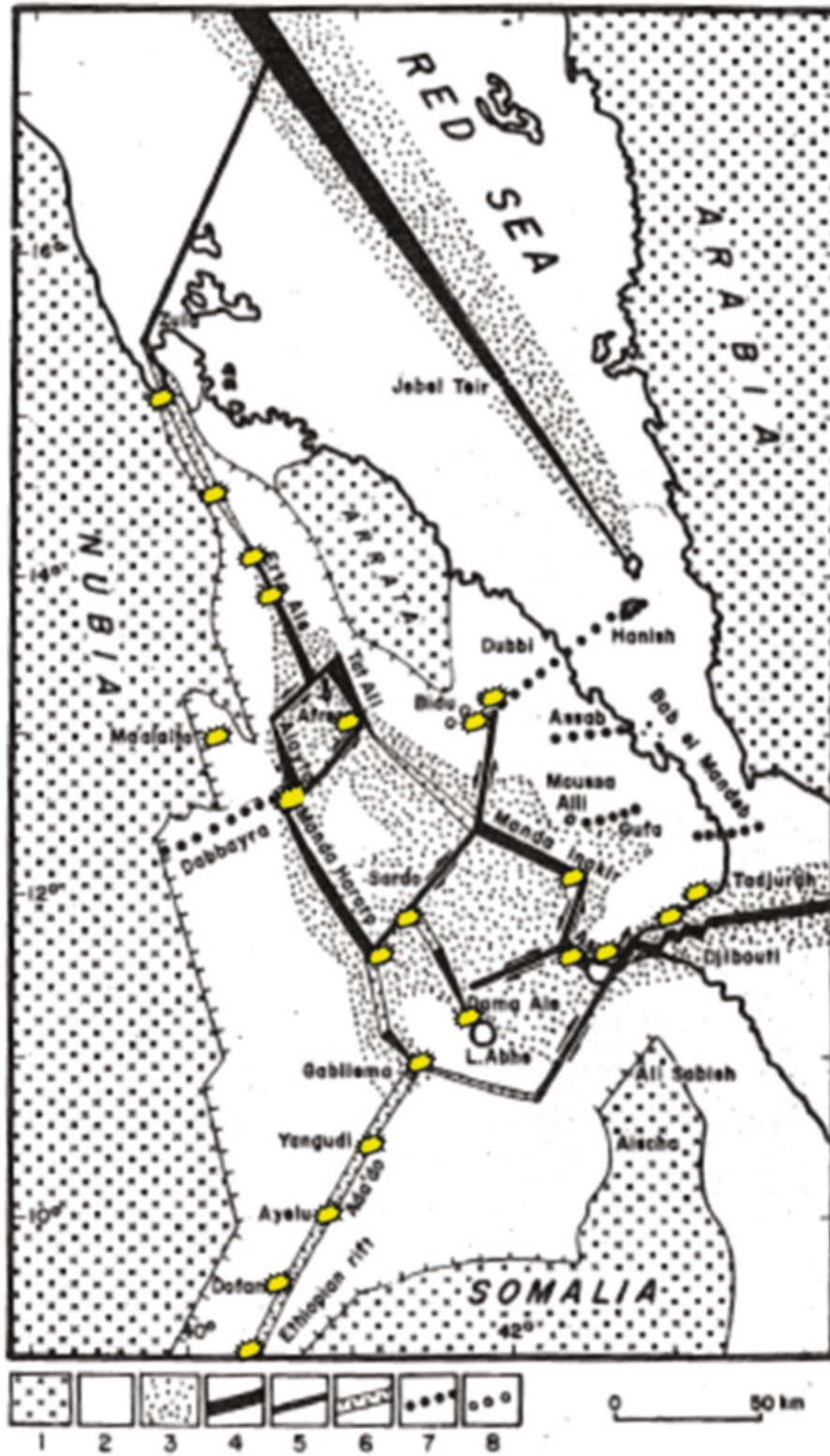
Many Afar sites have been shown to be of potential geothermal interest on the basis of geological and geodynamical criteria in this so-called “future Gulf region for geothermal energy” (Varet 2006). The vicinity of volcanic axial ranges (oceanic-type rift segments) with transverse fracture zones (surface expression of transform faults) should provide both heat sources and fractured reservoirs, the two most favourable conditions for high enthalpy geothermal development (Fig. 12.2).

North-eastern Ethiopia is also where the population suffers from severe droughts because of climate change, and from very low access to drinking water and energy. Geothermal power should satisfy these local needs as a first step, and later serve the grid or local energy intensive industries—as in Iceland with aluminium plants—because it enables modular development with the great advantage of progressive investment. Moreover, this technology creates local jobs. As a whole, geothermal appears for Afar as an efficient solution of resilience to climate change.

Because of the number of potential geothermal sites we examine only a few sites relevant to the various geological conditions.

12.1.2 Alid (Eritrea)

The Alid volcanic complex in Eritrea was studied for its geothermal potential as it represents one of the promising




 Favourable geothermal sites

Fig. 12.2 Geothermal sites in Afar, revisited selection by Varet (2006, 2010) on the basis of new geodynamic considerations, based on Barberi and Varet (1977) map of microplate boundaries. 1 Crystalline basement and Mesozoic cover; 2 Transition zone (thinned crust); 3 Oceanic crust (stratoid series in Afar, less than three million years old); 4 Accreting plate boundaries (mid oceanic ridges and axial volcanic ranges in Afar); 5 Inferred transform faults; 6 Active Ethiopian Rift axis; 7 Transverse volcanic ranges; 8 Central volcano

genuine energy resources of the country. After initial reconnaissance work by G. Marinelli, the site was investigated in depth by USGS, and the exploration work is presently continued by the Geological Survey of Eritrea (see Sect. 7.3).

Detailed studies of the hydrothermal manifestations in and around the dome (see Fig. 7.17) showed that a geothermal reservoir at a temperature of 225 °C developed in the Alid volcano-tectonic system, whereas geophysical surveys are in progress, together with detailed structural mapping (see fracture density map, Fig. 7.18), to locate targets for geothermal exploration drillings (Yohannes 2015). Besides Alid, Nabro volcano (NW of Assab) is also looked on as a target for future geothermal developments.

12.1.3 Dallol (North Afar, Ethiopia)

Because of the evaporation of a former southern branch of the Red Sea (200,000–25,000 years ago), the northern part of the depression is floored with thick (at least 1000 m) salt deposits, this allowing for the development of Sylvite deposits in addition to Halite. Numerous hot springs, explosion craters and fumaroles are reported at Dallol (Tazieff et al. 1970; Varet et al. 2012). The Dallol geothermal site is certainly the best known worldwide because of the spectacular features (Fig. 12.3) resulting from the interaction of hot geothermal fluids with the salt through which the spring occur.



Fig. 12.3 Black smoking fumaroles in Dallol, with successive stages of oxidation of the sulphurs offering a large variety of colours from *green* to *yellow* and *red* (photo Varet 2010)

The Dallol “dome” extends E–W, perpendicular to the rift axis. Rather than a real salt dome, it is a vertical uplift probably initiated by a magmatic intrusion. The regularly horizontal strata exposed in Dallol’s eroded hills confirm this hypothesis. A similar feature is observed in the northern tip of the Erta Ale range, on the western side of the Kibrit Ale volcano (Barberi and Varet 1970). Although no volcanic product is found in Dallol, geophysical data (magnetic and gravimetric) can be interpreted as resulting from a magmatic body (most probably basaltic), a few kilometres deep, underlying the sediments. With its location in the middle of the rift, right on the NNW alignment with the Erta Ale range, the presence of an active magmatic heat source is quite plausible.

Geophysical data also show E–W anomalies that can be interpreted as being the result of transverse faults. Hence, although the existence of a well-developed and active geothermal system is obvious, we cannot be certain that suitable conditions for true geothermal development are to be found because of the extremely salty environment (saturation in salt of the geothermal fluids). The UNDP report (UNDP 1973) concluded that Dallol was unsuitable for geothermal development on the basis of the geochemical content of the hot springs. After new observations of the Dallol site, Barberi and Varet concluded that this site should be reconsidered as suitable for geothermal exploration.

Phreatic explosions are well documented in the history of Dallol and its surroundings. On the top of the dome, a large crater—in which most of the active vents are located—results from a very large phreatic explosion probably a few hundred years old. Another phreatic explosion crater (100 m wide), in the Black Mountain site located SE of the Dallol dome, was observed in 1926. Between the Erta Ale range and Dallol, As Ale is also the expression of a former phreatic explosion, 55 m wide. New craters and pools, apparently linked to the 2005 seismic event, according to local observers, are found a few kilometres south of the dome, showing that phreatic explosions are still occurring (Varet 2010). This indicates the presence of a high-pressure, high-temperature (above 180 °C) geothermal reservoir currently active beneath this part of the salt plain. Considering the hydrogeological context in the basement slope of the Ethiopian escarpment, the Adigrat sandstones and the Jurassic limestones, the latter heavily karstified, both constitute efficient aquifers that would enable the infiltration of meteoric water, itself facilitated by the intense normal faulting (and transverse fractures) affecting the area. Under such conditions, a reasonably favourable geothermal model can be developed for the Dallol site where, underlying the salt plain and hypersaline geothermal system, there might be a deeper aquifer in the Jurassic limestone characterised by both low salinity and regular recharge by meteoric waters descending from the plateau. The presence of a high-pressure,

high-temperature reservoir is shown by the numerous past and present phreatic explosions, as well as by the steam vents aligned on NNW trending open fissures frequently reopened though the salt cover. Recent geological, geochemical and geophysical (MT) studies reported by Varet et al. (2012) confirm the presence of a high enthalpy (probably vapour dominated) geothermal system (Fig. 12.4). Exploration drilling in the area showed the difficulty of drilling through salt sediments affected by a geothermal system.

In addition to meeting local needs in the surrounding Afar villages, this energy production would also facilitate the re-opening of the Dallol potash mine. Instead of the costly ground mining techniques considered in previous feasibility studies, less expensive solution mining of potash deposits could benefit from the use of geothermal fluids (direct or through heat exchangers).

12.1.4 Tat’Ali Near Afdera (North Afar, Ethiopia)

Further south, another geothermal site may have developed around Lake Afrera, where the Erta Ale range ends, and the spreading is transferred to the two axial ranges of Alayta to the SW and Tat’Ali to the SE. Important hot springs found there are interpreted as the products of the heating of superficial groundwater crossing through the surrounding axis ranges by deeper geothermal reservoirs, the location of which remains to be identified by further exploration.

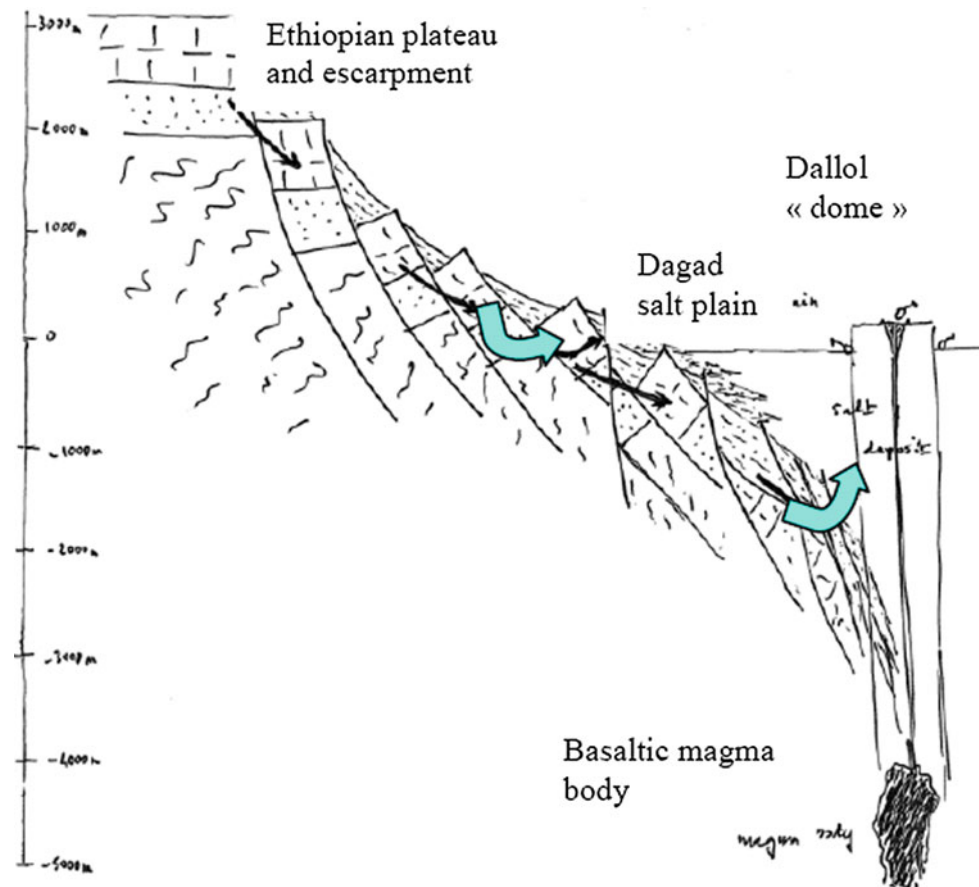
South of Tat’Ali, NNE-SSW normal and open faults cross through the dominant NNW-SSE trend between the centre of the range down to the south of Afdera massif. Numerous steam vents (Figs. 12.5 and 12.6) are found on some of these transverse faults, which indicate the presence of a dry steam reservoir beneath this area, which probably results from a southern major outflow from the central geothermal system of the Tat’Ali caldera.

This site is presently being studied by AGAP for a development that would first answer the growing needs of the Afrera small city (salt extractive industry, water pumping and desalinisation, etc.) and later feed the future needs of the electric grid to be built as an answer to the project of transport of the potash to the port of Tadjourah.

12.1.5 Dabbahu Near Teru (West Afar, Ethiopia)

In the area of transition between the two axial ranges of Alayta and Manda-Harraro (DDDBH TF) (see Figs. 6.78 and 11.4), the Dabbahu silicic centre developed with a fractionation sequence up to pantellerites, showing the presence of a shallow and active magma chamber (Barberi and Varet 1975). This is also the site of intense hydrothermal manifestations,

Fig. 12.4 Geological simplified model for Dallol geothermal system (Omenda et al. 2014). The target would be to tap the Jurassic limestone deep aquifer fed by the meteoritic water flowing down from the Ethiopian plateau



with numerous hot springs, fumaroles⁶ (Fig. 12.6) and silica deposits, notably along the sedimentary plains bordering the volcanic zones to the west. On the SW flank of Dabbahu, a great number of fumarole sites are “engineered” by the local Afar communities for condensing the water from the steam (Fig. 12.7).

These two sites were chosen as priority targets by AGAPI for the development of small size geothermal units answering the needs of local communities in the fast growing Afrera township and in the fertile Teru plain (estimated population over 100,000).

Manda-Harraro, the most active axial range in Afar, is surrounded by numerous fumaroles, hot grounds and hot springs. To the south of the range, rather intense NE–SW faulting, transverse to the regional NNW–SSE direction expresses a high permeability favourable to the development of a geothermal reservoir fed by the important Awash and Mille River basins. The apex of this system is located immediately south of the lava fields, whereas the Tendaho Geothermal Prospect was developed in the graben filled by recent unconsolidated sediments of the Awash River.

12.1.6 South Manda Harraro Geothermal Sites (Including Tendaho Graben, Central Afar, Ethiopia)

The Manda Harraro axial range was identified long ago as the most active spreading segment in Afar (Barberi and Varet 1977), an observation confirmed by the remarkable seismo-volcanic (2005–2011) during which a 75 km-long and up to 8 m-wide dike composed of 2–2.5 km³ of basaltic magma injected; as a result (this diking process being a continuous process on a geological scale), a huge quantity of energy was made available at shallow depth along this range.

In addition, considering that this is the place in Afar where the most important water inflow is available from both the basins of Mille River to the east and Awash River to the south, the next question is to locate the most suitable place in terms of permeability. Geological observations allowed identification of the area located along the prosecution of its axis affected by intense multiple fractures in at least three major directions (Figs. 12.8 and 12.9a).

This area also coincides with the most spectacular hydrothermal occurrences observed in Afar: hot springs, geysers, fumaroles and steaming grounds, together with well-developed hydrothermal deposits (Fig. 12.9b), and

⁶The Afar name is “Boina” meaning fumarole, erroneously given to Dabbahu.



Fig. 12.5 **a** The geothermally active normal and open fault at Tat'Ali, with alignment of steam vents, fumaroles and hot grounds with development of "geothermal grass" (Fiale) benefiting from the condensing water and alteration of the young basalt flows. Along the

same axis, the summit caldera of the Tat'Ali volcanic range is observed in the background, **b** Detailed view of a high temperature steam blowing hole along the fault seen in (a) (photos Varet 2016)

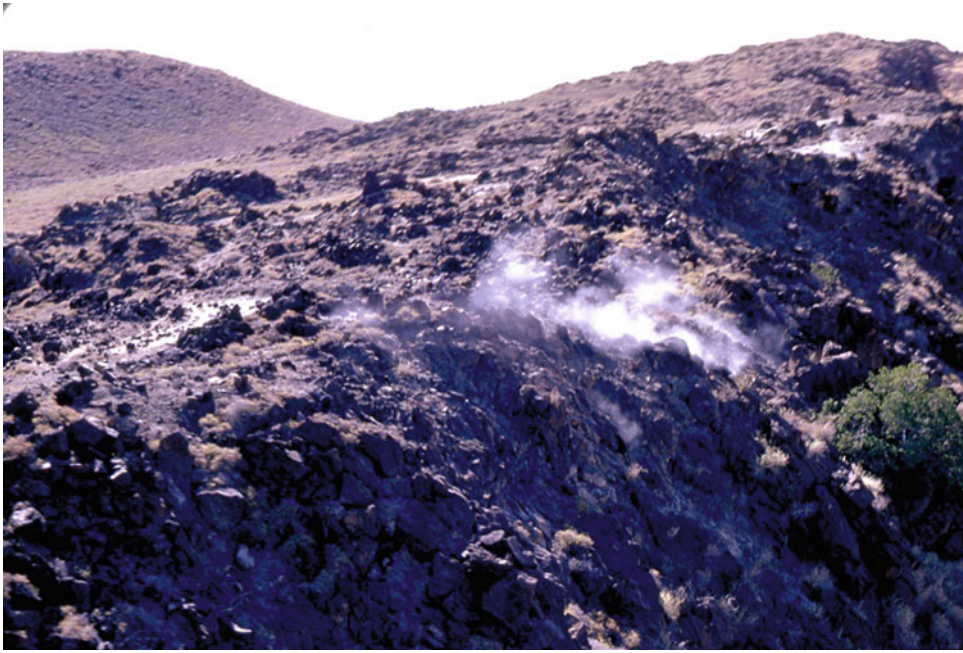


Fig. 12.6 Steaming fault in the Dabbahu massif (photo Varet 1969)



Fig. 12.7 One of the numerous steam condensing devices dug on a fumarole, used by the Afar local communities along Dabbahu SW flank (photo Varet 2016)

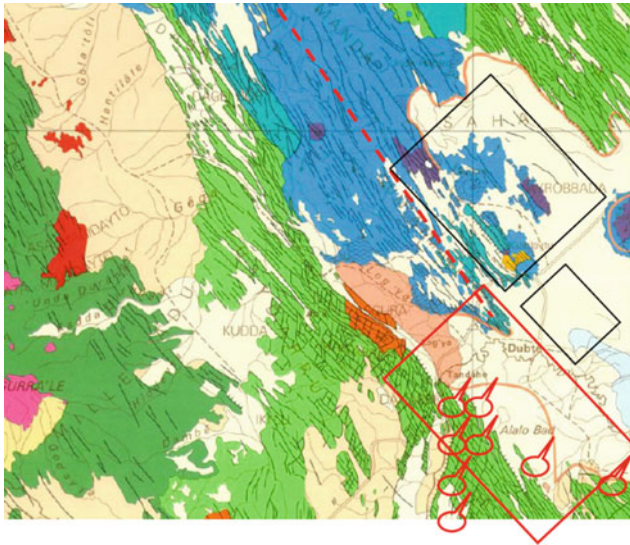


Fig. 12.8 Geological map of the southern part of Manda Hararo range and surrounding regions, including the Alalo Bad geothermal site located on the southern extension of the axial range axis (in red). Hydrothermal emergence sites are reported in red. Black rectangles indicate the exploration area defined for the Tendaho graben geothermal site under development. The target proposed by Omenda et al. (2014) is where the axis of the Manda Hararo range crosses with transverse fractures with development of thermal emergences drawn in red quadrangle

should be considered as a key target for locating a geothermal site. As a matter of fact, a very low resistivity zone (below $2 \Omega \text{ m}$), clearly elongated in a NNW–SSE trending direction, is observed at a depth of 7 km along the southern extension of the Manda Hararo axis, tracing a possible magmatic heat source (Kalberkamp 2010).

12.1.7 Dama Ale in Ethiopia and Lake Abhe in Djibouti

With its shallow magma chamber, the groundwater flow from the Awash through underlying faulted stratoid series, the abundant fumaroles in the crater and the numerous hot springs found at its lower flank, Dama Ale appears to be a promising high temperature geothermal target.

Hot springs are particularly well developed along the SE side of the Lake Abhe in Djibouti Republic where they form spectacular travertine chimneys which were mostly built in sublacustrine conditions when the lake level was a few tens of metres higher than it is now (Fig. 12.10).

However, the Djiboutian site is located too far from the magmatic heat source (35 km) to hope for direct incidence on the high temperature geothermal reservoir. The hydro-geochemical geothermometers indicating medium temperatures (110–140 °C) tend to confirm a simple convective transfer through normal faults of the surface manifestations.

The site is, however, being extensively studied by ODDEG (Office Djiboutien de l'Énergie Géothermique) with the support of ICEIDA (Iceland).

12.1.8 Asal in Djibouti Republic

Asal, the easternmost axial basaltic ranges of the Afar depression, was the first target for geothermal developments in Afar. BRGM (1970, 1973) identified the Asal Rift as a target of major geothermal interest. Surveys enabled a model to be proposed in which the shallow anomalous hot mantle along the Asal-Ghoubbet rift was to provide an efficient heat source with additional supply from a shallow magma chamber beneath the central part of the Asal shield volcano, whereas seawater circulation from Ghoubbet to Asal Lake (155 m) would provide fluids for the fractured reservoir.

Several groups of springs were identified: the Manda springs located on the eastern side of the lake emerging from recent basaltic flows, the Korili spring merging from the southern major fault system on the lake side, wadi Kalou springs south of the lake, and Alifita and Eadkorar spring areas on the northern side of the lake. Numerous fumaroles and steam vents were also mapped and studied (Fig. 12.12). Geochemical work was undertaken to examine the origin of these springs, the behaviour of the hydrogeological system and the geothermal fluids characteristics (BRGM 1973; Bosch et al. 1974; Fouillac et al. 1983).

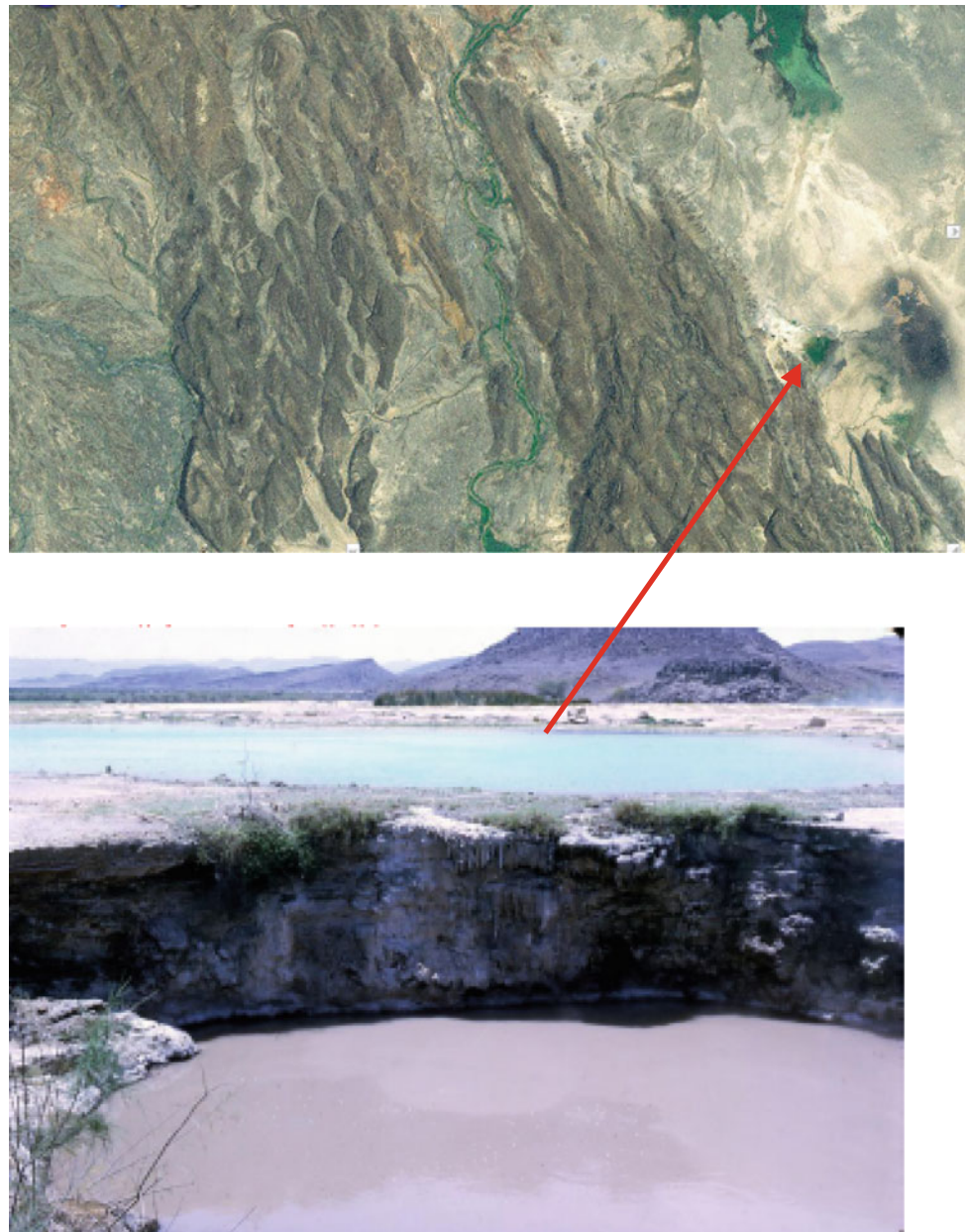
The importance of the flow of seawater from the Ghoubbet pass north-western shore into Asal Lake south-eastern shore (thanks to important open faults and fissures characterising the northern side of the axial rift) was emphasised. Avoiding drilling in the northern part of the rift where the system may have been kept cool at depth (Fig. 12.12), the site selection was oriented in the southern part of the rift, where the correlations between major elements and further studies of trace elements (such as lithium, strontium, bromine and boron), in addition to strontium isotopic analysis demonstrated the interaction of seawater with the basalt at high temperature and the effect of evaporation.

The EM⁷ method was applied by BRGM (1973); although of low penetration, it pointed out a superficial elongated conductor anomaly on which the first Asal1 well was located successfully (see location in Fig. 12.12). This anomaly correlates with several hyaloclastite deposits along a main fault zone in the southern part of the rift (Fig. 12.13).

Other conductors were also identified close to the rift axis. A gravimetric survey pointed out several heavy body anomalies;

⁷Electromagnetics

Fig. 12.9 (a) Satellite image of the area located immediately south from Manda Harraro range. Multiple faulting is observed in this area where the Awash River receives the Mille River tributary. (b) Alelo Bad hot springs pools and hydrothermal deposits, south Manda Harraro



those located in the central part of the rift correlate with dike injection and a magma chamber in the Fialé caldera area. Small local anomalies could be the result of an intensively fractured zone. Aeromagnetic and gravimetric modelling allowed mapping of the basement of the recent Quaternary basalts (the Dalha unit encountered in the wells), split into several compartments delimited by fault zones. An MT survey carried out by Balles-tracci and Benderitter (1980), completed with an AMT (audio-magnetotellurics) survey, faced difficulty in distinguishing the deep geothermal reservoir from the shallow reservoir (Barthes et al. 1980; Abdallah et al. 1981). Later on, an EM survey, focused on the axial part, was also limited in penetration to a few hundred metres (ORKUSTOFNUN 1988). The top of the conductor body delineates the ground seawater flow gradient

from Ghoubbet towards Lake Asal, with an “upflow” in the Fialé area. Later on, two magnetotelluric methods, MT5EX and low frequency, were engaged at a limited number of stations and appeared to provide useful complementary data.

Seismic reflection and PSV methods (Hirn 1988) confirmed that the geothermal reservoir identified in Asal1 was located on the intersection of main faults and was of the fractured type. From the observed seismicity concentrated in the Fialé area, a geothermal reservoir was located in the 2500–3000 m depth interval by REI (2008). This activity could be explained by the interaction of water circulations with the top of a magma chamber (Dobre et al. 2007a, b). More recently, a profile of the crustal structure through the rift by Vergne et al. (2012) showed (Fig. 12.14) that the



Fig. 12.10 Travertine chimney aligned along NE–SW emissive fissures parallel to the regional normal faulting on the SE shore of Lake Abhe (Djibouti Republic)

magma chamber beneath Fialé caldera could be as deep as 2000 m (see also Fig. 12.15).

Altogether, six deep wells with depths ranging from 1137 to 2105 m were drilled at Asal in two major campaigns (BRGM 1975; AQUATER 1989). A1, A3 and A6 are in the same area, located on the SW block inside the rift but away from the active volcanic axis and present seawater circulation. A4 and A5, located towards the central part of the rift, encountered the superficial underground seawater flow towards Asal between 250 and 280 m deep. The hydrothermal mineral assemblage is in good agreement with the measured temperatures in all wells (Zan et al. 1990), except A5. A3 and A6 temperature profiles are almost similar, with one intermediate (500–700 m) reservoir at a temperature of around 250 °C extending towards a deeper higher temperature reservoir (300 °C), and no clear cut was visible, whereas no deep reservoir was reached by A4 and A5. A high temperature reservoir was tapped by A3 at 1075 m and between 1225 and 1250 m, and at A6 between 1100 and 1300 m, with bottom hole temperatures of, respectively, 263.5 and 280 °C. At higher depths, A4 exhibited low permeability as well as A5 between 2000 and

2050 m, with bottom-hole temperatures above 345 °C (Fig. 12.14).

The deep liquid-dominated reservoir was produced three times for more than 9 months in total at A3. The first test provided 360 t/h of fluid at 12.5 bar at the wellhead with a production temperature of 265 °C and a vapour fraction of about 35%, which would allow the production of 10 MWe (AQUATER 1989). The total dissolved solids were 116 g/L with 1700 ppm non-condensable gases (mainly CO₂). The production data show an important decrease of the output, the bottom hole pressure dropping by 3.5 bar whereas scaling was observed in the wellbore and the surface equipment. Sample analysis showed metallic sulphide deposits (PbS, ZnS) at high pressure and amorphous silica with Mn and Fe at low pressure (BRGM 1975; VIRKIR-ORKINT 1990). Some calcite deposits were also detected. A 10 mm-thick scaling was measured by caliper in the flash zone and up to 6–8 mm in the wellhead. Reservoir engineering studies (Battistelli et al. 1991) concluded that the Asal 3 output decline was caused by wellbore scaling, certainly the major handicap of Asal deep reservoir, but that a decrease in average pressure could also result from the



Fig. 12.11 Open fissure affecting the floor of the lava lake occupying the Fialé caldera. Steam is emitted from the whole length of the fissure, with the Fiale “geothermal grass” growing thanks to the water condensation (photo Varet 2004)

limited extension of the reservoir because of fault boundaries in this fractured reservoir (as already pointed out by BRGM in 1981).

As a consequence, ISOR recommended REI to engage in the industrial project they offered to develop in the Fialé caldera, where better reservoir conditions would be expected. After the resignation of REI, the World Bank engaged an international consortium for a feasibility study including the drilling and test of four exploration wells at a depth of 2500 m at Fialé caldera and its immediate surroundings. As A5 was the only well drilled there, Varet (2004) had a further look at the data. This well, drilled in 1988 by Aquater, displays a particular profile with a strong temperature inversion: although the temperature increased sharply between 300 and 500 m, reaching 185 °C, it decreased to around 60 °C down at 1000 m from where it increased up to 359 °C at 2105 m.

A striking fact is that the hydrothermal mineral assemblage is in good agreement with the measured temperatures in all wells (Zan et al. 1990), except for A5.

This well showed a high temperature chlorite-epidote assemblage in the area subjected to the important temperature inversion. This was interpreted by Varet (2004) as resulting from the invasion of cold seawater in a pre-existing, well-developed, high temperature reservoir (200–300 °C), which should have existed at a depth of 500–1000 m. Another point is that between 1100 and 2105 m, the increase in temperature is rather linear from 100 to 259 °C, leaving no room for a deep geothermal reservoir. The profile would fit with the vicinity of a basaltic magma chamber, known at shallow depth from the 3D mapping described above (Fig. 12.15).

The 1978 seismotectonic crisis and volcanic eruption of Ardoukobba, which just followed the rifting episode with up to a 2-m opening along the axis of Asal-Ghoubbet (Ruegg et al. 1979), was followed by a 10-year period of fast rift opening (6 cm/year). A5 well was drilled just after that episode, and the geothermal reservoir was invaded by cold seawater as a result of this long-lasting distensive sequence. However, for 12 years after, the Fialé caldera was newly

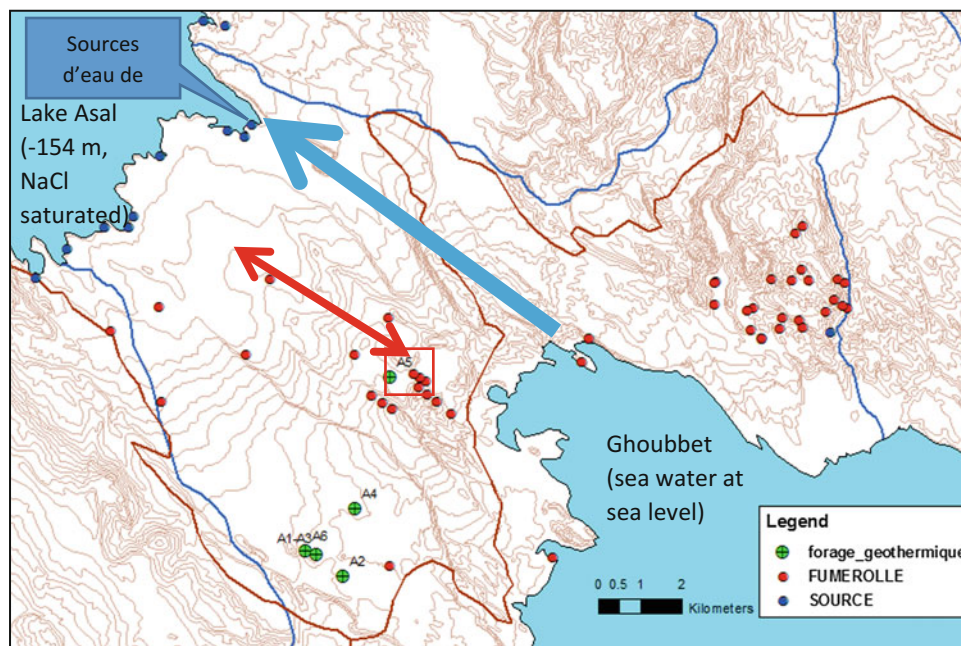


Fig. 12.12 Location of the active volcanic axis of the rift (*double red arrow*) and of the active fault along which an important ground seawater flow crosses through from Ghoubbet to Lake Asal (*blue arrow*). Asphalted road, drilled sites (in *green, numbered*) and main

fumaroles of the Asal rift are also reported on the topographic map. The *red square* shows the prospect for exploration drilling to be undertaken in 2015–2016 (from Varet 2014)



Fig. 12.13 Hyaloclastite massif outcropping on the western inner faulted side of Asal range. The *yellow* subaqueous deposit was later cut by basaltic dikes feeding the upper subaerial flows (photo Varet 2012)

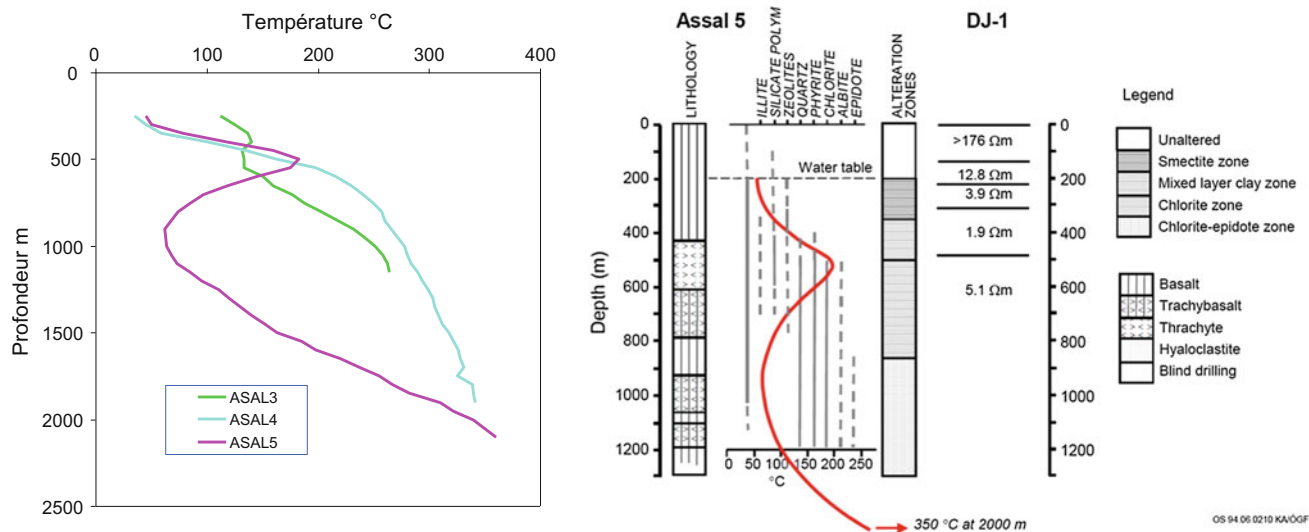


Fig. 12.14 Temperature profiles measured in the Asal wells A3–A5 (left). Note the inversion of temperature observed in the A5 well drilled in 1988 immediately NW of the Fialé caldera (Jalludin 2003). Note also that the hydrothermal mineral sequence (right, not at the same scale)

matches the resistivity profile but not the temperature profile, indicating a late inflow of cold seawater into a high temperature reservoir as observed by Anarson and Flovenz (1995)

replenished with magma at shallow depth, with several episodes of magma injection observed in the period 1998–2001 (Dobre et al. 2007a, b).

The fact that the Fialé caldera has apparently been quiet for the last 9 years indicates that the magma ceased to rise, and is in a process of slow cooling, with a surrounding high temperature magma-water contact zone that is now stabilised. As a consequence, an important amount of heat is being dissipated in the surrounding rocks and geothermal reservoir(s). The reservoir that was invaded by cold water during the 1978–1987 period, as observed in A5 in 1988, has encountered several events of abrupt heating for 10 years (1991–2001) because of the vicinity of magma injection and has been subjected for another 13 years to considerable heat dissipation from the huge mass of basaltic magma injected in that period.

If the interpretation proposed by Varet (2014) is correct, it has a direct impact on the conception of the drilling program engaged in the following month as part of the feasibility study:

1. The first action should be to engage a new thermal logging of A5 well. If we remember that it was drilled in 1988, it encountered cooling of the pre-existing reservoir during the 1978 event and the following 10 years of active extension. The cooled geothermal reservoir was not affected by any new heating event before 1991 when the first magma injection occurred in the centre of Fialé caldera. It should be noted that it is the 2001 event that

had the most effective influence at A5 location. With the further injection episodes, a new efficient heat source has been effective for the last 24 years. As a consequence, one should expect that the A5 reservoir in the interval 500–1000 m displays at present all the characteristics of an economic geothermal reservoir, with a suitable temperature (eventually above the previous range of 200–300 °C), a good fracture permeability and a moderate salt content (seawater composition slightly concentrated because of vapour leakage, as observed along open fissures at the surface of the lava lake).

2. Second, the reservoir has to be searched for at a shallow depth in the caldera surroundings, avoiding the NE margin where cold seawater flow is still intense because of the active nature of the “petit rift”, whereas no magmatic injection occurred in that part of the Asal rift floor.
3. Third, the drilling programme previously established by REI and taken for granted by the World Bank and associated banking consortium should be revisited. The deep wells planned at a depth of 2500 m and deviated at a depth of 2000 m up to 2800 m lengths may not only miss the target but also be at risk, as the chance to encounter magma in this depth range is rather high, as also shown by Houmed et al. (2012).
4. Fourth, a shallower drilling program should consider much earlier deviation (to be initiated at 500 m depth) in order to cross the maximum of open fissures in the reservoir at a depth of 500–1500 m.

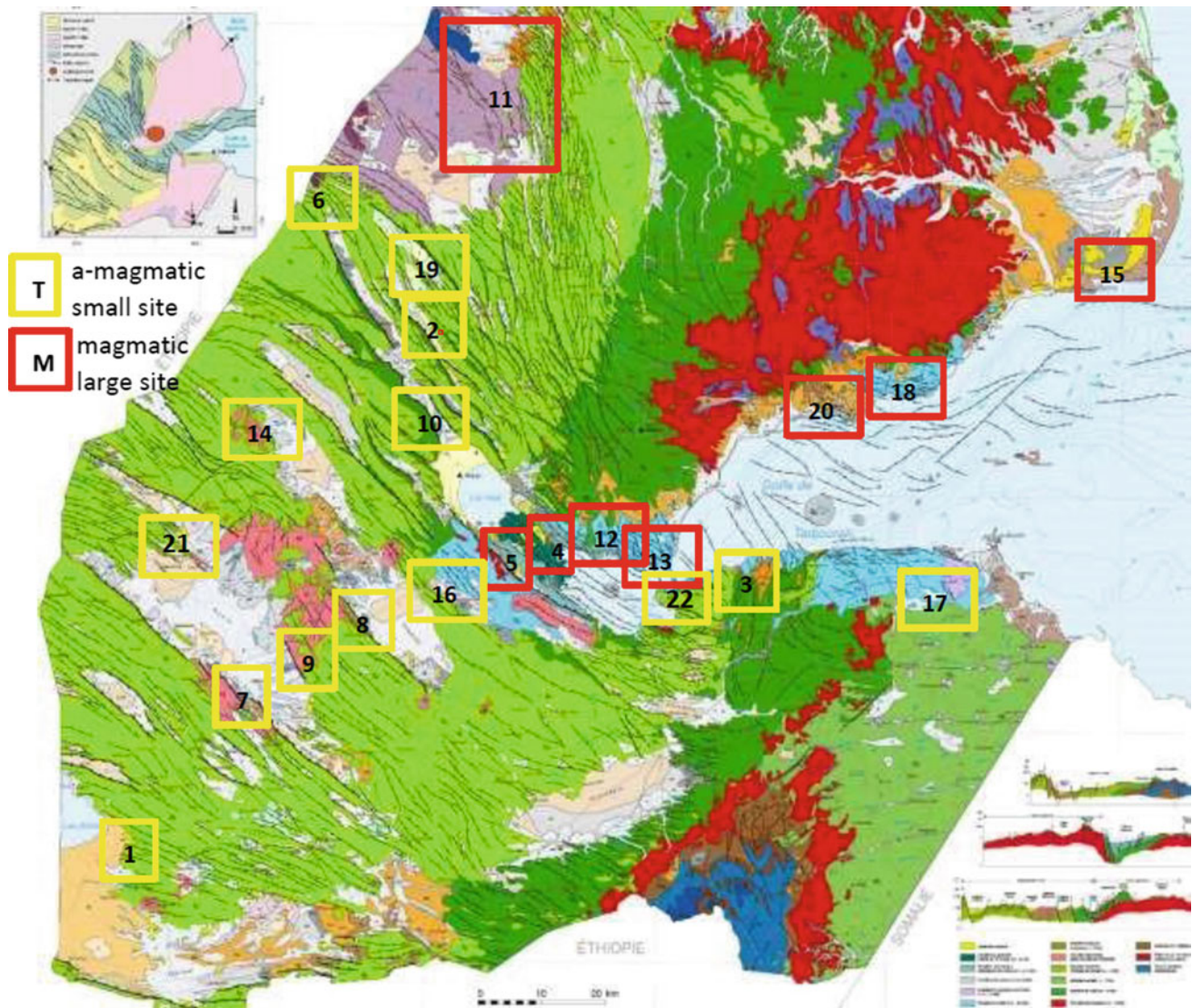


Fig. 12.15 Geological map of the Djibouti Republic showing the sites of major geothermal interest, with magmatic heat sources linked with the active ridge (“large sites”) shown as *red rectangles*. Amagmatic

hydrothermal sites on faults (“small sites”) are shown as *red circles*. *Note* that this map of “small sites” is not definitive and that other areas remain to be discovered and identified (ODDEG 2016)

12.1.9 Other Sites in Djibouti Republic

A new institute called ODDEG (Office Djiboutien de Développement de l’Energie Géothermique) was established in 2014, aiming to fulfil the electric production of the country from geothermal sources as defined in the 2035 vision of Djibouti Republic with a first unit of 50 MWe connected in 2019 and a second in 2035, this connection being facilitated by the new electric line to be built around the gulf connecting Obock and Tadjourah to Djibouti through Asal-Ghoubbet.

In addition to Asal, a second site is being identified that would bear a reservoir with the appropriate characteristics of at least 50 MWe that would replace Asal-Fialé in case of

problems on this site and bring another site to the stage of operational production of an additional 50 MWe by 2030. In addition, ODDEG could offer more advantageous options for the Djiboutian economy. Several sites located along the ridge between Obock and Asal, as far as Manda Inakir on land, have the necessary characteristics.

Besides large sites serving the electric grid, a specific approach for “small sites” answering local needs for villages or rural communities away from the national network can be considered. Frequently these pastoralist groups are located in the vicinity of thermal manifestations in order to benefit from these resources through artisanal devices (steam condensing for water condensation or use of hot springs for washing and irrigation). It also happened—as in PK20,

Baloo and Garapti-San – that wells drilled for water encountered problems because of the too high temperature of the targeted reservoir.

These are rather local convective systems, developed because of faults or open fissures crossing, frequently located in active seismic zones, affected by deformations (extension and strike-slip) of the stratoid series which is too old (3.5–1 million years) to provide a magmatic heat source. These purely hydrothermal systems are rising by thermal convection from the depths. It should, however, be possible to track these fluids at intermediate temperatures (120–180 °C) using shallow drillings (500–1000 m deep). ORC plants are more expensive than direct flash, but the diesel production they would replace is quite expensive! Developing small local units can also be considered for sites of larger potential where a local project answering present needs (small townships or pastoral communities) could also anticipate larger productions units, allowing the local populations to prepare themselves for such perspectives. This could be the case in Obock, Rouéli, Tadjourah, Arta or Abhe (Fig. 12.16).

This “small sites” option provides an answer to a social issue: there is no doubt that the areas in Djibouti suburbs, where poor populations tend to congregate (Balbala, for instance), result from migration from the most deprived rural areas, a phenomenon accelerated by climate change. Nomad pastoralists know it as they traditionally move to these geothermal sites when the climate gets too dry. Providing them such opportunities would be a strong answer to climate change.

Fig. 12.16 One of the numerous hot springs found south of Gawani along a NNE–SSW fault (MER direction) that limit the volcanic pile and the Awash sedimentary plain (Photo Varet 2015)



12.1.10 Gawani Area

Most probably geothermal indices are to be discovered along the northern end of the Ethiopian Rift Valley in southern Afar, as in Gabilema and Yangudi volcanic complexes. Hydrothermal activity is also known to occur further east and west, along the numerous faults observed in the area. However, near to the far more accessible Gawani surroundings, hydrothermal activity, with both active fumaroles in Abida caldera and many hot springs of Meteka south of the town (see Fig. 12.16), confirms the geothermal potential of the area.

Geochemical analysis carried on samples of these thermal emergences show the presence of two distinct components (ELC 1989): a water of alkali-bicarbonate composition with an outlet temperature of 40–50 °C and a water of alkali-chloride composition with an outlet temperature of 85–90 °C, interpreted as resulting from boiling NaHCO_3 waters inducing CaCO_3 precipitation. Geothermometric modelling allow the identification of temperatures of 100–125 °C, but the existence of the substantial boiling indicates the presence of a deep heat source at temperatures estimated at 235–255 °C. Significant hydrothermal deposits on the terraces that surround the hot springs (see Fig. 10.23) would require further study.

The geothermal model that can be deduced from these observations implies the development of an important magmatic heat source underneath both volcanoes, with a geothermal reservoir located in the fractured basaltic stratoid series and a cover made of recent hydrothermalised pyroclastites and clay-bearing lacustrine sediments.

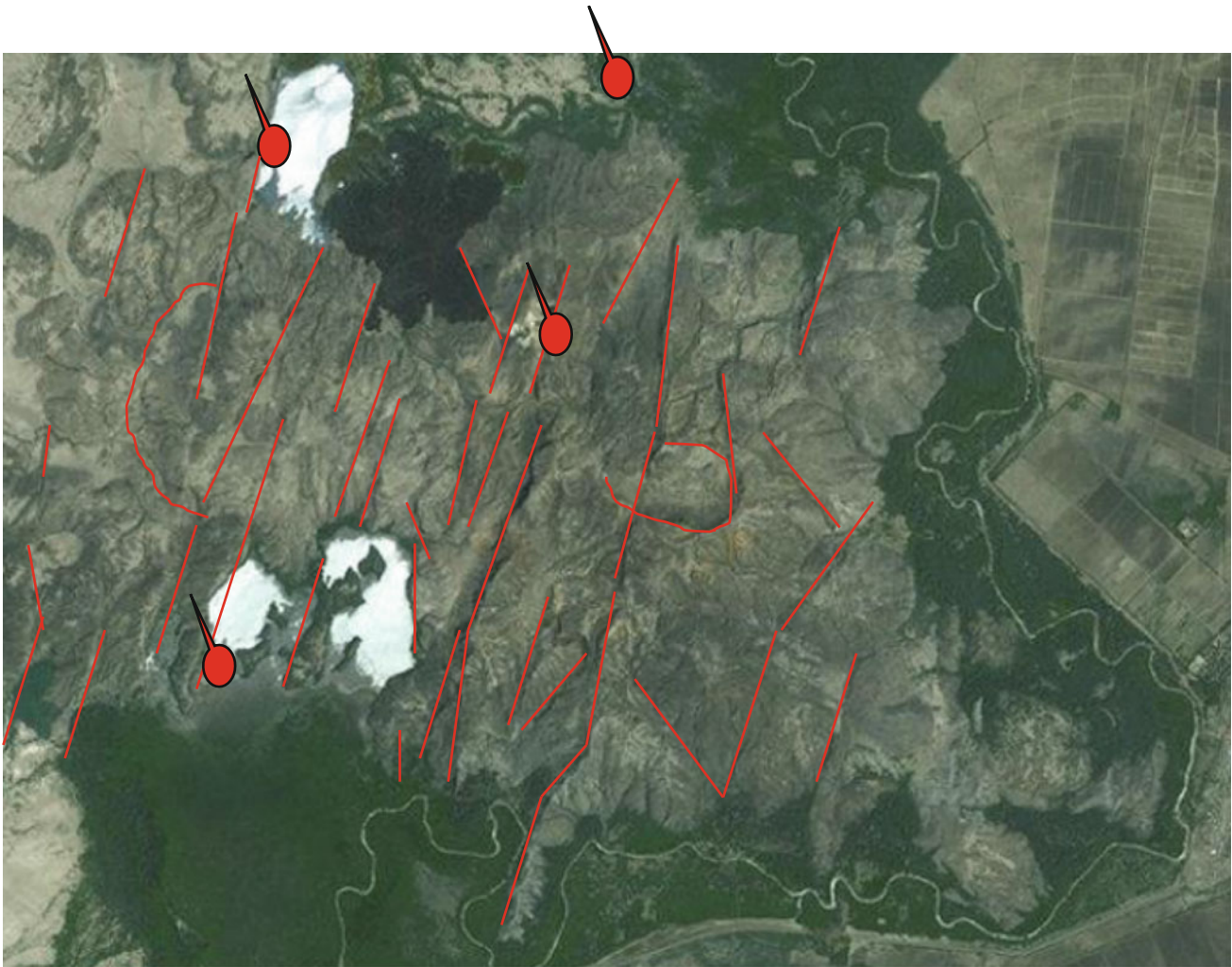


Fig. 12.17 Map showing the main faults cutting through the Dofan edifice and the major sites of hot springs or fumarolic activity. Satellite image from Global Mapper 16

A geothermal development could target both the superficial low temperature reservoir for direct uses and the deep reservoir for electricity production. This would require further geological, geochemical and geophysical investigation in order to target these reservoirs better.

12.1.11 Dofan

Dofan has long been identified as a geothermal target, known for both its fumarolic activity in the massif itself and the hot springs occurring along its margins. The sulphur of fumarolic origin, interstratified in porous friable trachyte, found in the northern crater, was even exploited industrially.

Important hot springs—at a temperature of around 50 °C—outflowing on the northern extremity of the volcano from recent, fractured scoriaceous basalts were analysed, together

with well waters and fumaroles (Figs. 12.17, 12.18, 12.19a and 12.19b) sampled in the central part of the edifice by ELC (1989). As a whole, two classes of fluids are observed, with bicarbonate waters (NaHCO_3) of relatively high pH (8.2–8.8) and chloride-sulphate waters. Water geothermometers indicate temperatures up to 130 °C whereas gas geothermometers in the fumaroles indicate temperatures of 200–280 °C.

Gas surveys (radon, CO_2) were carried out in the area, allowing the selection of drilling targets areas that still need to be confirmed by geophysical (MT-TEM⁸) surveys.

During our field visit in June 2016 we were shown by our local Afar guide an area in the sedimentary plain SW of Dofan

⁸Magnetotellurics-Transient Electromagnetics

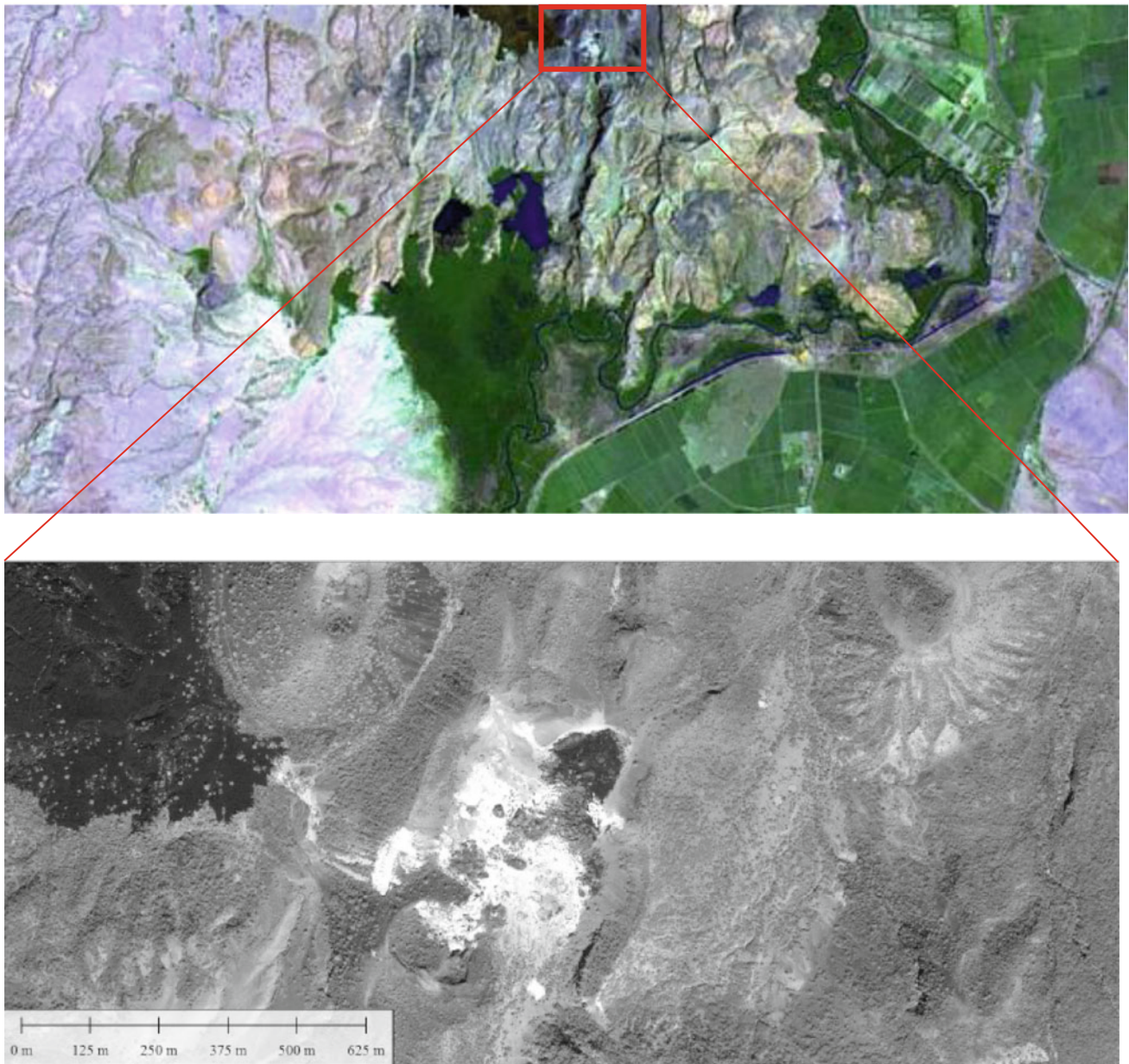


Fig. 12.18 Satellite image (Global Mapper 16) of the southern part of Dofan volcanic system showing the well-expressed axial graben and the domes and viscous flow prevailing in most parts of the edifice. Recent (*black*) flows are observed in the axial part. Hydrothermal zone appear in white

where a phreatic explosion occurred in 2005, indicating the existence of a shallow, steam-bearing, geothermal reservoir.

The geothermal models that result from the available data centre the drilling objectives on the 5 km-wide axial graben (see Fig. 12.18) where the thermal manifestations concentrate, as well as the soil anomalies (radon, CO₂, mercury) along the major normal faults limiting the rift-in-rift axis. Logically, the geothermal target is expected downstream rather than upstream, that is, on the northern side of the edifice. A high temperature (above 200 °C) reservoir is expected to occur in

the fractured stratoid series underlying the recent volcanic pile, with a cap rock made of ignimbrites and argillaceous sediments. Lower temperature reservoirs (50–140 °C) are also expected at shallow depths (not exceeding 500 m).

For 30 years Dofan has been considered as a high priority target for geothermal development, but no interest was placed on it until 2014 when the GRMF supported a request by the Ethiopian Geological Survey for a prefeasibility study. In 2015, the Dofan lease was allocated to Orpower. Orpower, a US private developer.



Fig. 12.19 (a) Detailed imagery (Global Mapper 16) of the central-northern part of the Dofan volcanic unit showing the highly hydrothermalised (*white deposits*) small summit caldera and the more recent craters along the axis and on both sides, north. The NW crater

gave a basaltic (probably historical) eruption (*black area*). (b) Photographs of the thermal springs (50 °C) outflowing from recent scoriaceous basalts in the northern part of Dofan geothermal site (photos Varet 2016)



Fig. 12.20 The Filwoha hot springs in the NE part of Fantale geothermal site. The hot spring emerge from a long fault cutting through a recent basalt flow, a few metres above the sedimentary filling of the downthrown compartment (photo Varet 2016)

12.1.12 Fantale

Several hot springs are observed north and south of the volcano, the most well-known being Filwoha in the Awash National Park NE of the volcanic centre (Fig. 12.20). The temperature of these springs never exceeds 50 °C.

Fumaroles (reaching a temperature of 95 °C) are present in the caldera and north of the volcano, south of Kasem

River (at a place called Techeda). These are dominantly bicarbonate waters, with NaHCO_3 composition and relatively high pH (6.2–8.8). Water geothermometers indicate temperatures ranging from 125 to 145 °C, whereas the gas geothermometers from the fumaroles indicate up to 260 °C. Fantale is therefore considered to be a geothermal target and a lease was allocated to Cluff Geothermal, a British Company for exploration drillings with the support of GRMF.

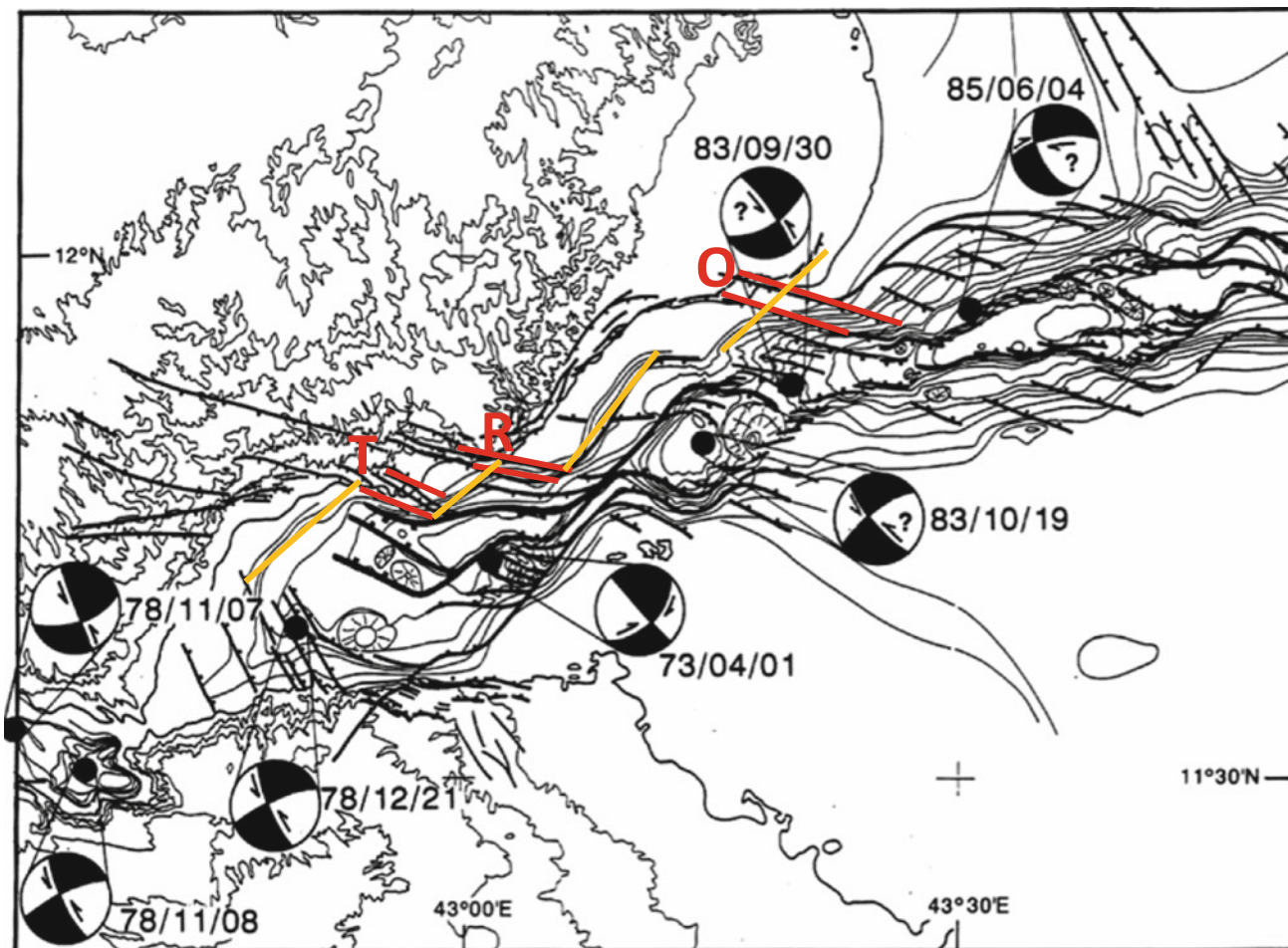


Fig. 12.21 Structural interpretative map of the (NNW–SSE) axial spreading segments and (NE–SW) leaky transform of the Gulf of Tadjourah (modified from Manighetti et al. 1997). Observe how the

faults of the active rift (*red*) and transform (*orange*) segments of the gulf's deep trough extend on land in the three sites of Tadjourah (*T*), Rouéli (*R*) and Obock (*O*)

12.1.13 Future Dreams: Drilling Through an Oceanic Ridge from Land

Afar western extremity along the Gulf of Tadjourah spreading segment permits observing inside the active spreading mechanism and supercritical geothermal resource derived from a nearby magmatic heat source from three sites: Tadjourah, Obock and Rouéli (Fig. 12.21).

Following the geological observations developed above, it can be seen that the western extension of the MOR of the Gulf of Aden is at a sufficiently short distance that it can be reached by deviated drilling from the coast. It was proposed by the author (Haga et al. 2012) that deviated research wells should be undertaken with two objectives (Fig. 12.22):

- First, to reach a conventional geothermal reservoir (200–250 °C) at a depths of around 2000 m for geothermal power generation answering local future needs

- Second, while pursuing at depth with deviated drilling 4–5 km long, to help the world research community in understanding, under ICDP (International Continental Drilling Programme), spreading mechanisms, magma generation in relation to extensive faulting as well as heat source development and heat transfer in oceanic systems.

From the Obock or Tadjourah coast, the final target should allow a reach to the base of the rift spreading axis whereas, from Rouéli, a leaky transform fault can be crossed allowing a touch from inside of both the shear and extensional faulting. Two heat sources can be expected: the hot anomalous mantle (1300 °C) located a few kilometres deep and more superficial magmatic chambers (above 1200 °C) could be crossed beneath the ridge, the leaky transform faults and the central volcano mapped in the vicinity of Obock.

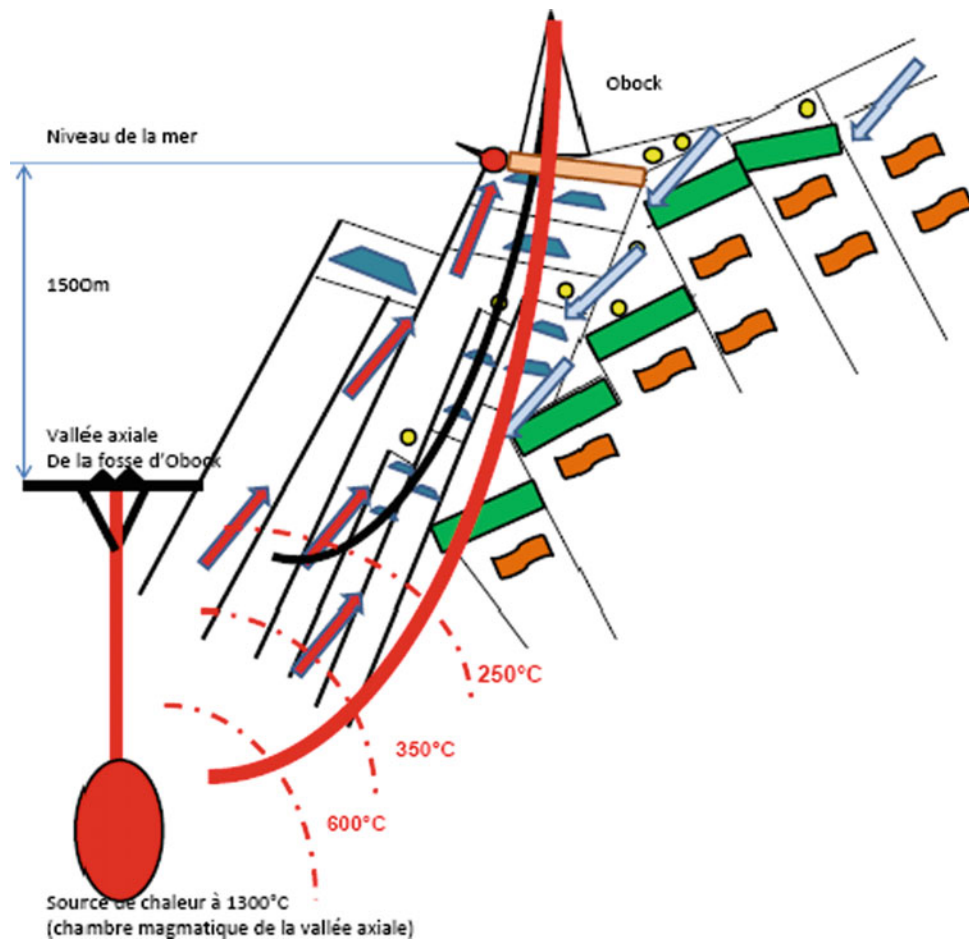


Fig. 12.22 Hypothetical interpretative scheme proposed for the Tadjourah, Obock (a S–N section in this case) and Rouéli (an E–W section in this case) ICDP deep well (in red) and “ordinary” geothermal well in black. The Mabla rhyolites (*marron*) and overlying Dalha basalts (*green*), intensively faulted and eroded along the Gulf of Tadjourah margin, are covered by the younger basalts (one to two million years old) emitted at the initial stage of the gulf opening. They are also affected by presently still active normal faults (trending E–W

and WNW–ESE), and transverse faults with normal components (trending NE–SW) along the gulf margins. The superficial geothermal reservoir (up to 220 °C) is expected to develop at a depth of 1000–2000 m in the Quaternary detrital formations also thanks to the important fractures developed in the two WNW and NE directions. Deeper supercritical fluids are expected to be met at 3000–4000 m depth while approaching the spreading axis under the sea floor

The geothermal model we have to work with presents the originality of being largely underneath the ocean. Surface indices along the shore are limited, and the most active part of the system clearly lies to the south and east, underneath the Gulf of Tadjourah, as the northern emerged part clearly belongs to more ancient, presently (and since four million years ago) inactive geological setting (now part of the Arabian plate). A hypothetical interpretative scheme is proposed in Fig. 12.22, where the relations between the submarine active rift segments and the potential deep-drilling sites of Tadjoura (T), Rouéli (R) and Obock (O) are shown:

- *The active ridge axis and related heat source*, at nearly 1300 °C, is mantellic or magmatic, located a few kilometres deep south of Tadjourah and Obock, each in its

specific oceanic axial valley of WNW–ESE direction, that is, oblique to the direction of the opening, which is N37°E according to Dauteuil et al. (2001). It should be noted that the NE–SW transverse faults, well developed along the Obock and Rouéli coastlines, are also of extensional character. They appear as the northern extension of the transform faults linking the Obock and Tadjourah rift segments through the small Maskali Rift. Hence, they also generate magmatic heat of mantellic origin (leaky transform faults). Nearby an anomalous mantle at 1300 °C, located, according to seismic evidence, at a depth not exceeding 6–7 km, is therefore expected on each of the sites at Tadjourah, Obock and Rouéli. Moreover, more superficial magma chambers are expected beneath nearby submarine central volcanoes.

A geothermal gradient of 20 °C/km at depth may therefore be expected in the wells.

- *A geothermal reservoir*, the temperature of which is above 210 °C at Obock according to thermal springs hydrogeochemistry may well be located at a depth of about 1000 m, and should develop in the faulted basaltic formations resulting from the early gulf opening (with good fracture permeability), but also in the interbedded detrital deposits, displaying a good matrix permeability. The intense fracturing developed along both WNW and NE directions, reactivated by the present seismicity, offers a particularly favorable context for the possible development of a geothermal reservoir. Higher temperature supercritical reservoirs are expected to be found at greater depth (around 2000 m).
- *The cover* is made of Quaternary formations, detrital and coral reef deposits and most probably hydrothermally altered units to be encountered a few hundred metres deep. The self-sealing process may have allowed the development of impermeable clay and silica-rich layers, although the active seismicity and faulting may regularly re-open these pluggings. Surface manifestations are more abundant in the rejuvenated fractured basaltic plateau margins of Rouéli than in the sedimentary plains of Tadjourah and Obock, where rapid sedimentation of the deltas of the northern wadies may obliterate the eventual leakages, less abundant in these softer units.
- *The feeding* of the reservoir is ensured by both meteoric water flowing from the upper faulted formations and oceanic water, which is certainly dominant at depths below sea level.

How would these sites fulfill the ICDP criteria?

Global Criterion: The unique geodynamic environment in the area can be tackled through the possibility of directly touching a real oceanic ridge by direct drilling onshore from a continent. This can solve problems of global significance. Although unique, this is without doubt an opportunity to understand better the actual geological structure of MORs. Moreover, this would be an attempt to build the first steps towards further prospective industrial developments offshore and in situ along these major energy producers from the inner Earth as future sources of geothermal power. In this respect, this is a real “World-Class” Geological Site!

International Criterion: Afar region as a whole is already a geological site of major international significance, with important work having been developed there by German, Italian and French scientific teams since the 1970–1980s, with renewed interest in the last 6 years because of the Manda Harraro-Dabbahu event (2005–2011), leading to continuous work by several scientific teams in the region extending from Afar to the Gulf of Aden. Hence, the

international collaboration is already extensive, involving the best possible science teams as well as local scientists. In this context, it would be a real opportunity for the pooling of resources and technology towards offshore exploitation of MOR geothermal resources.

Societal-Needs Criterion: Geothermal power production is of relevance to the people of the country itself as an immediate solution to the presently unsatisfied energy needs. In the long run, however, the incidence is of course much larger and concerns the whole world in its capacity to rely upon renewable, reliable and clean energy sources. In such circumstances, collaboration with industry represents an attractive target, although, at present, the site is not located in an industrial environment but rather in a to-be-developed region. Nevertheless, the site is open to a bright future because of the future railway link between central and northern Ethiopia with the sea through the future international port of Tadjourah.

Need-for-Drilling Criterion: Although the approach from the surface—already well developed through previous scientific work (geology, fluid geochemistry, geophysical hydrographic and oceanographic studies)—still needs to be fine tuned, there is no doubt that deep deviated drilling is the only way to tackle directly the actual problems yet to be understood and solved. Hence, we have clear proof of the necessity for drilling!

Depth-to-Cost Criterion: It is clear that, if one accepts the idea that looking after the actual functioning of MOR is of major scientific interest, and that approaching this question with a view to future economic developments (notably power production, but also eventually several minerals) is also valid, then the site proposed is optimal in terms of depth-to-cost criteria. This point, however, still needs to be well quantified through further engineering and economic studies. Balancing of costs and drilling design is yet to be established.

12.1.14 General Considerations on Geothermal Development Perspectives in Afar

Although there are major geothermal sites all along the EARV, several of which have already seen economic industrial developments, notably in Kenya, the Afar region has not yet demonstrated its capability. Although projects are under advanced feasibility in the Tendaho graben (Ethiopia) and Asal (Djibouti), Afar could possess the largest geothermal potential of the African continent. Because of its exceptional character as the fastest spreading part of the EARV, with additionally an emerged oceanic rift segment and the influence of active mantle plume, Afar certainly shares with Iceland the advantage of having the world’s highest geothermal potential.

Differing from Iceland, however, climate conditions are not generally favourable for a recharge of the geothermal

reservoir by meteoric water. Geothermal brines with corrosive and scaling effects prevail in northern and eastern Afar where hyper-saline lakes and salt deposits developed, which is typically the case at the bottom of endoreic basins with high evaporation in an arid climate where the axial ranges are located. Nevertheless, deep aquifers can be recharged by meteoric waters because of the vicinity of the high and humid Ethiopian plateau. Large water basins enable the recharging of the fractured and permeable formations located on the western side of the axial ranges where transverse fracture zones offer optimal conditions for geothermal reservoir development.

There is little doubt that Afar may, in the future, become a region of major renewable energy production. The transition period could, however, be difficult. The arid climate has not fostered social and economic development for the Afar population. As a first step, it is essential that geothermal development benefits local inhabitants. A well-adapted, probably specific, mode of development that involves the local population as much as possible should be considered. Afar workers presently building the artisanal steam condensers should, for instance, be offered employment in the drilling work. This sustainable development issue is a challenge for all, including local authorities, engineering and industrial firms, researchers and financing agencies. The capability of these agencies to support geothermal projects adapted to these specific conditions is a real challenge that regional programs should help to solve as soon as possible.

12.2 Mineral Resources

The EARV in general and Afar in particular holds a real potential for mineral raw materials. Little advantage is currently derived from these because of rare feasibility studies and the isolated situation of the region. However, because of the development of geothermal energy and new access and energy-related infrastructures, perspectives of exploitation are beginning to emerge.

12.2.1 Metallic Resources Associated with the Tectono-Magmatic and Geothermal Context

In Afar, a zone of rapid expansion, the volcanism is predominantly basaltic, tholeiitic with a differentiation that is rhyolitic in the north and centre, whereas alkali tendencies are more pronounced to the south under MER influence. Two typologies appear crucial from a metallogenic perspective:

1. In northern Afar, a fault is coated with magnetite and apatite (Barberi and Varet 1970); these mineralisations

linked with magmatic segregations are not dissimilar to the Asal1 borehole deposits (1971–1975) in the Republic of Djibouti. Once the geothermal deposit in this zone is exploited, as is expected, extraction of these metals (including zinc, lead, copper, silver and gold) could represent an economically viable resource. Such metallic deposits may also have developed naturally in active volcanic hydrothermal systems along the rift axis. They are simply too young to be found outcropping at the surface.

2. An epithermal gold-bearing phase is observed in the fissural basaltic series, in connection with the rhyolitic formations. They take the form of recent cherty veins deposited on open cracks and issuing from hydrothermal emergences (Figs. 12.23, 12.24 and 12.25). Several economically promising sites have already been identified in central-eastern Afar (Ethiopia, Djibouti) and have received an exploration license in Djibouti.⁹ As observed elsewhere in the world, some of them occur in active hydrothermal systems.

12.2.2 Mineral Resources Related to Marine or Lacustrine Evaporitic Contexts

Extensive tectonics brings about the formation of lacustrine sedimentary trenches throughout Afar as well as marine ones in its northern part. Climate fluctuations have allowed varied types of evaporitic sediments to accumulate. The silica and sodic volcanic environment affords conditions conducive to several types of deposit:

- Potash and rock salt (“white gold”) in northern Afar; the salt is mined, but transportation costs represent a handicap to the export of potash. In Djibouti, a mineral port is being constructed in the Ghoubbet bay by a Chinese company allowing to directly export the salt from lake Asal through marine routes.
- Gypsum, widespread throughout the Afar Rift, is well exploited in the Danakil Sea and Lake Asal surroundings
- Diatomite and powdery white limestone are quite common in many Afar grabens, but analysis needs to be done to select sites where pure diatomite or pure white limes are found in accessible conditions
- Hydrocarbons: the strong geothermal gradient favors the rapid and superficial maturation of the lacustrine deposits, rich in organic matter, but no commercial deposit has been found in Afar. Sedimentary basins being developed in the southern Red Sea and Gulf of Aden north and south of Tadjourah trench could provide off-shore targets.

⁹<http://www.agenceecofin.com/or/1403-18364-djibouti-pour-stratex-le-gisement-d-or-de-pandora-est-son-objectif-le-plus-attractif-sur-le-rift>.

Fig. 12.23 Fissures filled with silica (chalcedony and quartz) and calcite mineralised with metallic sulphides and gold in the eroded statoid series, eastern Afar, Djibouti Republic (photo IAVCEI, 2004)



12.2.3 Metallic Resources Associated with Synsedimentary Hydrothermal Activity

Manganese and barium deposits have been worked since the beginning of the twentieth century in En Kafala (northern Afar). Bonatti et al. (1972) have demonstrated the analogy of these deposits with those of the Red Sea, which is hydrothermal activity in a marine environment, in the vicinity of “black smokers”. The deposits are concentrated inside coralline formations (the former shores of the Danakil Sea).

No specific mineral exploration has been carried out on such targets for the last 50 years, and other deposits may be

found in other part of the Danakil Sea shorelines. In addition, analogues may be sought in similar geological environments, for example, in the coral formations found along the Gulf of Tadjourah.

Lastly, lithium, although not yet identified, might be concentrated on in the Afar context, where magmatic differentiation, high-temperature hydrothermal activity and evaporation are combined.

Besides the substances mentioned above, a potential exists for industrial rocks and minerals, derived from the products of volcanic activity: building stone, (ignimbrites...), pumice, perlite, zeolite and semi-precious stones (olivine, opal, etc.).

Fig. 12.24 Chalcedony and quartz veins with associated metallic mineralisation, some of which was associated with gold (photo Varet 2014). Hess Daba site, with M. Ali Barreh Adaweh (MERN, Djibouti)



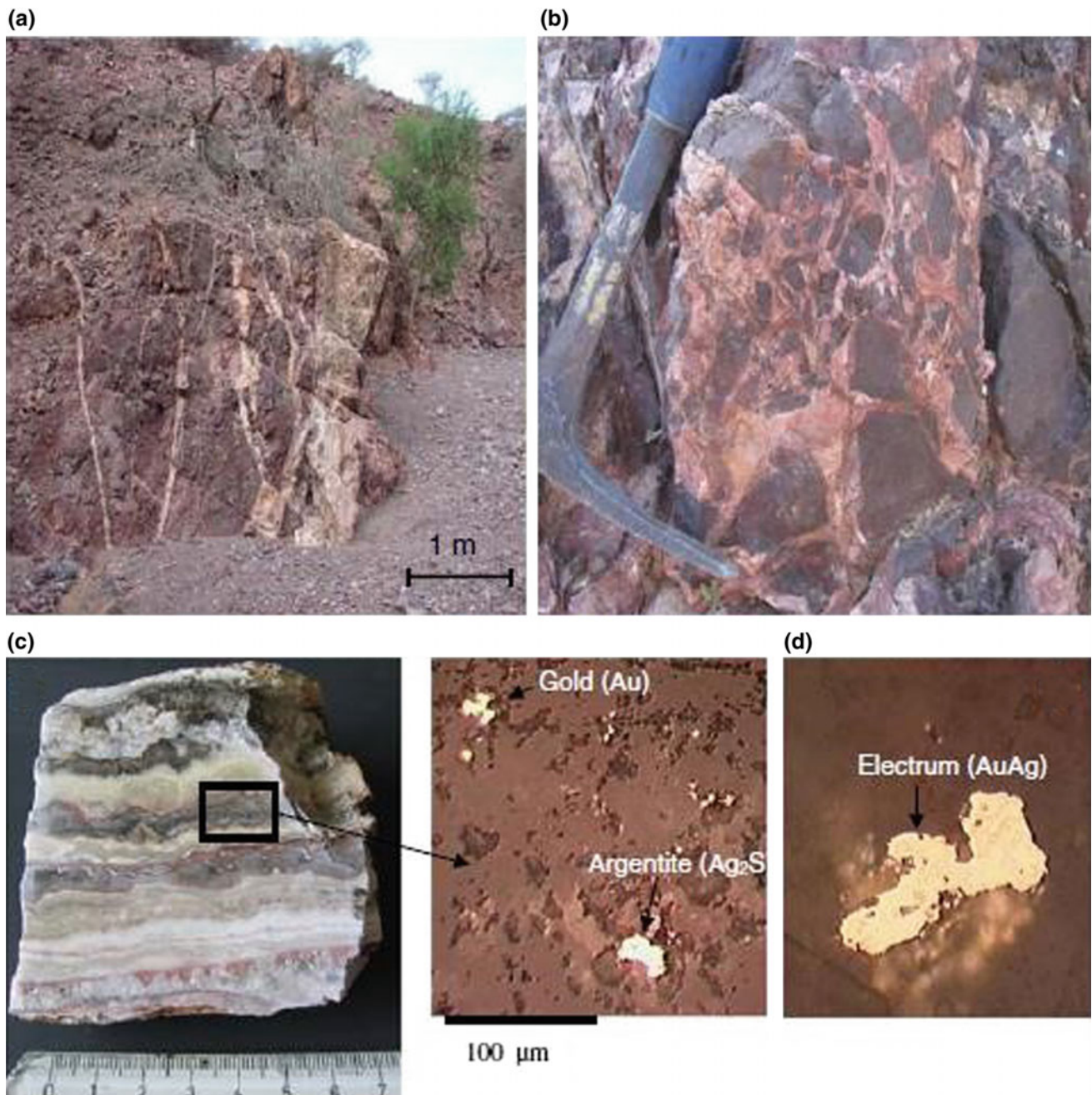


Fig. 12.25 Veins and breccias impregnated with silica in fissures affecting the Dalha basalts in Arta fault corridor (eastern Afar, Djibouti Republic). Gold and silver mineralisations observed under the

microscope appear as automorphous inclusions in the chalcedony gangue (Moussa et al. 2012)

References

- Abdallah A, Gérard A, Varet J (1981) Construction d'un modèle synthétique du champ géothermique d'Asal. Rapport BRGM/82-SDN-951-GTH, 25 pp, 10 maps
- AQUATER (1989). Geothermal exploration project. Republic of Djibouti. Final Report. ISERST 159p
- Amarson K, Flovenz OG (1995) Geothermal exploration by tem-soundings in the central Asal rift in Djibouti. World geothermal Congress, East Africa
- Ballestracci R, Benderitter Y (1980) Sondage magnétotellurique dans le rift d'Asal (République de Djibouti). C.R. Acad. Sc. Paris 290:77–80
- Barberi F, Varet J (1970) The Erta Ale volcanic range. Bull Volc 34:848–917
- Barberi F, Varet J (1975) Recent volcanic units of Afar and their structural significance. In: Pilger A, Rosler A (eds.), Afar depression of Ethiopia, proceedings of an international symposium on the Afar region and rift related problems, Bad Bergzabren, Germany, 1974, vol. 1, E. Schweizerbart'sche Verlagsbuchhandlung, Stuttgart, Germany, pp. 174–178
- Barberi F, Varet J (1977) Volcanism in Afar: small-scale plate tectonic implications. Bull Geol Soc Amer 88:1251–1266
- Barthes V, Gérard A, Varet J (1980) République de Djibouti, Champ géothermique d'Asal, synthèse des données disponibles au 1er juin 1980. Rapport BRGM/80-SGN-525-GTH42 p. 13 photos, 14 cartes
- Battistelli A, Rivera J, Ferragina C (1991) Reservoir engineering studies at the Asal field: Republic of Djibouti. Geoth Resour Counc Bull 280–289
- Bonatti E, Fisher DE, Joensuu O, Rydell HS, Beyth M (1972) Iron-manganese-barium deposit from the Northern Afar rift (Ethiopia). Econ Geol 67:717–730
- Bosch B, Deschamps J, Lopoukhine M, Marce A, et Vilbert C (1974) La zone géothermique du lac Asal (TFAI). Résultats de terrain et études expérimentales. Bull. BRGM II:367–383
- BRGM (1970) Reconnaissance géothermique du TFAI. Rapport BRGM/70-SGN-GTM. 59p
- BRGM (1973) Etude géothermique de la région du lac Asal, campagne 1972-1973. Rapport BRGM/73-SGN-144-GTH, 22p
- BRGM (1975) Territoire Français des Afars et des Issas: rapport de fin de sondage, interprétation des données géologiques de Asal 1 et Asal 2. Rapport BRGM/75-SGN-443-GTH. 19p
- Dauteuil O, Huchon P, Quemeneur F, Souriot T (2001) Propagation of an oblique spreading center; the western Gulf of Aden. Tectonophysics 332:423–442
- Dobre C, Manighetti I, Dorbath C, Dorbath L, Jacques E, Delmond J-C (2007a) Crustal structure and magmato-tectonic processes in an active rift (Asal-Ghoubbet, Afar, East Africa): 1. Insights from a 5-month seismological experiment. J Geophys Res 112
- Dobre C, Manighetti I, Dorbath L, Dorbath C, Bertil D, Delmond J-C (2007b) Crustal structure and magmato-tectonic processes in an active rift (Asal-Ghoubbet, Afar, East Africa): 2. Insights from a the 23 year recording of seismicity since the last rifting event. J Geophys Res 112
- Fouillac C, Fabriol R, et Lundt F (1983) Champ géothermique d'Asal. Synthèse des données disponibles au 1er janvier 1983. Rapport BRGM/83-SGN-022-GTH, 71 p
- Haga AO, Cheik HS, Varet J (2012) The Obock and Rouéli geothermal sites, Djibouti Republic. Proceedings of the 4th African Rift Geothermal Conference. Nairobi, Kenya, 21-23 November 2012, 9p
- Hirn A (1988) Etude sismique sur Asal. In: Champ géothermique d'Asal. Djibouti. Synthèse des données, 93CFG06, pp 56–60
- Houmed AM, Haga AO, Abdilahi S, Varet J (2012) The Asal geothermal site, Djibouti Republic (model update, 2012). Proceedings of the 4th African Rift Geothermal Conference. Nairobi, Kenya, 21–23 November 2012, 9p
- Jalludin M (2003) An overview of the geothermal prospections in the Republic of Djibouti. Results and perspectives. Kengen geothermal conference, Nairobi.
- Kalberkamp U (2010) Magnetotelluric measurements to explore for deeper structures of the Tendaho geothermal field, Afar, NE Ethiopia, Proceedings of the 23rd Schmucker-Weidelt-Colloquium for Electromagnetic Depth Research
- Manighetti I, Tapponnier P, Courtillot V, Gruszow S, Gillot P-Y (1997) Propagation of rifting along the Arabia-Somalia plate boundary: the gulfs of Aden and Tadjoura. J Geophys Res 102:2681–2710
- Moussa et al. (2012) First evidence of epithermal gold occurrence in the SE Afar Rift, Republic of Djibouti. Mineral Deposita 47:563–576
- Omenda P, Achieng J, Onyango S, Varet J (2014) The “Geothermal Village” concept: a new approach to geothermal development in rural Africa. Proceedings 5th African Rift Geothermal Conference, Arusha, Tanzania, 29–31
- Ruegg J-C, Lépine JC, Tarantola A (1979). Geodetic measurements of rifting associated with a seismo-volcanic crisis in Afar. Geophys. Res. Lett. 6:817– 820
- Tazieff H, Barberi F, Borsi S, Ferrara G, Marinelli G, Varet J (1970) Relationships between tectonics and magmatology in the Northern Afar (or Danakil) depression. Phil Trans Royal Soc London A 267:293–311
- UNDP (1973) Geology, geochemistry, and hydrology of the East Africa Rift System within Ethiopia. DDSF/ON/116. U.N. New York
- Varet J (2004) De l'Afar à la géothermie. In: Glénat (ed) Haroun Tazieff, une vie de feu, pp 85–94
- Varet J (2006) The Afar triangle: a future “gulf region” for world geothermal energy? In: ARGeo-C1—first east african rift geothermal conference—geothermal energy: an indigenous environmentally benign & renewable energy resource - Addis Abeba - Ethiopia, 24/11-02/12/2006
- Varet J (2010) Haroun Tazieff (1914-1998). Des années Afar au Secrétariat d'État (1967-1986): la difficile mutation institutionnelle. Bull COFRHIGEO, mars 2010, 26p
- Varet J (2014) Asal-Fialé geothermal field (Djibouti republic): a new interpretation for a geothermal reservoir in an actively spreading rift segment. Proceedings 5th African Rift geothermal Conference, Arusha, Tanzania, 29–31 October 2014
- Varet J, Chernet, T, Woldetinsae G, Arnason K (2012) Exploring for Geothermal Sites in Northern and Central Afar (Ethiopia). Proceedings of the 4th African Rift Geothermal Conference. Nairobi, Kenya, 21–23 November 2012, 7p
- Vergne J, Dobre C, Mohamed K, Dujardin A, Leroy S (2012) The lithospheric structure beneath mature continental rifts : New Insights from a dense seismic profile across the Asal-Ghoubbet Rift (Djibouti) Afar Rift Meeting, Addis-Ababa
- Yohannes E (2015) Geothermal exploration in Eritea Country update. Proceedings World Geothermal Congress Melbourne, Australia, 19–25 April 2015
- Zan L, Gianelli G, Passerini P, Troisi C, Haga AO (1990) Geothermal exploration in the Republic of Djibouti: thermal and geological data of the Hanle and Asal areas. Geothermics 19:58–561

The Afar depression is not just a well-defined geographical feature with its rather specific geological and climatic context. It is inhabited by a specific population, with its own language (of oriental Cushitic root) and culture (for instance, generally practicing Sunni Islam). Pastoralist, semi-nomadic with a strong identity, the Afar population is of the order of two million, spread over three countries: Ethiopia (where more than half live), Eritrea and Djibouti (less than half a million each).

Afar is the name they use in their language, whereas they are called Adal in Ethiopia (ge'ez:) which is the name of a political entity which was identified in the sixteenth century, or Dankali (Arabic:) and Danakil when plural by the Arabs.

National boundaries between Ethiopia, Djibouti and Eritrea were defined between 1891 and 1955, and with the independence of Eritrea in 1993, and as a result, Afar, despite the continuity of the land, pastures, language and culture, was split between these three national entities.

In Ethiopia, since the creation of the Federal Democratic Republic (1993), Afar became one of the Regional States, with its own administration, police, education system, and even a university built in the newly built capital of Semara (central Afar). The Regional State is divided into 5 zones and 30 Woredas (Fig. 13.1).

In Eritrea, the Afar region, which extends along the Red Sea coast from Mersa Fatma to the boundary with Djibouti, is split into two (of the six) political regions of the country: the Southern Red Sea (with Assab as capital) which corre-

sponds to the “Danakil Alps”, and the Northern Red Sea (with Massawa as capital) which includes the northern extremity of the Danakil depression (including, for instance, the Alid volcano and geothermal site).

In Djibouti, despite the fact that the largest part of the territory is populated by Afars (northern and western parts of the country), the majority of the population is located in the capital and is dominantly Somali (mainly Issas). Despite some political reforms, ethnic Issas presently dominate executive decision-making, the civil service, and the ruling party, and this has bred resentment for the Afars. The signing in May 2001 of an agreement between the Djibouti government and the radical fraction of the Afar organisation FRUD (*Front pour la Restauration de l'Unité et de la Démocratie*) at least temporarily eased tensions in the three countries, the development of education, telecommunication, transport facilities, and diversification of the economic activities (like road and construction building, hotels, restaurants, plantations, mines...) induced a mixing of the Afars with populations from the surroundings. Nowadays, in several Afar cities, Coptic churches co-exist with the mosqs, both recently built. With time, the Afar region, crossed by numerous communication routes, is becoming an international melting pot, despite its arid and hot climate (peaking 50 °C in summer). As a whole, despite having been named “the cruelest place on earth” by the National Geographic, Afar people prove to be the most hospitable.

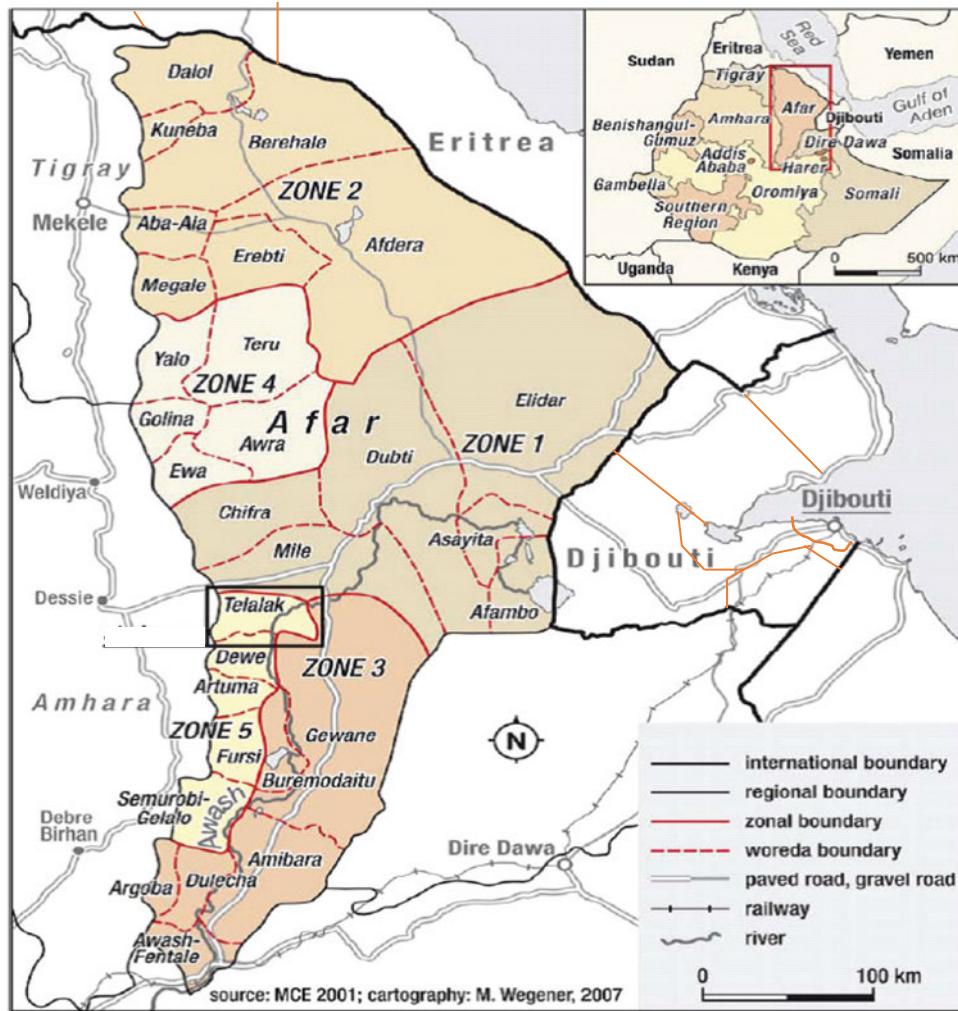


Fig. 13.1 Afar regional state: zones (5) and Woreda subdivisions. Subdivisions in Djibouti and Eritrea are also drawn (*orange lines*)

Whatever the country, the capability for the Afars to take control of their affairs, including the political and economic development of their respective sub-regions, remains a

challenge. Knowledge of the Earth resources and development of education and professional training should be powerful keys. It is hoped that this book can contribute.

Conclusion

Geologically, Afar represents one of the most significant treasures of Planet Earth. It has features that are of major importance for understanding how the Earth crust forms, how the mantle interferes with the Earth's crust, how volcanoes and faults work, how geothermal systems develop, how mineral resources are formed and renewed and how life and even mankind appeared.

For these reasons and a few others, despite its arid climate and the present stage of its population deeply affected by drought and climate change, it is also an area of major importance for the future of humanity. The Afar population—that offers to the world an example of adaptation and resilience to the worst climate conditions on Earth—now can seize the opportunity to support a radical transition towards resilience imposed by climate change. The perspective of inventing there a really sustainable development offers enormous possibilities for science, technology, education and transfer of know-how.

In the coming years, areas where sustainable sources of energy and minerals/metals are not only made available but also renewed by active geological processes could become the new privileged centres for planetary development.

Differing from previous economic revolutions based on exploitation of fossil fuels and exhaustible mineral resources, areas displaying environmentally friendly sustainable sources could become the new key development centres.

Besides this, locally, the ecological transition that is required worldwide allows for direct development to occur, benefitting from newly available technologies of the future (mini-grid, cascade uses, ORC production, intelligent systems, etc.), without passing through the unnecessary steps of fossil fuels and nuclear energy which have characterised the present and past steps of “development”.

A sustainable development cannot be achieved without taking into account the economic and social dimensions. The strategic position of this area in the world, the fast economic growth in Ethiopia and Djibouti and the introduction of appropriate technologies should ensure economic stability. The social dimension relies on the capability of the Afar population to become active in these developments. May this book contribute to facilitate these issues for the benefit of the Afar population which deserves it, and for the broader interests of mankind.

References

- Abbate E, Passerini P, Leonardo Z (1995) Strike-slip faults in a rift area: a transect in the Afar triangle, East Africa. *Tectonophysics* 241:67–97
- Abdallah A, Courtillot V, Kasser M, Le Dain AY, Lépine J-C, Robineau B, Ruegg J-C, Tapponnier P, Tarantola A (1979) Afar seismicity and volcanism: relevance to the mechanics of accreting plate boundaries. *Nature* 282:17–23
- Abdelsalam MG, Stern R (1996) Sutures and shear zones in the Arabian-Nubian Shield. *J Afr Earth Sci* 23:289–310
- Abebe B, Boccaletti M, Mazzuoli R, Bonini M, Tortorici L, Trua T (1998a) Geological map of the Lake Ziway-Asela region (Main Ethiopian Rift), scale 1:50,000. *Cons Naz delle Ric, ARCA*. Florence, Italy
- Abebe T, Mazzarini F, Innocenti F, Manetti P (1998) The Yerer-Tullu Wellel volcanotectonic lineament: a transtensional structure in central Ethiopia and the associated magmatic activity. *J Afr Earth Sci* 26(1):135–150
- Abell PI, Williams MJ (1989) Oxygen and carbon isotope ratios in gastropod shells as indicators of paleoenvironments in the Afar region of Ethiopia. *Palaeo Palaeo Palaeo* 74:265–278
- Abraha M (2006) Geothermal exploration opportunities. *GRC Trans* 30:643–647
- Acocella V, Korme T (2002) Holocene extension direction along the Main Ethiopian Rift, East Africa. *Terra Nova* 14:191–197
- Acocella V, Korme T, Salvini F (2003) Formation of normal faults along the axial zone of the Ethiopian Rift. *J Struct Geol* 25:503–513
- Acocella V, Abebe B, Korme T, Barberi F (2008) Structure of Tendaho Graben and Manda Hararo Rift: implications for the evolution of the southern Red Sea propagator in Central Afar. *Tectonics* 27:TC4016.
- Acton GD, Stein S (1991) Block rotation and continental extension in Afar: a comparison to oceanic microplate systems. *Tectonics* 10:501–526
- Acton G, Tessema A, Jackson M, Bilham R (2000) The tectonic and geomagnetic significance of paleomagnetic observations from volcanic rocks from central Afar. *Earth Planet Sci Lett* 180:225–241
- Allard P, Tazieff H, Dajlevic D (1979) Observations of sea-floor spreading in Afar during the November 1978 fissure eruption. *Nature* 279:30–33
- Almond DC (1986) Geological evolution of the Afro-Arabian dome. *Tectonophysics* 331(1986):302–333
- Arnarson K (2008) The Asal Geothermal Field, Djibouti. *Geophys Surf Exp. ISOR*
- ArRajehi A et al. (2010) Geodetic constraints on present-day motion of the Arabian plate: implication for Red Sea and Gulf of Aden rifting. *Tectonics* 29:TC3011
- Asaye M, Tassew M (2006) Ethiopia geothermal activities—summary of rehabilitation of Alutu-Langano geothermal power plant and Tendaho feasibility study. *GRC Trans* 30:649–653
- Asfaw LM (1998) Environmental hazard from fissures in the Main Ethiopian Rift. *J Afr Earth Sci* 27(3/4):481–490
- Asfaw B, Ebinger C, Harding D, White T, Woldegabriel G (1990) Space-based imagery in paleoanthropological research—An Ethiopian example. *Nat Geogr Res* 6:418–434
- Asfaw LM, Beyene H, Mkonnen A, Oli T (2006) Vertical deformation in the Main Ethiopian Rift: levelling results in its northern part, 1995–2004. In: Yirgu G, Ebinger CJ, Maguire PKH (eds) *The Afar Volcanic Province within the East African Rift System*. Geological Society of London, Special Pub. 259, pp 185–190
- Asrat A, Berbey P, Gleizes G (2001) The Precambrian geology of Ethiopia: a review. *Afr Geosci Rev* 8:271–288
- Aubry A (1855) Observations géologiques sur le pays Danakil, Somalie, le Royaume du Choa et les pays Galla. *Bull Soc Geol Fr* XIV
- Ayalew D, Barbey P, Marty B, Reisberg L, Yirgu G, Pik R (2002) Source, genesis and timing of giant ignimbrite deposits associated with Ethiopian continental flood basalts. *Geochim Cosmochim Acta* 66:1429–1448
- Ayalew D, Ebinger C, Bourdon E, Wolfenden E, Yirgu G, Grassineau N (2006) Temporal compositional variation of early syn-rift rhyolites along the western Red Sea margin and northern Main Ethiopian rift. In: Yirgu G, Ebinger CJ, Maguire PKH (eds) *The Afar Volcanic Province within the East African Rift System*. Geological Society of London, Special Pub. 259, pp 121–130
- Ayele A (1995) Earthquake catalogue of the Horn of Africa for the period 1960–1993, Rep. 3–95, pp 1–9, *Seismol. Dep., Uppsala Univ., Uppsala*
- Ayele A, Kulhanek O (1997) Spatial and temporal variations of seismicity in the Horn of Africa from 1960 to 1993. *Geophys J Int* 130:805–810
- Ayele A, Arvidsson R (1998) Fault mechanisms and tectonic implication of the 1985–1987 earthquake sequence in south western Ethiopia. *J Seismol* 1:383–394
- Ayele A (2000) Normal left-oblique fault mechanisms as an indication of sinistral deformation between the Nubia and Somalia plates in the Main Ethiopian Rift. *J Afr Earth Sci* 31(2):359–368
- Ayele A, Kulhanek O (2000) Reassessment of source parameters for three major earthquakes in East African rift system from historical seismograms and bulletins. *Ann Geofis* 43:81–94
- Ayele A, Stuart G, Kendall JM (2004) Insights into rifting from shear-wave splitting in press: an example from Ethiopia. *Geophys J Int* 157:354–362
- Ayele A, Stuart GW, Bastow ID, Keir D (2006a) The August 2002 earthquake sequence in north Afar: Insights into the neotectonics of the Danakil microplate. *J Afr Earth Sci*
- Ayele A, Nyblade AA, Langston CA, Cara M, Leveque J-J (2006b) New evidence for Afro-Arabian plate separation in southern Afar.

- In: Yirgu G, Ebinger CJ, Maguire PKH (eds) The Afar Volcanic Province within the East African Rift System. *Geol. Soc. Spec. Publ.*, 259, pp 133–142
- Ayele A et al (2007) The volcano-seismic crisis in Afar, Ethiopia, starting September 2005. *Earth Planet Sci Lett* 255:177–187
- Baker J, Snee L, Menzies M (1996) A brief Oligocene period of flood volcanism in Yemen. *Earth Planet Sci Lett* 138:39–49
- Bannert D (1972) Plate drift in the Afar and Issas Territory and Eastern Ethiopia as seen on space photography, *NASA, TN. D-6277*, 28p
- Barberi F, Tazieff H, Varet J (1972) Volcanism in the Afar depression: its tectonic and magmatic significance. *Tectonophysics* 15:19–29
- Barberi F, Borsi S, Ferrara G, Marinelli G, Santacroce R, Tazieff H, Varet J (1972) Evolution of the Danakil Depression (Afar Ethiopia) in light of radiometric age determination. *J Geol* 80:720–729
- Barberi F, Santacroce R, Varet J (1974) Peralkaline silicic volcanic rocks of the Afar Depression. *Bull Volcan* 38:755–790
- Barberi F, Santacroce R, Ferrara G, Varet J (1974) Evolution of Afar in light of K/Ar age determinations. *Afar Symposium, Bad Bergzabern*, April 1–6 (abstract)
- Barberi F, Bonatti E, Marinelli G, Varet J (1974) Transverse tectonics during the split of a continent data from the Afar Rift. *Tectonophysics* 23:17–29
- Barberi F, Ferrara G, Santacroce R, Treuil M, Varet J (1975) A transitional basalt-pantellerite sequence of fractional crystallisation, the Boina centre (Afar rift, Ethiopia). *J Petrol* 16:22–56
- Barberi F, Ferrara G, Santacroce R, Varet J (1975) Structural evolution of the Afar triple junction. In: Pilger A, Rösler A (eds) *Afar Depression of Ethiopia*, Stuttgart (Schweizerbart), pp 38–54
- Barberi F, Civetta L, Varet J (1979) Sr isotopic composition of Afar volcanics and its implication to mantle evolution. *Earth Planet Sci Lett*
- Barberi F, Santacroce R (1980) The Afar Stratoid Series and the magmatic evolution of the East African rift system. *Bull Soc Geol Fr* 6:891–899
- Barberi F, Varet J (1975) Volcanological research in Afar (L. R. Wager prize summary lecture). *Bull Volc* 39(2):166–174
- Barberi F, Varet J (1975) Recent volcanic units of Afar and their structural significance. In: Pilger A, Rösler A (eds) *Afar depression of Ethiopia, proceedings of an international symposium on the Afar region and rift related problems*, Bad Bergzabren, Germany, 1974, vol 1, E. Schweizerbart'sche Verlagsbuchhandlung, Stuttgart, Germany, pp 174–178
- Barrat JA, Fourcade S, Jahn BM, Cheminee JL, Capdevila R (1998) Isotope (Sr, Nd, Pb, O) and trace element geochemistry of volcanics from the Erta' Ale range (Ethiopia). *J Volcanol Geothermal Res* 80:85–100
- Barrat J-A, Jahn BM, Joron J-L, Auvray B, Hamdi H (1990) Mantle heterogeneity in northeastern Africa: evidence from Nd isotopic compositions and hygromagmaphile element geochemistry of basaltic rocks from the Gulf of Tadjoura and southern Red Sea regions. *Earth Planet Sci Lett* 101:233–247
- Bastow I, Stuart GW, Kendall J-M, Ebinger C (2005) Upper mantle seismic structure in a region of incipient continental breakup: northern Ethiopian rift. *Geophys J Int* 162:479–493
- Bastow ID, Pilidou S, Kendall J-M, Stuart GW (2010) Melt-induced seismic anisotropy and magma assisted rifting in Ethiopia: evidence from surface waves. *Geochem Geophys, Geosyst*, p 11
- Baye AY (2009) Hydrogeological and hydrogeochemical framework of complex volcanic system in the Upper Awash River Basin, Central Ethiopia. Thesis, Univ. Poitiers, 218p
- Bellahsen N, Faccenna C, Funicicello F, Daniel JM, Jolivet L (2003) Why did Arabia separate from Africa? Insights from 3-D laboratory experiments. *Earth planet Sci Lett* 216:365–381
- Bendick B, McClusky S, Bilham R, Asfaw L, Klempere S (2006) Distributed Nubia-Somalia relative motion and dyke intrusion in the Main Ethiopian rift. *Geophys J Int* 165:303–310
- Benoit MH, Nyblade AA, VanDecar JC, Gurrola H (2003) Upper mantle P wave velocity structure and transition zone thickness beneath the Arabian Shield. *Geophys Res Lett* 30(10):1531
- Benoit MH, Nyblade AA, Owens TJ, Stuart G (2006) Mantle transition zone structure and upper mantle S velocity variations beneath Ethiopia: evidence for a broad, deep-seated thermal anomaly. *Geochem Geophys Geosyst* 7(11):Q11013
- Benoit MH, Nyblade AA, Pasyanos ME (2006) Crustal thinning between the Ethiopian and East African plateaus from modeling Rayleigh wave dispersion. *Geophys Res Lett* 33(13):L13301
- Benoit MH, Nyblade AA, VanDecar JC (2006) Upper mantle P wave speed variations beneath Ethiopia and the origin of the Afar Hotspot. *Geology* 34:329–332
- Berckhemer H, Baier B, Bartelson H, Behle A, Burkhardt H, Gebrande H, Makris J, Menzel H, Miller H, Veas R (1975) Deep seismic soundings in the Afar region and on the highland of Ethiopia. In: Pilger A, Rösler A (eds) *Afar between continental and oceanic rifting*: Stuttgart, Schweizerbart, pp 89–107
- Berhe SM (1990) Ophiolites in northeast and east Africa: implication for Proterozoic crustal growth. *J Geol Soc London* 147:41–57
- Berhe S, Kazmin V (1978) Nazret sheet NC37–15: Addis Ababa. *Ethiopi Inst Geol Surv scale 1(250):000*
- Berhe SM, Desta B, Nicoletti M, Teferra M (1987) Geology, geochronology and geodynamic implications of Cenozoic magmatic province in W and SE Ethiopia. *J Geol Soc London* 144:213–226
- Beyth M (1991) 'Smooth' and 'rough' propagation of spreading Southern Red Sea-Afar Depression. *J Afr Earth Sci* 13:157–171
- Bilham R, Bendick R, Larson K, Braun J, Tesfaye S, Mohr P, Asfaw L (1999) Secular and tidal strain across the Ethiopian rift. *Geophys Res Lett* 27:2789–2984
- Bizouard H, Barberi F, Varet J (1976) Minéralogie des séries volcaniques axiales de l'Afar/précisions sur les processus et les conditions de fractionnement des magmas basaltiques dans les zones d'accrétion
- Bizouard H, Barberi F, Varet J (1979) The magmatic expression of the Afar spreading axis: mineralogy and petrology of Erta Ale and Boina series. *Earth Planet Sci Lett*
- Boccaletti M, Bonini M, Mazzuoli R, Abebe B, Piccardi L, Tortorici L (1998) Quaternary oblique extensional tectonics in the Ethiopian Rift (Horn of Africa). *Tectonophysics* 287:97–116
- Boccaletti M, Mazzuoli R, Bonini M, Trua T, Abebe B (1999) Plio-Quaternary volcanotectonic activity in the northern sector of the Main Ethiopian rift: Relationships with oblique rifting. *J Afr Earth Sci* 29:679–698
- Bohannon R, Naeser C, Schmidt D, Zimmermann R (1989) The timing of uplift, volcanism, and rifting peripheral to the Red Sea: a case for passive rifting. *J Geophys Res* 94:1683–1701
- Bonini M, Souriot T, Boccaletti M, Brun J-P (1997) Successive orthogonal and oblique extension episodes in a rift zone: laboratory experiments with application to the Ethiopian rift. *Tectonics* 16:347–363
- Bonnefille R, Vincens A, Buchet G (1987) Palynology, stratigraphy and paleoenvironment of a Pliocene hominid site (2.9–3.3 M.Y.) at Hadar, Ethiopia. *Palaeo Palaeo Palaeo* 60:249–281
- Bosellini A, Russo A, Assefa G (2001) The Mesozoic succession of Dire Dawa, Harar province, Ethiopia. *J Afr Earth Sci* 32:403–417
- Bosworth W, Strecker MR (1997) Stress field changes in the Afro-Arabian Rift system during the miocene to recent period. In: Fuchs K, Altherr R, Mueller B, Prodehl C (eds) *Structure and dynamic processes in the lithosphere of the Afro-Arabian Rift System*, *Tectonophysics* 278, 47–62
- Bott MHP (1980) Crustal doming and the mechanism of continental rifting. *Tectonophysics* 73:1–8
- Bott W, Smith B, Oakes G, Sikander A, Ibrahim A (1992) The tectonic framework and regional hydrocarbon prospectivity of the Gulf of Aden. *J Petroleum Geol* 15:211–243

- BP Exploration (1992) Southern Red Sea. Reg Rev. Ext. 64264
- Braunmiller J, Nabelek J (1990) The 1989 Ethiopia earthquake sequence. EOS Trans AGU 71:1480
- BRGM (1975) Territoire Français des Afars et des Issas: rapport de fin de sondage: résultats des premiers essais de production. *Rapport BRGM/75-SGN-442-GTH*. 18p
- BRGM (1975) Territoire Français des Afars et des Issas: rapport de fin de sondage, interprétation des données géologiques de Asal 1 et Asal 2. *Rapport BRGM/75-SGN-443-GTH*. 19p
- Buck WR (2004) Consequences of athenospheric variability on continental rifting. In: Karner GD, Taylor B, Driscoll N, Kohlstedt D (eds) Rheology and deformation of the lithosphere at continental margins. Columbia University Press, New York, pp 1–30
- Buck WR (2006) The role of magma in the development of the Afro-Arabian Rift System. In: Yirgu G, Ebinger CJ, Maguire PKH (eds) The Afar Volcanic Province within the East African Rift System. Geol. Soc. London, Special Pub. 259, pp 43–54
- Calais E, DeMets C, Nocquet J-M (2003) Evidence for post-3.16 Ma change in Nubia–Eurasia–North America plate motions. *Earth Planet Sci Lett* 216:81–92
- Calais E, Ebinger C, Hartnady C, Nocquet JM (2006) Kinematics of the East African rift from GPS and earthquake slip vector data. In: Yirgu G, Ebinger CJ, Maguire PKH (eds) The Afar Volcanic Province within the East African Rift System. Geol. Soc. Spec. Publ. 259, 9–22
- Camp VE, Roobol MJ (1992) Upwelling asthenosphere beneath western Arabia and its regional implications. *J Geophys Res* 97:15255–15271
- Casey M, Ebinger C, Keir D, Gloaguen R, Mohamed F (2006) Strain accommodation in transitional rifts: extension by magma intrusion and faulting in Ethiopian rift magmatic segments. In: Yirgu G, Ebinger CJ, Maguire PKH (eds) The Afar Volcanic Province within the East African Rift System. Geol. Soc. Spec. Publ. 259, 143–164
- Cattin R, Doubre C, De Chabaliere J-B, Vigny C, King G, Avouac J-P, Ruegg J-C (2004) Numerical modelling of Quaternary deformation and post-rifting displacement in the Asal-Ghoubbet Rift (Djibouti, Aar). *Earth Planet Sci Lett* 239:352–367
- Cattin R, Doubre C, De Chabaliere J-B, King G, Vigny C, Avouac J-P, Ruegg J-C (2005) Thermo-mechanical modelling of quaternary deformation and post-seismic displacement in the Asal-Ghoubbet (Djibouti, Afar). *Earth Planet Sci Lett* 239:352–367
- CFG (1993) Champ géothermique d'Asal. Djibouti. Synthèse des données. *93CFG06*. 87p
- Chang S-J, Merino M, van der Lee S, Stein S, Stein C (2011) Mantle flow beneath Arabia offset from the opening Red Sea. *Geophys Res. Lett*
- Chang S-J, van der Lee S, Flanagan MP, Bedle H, Marone F, Matzel EM, Pasyanos ME, Rodgers AJ, Romanowicz B, Schmid C (2010) Joint inversion for 3- dimensional S-velocity mantle structure along the Tethyan margin. *J Geophys Res* 115
- Chorowicz J, Collet B, Bonavia F, Korme T (1999) Left-lateral strike-slip tectonic and gravity induced individualisation of wide continental blocks in the western Afar margin. *Ecologiae Geologicae Helveticae* 92:149–158
- Christiansen TB, Schaefer H-U, Schoenfeld M (1975) Geology of southern and central Afar, Ethiopia. In: Pilger A, Rosler A (eds) Afar depression of Ethiopia, proceedings of an international symposium on the Afar region and rift related problems, Bad Bergzabren, Germany, 1974, vol 1, E. Schweizerbart'sche Verlagsbuchhandlung, Stuttgart, Germany, pp 259–277
- Chu D, Gordon RG (1998) Current plate motions across the Red Sea. *Geophys J Int* 135:313–328
- Chu C, Gordon R (1999) Evidence for motion between Nubia and Somalia along the Southwest Indian Ridge. *Nature* 398:64–67
- Cerling TE, Hay RL, O'Neil JR (1977) Isotopic evidence for dramatic climatic changes in East Africa during Pleistocene. *Nature* 267:137–138
- Cochran JR (1981) The Gulf of Aden: structure and evolution of a young ocean basin and continental margin. *J Geophys Res* 86:263–288
- Cochran JR (1981) Pre-sea floor spreading development of the Gulf of Aden. *Oceanol Acta Suppl* 4:155–165
- Cochran J (1982) The magnetic quiet zone in the eastern Gulf of Aden: Implications for the early development of the margin. *Royal Astr Soc Geophys J* 68:171–201
- Cochran J (1983) A model for development of the Red Sea. *Amer Assoc Petrol Geol Bull* 67:41–69
- Cochran J, Martinez F (1988) Evidence from the northern Red Sea on the transition from continental to oceanic rifting. *Tectonophysics* 153:25–53
- Coleman RG (1974) Geologic background of the Red Sea. In: Burk CA, Drake DL (eds) The geology of continental margins. Springer, New York, pp 743–751
- Coleman RG, McGuire AV (1988) Magma systems related to the Red Sea opening. *Tectonophysics* 150:77–100
- Constable SC, Parker RL, Constable CG (1987) Occam's inversion: a practical algorithm for generating smooth models from electromagnetic sounding data. *Geophysics* 52:289–300
- Cornwell DG, MacKenzie GD, England RW, Maguire PKH, Asfaw LM, Oluma B (2006) Northern Main Ethiopian Rift crustal structure from new high-precision gravity data. In: Yirgu G, Ebinger CJ, Maguire PKH (eds) The Afar Volcanic Province within the East African Rift System. Geological Society of London, Special Pub. 259, pp 307–322
- Correia H, Demange J, Fabriol R, Gérard A, Varet J (1983) Champ géothermique d'Asal. Synthèse des données disponibles au 1er janvier 1983. *Rapport BRGM/83-SGN-022-GTH* 71p. 10 cartes
- Coulie E, Quidelleur X, Gillot PY, Courtillot V, Lefevre JC, Chiesa S (2003) Comparative K-Ar and Ar-Ar dating of Ethiopian and Yemenite Oligocene volcanism: implications for timing and duration of the Ethiopian traps. *Earth Planet Sci Lett* 206:477–492
- Courtillot V, Achache J, Landre F, Bonhommet N, Montigny R, Feraud G (1984) Episodic spreading and rift propagation—new Paleomagnetic and geochronological data from the Afar nascent passive margin. *J Geophys Res* 89:3315–3333
- Crane K, Bonatti E (1987) The role of fracture zones during early Red Sea rifting. Structural analysis using space shuttle radar and Landsat imagery. *J Geol Soc London* 144:407–420
- D'Acremont E, Leroy S, Beslier M-O, Bellahsen N, Fournier M, Robin C, Maia M, Gente P (2005) Structure and evolution of the eastern Gulf of Aden conjugate margins from seismic reflection data. *Geoph J Int* 160(3):869–890
- Daly E, Keir D, Ebinger CJ, Stuart GW, Bastow ID, Ayele A (2008) Crustal tomographic imaging of a transitional continental rift: the Ethiopian rift. *Geoph J Int* 172(3):1033–1048
- D'Amore F, Giusti D, Gizaw B (1997) The geochemical assesment of Northern Tendaho Rift, Ethiopia. *Proceedings of 22th Stanford Reservoir engineering*, pp 435–445
- Davison I, Al'Kadasi M, Al'Khirbash S, Al'Subbary AK, Baker J, Blakey S, Bosence D, Dart C, Heaton R, McClay K, Menzies M, Nichols G, Owen L, Yelland A (1994) Geological evolution of the southeastern Red-Sea rift margin, Republic of Yemen. *Geol Soc Am Bull* 106:1474–1493
- Debayle E, Lèveque J-J, Cara M (2001) Seismic evidence for a deeply rooted low-velocity anomaly in the upper mantle beneath the northeastern Afro-Arabiancontinent. *Earth Planet Sci Lett* 193:423–436
- De Fino M, La Volpe L, Lirer L, Varet J (1973) Geology and petrology of Manda-Inakir range and Moussa Alli volcano, central eastern

- Afar (Ethiopia and T.F.A.I.). *Rev Geog Phys Géol Dyn* (2)15:373–386
- De Fino M, La Volpe L, Lirer L (1973) Volcanology and petrology of the Assab range (Ethiopia). *Bull Volc* 37–1:1–16
- De Fino M, La Volpe L, Lirer L (1973) Geology and volcanology of the Edd-Bahar Assoli area (Ethiopia). *Bull Volc* 41–1:32–42
- Delibrias C, Faure H, Gasse F, Marinelli G, Varet J (1971) Le lac Afrera à l'Holocène (Afar, Ethiopie). *Comm. VII^e Cong. Panafricain Préhit. Et. Quat. Addis Abeba*
- Delibrias G, Marinelli G, Stieltjes L (1975) Spreading rate of the Asal Rift: a geological approach, *Stuttgart*. In: Pilger A, Rösler A (eds) *Afar Depression of Ethiopia, Proceedings of an International Symposium on the Afar Region and Related Rift Problems*, Bad Bergzabern, F.R. Germany, 1–6 April 1974
- Deniel C, Vidal P, Coulon C, Vellutini PJ (1994) Temporal evolution of mantle sources during continental rifting—the volcanism of Djibouti (Afar). *J Geophys Res* 99:2853–2869
- Déprez A, Doubre C, Masson F, Ulrich P (2013) Seismic and aseismic deformation along the East African Rift from reanalysing of the GPS velocity field of Africa. *Geophys J Int* 193:1353–1369
- Derakhshani R, Farhoudi G (2005) Existence of the Oman Line in the Empty Quarter of Saudi Arabia and its Continuation in the Red Sea. *J Appl Sci* 5:745–752
- Dixon TH, Ivins ER, Franklin BJ (1989) Topographic and volcanic asymmetry around the Red Sea: constraints on rift models. *Tectonics* 8:1193–1216
- Doubre C, Peltzer G (2007) Fluid-controlled faulting process in the Asal rift, Djibouti, from 8 yr of radar interferometry observations. *Geology* 35(1):69–72
- Doubre C, Manighetti I, Dorbath C, Dorbath L, Jacques E, Delmond J-C (2007) Crustal structure and magmato-tectonic processes in an active rift (Asal-Ghoubbet, Afar, East Africa): 1. Insights from a 5-month seismological experiment. *J Geophys Res* 112
- Doubre C, Manighetti I, Dorbath L, Dorbath C, Bertil D, Delmond J-C (2007) Crustal structure and magmato-tectonic processes in an active rift (Asal-Ghoubbet, Afar, East Africa): 2. Insights from a the 23 year recording of seismicity since the last rifting event. *J Geophys Res* 112
- Drury SA, Kelley SP, Berhe SM, Collier RE, Abraha M (1994) Structures related to Red Sea evolution in northern Eritrea. *Tectonics* 13:1371–1380
- Duffield WA, Jackson MD, Smith JG, Lowenstern JB, Clyne MA (1996) Structural doming over an upper crustal magma body at Alid, Eritrea. *EOS Trans Am Geophys Union* 77:F792
- Dugda M, Nyblade A, Julia J, Langston CA, Ammon C, Simiyu S (2005) Crustal structure in Ethiopia and Kenya from receiver function analyses: implication for rift development in eastern Africa. *J geophys Res* 110:B01303
- Dugda MT, Nyblade AA (2006) New constraints on crustal structure in eastern Afar from the analysis of receiver functions and surface wave dispersion in Djibouti. In: Yirgu G, Ebinger CJ, Maguire PKH (eds) *The Afar Volcanic Province within the East African Rift System*. Geological Society of London, Special Pub. 259, pp 239–251
- Dugda MT, Nyblade Andrew A, Julia Jordi (2007) Thin lithosphere beneath the Ethiopian plateau revealed by a joint inversion of rayleigh wave group velocities and receiver functions. *J Geophys Res* 112(b8):B08305
- Drury G, S A, Kelley SP, Berhe SM, Collier R, Araha M, (1994) Structures related to Red Sea evolution in northern Eritrea. *Tectonics* 13:1371–1380
- Ebinger C, Bechtel T, Forsyth D, Bowin C (1989) Effective elastic plate thickness beneath the East-African and Afar plateaus and dynamic compensation of the uplifts. *J geophys Res* 94:2883–2901
- Ebinger CJ, Hayward NJ (1996) Soft plates and hot spots: views from Afar. *J Geophys Res* 101:21,859–21,876
- Ebinger CJ, Jackson JA, Foster AN, Hayward NJ (1999) Extensional basin geometry and the elastic lithosphere. *Phil Trans R Soc London Series A* 357:741–762
- Ebinger C, Yemane T, Harding D, Tesfaye S, Rex D, Kelley S (2000) Rift deflection, migration, and propagation: linkage of the Ethiopian and Eastern rifts Africa. *Geol Soc Am Bull* 102:163–176
- Ebinger CJ, Casey M (2001) Continental breakup in magmatic provinces: an Ethiopian example. *Geology* 29:527–530
- Ebinger CJ (2005) Continental breakup: the East African Perspective. *Astron Geophys* 46(2):2.16–2.21
- Egloff F et al (1991) Contrasting structural styles of the eastern and western margins of the southern Red Sea: the 1988 SONNE experiment. *Tectonophysics* 198:329–353
- Evans J, Achauer U (1993) Teleseismic tomography using the ACH method: theory and application to continental scale studies. In: Iyer E, Hirahara (eds) *Seismic tomography: theory and practice*. Chapman and Hall, New York.
- Fantozzi PL (1996) Transition from continental to oceanic rifting in the Gulf of Aden: Structural evidence from field mapping in Somalia and Yemen. *Tectonophysics* 259:285–311
- Fernandes R, Ambrosius B, Noomen R, Bastos L, Combrinck L, Miranda J, Spakman W (2004) Angular velocities of Nubia and Somalia from continuous GPS data: Implications on present-day relative kinematics. *Earth Planet Sci Lett* 222:197–208
- Foster AN, Jackson JA (1998) Source parameters of large African earthquakes: implications for crustal rheology and regional kinematics. *Geophys J Int* 134:422–448
- Franzosa H, Helga M, Helgadóttir HM, Óskarsson F (2015) Surface Exploration and First Conceptual Model of the Dallol Geothermal Area, Northern Afar, Ethiopia. *Proceedings World Geothermal Congress 2015 Melbourne, Australia, 19-25 April 2015*
- Gadalia A, Varet J (1983) Le rhyolites miocènes de l'Est de l'Afar. *Bull. Soc. Geol. Fr.* 7, XXV:139–153
- Gangopadhyay A, Pulliam J, Sen MK (2007) Waveform modelling of teleseismic S, Sp, SsPmP, and shear-coupled PL waves for crust- and upper-mantle velocity structure beneath Africa. *Geoph J Int* 170 (3):1210–1226
- Garfunkel Z, Beyth M (2006) Constraints on the structural development of Afar imposed by the kinematics of the major surrounding plates. In: Yirgu G, Ebinger CJ, Maguire PKH (eds) *The Afar Volcanic Province within the East African Rift System*. *Geol. Soc. Spec. Publ.* 259, 259:23–42
- Gashawbeza EM, Klempere SL, Nyblade AA, Walker KT, Keranen KM (2004) Shear-wave splitting in Ethiopia: precambrian mantle anisotropy locally modified by Neogene rifting. *Geophys Res, Lett*, p 31
- Gass IG (1970) The evolution of volcanism in the junction area of the Red Sea, Gulf Aden and Ethiopian Rifts. *Phil Trans R Soc London* 267:369–381
- Gasse F, Fontes JC (1989) Palaeoenvironments and palaeohydrology of a tropical closed lake (Lake Asal, Djibouti) since 10,000 yr B. P. *Palaeogeogr Palaeoclimatol Palaeoecol* 69:67–102
- Gasse F, Richard O, Robbe D, Rognon P, Williams MAJ (1980) Evolution tectonique et climatique de l'Afar central d'après les sédiments plio-pleistocènes. *Bull Soc Geol France* 6:987–1001
- Gasse F, Fournier M (1983) Sédiments plio-quatérnaires et tectonique en bordure du Golfe de Tadjoura, République de Djibouti. *Bull Centres Rech Explo- Prod Elf-Aquitaine* 7:285–300
- Gerlach TM (1989) Degassing of carbon dioxide from basaltic magma at spreading centers: I. Afar transitional basalts. *J Volc Geoth Res* 39:211–219
- Ghebreab W, Talbot C (2000) Red Sea extension influenced by Pan-African tectonic grain in eastern Eritrea. *J Struc Geol* 22:931–946

- Gillespie R, Street-Perrott FA, Switsur R (1983) Post-glacial arid episodes in Ethiopia have implications for climate predictions. *Nature* 306:680–683
- Girdler RW (1962) Initiation of continental drift. *Nature* 194:521–524
- Girdler RW (1965) The role of translational and rotational movements in the formation of the Red Sea and Gulf of Aden. *Int. Upper Mantle Project Symposium. The World Rift System. Geol Surv Canada*, 65–76
- Girdler RW (1991) The Afro-Arabian Rift system: an overview. *Tectonophysics* 197:139–153
- Girdler RW, Styles P (1974) Sea-floor spreading in the western Gulf of Aden. *Nature* 271:615–617
- Gonfiantini R, Borsi S, Ferrara G (1973) Isotopic composition of waters from the Danakil Depression, Ethiopia. *Earth Plant Sci Lett* 18:13–21
- Gouin P, Mohr PA (1964) Gravity traverses in Ethiopia. *Bull Geophys Obs Addis Abeba* 3(3):185–240
- Gray T (1980) Environmental reconstruction of the Hadar Formation (Afar, Ethiopia). Ph.D. Thesis. Case Western Reserve University, Cleveland, USA
- Gupta A, Scholz CH (2000) Brittle strain regime transition in the Afar depression: implications for fault growth and seafloor spreading. *Geology* 28:1087–1090
- Guiraud R, Bosworth W (2005) Phanerozoic geological evolution of Northern and Central Africa: an overview. *J Afr Earth Sci*.
- Gurnis M, Mitrovica JX, Su WJ, van Heijst H (2000) Constraining mantle density structure using geological evidence of surface uplift rates: the case of the African plume. *Geochem Geophys Geosyst* 1 (7).
- Hadiouche O, Jobert N, Montagner J-P (1989) Anisotropy of the African continent inferred from surface waves. *Phys Earth planet Int* 58:61–81
- Hailemichael M, Aronson J, Savin S, Tevesz M, Walter R (1996) Oxygen isotope evidence from gastropod shells on the character of the Pliocene lake at Hadar. *Geol Soc Am Abstr* 28[6]
- Hailemichael M, Aronson J, Savin S, Tevesz M, Walter R, Carter J (1997) Tectonic evolution of the Western Afar/Ethiopian Plateau margin, 3.4–2.3 mya. Inferred from isotopic study of Hadar paleosols and lacustrine deposits. *International symposium on flood basalts, rifting and paleoclimates in the Ethiopian Rift and the Afar Depression. Addis Ababa, Ethiopia*
- Hamling I, Wright T, Calais E, Bennati L, Lewi E (2010) Stress transfer between thirteen successive dyke intrusions in Ethiopia. *Nat Geosc Lett*
- Hammond J, Kendall M, Angus D, Wookey J (2010) Interpreting spatial variations in anisotropy: insights into the Main Ethiopian Rift from SKS waveform modelling. *Geophys J Int*
- Harris WC (1844) *The highlands of Ethiopia*, vol 3. Longman, New York
- Hart W, WoldeGabriel G, Walter R, Mertzman S (1989) Basaltic volcanism in Ethiopia: constraints on continental rifting and mantle interactions. *J Geophys Res* 94:7731–7748
- Hayward NJ, Ebinger CJ (1996) Variations in the long-axis segmentation of the Afar rift system. *Tectonics* 15:244–257
- Hebert L, Langston C (1984) Crustal thickness estimate at AAE (Addis Ababa, Ethiopia) and NAI (Nairobi, Kenya using teleseismic P-wave conversions). *Tectonophysics* 111:299–327
- Hébert H, Deplus C, Huchon P, Khanbari K (2001) Lithospheric structure of a nascent spreading ridge inferred from gravity data: the western Gulf of Aden. *J Geophys Res* 106:26,345–26,364
- Hendrie DB, Kusznir NJ, Morley CK, Ebinger CJ (1994) Cenozoic extension in northern Kenya: a quantitative model of rift basin development in the Turkana region. *Tectonophysics* 236:409–438
- Hillaire-Marcel C, Taieb M, Tiercelin J, Page N (1982) A 1.2 Mys record of isotopic changes in a late Pliocene Rift Lake, Ethiopia. *Nature* 296:640–642
- Hirn A, Lépine J-C, Sapine M (1993) Triple junction and ridge hot spots: Earthquakes, faults, and volcanism in Afar, the Azores, and Iceland. *J Geophys Res* 98:11995–12001
- Hjartarson G, Gisladottir V, Gislason G, Olafsson K (2010) Geothermal Development in the Assal Area, Djibouti. *Proceedings World Geothermal Congress, Bali* 8p.
- Houmed AM, Haga AO, Abdilahi S, Varet J (2012) Proposal for new geothermal models and sites hierarchy in Djibouti Republic. *Proceedings of the 4th African Rift Geothermal Conference. Nairobi, Kenya, 21–23 November 2012*, 10pp
- Houmed AM, Haga AO, Abdilahi S, Varet J (2012) The Asal geothermal site, Djibouti Republic (model update, 2012). *Proceedings of the 4th African Rift Geothermal Conference. Nairobi, Kenya, 21–23 November 2012*, 9p.
- Houmed AM, Haga AO, Varet J (2012) A revised approach to the Hanlé-Gaggadé (Djibouti Republic): the Garabbayis geothermal site. *Proceedings of the 4th African Rift Geothermal Conference. Nairobi, Kenya, 21–23 November 2012*, 7p.
- Houmed AM, Haga AO, Abdilahi S, Varet J (2012) Nord-Ghoubbet geothermal site, Djibouti Republic. *Proceedings of the 4th African Rift Geothermal Conference. Nairobi, Kenya, 21–23 November 2012*, 7p
- Hughes GW, Osman V, Zaid BR (1991) Evidence for middle Oligocene rifting of the Gulf of Aden and for late Oligocene rifting of the southern Red Sea. *Mar Petrol Geol* 8:354–358
- Hunegnaw A, Sage L, Gonnard R (1998) Hydrocarbon potential of the intracratonic Ogaden Basin SE Ethiopia. *J Petrol Geol* 21:401–425
- Izzeldin AY (1987) Seismic, gravity and magnetic surveys in the central part of the Red Sea, their interpretation and implications for the structure and evolution of the Red Sea. *Tectonophysics* 143:269–306
- Jestin F, Huchon P, Gaulier JM (1994) The Somalia plate and the East African Rift System: present-day kinematics. *Geophys J Int* 116:637–654
- Joffe S, Garfunkel Z (1987) Plate kinematics of the circum Red Sea—a re-evaluation. *Tectonophysics* 141:5–22
- Johanson DC, Taieb M (1976) Plio-Pleistocene hominid discoveries in Hadar, Ethiopia. *Nature* 260:293–297
- Johnston (1884) *Travel in southern Ethiopia through the country of Adal and the kingdom of Shoa*. London
- Jones P (1976) Age of the lower flood basalts of the Ethiopian plateau. *Nature* 261:567–569
- Kasser M, Ruegg J-C, Lépine J-C (1987) Geodetic measurements on the Asal Rift (Djibouti): Twelve years of observations. *J Geodyn* 7:221–226
- Kazmin V (1975) Explanatory note to the geology of Ethiopia. *Ethiopian Inst Geol Surv Addis Ababa* 2:35
- Kazmin VG, Byakov AF (2000) Magmatism and crustal accretion in continental rifts. *J Afr Earth Sci* 30:555–568
- Kebede F, Kim W-Y, Kulha'nek O (1989) Dynamic source parameters of the March–May 1969 Serdo earthquakes in central Afar, Ethiopia, deduced from teleseismic body waves. *J Geophys Res* 94:5603–5614
- Kebede F, Kulhanek O (1991) Recent seismicity of the East African rift system and its implications. *Phys Earth Planet Int* 68:259–273
- Kebede F, Kulhanek O (1994) Spatial and temporal variations of b-values along the East African rift system and southern Red Sea. *Phys Earth Planet Int* 83:249–264
- Kebede F, Travi Y, Rozanski K (2008) The 18O and 2H enrichment of Ethiopian lakes. *J Hydrol* 365:173–182
- Keir D, Kendall JM, Ebinger CJ, Stuart GW (2005) Variations in late syn-rift melt alignment inferred from shear-wave splitting in crustal

- earthquakes beneath the Ethiopian Rift. *Geophys Res Lett* 32. Art. No. L23308.
- Keir D, Ebinger CJ, Stuart GW, Daly E, Ayele A (2006) Strain accommodation by magmatism and faulting at continental breakup: seismicity of the northern Ethiopian rift. *J geophys Res* 111
- Keir D, Hamling JJ, Ayele A, Calais E, Ebinger C, Wright TJ, Jacques E, Mohamed K, Hammond JOS, Belachew M, Baker E, Rowland JV, Lewi E, Bennati L (2009) Evidence for focused magmatic accretion at segment centers from lateral dike injections captured beneath the Red Sea rift in Afar. *Geology* 37:59–62
- Keir D, Bastow ID, Whaler KA, Daly E, Cornwall DG, Hautot S (2009) Lower crustal earthquakes near the Ethiopian rift induced by magmatic processes. *Geochem Geophys Geosyst* 10:Q0AB02
- Keir D et al (2011) Mapping the evolving strain field during continental breakup from crustal anisotropy in the Afar Depression. *Nat Comm* 2:285
- Keller GR, Harder SH, O'Reilly B, Mickus K, Tadesse K, Maguire PKM, The EAGLE Working Group (2004) A preliminary analysis of crustal structure variations along the Ethiopian Rift. In: Yirgu G et al. (eds) *Proceedings of the International Conference on the East African Rift System*, Addis Ababa, Ethiopia, Ethiopian Geoscience and Mineral Engineering Association, 97–101
- Kendall J-M (2000) Seismic anisotropy in the boundary layers of the mantle. In: Karato S, Stixrude L, Liebermann RC, Masters TG, Forte AM (eds) *Earth's Deep Interior: Atomic to the Global Scale*. Geophysical Monograph Series, 117, Am Geophys Union, 149–175.
- Kendall J-M, Stuart G, Ebinger C, Bastow I, Keir D (2005) Magma-assisted rifting in Ethiopia. *Nature* 433:146–148
- Kendall J-M, Pilidou S, Keir D, Bastow ID, Stuart GW, Ayele A (2006) Temporal compositional variation of early syn-rift rhyolites along the western Red Sea margin and northern Main Ethiopian rift. In: Yirgu G, Ebinger CJ, Maguire PKH (eds) *The Afar Volcanic Province within the East African Rift System*. *Geol Soc London, Special Pub.* 259:55–72
- Kendall J-M, Stuart GW, Ebinger CJ, Bastow ID, Keir D (2005) Magma-assisted rifting in Ethiopia. *Nature* 433:146–148
- Kenea N, Ebinger C, Rex DC (2001) Late Oligocene volcanism and extension in the southern Red Sea hills, Sudan. *J Geol Soc* 158:285–294
- Keranen K, Klemperer S, Gloaguen R, EAGLE Working Group (2004) Three-dimensional seismic imaging of a protoridge axis in the Main Ethiopian rift. *Geology* 32:949–952
- Kidane T, Courtillot V, Manighetti I, Audin L, Lahitte P, Quidelleur X, Gillot P-Y, Gallet Y, Carluat J, Haile T (2003) New paleomagnetic and geochronologic results from Ethiopian Afar: block rotations linked to rift overlap and propagation and determination of 2 Ma reference pole for stable Africa. *J Geophys Res* 108:1–32
- Kidane T, Platzman E, Ebinger C, Abebe B, Rochette P (2006) Paleomagnetic constraints on Continental Breakup: Observations from the Main Ethiopian rift. In: Yirgu G, Ebinger CJ, Maguire PKH (eds) *The Afar Volcanic Province within the East African Rift System*. *Geol. Soc. Spec. Publ.*, 259:165–184
- Kidane T, Otofujii Y-I, Komatsu Y, Shibasaki H, Rowland J (2009) Paleomagnetism of the Fentale-magmatic segment, main Ethiopian Rift: new evidence for counterclockwise block rotation linked to transensional deformation. *Phys Earth Planet Int* 176:109–123
- Kimbel WH, Johanson DC, Rak Y (1994) The 1st skull and other new discoveries of *Australopithecus-Afarensis* at Hadar, Ethiopia. *Nature* 368:449–451
- Kimbel W, Walter R, Johanson D, Reed K, Aronson J, Assefa Z, Marean C, Eck G, Bobe R, Hovers E, Rak Y, Voldra C, Yemane T, York D, Chen Y, Evensen N, Smith P (1996) Late Pliocene Homo and Oldowan tools from the Hadar Formation (Kada Hadar Member), Ethiopia. *J Hum Evol* 31:549–561
- Knox R, Nyblade A, Langston C (1999) Upper mantle S velocities beneath Afar and western Saudi Arabia from Rayleigh wave dispersion. *Geoph Res Lett* 25:4233–4236
- Korme T, Chorowicz J, Collet B, Bonavia FF (1997) Volcanic vents rooted on extension fractures and their geodynamic implications in the Ethiopian Rift. *J Volcanol Geotherm Res* 79:205–222
- Kreemer C, Holt WE, Haines AJ (2003) An integrated global model of present day plate motions and plate boundary deformation. *Geophys J Int* 154:8–34
- Kursten MOC (1975) Tectonic inventory of the Danakil Depression. In: Pilger A, Rosler A (eds) *Afar depression of Ethiopia, proceedings of an international symposium on the Afar region and rift related problems*, Bad Bergzabren, Germany, 1974, vol 1, E. Schweizerbart'sche Verlagsbuchhandlung, Stuttgart, Germany, pp 170–173
- Lahitte P, Coule M, Mercier N, Kidene T, Gillot PY (2001) K-Ar and TL volcanism chronology of the southern ends of the Red Sea spreading in Afar since 300 ka. *Earth Planet Sci* 332:13–20
- Lahitte P, Gillot P-Y, Courtillot V (2003) Silicic central volcanoes as precursors to rift propagation: the Afar case. *Earth Planet Sci Lett* 207:103–116
- Laughton AS (1966) *Phil Trans R Soc Lond A* 267:150
- Le Pichon X, Francheteau J (1978) A plate-tectonic analysis of the Red Sea-Gulf of Aden area. *Tectonophysics* 46:369–406
- Lepine J-C, Ruegg J-C, Steinmetz L (1972) Seismic profiles in the Djibouti area. *Tectonophysics* 15:59–64
- Lepine J-C, Hirn A (1992) Seismotectonics in the Republic of Djibouti linking the Afar Depression and the Gulf of Aden. *Tectonophysics* 209:65–86
- Leroy S, Gente P, Fournier M, d'Acremont E, Patriat P, Beslier M-O, Bellahsen N, Maia M, Blais A, Perrot J, Al-Kathiri A, Merkouriev S, Fleury J-M, Ruellan P-Y, Lepvrier C, Huchon P (2004) From rifting to spreading in the eastern Gulf of Aden: a geophysical survey of a young oceanic basin from margin to margin. *Terra Nova* 16:185–192
- Leroy S, d'Acremont E, Tiberi C, Basuyau C, Autin J, Lucazeau F, Sloan H (2010) Recent off-axis volcanism in the eastern Gulf of Aden: implications for plume–ridge interaction. *Earth Planet Sci Lett* 293:140–153
- Le Turdu C et al (1999) The Ziway-Shala lake basin system, Main Ethiopian rift: influence of volcanism, tectonics, and climatic forcing on basin formation and sedimentation. *Palaeo* 150:135–177
- Lin S-C, Kuo B-Y, Chiao L-Y, van Keken PE (2005) Thermal plume models and melt generation in East Africa: a dynamic modeling approach. *Earth Planet Sci Lett* 237:175–192
- Lithgow-Bertelloni C, Silver PG (1998) Dynamic topography, plate driving forces and the African superswell. *Nature* 395:269–272
- Lucazeau F, Leroy S, Autin J, Bonneville A, Goutorbe B, Watremez L, d'Acremont E, Düsünur D, Rolandone F, Huchon P, Bellahsen N, Tuchais P (2009) Post-rift volcanism and high heat-flow at the ocean-continent transition of the eastern Gulf of Aden. *Terra Nova* 21:285–292
- Lupi L (2010) *Dancalia, l'esplorazione del Afar, un'avventura italiana, IGM Firenze*, 2 vol, 1488p
- Mackenzie GD, Thybo H, Maguire PKH (2005) Crustal velocity structure across the Main Ethiopian Rift: results from two-dimensional wide-angle seismic modelling. *Geophys J Int* 162:994–1006
- Maguire P et al (2003) Geophysical project in Ethiopia studies continental breakup, EOS. *Trans Am Geophys Un* 84:337–340
- Maguire PKH et al (2006) Crustal structure of the northern Main Ethiopian Rift from the EAGLE controlled source survey; a snapshot of incipient lithospheric break-up. In: Yirgu G, Ebinger CJ, Maguire PKH (eds) *The Afar Volcanic Province within the East African Rift System*. *Geol. Soc. Spec. Publ.*, 259:269–292

- Mahatsente R, Jentzsch G, Jahr T (1999) Crustal structure of the Main Ethiopian rift from gravity data: 3-dimensional modeling. *Tectonophysics* 313:363–382
- Makris J (1975) Afar and Iceland—a geophysical comparison. In: Pilger A, Rosler A (eds) *Afar depression of Ethiopia, proceedings of an international symposium on the Afar region and rift related problems*, Bad Bergzabren, Germany, 1974, vol 1, E. Schweizerbart'sche Verlagsbuchhandlung, Stuttgart, Germany, pp 379–390.
- Makris J, Ginzburg A (1987) The Afar Depression: Transition between continental rifting and sea-floor spreading. *Tectonophysics* 141:199–214
- Makris MJ, Rihm R (1991) Shear controlled evolution of the Red Sea: pull-apart model. *Tectonophysics* 198:441–466
- Manighetti I, King GCP, Gaudemer Y, Scholtz CH, Doubre C (2001) Slip accumulation and lateral propagation of active normal faults in Afar. *J Geophys Res* 106:13,667–13,696
- Manighetti I, Tapponnier P, Courtillot V, Gallet Y, Jacques E, Gillot Y (2001) Strain transfer between disconnected, propagating rifts in Afar. *J Geophys Res* 106:13,613–13,665
- Marinelli G (1971) La province géothermique de la dépression Danakil. *Ann. Mines*, mai 1971
- Marone F, van der Lee S, Giardini D (2004) Three-dimensional upper-mantle S-velocity model for the Eurasia-Africa plate boundary region. *Geophys J Int* 158:109–130
- Marone F, van der Meijde M, van der Lee S, Giardini D (2003) Joint inversion of local, regional and teleseismic data for crustal thickness in the Eurasia-Africa plate boundary region. *Geophys J Int* 154:499–514
- Martini M (1969) La geochimica del Lago Giuletti. *Rend Soc Ital Mineral Petrol* 25:67–78
- Martini M (1969) Studio di Prodotti fumarolici di alcuni vulcani della catena dell'Erta Ale (Ethiopia). *Rend Soc Ital Mineral Petrol* 25:1–16
- McClusky S, Reilinger R, Mahmoud S, Ben Sari D, Tealeb A (2003) GPS constraints on Africa (Nubia) and Arabia plate motions. *Geoph J Int* 155:126–138
- McClusky S, Reilinger R, Ogubazghi G, Amlison A, Healed B, Vernant P, Sholna J, Fisseha S, Asfaw L, Bendick R, Kogan L (2010) Kinematics of the southern Red Sea—Afar triple Junction and implications for plate dynamics. *Geophys Res Lett* 37(5)
- McConnel RB (1975) The structural setting of the Afar depression. In *7th Colloquium on African Geology*, Firenze, *Travaux des laboratoires des sciences de la terre, Serie B11*, 116–117
- McKenzie DP, Davies D, Molnar P (1972) Plate tectonics of the Red Sea and East Africa. *Nature* 224:125–133
- Mechie J, Prodehl C (1988) Crustal and uppermost mantle structure beneath the Afro-Arabian Rift System. *Tectonophysics* 153:103–121
- Meshesha D, Shinjo R (2008) Rethinking geochemical feature of the Afar and Kenya mantle plumes and geodynamics implications. *J Geophys Res* 113
- Menzies M, Gallagher K, Yelland A, Hurford A (1997) Volcanic and non-volcanic rifted margins of the Red Sea and Gulf of Aden. *Geoch Cosmoch Acta* 61:2511–2527
- Mlynarski M, Zlotnicki J (2001) Fluid circulation in the active emerged Asal Rift (east Africa, Djibouti) inferred from self-potential and Telluric-Telluric prospecting. *Tectonophysics* 339:455–472
- Mohr PA (1962) The Ethiopian rift system. *Bull Geophys Observatory Addis Ababa* 5:33–62
- Mohr P (1983) Ethiopian flood basalt province. *Nature* 303:577–584
- Mohr P (1983) The Morton-Black hypothesis for the thinning of continental crust—revisited in western Afar. *Tectonophysics* 94:509–528
- Mohr PA, Zanettin B (1988) The Ethiopian flood basalt province. In: MacDougall JD (ed) *Continental Flood Basalts*. Kluwer Academic, Dordrecht, pp 63–110
- Mohr P (1989) Nature of the crust under Afar—new igneous not thinned continental. *Tectonophysics* 167:1–11
- Montenat C, Ott d'Estevou P, Purser BH (1998) The Suez Rift and the north-western Red Sea Neogene sedimentation and tectonic evolution. In: Purser BH (ed) *Dynamics and methods of study of sedimentary*. Oxford and IBH Publishing Company, New Delhi, India, pp 173–199
- Morbiddelli L, Nicoletti M, Petrucciani C, Piccirillo E (1975) Ethiopian southeastern plateau and related escarpment: K/Ar ages of the main volcanic events. In: Pilger A, Rösler A (eds) *Afar between continental and oceanic rifting*. Schweizerbart, Stuttgart, pp 362–370
- Morgan WJ (1968) Rises, trenches, great faults and crustal blocks. *J Geophys Res* 73:1959
- Morton WH, Black R (1975) Crustal attenuation in Afar. In: Pilger A, Rosler A (eds) *Afar Depression of Ethiopia*. Schweizerbart, Stuttgart, pp 55–61
- Morton W, Rex D, Mitchell J, Mohr P (1979) Riftward younging of volcanic units in the Addis Ababa region, Ethiopian rift valley. *Nature* 280:284–288
- Nesbitt LM (1934) Desert and Forest: the exploration of Abyssinian Danakil (London: *Jonathan Cape*) 450 pp. (Also published in 1935 by A. A. Knopf, New York, under the title 'Hell-hole of creation: the exploration of the Abyssinian Danakil')
- Noir J, Jacques E, Békri S, Adler PM, Tapponnier P, King GCP (1997) Fluid flow triggered migration of events in the 1989 Dobi earthquake sequence of Central Afar. *Geophys Res Lett* 24:2335–2338
- Nooner SL, Bennati L, Calais E, Buck WR, Hamling IJ, Wright TJ, Lewi E (2009) Post rifting relaxation in the Afar Region. *Ethiopia Geophys Res Lett* 36:L21308
- Nyblade AA, Robinson SW (1994) The African superswell. *Geophys Res Lett* 21:765–768
- Nyblade A, Knox R, Gurrola H (2000) Mantle transition zone thickness beneath Afar: implications for the origin of the Afar hotspot. *Geophys J Int* 142:615–619
- Nyblade A, Brazier RA (2002) Precambrian lithosphere controls on the development of the east African rift system. *Geology* 30:755–758
- Omenda, P, Achieng J, Onyango S, Varet, J (2014) The “Geothermal Village” Concept: a new approach to geothermal development in rural Africa. *Proceedings 5th African Rift geothermal Conference*, Arusha, Tanzania, 29–31 October 2014
- O'Neill C, Müller D, Steinberger B (2005) On the uncertainties in hot spot reconstructions and the significance of moving hot spot reference frames. *Geochem Geophys Geosyst* 6
- Onyango S, Varet J (2014) For a new social gender-based approach to geothermal development. *Proceedings 5th African Rift geothermal Conference*, Arusha, Tanzania, 29–31 October 2014
- Pallister JS (1987) Magmatic history of Red Sea rifting; perspective from the central Saudi Arabian coastal plain. *Geol Soc Am Bull* 98:400–417
- Pan M, Sjoeborg LE, Asfaw LM, Asenjo E, Alemu A, Hunegnaw A (2002) An analysis of the Ethiopian rift valley GPS campaigns in 1994 and 1999. *J Geodyn* 33:333–343
- Park Y, Nyblade AA, Rodgers AJ, Al-Amri A (2007) Upper mantle structure beneath the Arabian Peninsula and northern Red Sea from teleseismic body wave tomography: implication for the origin of Cenozoic uplift and volcanism in the Arabian Shield. *Geochem Geophys Geosyst* 8:Q06021
- Park Y, Nyblade AA, Rodgers AJ, Al-Amri A (2008) S wave velocity structure of the Arabian Shield upper mantle from Rayleigh wave tomography. *Geochem Geophys Geosyst* 9:Q07020
- Pik R, Marty B, Carignan J, Lavé J (2003) Stability of the upper Nile drainage network (Ethiopia) deduced from (U-Th)/He thermochronometry: implications for uplift and erosion of the Afar plume dome. *Earth planet Sci Lett* 215:73–88

- Pilger A, Rosler (1974) Afar between continental and oceanic rifting. Proceeding of the International Symposium on the Afar Region and related rift problems held in Bad Bergzabern, Germany. 1–6 April 1974
- Pinzuti P, Manighetti I, Humler E, Carlucci J (2001) Magmato-tectonic evolution of Asal Rift, Afar depression. *Eos Trans AGU* 82(47)
- Pizzi A, Coltorti M, Abebe B, Disperati L, Sacchi G, Salvini R (2006) The Wonji Fault Belt (Main Ethiopian Rift, Ethiopia): structural and geomorphological constraints and GPS monitoring. In: Yirgu G, G C, Ebinger CJ, Maguire PKH (eds) *The Afar Volcanic Province within the East African Rift System*. Geol. Soc. London, Spec. Pub. 259:191–208
- Prodehl C, Fuchs K, Mechie J (1997) Seismic-refraction studies of the Afro-Arabian Rift system—a brief review. *Tectonophysics* 278:1–13
- Purcell PG (1976) The marda fault zone, Ethiopia. *Nature* 261:569–571
- Radosevich SC, Rerallack G, Taieb M (1992) Reassessment of the paleoenvironment and preservation of hominid fossils from Hadar, Ethiopia. *Am J Phys Anthropol* 87:15–27
- Redfield TF, Wheeler WH, Often M (2003) A kinematic model for the development of the Afar Depression and its paleogeographic implications. *Earth Planet Sci Lett* 6831:1–16
- Reilinger R, McClusky S, Vernant P, Lawrence S, Ergintav S, Cakmak R, Ozener H, Kadirov F, Guliev I, Stepanyan R, Nadariya M, Hahubia G, Mahmoud S, Sakr K, ArRajehi A, Paradissis D, Al-Aydrus A, Prilepin M, Guseva T, Evren E, Dmitrova A, Filikov SV, Gomez F, Al-Ghazzi R, Karam G (2006) GPS constraints on continental deformation in the Africa–Arabia–Eurasia continental collision zone and implications for the dynamics of plate interactions. *J Geophys Res* 111:B05411
- Renne P, Walter R, Verosub K, Sweitzer M, Aronson J (1993) New data from Hadar (Ethiopia) support orbitally tuned time scale to 3.3 Ma. *Geophys Res Lett* 20:1067–1070
- Richard O (1979) Etude de la transition dorsale océanique–rift émergé: Le Golfe de Tadjoura (République de Djibouti). Approche géologique, géochronologique et pétrologique, Thèse, 149 pp., Univ. Paris XI-Orsay, Paris, France.
- Ritsema J, Nyblade AA, Owens TJ, Langston CA (1998) Upper mantle seismic velocity structure beneath Tanzania, east Africa: Implications for the stability of cratonic lithosphere. *J Geophys Res* 103:21201–21213
- Ritsema J, van Heijst H (2000) New seismic model of the upper mantle beneath Africa. *Geology* 28:63–66
- Ritsema J, Allen R (2003) The elusive mantle plume. *Earth Planet Sci Lett* 207:1–12
- Robertson Research (1993) UNDP/The World Bank, Red Sea/Gulf of Aden Regional Hydrocarbon Study Project report: Llandudno, Roberston Research, 121 p
- Rogers NW (2006) Basaltic magmatism and the geodynamics of the East African Rift System. In: Yirgu G, Ebinger CJ, Maguire PKH (eds) *The Afar Volcanic Province within the East African Rift System*. Geol. Soc. London, Spec. Pub. 259, pp 77–94
- Roeser HA (1975) A detailed magnetic survey of the southern Red Sea. *Geol Jahrb D13*:131–153
- Rognon P (1975) Tectonic deformation in central Afar basins in the upper Pleistocene and Holocene periods, from the study of lacustrine deposits. In: Pilger A, Rosler A (eds) *Afar depression of Ethiopia, proceedings of an international symposium on the Afar region and rift related problems, Bad Bergzabern, Germany, 1974, vol 1*, E. Schweizerbart'sche Verlagsbuchhandlung, Stuttgart, Germany, pp 198–200
- Rooney TO, Furman T, Yirgu G, Ayalew D (2005) Structure of the Ethiopian lithosphere: Xenolith evidence in the Main Ethiopian Rift. *Geochem Cosmochim Acta* 69:3889–3910
- Rouby D, Souriot T, Brun JP, Cobbod PR (1996) Displacements, strains, and rotations within the Afar Depression (Djibouti) from restoration in map view. *Tectonics* 15:952–965
- Roux J, Varet J (1975) Alkali feldspar liquid equilibrium relationships in peralkaline oversaturated systems and volcanic rocks. *Contrib Mineral Petrol* 49:67–81
- Rubin AM, Pollard DD (1988) Dike-induced faulting on rift zones of Iceland and Afar. *Geology* 16:413–417
- Ruegg J-C (1975) Main results about the crustal and upper mantle structure of the Djibouti region TFAL. In: Pilger A, Rösler A (eds) *Afar between continental and oceanic rifting*. Stuttgart, Schweizerbart, pp 89–107
- Ruegg JC, Kasser M, Lépine JC, Tarantola A (1979) Geodetic measurements of rifting associated with a seismo–volcanic crisis in Afar. *Geophys Res Lett* 6:817–820
- Ruegg J-C, Lépine J-C, Tarantola A (1979) Geodetic measurements of rifting associated with a seismo-volcanic crisis in Afar. *Geophys Res Lett* 6:817–820
- Ruegg J-C, Kasser M, Lépine J-C (1987) Strain accumulation across the Asal-Ghoubbet Rift, Djibouti, East Africa. *J Geophys Res* 89:6237–6246
- Ruppel E (1934) Skizze der geologischen formationen Abyssiniens. *Mus. Senckenberg*. 1
- Sanjuan B, Michard G, Michard A (1990) Origine des substances dissoutes dans les eaux des sources thermales et des forages de la région Asal-Goubbet (République de Djibouti). *J Volc Geoth Res* 43:333–352
- Schilling J-G, Kingsley R, Hanan B, McCully B (1992) Nd-Sr-Os isotopic variations along the Gulf of Aden: evidence for mantle-plume lithosphere interaction. *J Geophys Res* 97:10,927–10,966
- Sicilia D, Montagner J-P, Cara M, Stutzmann E, Debayle E, Lépine J-C, Leveque J-J, Beucler E, Sebai A, Roullet G, Ayele A, Sholan JM (2008) Upper mantle structure of shear-wave velocities and stratification of anisotropy in the Afar Hotspot region. *Tectonophysics* 462:164–177
- Sigmundsson F (1992) Tectonic implications of the 1989 Afar earthquake sequence. *Geophys Res Lett* 19:877–880
- Shackleton RM (1986) Precambrian collision tectonics in Africa. In: Coward MP, Ries AC (eds) *Collision Tectonics*. Geol. Soc., London, spec. pub., 19:329–349
- Sleep NH, Ebinger CJ, Kendall J-M (2002) Deflection of mantle plume material by cratonic keels. In: Fowler CMR, Ebinger CJ, Hawkesworth CJ (eds) *The early earth: physical, chemical and biological development*. Geol. Soc. Spec. Publ., 199, pp 135–150
- Smithsonian Institution (1992a) Erta `Ale (Ethiopia). *Bull Glob Volcanism Netw* 17:5
- Smithsonian Institution (1992b) Erta `Ale (Ethiopia). *Bull Glob Volcanism Netw* 17:4
- Smithsonian Institution (1992c) Erta `Ale (Ethiopia). *Bull Glob Volcanism Netw* 17:2
- Smithsonian Institution (1995) Erta `Ale (Ethiopia). *Bull Glob Volcanism Netw* 20:11
- Souleiman H, Houmed AM, Khaireh A, Haga AO, Abdillahi SO, Aye F (2012) Geothermal Development in Djibouti Republic: A Country Report. Proceedings of the 4th African Rift Geothermal Conference. Nairobi, Kenya, 21–23 November 2012, 7p
- Souriot T, Brun J-P (1992) Faulting and block rotation in the Afar triangle, East Africa: the Danakil crank-arm model. *Geology* 20:911–924
- Stein R, Briole P, Ruegg J-C, Tapponnier P, Gasse F (1991) Contemporary, Holocene, and Quaternary deformation of the Asal Rift, Djibouti: Implications for the mechanics of slow spreading ridges. *J Geophys Res* 96:21789–21806

- Stern RJ, Nielsen KC, Best E, Sultan M, Arvidson RE, Kroner A (1990) Orientation of the late Precambrian sutures in the Arabian-Nubian Shield. *Geology* 18:1103–1106
- Stieltjes L (1980) Carte géologique du rift d'Asal, République de Djibouti, Afar, East Africa. CNRS, BRGM, Paris, Orléans
- Stuart GW, Bastow ID, Ebinger CJ (2006) Crustal structure of the northern Main Ethiopian Rift from receiver function studies. In: Yirgu G, Ebinger CJ, Maguire PKH (eds) *The Afar Volcanic Province within the East African Rift System*. Geol. Soc. London, Spec. Pub. 259, pp 253–267
- Supan A (1927) *Grünzüge der Physischen Erdkunde. W. de Gruyter & Co, Berlin*, t.1. 495p
- Sultan M, Becker R, Arvidson RE, Shore P, Stern RJ, El Alfy Z, Guinness EA (1992) Nature of the Red Sea crust: a controversy revisited. *Geology* 20:593–596
- Talbot C, Ghebreab W (1997) Red Sea detachment and basement core complexes in Eritrea. In: *Geology* P, Armijo R, Manighetti I, Courtillot V (1990) Bookshelf faulting and horizontal block rotations between overlapping rift zones in southern Afar. *Geophys. Res. Lett.* 17:1–4
- Tarantola A, Ruegg J-C, Le'pine J-C (1979) Geodetic evidence for rifting in Afar: a brittle-elastic model of the behaviour of the lithosphere. *Earth Planet Sci Lett* 45:435–444
- Tarantola A, Ruegg J-C, Lépine J-P (1980) Geodetic evidence for rifting in Afar, 2. Vertical displacements. *Earth Planet Sci Lett* 48:363–370
- Tazieff H (1952) Une récente champagne océanographique dans la Mer rouge. *Bull Soc Belge Geol Pal Hyd* 61:84–90
- Tazieff H (1973) The Erta `Ale volcano. *Rev Geogr Phys Geol Dyn* 15:437–441
- Tazieff H, Varet J (1969) Pétrographie et tectonique de l'Afar septentrional (Ethiopie). *Colloque Géol. Africaine Clermont-Ferrand* (résumé), Ann. Fac. Sc. Clermont, no 41, p 54
- Tazieff H, Varet J (1969) Signification tectonique et magmatique de l'Afar septentrional (Ethiopie). *Rev Géog Phys Geol Dyn* 2 (11):429–450
- Tesfaye S, Kusky TT, Harding D (2003) Early Continental breakup boundary and migration of the Afar triple junction, Ethiopia. *Geol Soc Am Bull* 115:1053–1067
- Tesfaye S, Rowan MG, Mueller K, Trudgill BD, Harding DJ (2008) Relay and accommodation zones in the Dobe and Hanle grabens, central Afar, Ethiopia and Djibouti. *J Geol Soc* 165(2):535–547. doi:10.1144/0016-76492007-093
- Tiberi C, Ebinger C, Ballu V, Stuart G, Oluma B (2005) Inverse models of gravity data from the Red Sea—Aden—East African Rift triple junction zone. *Geophys J Int* 163:775–787
- UNESCO-CGGM (2000) Geological map of the world, 2nd edn. BRGM, Paris
- Vail JR (1985) Pan-African (late Precambrian) tectonic terranes and reconstruction of the Arabian-Nubian Shield. *Geology* 13 (1985):839–842
- Van Ngoc P, Boyer D, Le Moue'l J-L, Courtillot V (1981) Identification of a magma chamber in the Ghoubbet-Asal Rift (Djibouti) from a magnetotelluric experiment. *Earth Planet Sci Lett* 52:372–380
- Varet J (1971) Erta'Ale volcanic activity. Smithsonian Institution, Center for short-lived Phenomena. Event 22–71, 18/2/71, cards no 1132–1133 and 1308
- Varet J (1971) Erta'Ale activity (Afar, Ethiopia). *Bull Geophys Obs Addis Ababa* 13:115–119
- Varet J (1971) Sur l'activité récente de l'Erta'Ale (Dankalie, Ethiopie). *C R Ac Sci Paris t. 272*, pp 1964–1967
- Varet J (1972) Erta Ale volcanic activity. Smithsonian Institution, Center for short-lived Phenomena. Event 16–72, 6/3/72, card No 1363
- Varet J (1972) Erta Ale volcanic activity—*Smithson*. Instit Cent for short lived phenomena. Event 16–72, Cards no 1390 and 1390 A
- Varet J (1975) Carte géologique de l'Afar central et méridional, CNR-CNRS, 1/500 000 *Géotechnip*
- Varet J (1975) L'Afar, un "point chaud" de la géophysique. *La Recherche* 62:1018–1026
- Varet J (1976) Introduction: accréation de nouvelle croûte en domaine suhaérien exemple de l'Afar. *Bull Soc Géol France* 18(4):825–828
- Varet J (1978) Geology of central and southern Afar (Ethiopia and Djibouti Republic), map and 124 pp. report, Centre Natl. de la Rec. Sci., Paris.
- Varet J (1978) La géothermie dans le développement futur de l'Ethiopie. SINET—Addis Abeba—Ethiopie
- Varet J, Barberi F (1975) Nature of the Afar crust: a discussion. In: Pilger A, Rosler A (eds) *Afar depression of Ethiopia*. Stuttgart (Schweizerbart), pp 375–378
- Varet J, Barberi F (1976) Traçé des frontières de plaques en Afar: discussion à partir des données volcanologiques. *Bull Soc Géol France* 18(4):831–846
- Varet J, Barberi F (1978) The Afar rift junction. In: Neunan, Rarnberg (eds) *Petrology and geochemistry of continental rifts*, pp 55–69
- Varet J, Gasse F (1978) Geology of central and meridional Afar. Ed. CNRS, 140 p
- Varet J, Stieljes L, Joron JL, Treuil M (1976) Le rift d'Asal, segment de dorsale émergé : discussion pétrologique et géochimique. *Bull Soc Géol France* 18(4):851–862
- Varet J, Delattre JN, Gerard A, Mennechet C (1979) Etude des variations du champ de pesanteur entre 1973 et 1979 dans la région de L'Ardoukoba (République de Djibouti)
- Varet J, Ballestracci R, Benderitter Y (1980) Sondage magnétotellurique dans le rift d'Assal (République de Djibouti). *CR Acad Sci* 290:77–80
- Varet J, Chernet T, Woldetinsae G, Arnason K (2012) Exploring for Geothermal Sites in Northern and Central Afar (Ethiopia). *Proceedings of the 4th African Rift Geothermal Conference*. Nairobi, Kenya, 21–23 November 2012, 7 p
- Vellutini P (1990) The Manda-Inakir Rift, Republic of Djibouti: a comparison with the Asal Rift and its geodynamic interpretation. *Tectonophysics* 172(1990):141–153
- Vellutini P, Piguët P, Recroix F (1995) Carte géologique de la République de Djibouti au 1/100,000. Feuille de Dorra. In: *Notice explicative*. (BRGM, eds). Service Géologique National, Orléans, 85 pp
- Vigier N, Bourdon B, Joron J-L, Alle`gre CJ (1999) U-decay series and trace element systematics in the 1978 eruption of Arduko`ba, Asal Rift: Timescale of magma crystallization, *Earth Planet Sci Lett* 174:81–97
- Vigny C, Huchon P, Ruegg JC, Khanbari K, Asfaw L (2006) New GPS data in Yemen confirm slow Arabia plate motion. *J Geophys Res* 111:B02402
- Vigny C, Huchon P, Ruegg J-C, Khanbari K, Asfaw LM (2006) Confirmation of Arabia plate slow motion by new GPS data in Yemen. *J Geophys Res* 111:B02402
- Vincent EA (1975) Presentation of the Wager prize to F. Barberi and J. Varet. *Bull Volc* 30(2):162–166
- Voggenreiter W, Hötzl H, Mechie J (1988) Low-angle detachment origin for the Red Sea rift system. *Tectonophysics* 150:51–75
- Vauchez A, Tommasi A, Barruol G, Maumus J (2000) Upper mantle deformation and seismic anisotropy in continental rifts. *Phys Chem Earth* 25:111–117
- Wagner G, Lagston C (1988) East African earthquake body wave inversion with implications for continental structure and deformation. *Geophys J* 94:503–518
- Walker K, Nyblade AA, Klemperer SL, Bokelmann GHR, Owens TJ (2003) On the relationship between extension and anisotropy:

- constraints from shear wave splitting across the East Africa Plateau. *J Geophys Res* 109. doi:10.1029/2003JB002866
- Walter RC (1981) The volcanic history of the Hadar early man site and the surrounding Afar region of Ethiopia. Ph.D. dissertation, Case Western Reserve University, USA
- Walter RC, Aronson JL (1982) Revisions of K/Ar ages for the Hadar hominid site, Ethiopia. *Nature* 296:122–127
- Watchorn F, Nichols GJ, Bosence DWJ (1998) Rift related sedimentation and stratigraphy, southern Yemen (Gulf of Aden). In: Purser BH, Bosence DWJ (eds) *Sedimentation and Tectonics of Rift Basins: Red Sea–Gulf of Aden*. Chapman and Hall, London, 663 p
- Wegener A (1929) *Die Entstehung der Kontinente und Ozeane* (4th edn). Friedrich Vieweg & Sohn Akt. Ges, Braunschweig
- Whaler KA, Hautot S (2006) The electrical resistivity structure of the crust beneath the northern Main Ethiopian Rift. In: Yirgu G, Ebinger CJ, Maguire PKH (eds) *The Afar Volcanic Province within the East African Rift System*. Geol. So. London, Spec. Pub. 259:293–306
- Williams MA, Bishop PM, Dakin F (1977) Late Quaternary lake levels in southern Afar and the adjacent Ethiopian Rift. *Nature* 267:690–693
- Williams FM, Williams MA, Aumento J (2004) Tensional fissures and crustal extension rates in the northern part of the Main Ethiopian Rift. *J Afr Earth Sci* 38:183–197
- Wolde B (1996) Spatial and temporal variations in the compositions of Upper Miocene to Recent basic lavas in the northern Main Ethiopian Rift: implications for the causes of Cenozoic magmatism in Ethiopia. *Geol Rundsch* 85:380–389
- WoldeGabriel G, Aronson JL, Walter RC (1990) Geology, geochronology and rift basin development in the central sector of the Main Ethiopian Rift. *Geol Soc Am Bull* 102:439–485
- WoldeGabriel G, Aronson J, Walter R (1990) Tectonic development of the Main Ethiopian rift. *Geol Soc Am Bull* 102:439–458
- WoldeGabriel G, Yemane T, Suwa G, White T, Asfaw B (1991) Age of volcanism and rifting in the Buri-Soyoma are, Amaro Horst, southern main Ethiopian Rift: geo- and biochronologic data. *J Afr Earth Sci* 13:437–447
- WoldeGabriel G, White T, Suwa G, Renne P, de Heinzelin J, Hart W, Heiken G (1994) Ecological and temporal placement of early Pliocene hominids at Aramis, Ethiopia. *Nature* 371:330–333
- Woldetinsae G, Götze H-J (2005) Gravity field and isostatic state of Ethiopia and its adjacent areas. *J Afr Earth Sci* 41:103–117
- Yemane T (1997) *Stratigraphy and Sedimentology of the Hadar Formation, Afar, Ethiopia* (Ph.D. thesis), Ames, Iowa State University, 182 p
- Yirgu G, Ayele A, Ayalew D (2006) Recent seismovolcanic crisis in Northern Afar, Ethiopia. *Eos* 87(33):325–336
- Zanettin B, Justin-Visentin E (1975) Tectonical and volcanological evolution of the western Afar margin (Ethiopia). In: Pilger A, Rosler A (eds) *Afar Depression of Ethiopia*. Schweizerbart, Stuttgart, pp 300–309